ISSN 1007-9327 (print)
ISSN 2219-2840 (online)

World Journal of *Gastroenterology*

World J Gastroenterol 2017 November 7; 23(41): 7347-7494

Published by Baishideng Publishing Group Inc

World Journal of Gastroenterology

A peer-reviewed, online, open-access journal of gastroenterology and hepatology

Editorial Board

2014-2017

The *World Journal of Gastroenterology* Editorial Board consists of 1353 members, representing a team of worldwide experts in gastroenterology and hepatology. They are from 68 countries, including Albania (1), Algeria (1), Argentina (7), Australia (31), Austria (9), Belgium (10), Brazil (20), Brunei Darussalam (1), Bulgaria (2), Cambodia (1), Canada (25), Chile (4), China (161), Croatia (1), Cuba (1), Czech (6), Denmark (2), Egypt (9), Estonia (2), Finland (6), France (17), Germany (56), Greece (31), Guatemala (1), Hungary (14), Iceland (1), India (33), Indonesia (2), Iran (10), Ireland (9), Israel (18), Italy (195), Japan (151), Jordan (1), Kuwait (1), Lebanon (7), Lithuania (1), Malaysia (1), Mexico (10), Morocco (1), Netherlands (5), New Zealand (4), Nigeria (3), Norway (6), Pakistan (6), Poland (12), Portugal (8), Puerto Rico (1), Qatar (1), Romania (10), Russia (3), Saudi Arabia (2), Singapore (7), Slovenia (2), South Korea (64), Spain (51), Sri Lanka (1), Sudan (1), Sweden (12), Switzerland (5), Thailand (7), Trinidad and Tobago (1), Tunisia (2), Turkey (56), United Kingdom (47), United States (173), Venezuela (1), and Vietnam (1).

Austria

Felix Aigner, *Innsbruck*
Gabriela A Berlakovich, *Vienna*
Herwig R Cerwenka, *Graz*
Peter Ferenci, *Wien*
Alfred Gangl, *Vienna*
Kurt Lenz, *Linz*
Markus Peck-Radosavljevic, *Vienna*
Markus Raderer, *Vienna*
Stefan Riss, *Vienna*

Belgium

Michael George Adler, *Brussels*
Benedicte Y De Winter, *Antwerp*
Mark De Ridder, *Jette*
Olivier Detry, *Liege*
Denis Dufrane Dufrane, *Brussels*
Nikos Kotzampassakis, *Liège*
Geert KMM Robaeys, *Genk*
Xavier Sagaert, *Leuven*
Peter Starkel, *Brussels*
Eddie Wisse, *Keerbergen*

Brazil

SMP Balzan, *Santa Cruz do Sul*
JLF Caboclo, *Sao jose do rio preto*
Fábio Guilherme Campos, *Sao Paulo*
Claudia RL Cardoso, *Rio de Janeiro*
Roberto J Carvalho-Filho, *Sao Paulo*
Carla Daltro, *Salvador*
José Sebastiao dos Santos, *Ribeirao Preto*
Eduardo LR Mello, *Rio de Janeiro*
Sthela Maria Murad-Regadas, *Fortaleza*
Claudia PMS Oliveira, *Sao Paulo*
Júlio C Pereira-Lima, *Porto Alegre*
Marcos V Perini, *Sao Paulo*
Vietla Satyanarayana Rao, *Fortaleza*
Raquel Rocha, *Salvador*
AC Simoes e Silva, *Belo Horizonte*
Mauricio F Silva, *Porto Alefre*
Aytan Miranda Sipahi, *Sao Paulo*
Rosa Leonôra Salerno Soares, *Niterói*
Cristiane Valle Tovo, *Porto Alegre*
Eduardo Garcia Vilela, *Belo Horizonte*

Brunei Darussalam

Vui Heng Chong, *Bandar Seri Begawan*

Bulgaria

Tanya Kirilova Kadiyska, *Sofia*
Mihaela Petrova, *Sofia*

Cambodia

Francois Rouet, *Phnom Penh*

Canada

Brian Bressler, *Vancouver*
Frank J Burczynski, *Winnipeg*
Wangxue Chen, *Ottawa*
Francesco Crea, *Vancouver*
Mirko Diksic, *Montreal*
Jane A Foster, *Hamilton*
Hugh J Freeman, *Vancouver*
Shahrokh M Ghobadloo, *Ottawa*
Yuewen Gong, *Winnipeg*
Philip H Gordon, *Quebec*
Rakesh Kumar, *Edmonton*
Wolfgang A Kunze, *Hamilton*
Patrick Labonte, *Laval*
Zhikang Peng, *Winnipeg*
Jayadev Raju, *Ottawa*
Maitreyi Raman, *Calgary*
Giada Sebastiani, *Montreal*
Maida J Sewitch, *Montreal*
Eldon A Shaffer, *Alberta*
Christopher W Teshima, *Edmonton*
Jean Sévigny, *Québec*
Pingchang Yang, *Hamilton*
Pingchang Yang, *Hamilton*
Eric M Yoshida, *Vancouver*
Bin Zheng, *Edmonton*

Chile

Marcelo A Beltran, *La Serena*
Flavio Nervi, *Santiago*
Adolfo Parra-Blanco, *Santiago*
Alejandro Soza, *Santiago*

China

Zhao-Xiang Bian, *Hong Kong*
San-Jun Cai, *Shanghai*
Guang-Wen Cao, *Shanghai*
Long Chen, *Nanjing*
Ru-Fu Chen, *Guangzhou*
George G Chen, *Hong Kong*
Li-Bo Chen, *Wuhan*
Jia-Xu Chen, *Beijing*
Hong-Song Chen, *Beijing*
Lin Chen, *Beijing*
Yang-Chao Chen, *Hong Kong*
Zhen Chen, *Shanghai*
Ying-Sheng Cheng, *Shanghai*
Kent-Man Chu, *Hong Kong*
Zhi-Jun Dai, *Xi'an*
Jing-Yu Deng, *Tianjin*
Yi-Qi Du, *Shanghai*
Zhi Du, *Tianjin*
Hani El-Nezami, *Hong Kong*
Bao-Ying Fei, *Hangzhou*
Chang-Ming Gao, *Nanjing*
Jian-Ping Gong, *Chongqing*
Zuo-Jiong Gong, *Wuhan*
Jing-Shan Gong, *Shenzhen*
Guo-Li Gu, *Beijing*
Yong-Song Guan, *Chengdu*
Mao-Lin Guo, *Luoyang*
Jun-Ming Guo, *Ningbo*
Yan-Mei Guo, *Shanghai*
Xiao-Zhong Guo, *Shenyang*
Guo-Hong Han, *Xi'an*
Ming-Liang He, *Hong Kong*
Peng Hou, *Xi'an*
Zhao-Hui Huang, *Wuxi*
Feng Ji, *Hangzhou*
Simon Law, *Hong Kong*
Yu-Yuan Li, *Guangzhou*
Meng-Sen Li, *Haikou*
Shu-De Li, *Shanghai*
Zong-Fang Li, *Xi'an*
Qing-Quan Li, *Shanghai*
Kang Li, *Lasa*
Han Liang, *Tianjin*
Xing'e Liu, *Hangzhou*
Zheng-Wen Liu, *Xi'an*
Xiao-Fang Liu, *Yantai*
Bin Liu, *Tianjin*
Quan-Da Liu, *Beijing*
Hai-Feng Liu, *Beijing*
Fei Liu, *Shanghai*
Ai-Guo Lu, *Shanghai*
He-Sheng Luo, *Wuhan*
Xiao-Peng Ma, *Shanghai*
Yong Meng, *Shantou*
Ke-Jun Nan, *Xi'an*
Siew Chien Ng, *Hong Kong*
Simon SM Ng, *Hong Kong*
Zhao-Shan Niu, *Qingdao*
Bo-Rong Pan, *Xi'an*
Di Qu, *Shanghai*
Rui-Hua Shi, *Nanjing*
Bao-Min Shi, *Shanghai*
Xiao-Dong Sun, *Hangzhou*
Si-Yu Sun, *Shenyang*
Guang-Hong Tan, *Haikou*
Wen-Fu Tang, *Chengdu*
Anthony YB Teoh, *Hong Kong*
Wei-Dong Tong, *Chongqing*
Eric Tse, *Hong Kong*
Hong Tu, *Shanghai*
Rong Tu, *Haikou*
Jian-She Wang, *Shanghai*
Kai Wang, *Jinan*
Xiao-Ping Wang, *Xianyang*
Dao-Rong Wang, *Yangzhou*
De-Sheng Wang, *Xi'an*
Chun-You Wang, *Wuhan*
Ge Wang, *Chongqing*
Xi-Shan Wang, *Harbin*
Wei-hong Wang, *Beijing*
Zhen-Ning Wang, *Shenyang*
Wai Man Raymond Wong, *Hong Kong*
Chun-Ming Wong, *Hong Kong*
Jian Wu, *Shanghai*
Sheng-Li Wu, *Xi'an*
Wu-Jun Wu, *Xi'an*
Bing Xia, *Wuhan*
Qing Xia, *Chengdu*
Yan Xin, *Shenyang*
Dong-Ping Xu, *Beijing*
Jian-Min Xu, *Shanghai*
Wei Xu, *Changchun*
Ming Yan, *Jinan*
Xin-Min Yan, *Kunming*
Yi-Qun Yan, *Shanghai*
Feng Yang, *Shanghai*
Yong-Ping Yang, *Beijing*
He-Rui Yao, *Guangzhou*
Thomas Yau, *Hong Kong*
Winnie Yeo, *Hong Kong*
Jing You, *Kunming*
Jian-Qing Yu, *Wuhan*
Ying-Yan Yu, *Shanghai*
Wei-Zheng Zeng, *Chengdu*
Zong-Ming Zhang, *Beijing*

Dian-Liang Zhang, *Qingdao*
Ya-Ping Zhang, *Shijiazhuang*
You-Cheng Zhang, *Lanzhou*
Jian-Zhong Zhang, *Beijing*
Ji-Yuan Zhang, *Beijing*
Hai-Tao Zhao, *Beijing*
Jian Zhao, *Shanghai*
Jian-Hong Zhong, *Nanning*
Ying-Qiang Zhong, *Guangzhou*
Ping-Hong Zhou, *Shanghai*
Yan-Ming Zhou, *Xiamen*
Tong Zhou, *Nanchong*
Li-Ming Zhou, *Chengdu*
Guo-Xiong Zhou, *Nantong*
Feng-Shang Zhu, *Shanghai*
Jiang-Fan Zhu, *Shanghai*
Zhao-Hui Zhu, *Beijing*

Croatia

Tajana Filipec Kanizaj, *Zagreb*

Cuba

Damian Casadesus, *Havana*

Czech

Jan Bures, *Hradec Kralove*
Marcela Kopacova, *Hradec Kralove*
Otto Kucera, *Hradec Kralove*
Marek Minarik, *Prague*
Pavel Soucek, *Prague*
Miroslav Zavoral, *Prague*

Denmark

Vibeke Andersen, *Odense*
E Michael Danielsen, *Copenhagen*

Egypt

Mohamed MM Abdel-Latif, *Assiut*
Hussein Atta, *Cairo*
Ashraf Elbahrawy, *Cairo*
Mortada Hassan El-Shabrawi, *Cairo*
Mona El Said El-Raziky, *Cairo*
Elrashdy M Redwan, *New Borg Alrab*
Zeinab Nabil Ahmed Said, *Cairo*
Ragaa HM Salama, *Assiut*
Maha Maher Shehata, *Mansoura*
Mostafa Sira, *Menofiya*

Estonia

Margus Lember, *Tartu*
Tamara Vorobjova, *Tartu*

Finland

Marko Kalliomäki, *Turku*
Thomas Kietzmann, *Oulu*
Kaija-Leena Kolho, *Helsinki*
Eija Korkeila, *Turku*
Heikki Makisalo, *Helsinki*
Tanja Pessi, *Tampere*

France

Armando Abergel Clermont, *Ferrand*
Elie K Chouillard, *Polssy*
Pierre Cordelier, *Toulouse*
Pascal P Crenn, *Garches*
Catherine Daniel, *Lille*
Fanny Daniel, *Paris*
Cedric Dray, *Toulouse*
Benoit Foligne, *Lille*
Jean-Noel Freund, *Strasbourg*
Nathalie Janel, *Paris*
Majid Khatib, *Bordeaux*
Jacques Marescaux, *Strasbourg*
Jean-Claude Marie, *Paris*
Hang Nguyen, *Clermont-Ferrand*
Hugo Perazzo, *Paris*
Alain L Servin, *Chatenay-Malabry*
Chang Xian Zhang, *Lyon*

Germany

Stavros A Antoniou, *Monchengladbach*
Erwin Biecker, *Siegburg*
Hubert E Blum, *Freiburg*
Thomas Bock, *Berlin*
Katja Breitkopf-Heinlein, *Mannheim*
Elke Cario, *Essen*
Güralp Onur Ceyhan, *Munich*
Angel Cid-Arregui, *Heidelberg*
Michael Clemens Roggendorf, *München*
Christoph F Dietrich, *Bad Mergentheim*
Valentin Fuhrmann, *Hamburg*
Nikolaus Gassler, *Aachen*
Andreas Geier, *Wuerzburg*
Markus Gerhard, *Munich*
Anton Gillessen, *Muenster*
Thorsten Oliver Goetze, *Offenbach*
Daniel Nils Gotthardt, *Heidelberg*
Robert Grützmann, *Dresden*
Thilo Hackert, *Heidelberg*
Joerg Haier, *Muenster*
Claus Hellerbrand, *Regensburg*
Harald Peter Hoensch, *Darmstadt*
Jens Hoeppner, *Freiburg*
Richard Hummel, *Muenster*
Jakob Robert Izbicki, *Hamburg*
Gernot Maximilian Kaiser, *Essen*
Matthias Kapischke, *Hamburg*
Michael Keese, *Frankfurt*
Andrej Khandoga, *Munich*
Jorg Kleeff, *Munich*
Alfred Koenigsrainer, *Tuebingen*
Peter Christopher Konturek, *Saalfeld*
Michael Linnebacher, *Rostock*
Stefan Maier, *Kaufbeuren*
Oliver Mann, *Hamburg*
Marc E Martignoni, *Munic*
Thomas Minor, *Bonn*
Oliver Moeschler, *Osnabrueck*
Jonas Mudter, *Eutin*
Sebastian Mueller, *Heidelberg*
Matthias Ocker, *Berlin*
Andreas Ommer, *Essen*
Albrecht Piiper, *Frankfurt*
Esther Raskopf, *Bonn*
Christoph Reichel, *Bad Brückenau*
Elke Roeb, *Giessen*
Udo Rolle, *Frankfurt*
Karl-Herbert Schafer, *Zweibrücken*
Andreas G Schreyer, *Regensburg*
Manuel A Silva, *Penzberg*
Georgios C Sotiropoulos, *Essen*
Ulrike S Stein, *Berlin*
Dirk Uhlmann, *Leipzig*
Michael Weiss, *Halle*
Hong-Lei Weng, *Mannheim*
Karsten Wursthorn, *Hamburg*

Greece

Alexandra Alexopoulou, *Athens*
Nikolaos Antonakopoulos, *Athens*
Stelios F Assimakopoulos, *Patras*
Grigoris Chatzimavroudis, *Thessaloniki*
Evangelos Cholongitas, *Thessaloniki*
Gregory Christodoulidis, *Larisa*
George N Dalekos, *Larissa*
Maria Gazouli, *Athens*
Urania Georgopoulou, *Athens*
Eleni Gigi, *Thessaloniki*
Stavros Gourgiotis, *Athens*
Leontios J Hadjileontiadis, *Thessaloniki*
Thomas Hyphantis, *Ioannina*
Ioannis Kanellos, *Thessaloniki*
Stylianos Karatapanis, *Rhodes*
Michael Koutsilieris, *Athens*
Spiros D Ladas, *Athens*
Theodoros K Liakakos, *Athens*
Emanuel K Manesis, *Athens*
Spilios Manolakopoulos, *Athens*
Gerassimos John Mantzaris, *Athens*
Athanasios D Marinis, *Piraeus*
Nikolaos Ioannis Nikiteas, *Athens*
Konstantinos X Papamichael, *Athens*
George Sgourakis, *Athens*
Konstantinos C Thomopoulos, *Patras*
Konstantinos Triantafyllou, *Athens*
Christos Triantos, *Patras*
Georgios Zacharakis, *Athens*
Petros Zezos, *Alexandroupolis*
Demosthenes E Ziogas, *Ioannina*

Guatemala

Carlos Maria Parellada, *Guatemala*

Hungary

Mihaly Boros, *Szeged*
Tamás Decsi, *Pécs*
Gyula Farkas, *Szeged*
Andrea Furka, *Debrecen*
Y vette Mandi, *Szeged*
Peter L Lakatos, *Budapest*
Pal Miheller, *Budapest*
Tamás Molnar, *Szeged*
Attila Olah, *Gyor*
Maria Papp, *Debrecen*
Zoltan Rakonczay, *Szeged*

Ferenc Sipos, *Budapest*
Miklós Tanyi, *Debrecen*
Tibor Wittmann, *Szeged*

Iceland

Tryggvi Bjorn Stefánsson, *Reykjavík*

India

Brij B Agarwal, *New Delhi*
Deepak N Amarapurkar, *Mumbai*
Shams ul Bari, *Srinagar*
Sriparna Basu, *Varanasi*
Runu Chakravarty, *Kolkata*
Devendra C Desai, *Mumbai*
Nutan D Desai, *Mumbai*
Suneela Sunil Dhaneshwar, *Pune*
Radha K Dhiman, *Chandigarh*
Pankaj Garg, *Mohali*
Uday C Ghoshal, *Lucknow*
Kalpesh Jani, *Vadodara*
Premashis Kar, *New Delhi*
Jyotdeep Kaur, *Chandigarh*
Rakesh Kochhar, *Chandigarh*
Pradyumna K Mishra, *Mumbai*
Asish K Mukhopadhyay, *Kolkata*
Imtiyaz Murtaza, *Srinagar*
P Nagarajan, *New Delhi*
Samiran Nundy, *Delhi*
Gopal Pande, *Hyderabad*
Benjamin Perakath, *Vellore*
Arun Prasad, *New Delhi*
D Nageshwar Reddy, *Hyderabad*
Lekha Saha, *Chandigarh*
Sundeep Singh Saluja, *New Delhi*
Mahesh Prakash Sharma, *New Delhi*
Sadiq Saleem Sikora, *Bangalore*
Sarman Singh, *New Delhi*
Rajeev Sinha, *Jhansi*
Rupjyoti Talukdar, *Hyderabad*
Rakesh Kumar Tandon, *New Delhi*
Narayanan Thirumoorthy, *Coimbatore*

Indonesia

David Handojo Muljono, *Jakarta*
Andi Utama, *Jakarta*

Iran

Arezoo Aghakhani, *Tehran*
Seyed Mohsen Dehghani, *Shiraz*
Ahad Eshraghian, *Shiraz*
Hossein Khedmat, *Tehran*
Sadegh Massarrat, *Tehran*
Marjan Mohammadi, *Tehran*
Roja Rahimi, *Tehran*
Farzaneh Sabahi, *Tehran*
Majid Sadeghizadeh, *Tehran*
Farideh Siavoshi, *Tehran*

Ireland

Gary Alan Bass, *Dublin*
David J Brayden, *Dublin*
Ronan A Cahill, *Dublin*
Glen A Doherty, *Dublin*
Liam J Fanning, *Cork*
Barry Philip McMahon, *Dublin*
RossMcManus, *Dublin*
Dervla O'Malley, *Cork*
Sinead M Smith, *Dublin*

Israel

Dan Carter, *Ramat Gan*
Jorge-Shmuel Delgado, *Metar*
Eli Magen, *Ashdod*
Nitsan Maharshak, *Tel Aviv*
Shaul Mordechai, *Beer Sheva*
Menachem Moshkowitz, *Tel Aviv*
William Bahij Nseir, *Nazareth*
Shimon Reif, *Jerusalem*
Ram Reifen, *Rehovot*
Ariella Bar-Gil Shitrit, *Jerusalem*
Noam Shussman, *Jerusalem*
Igor Sukhotnik, *Haifa*
Nir Wasserberg, *Petach Tiqwa*
Jacob Yahav, *Rehovot*
Doron Levi Zamir, *Gedera*
Shira Zelber-Sagi, *Haifa*
Romy Zemel, *Petach-Tikva*

Italy

Ludovico Abenavoli, *Catanzaro*
Luigi Elio Adinolfi, *Naples*
Carlo Virginio Agostoni, *Milan*
Anna Alisi, *Rome*
Piero Luigi Almasio, *Palermo*
Donato Francesco Altomare, *Bari*
Amedeo Amedei, *Florence*
Pietro Andreone, *Bologna*
Imerio Angriman, *Padova*
Vito Annese, *Florence*
Paolo Aurello, *Rome*
Salavtore Auricchio, *Naples*
Gian Luca Baiocchi, *Brescia*
Gianpaolo Balzano, *Milan*
Antonio Basoli, *Rome*
Gabrio Bassotti, *San Sisto*
Mauro Bernardi, *Bologna*
Alberto Biondi, *Rome*
Ennio Biscaldi, *Genova*
Massimo Bolognesi, *Padua*
Luigi Bonavina, *Milano*
Aldo Bove, *Chieti*
Raffaele Bruno, *Pavia*
Luigi Brusciano, *Napoli*
Giuseppe Cabibbo, *Palermo*
Carlo Calabrese, *Bologna*
Daniele Calistri, *Meldola*
Vincenza Calvaruso, *Palermo*
Lorenzo Camellini, *Reggio Emilia*
Marco Candela, *Bologna*
Raffaele Capasso, *Naples*
Lucia Carulli, *Modena*
Renato David Caviglia, *Rome*
Luigina Cellini, *Chieti*
Giuseppe Chiarioni, *Verona*
Claudio Chiesa, *Rome*
Michele Cicala, *Roma*
Rachele Ciccocioppo, *Pavia*
Sandro Contini, *Parma*
Gaetano Corso, *Foggia*
Renato Costi, *Parma*
Alessandro Cucchetti, *Bologna*
Rosario Cuomo, *Napoli*
Giuseppe Currò, *Messina*
Paola De Nardi, *Milano*
Giovanni D De Palma, *Naples*
Raffaele De Palma, *Napoli*
Giuseppina De Petro, *Brescia*
Valli De Re, *Aviano*
Paolo De Simone, *Pisa*
Giuliana Decorti, *Trieste*
Emanuele Miraglia del Giudice, *Napoli*
Isidoro Di Carlo, *Catania*
Matteo Nicola Dario Di Minno, *Naples*
Massimo Donadelli, *Verona*
Mirko D'Onofrio, *Verona*
Maria Pina Dore, *Sassari*
Luca Elli, *Milano*
Massimiliano Fabozzi, *Aosta*
Massimo Falconi, *Ancona*
Ezio Falletto, *Turin*
Silvia Fargion, *Milan*
Matteo Fassan, *Verona*
Gianfranco Delle Fave, *Roma*
Alessandro Federico, *Naples*
Francesco Feo, *Sassari*
Davide Festi, *Bologna*
Natale Figura, *Siena*
Vincenzo Formica, *Rome*
Mirella Fraquelli, *Milan*
Marzio Frazzoni, *Modena*
Walter Fries, *Messina*
Gennaro Galizia, *Naples*
Andrea Galli, *Florence*
Matteo Garcovich, *Rome*
Eugenio Gaudio, *Rome*
Paola Ghiorzo, *Genoa*
Edoardo G Giannini, *Genova*
Luca Gianotti, *Monza*
Maria Cecilia Giron, *Padova*
Alberto Grassi, *Rimini*
Gabriele Grassi, *Trieste*
Francesco Greco, *Bergamo*
Luigi Greco, *Naples*
Antonio Grieco, *Rome*
Fabio Grizzi, *Rozzano*
Laurino Grossi, *Pescara*
Salvatore Gruttadauria, *Palermo*
Simone Guglielmetti, *Milan*
Tiberiu Hershcovici, *Jerusalem*
Calogero Iacono, *Verona*
Enzo Ierardi, *Bari*
Amedeo Indriolo, *Bergamo*
Raffaele Iorio, *Naples*
Paola Iovino, *Salerno*
Angelo A Izzo, *Naples*
Loreta Kondili, *Rome*
Filippo La Torre, *Rome*
Giuseppe La Torre, *Rome*
Giovanni Latella, *L'Aquila*
Salvatore Leonardi, *Catania*
Massimo Libra, *Catania*
Anna Licata, *Palermo*
C armela Loguercio, *Naples*
Amedeo Lonardo, *Modena*
Carmelo Luigiano, *Catania*
Francesco Luzza, *Catanzaro*
Giovanni Maconi, *Milano*
Antonio Macrì, *Messina*
Mariano Malaguarnera, *Catania*

Francesco Manguso, *Napoli*
Tommaso Maria Manzia, *Rome*
Daniele Marrelli, *Siena*
Gabriele Masselli, *Rome*
Sara Massironi, *Milan*
Giuseppe Mazzarella, *Avellino*
Michele Milella, *Rome*
Giovanni Milito, *Rome*
Antonella d'Arminio Monforte, *Milan*
Fabrizio Montecucco, *Genoa*
Giovanni Monteleone, *Rome*
Mario Morino, *Torino*
Vincenzo La Mura, *Milan*
Gerardo Nardone, *Naples*
Riccardo Nascimbeni, *Brescia*
Gabriella Nesi, *Florence*
Giuseppe Nigri, *Rome*
Erica Novo, *Turin*
Veronica Ojetti, *Rome*
Michele Orditura, *Naples*
Fabio Pace, *Seriate*
Lucia Pacifico, *Rome*
Omero Alessandro Paoluzi, *Rome*
Valerio Pazienza, *San Giovanni Rotondo*
Rinaldo Pellicano, *Turin*
Adriano M Pellicelli, *Rome*
Nadia Peparini, *Ciampino*
Mario Pescatori, *Rome*
Antonio Picardi, *Rome*
Alberto Pilotto, *Padova*
Alberto Piperno, *Monza*
Anna Chiara Piscaglia, *Rome*
Maurizio Pompili, *Rome*
Francesca Romana Ponziani, *Rome*
Cosimo Prantera, *Rome*
Girolamo Ranieri, *Bari*
Carlo Ratto, *Tome*
Barbara Renga, *Perugia*
Alessandro Repici, *Rozzano*
Maria Elena Riccioni, *Rome*
Lucia Ricci-Vitiani, *Rome*
Luciana Rigoli, *Messina*
Mario Rizzetto, *Torino*
Ballarin Roberto, *Modena*
Roberto G Romanelli, *Florence*
Claudio Romano, *Messina*
Luca Roncucci, *Modena*
Cesare Ruffolo, *Treviso*
L ucia Sacchetti, *Napoli*
Rodolfo Sacco, *Pisa*
Lapo Sali, *Florence*
Romina Salpini, *Rome*
Giulio Aniello, *Santoro Treviso*
Armando Santoro, *Rozzano*
Edoardo Savarino, *Padua*
Marco Senzolo, *Padua*
Annalucia Serafino, *Rome*
Giuseppe S Sica, *Rome*
Pierpaolo Sileri, *Rome*
Cosimo Sperti, *Padua*
Vincenzo Stanghellini, *Bologna*
Cristina Stasi, *Florence*
Gabriele Stocco, *Trieste*
Roberto Tarquini, *Florence*
Mario Testini, *Bari*
Guido Torzilli, *Milan*
Guido Alberto Massimo, *Tiberio Brescia*
Giuseppe Toffoli, *Aviano*
Alberto Tommasini, *Trieste*
Francesco Tonelli, *Florence*
Cesare Tosetti Porretta, *Terme*
Lucio Trevisani, *Cona*
Guglielmo M Trovato, *Catania*
Mariapia Vairetti, *Pavia*
Luca Vittorio Valenti, *Milano*
Mariateresa T Ventura, *Bari*
Giuseppe Verlato, *Verona*
Alessandro Vitale, *Padova*
Marco Vivarelli, *Ancona*
Giovanni Li Volti, *Catania*
Giuseppe Zanotti, *Padua*
Vincenzo Zara, *Lecce*
Gianguglielmo Zehender, *Milan*
Anna Linda Zignego, *Florence*
Rocco Antonio Zoccali, *Messina*
Angelo Zullo, *Rome*

Japan

Yasushi Adachi, *Sapporo*
Takafumi Ando, *Nagoya*
Masahiro Arai, *Tokyo*
Makoto Arai, *Chiba*
Takaaki Arigami, *Kagoshima*
Itaru Endo,*Yokohama*
Munechika Enjoji, *Fukuoka*
Shunji Fujimori, *Tokyo*
Yasuhiro Fujino, *Akashi*
Toshiyoshi Fujiwara, *Okayama*
Yosuke Fukunaga, *Tokyo*
Toshio Fukusato, *Tokyo*
Takahisa Furuta, *Hamamatsu*
Osamu Handa, *Kyoto*
Naoki Hashimoto, *Osaka*
Yoichi Hiasa, *Toon*
Masatsugu Hiraki, *Saga*
Satoshi Hirano, *Sapporo*
Keiji Hirata, *Fukuoka*
Toru Hiyama, *Higashihiroshima*
Akira Hokama, *Nishihara*
Shu Hoteya, *Tokyo*
Masao Ichinose, *Wakayama*
Tatsuya Ide, *Kurume*
Masahiro Iizuka, *Akita*
Toshiro Iizuka, *Tokyo*
Kenichi Ikejima, *Tokyo*
Tetsuya Ikemoto, *Tokushima*
Hiroyuki Imaeda, *Saitama*
Atsushi Imagawa, *Kan-onji*
Hiroo Imazu, *Tokyo*
Akio Inui, *Kagoshima*
Shuji Isaji, *Tsu*
Toru Ishikawa, *Niigata*
Toshiyuki Ishiwata, *Tokyo*
Soichi Itaba, *Kitakyushu*
Yoshiaki Iwasaki, *Okayama*
Tatehiro Kagawa, *Isehara*
Satoru Kakizaki, *Maebashi*
Naomi Kakushima, *Shizuoka*
Terumi Kamisawa, *Tokyo*
Akihide Kamiya, *Isehara*
Osamu Kanauchi, *Tokyo*
Tatsuo Kanda, *Chiba*
Shin Kariya, *Okayama*
Shigeyuki Kawa, *Matsumoto*
Takumi Kawaguchi, *Kurume*
Takashi Kawai, *Tokyo*
Soo Ryang Kim, *Kobe*
Shinsuke Kiriyama, *Gunma*
Tsuneo Kitamura, *Urayasu*
Masayuki Kitano, *Osakasayama*
Hirotoshi Kobayashi, *Tokyo*
Hironori Koga, *Kurume*
Takashi Kojima, *Sapporo*
Satoshi Kokura, *Kyoto*
Shuhei Komatsu, *Kyoto*
Tadashi Kondo, *Tokyo*
Yasuteru Kondo, *Sendai*
Yasuhiro Kuramitsu, *Yamaguchi*
Yukinori Kurokawa, *Osaka*
Shin Maeda, *Yokohama*
Koutarou Maeda, *Toyoake*
Hitoshi Maruyama, *Chiba*
Atsushi Masamune, *Sendai*
Hiroyuki Matsubayashi, *Suntogun*
Akihisa Matsuda, *Inzai*
Hirofumi Matsui, *Tsukuba*
Akira Matsumori, *Kyoto*
Yoichi Matsuo, *Nagoya*
Y Matsuzaki, *Ami*
Toshihiro Mitaka, *Sapporo*
Kouichi Miura, *Akita*
Shinichi Miyagawa, *Matumoto*
Eiji Miyoshi, *Suita*
Toru Mizuguchi, *Sapporo*
Nobumasa Mizuno, *Nagoya*
Zenichi Morise, *Nagoya*
Tomohiko Moriyama, *Fukuoka*
Kunihiko Murase, *Tusima*
Michihiro Mutoh, *Tsukiji*
Akihito Nagahara, *Tokyo*
Hikaru Nagahara, *Tokyo*
Hidenari Nagai, *Tokyo*
Koichi Nagata, *Shimotsuke-shi*
Masaki Nagaya, *Kawasaki*
Hisato Nakajima, *Nishi-Shinbashi*
Toshifusa Nakajima, *Tokyo*
Hiroshi Nakano, *Kawasaki*
Hiroshi Nakase, *Kyoto*
Toshiyuki Nakayama, *Nagasaki*
Takahiro Nakazawa, *Nagoya*
Shoji Natsugoe, *Kagoshima City*
Tsutomu Nishida, *Suita*
Shuji Nomoto, *Naogya*
Sachiyo Nomura, *Tokyo*
Takeshi Ogura, *Takatsukishi*
Nobuhiro Ohkohchi, *Tsukuba*
Toshifumi Ohkusa, *Kashiwa*
Hirohide Ohnishi, *Akita*
Teruo Okano, *Tokyo*
Satoshi Osawa, *Hamamatsu*
Motoyuki Otsuka, *Tokyo*
Michitaka Ozaki, *Sapporo*
Satoru Saito, *Yokohama*
Chouhei Sakakura, *Kyoto*
Naoaki Sakata, *Sendai*
Ken Sato, *Maebashi*
Toshiro Sato, *Tokyo*
Tomoyuki Shibata, *Toyoake*
H Shimada, *Tokyo*
Tomohiko Shimatani, *Kure*
Yukihiro Shimizu, *Nanto*
Tadashi Shimoyama, *Hirosaki*
Masayuki Sho, *Nara*
Ikuo Shoji, *Kobe*
Atsushi Sofuni, *Tokyo*
Takeshi Suda, *Niigata*
M Sugimoto, *Hamamatsu*
Ken Sugimoto, *Hamamatsu*
Haruhiko Sugimura, *Hamamatsu*
Shoichiro Sumi, *Kyoto*
Hidekazu Suzuki, *Tokyo*
Masahiro Tajika, *Nagoya*
Hitoshi Takagi, *Takasaki*
Toru Takahashi, *Niigata*

Yoshihisa Takahashi, *Tokyo*
Shinsuke Takeno, *Fukuoka*
Akihiro Tamori, *Osaka*
Kyosuke Tanaka, *Tsu*
Shinji Tanaka, *Hiroshima*
Atsushi Tanaka, *Tokyo*
Yasuhito Tanaka, *Nagoya*
Shinji Tanaka, *Tokyo*
Minoru Tomizawa, *Yotsukaido City*
Kyoko Tsukiyama-Kohara, *Kagoshima*
Takuya Watanabe, *Niigata*
Kazuhiro Watanabe, *Sendai*
Satoshi Yamagiwa, *Niigata*
Takayuki Yamamoto, *Yokkaichi*
Hiroshi Yamamoto, *Otsu*
Kosho Yamanouchi, *Nagasaki*
Ichiro Yasuda, *Gifu*
Yutaka Yata, *Maebashi-city*
Shin-ichi Yokota, *Sapporo*
Norimasa Yoshida, *Kyoto*
Hiroshi Yoshida, *Tama-City*
Hitoshi Yoshiji, *Kashihara*
Kazuhiko Yoshimatsu, *Tokyo*
Kentaro Yoshioka, *Toyoake*
Nobuhiro Zaima, *Nara*

Jordan

Khaled Ali Jadallah, *Irbid*

Kuwait

Islam Khan, *Kuwait*

Lebanon

Bassam N Abboud, *Beirut*
Kassem A Barada, *Beirut*
Marwan Ghosn, *Beirut*
Iyad A Issa, *Beirut*
Fadi H Mourad, *Beirut*
AIa Sharara, *Beirut*
Rita Slim, *Beirut*

Lithuania

Antanas Mickevicius, *Kaunas*

Malaysia

Huck Joo Tan, *Petaling Jaya*

Mexico

Richard A Awad, *Mexico City*
Carlos R Camara-Lemarroy, *Monterrey*
Norberto C Chavez-Tapia, *Mexico City*
Wolfgang Gaertner, *Mexico City*
Diego Garcia-Compean, *Monterrey*
Arturo Panduro, *Guadalajara*
OT Teramoto-Matsubara, *Mexico City*
Felix Tellez-Avila, *Mexico City*
Omar Vergara-Fernandez, *Mexico City*
Saúl Villa-Trevino, *Cuidad de México*

Morocco

Samir Ahboucha, *Khouribga*

Netherlands

Robert J de Knegt, *Rotterdam*
Tom Johannes Gerardus Gevers, *Nijmegen*
Menno Hoekstra, *Leiden*
BW Marcel Spanier, *Arnhem*
Karel van Erpecum, *Utrecht*

New Zealand

Leo K Cheng, *Auckland*
Andrew Stewart Day, *Christchurch*
Jonathan Barnes Koea, *Auckland*
Max Petrov, *Auckland*

Nigeria

Olufunmilayo Adenike Lesi, *Lagos*
Jesse Abiodun Otegbayo, *Ibadan*
Stella Ifeanyi Smith, *Lagos*

Norway

Trond Berg, *Oslo*
Trond Arnulf Buanes, *Krokkleiva*
Thomas de Lange, *Rud*
Magdy El-Salhy, *Stord*
Rasmus Goll, *Tromso*
Dag Arne Lihaug Hoff, *Aalesund*

Pakistan

Zaigham Abbas, *Karachi*
Usman A Ashfaq, *Faisalabad*
Muhammad Adnan Bawany, *Hyderabad*
Muhammad Idrees, *Lahore*
Saeed Sadiq Hamid, *Karachi*
Yasir Waheed, *Islamabad*

Poland

Thomas Brzozowski, *Cracow*
Magdalena Chmiela, *Lodz*
Krzysztof Jonderko, *Sosnowiec*
Anna Kasicka-Jonderko, *Sosnowiec*
Michal Kukla, *Katowice*
Tomasz Hubert Mach, *Krakow*
Agata Mulak, *Wroclaw*
Danuta Owczarek, *Kraków*
Piotr Socha, *Warsaw*
Piotr Stalke, *Gdansk*
Julian Teodor Swierczynski, *Gdansk*
Anna M Zawilak-Pawlik, *Wroclaw*

Portugal

Marie Isabelle Cremers, *Setubal*
Ceu Figueiredo, *Porto*
Ana Isabel Lopes, *LIsbon*
M Paula Macedo, *Lisboa*
Ricardo Marcos, *Porto*
Rui T Marinho, *Lisboa*
Guida Portela-Gomes, *Estoril*
Filipa F Vale, *Lisbon*

Puerto Rico

Caroline B Appleyard, *Ponce*

Qatar

Abdulbari Bener, *Doha*

Romania

Mihai Ciocirlan, *Bucharest*
Dan LucianDumitrascu, *Cluj-Napoca*
Carmen Fierbinteanu-Braticevici, *Bucharest*
Romeo G Mihaila, *Sibiu*
Lucian Negreanu, *Bucharest*
Adrian Saftoiu, *Craiova*
Andrada Seicean, *Cluj-Napoca*
Ioan Sporea, *Timisoara*
Letiția Adela Maria Streba, *Craiova*
Anca Trifan, *Iasi*

Russia

Victor Pasechnikov, *Stavropol*
Vasiliy Ivanovich Reshetnyak, *Moscow*
Vitaly Skoropad, *Obninsk*

Saudi Arabia

Abdul-Wahed N Meshikhes, *Dammam*
M Ezzedien Rabie, *Khamis Mushait*

Singapore

Brian KP Goh, *Singapore*
Richie Soong, *Singapore*
Ker-Kan Tan, *Singapore*
Kok-Yang Tan, *Singapore*
Yee-Joo Tan, *Singapore*
Mark Wong, *Singapore*
Hong Ping Xia, *Singapore*

Slovenia

Matjaz Homan, *Ljubljana*
Martina Perse, *Ljubljana*

South Korea

Sang Hoon Ahn, *Seoul*
Soon Koo Baik, *Wonju*
Soo-Cheon Chae, *Iksan*
Byung-Ho Choe, *Daegu*

Suck Chei Choi, *Iksan*
Hoon Jai Chun, *Seoul*
Yeun-Jun Chung, *Seoul*
Young-Hwa Chung, *Seoul*
Ki-Baik Hahm, *Seongnam*
Sang Young Han, *Busan*
Seok Joo Han, *Seoul*
Seung-Heon Hong, *Iksan*
Jin-Hyeok Hwang, *Seoungnam*
Jeong Won Jang, *Seoul*
Jin-Young Jang, *Seoul*
Dae-Won Jun, *Seoul*
Young Do Jung, *Kwangju*
Gyeong Hoon Kang, *Seoul*
Sung-Bum Kang, *Seoul*
Koo Jeong Kang, *Daegu*
Ki Mun Kang, *Jinju*
Chang Moo Kang, *Seodaemun-gu*
Gwang Ha Kim, *Busan*
Sang Soo Kim, *Goyang-si*
Jin Cheon Kim, *Seoul*
Tae Il Kim, *Seoul*
Jin Hong Kim, *Suwon*
Kyung Mo Kim, *Seoul*
Kyongmin Kim, *Suwon*
Hyung-Ho Kim, *Seongnam*
Seoung Hoon Kim, *Goyang*
Sang Il Kim, *Seoul*
Hyun-Soo Kim, *Wonju*
Jung Mogg Kim, *Seoul*
Dong Yi Kim, *Gwangju*
Kyun-Hwan Kim, *Seoul*
Jong-Han Kim, *Ansan*
Ja-Lok Ku, *Seoul*
Kyu Taek Lee, *Seoul*
Hae-Wan Lee, *Chuncheon*
Inchul Lee, *Seoul*
Jung Eun Lee, *Seoul*
Sang Chul Lee, *Daejeon*
Song Woo Lee, *Ansan-si*
Hyuk-Joon Lee, *Seoul*
Seong-Wook Lee, *Yongin*
Kil Yeon Lee, *Seoul*
Jong-Inn Lee, *Seoul*
Kyung A Lee, *Seoul*
Jong-Baeck Lim, *Seoul*
Eun-Yi Moon, *Seoul*
SH Noh, *Seoul*
Seung Woon Paik, *Seoul*
Won Sang Park, *Seoul*
Sung-Joo Park, *Iksan*
Kyung Sik Park, *Daegu*
Se Hoon Park, *Seoul*
Yoonkyung Park, *Gwangju*
Seung-Wan Ryu, *Daegu*
Dong Wan Seo, *Seoul*
Il Han Song, *Cheonan*
Myeong Jun Song, *Daejeon*
Yun Kyoung Yim, *Daejeon*
Dae-Yeul Yu *Daejeon*

Spain

Mariam Aguas, *Valencia*
Raul J Andrade, *Málaga*
Antonio Arroyo, *Elche*
Josep M Bordas, *Barcelona*
Lisardo Boscá, *Madrid*
Ricardo Robles Campos, *Murcia*
Jordi Camps, *Reus*
Carlos Cervera *Barcelona*
Alfonso Clemente, *Granada*
Pilar Codoner-Franch, *Valencia*
Fernando J Corrales, *Pamplona*
Fermin Sánchez de Medina, *Granada*
Alberto Herreros de Tejada, *Majadahonda*
Enrique de-Madaria, *Alicante*
JE Dominguez-Munoz, *Santiago de Compostela*
Vicente Felipo, *Valencia*
CM Fernandez-Rodriguez, *Madrid*
Carmen Frontela-Saseta, *Murcia*
Julio Galvez, *Granada*
Maria Teresa García, *Vigo*
MI Garcia-Fernandez, *Málaga*
Emilio Gonzalez-Reimers, *La Laguna*
Marcel Jimenez, *Bellaterra*
Angel Lanas, *Zaragoza*
Juan Ramón Larrubia, *Guadalajara*
Antonio Lopez-Sanroman, *Madrid*
Vicente Lorenzo-Zuniga, *Badalona*
Alfredo J Lucendo, *Tomelloso*
Vicenta Soledad Martinez-Zorzano, *Vigo*
José Manuel Martin-Villa, *Madrid*
Julio Mayol, *Madrid*
Manuel Morales-Ruiz, *Barcelona*
Alfredo Moreno-Egea, *Murcia*
Albert Pares, *Barcelona*
Maria Pellise, *Barcelona*
José Perea, *Madrid*
Miguel Angel Plaza, *Zaragoza*
María J Pozo, *Cáceres*
Enrique Quintero, *La Laguna*
Jose M Ramia, *Madrid*
Francisco Rodriguez-Frias, *Barcelona*
Silvia Ruiz-Gaspa, *Barcelona*
Xavier Serra-Aracil, *Barcelona*
Vincent Soriano, *Madrid*
Javier Suarez, *Pamplona*
Carlos Taxonera, *Madrid*
M Isabel Torres, *Jaén*
Manuel Vazquez-Carrera, *Barcelona*
Benito Velayos, *Valladolid*
Silvia Vidal, *Barcelona*

Sri Lanka

Arjuna Priyadarsin De Silva, *Colombo*

Sudan

Ishag Adam, *Khartoum*

Sweden

Roland G Andersson, *Lund*
Bergthor Björnsson, *Linkoping*
Johan Christopher Bohr, *Örebro*
Mauro D'Amato, *Stockholm*
Thomas Franzen, *Norrkoping*
Evangelos Kalaitzakis, *Lund*
Riadh Sadik, *Gothenburg*
Per Anders Sandstrom, *Linkoping*
Ervin Toth, *Malmö*
Konstantinos Tsimogiannis, *Vasteras*
Apostolos V Tsolakis, *Uppsala*

Switzerland

Gieri Cathomas, *Liestal*
Jean Louis Frossard, *Geneve*
Christian Toso, *Geneva*
Stephan Robert Vavricka, *Zurich*
Dominique Velin, *Lausanne*

Thailand

Thawatchai Akaraviputh, *Bangkok*
P Yoysungnoen Chintana, *Pathumthani*
Veerapol Kukongviriyapan, *Muang*
Vijittra Leardkamolkarn, *Bangkok*
Varut Lohsiriwat, *Bangkok*
Somchai Pinlaor, *Khaon Kaen*
D Wattanasirichaigoon, *Bangkok*

Trinidad and Tobago

B Shivananda Nayak, *Mount Hope*

Tunisia

Ibtissem Ghedira, *Sousse*
Lilia Zouiten-Mekki, *Tunis*

Turkey

Sami Akbulut, *Diyarbakir*
Inci Alican, *Istanbul*
Mustafa Altindis, *Sakarya*
Mutay Aslan, *Antalya*
Oktar Asoglu, *Istanbul*
Yasemin Hatice Balaban, *Istanbul*
Metin Basaranoglu, *Ankara*
Yusuf Bayraktar, *Ankara*
Süleyman Bayram, *Adiyaman*
Ahmet Bilici, *Istanbul*
Ahmet Sedat Boyacioglu, *Ankara*
Züleyha Akkan Cetinkaya, *Kocaeli*
Cavit Col, *Bolu*
Yasar Colak, *Istanbul*
Cagatay Erden Daphan, *Kirikkale*
Mehmet Demir, *Hatay*
Ahmet Merih Dobrucali, *Istanbul*
Gülsüm Ozlem Elpek, *Antalya*
Ayse Basak Engin, *Ankara*
Eren Ersoy, *Ankara*
Osman Ersoy, *Ankara*
Yusuf Ziya Erzin, *Istanbul*
Mukaddes Esrefoglu, *Istanbul*
Levent Filik, *Ankara*
Ozgur Harmanci, *Ankara*
Koray Hekimoglu, *Ankara*
Abdurrahman Kadayifci, *Gaziantep*
Cem Kalayci, *Istanbul*
Selin Kapan, *Istanbul*
Huseyin Kayadibi, *Adana*
Sabahattin Kaymakoglu, *Istanbul*
Metin Kement, *Istanbul*
Mevlut Kurt, *Bolu*
Resat Ozaras, *Istanbul*

Elvan Ozbek, *Adapazari*
Cengiz Ozcan, *Mersin*
Hasan Ozen, *Ankara*
Halil Ozguc, *Bursa*
Mehmet Ozturk, *Izmir*
Orhan V Ozkan, *Sakarya*
Semra Paydas, *Adana*
Ozlem Durmaz Suoglu, *Istanbul*
Ilker Tasci, *Ankara*
Müge Tecder-ünal, *Ankara*
Mesut Tez, *Ankara*
Serdar Topaloglu, *Trabzon*
Murat Toruner, *Ankara*
Gokhan Tumgor, *Adana*
Oguz Uskudar, *Adana*
Mehmet Yalniz, *Elazig*
Mehmet Yaman, *Elazig*
Veli Yazisiz, *Antalya*
Yusuf Yilmaz, *Istanbul*
Ozlem Yilmaz, *Izmir*
Oya Yucel, *Istanbul*
Ilhami Yuksel, *Ankara*

United Kingdom

Nadeem Ahmad Afzal, *Southampton*
Navneet K Ahluwalia, *Stockport*
Yeng S Ang, *Lancashire*
Ramesh P Arasaradnam, *Coventry*
Ian Leonard Phillip Beales, *Norwich*
John Beynon, *Swansea*
Barbara Braden, *Oxford*
Simon Bramhall, *Birmingham*
Geoffrey Burnstock, *London*
Ian Chau, *Sutton*
Thean Soon Chew, *London*
Helen G Coleman, *Belfast*
Anil Dhawan, *London*
Sunil Dolwani, *Cardiff*
Piers Gatenby, *London*
Anil T George, *London*
Pasquale Giordano, *London*
Paul Henderson, *Edinburgh*
Georgina Louise Hold, *Aberdeen*
Stefan Hubscher, *Birmingham*
Robin D Hughes, *London*
Nusrat Husain, *Manchester*
Matt W Johnson, *Luton*
Konrad Koss, *Macclesfield*
Anastasios Koulaouzidis, *Edinburgh*
Simon Lal, *Salford*
John S Leeds, *Aberdeen*
Hongxiang Liu, *Cambridge*
Michael Joseph McGarvey, *London*
Michael Anthony Mendall, *London*
Alexander H Mirnezami, *Southampton*
J Bernadette Moore, *Guildford*
Claudio Nicoletti, *Norwich*
Savvas Papagrigoriadis, *London*
David Mark Pritchard, *Liverpool*
James A Ross, *Edinburgh*
Kamran Rostami, *Worcester*
Xiong Z Ruan, *London*
Dina Tiniakos, *Newcastle upon Tyne*
Frank I Tovey, *London*
Dhiraj Tripathi, *Birmingham*
Vamsi R Velchuru, *Great Yarmouth*
Nicholas T Ventham, *Edinburgh*
Diego Vergani, *London*
Jack Westwood Winter, *Glasgow*
Terence Wong, *London*
Ling Yang, *Oxford*

United States

Daniel E Abbott, *Cincinnati*
Ghassan K Abou-Alfa, *New York*
Julian Abrams, *New York*
David William Adelson, *Los Angeles*
Jonathan Steven Alexander, *Shreveport*
Tauseef Ali, *Oklahoma City*
Mohamed R Ali, *Sacramento*
Rajagopal N Aravalli, *Minneapolis*
Hassan Ashktorab, *Washington*
Shashi Bala, *Worcester*
Charles F Barish, *Raleigh*
P Patrick Basu, *New York*
Robert L Bell, *Berkeley Heights*
David Bentrem, *Chicago*
Henry J Binder, *New Haven*
Joshua Bleier, *Philadelphia*
Wojciech Blonski, *Johnson City*
Kenneth Boorom, *Corvallis*
Brian Boulay, *Chicago*
Carla W Brady, *Durham*
Kyle E Brown, *Iowa City*
Adeel AButt, *Pittsburgh*
Weibiao Cao, *Providence*
Andrea Castillo, *Cheney*
Fernando J Castro, *Weston*
Adam S Cheifetz, *Boston*
Adam S Cheifetz, *Boston*
Xiaoxin Luke Chen, *Durham*
Ramsey Cheung, *Palo Alto*
Parimal Chowdhury, *Little Rock*
Edward John Ciaccio, *New York*
Dahn L Clemens, *Omaha*
Yingzi Cong, *Galveston*
Laura Iris Cosen-Binker, *Boston*
Joseph John Cullen, *Lowa*
Mark J Czaja, *Bronx*
Mariana D Dabeva, *Bronx*
Christopher James Damman, *Seattle*
Isabelle G De Plaen, *Chicago*
Abhishek Deshpande, *Cleveland*
Punita Dhawan, *Nashville*
Hui Dong, *La Jolla*
Wael El-Rifai, *Nashville*
Sukru H Emre, *New Haven*
Paul Feuerstadt, *Hamden*
Josef E Fischer, *Boston*
Laurie N Fishman, *Boston*
Joseph Che Forbi, *Atlanta*
Temitope Foster, *Atlanta*
AmyEFoxx-Orenstein, *Scottsdale*
Daniel E Freedberg, *New York*
Shai Friedland, *Palo Alto*
Virgilio George, *Indianapolis*
Ajay Goel, *Dallas*
Oliver Grundmann, *Gainesville*
Stefano Guandalini, *Chicago*
Chakshu Gupta, *St. Joseph*
Grigoriy E Gurvits, *New York*
Xiaonan Han, *Cincinnati*
Mohamed Hassan, *Jackson*
Martin Hauer-Jensen, *Little Rock*
Koichi Hayano, *Boston*
Yingli Hee, *Atlanta*
Samuel B Ho, *San Diego*
Jason Ken Hou, *Houston*
Lifang Hou, *Chicago*
K-Qin Hu, *Orange*
Jamal A Ibdah, *Columbia*
Robert Thomas Jensen, *Bethesda*
Huanguang "Charlie" Jia, *Gainesville*
Rome Jutabha, *Los Angeles*
Andreas M Kaiser, *Los Angeles*
Avinash Kambadakone, *Boston*
David Edward Kaplan, *Philadelphia*
Randeep Kashyap, *Rochester*
Rashmi Kaul, *Tulsa*
Ali Keshavarzian, *Chicago*
Amir Maqbul Khan, *Marshall*
Nabeel Hasan Khan, *New Orleans*
Sahil Khanna, *Rochester*
Kusum K Kharbanda, *Omaha*
Hyun Sik Kim, *Pittsburgh*
Joseph Kim, *Duarte*
Jae S Kim, *Gainesville*
Miran Kim, *Providence*
Timothy R Koch, *Washington*
Burton I Korelitz, *New York*
Betsy Kren, *Minneapolis*
Shiu-Ming Kuo, *Buffalo*
Michelle Lai, *Boston*
Andreas Larentzakis, *Boston*
Edward Wolfgang Lee, *Los Angeles*
Daniel A Leffler, *Boston*
Michael Leitman, *New York*
Suthat Liangpunsakul, *Indianapolis*
Joseph K Lim, *New Haven*
Elaine Y Lin, *Bronx*
Henry C Lin, *Albuquerque*
Rohit Loomba, *La Jolla*
James David Luketich, *Pittsburgh*
Mohammad F Madhoun, *Oklahoma City*
Thomas C Mahl, *Buffalo*
Ashish Malhotra, *Bettendorf*
Pranoti Mandrekar, *Worcester*
John Marks, *Wynnewood*
Wendy M Mars, *Pittsburgh*
Julien Vahe Matricon, *San Antonio*
Craig J McClain, *Louisville*
George K Michalopoulos, *Pittsburgh*
Tamir Miloh, *Phoenix*
Ayse Leyla Mindikoglu, *Baltimore*
Huanbiao Mo, *Denton*
Klaus Monkemuller, *Birmingham*
John Morton, *Stanford*
Adnan Muhammad, *Tampa*
Michael J Nowicki, *Jackson*
Patrick I Okolo, *Baltimore*
Giusepp Orlando, *Winston Salem*
Natalia A Osna, *Omaha*
Virendra N Pandey, *Newark*
Mansour A Parsi, *Cleveland*
Michael F Picco, *Jacksonville*
Daniel S Pratt, *Boston*
Xiaofa Qin, *Newark*
Janardan K Reddy, *Chicago*
Victor E Reyes, *Galveston*
Jon Marc Rhoads, *Houston*
Giulia Roda, *New York*
Jean-Francois Armand Rossignol, *Tampa*
Paul A Rufo, *Boston*
Madhusudana Girija Sanal, *New York*
Miguel Saps, *Chicago*
Sushil Sarna, *Galveston*
Ann O Scheimann, *Baltimore*
Bernd Schnabl, *La Jolla*

World Journal of Gastroenterology

Contents Weekly Volume 23 Number 41 November 7, 2017

ORIGINAL ARTICLE

Basic Study

Retrospective Cohort Study

Retrospective Study

Observational Study

World Journal of Gastroenterology
Volume 23 Number 36 November 7, 2017

Contents

NAME OF JOURNAL
World Journal of Gastroenterology

ISSN
ISSN 1007-9327 (print)
ISSN 2219-2840 (online)

LAUNCH DATE
October 1, 1995

FREQUENCY
Weekly

EDITORIAL OFFICE
Jin-Lei Wang, Director
Yuan Qi, Vice Director
Ze-Mao Gong, Vice Director
World Journal of Gastroenterology
Baishideng Publishing Group Inc
7901 Stoneridge Drive, Suite 501,
Pleasanton, CA 94588, USA
Telephone: +1-925-2238242
Fax: +1-925-2238243
E-mail: editorialoffice@wjgnet.com
Help Desk: http://www.f6publishing.com/helpdesk
http://www.wjgnet.com

PUBLISHER
Baishideng Publishing Group Inc
7901 Stoneridge Drive, Suite 501,
Pleasanton, CA 94588, USA
Telephone: +1-925-2238242
Fax: +1-925-2238243
E-mail: bpgoffice@wjgnet.com
Help Desk: http://www.f6publishing.com/helpdesk
http://www.wjgnet.com

PUBLICATION DATE
November 7, 2017

INSTRUCTIONS TO AUTHORS
Full instructions are available online at http://www.wjgnet.com/bpg/gerinfo/204

ONLINE SUBMISSION
http://www.f6publishing.com

World Journal of Gastroenterology

Submit a Manuscript: http://www.f6publishing.com

World J Gastroenterol 2017 November 7; 23(41): 7347-7358

DOI: 10.3748/wjg.v23.i41.7347

ISSN 1007-9327 (print) ISSN 2219-2840 (online)

ORIGINAL ARTICLE

Basic Study

Reabsorption of iron into acutely damaged rat liver: A role for ferritins

Ihtzaz Ahmed Malik, Jörg Wilting, Giuliano Ramadori, Naila Naz

Ihtzaz Ahmed Malik, Jörg Wilting, Institute of Anatomy and Cell Biology, University Medical Center, D-37075 Goettingen, Germany

Giuliano Ramadori, Department of Gastroenterology and Endocrinology, University Medical Center, D-37075 Goettingen, Germany

Naila Naz, Faculty of Life Sciences, The University of Manchester, Manchester M13 9PL, United Kingdom

ORCID number: Ihtzaz Ahmed Malik (0000-0002-6712-0838); Jörg Wilting (0000-0001-8337-2296); Giuliano Ramadori (0000-0002-7921-7186); Naila Naz (0000-0002-8864-0250).

Author contributions: Malik IA, Ramadori G and Naz N designed the study; Malik IA and Naz N performed the experiments; Malik IA, Ramadori G and Naz N analyzed the data and wrote manuscript; Wilting J assisted to interpret the data and improved the manuscript; Ramadori G and Naz N contributed equally to this work.

Support by the German Research Foundation, and the Open Access Publication Funds of the Göttingen University.

Institutional review board statement: The studies were performed according to the guidelines of good scientific practice.

Institutional animal care and use committee statement: The animal studies were reviewed and approved by the committee of the Central Institute for Animal Experiments of the University of Goettingen, and the Lower Saxony State Office for Consumer Protection and Food Safety (Study No. 33.9-42502-04-13/1086).

Conflict-of-interest statement: The authors declare that no actual or potential conflict-of-interest in relation to this article exists.

Data sharing statement: The data were obtained, analyzed and used by the authors only.

Manuscript source: Unsolicited manuscript

Correspondence to: Ihtzaz Ahmed Malik, PhD, Institute of Anatomy and Cell Biology, University Medical Center Goettingen, Kreuzbergring 36, D-37075 Goettingen, Germany. i.malik@med.uni-goettingen.de
Telephone: +49-551-398982
Fax: +49-551-397067

Received: July 16, 2017
Peer-review started: July 21, 2017
First decision: August 10, 2017
Revised: August 22, 2017
Accepted: September 13, 2017
Article in press: September 13, 2017
Published online: November 7, 2017

Abstract

AIM

To studied iron metabolism in liver, spleen, and serum after acute liver-damage, in relation to surrogate markers for liver-damage and repair.

METHODS

Rats received intraperitoneal injection of the hepatotoxin thioacetamide (TAA), and were sacrificed regularly between 1 and 96 h thereafter. Serum levels of transaminases and iron were measured using conventional laboratory assays. Liver tissue was used for conventional histology, immunohistology, and iron staining. The expression of acute-phase cytokines, ferritin light chain (FTL), and ferritin heavy chain (FTH)

was investigated in the liver by qRT-PCR. Western blotting was used to investigate FTL and FTH in liver tissue and serum. Liver and spleen tissue was also used to determine iron concentrations.

RESULTS

After a short initial decrease, iron serum concentrations increased in parallel with serum transaminase (aspartate aminotransferase and alanine aminotransferase) levels, which reached a maximum at 48 h, and decreased thereafter. Similarly, after 48 h a significant increase in FTL, and after 72h in FTH was detected in serum. While earliest morphological signs of inflammation in liver were visible after 6 h, increased expression of the two acute-phase cytokines IFN-γ (1h) and IL-1β (3h) was detectable earlier, with maximum values after 12-24 h. Iron concentrations in liver tissue increased steadily between 1 h and 48 h, and remained high at 96 h. In contrast, spleen iron concentrations remained unchanged until 48 h, and increased mildly thereafter (96 h). Although tissue iron staining was negative, hepatic FTL and FTH protein levels were strongly elevated. Our results reveal effects on hepatic iron concentrations after direct liver injury by TAA. The increase of liver iron concentrations may be due to the uptake of a significant proportion of the metal by healthy hepatocytes, and only to a minor extent by macrophages, as spleen iron concentrations do not increase in parallel. The temporary increase of iron, FTH and transaminases in serum is obviously due to their release by damaged hepatocytes.

CONCLUSION

Increased liver iron levels may be the consequence of hepatocyte damage. Iron released into serum by damaged hepatocytes is obviously transported back and stored via ferritins.

Key words: Iron metabolism; Ferritin; Liver; Cytokines; Acute liver damage

Core tip: In humans, an increase in hepatic iron concentration is caused by chronic hepatitis-C infection, alcohol abuse, and non-alcoholic fatty liver disease. The pathophysiology behind increased liver iron concentrations caused by acute liver damage has remained obscure. Using thioacetamide-injection in rats, we demonstrate that the increase in liver iron may be a consequence rather than the cause of hepatocyte damage. Thereby, iron is released into serum by damaged hepatocytes during acute liver damage, and reabsorbed by remaining hepatocytes (but not spleen) by means of ferritin L and ferritin H subunits. Our studies also show that ferritin H is a promising surrogate marker for damaged hepatocytes.

Malik IA, Wilting J, Ramadori G, Naz N. Reabsorption of iron into acutely damaged rat liver: A role for ferritins. *World J Gastroenterol* 2017; 23(41): 7347-7358 Available from: URL: http://www.wjgnet.com/1007-9327/full/v23/i41/7347.htm DOI: http://dx.doi.org/10.3748/wjg.v23.i41.7347

INTRODUCTION

Iron is an essential and the most abundant trace element for human physiology. It is required not only for erythropoiesis and oxygen transport, but also for enzymatic functions[1,2]. Human body contains 50 mg iron per kg body weight. The daily intestinal (duodenal) iron uptake is 1-2 mg, which compensates for the iron loss by sloughing off of intestinal and epidermal cells. In fact, 65% of the iron is bound to hemoglobin (2300 mg), and most of the non-hemoglobin iron is stored in the liver[1,3-5]. Hepatocytes are responsible for the uptake of ionic iron, which reaches the portal blood from the intestine, and is transported to the liver as transferrin-iron[1,3,6]. A small amount of iron is also taken up by Kupffer cells, which have the important function of clearing aged erythrocytes[2,5,7]. In normal plasma, transferrin iron-binding sites are saturated to about one third. The remaining iron-binding capacity serves as a buffer for conditions where iron concentrations increase acutely, which may induce tissue damage due to iron toxicity[8-10].

The hepatocytes capture about 80% of transferrin-bound iron through caging receptors, made up of the ferritin (FT) subunits ferritin heavy chain (FTH) and ferritin light chain (FTL)[6,8,11-13]. However, in contrast to other cells, hepatocytes not only synthesize FTL as a component of the iron cage, but also as a secreted serum protein[14]. As serum ferritin is reported to be exclusively FTL, and not FTH[14,15], its synthesis and secretion in the liver is differentially regulated[16], mainly at post-transcriptional levels[12].

In all tissues, iron is the main stimulus for FTL gene expression. An increase in synthesis and secretion of FTL has been demonstrated in the liver in a model of acute-phase response[14,17], and in hepatocytes *in vitro* by different acute-phase cytokines including interleukin-6 (IL-6)[14]. Cytokines are known to be responsible for dramatic changes of hepatic protein synthesis, including upregulation of hepcidin[17], lactoferrin[18], and lipocalin-2[19]. These low molecular weight proteins are involved in the control of iron metabolism, as a reaction to extrahepatic tissue damage.

Experimentally, the generation of a systemic acute-phase reaction, by means of turpentine oil-induced sterile intramuscular abscesses, was shown to be accompanied by elevated hepatic iron concentrations. This was attributed to increased iron-uptake into

hepatocytes[20], which could also be observed *in vitro*[15]. Similarly, increased hepatic iron storage, in addition to elevated serum cytokine levels, has been reported in human liver diseases caused by viruses, alcohol consumption or overweight[21,22]. These alterations were shown to be reversible after elimination of the noxae, as is the case after successful treatment of hepatitis C[23,24]. An increased absorption of dietary-iron in the intestine has been postulated to cause NAFLD/NASH in humans[25], however, the mechanisms underlying the increase of the iron deposition in the liver during acute-phase reaction are still poorly understood.

Here, we have studied changes in the expression of FTH and FTL, various acute-phase cytokines, as well as iron concentrations in liver and spleen after intraperitoneal administration of thioacetamide (TAA), in parallel with serological markers for liver damage and repair. We provide evidence for the hypothesis that the increase of liver iron concentrations may be rather the consequence than the cause of hepatocyte damage.

MATERIALS AND METHODS

Materials and chemicals were bought from Merck (Darmstadt, Germany), Applichem (Darmstadt, Germany) and Sigma (Steinheim, Germany). Details for each chemical and material are noted in the appropriate sections.

Rat model of hepatic acute-phase reaction

Male Sprague-Dawley rats weighing 200-220 g were purchased from Charles River (Sulzfeld, Germany) and Harlan Winkelmann (Borchen, Germany). The animals were kept according to our institutional guidelines and the rules of the German Law for the Protection of Animals. The experiments were approved by the committee on animal protection of the University of Goettingen and the Lower Saxony State Office for Consumer Protection and Food Safety (Study no. 33.9-42502-04-13/1086).

The rats were divided into a control group (n = 12) and an experiment group (n = 32). Five animals were kept per cage following a 12:12-hour (h) light-dark cycle. They had unrestricted access to food and water. An intraperitoneal (ip) injection of thioacetamide (TAA) (prepared freshly, dissolved in sterile NaCl) with a dose of 500 mg/kg body weight was given to each rat as described before[26]. Control rats were injected with the same volume of NaCl. Rats were sacrificed after 1, 3, 6, 12, 24, 48, 72, and 96 h under pentobarbital anesthesia. Serum, liver and spleen were snap frozen in liquid nitrogen and stored at -80 ℃.

Measurement of liver enzymes in serum

Blood samples from the *inferior vena cava* were collected from control and experimental rats after 1, 3, 6, 12, 24, 48, 72, and 96 h. Serum was used for the determination of alkaline phosphatase with a standard p-nitrophenolphosphate photometric assay (Roche, Mannheim, Germany). Aspartate aminotransferase (AST) and alanine aminotransferase (ALT) activities were measured by using analysis kits (DiaSys, Karben, Germany) according to the manufacturer's instructions.

Histopathology

Histopathology was performed on 5 μm acetone-fixed cryostat sections (Reichert Jung, Wetzlar, Germany) as described previously[20,27]. Briefly, the cryostat sections were washed with phosphate-buffered saline (PBS), and stained with hematoxylin for 5 minutes. Thereafter, tissues were stained with 1% eosin followed by short washing with 100% alcohol. Tissues were then transferred into xylol and mounted.

Measurement of serum and tissue iron levels

Serum and tissue iron levels were measured with a colorimetric ferrozine-based assay[28] following the company's protocol, through facility service provided by the University Medical School, Goettingen. The hepatic tissue iron concentrations were measured from liver homogenates, which were prepared as described earlier[20].

Prussian blue iron staining of liver and spleen

5 μm thick air-dried cryostat sections (Reichert Jung, Wetzlar, Germany) were stained for iron using the Prussian blue method. Fixation was performed by incubating the slides in ice-cold methanol (-20 ℃) for 10 min, and ice-cold acetone (-20 ℃) for 10 s. The sections were stained for iron by using iron-stain kit from Sigma-Aldrich (Munich, Germany), according to the manufacturer's instructions.

RNA isolation from liver tissue and real-time PCR

RNA was isolated from all control and TAA-treated rat livers as described previously[17]. Briefly, mRNA was converted into cDNA with Superscript kit (Invitrogen, CA). ABI Prism Sequence Detection System 7000 (Applied Biosystems, Foster City, CA) was used for real-time PCR. The primers used in this study are presented in Table 1. They were synthesized by Invitrogen. *Ubiquitin C* (UBC) served as housekeeping gene, and was used to normalize the values of the genes of interest. The normalized values for TAA-treated rats were compared with saline-treated controls, and the relative expression was plotted against the observation time. The results represent at least three experiments performed as duplicates.

Western blot analysis of liver tissue and serum proteins

Serum and total liver protein from all control and TAA-treated rats (time points: 1, 3, 6, 12, 24, 48, 72, 96

Table 1 Primers used for polymerase chain reaction

Primer	5′ → 3′ Forward	5′ → 3′ Reverse
UBC	CAC CAA GAA GGT CAA ACA GGA A	AAG ACA CCT CCC CAT CAA ACC
Ferritin H	GCCCTGAAGAACTTTGCCAAAT	TGCAGGAAGATTCGTCCACCT
Ferritin L	AACCACCTGACCAACCTCCGTA	TCAGAGTGAGGCGCTCAAAGAG
IL-6	GTCAACTCCATCTGCCCTTCAG	GGCAGTGGCTGTCAACAACAT
IL-1β	TACCTATGTCTTGCCCGTGGAG	ATCATCCCACGAGTCACAGAGG
TNF-α	ACAAGGCTGCCCCGACTAT	CTCCTGGTATGAAGTGGCAAATC
IFN-γ	GAACTGGCAAAAGGACGGTA	CTGATGGCCTGGTTGTCTTT

Table 2 Antibodies used in this study

Antibodies	Company	Reference	Dilution
FTH	Santa Cruz	SC-25617	1:100
FTH	LS Bio	LS-C23537	1:250
FTL	Abcam	AB-69090	1:1000
FTL	Santa Cruz	SC-14422	1:100
FTL peptide	Santa Cruz	SC-14422	1:50
β-actin	Sigma	A-2228	1:4000

h) was used for Western blot analysis as described before[20]. Shortly, for total liver protein isolation, hepatic tissue probes were lysed in RIPA buffer (25 mM Tris-HCl pH 7.6, 150 mmol/L NaCl, 1% NP-40, 1% sodium deoxycholate, 0.1% SDS). The Bradford method was used to measure protein concentrations. 50 μg of protein either from tissue or serum samples were used in sodium dodecyl sulfate polyacrylamide gel electrophoresis (NuPAGE, Novex 4%-12%, Bis-Tris gel, Invitrogen), under reducing conditions. Then, proteins were transferred to nitrocellulose membranes, and Western blot analysis was performed with antibodies listed in Table 2. Immunodetection was performed according to the ECL Western blotting protocol (Amersham, GE Healthcare, United States).

Immunohistochemistry of liver tissue

5 μm hepatic cryostat sections (Reichert Jung, Wetzlar, Germany) from control and TAA-injected animals were used for immunodetection of FTL and FTH as described before[27]. Fixation was performed with ice-cold methanol (-20 ℃) for 10 min, and ice-cold acetone (-20 ℃) for 10 s. The sections were incubated with PBS containing glucose/glucose oxidase/sodium azide to inhibit endogenous peroxidase reactions. Nonspecific staining was minimized by incubation with fetal calf serum (FCS) for 30 min. Commercially available antibodies for FTL (Abcam, UK and Santa Cruz, United States) and FTH (LS Bio and Santa Cruz, United States) were used for immunostaining. The sections were incubated with primary antibodies overnight at 4 ℃. (For details see Table 2). Negative controls were performed with isotype-specific IgGs. Next day, sections were washed with PBS, and incubated with peroxidase-conjugated anti-rabbit/anti-mouse IgG (Dako, Hamburg, Germany), pre-absorbed with normal rat serum to minimize cross-reactivities. Peroxidase reaction was performed with 3,3′-diaminobenzidine (0.5 mg/mL) and H_2O_2 (0.01%) for 10 min. Meyer's hemalaun solution was used for counter-staining.

Statistical analyses

Student's *t* test and One-way ANOVA with Dennett's post-test were performed using Graph Pad Prism version 4.00 for Windows (Graph Pad Software, San Diego, CA, www.graphpad.com). Experimental errors are shown as SEM. Statistical significance was accepted at: $^{a}P \leqslant 0.05$; $^{b}P \leqslant 0.01$; $^{c}P \leqslant 0.001$.

RESULTS

Measurement of liver damage in TAA-treated animals

Liver damage was analyzed by measuring the amount of circulating liver enzymes at various times after TAA injection. The serum levels of aspartate aminotransferase (AST) reached to their peak (8301 ± 1007 U/L) after 48 h of TAA injection with a statistical significant of $P = 0.001$. Similarly, compared to controls (54 ± 1.4 U/L), serum activity of alanine aminotransferase (ALT) was significantly elevated with a maximum at 48 h (1389 ± 121 U/L; $P < 0.001$) (Figure 1 A and B). Correspondingly, in liver tissue sections of TAA-injected animals we have previously observed immigration of inflammatory cells over time, staring in portal areas and extending into pericentral areas, reaching a maximal infiltration at 48 h, and declining thereafter until complete disappearance at 96 h[26].

Changes in hepatic gene expression of major acute-phase cytokines

The changes in mRNA levels of major acute-phase cytokines (APC) were measured by qPCR in TAA-treated rats at different time points compared to controls. An early up-regulation of the expression of several APCs was observed (Figure 2). IFN-γ started to increase first. A significant induction was observed after 1h, and a maximum (13.7 ± 2.64 - fold) after 12

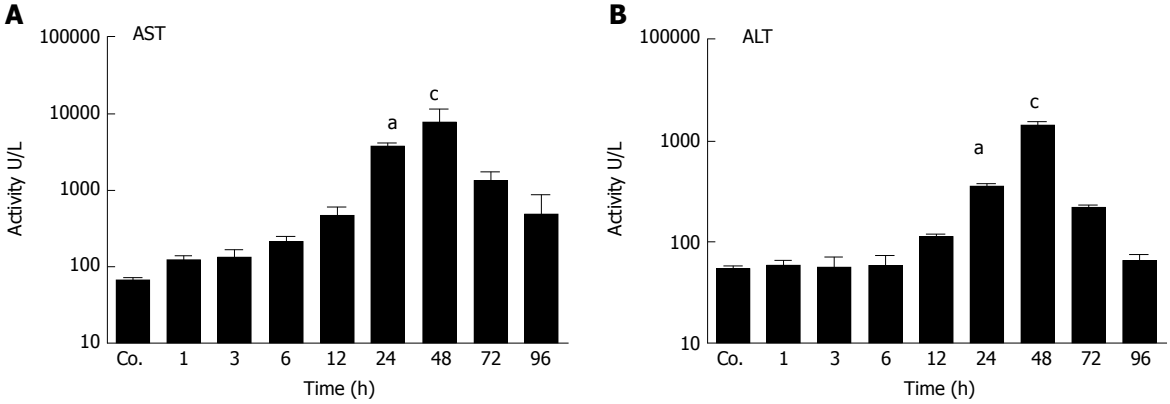

Figure 1 Serum enzyme levels in control and thioacetamide-injected rats. Serum aspartate aminotransferase (AST) (A) and alanine aminotransferase (ALT) (B) levels showed a statically significant ($^{a}P \leq 0.05$; $^{c}P \leq 0.001$) increase at 24 and 48 h followed by a decrease thereafter. Results represent mean values ± SEM, measured in duplicate in four animals for each time point, compared to controls (Co.).

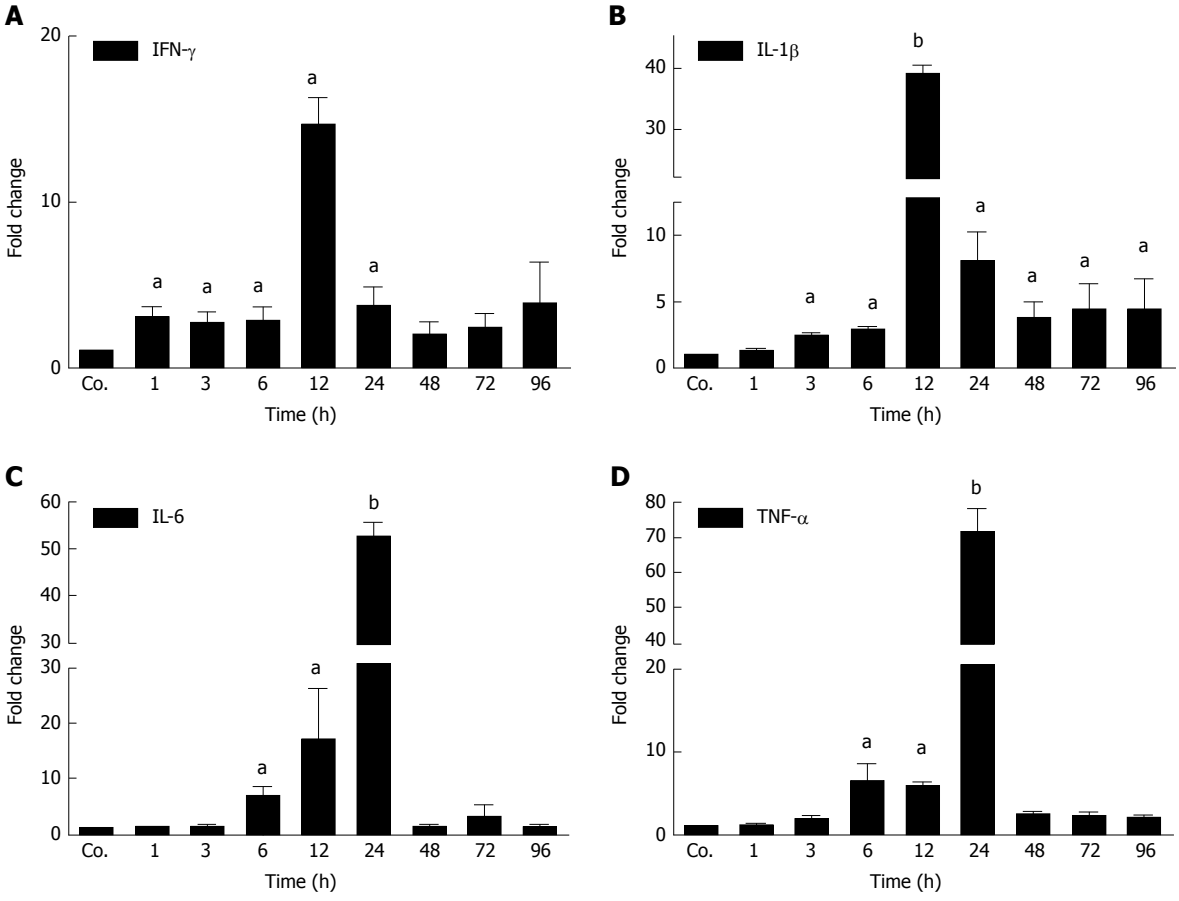

Figure 2 Early up-regulation of the expression of several acute-phase cytokines was observed. A-D: Significant increase of mRNA expression of acute-phase cytokines (IFN-γ, IL-1β, IL-6, TNF-α) in liver of thioacetamide -injected rats after various time points ($^{a}P \leq 0.05$; $^{b}P \leq 0.01$). Real-time PCR was normalized to GAPDH. Results represent mean values ± SEM, measured in duplicate in four animals for each time point, compared to controls (Co.).

h of TAA-administration. The levels of IFN-γ decreased thereafter, and turned to normal after 24 h. We also measured a significant induction of the expression of IL-1β with a maximum (41 ± 2.2 - fold) after 12 h. Thereafter, levels decreased but remained significantly elevated throughout the course of the study (until 96 h). Upregulation of both IL-6 and TNF-α started later (6 h) and reached a maximum after 24 h with an increase of 55 ± 2.1 and 69 ± 5 - fold, respectively. Expression decreased thereafter (Figure 2).

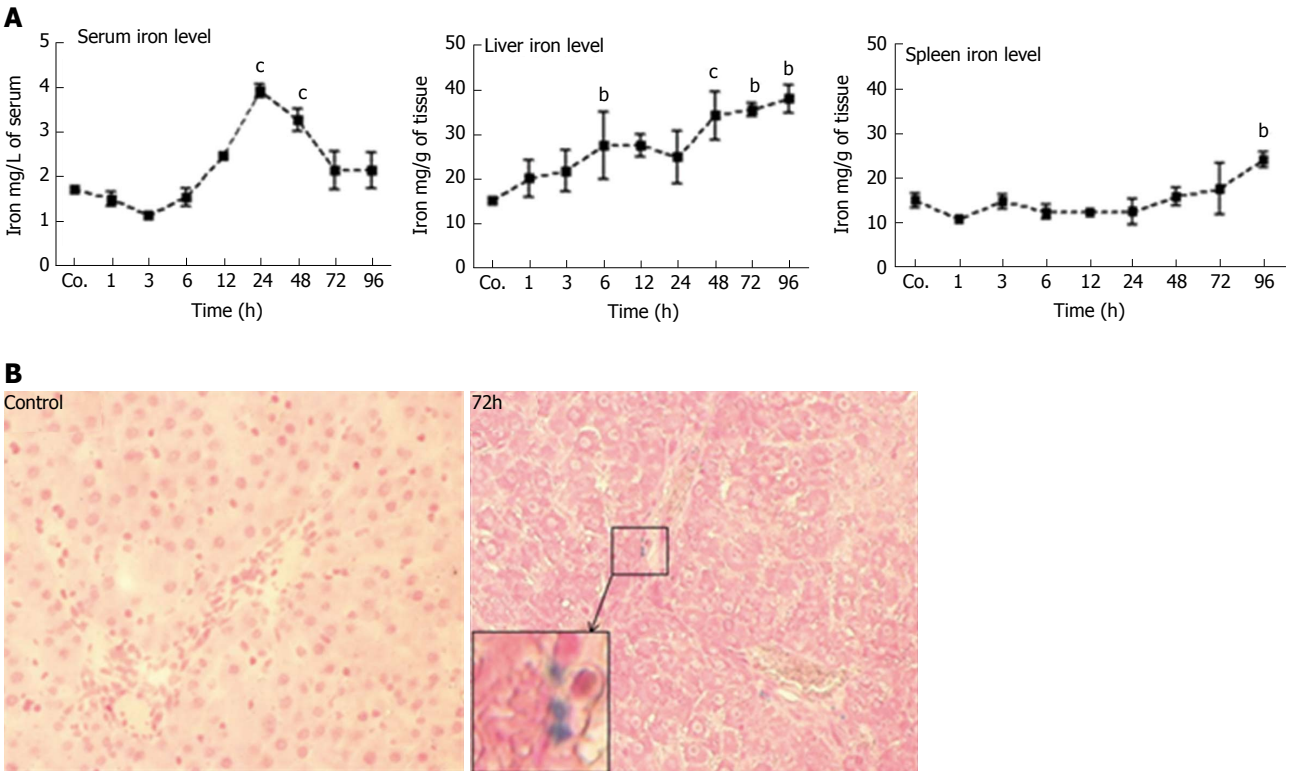

Figure 3 Measurement of serum, hepatic and splenic iron levels. A: Serum, liver and spleen iron levels at various time points after TAA injection in rats, as compared to controls (Co.). A mild decrease in serum iron levels was followed by a significant ($^{c}P \leq 0.001$) increase at 24 h and 48 h after TAA injection. Liver iron levels showed a significant ($^{b}P \leq 0.01$; $^{c}P \leq 0.001$) increase almost throughout the whole course of the study (a clear tendency is seen already after 1 h and 3 h). However, splenic iron content increased significantly ($^{b}P \leq 0.01$) only after 96 h. Results show mean ± SEM of each four animals; B: Prussian blue iron staining in liver of control and TAA-injected rats. Inset shows a higher magnification of the boxed area. A few positive cells are visible in rats after 72 h. Original magnification × 200.

Measurement of serum, hepatic and splenic iron levels

Compared to control serum iron levels (1.7 ± 0.03 mg/L), a slight but non-significant decrease (1.4 ± 0.1 mg/L) was observed shortly (1 h) after TAA injection. Values remained below controls until 6 h. Thereafter, serum iron level started to increase (2.4 ± 0.04 mg/L at 12h after TAA injection), reached a maximum after 24 h (3.97 ± 0.2 mg/L; $P = 0.0010$), and remained significantly elevated until 48 h. Then, serum iron decreased and returned to control levels at 72 - 96 h (Figure 3A). Compared to control animals (15.2 ± 0.9 mg/g), hepatic iron concentrations started to increase immediately (1 h) after TAA-administration, and progressively increased throughout the course of the study. The most prominent elevation (38 ± 3.1 mg/g; $P = 0.030$) was measured during 48 - 96 h after TAA injection (Figure 3A).

In contrast, splenic iron showed a tendency to decrease 1 h after TAA administration, and compared to control levels of 15 ± 1 mg/g, a mild decrease was observed during most of the investigated time points (3 - 24 h). Splenic iron concentrations reached normal levels after 48 - 72 h, which was followed by a mild but significant increase (23 ± 1 mg/g) at 96 h after TAA injection (Figure 3A).

Prussian blue staining of hepatic and splenic tissue

After having measured a significant increase in iron concentration in liver homogenates, we sought to detect iron in liver cells by histological staining methods. However, the applied method did not consistently detect iron in the specimens, obviously due to insufficient sensitivity. We could only detect iron in a few nucleated cells 72 h after TAA-administration in liver (Figure 3B), but never in spleen.

Changes in hepatic and serum levels of FTL and FTH

Our qRT-PCR analysis of total liver RNA showed a mild increase of mRNA expression of the iron storage protein FTH after 3 h - 48 h of TAA-injection, and a significant increase after 72 h (4.9 ± 2.6 - fold; $P \leq 0.01$) (Figure 4A). Additionally, a significant increase of the expression of FTL was noted after 48 h (7.8 ± 3.18 - fold; $P \leq 0.001$) (Figure 4A).

Western blot analysis of total protein from hepatic tissue lysates demonstrated an almost constant increase in the content of FTL and FTH beginning early (3 h - 6 h after TAA-injection), reaching a maximum

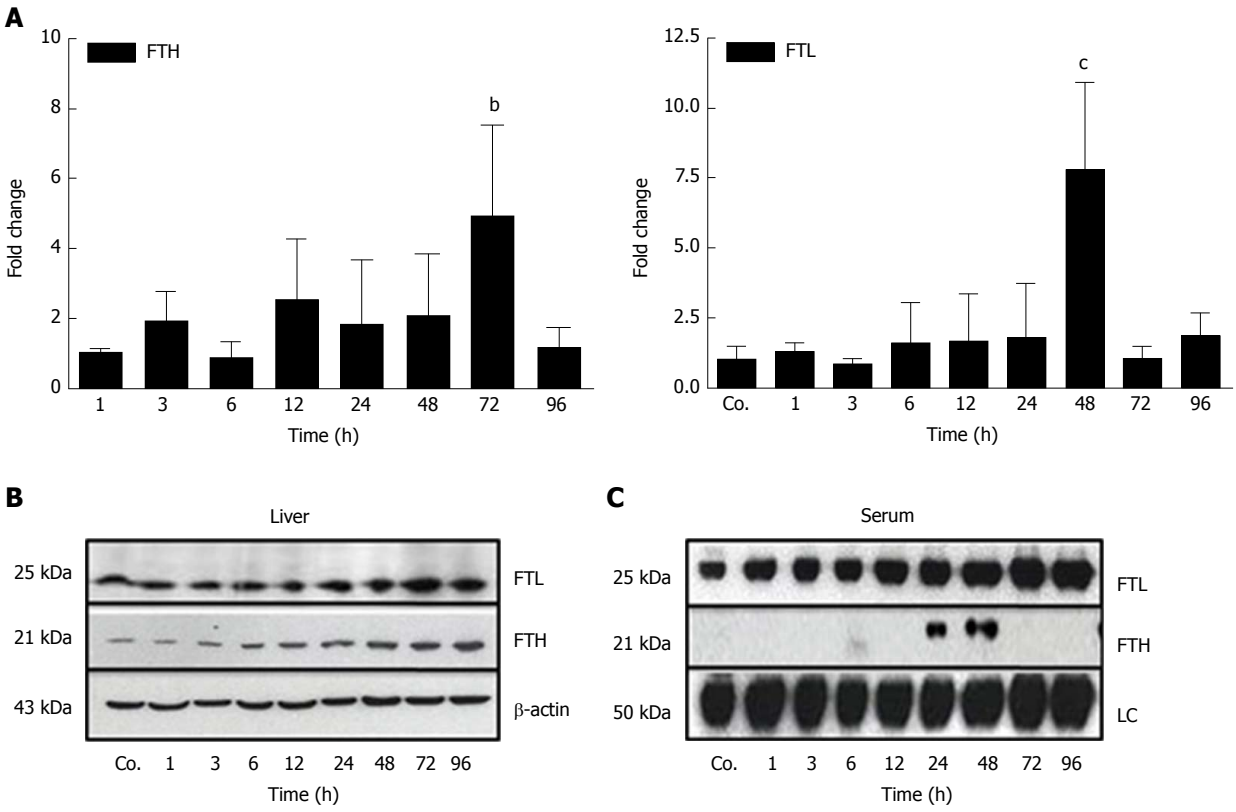

Figure 4 Changes in hepatic and serum levels of ferritin heavy chain and ferritin light chain after thioacetamide-induced liver damage. A: Significant ($^{b}P \leq 0.01$; $^{c}P \leq 0.001$) fold-change of hepatic mRNA expression of ferritin heavy chain (FTH) and ferritin light chain (FTL) in TAA-injected animals *vs* controls (Co.) after 72 h and 48 h, respectively, analyzed by qPCR and normalized against the house-keeping gene *UBC*. Results represent mean values ± SEM of each four animals per group. Controls were set as 1; B, C: Western blot analysis of FTL and FTH in total liver and in serum of control (Co.) and TAA-injected animals at indicated time points. β-actin (about 43 kDa) was used as loading control for liver tissue, while in serum the loading control (LC) represents an internal control (about 50 kDa).

at 72 h and 96 h, respectively (Figure 4B). Thereby, hepatic expression of FTL was more abundant compared to FTH (Figure 4B). Such quantitative difference became even more clearly visible in sera from control and TAA-treated animals (Figure 4C). Western blots revealed expression of FTL, but not FTH, in control animals. Thereby, FTL increased progressively after TAA injection with a maximum level at 96 h, whereas FTH became positive only at 24 h and 48 h after TAA injection (Figure 4C). These data clearly show differential regulation and release of FTH and FTL in damaged liver.

Immunolocalization of FTL and FTH in liver of control and TAA-injected animals

Immunohistochemical analysis of normal liver revealed weak granular FTL positivity mainly in the cytoplasm of hepatic cells. Immunoreactivity strongly increased in non-damaged liver areas after 48 h in TAA-treated rats. An intense signal was still visible at 72 h (Figure 5), although at this time point liver recovery has started to take place (Figure 1).

Immunostaining for FTH in liver tissue revealed a weak and almost homogenous staining pattern in control rats, and positivity in specific areas was found to increase most strongly at 48 h after TAA injection (Figure 6). Thereby, the regions of strongest staining obviously correlate to the pattern of inflammatory cells that invade the liver after TAA administration.

DISCUSSION

In animals, biochemical and histological effects of TAA-induced liver damage have been widely studied, and are highly similar to human acute liver damage[29]. However, the iron metabolism in the liver during acute-phase reaction is still poorly understood. In the present study, we administered TAA to rats using single intraperitoneal injection to induce reversible liver damage. The success of the method was confirmed by measurements of circulating hepatic enzymes (AST, ALT), and the typical pattern of inflammatory cells invading the liver from portal to central fields. Serum levels of AST and ALT were found to be highest at 24 h and 48h after TAA injection, and decreased to baseline levels at 72 h and 96 h, indicating liver damage followed by recovery. Previous studies have demonstrated similar results when TAA was administered in rats

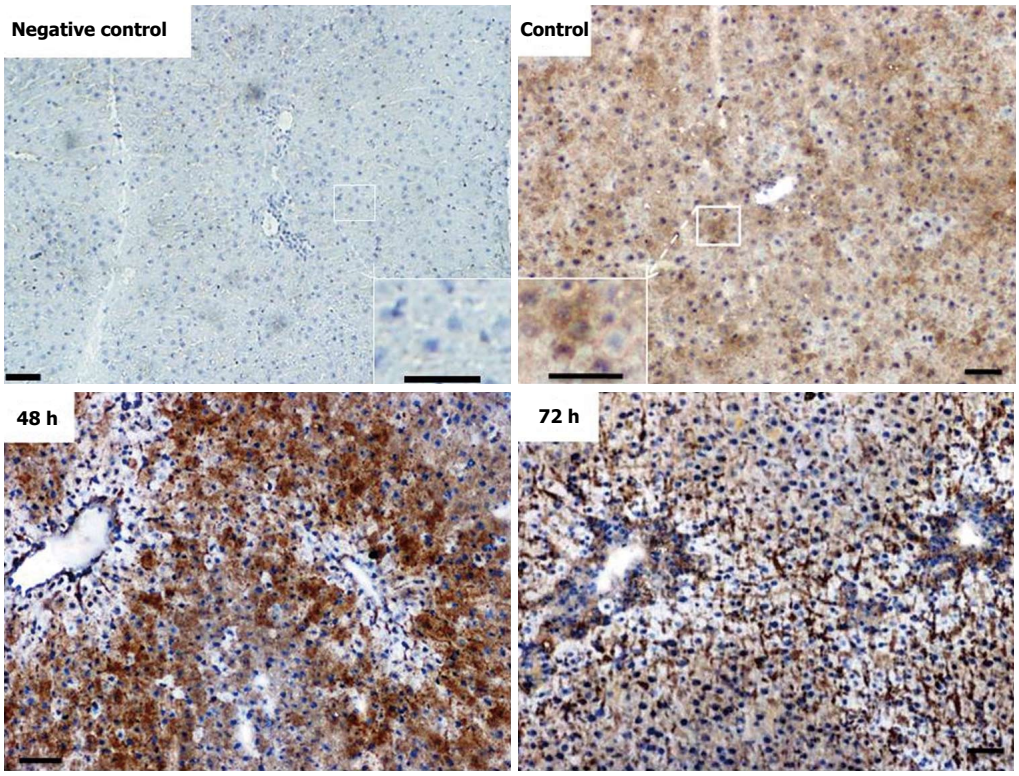

Figure 5 Immunoperoxidase staining of ferritin light chain in cryostat sections of rat liver from control and thioacetamide-injected animals. Insets show higher magnification of corresponding areas. Negative control represents the omission of primary antibodies. Note massive increase in signal intensity after 48 h and 72 h. Original magnification × 100; bar = 50 μm.

intravenously[30] or intraperitoneally[26]. Here we have also shown upregulation of hepatic gene expression of acute-phase cytokines (APCs) IFN-γ, IL-1β, IL6, and TNF-α; starting with IFN-γ after 1 h and IL-1β after 3 h of TAA injection. IL-6 and TNF-α expression increased after 6 h, when hepatic damage becomes overt in histological sections.

Increased serum iron levels may be attributed to damage of liver cells

In parallel with the early increase of IFN-γ and IL-1β expression, a mild decrease of the serum iron concentration, together with an increase of liver iron concentrations was detected. However, serum iron levels increased after 24 h and 48 h of TAA administration, corresponding to the peak levels of serum transaminases. Interestingly, in contrast to FTL, which increased almost constantly, FTH protein was only detectable in serum at these time points. We assume that the extensive damage of hepatocytes, demonstrated by the massive release of intracellular enzymes and of FTH into the serum may also be responsible for the increased serum iron levels after 24 h and 48 h of TAA injection.

The extremely high expression of APCs after 12 h - 24 h may additionally have induced the increase of tissue iron concentrations, which is also supported by results obtained with intramuscular administration of turpentine oil[17,31]. Hepatic iron accumulates in parallel to the increase of the two ferritin subtypes FTH and FTL. Both FTH and FTL have been reported to be intracellular proteins, and in fact, until recently the mature form of serum ferritin was unidentified, as it was its source. We recently identified FTL as the sole ferritin species in serum, and also demonstrated that it is a secreted acute-phase protein[14]. In contrast, FTH remains intracellularly located, despite its similar reactivity under acute-phase conditions. In fact, gene expression of both of the FT forms is modulated not only by iron itself, but also by acute-phase mediators[14,15]. The increase in ferritin expression and production may be attributed to the increased uptake of iron, released from damaged liver cells, by healthy hepatocytes. The role of FTL appears to be more important in this case, because it does not only store increasing amounts of iron in the 'stressed' hepatocytes together with FTH, but is also secreted to transport iron in the serum. This phenomenon seems to be specific for liver and not for other organs.

Indeed, ferritin was discovered as a cytosolic iron storage protein[32-34]. However, the localization of ferritins within the cell is discussed controversially. Previously, we reported the nuclear localization of iron transport proteins including FTH in rat liver under

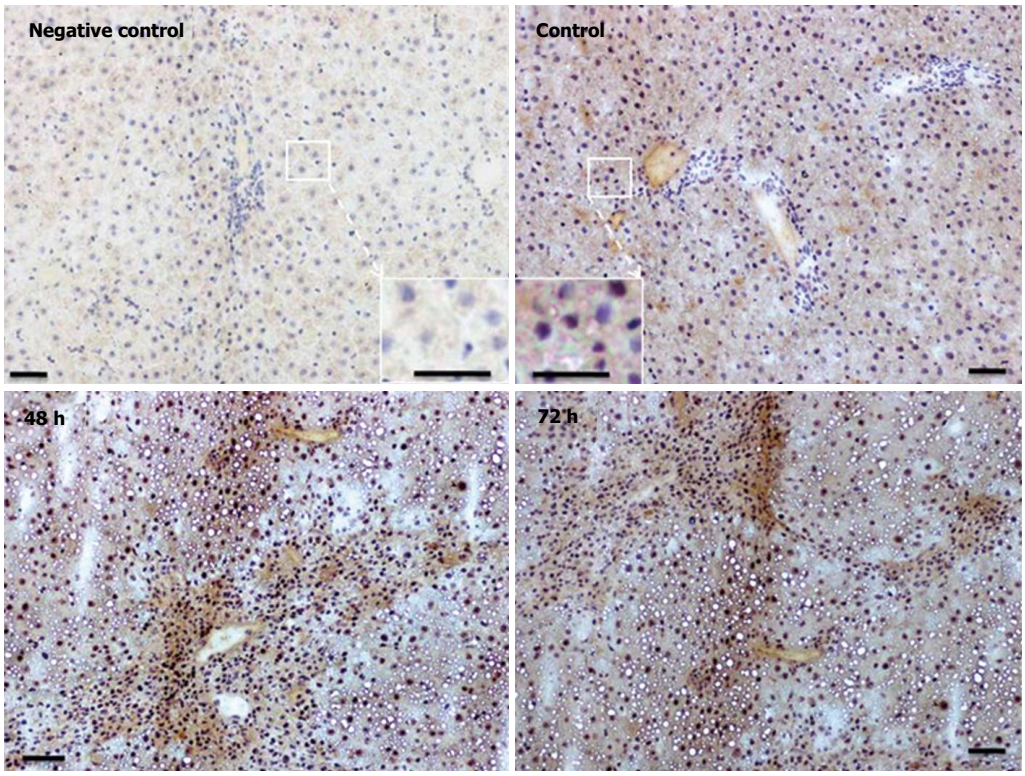

Figure 6 Immunodetection of ferritin heavy chain in cryostat sections of rat liver from control and thioacetamide-injected animals utilizing peroxidase-conjugated secondary antibodies. Insets show higher magnification of corresponding areas. Negative control represents the omission of primary antibodies. Note increase in signal intensity after 48 h and 72 h. Original magnification × 100; bar = 50 μm.

normal and acute-phase conditions[20,16]. In the same line of evidence, presence of nuclear FTH has been described in human astrocytoma cell-lines[35], in corneal epithelial cells[36], and in murine hepatocytes in iron overload settings[37]. Differential localization of FTH and FTL as well as quantitative differences are obviously related to their distinct roles in the liver. Thereby, nuclear FTH suggests an important role of iron for the activation of nuclear enzymes, which are involved in DNA synthesis and repair, and also in the modulation and initiation of transcription[38].

Spleen does not accumulate iron in acute liver damage

We also sought to study the functions of the spleen in iron metabolism after TAA-induced hepatocellular damage. The spleen represents a major organ of the reticuloendothelial system, and is responsible for the uptake and clearing of corpuscular matter from the blood circulation. In contrast to liver, we could not detect increased iron levels in the spleen, neither at early time points nor during the period of most severe liver damage. Only after 96 h, a mild but significant increase was noted. Although iron is supposed to be sequestered in the cells of the reticuloendothelial system we assume that under acute-phase conditions most of the serum iron is taken up by 'stressed' hepatocytes[15,20]. Although our direct iron staining in liver tissue was hardly successful, two significant findings support our assumption: Ⅰ) the increase of ferritins in hepatocytes, and Ⅱ) the lack of increase of splenic iron concentrations when liver iron is increased.

Acute-phase reaction can be subdivided into early and late stages

TAA administration induces an acute-phase reaction in the liver, which starts very early[39,40]. Thereby, liver macrophages obviously act as a first-line defense barrier. Inhibition of macrophages has been reported to aggravate liver damage in the rat model[41]. We and others have shown that liver macrophages are the first source of acute-phase mediators, *e.g.,* when toxins like CCl_4[42], acetaminophen[43], corpuscular matter, gadolinium or zymosan[44], and the bacterial polysaccharide (LPS)[18] are used to induce an acute-phase response in liver. At the same time, a massive production of chemoattractants is induced by the toxins in cells of the portal vessels and the portal fields, which may account for the recruitment of inflammatory cells and for hepatocellular damage[26]. We assume that hepatocytes "spared" from this damage take over the functions of damaged cells and maintain the acute-phase response. This may explain why we observed

changes in the synthesis of ferritins after liver damage, which are similar to those in the liver when the tissue damage takes place in extrahepatic sites[17]. The hypothesis is further supported by the detection of FTH and increased levels of FTL in serum, and in non-damaged areas of the liver. Thereby, although histological examinations of the liver indicate complete recovery 96 h after TAA administration, the increased iron and ferritin concentrations suggest that this is not yet the case.

In conclusion, our results show that damaging noxae like TAA induce a hepatic acute-phase reaction before and during the appearance of acute hepatocellular damage. Iron is taken up by the surviving (spared) liver cells during the phases of damage and recovery. Iron released into serum by damaged cells may be transported to and stored in liver cells *via* FTL and FTH. Moreover, FTL is not only a marker of iron deposition but also a potential clinical marker for both acute and "chronic" liver damage, as it is not only a component of the iron "cage" within the tissue, but also a secretory protein in response to locally produced acute-phase cytokines.

COMMENTS

Background

The liver has a pivotal role in the homeostasis of iron under physiological conditions, including its storage and distribution to various organs according to their actual needs. The liver also has a central role in iron metabolism during the acute-phase reaction following tissue damage in extra-hepatic organs. Under these conditions, liver does not only increase its iron uptake, but also synthesizes the major iron-transport proteins ferritin (FT) and transferrin, in addition to lipocalin-2, lactoferrin and hepcidin, which are acute-phase proteins involved in systemic and local iron metabolism. Changes of iron metabolism induced by directly liver-damaging noxae like viruses, alcohol, and xenobiotics still need to be investigated.

Research frontiers

The authors provide evidence that the increase in liver iron concentrations after acute liver damage may be rather the consequence than the cause of hepatocyte loss; and that ferritin heavy chain (FTH) is a surrogate marker for hepatocyte damage in serum.

Innovations and breakthroughs

They results show that liver damage by thioacetamide induces a hepatic acute-phase reaction, as seen by early upregulation of cytokines followed by morphologically visible acute hepatocellular damage. Iron is taken up by the surviving (spared) hepatocytes during the phases of damage and recovery. Iron released into serum by dying cells is obviously transported back and stored in liver cells *via* FTL and FTH.

Applications

The current study increases our understanding of hyperferritinemia and hypersideremia associated with hepatic iron-overload found in non-alcoholic fatty liver disease, non-alcoholic steato-hepatitis, alcoholic liver disease, and chronic hepatitis-C. Moreover, we show that FTL is not only a marker for iron deposition, but also a potential clinical marker for both acute and chronic liver damage, as it is not only a component of the iron 'cage' within the tissue, but also a secreted protein in response to locally produced acute-phase cytokines.

Terminology

Ferritin is an intracellular protein, mainly functioning as an iron storage protein. It is made up of two subunits known as FTH and FTL. The two subunits are highly conserved, but independently and differently regulated both at transcriptional and posttranscriptional levels.

Peer-review

Article "Reabsorption of iron into acutely damaged rat liver: a role for ferritins" by Malik *et al* according to my opinion, is acceptable for publication without additional revision. This article is very interesting for persons involved in the field of hepatology This basic study try to explain what's happened with the iron during acute liver injury.

ACKNOWLEDGMENTS

We'd like to acknowledge the expert technical assistance of Mrs. D. Gerke.

REFERENCES

1 **Frazer DM**, Anderson GJ. Iron imports. I. Intestinal iron absorption and its regulation. *Am J Physiol Gastrointest Liver Physiol* 2005; **289**: G631-G635 [PMID: 16160078 DOI: 10.1152/ajpgi.00220.2005]
2 **Ganz T**, Nemeth E. Iron metabolism: interactions with normal and disordered erythropoiesis. *Cold Spring Harb Perspect Med* 2012; **2**: a011668 [PMID: 22553501 DOI: 10.1101/cshperspect.a011668]
3 **Anderson GJ**, Frazer DM. Hepatic iron metabolism. *Semin Liver Dis* 2005; **25**: 420-432 [PMID: 16315136 DOI: 10.1055/s-2005-923314]
4 **Cairo G**, Bernuzzi F, Recalcati S. A precious metal: Iron, an essential nutrient for all cells. *Genes Nutr* 2006; **1**: 25-39 [PMID: 18850218 DOI: 10.1007/BF02829934]
5 **Muckenthaler MU**, Rivella S, Hentze MW, Galy B. A Red Carpet for Iron Metabolism. *Cell* 2017; **168**: 344-361 [PMID: 28129536 DOI: 10.1016/j.cell.2016.12.034]
6 **Graham RM**, Reutens GM, Herbison CE, Delima RD, Chua AC, Olynyk JK, Trinder D. Transferrin receptor 2 mediates uptake of transferrin-bound and non-transferrin-bound iron. *J Hepatol* 2008; **48**: 327-334 [PMID: 18083267 DOI: 10.1016/j.jhep.2007.10.009]
7 **Cairo G**, Recalcati S, Mantovani A, Locati M. Iron trafficking and metabolism in macrophages: contribution to the polarized phenotype. *Trends Immunol* 2011; **32**: 241-247 [PMID: 21514223 DOI: 10.1016/j.it.2011.03.007]
8 **Darshan D**, Vanoaica L, Richman L, Beermann F, Kühn LC. Conditional deletion of ferritin H in mice induces loss of iron storage and liver damage. *Hepatology* 2009; **50**: 852-860 [PMID: 19492434 DOI: 10.1002/hep.23058]
9 **Kaplan J**, Ward DM. The essential nature of iron usage and regulation. *Curr Biol* 2013; **23**: R642-R646 [PMID: 23928078 DOI: 10.1016/j.cub.2013.05.033]
10 **Ramm GA**, Ruddell RG. Iron homeostasis, hepatocellular injury, and fibrogenesis in hemochromatosis: the role of inflammation in a noninflammatory liver disease. *Semin Liver Dis* 2010; **30**: 271-287 [PMID: 20665379 DOI: 10.1055/s-0030-1255356]
11 **Levi S**, Yewdall SJ, Harrison PM, Santambrogio P, Cozzi A, Rovida E, Albertini A, Arosio P. Evidence of H- and L-chains have co-operative roles in the iron-uptake mechanism of human ferritin. *Biochem J* 1992; **288** (Pt 2): 591-596 [PMID: 1463463]
12 **Sammarco MC**, Ditch S, Banerjee A, Grabczyk E. Ferritin L and H subunits are differentially regulated on a post-transcriptional level. *J Biol Chem* 2008; **283**: 4578-4587 [PMID: 18160403 DOI: 10.1074/jbc.M703456200]
13 **Sargent PJ**, Farnaud S, Evans RW. Structure/function overview

of proteins involved in iron storage and transport. *Curr Med Chem* 2005; **12**: 2683-2693 [PMID: 16305465]
14 **Naz N**, Moriconi F, Ahmad S, Amanzada A, Khan S, Mihm S, Ramadori G, Malik IA. Ferritin L is the sole serum ferritin constituent and a positive hepatic acute-phase protein. *Shock* 2013; **39**: 520-526 [PMID: 23524846 DOI: 10.1097/SHK.0b013e31829266b9]
15 **Ahmad S**, Sultan S, Naz N, Ahmad G, Alwahsh SM, Cameron S, Moriconi F, Ramadori G, Malik IA. Regulation of iron uptake in primary culture rat hepatocytes: the role of acute-phase cytokines. *Shock* 2014; **41**: 337-345 [PMID: 24365882 DOI: 10.1097/SHK.0000000000000107]
16 **Ahmad S**, Moriconi F, Naz N, Sultan S, Sheikh N, Ramadori G, Malik IA. Ferritin L and Ferritin H are differentially located within hepatic and extra hepatic organs under physiological and acute phase conditions. *Int J Clin Exp Pathol* 2013; **6**: 622-629 [PMID: 23573308]
17 **Sheikh N**, Dudas J, Ramadori G. Changes of gene expression of iron regulatory proteins during turpentine oil-induced acute-phase response in the rat. *Lab Invest* 2007; **87**: 713-725 [PMID: 17417667 DOI: 10.1038/labinvest.3700553]
18 **Ahmad G**, Sial GZ, Ramadori P, Dudas J, Batusic DS, Ramadori G. Changes of hepatic lactoferrin gene expression in two mouse models of the acute phase reaction. *Int J Biochem Cell Biol* 2011; **43**: 1822-1832 [PMID: 21963450 DOI: 10.1016/j.biocel.2011.09.002]
19 **Sultan S,** Pascucci M, Ahmad S, Malik IA, Bianchi A, Ramadori P, Ahmad G, Ramadori G. LIPOCALIN-2 is a major acute-phase protein in a rat and mouse model of sterile abscess. *Shock* 2012; **37**: 191-196 [PMID: 22249220 DOI: 10.1097/SHK.0b013e31823918c2]
20 **Naz N**, Malik IA, Sheikh N, Ahmad S, Khan S, Blaschke M, Schultze F, Ramadori G. Ferroportin-1 is a ‚nuclear'-negative acute-phase protein in rat liver: a comparison with other iron-transport proteins. *Lab Invest* 2012; **92**: 842-856 [PMID: 22469696 DOI: 10.1038/labinvest.2012.52]
21 **Miura K**, Taura K, Kodama Y, Schnabl B, Brenner DA. Hepatitis C virus-induced oxidative stress suppresses hepcidin expression through increased histone deacetylase activity. *Hepatology* 2008; **48**: 1420-1429 [PMID: 18671304 DOI: 10.1002/hep.22486]
22 **Pietrangelo A**. Iron in NASH, chronic liver diseases and HCC: how much iron is too much? *J Hepatol* 2009; **50**: 249-251 [PMID: 19070915 DOI: 10.1016/j.jhep.2008.11.011]
23 **Amanzada A**, Schneider S, Moriconi F, Lindhorst A, Suermann T, van Thiel DH, Mihm S, Ramadori G. Early anemia and rapid virological response improve the predictive efficiency of IL28B-genotype for treatment outcome to antiviral combination therapy in patients infected with chronic HCV genotype 1. *J Med Virol* 2012; **84**: 1208-1216 [PMID: 22711348 DOI: 10.1002/jmv.23323]
24 **Amanzada A**, Goralczyk AD, Moriconi F, van Thiel DH, Ramadori G, Mihm S. Vitamin D status and serum ferritin concentration in chronic hepatitis C virus type 1 infection. *J Med Virol* 2013; **85**: 1534-1541 [PMID: 23852677 DOI: 10.1002/jmv.23632]
25 **Kowdley KV**, Belt P, Wilson LA, Yeh MM, Neuschwander-Tetri BA, Chalasani N, Sanyal AJ, Nelson JE; NASH Clinical Research Network. Serum ferritin is an independent predictor of histologic severity and advanced fibrosis in patients with nonalcoholic fatty liver disease. *Hepatology* 2012; **55**: 77-85 [PMID: 21953442 DOI: 10.1002/hep.24706]
26 **Amanzada A**, Moriconi F, Mansuroglu T, Cameron S, Ramadori G, Malik IA. Induction of chemokines and cytokines before neutrophils and macrophage recruitment in different regions of rat liver after TAA administration. *Lab Invest* 2014; **94**: 235-247 [PMID: 24276236 DOI: 10.1038/labinvest.2013.134]
27 **Malik IA**, Moriconi F, Sheikh N, Naz N, Khan S, Dudas J, Mansuroglu T, Hess CF, Rave-Fränk M, Christiansen H, Ramadori G. Single-dose gamma-irradiation induces up-regulation of chemokine gene expression and recruitment of granulocytes into the portal area but not into other regions of rat hepatic tissue. *Am J Pathol* 2010; **176**: 1801-1815 [PMID: 20185578 DOI: 10.2353/ajpath.2010.090505]
28 **Riemer J**, Hoepken HH, Czerwinska H, Robinson SR, Dringen R. Colorimetric ferrozine-based assay for the quantitation of iron in cultured cells. *Anal Biochem* 2004; **331**: 370-375 [PMID: 15265744 DOI: 10.1016/j.ab.2004.03.049]
29 **Rahman TM**, Hodgson HJ. The effects of early and late administration of inhibitors of inducible nitric oxide synthase in a thioacetamide-induced model of acute hepatic failure in the rat. *J Hepatol* 2003; **38**: 583-590 [PMID: 12713868 DOI: 10.1016/S0168-8278(03)00050-3]
30 **Chen TM**, Subeq YM, Lee RP, Chiou TW, Hsu BG. Single dose intravenous thioacetamide administration as a model of acute liver damage in rats. *Int J Exp Pathol* 2008; **89**: 223-231 [PMID: 18422601 DOI: 10.1111/j.1365-2613.2008.00576.x]
31 **Malik IA**, Naz N, Sheikh N, Khan S, Moriconi F, Blaschke M, Ramadori G. Comparison of changes in gene expression of transferrin receptor-1 and other iron-regulatory proteins in rat liver and brain during acute-phase response. *Cell Tissue Res* 2011; **344**: 299-312 [PMID: 21437659 DOI: 10.1007/s00441-011-1152-3]
32 **Cairo G**, Tacchini L, Schiaffonati L, Rappocciolo E, Ventura E, Pietrangelo A. Translational regulation of ferritin synthesis in rat liver. Effects of chronic dietary iron overload. *Biochem J* 1989; **264**: 925-928 [PMID: 2619720]
33 **Cairo G**, Rappocciolo E, Tacchini L, Schiaffonati L. Expression of the genes for the ferritin H and L subunits in rat liver and heart. Evidence for tissue-specific regulations at pre- and post-translational levels. *Biochem J* 1991; **275** (Pt 3): 813-816 [PMID: 2039459]
34 **Meyron-Holtz EG**, Moshe-Belizowski S, Cohen LA. A possible role for secreted ferritin in tissue iron distribution. *J Neural Transm* (Vienna) 2011; **118**: 337-347 [PMID: 21298454 DOI: 10.1007/s00702-011-0582-0]
35 **Surguladze N**, Patton S, Cozzi A, Fried MG, Connor JR. Characterization of nuclear ferritin and mechanism of translocation. *Biochem J* 2005; **388**: 731-740 [PMID: 15675895 DOI: 10.1042/BJ20041853]
36 **Cai CX**, Linsenmayer TF. Nuclear translocation of ferritin in corneal epithelial cells. *J Cell Sci* 2001; **114**: 2327-2334 [PMID: 11493671]
37 **Smith AG**, Carthew P, Francis JE, Edwards RE, Dinsdale D. Characterization and accumulation of ferritin in hepatocyte nuclei of mice with iron overload. *Hepatology* 1990; **12**: 1399-1405 [PMID: 2258156 DOI: 10.1002/hep.1840120622]
38 **Thompson KJ**, Fried MG, Ye Z, Boyer P, Connor JR. Regulation, mechanisms and proposed function of ferritin translocation to cell nuclei. *J Cell Sci* 2002; **115**: 2165-2177 [PMID: 11973357]
39 **Izawa T**, Murakami H, Wijesundera KK, Golbar HM, Kuwamura M, Yamate J. Inflammatory regulation of iron metabolism during thioacetamide-induced acute liver injury in rats. *Exp Toxicol Pathol* 2014; **66**: 155-162 [PMID: 24373749 DOI: 10.1016/j.etp.2013.12.002]
40 **Kuramochi M**, Izawa T, Pervin M, Bondoc A, Kuwamura M, Yamate J. The kinetics of damage-associated molecular patterns (DAMPs) and toll-like receptors during thioacetamide-induced acute liver injury in rats. *Exp Toxicol Pathol* 2016; **68**: 471-477 [PMID: 27522298 DOI: 10.1016/j.etp.2016.06.005]
41 **Golbar HM**, Izawa T, Wijesundera KK, Bondoc A, Tennakoon AH, Kuwamura M, Yamate J. Depletion of Hepatic Macrophages Aggravates Liver Lesions Induced in Rats by Thioacetamide (TAA). *Toxicol Pathol* 2016; **44**: 246-258 [PMID: 26957569 DOI: 10.1177/0192623315621191]
42 **Neubauer K**, Lindhorst A, Tron K, Ramadori G, Saile B. Decrease of PECAM-1-gene-expression induced by proinflammatory cytokines IFN-gamma and IFN-alpha is reversed by TGF-beta in sinusoidal endothelial cells and hepatic mononuclear phagocytes. *BMC Physiol* 2008; **8**: 9 [PMID: 18466611 DOI: 10.1186/1472-6793-8-9]

43 **Woolbright BL**, Jaeschke H. Role of the inflammasome in acetaminophen-induced liver injury and acute liver failure. *J Hepatol* 2017; **66**: 836-848 [PMID: 27913221 DOI: 10.1016/j.jhep.2016.11.017]
44 **Moriconi F**, Ahmad G, Ramadori P, Malik I, Sheikh N, Merli M, Riggio O, Dudas J, Ramadori G. Phagocytosis of gadolinium chloride or zymosan induces simultaneous upregulation of hepcidin- and downregulation of hemojuvelin- and Fpn-1-gene expression in murine liver. *Lab Invest* 2009; **89**: 1252-1260 [PMID: 19721414 DOI: 10.1038/labinvest.2009.92]

P- Reviewer: Markic D, Paraskevas KI **S- Editor**: Qi Y
L- Editor: A **E- Editor**: Huang Y

World Journal of Gastroenterology

Submit a Manuscript: http://www.f6publishing.com

World J Gastroenterol 2017 November 7; 23(41): 7359-7368

DOI: 10.3748/wjg.v23.i41.7359

ISSN 1007-9327 (print) ISSN 2219-2840 (online)

ORIGINAL ARTICLE

Basic Study

Region-dependent effects of diabetes and insulin-replacement on neuronal nitric oxide synthase- and heme oxygenase-immunoreactive submucous neurons

Nikolett Bódi, Zita Szalai, Lalitha Chandrakumar, Mária Bagyánszki

Nikolett Bódi, Zita Szalai, Lalitha Chandrakumar, Mária Bagyánszki, Department of Physiology, Anatomy and Neuroscience, Faculty of Science and Informatics, University of Szeged, H-6726 Szeged, Hungary

ORCID number: Nikolett Bódi (0000-0002-9774-1387); Zita Szalai (0000-0002-8722-0211); Lalitha Chandrakumar (0000-0003-3674-5306); Mária Bagyánszki (0000-0003-3533-9461).

Author contributions: Bódi N designed the research and performed the majority of experiments; Szalai Z and Chandrakumar L participated in experiments; Bódi N and Bagyánszki M coordinated the research and analyzed the data; Bódi N, Szalai Z and Bagyánszki M wrote the paper.

Supported by the Hungarian Scientific Research Fund, OTKA grant, No.PD 108309 (Nikolett Bódi); by the János Bolyai Research Scholarship of the Hungarian Academy of Sciences (Mária Bagyánszki); and by the Stipendium Hungaricum Scholarship, No. 2015-SH-500041, Tempus Public Foundation (Lalitha Chandrakumar).

Institutional review board statement: The study was reviewed and approved by the University of Szeged Faculty of Science and Informatics Dept. of Physiology, Anatomy and Neuroscience.

Conflict-of-interest statement: No conflict of interest.

Data sharing statement: Technical appendix, statistical code, and dataset available from the corresponding author, Mária Bagyánszki at bmarcsi@bio.u-szeged.hu

Manuscript source: Unsolicited Manuscript

Correspondence to: Mária Bagyánszki, PhD, Associate Professor, Department of Physiology, Anatomy and Neuroscience, Faculty of Science and Informatics, University of Szeged, Közép fasor 52, H-6726 Szeged, Hungary. bmarcsi@bio.u-szeged.hu
Telephone: +36-62-544123
Fax: +36-62-544291

Received: June 15, 2017
Peer-review started: June 16, 2017
First decision: July 13, 2017
Revised: July 26, 2017
Accepted: August 25, 2017
Article in press: August 25, 2017
Published online: November 7, 2017

Abstract

AIM

To investigate the intestinal segment-specific effects of diabetes and insulin replacement on the density of different subpopulations of submucous neurons.

METHODS

Ten weeks after the onset of type 1 diabetes samples were taken from the duodenum, ileum and colon of streptozotocin-induce diabetic, insulin-treated diabetic and sex- and age-matched control rats. Whole-mount preparations of submucous plexus were prepared from the different gut segments for quantitative fluorescent immunohistochemistry. The following double-

immunostainings were performed: neuronal nitric oxide synthase (nNOS) and HuC/D, heme oxygenase (HO) 1 and peripherin, as well as HO2 and peripherin. The density of nNOS-, HO1- and HO2-immunoreactive (IR) neurons was determined as a percentage of the total number of submucous neurons.

RESULTS

The total number of submucous neurons and the proportion of nNOS-, HO1- and HO2-IR subpopulations were not affected in the duodenal ganglia of control, diabetic and insulin-treated rats. While the total neuronal number did not change in either the ileum or the colon, the density of nitrergic neurons exhibited a 2- and 3-fold increase in the diabetic ileum and colon, respectively, which was further enhanced after insulin replacement. The presence of HO1- and HO2-IR submucous neurons was robust in the colon of controls (38.4%-50.8%), whereas it was significantly lower in the small intestinal segments (0.0%-4.2%, $P < 0.0001$). Under pathophysiological conditions the only alteration detected was an increase in the ileum and a decrease in the colon of the proportion of HO-IR neurons in insulin-treated diabetic animals.

CONCLUSION

Diabetes and immediate insulin replacement induce the most pronounced region-specific alterations of nNOS-, HO1- and HO2-IR submucous neuronal density in the distal parts of the gut.

Key words: Nitrergic neurons; Heme oxygenase 1; Heme oxygenase 2; Submucous neurons; Gut region-specificity; Diabetes; Insulin

Core tip: Our present findings demonstrate for the first time the segment–specific alterations of the proportion of nitrergic, heme oxygenase (HO)1-immunoreactive (IR) and HO2-IR neurons in the submucous plexus of control, diabetic and insulin-treated diabetic rats. Our results suggest that duodenal nitrergic neurons are not affected, but ileal and colonic ones are induced to change their neurochemical character in diabetes and insulin replacement. The colonic ganglia are abundant in HO-IR neurons in both controls and diabetics, whereas insulin treatment decreases their proportion. In contrast to the colon, the low amount of HO-IR ileal neurons was increased by insulin-treatment.

Bódi N, Szalai Z, Chandrakumar L, Bagyánszki M. Region-dependent effects of diabetes and insulin-replacement on neuronal nitric oxide synthase- and heme oxygenase-immunoreactive submucous neurons. *World J Gastroenterol* 2017; 23(41): 7359-7368 Available from: URL: http://www.wjgnet.com/1007-9327/full/v23/i41/7359.htm DOI: http://dx.doi.org/10.3748/wjg.v23.i41.7359

INTRODUCTION

Diabetes has widespread effects on gastrointestinal (GI) function causing different GI symptoms, including nausea, vomiting, abdominal pain, constipation or diarrhoea[1]. The functional impairments of the GI tract in diabetes are studied intensively; however, the complexity of diabetes-related pathophysiological consequences hinders the attainment of clear findings about the underlying mechanisms and alterations. An increasing body of evidence confirms that the impaired function of the enteric nervous system (ENS) is closely related to the GI syndromes of diabetic patients[2-4]. The ENS is an autonomous entity structured as two major ganglionated plexi, *i.e.,* the myenteric and the submucosal plexi. The myenteric plexus regulates intestinal motility[5]. It is more difficult to determine the functions of submucous neurons because of differences in the organization and function of the submucous plexus: it is more complex in large mammals with at least two distinct nerve networks than in small rodents. Submucous neurons regulate electrolyte absorption across the mucosa, blood flow and mucosal secretion in small rodents[6,7], moreover in large mammals it is involved both in mucosal and motility processes[8,9].

The alterations in the number of inhibitory neurons including nitrergic neurons in diabetes and their responsiveness to insulin treatment have been intensively studied, but these investigations mainly target the myenteric plexus. Furthermore, a region-specific susceptibility of the nitrergic neurons to diabetes- as well as insulin-related damages was identified in the myenteric plexus[10-12].

In contrast to the intense interest in the neurochemical characterization of myenteric neurons in non-diabetic and diabetic state, the submucous plexus is poorly investigated in diabetes. A decreased total and an unchanged nitrergic submucous neuronal density were found in the jejunum and ileum in streptozotocin-induced (STZ) diabetes as compared to the controls[13,14], but we have no information about the effects of insulin treatment on the submucous neurons.

Long-lasting hyperglycemia can lead to oxidative stress, an imbalance between the increased production of reactive oxygen and nitrogen species (RONS) and the decrease of antioxidant defence mechanisms, which have been implicated in the damage of the ENS such as quantitative and neurochemical changes of the enteric neurons. The systemic oxidative state in type 2 diabetic patients was proved by the determination of serum oxidative stress markers including increased

malondialdehyde level and superoxide dismutase activity, decreased glutathione reductase, glutathione peroxidase, glucose-6-phosphate dehydrogenase enzyme activities and glutathione level[15]. This oxidative state was further confirmed by the results from diabetic duodenum and colon of human patients or rats, where it led to the apoptosis of enteric neurons and to neuronal remodelling in the ENS[16,17].

The heme catabolizing heme oxygenase (HO) enzyme plays an essential role in antioxidant defence mechanisms. This enzyme has two main isoforms including the inducible HO1 and the constitutive HO2. Of the two, HO2 is described as the isoform widely expressed in the neuronal and non-neuronal cell types of the healthy GI tract, and both HO1 and HO2 can be co-localized with neuronal nitric oxide synthase (nNOS)[18-21]. In diabetic rat ileum, the nitrergic myenteric neurons containing HO2 were more resistant to the effect of experimentally induced diabetes on cell body size[22]. However, the detailed characterization of the changes of HO1-immunoreactive (HO1-IR) and HO2-IR submucous neurons in the different gut regions of diabetic and insulin-treated diabetic rats has not been accomplished.

In view of the interest in understanding the gut segment-dependent changes in the submucous plexus in diabetes and insulin-treated diabetes, our study aimed to reveal the region-specific alterations in the density of neurons containing nNOS as well as HO1 or HO2 enzymes in the different segments of the small and large intestine of control, diabetic and insulin-treated diabetic rats.

MATERIALS AND METHODS

Animal model

Adult male Wistar rats (Crl:WI BR; Toxi-Coop Zrt.) weighing 210–260 g, kept on standard laboratory chow (Farmer-Mix Kft., Zsámbék) and with free access to drinking water were used throughout the experiments. The rats were divided randomly into three groups: STZ-induced diabetics (diabetics; n = 6), insulin-treated STZ-induced diabetics (insulin-treated diabetics; n = 4) and sex- and age-matched controls (n = 5). Hyperglycaemia was induced as described previously[10,23]. The animals were considered diabetic if the non-fasting blood glucose concentration was 18 mmol/L. From this time on, one group of hyperglycaemic rats received a subcutaneous injection of insulin (Humulin M3, Eli Lilly Nederland) each morning (2 IU) and afternoon (2 IU). The blood glucose level and weight of each animal were measured weekly. In all procedures involving experimental animals, the principles of laboratory animal care (NIH Publication No. 85-23, revised 1985) were strictly followed, and all the experiments were approved in advance by the Local Ethics Committee for Animal Research Studies at the University of Szeged.

Tissue handling

Ten weeks after the onset of diabetes, the animals were killed by cervical dislocation under chloral hydrate anaesthesia (375 mg/kg i.p.). The gut segments of control, diabetic and insulin-treated diabetic rats were dissected and rinsed in 0.05 mol/L phosphate buffer (PB, pH 7.4). Samples were taken from the duodenum (1 cm distal to the pylorus), the ileum (1 cm proximal to the ileocecal junction), and the proximal colon and processed for immunohistochemical studies. For double-labelling fluorescent immunohistochemistry, the intestinal segments were cut along the mesentery, pinched flat and fixed overnight at 4 ℃ in 4% paraformaldehyde solution buffered with 0.1 mol/L PB (pH 7.4). The samples were then washed, and to obtain the whole-mounts of the submucous plexus, the muscular layers of the gut wall were removed, and the mucosa was extracted by scrapping with a small spatula under an Olympus SD30 stereomicroscope.

Double-labelling fluorescent immunohistochemistry

For quantitative immunohistochemistry, whole-mount preparations derived from different gut segments were double-immunostained with nNOS and HuC/D, HO1 and peripherin, as well as HO2 and peripherin. Briefly, after blocking the preparations in PB containing 0.1% bovine serum albumin, 10% normal goat serum and 0.3% Triton X-100, they were incubated overnight with anti-nNOS (rabbit; Cayman Chemical, Ann Arbor, MI, the United States of America; final dilution 1:200) in combination with anti-HuC/D (mouse; Molecular Probes, Eugene, OR, the United States of America; final dilution 1:50), anti-HO1 (mouse; Novus Biologicals Europe, Abington, United Kingdom; final dilution 1:200) or anti-HO2 (mouse; Santa Cruz Biotechnology, Inc., Dallas, TX, the United States of America; final dilution 1:50) in combination with anti-peripherin (rabbit; Millipore, Temecula, CA, the United States of America; final dilution 1:400) primary antibodies. After washing in PB, whole-mounts were incubated with anti-rabbit Alexa Fluor 488 (Life Technologies Corporation, Molecular Probes, Inc., Eugene, OR, the United States of America; final dilution 1:200) and anti-mouse Cy™3 (Jackson ImmunoResearch Laboratories, Inc., Baltimore Pike, PA, the United States of America; final dilution 1:200) secondary antibodies for 4 h. All incubations were carried out at room temperature. Negative controls were performed by omitting the primary antibody, when no immunoreactivity was observed. Whole-mounts were mounted on slides in EverBrite™ Mounting Medium (Biotium, Inc., Hayward, CA, the United States of America), observed and photographed with an Olympus BX51 fluorescent microscope equipped with an Olympus DP70 camera. One hundred submucous ganglia were taken from

Table 1 Weight and glycaemic characteristics of the three experimental groups of rats

	Weight (g)		Blood glucose level (mmol/L)	
	Initial	Final	Initial	Average
Controls (n = 5)	232.2 ± 7.29	486 ± 4.93[a]	7.08 ± 0.22	6.3 ± 0.13
Diabetics (n = 6)	235.3 ± 10.48	382.7 ± 3.53[a,b]	6.6 ± 0.1	23.31 ± 0.53[a,b]
Insulin-treated diabetics (n = 4)	251.5 ± 4.35	481.5 ± 13.4[a,c]	6.65 ± 0.18	9.48 ± 0.14[a,b,c]

Data are expressed as mean ± SE; [a]$P < 0.0001$ *vs* initial, [b]$P < 0.0001$ *vs* final controls, and [c]$P < 0.0001$ *vs* final diabetics.

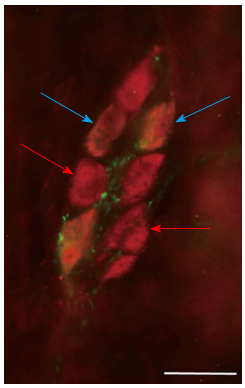

Figure 1 Representative fluorescent micrograph of a whole-mount preparation of submucous ganglia from the colon of a diabetic rat after nNOS-HuC/D double-labelling immunohistochemistry. Red arrows indicate neurons labelled for HuC/D only, blue arrows show neurons double-labelled for both nNOS and HuC/D; Scale bar: 50 μm.

each intestinal segment in each experimental group and we counted the nNOS-, HO1- and HO2-IR neurons and the HuC/D- and peripherin-IR neurons to yield the total number of submucous neurons. We determined the nNOS-, HO1- and HO2-IR neurons as a percentage of the total number of neurons.

Statistical analysis

Statistical analysis was performed with one-way ANOVA and the Newman–Keuls test. All analyses were carried out with GraphPad Prism 6.0 (GraphPad Software, La Jolla, CA, the United States of America). A probability of $P < 0.05$ was set as the level of significance. All data were expressed as mean ± SE.

RESULTS

Pathophysiological characteristics of diabetes

According to the data shown in Table 1, STZ promoted hyperglycaemia in the diabetic rats (23.31 ± 0.53 mmol/L), but the insulin treatment prevented the extremely high blood glucose concentration (9.48 ± 0.14 mmol/L). The weight of the animals significantly increased in all groups during the ten weeks of the experiment, but the final body weight of diabetic rats was less elevated compared to the control and the insulin-treated diabetic animals.

Proportion of nNOS-IR neurons

To determine the proportion of nNOS-IR neurons in the total submucous neuronal number, nNOS and HuC/D double-labelling fluorescent immunohistochemistry was applied, as shown in the representative micrograph (Figure 1). In the total number of neurons, no changes were found between the different gut segments within the control group or among the three experimental groups in the duodenal, ileal or colonic intestinal regions (data are not shown). The proportion of nitrergic neurons in the total neuronal number did not show any differences between the three investigated gut segments of controls (Figure 2A). STZ treatment resulted in an increase in the proportion of nitrergic neurons in the distal intestinal segments (in the ileum and colon) but not in the duodenum. The proportion of the nitrergic subpopulation exhibited a 2-fold increase in the ileum (12% *vs* 6% in controls), whereas a 3-fold increase was observed in the colon of diabetics (22% *vs* 8% in controls; Figure 2B). The insulin treatment had no effect on the proportion of duodenal and colonic nitrergic submucous neurons which, however, was found to increase significantly in the ileal segment as compared to the diabetic rats.

Proportion of HO1-IR neurons

To visualize and quantify the occurrence of HO1-IR submucous neurons, HO1 immunohistochemistry was used combined with peripherin as pan-neuronal marker (Figure 3).

The distribution of HO1-IR submucous neurons as compared to total neuronal number demonstrated region-dependent differences in the three examined segments even in the controls. The proportion of duodenal and ileal HO1-IR submucous neurons was only 4% and 0%, respectively, but the occurrence of HO1-IR neurons was extremely robust in the colon (51%; $P < 0.0001$; Figure 4A). In the diabetics, results similar to the controls were obtained along the intestinal tract, with HO1-IR neurons seldom occurring in the small intestine and present in abundance in the large intestine (Figure 4B). In the duodenal segment no change was induced by the insulin treatment in the presence of HO1-IR neurons, whereas in the ileum quantitative analysis of the HO1-IR submucous subpopulation revealed a significant increase in the proportion of these neurons in the insulin-treated diabetic group (6%) as compared to the control group (0%). In the colonic submucous ganglia we found a significant decrease in the insulin-treated diabetics

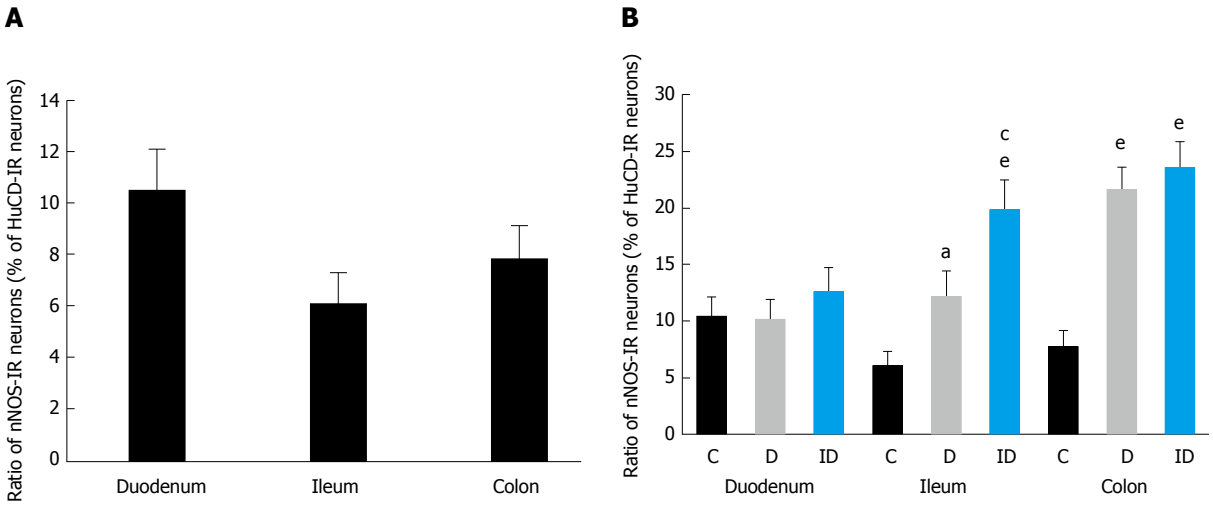

Figure 2 Proportion of nitric oxide synthase-immunoreactive neurons related to the total number of submucous neurons in the duodenum, ileum and colon. A: Only in controls; B: in control, diabetic and insulin-treated diabetic rats. Data are expressed as mean ± SE; $^{a}P < 0.05$ and $^{e}P < 0.0001$ *vs* controls, $^{c}P < 0.05$ *vs* diabetics. IR: Immunoreactive; C: Controls; D: Diabetics; ID: Insulin-treated diabetics.

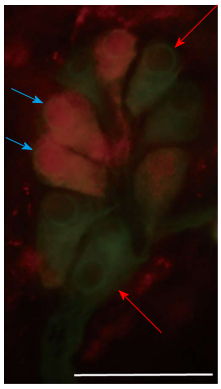

Figure 3 Representative fluorescent micrograph of a whole-mount preparation of submucous ganglia from the colon of a control rat after HO1-peripherin double-labelling immunohistochemistry. Red arrows indicate neurons labelled for peripherin only, blue arrows show neurons double-labelled for both HO1 and peripherin; Scale bar: 50 μm.

(14%) as compared to the control (51%) or the diabetic (38%) groups (Figure 4B).

Proportion of HO2-IR neurons

The occurrence of HO2-IR submucous neurons was also calculated as the proportion of peripherin-stained total submucous neuronal number (Figure 5). In the controls, the HO2-IR neurons demonstrated a distribution similar to that of the HO1-IR submucous neurons. In the segments of small intestine, a low level of HO2-IR neurons was detected (4% in the duodenum, 1% in the ileum), but in the colon this proportion was significantly higher (38%; $P < 0.0001$; Figure 6A). In the diabetics, results similar to the controls were obtained along the intestine; the marked differences in the ratio of HO2-IR neurons between the different gut segments remained unchanged (Figure 6B).

Immediate insulin replacement had no effect on the abundance of HO2-IR neurons in the duodenum. Although the ileal segment showed the lowest proportion of HO2-IR neurons compared to the other two control regions, a significant increase in their numbers was found in the ileum after insulin replacement (17%) compared to the control (1%) and the diabetic rats (6%). The proportion of colonic HO2-IR neurons showed a pattern similar to that of the HO1-IR neurons in the same segment. The ten-week insulin treatment reduced the proportion of HO2-IR neurons (28%) below control level, and this decrease was significant as compared to the diabetic group (52%; Figure 6B).

DISCUSSION

In the present study we investigated the nitrergic subpopulation of submucous neurons similarly to our earlier study on the myenteric plexus. In that study we published the gut region-dependent quantitative changes of the total population and the nitrergic subpopulation of myenteric neurons in STZ-induced diabetic and insulin-treated diabetic rats[10]. In the present study we demonstrate that the total submucous neuronal number is similar in the duodenum, ileum and colon in the controls, and remains unchanged in diabetes as well as after insulin replacement. This is in agreement with the observation of da Silva *et al*[24], however their investigations are limited to the ileum. Our data reflect that STZ-induced diabetes does not induce degenerative changes in the total population of submucous neurons, unlike our previous data about the myenteric plexus. Oxidative stress is known to be induced by hyperglycaemia in diabetes *via* the mitochondrial overproduction of RONS, which leads to an imbalance between free radical production and antioxidant defense molecules

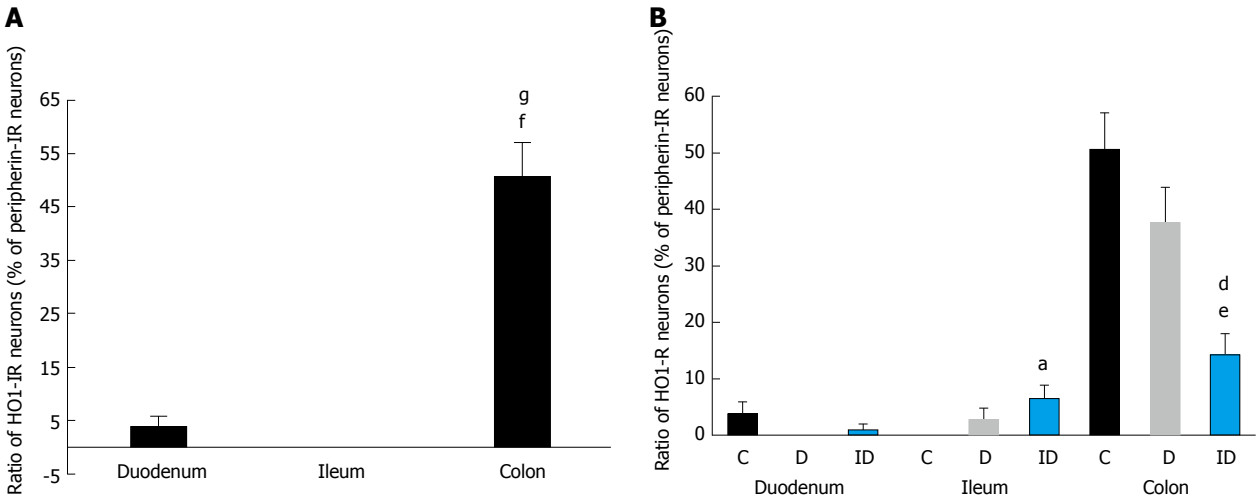

Figure 4 Proportion of HO1-immunoreactive neurons related to the total number of submucous neurons in the duodenum, ileum and colon. A: Only in controls; B: In control, diabetic and insulin-treated diabetic rats. Data are expressed as mean ± SE; $^{f}P < 0.0001$ *vs* control duodenum; $^{g}P < 0.0001$ *vs* control ileum, $^{a}P < 0.05$ and $^{e}P < 0.0001$ *vs* controls, and $^{d}P < 0.01$ *vs* diabetics. IR: Immunoreactive; C: Controls; D: Diabetics; ID: Insulin-treated diabetics.

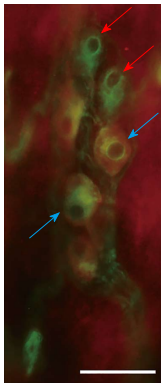

Figure 5 Representative fluorescent micrograph of a whole-mount preparation of submucous ganglia from the colon of a control rat after HO2-peripherin double-labelling immunohistochemistry. Red arrows indicate neurons labelled for peripherin only, blue arrows show neurons double-labelled for both HO2 and peripherin; Scale bar: 50 μm.

or mechanisms[15-17]. We suggest, in accordance with the opinion of Lopes *et al*[13], that submucous neurons may have greater resistance to RONS under diabetic conditions.

In non-diabetic state, nitrergic myenteric and submucous neurons have been examined along the gut in different rodent species, and it has been described that the myenteric plexus has more nitrergic neurons as compared to the submucous plexus[25-27]. Using the same rat model of type 1 diabetes as Izbéki *et al*[10], the gut segment-specific alterations in the two ganglionated plexi can be compared. According to the investigation of the myenteric plexus in the controls, the ileum contained the lowest proportion of nitrergic neurons[10], but we found no region-specific differences in the submucous plexus in accordance with other findings[28,29]. We have revealed different effects of hyperglycaemia on the ratio of nitrergic neurons in the two plexi; a significant decrease was seen in all segments of the myenteric plexus, but, with the exception of the duodenum, an increase was found in the ileal and colonic submucous ganglia. Our results demonstrate that not only total neuronal density but also the nitrergic subpopulation of the two plexi are affected in a different way by the diabetic state.

Because of the unchanged total neuronal number in submucous ganglia, alterations of the neurochemical character as an adaptation to diabetes-related oxidative stress is suggested to be in the background of these modifications. Neurochemical changes as an answer of the ENS to pathological conditions including Crohn's disease, ulcerative colitis or Parkinson's disease are known[30-32]. Moreover, there is evidence that diabetic neuropathy and changes in neurochemical coding can occur in the submucous plexus of the ENS[13,14]. We found a similar result in another pathological rat model, in chronic ethanol-consumption, where the total myenteric neuronal number remained constant, but the density of nitrergic neurons was changed[33,34]. Previous studies showed that there are few nitrergic neurons in the submucous ganglia, the submucous plexus is more abundant in vasoactive intestinal polypeptide (VIP)-IR neurons as compared to the myenteric plexus, and there is a high proportion of VIP and nNOS co-localizing neurons in both plexi[14,35]. Lin *et al*[36] demonstrated that colonic VIP-IR submucous neurons start to express nNOS during culturing as a form of functional plasticity.

Our results reported here show gut segment-specific alterations of not only the nitrergic, but also the HO1-IR and HO2-IR submucous neurons, and these alterations become increasingly pronounced along the proximo-distal axis of the gut. An important finding of this study is that HO1-IR and HO2-IR neurons are more abundant in the colon (about half

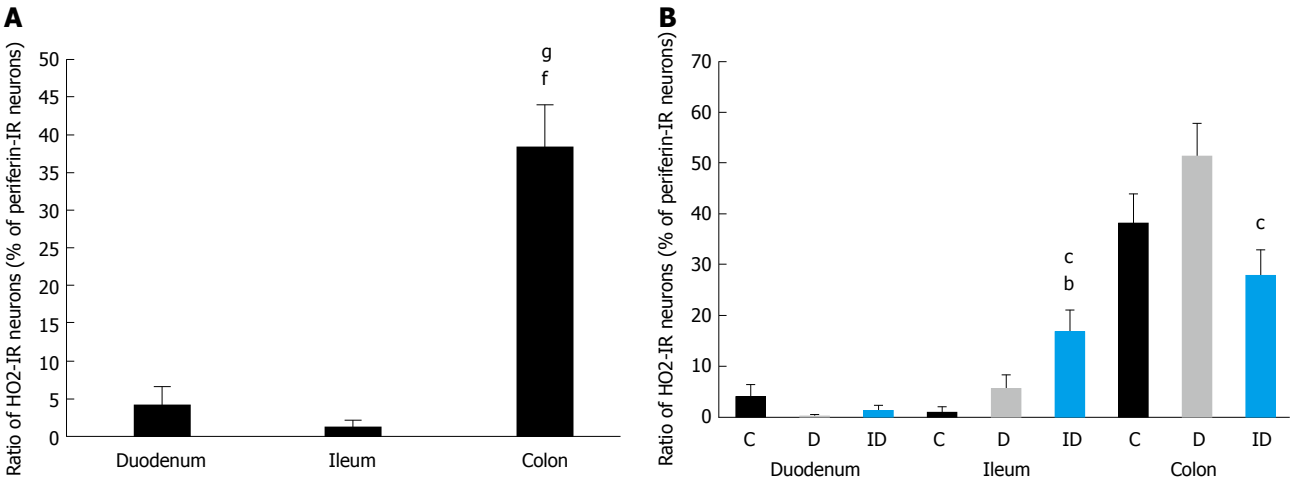

Figure 6 Proportion of HO2-immunoreactive neurons related to the total number of submucous neurons in the duodenum, ileum and colon. A: Only in controls; B: In control, diabetic and insulin-treated diabetic rats. Data are expressed as mean ± SE; $^{f}P < 0.0001$ *vs* control duodenum, $^{g}P < 0.0001$ *vs* control ileum, $^{b}P < 0.001$ *vs* controls, and $^{c}P < 0.05$ *vs* diabetics; C: Controls; D: Diabetics. IR: Immunoreactive; ID: Insulin-treated diabetics.

of the colonic neurons was HO-IR) than in the small intestinal segments (about 0%-5%) in the controls, and STZ treatment did not result in any significant changes in the investigated regions. The question arises as to what the reasons underlying these differences are. In non-diabetic state, more RONS are generated in the colon then in the small intestine[37]. It is possible that under worsening oxidative circumstances the pro-oxidant basal state in the colon acts as a preconditioning factor inducing the higher physiological activity of both isoforms of the antioxidant HO enzymes. This mechanism may play a role in the protection of this segment against neuronal cell loss regarding the total submucous neuronal number in diabetic condition, in contrast to earlier findings in the colonic myenteric ganglia. The neuroprotective, anti-apoptotic effects of the HO1 enzyme in oxidative stress were proved in the central ENS[38,39]. However, we did not investigate the co-localization of nNOS with HO in these neurons, despite earlier findings demonstrating the beneficial effects of the coexistence of these enzymes on the myenteric neurons[22]. Moreover, former studies visualized nNOS-HO2-IR neurons in the submucous ganglia[19,20,40], which suggests a protective role of HO, and may contribute to our results revealing the increasing proportion of nitrergic neurons in the diabetic ileum and colon.

The data about the effects of insulin are contradictory. While early insulin replacement was preventive to the total population of colonic myenteric neurons[10], we found no changes in the three intestinal regions in the total number of submucous neurons of insulin-treated diabetic rats. The density of nitrergic neurons showed similar patterns in the two plexi after insulin replacement, an increase was found from proximal to distal direction, which means significant changes in the ileum and the colon as compared to untreated diabetic rats.

As in the case of the nitrergic subpopulation, not the duodenal, but the ileal and colonic HO1- and HO2-IR submucous neurons responded to insulin treatment, but in an opposite way. However, there were no differences between the control and diabetic groups in these two regions and we found an increased density in the ileum, but a decreased abundance in the colon of insulin-treated diabetic rats.

Our results suggest that the three investigated gut segments have different levels of responsiveness to immediate insulin replacement in diabetes regarding the nitrergic and HO-IR subpopulation of submucous neurons. This is confirmed by our earlier findings in the myenteric neurons and in their microenvironment including the capillary endothelium adjacent to the myenteric ganglia[23]. The environmental changes of submucous ganglia were described, such as the alteration of the faeces-associated microbiota in diabetes and insulin-treatment[41]. Moreover, microangiopathy as a complication of diabetes in submucosal vessels of the GI tract was identified on duodenal and colon samples from diabetic patients[42,43]. On the other hand, our results are in accordance with the previous contradictory data about the beneficial or harmful effects of insulin. Insulin was shown to induce DNA damage through the enhanced production of RONS and to increase the risk of cancer in different cell types[44,45]. But insulin therapy decreased vascular superoxide overproduction in diabetic rats generated by NADPH oxidase, NOS or xanthine oxidase[46]. It is important to mention that the nitric oxide produced by NOS and the carbon monoxide generated by HO enzymes may have either pro-oxidant or antioxidant effects depending on the microenvironment, the duration of production and

the amount of these gases[47-49].

This complex background makes it difficult to understand the details of our recent findings, and further experiments are needed to explore the mechanisms of physiological and pathological events in the submucous neurons in diabetes and insulin replacement, their relationships and communication with their environment.

In summary, our present study provides evidence for the first time that the neurochemical character of the nitrergic submucous neurons exhibits gut region-dependent changes in diabetic and insulin-treated diabetic rats. In addition, we prove that HO1-IR and HO2-IR submucous neurons are present in small amounts in the small intestine, but in high abundance in the colon of control and diabetic rats, and they have segment-specific responsiveness to immediate insulin replacement.

COMMENTS

Background

In diabetic rat ileum, the nitrergic myenteric neurons containing heme oxygenase (HO) 2 were more resistant to the effect of experimentally induced diabetes on cell body size. However, the detailed characterization of the changes of HO1-immunoreactive (HO1-IR) and HO2-IR submucous neurons in the different gut regions of diabetic and insulin-treated diabetic rats has not been accomplished.

Research frontiers

This study aimed to reveal the region-specific alterations in the density of neurons containing nNOS as well as HO1 or HO2 enzymes in the different segments of the small and large intestine of control, diabetic and insulin-treated diabetic rats.

Innovations and breakthroughs

The authors prove that HO1-IR and HO2-IR submucous neurons are present in small amounts in the small intestine, but in high abundance in the colon of control and diabetic rats, and they have segment-specific responsiveness to immediate insulin replacement.

Peer-review

This is a good experimental research and suitable for publication. The findings are of interest and original.

ACKNOWLEDGMENTS

We thank our teacher, Professor Éva Fekete for her valuable support and guidance in the research work.

REFERENCES

1 **Azpiroz F**, Malagelada C. Diabetic neuropathy in the gut: pathogenesis and diagnosis. *Diabetologia* 2016; **59**: 404-408 [PMID: 26643877 DOI: 10.1007/s00125-015-3831-1]

2 **Horváth VJ**, Putz Z, Izbéki F, Körei AE, Gerő L, Lengyel C, Kempler P, Várkonyi T. Diabetes-related dysfunction of the small intestine and the colon: focus on motility. *Curr Diab Rep* 2015; **15**: 94 [PMID: 26374571 DOI: 10.1007/s11892-015-0672-8]

3 **Yarandi SS**, Srinivasan S. Diabetic gastrointestinal motility disorders and the role of enteric nervous system: current status and future directions. *Neurogastroenterol Motil* 2014; **26**: 611-624 [PMID: 24661628 DOI: 10.1111/nmo.12330]

4 **Uranga-Ocio JA**, Bastús-Díez S, Delkáder-Palacios D, García-Cristóbal N, Leal-García MÁ, Abalo-Delgado R. Enteric neuropathy associated to diabetes mellitus. *Rev Esp Enferm Dig* 2015; **107**: 366-373 [PMID: 26031865]

5 **Furness JB**. The enteric nervous system and neurogastroenterology. *Nat Rev Gastroenterol Hepatol* 2012; **9**: 286-294 [PMID: 22392290 DOI: 10.1038/nrgastro.2012.32]

6 **Furness JB**. The enteric nervous system: normal functions and enteric neuropathies. *Neurogastroenterol Motil* 2008; **20** Suppl 1: 32-38 [PMID: 18402640 DOI: 10.1111/j.1365-2982.2008.01094.x]

7 **Andres H**, Rock R, Bridges RJ, Rummel W, Schreiner J. Submucosal plexus and electrolyte transport across rat colonic mucosa. *J Physiol* 1985; **364**: 301-312 [PMID: 2411917 DOI: 10.1113/jphysiol.1985.sp015746]

8 **Timmermans JP**, Hens J, Adriaensen D. Outer submucous plexus: an intrinsic nerve network involved in both secretory and motility processes in the intestine of large mammals and humans. *Anat Rec* 2001; **262**: 71-78 [PMID: 11146430]

9 **Krueger D**, Michel K, Zeller F, Demir IE, Ceyhan GO, Slotta-Huspenina J, Schemann M. Neural influences on human intestinal epithelium in vitro. *J Physiol* 2016; **594**: 357-372 [PMID: 26527433 DOI: 10.1113/JP271493]

10 **Izbéki F**, Wittman T, Rosztóczy A, Linke N, Bódi N, Fekete E, Bagyánszki M. Immediate insulin treatment prevents gut motility alterations and loss of nitrergic neurons in the ileum and colon of rats with streptozotocin-induced diabetes. *Diabetes Res Clin Pract* 2008; **80**: 192-198 [PMID: 18242757 DOI: 10.1016/j.diabres.2007.12.013]

11 **Bagyánszki M**, Bódi N. Diabetes-related alterations in the enteric nervous system and its microenvironment. *World J Diabetes* 2012; **3**: 80-93 [PMID: 22645637 DOI: 10.4239/wjd.v3.i5.80]

12 **de Mello ST**, de Miranda Neto MH, Zanoni JN, Furlan MM. Effects of insulin treatment on HuC/HuD, NADH diaphorase, and nNOS-positive myoenteric neurons of the duodenum of adult rats with acute diabetes. *Dig Dis Sci* 2009; **54**: 731-737 [PMID: 18661235 DOI: 10.1007/s10620-008-0430-8]

13 **Lopes CR**, Ferreira PE, Zanoni JN, Alves AM, Alves EP, Buttow NC. Neuroprotective effect of quercetin on the duodenum enteric nervous system of streptozotocin-induced diabetic rats. *Dig Dis Sci* 2012; **57**: 3106-3115 [PMID: 22878915 DOI: 10.1007/s10620-012-2300-7]

14 **Hermes-Uliana C**, Panizzon CP, Trevizan AR, Sehaber CC, Ramalho FV, Martins HA, Zanoni JN. Is L-glutathione more effective than L-glutamine in preventing enteric diabetic neuropathy? *Dig Dis Sci* 2014; **59**: 937-948 [PMID: 24370785 DOI: 10.1007/s10620-013-2993-2]

15 **Aouacheri O**, Saka S, Krim M, Messaadia A, Maidi I. The investigation of the oxidative stress-related parameters in type 2 diabetes mellitus. *Can J Diabetes* 2015; **39**: 44-49 [PMID: 25065473 DOI: 10.1016/j.jcjd.2014.03.002]

16 **Jancsó Z**, Bódi N, Borsos B, Fekete É, Hermesz E. Gut region-specific accumulation of reactive oxygen species leads to regionally distinct activation of antioxidant and apoptotic marker molecules in rats with STZ-induced diabetes. *Int J Biochem Cell Biol* 2015; **62**: 125-131 [PMID: 25794426 DOI: 10.1016/j.biocel.2015.03.005]

17 **Chandrasekharan B**, Anitha M, Blatt R, Shahnavaz N, Kooby D, Staley C, Mwangi S, Jones DP, Sitaraman SV, Srinivasan S. Colonic motor dysfunction in human diabetes is associated with enteric neuronal loss and increased oxidative stress. *Neurogastroenterol Motil* 2011; **23**: 131-138, e26 [PMID: 20939847 DOI: 10.1111/j.1365-2982.2010.01611.x]

18 **Gibbons SJ**, Farrugia G. The role of carbon monoxide in the

gastrointestinal tract. *J Physiol* 2004; **556**: 325-336 [PMID: 14766943 DOI: 10.1113/jphysiol.2003.056556]
19 **Donat ME**, Wong K, Staines WA, Krantis A. Heme oxygenase immunoreactive neurons in the rat intestine and their relationship to nitrergic neurons. *J Auton Nerv Syst* 1999; **77**: 4-12 [PMID: 10494744 DOI: 10.1016/S0165-1838(99)00023-5]
20 **Battish R**, Cao GY, Lynn RB, Chakder S, Rattan S. Heme oxygenase-2 distribution in anorectum: colocalization with neuronal nitric oxide synthase. *Am J Physiol Gastrointest Liver Physiol* 2000; **278**: G148-G155 [PMID: 10644573]
21 **Ny L**, Alm P, Larsson B, Andersson KE. Morphological relations between haem oxygenases, NO-synthase and VIP in the canine and feline gastrointestinal tracts. *J Auton Nerv Syst* 1997; **65**: 49-56 [PMID: 9258872 DOI: 10.1016/S0165-1838(97)00034-9]
22 **Shotton HR**, Lincoln J. Diabetes only affects nitric oxide synthase-containing myenteric neurons that do not contain heme oxygenase 2. *Brain Res* 2006; **1068**: 248-256 [PMID: 16375869 DOI: 10.1016/j.brainres.2005.11.057]
23 **Bódi N**, Talapka P, Poles MZ, Hermesz E, Jancsó Z, Katarova Z, Izbéki F, Wittmann T, Fekete É, Bagyánszki M. Gut region-specific diabetic damage to the capillary endothelium adjacent to the myenteric plexus. *Microcirculation* 2012; **19**: 316-326 [PMID: 22296580 DOI: 10.1111/j.1549-8719.2012.00164.x]
24 **da Silva GG**, Zanoni JN, Buttow NC. Neuroprotective action of Ginkgo biloba on the enteric nervous system of diabetic rats. *World J Gastroenterol* 2011; **17**: 898-905 [PMID: 21412498 DOI: 10.3748/wjg.v17.i7.898]
25 **Ekblad E**, Mulder H, Uddman R, Sundler F. NOS-containing neurons in the rat gut and coeliac ganglia. *Neuropharmacology* 1994; **33**: 1323-1331 [PMID: 7532815 DOI: 10.1016/0028-3908(94)90032-9]
26 **Ekblad E**, Alm P, Sundler F. Distribution, origin and projections of nitric oxide synthase-containing neurons in gut and pancreas. *Neuroscience* 1994; **63**: 233-248 [PMID: 7534882 DOI: 10.1016/0306-4522(94)90019-1]
27 **Costa M**, Furness JB, Pompolo S, Brookes SJ, Bornstein JC, Bredt DS, Snyder SH. Projections and chemical coding of neurons with immunoreactivity for nitric oxide synthase in the guinea-pig small intestine. *Neurosci Lett* 1992; **148**: 121-125 [PMID: 1284439 DOI: 10.1016/0304-3940(92)90819-S]
28 **Chino Y**, Fujimura M, Kitahama K, Fujimiya M. Colocalization of NO and VIP in neurons of the submucous plexus in the rat intestine. *Peptides* 2002; **23**: 2245-2250 [PMID: 12535705 DOI: 10.1016/S0196-9781(02)00264-4]
29 **Sayegh AI**, Ritter RC. Morphology and distribution of nitric oxide synthase-, neurokinin-1 receptor-, calretinin-, calbindin-, and neurofilament-M-immunoreactive neurons in the myenteric and submucosal plexuses of the rat small intestine. *Anat Rec A Discov Mol Cell Evol Biol* 2003; **271**: 209-216 [PMID: 12552637 DOI: 10.1002/ar.a.10024]
30 **Schneider J**, Jehle EC, Starlinger MJ, Neunlist M, Michel K, Hoppe S, Schemann M. Neurotransmitter coding of enteric neurones in the submucous plexus is changed in non-inflamed rectum of patients with Crohn's disease. *Neurogastroenterol Motil* 2001; **13**: 255-264 [PMID: 11437988 DOI: 10.1046/j.1365-2982.2001.00265.x]
31 **Chaumette T**, Lebouvier T, Aubert P, Lardeux B, Qin C, Li Q, Accary D, Bézard E, Bruley des Varannes S, Derkinderen P, Neunlist M. Neurochemical plasticity in the enteric nervous system of a primate animal model of experimental Parkinsonism. *Neurogastroenterol Motil* 2009; **21**: 215-222 [PMID: 19077145 DOI: 10.1111/j.1365-2982.2008.01226.x]
32 **Neunlist M**, Aubert P, Toquet C, Oreshkova T, Barouk J, Lehur PA, Schemann M, Galmiche JP. Changes in chemical coding of myenteric neurones in ulcerative colitis. *Gut* 2003; **52**: 84-90 [PMID: 12477766 DOI: 10.1136/gut.52.1.84]
33 **Krecsmarik M**, Izbéki F, Bagyánszki M, Linke N, Bódi N, Kaszaki J, Katarova Z, Szabó A, Fekete E, Wittmann T. Chronic ethanol exposure impairs neuronal nitric oxide synthase in the rat intestine. *Alcohol Clin Exp Res* 2006; **30**: 967-973 [PMID: 16737454 DOI: 10.1111/j.1530-0277.2006.00110.x]
34 **Bagyánszki M**, Bódi N. Gut region-dependent alterations of nitrergic myenteric neurons after chronic alcohol consumption. *World J Gastrointest Pathophysiol* 2015; **6**: 51-57 [PMID: 26301118 DOI: 10.4291/wjgp.v6.i3.51]
35 **Aimi Y**, Kimura H, Kinoshita T, Minami Y, Fujimura M, Vincent SR. Histochemical localization of nitric oxide synthase in rat enteric nervous system. *Neuroscience* 1993; **53**: 553-560 [PMID: 7684113 DOI: 10.1016/0306-4522(93)90220-A]
36 **Lin Z**, Sandgren K, Ekblad E. Increased expression of nitric oxide synthase in cultured neurons from adult rat colonic submucous ganglia. *Auton Neurosci* 2004; **114**: 29-38 [PMID: 15331042 DOI: 10.1016/j.autneu.2004.06.002]
37 **Sanders LM**, Henderson CE, Hong MY, Barhoumi R, Burghardt RC, Carroll RJ, Turner ND, Chapkin RS, Lupton JR. Pro-oxidant environment of the colon compared to the small intestine may contribute to greater cancer susceptibility. *Cancer Lett* 2004; **208**: 155-161 [PMID: 15142673 DOI: 10.1016/j.canlet.2003.12.007]
38 **Al-Owais MM**, Dallas ML, Boyle JP, Scragg JL, Peers C. Heme Oxygenase-1 Influences Apoptosis via CO-mediated Inhibition of K+ Channels. *Adv Exp Med Biol* 2015; **860**: 343-351 [PMID: 26303499 DOI: 10.1007/978-3-319-18440-1_39]
39 **Chen L**, Wang L, Zhang X, Cui L, Xing Y, Dong L, Liu Z, Li Y, Zhang X, Wang C, Bai X, Zhang J, Zhang L, Zhao X. The protection by octreotide against experimental ischemic stroke: up-regulated transcription factor Nrf2, HO-1 and down-regulated NF-κB expression. *Brain Res* 2012; **1475**: 80-87 [PMID: 22885292 DOI: 10.1016/j.brainres.2012.07.052]
40 **Miller SM**, Reed D, Sarr MG, Farrugia G, Szurszewski JH. Haem oxygenase in enteric nervous system of human stomach and jejunum and co-localization with nitric oxide synthase. *Neurogastroenterol Motil* 2001; **13**: 121-131 [PMID: 11298990 DOI: 10.1046/j.1365-2982.2001.00255.x]
41 **Wirth R**, Bódi N, Maróti G, Bagyánszki M, Talapka P, Fekete É, Bagi Z, Kovács KL. Regionally distinct alterations in the composition of the gut microbiota in rats with streptozotocin-induced diabetes. *PLoS One* 2014; **9**: e110440 [PMID: 25469509 DOI: 10.1371/journal.pone.0110440]
42 **Sasor A**, Ohlsson B. Microangiopathy is common in submucosal vessels of the colon in patients with diabetes mellitus. *Rev Diabet Stud* 2014; **11**: 175-180 [PMID: 25396405 DOI: 10.1900/RDS.2014.11.175]
43 **De Las Casas LE**, Finley JL. Diabetic microangiopathy in the small bowel. *Histopathology* 1999; **35**: 267-270 [PMID: 10469219 DOI: 10.1046/j.1365-2559.1999.00702.x]
44 **Othman EM**, Kreissl MC, Kaiser FR, Arias-Loza PA, Stopper H. Insulin-mediated oxidative stress and DNA damage in LLC-PK1 pig kidney cell line, female rat primary kidney cells, and male ZDF rat kidneys in vivo. *Endocrinology* 2013; **154**: 1434-1443 [PMID: 23456362 DOI: 10.1210/en.2012-1768]
45 **Othman EM**, Leyh A, Stopper H. Insulin mediated DNA damage in mammalian colon cells and human lymphocytes in vitro. *Mutat Res* 2013; **745-746**: 34-39 [PMID: 23524287 DOI: 10.1016/j.mrfmmm.2013.03.006]
46 **Malardé L**, Rebillard A, Le Douairon-Lahaye S, Vincent S, Zguira MS, Lemoine-Morel S, Gratas-Delamarche A, Groussard C. Superoxide production pathways in aortas of diabetic rats: beneficial effects of insulin therapy and endurance training. *Mol Cell Biochem* 2014; **389**: 113-118 [PMID: 24374791 DOI: 10.1007/s11010-013-1932-z]
47 **Rivera LR**, Poole DP, Thacker M, Furness JB. The involvement of nitric oxide synthase neurons in enteric neuropathies. *Neurogastroenterol Motil* 2011; **23**: 980-988 [PMID: 21895878 DOI: 10.1111/j.1365-2982.2011.01780.x]
48 **Chen S**, Khan ZA, Barbin Y, Chakrabarti S. Pro-oxidant role of heme oxygenase in mediating glucose-induced endothelial cell

damage. *Free Radic Res* 2004; **38**: 1301-1310 [PMID: 15763954 DOI: 10.1080/10715760400017228]

49 **da Silva JL**, Morishita T, Escalante B, Staudinger R, Drummond G, Goligorsky MS, Lutton JD, Abraham NG. Dual role of heme oxygenase in epithelial cell injury: contrasting effects of short-term and long-term exposure to oxidant stress. *J Lab Clin Med* 1996; **128**: 290-296 [PMID: 8783636 DOI: 10.1016/S0022-2143(96)90030-X]

P- Reviewer: Dinc M, Tomkin GH **S- Editor**: Qi Y
L- Editor: A **E- Editor**: Huang Y

World Journal of Gastroenterology

Submit a Manuscript: http://www.f6publishing.com

World J Gastroenterol 2017 November 7; 23(41): 7369-7386

DOI: 10.3748/wjg.v23.i41.7369

ISSN 1007-9327 (print) ISSN 2219-2840 (online)

ORIGINAL ARTICLE

Basic Study

Parallel mRNA, proteomics and miRNA expression analysis in cell line models of the intestine

Finbarr O'Sullivan, Joanne Keenan, Sinead Aherne, Fiona O'Neill, Colin Clarke, Michael Henry, Paula Meleady, Laura Breen, Niall Barron, Martin Clynes, Karina Horgan, Padraig Doolan, Richard Murphy

Finbarr O'Sullivan, Joanne Keenan, Sinead Aherne, Fiona O'Neill, Michael Henry, Paula Meleady, Laura Breen, Niall Barron, Martin Clynes, Padraig Doolan, National Institute for Cellular Biotechnology, Dublin City University, Dublin D09 W6Y4, Ireland

Colin Clarke, National Institute for Bioprocessing Research & Training, Blackrock, Dublin A94 X099, Ireland

Karina Horgan, Richard Murphy, Alltech, Dunboyne, Meath, A86 X006, Ireland

Author contributions: O'Sullivan F was involved at all stages of the research and co-wrote the manuscript; Doolan P coordinated the analysis of the triomic dataset and co-wrote the manuscript; Keenan J and Breen L performed the cell culture and prepared samples for analysis; Aherne S and O'Neill F performed the microarray experiments; Henry M and Meleady P performed the proteomic experiments; Clarke C and Barron N performed bioinformatics analysis on the data; Murphy R designed and coordinated the research programme with help from Clynes M and Horgan K; All authors read and reviewed the manuscript; Doolan P and Murphy R contributed equally to this work and are joint-last Authors.

Supported by A Strategic Alliance Programme between Alltech Ltd. and DCU and also Enterprise Ireland Innovation Partnership Grant (IP 2015 0375).

Conflict-of-interest statement: The authors declare they have no conflicts of interest.

Data sharing statement: All data generated or analysed during this study are included in this published article and its supplementary information files.

Manuscript source: Unsolicited manuscript

Correspondence to: Finbarr O'Sullivan, PhD, Associate Director, National Institute for Cellular Biotechnology, Dublin City University, Dublin D09 W6Y4, Ireland. finbarr.osullivan@dcu.ie
Telephone: +353-1-7005700

Received: May 16, 2017
Peer-review started: May 18, 2017
First decision: June 22, 2017
Revised: July 7, 2017
Accepted: August 8, 2017
Article in press: August 8, 2017
Published online: November 7, 2017

Abstract

AIM

To identify miRNA-regulated proteins differentially expressed between Caco2 and HT-29: two principal cell line models of the intestine.

METHODS

Exponentially growing Caco-2 and HT-29 cells were harvested and prepared for mRNA, miRNA and proteomic profiling. mRNA microarray profiling analysis was carried out using the Affymetrix GeneChip Human Gene 1.0 ST array. miRNA microarray profiling analysis was carried out using the Affymetrix Genechip miRNA 3.0 array. Quantitative Label-free LC-MS/MS proteomic analysis was performed using a Dionex Ultimate 3000 RSLCnano system coupled to a hybrid linear ion

trap/Orbitrap mass spectrometer. Peptide identities were validated in Proteome Discoverer 2.1 and were subsequently imported into Progenesis QI software for further analysis. Hierarchical cluster analysis for all three parallel datasets (miRNA, proteomics, mRNA) was conducted in the R software environment using the Euclidean distance measure and Ward's clustering algorithm. The prediction of miRNA and oppositely correlated protein/mRNA interactions was performed using TargetScan 6.1. GO biological process, molecular function and cellular component enrichment analysis was carried out for the DE miRNA, protein and mRNA lists *via* the Pathway Studio 11.3 Web interface using their Mammalian database.

RESULTS

Differential expression (DE) profiling comparing the intestinal cell lines HT-29 and Caco-2 identified 1795 Genes, 168 Proteins and 160 miRNAs as DE between the two cell lines. At the gene level, 1084 genes were upregulated and 711 were downregulated in the Caco-2 cell line relative to the HT-29 cell line. At the protein level, 57 proteins were found to be upregulated and 111 downregulated in the Caco-2 cell line relative to the HT-29 cell line. Finally, at the miRNAs level, 104 were upregulated and 56 downregulated in the Caco-2 cell line relative to the HT-29 cell line. Gene ontology (GO) analysis of the DE mRNA identified cell adhesion, migration and ECM organization, cellular lipid and cholesterol metabolic processes, small molecule transport and a range of responses to external stimuli, while similar analysis of the DE protein list identified gene expression/transcription, epigenetic mechanisms, DNA replication, differentiation and translation ontology categories. The DE protein and gene lists were found to share 15 biological processes including for example epithelial cell differentiation [P value $\leqslant$ 1.81613E-08 (protein list); $P \leqslant 0.000434311$ (gene list)] and actin filament bundle assembly [P value $\leqslant 0.001582797$ (protein list); $P \leqslant 0.002733714$ (gene list)]. Analysis was conducted on the three data streams acquired in parallel to identify targets undergoing potential miRNA translational repression identified 34 proteins, whose respective mRNAs were detected but no change in expression was observed. Of these 34 proteins, 27 proteins downregulated in the Caco-2 cell line relative to the HT-29 cell line and predicted to be targeted by 19 unique anti-correlated/upregulated microRNAs and 7 proteins upregulated in the Caco-2 cell line relative to the HT-29 cell line and predicted to be targeted by 15 unique anti-correlated/downregulated microRNAs.

CONCLUSION

This first study providing "tri-omics" analysis of the principal intestinal cell line models Caco-2 and HT-29 has identified 34 proteins potentially undergoing miRNA translational repression.

Key words: Caco-2; HT-29; Microarray; Proteomics; miRNA; Targetscan; Gene ontology

Core tip: Unique triomics analysis of Caco-2 and HT-29, two commonly used *in vitro* cell lines models of the intestine, was conducted. This analysis not only provided data on differentially expressed mRNAs, miRNAs and proteins but also allowed the identification of miRNA-regulated proteins differentially expressed between these two cell lines.

O'Sullivan F, Keenan J, Aherne S, O'Neill F, Clarke C, Henry M, Meleady P, Breen L, Barron N, Clynes M, Horgan K, Doolan P, Murphy R. Parallel mRNA, proteomics and miRNA expression analysis in cell line models of the intestine. *World J Gastroenterol* 2017; 23(41): 7369-7386 Available from: URL: http://www.wjgnet.com/1007-9327/full/v23/i41/7369.htm DOI: http://dx.doi.org/10.3748/wjg.v23.i41.7369

INTRODUCTION

In recent years both research and industry, particularly in the areas of pharmacology and nutrition, have steadily increased their use of *in vitro* cell models as an alternative to animal testing. This increase has been driven in part by the principles of the 3Rs (Replacement, Reduction and Refinement) and associated legislation, for example Article 4 of EU Directive 2010/63/EU. In addition there has been a growing use of automated high throughput techniques in the laboratory which has also increased the use of such *in vitro* cell lines. Thus there has been increased interest in the development of suitable intestinal *in vitro* models. These models are key to obtaining new information on intestinal toxicity, microbial infections, bioavailability of new food additives or new drugs as well as intestinal-related diseases[1-5].

The intestinal epithelium contains a number of specialised cell types; absorptive enterocytes (the principle intestinal cell type), goblet cells (mucin secreting), enteroendocrine cells, Paneth cells, tuft cells and M(or microfold) cells[6]. However the *in vitro* primary culture of intestinal epithelium is difficult, hence the use of intestinal cell lines allow for robust, reproducible *in vitro* culture models. Two cell lines, derived human from colonic adenocarcinomas, commonly used for the creation of such models are Caco-2 and HT-29.

The Caco-2 cell line can differentiate spontaneously to yield a polarised monolayer shown to express several characteristics and markers of enterocytes[7,8]. Thus Caco-2 cells have become a cell line of choice in the making of *in vitro* models of the intestine[9,10]. HT29 cell line is heterogeneous, consisting of a main population of undifferentiated cells and a smaller subpopulation capable of producing mucus[11-13]. Using glucose-free conditions, the HT-29 line can be differentiated to an

enterocyte phenotype. In addition various selection procedures have generated homogeneous mucin-secreting populations[11,13-15]. These two cell lines form the basis of numerous models of the intestine either as single cell models or advanced multicellular models[16-18]. However, the creation of suitable complex *in vitro* models requires that cell lines used are well characterised; this includes an understanding of the molecular controls within the cells.

There is an increasing recognition of the importance of the post-transcriptional control by miRNA of cell processes such as proliferation, differentiation, and apoptosis. The importance of miRNA in intestinal development and behaviour has been implicated in a number of studies[19,20]. In addition, the miRNAs miR-99b, miR-125a-5p and miR-1269 have been identified as having a potential role in determining Caco-2 and HT-29 behaviour[21].

miRNA exerts its control by either interfering with protein initiation and elongation or by the degradation of the target mRNA[22-25]. An additional complexity of this control mechanism is that a single mRNA can be co-operatively targeted by multiple miRNAs, while a single miRNA can target multiple mRNAs[26,27]. A number of algorithms exist to predict the potential targets of miRNAs for example miRanda, TargetScan and PicTar[28-30]. These algorithms generally function by their ability to recognise regions of sequence complementarity to miRNA seed regions (nucleotides 2-7 of the miRNA) in the 3'UTR of target mRNAs and the thermodynamic feasibility of such binding.

However, validation by experimental means is often required to determine the most significant miRNAs responsible for an observed effect within a biological system. This study uniquely uses a tri-omics approach combining the expression profiles of mRNA, miRNA and proteomics generated in parallel to identify potential miRNAs controlling translational repression and thus cell behaviour. As we have previously noted[31], the use of solitary profiling methodologies (including proteomic mass spectrometry, mRNA microarrays *etc.*) is prone to several distinct disadvantages when used in isolation. For example, gene expression analysis using microarrays is capable of identifying a wide coverage of mRNAs but post-transcriptional processes will not be captured using just this method. The availability of a combined profiling approach could also reduce the possibilities of false positive/negative rates associated with purely in-silico prediction analyses. Additionally, studies examining the role of miRNAs typically rely heavily on computational methods to predict miRNA interaction and prioritise potential direct targets.

This study uses the availability of data on multiple levels to identify potential interacting miRNA-protein networks that would not have been identified by a single dataset, allowing us to provide new information for the characterising of these two cell lines.

MATERIALS AND METHODS

Cell culture

The human colon carcinoma cell lines Caco-2 (cat. HTB37) was obtained from the American Type Culture Collection) and HT-29 (cat. 91072201) was obtained from Public Health England Culture collection. HT-29 and Caco-2 were maintained in MEM supplemented with 1% L-glutamine and 5% or 10% FBS respectively under normal conditions (37 ℃, 5% CO_2). Caco-2 cells were allowed to reach a maximum confluency of 60%-70% before trypsinizing to ensure that spontaneous differentiation was not occurring. Both cell lines were tested and found to be mycoplasma negative. All chemicals (unless otherwise stated), glutamine and cell culture media were obtained from Sigma (Poole, United Kingdom). FBS and HBSS were obtained from Invitrogen-ThermoFisher Scientific. Exponentially growing cells were set up in 25 cm^2 flasks (Corning) for RNA extraction or 75 cm^2 flasks (Corning) for protein extraction.

Affymetrix miRNA microarray analysis of miRNA expression

Total RNA was extracted from triplicate biological replicate samples using the Qiagen miRNeasy kit according to the manufacturer's instructions. RNA quantity was assessed using the NanoDrop ND-1000 spectrophotometer and RNA quality assayed using the Agilent RNA 6000 NANO KIT and Agilent Bioanalyzer (Agilent, Santa Clara, CA, United States). The FlashTag Biotin HSR RNA Labelling Kit (Affymetrix, Santa Clara, CA, United States) was used to label a total of 500 ng of total RNA according to manufacturer's procedure. The GeneChip Scanner 3000 7G System and reagents from Affymetrix were used to hybridize, wash, stain and scan the Genechip miRNA 3.0 arrays (Affymetrix, Santa Clara, CA, United States).

Microarray profiling and associated bioinformatics analysis

Gene expression analysis was carried out on the Affymetrix GeneChip Human Gene 1.0 ST array according to the manufacturer's instructions (Affymetrix, Santa Clara, CA, United States). The methodology and criteria used for total RNA purification, ssDNA sample processing and hybridisation to human microarrays have been previously described[32]. All microarray data were pre-processed as described previously. Prior to data analysis, probesets that did not reach the detection threshold (fluorescence level $\geqslant$ log2 (100) for at least 1 sample) were identified and designated undetected. The remaining probesets were considered

differentially expressed between the two cell types if a fold change ⩾ 1.2 in either direction along with a BH adjusted *P* value ⩽ 0.05 was observed

Proteomics profiling and associated bioinformatics analysis

Exponentially growing cells were harvested and pelleted by centrifugation. Cells were washed with ice cold PBS, cell pellets were then snap frozen and stored at -80 ℃ until required. Cell lysis was carried out using a buffer containing 7 mol/L Urea, 2 mol/L Thiourea, 4% CHAPS, 30 mmol/L Tris, pH 8.5, 1x HALT protease inhibitors (Thermo Fisher Scientific) and incubated on ice for 20 min with occasional vortexing. Sample lysates were centrifuged at 14000 × for 15 min at 4 ℃. The supernatant was transferred to a new microcentrifuge tube and protein concentration was determined using the Quick StartTM Bradford Protein Assay (BioRad).

Protein samples from the cell lysates were cleaned up using the ReadyPrep 2D Cleanup Kit (BioRad). Pellets were then resuspended in a buffer containing 6 M Urea, 2 mol/L Thiourea, 30 mmol/L Tris, pH 8.5. 20 μg from each sample was reduced with dithiothreitol to a final concentration of 5 mmol/L for 20 min at 56 ℃ followed by alkylation with iodoacetamide to a final concentration of 15 mmol/L, and incubated in the dark for 20 min at room temperature. Protein samples were tryptically digested (sequence grade, Promega) at a ratio of 50:1 protein/enzyme w/v at 37 ℃ overnight. Trifluoroacetic acid (TFA) was added to a final concentration of 0.5% to each sample to inactivate the trypsin. The digested peptide samples were then concentrated with C18 spin columns (Pierce, Thermo Fisher Scientific) and eluted peptides were gently dried with a vacuum evaporator (SpeedVac).

LC-MS/MS analysis

Dried peptides were re-solubilised in 25 μL of LC-MS grade water with 0.1% FA and 2% Acetonitrile (ACN). Peptides were separated and analysed using a Dionex Ultimate 3000 RSLCnano system (Thermo Fisher Scientific) coupled to a hybrid linear ion trap/Orbitrap mass spectrometer (LTQ Orbitrap XL; Thermo Fisher Scientific).

A 5 μL injection of sample was picked up using the autosampler and loaded onto a C18 trap column (C18 PepMap, 300 μm ID × 5 mm, 5 μm particle size, 100 Å pore size; Thermo Fisher Scientific). The sample was desalted for 3 minutes using a flow rate of 25 μL/min in 0.1% TFA containing 2% ACN. The trap column was then switched online with the analytical column [PepMap C18, 75 μm ID × 250 mm, 3 μm particle and 100 Å pore size; (Thermo Fisher Scientific)] using a column oven at 35°C and peptides were eluted with the following binary gradients of: Mobile Phase Buffer A and Mobile Phase Buffer B: 0%-25% solvent B in 240 min and 25%-50% solvent B in a further 60 min, where solvent A consisted of 2% acetonitrile (ACN) and 0.1% formic acid in water and solvent B consisted of 80% ACN and 0.08% formic acid in water. The column flow rate was set to 300 nL/min. Data was acquired with Xcalibur software, version 2.0.7 (Thermo Fisher Scientific).

The LTQ Orbitrap XL was operated in data-dependent and externally calibrated. Survey MS scans were acquired in the Orbitrap in the 400-1800 m/z range with the resolution set to a value of 30000 at m/z 400. Up to three of the most intense ions (1+, 2+ and 3+) per scan were CID fragmented in the linear ion trap. Dynamic exclusion was enabled with a repeat count of 1, repeat duration of 30 s, exclusion list size of 500 and exclusion duration of 40 s. The minimum signal was set to 500. All tandem mass spectra were collected using a normalised collision energy of 35%, an isolation window of 2 m/z with an activation time of 30 ms.

Quantitative label-free LC-MS/MS data analysis

The raw MS data files obtained were processed using Progenesis QI for Proteomics software (version 2.0; Non-Linear Dynamics, a Waters company, Newcastle upon Tyne, United Kingdom). Peptide LC retention times from all MS data files were aligned to an assigned reference run as previously described[31]. The samples from the two experimental groups were then set up within the Progenesis software for differential analysis. Peptide features were filtered using the following parameters; (1)peptide features with ANOVA ⩽ 0.05 between experimental groups; and (2)mass peaks with charge states from +1 to +3 and greater than one isotope per peptide. For the proteomic analysis a mascot generic file (mgf) was then generated from all exported MS/MS spectra which was used for peptide and protein identification *via* Proteome Discoverer 2.1 using Sequest HT (Thermo Fisher Scientific) and Percolator against the human Swissprot database containing 23053 sequences. The following search parameters were used for protein identification: (1)peptide mass tolerance set to 20 ppm; (2)MS/MS mass tolerance set to 0.6 Da; (3)up to two missed cleavages were allowed; (4)carbamidomethylation of cysteine set as a fixed modification; and (5)methionine oxidation was set as variable modifications. Only high confident peptide identifications with an FDR ⩽ 0.01 [identified using a SEQUEST HT workflow coupled with Percolator validation in Proteome Discoverer 2.1 (Thermo Fisher Scientific)] were imported into Progenesis QI software for further analysis. A statistical criteria of ANOVA *P* value less than 0.05, a minimum of two peptides matched to a protein and a ⩾ 1.2 fold change between the two cell lines (HT-29 and Caco-2) was used as the criteria for identification as a differentially expressed protein. Data visualisation was achieved using a heatmap which were generated using

ggplot package in R to show the distribution of all identified proteins based on statistics and fold-change across all of the samples used in the analysis.

Bioinformatics QC analysis, miRNA target prediction and GO analysis

Hierarchical cluster analysis (HCA) for all three parallel datasets (miRNA, proteomics, mRNA) was conducted in the R software environment (provided in the public domain by R Foundation for Statistical Computing, Vienna, Austria, available at http://www.r-project.org/) using the Euclidean distance measure and Ward's clustering algorithm. The prediction of miRNA and oppositely correlated protein/mRNA interactions was performed using TargetScan 6.1 (www.targetscan.org/vert_61/) and has been described previously[32]. miRNA Names (*e.g.,* hsa-miR-375) were annotated to miRNA Accession IDs (*e.g.,* MI0000783) using miRBase (http://www.mirbase.org/) for GO analysis. GO biological process, molecular function and cellular component enrichment analysis was carried out for the DE miRNA, protein and mRNA lists *via* the Pathway Studio 11.3 Web interface (https://www.elsevier.com/solutions/pathway-studio-biological-research) using their Mammalian database and has been described previously[33].

RESULTS

Data analysis methodology of combined omics/"Tri-omics" expression profiling approach

Figure 1 describes the data analysis strategy employed in this study. Differential expression (DE) profiling of HT-29 and Caco-2 cell line triplicate samples at the miRNA, protein and mRNA levels identified three separate datasets of 160 DE miRNAs, 168 DE proteins and 1795 DE mRNA transcripts (Stage 1: Supplementary Tables 1-3). Enrichment analysis against GO was conducted using the literature mining software Pathway Studio Web for the three resulting lists to determine if any biological processes were overrepresented (Stage 2: Supplementary Tables 4-6). The availability of all three data streams acquired in parallel was essential for the identification of our priority candidates - targets undergoing potential miRNA translational repression.

Prior to target prediction against the DE miRNA list, we separated miRNA, protein and mRNA targets into three groups of interest (Stage 3). "Group 1" contains those targets where a degree of post-transcriptional regulation was observed (possibly *via* miRNA mediated translational repression) which may contribute to phenotypic differences between these two cell lines and were considered the most interesting group studied. The 34 proteins in Group 1 were DE between HT-29 and Caco-2, their respective mRNAs were expressed above the microarray detection threshold but no change in mRNA expression was observed and were predicted to be targeted by 34 DE microRNAs whose expression was correlated in the opposite direction. This group comprised 27 proteins downregulated in the Caco-2 cell line relative to the HT-29 cell line and predicted to be targeted by 19 unique anti-correlated/upregulated microRNAs (Table 1) and 7 proteins upregulated in the Caco-2 cell line relative to the HT-29 cell line and predicted to be targeted by 15 unique anti-correlated/downregulated microRNAs (Table 2).

The second group of candidates (referred to as "Group 2") were comprised of DE protein targets where the matching mRNA transcript was DE in the matching direction. These "Group 2" candidates follow the classical mRNA-protein expression control model (*i.e.*, non-miR-based expression control) and are detailed in Supplementary Table 7.

The third group of candidates ("Group 3"; detailed in Supplementary Table 8) were comprised of DE protein targets where (1) the matching mRNA transcripts were not DE in the same direction or (2) where the mRNA probeset was under the detection threshold or (3) not present on the chip and finally (4) microRNAs predicted to target these proteins (using Targetscan) were not identified as DE between the two cell lines. The role of miRNA in control of expression of these "Group 3" candidates is therefore unclear and these proteins are considered lowest-priority of the three groups studied, for the purposes of the analysis presented here.

Combined omics/"Tri-omics" expression profiling identifies three interesting DE candidate groups that characterise the differences between HT-29 and Caco-2

Tri-omics expression profiling using the three methodologies outlined identified 160 DE miRNAs, 168 DE Proteins and 1795 DE Genes from a comparison of the HT-29 and Caco-2 cell lines.

Bioinformatics analysis of the microRNA profiling data (as outlined) on the HT-29 and Caco-2 cell lines identified 1550 probesets (772 upregulated, 778 downregulated) as differentially expressed (DE). These 1550 DE probesets were species-annotated to 221 human-specific probesets (140 upregulated, 71 downregulated) and further reduced to 160 DE mature non-star human miRNAs (104 upregulated, 56 downregulated (Supplementary Table 1). Bioinformatics analysis (as outlined) of the proteomics profiling data identified a total of 168 annotated DE proteins (57 upregulated, 111 downregulated) between the HT-29 and Caco-2 cell lines (Supplementary Table 2). Bioinformatics analysis (as outlined) of the microarray profiling data identified 1795 probesets (1084 upregulated, 711 downregulated) as differentially

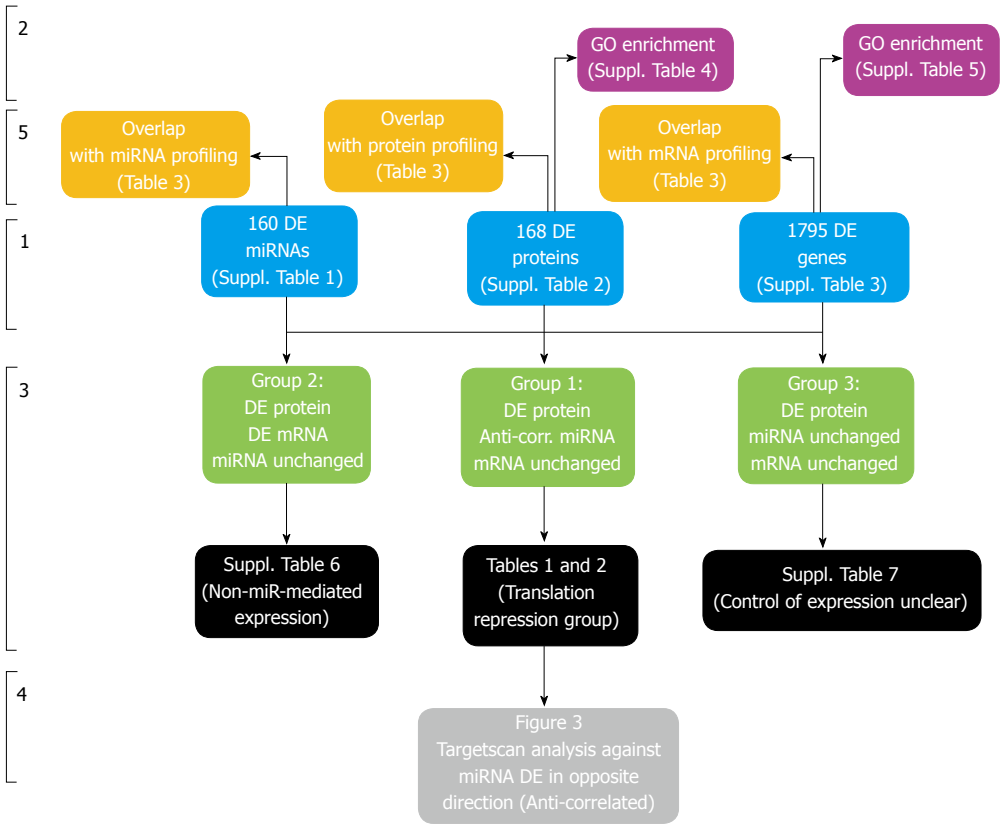

Figure 1 Overview of Tri-Omics data analysis approach. Stage 1: Differential expression analysis of "Tri-Omics" data (miRNA, protein, mRNA) between HT-29 and Caco-2 cell lines (for a full list of results, including fold-changes and associated *P* value statistics, see Supplementary Tables 1-3). Stage 2: Enrichment analysis using Pathway Studio to determine overrepresented GO biological processes in the DE miRNA, protein and mRNA lists (see Supplementary Tables 4-6). Stage 3: Integration of three parallel datasets to generate 3 groups of interesting candidates; (1) Potential targets of miRNA translational repression (protein DE without mRNA change and targeted by anti-correlated miRNA): see Table 1 (Downregulated Proteins targeted by Upregulated miRNAs) and Table 2 (Upregulated Proteins targeted by Downregulated miRNAs); (2) Non- microRNA-mediated gene-protein expression (matching mRNA transcripts and proteins were DE, no corresponding anti-correlated microRNA data or results were below detection level): see Supplementary Table 7 and (3) Targets where control of differential protein expression was unclear (protein DE without mRNA or corresponding targeting microRNA change). Stage 4: TargetScan analysis of both groups against miRNAs DE in the opposite direction. Stage 5: Overlap analysis of Supplementary Tables 1-3 with published profiling studies on same cell lines: see Table 3.

expressed (DE) between the HT-29 and Caco-2 cell lines (Supplementary Table 3).

Two-way hierarchical HCA clustering analysis as outlined on the HT-29 and Caco-2 cell line samples confirms that the DE (miRNA, proteomics, miRNA) candidates separate the samples into their respective replicate groups, indicating that they are of sufficient quality to yield high-priority candidates for phenotypic characterisation between both cell lines (Figure 2). For (A) miRNA and (C) mRNA, red indicates diminished expression and green indicates increased expression for all three replicate groups, while for (B) proteomics blue indicates diminished expression and red indicates increased expression for all three replicates in each group.

A TargetScan prediction analysis for (A) post-transcriptionally downregulated (green) proteins and anti-correlated/upregulated (red) miRNAs and (B) post-transcriptionally upregulated (red) proteins and anti-correlated/downregulated (green) miRNAs is shown in Figure 3. The prioritisation of these targets was possible only through integration of the miRNA, protein and mRNA datasets.

GO enrichment analysis identifies overrepresented GO categories related to cell differentiation, actin assembly and cytoskeleton organization shared between DE protein and gene lists

GO biological processes found to be overrepresented within the DE protein list included gene expression/transcription, epigenetic mechanisms, DNA replication, differentiation and translation (Supplementary Table 4).

A similar analysis of the DE mRNAs identified cell adhesion, migration and ECM organization, cellular lipid and cholesterol metabolic processes, small molecule transport and a range of responses to external stimuli to be the most significantly-enriched GO categories from this list (Supplementary Table 5).

Fifty shared biological processes were enriched by the DE protein and microarray datasets, including epithelial cell differentiation [*P* value $\leqslant$ 1.81613E-08 (protein list); *P* $\leqslant$ 0.000434311 (gene list), actin

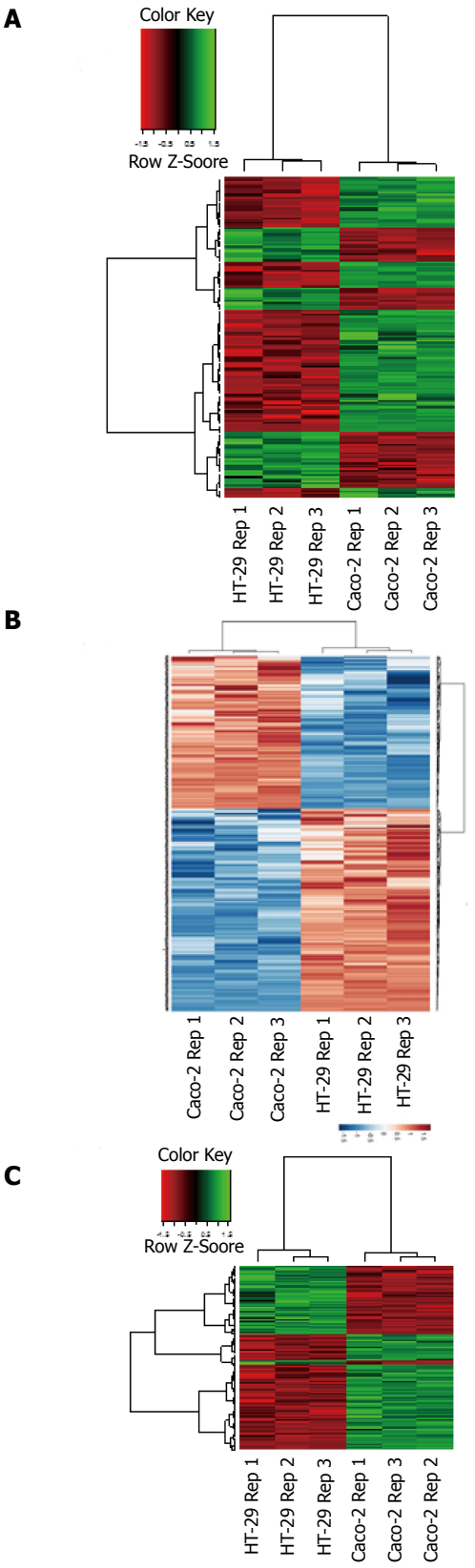

Figure 2 Bioinformatics QC analysis of HT-29 and Caco-2 replicates. 2-way hierarchical HCA clustering analysis on the HT-29 and Caco-2 cell line replicates using (A) DE miRNA probeset list (160 probesets) (B) DE proteomics list (168 proteins) and (C) DE mRNA probeset list (1795 probesets) confirms that the DE candidates separate the samples into their respective cell line replicate groups. For (A) and (C), red indicates diminished expression and green indicates increased expression for all three replicate groups; for (B) blue indicates diminished expression and red indicates increased expression for all three replicate groups.

filament bundle assembly [*P* value ⩽ 0.001582797 (protein list); *P* ⩽ 0.002733714 (gene list)], cell morphogenesis involved in differentiation [*P* value ⩽ 0.003493544 (protein list); *P* ⩽ 0.005671882 (gene list)] and cytoskeleton organization [*P* value ⩽ 0.004078084 (protein list); *P* ⩽ 0.005154161 (gene list)].

GO analysis using the 160 DE microRNA list of entities did not identify any enriched biological processes in the Pathway Studio Web database.

Integration of 3 parallel datasets identifies a priority group of 37 DE proteins and 44 associated miRs that may characterise phenotypic differences between HT-29 and Caco-2

The availability of all three level of expression data (miRNA, protein, mRNA) acquired in parallel on identical cell line samples was essential for the identification of our priority candidates for characterisation of the differences between the HT-29 and Caco-2 cell lines - protein targets that could undergo potential miRNA translational repression.

These potential targets of miRNA translational repression were identified as differentially-expressed (DE) proteins that could be targeted by a DE miRNA in the opposite direction (anti-correlated miRNA) and where the corresponding gene transcript was unchanged (protein DE without mRNA change and targeted by anti-correlated miRNA). From this 3-way overlap analysis, a total of 34 DE proteins and 34 DE microRNAs were identified to be of interest (Tables 1 and 2). Table 1 (Downregulated Proteins targeted by Upregulated miRNAs) displays the 27 proteins observed to be downregulated in the Caco-2 cell line relative to the HT-29 cell line and predicted to be targeted by 19 unique anti-correlated/upregulated microRNAs. Table 2 (Upregulated Proteins targeted by Downregulated miRNAs) contains the 7 proteins upregulated in the Caco-2 cell line relative to the HT-29 cell line and predicted to be targeted by 15 unique anti-correlated/downregulated microRNAs. Annotation information and associated statistical data for both DE proteins and microRNAs are included.

Integration of 3 parallel datasets identifies a group of 36 DE proteins and corresponding mRNA transcripts that may characterise phenotypic differences between HT-29 and Caco-2 that are not miR-mediated

The data-overlapping strategy similarly identified a group of 35 DE proteins (16 upregulated in Caco-2 relative to HT-29 and 19 downregulated in Caco-2 relative to HT-29) where the corresponding gene transcript was also DE in the direction and where the protein was not predicted to be targeted by any of the DE microRNAs (or where the DE miRNA data results were below detection levels). These proteins and genes (listed together with their attendant annotation information and associated statistical results in Supplementary Table 6) were considered to follow the standard molecular model for gene-protein expression,

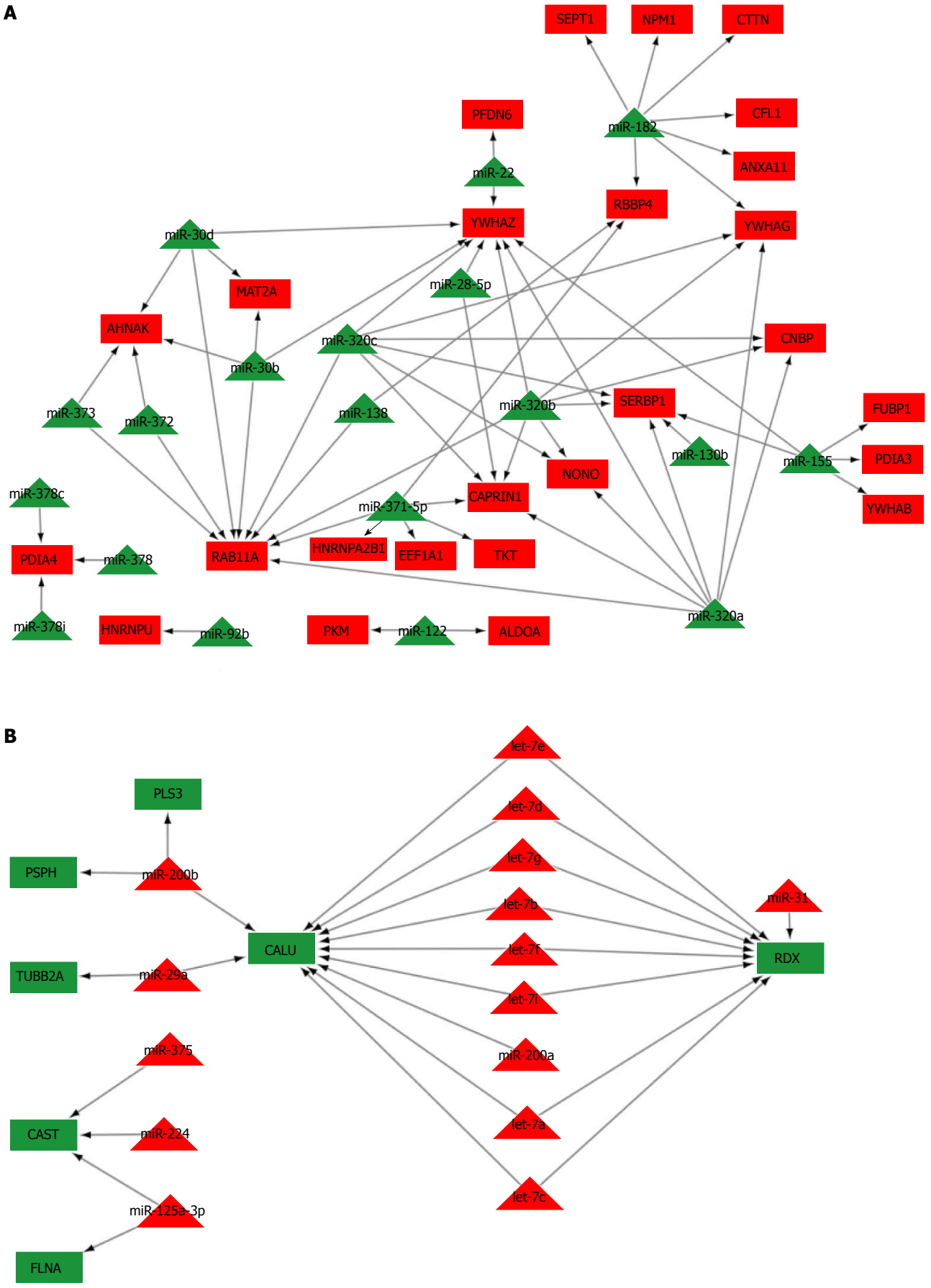

Figure 3 Summary of TargetScan predicted miRNA targets. A: TargetScan prediction analysis for post-transcriptionally downregulated (green) proteins and anti-correlated/upregulated (red) miRNAs; B: TargetScan prediction analysis for post-transcriptionally upregulated (red) proteins and anti-correlated/downregulated (green) miRNAs. The prioritisation of these targets was possible only through integration of the miRNA, protein and mRNA datasets.

Table 1 Twenty-seven downregulated proteins with no DE mRNA targeted by 19 upregulated miRNAs

Protein					microRNA					
Uniprot	Symbol	Title	Linear FC	Adj. *P* value	miRBase ID	logFC	LinFC	AveExpr	*P* value	Adj. *P* value
Q09666	AHNAK	Neuroblast differentiation-associated protein AHNAK	1.66	0.02036	hsa-miR-30b	1.39	2.62	10.38	5.04E-04	0.011296975
					hsa-miR-30d	1.36	2.56	11.05	1.17E-04	0.003668745
					hsa-miR-372	12.21	4743.91	7.03	6.55E-11	2.27E-07
					hsa-miR-373	12.12	4451.32	7.23	2.25E-11	1.88E-07
P04075	ALDOA	Fructose-bisphosphate aldolase A	2.03	0.00001	hsa-miR-122	5.85	57.63	5.04	3.71E-05	0.001621788
P50995	ANXA11	Annexin A11	4.57	0.00012	hsa-miR-182	1.09	2.13	12.01	2.48E-04	0.006341084
Q14444	CAPRIN1	Caprin-1	1.42	0.00658	hsa-miR-28-5p	1.16	2.24	9.32	7.05E-05	0.002531521
					hsa-miR-320a	1.46	2.76	12.49	2.74E-05	0.001333363
					hsa-miR-320b	1.46	2.76	12.49	4.80E-05	0.001959043
					hsa-miR-320c	1.46	2.74	12.35	5.43E-05	0.002111768
					hsa-miR-371-5p	11.89	3799.61	7.79	1.04E-10	2.62E-07
P23528	CFL1	Cofilin-1	1.53	0.00962	hsa-miR-182	1.09	2.13	12.01	2.48E-04	0.006341084
P62633	CNBP	Cellular nucleic acid-binding protein	1.79	0.00064	hsa-miR-320a	1.46	2.76	12.49	2.74E-05	0.001333363
					hsa-miR-320b	1.46	2.76	12.49	4.80E-05	0.001959043
					hsa-miR-320c	1.46	2.74	12.35	5.43E-05	0.002111768
Q14247	CTTN	Src substrate cortactin	1.33	0.00716	hsa-miR-182	1.09	2.13	12.01	2.48E-04	0.006341084
P68104	EEF1A1	Elongation factor 1-alpha 1	1.46	0.01148	hsa-miR-371-5p	11.89	3799.61	7.79	1.04E-10	2.62E-07
P06733	ENO1	Alpha-enolase	2.06	0.00015	hsa-miR-22	1.96	3.9	10.84	1.01E-04	0.003309338
Q96AE4	FUBP1	Far upstream element-binding protein 1	2.17	0.00290	hsa-miR-155	1.85	3.61	9.51	5.54E-05	0.002127503
P22626	HNRNPA2B1	Heterogeneous nuclear ribonucleoproteins A2/B1	1.72	0.00053	hsa-miR-371-5p	11.89	3799.61	7.79	1.04E-10	2.62E-07
Q00839	HNRNPU	Heterogeneous nuclear ribonucleoprotein U	4.51	0.00152	hsa-miR-92b	1.22	2.33	6.95	4.51E-04	0.010275397
					hsa-miR-122	5.85	57.63	5.04	3.71E-05	0.001621788
P31153	MAT2A	S-adenosylmethionine synthase isoform type-2	1.92	0.00023	hsa-miR-30b	1.39	2.62	10.38	5.04E-04	0.011296975
					hsa-miR-30d	1.36	2.56	11.05	1.17E-04	0.003668745
Q15233	NONO	Non-POU domain-containing octamer-binding protein	2.74	0.00522	hsa-miR-320a	1.46	2.76	12.49	2.74E-05	0.001333363
					hsa-miR-320b	1.46	2.76	12.49	4.80E-05	0.001959043
					hsa-miR-320c	1.46	2.74	12.35	5.43E-05	0.002111768
P06748	NPM1	Nucleophosmin	1.51	0.01869	hsa-miR-182	1.09	2.13	12.01	2.48E-04	0.006341084
P30101	PDIA3	Protein disulfide-isomerase A3	1.84	0.00465	hsa-miR-155	1.85	3.61	9.51	5.54E-05	0.002127503
P13667	PDIA4	Protein disulfide-isomerase A4	1.74	0.00006	hsa-miR-378	1.35	2.55	11.31	7.79E-05	0.002720502
					hsa-miR-378c	1.17	2.25	10.21	5.74E-04	0.012576882
					hsa-miR-378i	0.85	1.80	9.00	7.98E-04	0.01627753
O15212	PFDN6	Prefoldin subunit 6	2.26	0.02810	hsa-miR-22	1.96	3.90	10.84	1.01E-04	0.003309338
P14618	PKM	Pyruvate kinase PKM	1.91	0.00020	hsa-miR-122	5.85	57.63	5.04	3.71E-05	0.001621788
P62491	RAB11A	Ras-related protein Rab-11A	1.74	0.00318	hsa-miR-138	5.84	57.23	4.36	6.08E-08	2.62E-05
					hsa-miR-30b	1.39	2.62	10.38	5.04E-04	0.011296975
					hsa-miR-30d	1.36	2.56	11.05	1.17E-04	0.003668745
					hsa-miR-320a	1.46	2.76	12.49	2.74E-05	0.001333363
					hsa-miR-320b	1.46	2.76	12.49	4.80E-05	0.001959043
					hsa-miR-320c	1.46	2.74	12.35	5.43E-05	0.002111768
					hsa-miR-371-5p	11.89	3799.61	7.79	1.04E-10	2.62E-07
					hsa-miR-372	12.21	4743.91	7.03	6.55E-11	2.27E-07
					hsa-miR-373	12.12	4451.32	7.23	2.25E-11	1.88E-07
Q09028	RBBP4	Histone-binding protein RBBP4	1.76	0.00339	hsa-miR-138	5.84	57.23	4.36	6.08E-08	2.62E-05
					hsa-miR-138	5.84	57.23	4.36	6.08E-08	2.62E-05
					hsa-miR-182	1.09	2.13	12.01	2.48E-04	0.006341084
					hsa-miR-371-5p	11.89	3799.61	7.79	1.04E-10	2.62E-07
Q9UHD8	9-Sep	Septin-9	1.98	0.00016	hsa-miR-182	1.09	2.13	12.01	2.48E-04	0.006341084
Q8NC51	SERBP1	Plasminogen activator inhibitor 1 RNA-binding protein	2.35	0.00473	hsa-miR-130b	1.77	3.42	11.03	2.57E-05	0.00127274
					hsa-miR-155	1.85	3.61	9.51	5.54E-05	0.002127503
					hsa-miR-320a	1.46	2.76	12.49	2.74E-05	0.001333363
					hsa-miR-320b	1.46	2.76	12.49	4.80E-05	0.001959043
					hsa-miR-320c	1.46	2.74	12.35	5.43E-05	0.002111768
P29401	TKT	Transketolase	1.56	0.00000	hsa-miR-371-5p	11.89	3799.61	7.79	1.04E-10	2.62E-07
P31946	YWHAB	14-3-3 protein beta/alpha	1.35	0.01490	hsa-miR-155	1.85	3.61	9.51	5.54E-05	0.002127503
P61981	YWHAG	14-3-3 protein gamma	2.05	0.00007	hsa-miR-182	1.09	2.13	12.01	2.48E-04	0.006341084
					hsa-miR-320a	1.46	2.76	12.49	2.74E-05	0.001333363
					hsa-miR-320b	1.46	2.76	12.49	4.80E-05	0.001959043
					hsa-miR-320c	1.46	2.74	12.35	5.43E-05	0.002111768

P63104	YWHAZ	14-3-3 protein zeta/delta	2.52	0.00005	hsa-miR-155	1.85	3.61	9.51	5.54E-05	0.002127503
					hsa-miR-22	1.96	3.90	10.84	1.01E-04	0.003309338
					hsa-miR-28-5p	1.16	2.24	9.32	7.05E-05	0.002531521
					hsa-miR-30b	1.39	2.62	10.38	5.04E-04	0.011296975
					hsa-miR-30d	1.36	2.56	11.05	1.17E-04	0.003668745
					hsa-miR-320a	1.46	2.76	12.49	2.74E-05	0.001333363
					hsa-miR-320b	1.46	2.76	12.49	4.80E-05	0.001959043
					hsa-miR-320c	1.46	2.74	12.35	5.43E-05	0.002111768

Twenty-seven proteins found downregulated in the Caco-2 cell line relative to the HT-29 cell line and predicted to be targeted by 19 unique anti-correlated/upregulated microRNAs.

without being miRNA-mediated (matching mRNA transcripts & proteins were DE (36), no corresponding anti-correlated miRNA data).

Integration of 3 parallel datasets identifies a group of 132 DE proteins where the control of differential protein expression was unclear

Finally, the data-overlapping strategy identified a list of 132 DE proteins (40 upregulated in Caco-2 relative to HT-29 and 92 downregulated in Caco-2 relative to HT-29) where the corresponding gene transcript was (1) not changing or probeset expression levels were below the detection threshold and (2) were not predicted to be targeted by any of the DE microRNAs, or where the DE miRNA data results were below detection levels. As a result, the control of expression of these proteins (listed together with their attendant annotation information and associated statistical results in Supplementary Table 7) is currently unclear (protein DE without mRNA or corresponding targeting miRNA change).

DISCUSSION

Data analysis methodology identifies unique targets involved in actin organisation

The utilisation of three expression profiling technologies (miRNA, proteomics, mRNA) in parallel as part of an integrative methodology on replicate HT-29 and Caco-2 cell lines provides a unique opportunity for characterising these two cell lines, complementing and adding to the previous literature. A total of 37 differentially-expressed proteins and targeting miRNAs were identified as a result of this unique approach, which has (to our knowledge) never before been employed on analysing these two key intestinal cell line models and which will assist in characterising miRNA/protein regulatory networks that may contribute to their respective phenotypic differences.

The key aspect of the experimental design is the combination of data from multiple expression profiling methods and in-silico prediction to study potential miRNA-protein networks that may give rise to differences between the two cell lines. We have previously shown that the use of such a combined data can address some of the disadvantages of solitary profiling methodologies, while also allowing us to identify potential interacting miRNA-protein networks that would not have been identified by a single dataset[31]. As a result, we have prioritised our discussion of these potential interacting networks (whose identification is possible only *via* the integration of the "tri-omics" (miRNA, protein, mRNA) datasets) which may undergo classical miRNA-mediated translation repression when comparing mucin-producing HT-29 cell phenotype to the more absorptive Caco-2 cell phenotype.

When differing gene- and protein-expression profiles between the cell lines were compared, the key areas of common ontological enrichment between the larger, non-overlapped DE gene and protein lists were in cytoskeleton organization and actin filament bundle assembly, possibly pointing to differences in the shape, support and movement of the cells. We have focused our discussion on a selection of these DE protein and miRNA targets that have demonstrated potential roles in cytoskeleton organization and biogenesis.

Cofilin1 (CFL1), which was downregulated at the protein level in the Caco-2 cell line relative to HT-29 and is targeted by the upregulated miR-182 (Table 1), is part of the ADF/cofilin family of actin-binding proteins which disassemble actin filaments. The role of CFL1 in positively regulating actin filament depolymerisation and severing as well as in cytoskeleton organization, function & biogenesis has been extensively reviewed[34-36]. It has been previously reported that CFL1 levels increase transiently in Caco-2 cells during early differentiation and that this may be linked to the changes required in the actin cytoskeleton[37]. Additionally, several groups have reported that CFL1 has been shown to positively regulate lamellipodium formation and cytoskeletal protein actin projections on the leading edge of highly mobile cells[38-44], although a recent study[45], indicated that it may both inhibit and promote lamellipodium formation. Loss of Cofilin1 has also been shown to hinder apical constriction in mouse endothelial cells[46].

Also targeted by the upregulated miR-182 was the downregulated (in Caco-2 relative to HT-29) protein Cortactin (CTTN)(Table 1), which is a monomeric protein located in the cytoplasm of cells that can be activated by external stimuli to promote actin filament branching and rearrangement of the actin cytoskeleton[47,48] and lamellipodium formation[49,50].

Proteins that were upregulated (in the Caco-2

Table 2 Seven upregulated proteins with no DE mRNA targeted by 15 downregulated miRNAs

Protein					microRNA					
Uniprot	Symbol	Title	Linear FC	Adj. *P* value	miRBase ID	logFC	LinFC	AveExpr	*P* Value	Adj. *P* value
O43852	CALU	Calumenin	1.86	0.0162	hsa-let-7a	-1.44	-2.72	12.58	1.30E-04	0.00396
					hsa-let-7b	-2.61	-6.11	12.84	1.71E-06	0.00017
					hsa-let-7c	-3.45	-10.94	11.26	2.39E-06	0.00021
					hsa-let-7d	-2.66	-6.34	12.12	2.20E-06	0.00020
					hsa-let-7e	-1.40	-2.65	12.39	6.41E-05	0.00236
					hsa-let-7f	-2.85	-7.20	8.75	5.04E-06	0.00034
					hsa-let-7g	-1.06	-2.08	8.90	2.99E-04	0.00737
					hsa-let-7i	-2.31	-4.95	10.22	2.35E-06	0.00021
					hsa-miR-29a	-1.63	-3.09	9.69	1.14E-04	0.00361
					hsa-miR-200a	-2.68	-6.43	9.16	4.14E-04	0.00965
					hsa-miR-200b	-2.54	-5.81	10.40	2.63E-05	0.00129
P20810	CAST	Calpastatin	2.39	0.00011	hsa-miR-125a-3p	-3.14	-8.83	5.84	3.26E-05	0.00150
					hsa-miR-224	-2.44	-5.42	7.35	8.21E-04	0.01667
					hsa-miR-375	-4.06	-16.67	8.29	1.50E-05	0.00083
P21333	FLNA	Filamin-A	3.59	0.00048	hsa-miR-125a-3p	-3.14	-8.83	5.84	3.26E-05	0.00150
P13797	PLS3	Plastin-3	5.88	0.00006	hsa-miR-200b	-2.54	-5.81	10.40	2.63E-05	0.00129
P78330	PSPH	Phosphoserine phosphatase	2.22	0.0004	hsa-miR-200b	-2.54	-5.81	10.40	2.63E-05	0.00129
P35241	RDX	Radixin	5.57	0.00012	hsa-let-7a	-1.44	-2.72	12.58	1.30E-04	0.00396
					hsa-let-7b	-2.61	-6.11	12.84	1.71E-06	0.00017
					hsa-let-7c	-3.45	-10.94	11.26	2.39E-06	0.00021
					hsa-let-7d	-2.66	-6.34	12.12	2.20E-06	0.00020
					hsa-let-7e	-1.40	-2.65	12.39	6.41E-05	0.00236
					hsa-let-7f	-2.85	-7.20	8.75	5.04E-06	0.00034
					hsa-let-7g	-1.06	-2.08	8.90	2.99E-04	0.00737
					hsa-let-7i	-2.31	-4.95	10.22	2.35E-06	0.00021
					hsa-miR-31	-1.94	-3.83	12.79	7.91E-05	0.00274
Q13885	TUBB2A	Tubulin beta-2A chain	1.46	0.00388	hsa-miR-29a	-1.63	-3.09	9.69	1.14E-04	0.00361

Seven proteins found upregulated in the Caco-2 cell line relative to the HT-29 cell line and predicted to be targeted by 15 unique anti-correlated/downregulated microRNAs.

cell line relative to HT-29) included the actin binding protein Radixin (upregulated 5.57 fold) which was targeted by several DE members of the let-7 miRNA family, as well as miR-31 (Table 2). Radixin is one of three members of the ERM family of proteins, which have a number of roles in the stabilisation and regulation of the membrane cytoskeleton interface[51]. Radixin has been found to be important in the linking of ABCC2 (MRP2) and P-glycoprotein to the actin cytoskeleton in Caco-2 and murine small intestinal cells respectively[52,53].

In addition to roles involving the actin cytoskeleton, the group of 37 proteins also includes those with metabolic functions, such as α-Enolase (Eno1) which catalyses 2-phosphoglycerate to phosphoenolpyruvate in glycolysis, is expressed at a 2.06 fold lower level in Caco-2 cells relative to HT-29 cells and is potentially targeted by miR-22 (Table 1). Down regulation of α-enolase has previously been reported as increasing and then decreasing in early differentiating Caco-2 cells and decreased in formula fed preterm pigs developing necrotizing enterocolitis[37,54]. NONO (2.74 fold lower in Caco-2 v's HT-29, Table 1) is involved in regulating androgen receptor and carbonic anhydrase activity[55,56].

Identification of differentially expressed miRNA

The profiling of miRNA expression in Caco-2 compared to HT-29 found 160 miRNAs differentially expressed, a number of which (for example miR-152, miR-99b, miR-125a-5p, miR-10a, miR-196b, miR-222) have been previously identified with intestinal differentiation, function and immune response in a number of species[19-21,57-59]. While in the top 10 upregulated miRNAs in Caco-2 compared to HT-29, an association with cell viability and proliferation has been reported previously for example miR-372 (4743.91 fold up), miR-373 (4451.32 fold up)and miR-122 (57.63 fold up)[60-62]. Similarly among the top 10 downregulated miRNAs in Caco-2 compared to HT-29, there is again an association with cell viability and proliferation for example miR-10a (46.76 fold down), miR-935 (13.38 fold down)[63,64].

Identification of differentially expressed mRNA

A total of 1795 differentially expressed mRNA transcripts were identified DE between HT-29 and Caco-2 cells, comprising of 1084 upregulated and 711 downregulated transcripts (Supplementary Table 3).

GO analysis found that biological processes linked to lipid metabolism, extracellular matrix organisation,

cell adhesion and cytoskeleton were over represented. This enrichment for processes linked to cytoskeleton can be seen in a number of targets both down and up regulated.

For example, Moesin, is one of the largest down regulated transcripts (173 fold) in Caco-2 compared to HT-29 (Supplementary Table 3). Which in addition to being down regulated at transcript level, was also downregulated at a protein level (6.48 fold) in Caco-2 compared to HT-29 (Supplementary Table 2). Moesin is a member of the ERM family of proteins and is involved in regulating actin filament depolymerisation along with apical junction assembly and focal adhesion assembly[51]. Moesin often shows different cellular distribution and expression from the other two ERM proteins, radxin and ezrin[65]. It has been previously reported that it is not expressed Caco-2 or in normal colorectal mucosa epithelial cells[52,66].

Similarly, Galectin 4 (LGALS4), whose transcript was down regulated in Caco-2 compared to HT-29 (109 fold, Supplementary Table 3), has as one of its principal functions the improved stabilisation of the apical membrane rafts and the trafficking of apical cell membrane[67,68]. Variable staining for Galectin 4 has been reported in gut villi, with the upper 1/4 of the villus showing negative staining[69]. Galectin 4 is expressed after confluence in Caco-2 cells along with the formation of brush boarder[68]. Galectin 4 linked to the segregation of glycolproteins for apical secretion in HT-29 cells[68].

The Ca^{2+} binding protein Calbindin 2 (CALB2), also known as Calretinin was down regulated 102 fold in Caco-2 compared to HT-29 cells (Supplementary Table 3). The exact role of calretinin in intestinal epithelia is unknown but it is believed to have roles in the stabilisation of cytokeratins and microtubules, differentiation status and butyrate response[70-72]. The expression profile obtained is in agreement with previous studies which report expression in undifferentiated colon adenocarcinoma cell lines (*e.g.,* HT-29) and no expression in for normal differentiated colon epithelial cells and more differentiated cell lines (*e.g.,* Caco-2) studies[71].

In case of transcripts that were up regulated in Caco-2 relative to HT-29, again a number of targets were linked to cytoskeleton function, for example Fibronectin1 (FN1), whose, mRNA was upregulated 441 fold in the Caco-2 cell line relative to HT-29 (Supplementary Table 3). In addition to having an elevated transcript, fibronectin protein was upregulated 5.15 fold up at a protein in Caco-2 relative to HT-29. Fibronectin is a glycoprotein of the extracellular matrix that binds to membrane-spanning receptor integrins and plays a major role in cell adhesion and actin cytoskeleton organisation[73]. Previously the differentiation of Caco-2 cells has been associated with a down regulation of fibronectin[74,75], but our studies were on proliferating cells.

Another transcript with associated cytoskeleton function that was upregulated was BicC 1 (up regulated 206.75 fold in the Caco-2 cell line relative to HT-29, Supplementary Table 3). BicC1 is believed to bind and regulate mRNA translation *via* a number of mechanisms such as clustering of target mRNAs or as a chaperone which recruits specific miRNA precursors and Dicer to target mRNAs and subsequently transfers these to AGO for silencing[76,77]. Its expression has been linked positively to the formation of E-cadherin adherens junctions and cortical actin distribution[78].

Also upregulated (192.74 fold) at a transcript level was LRP2 also know Megalin, a member of the low density lipoprotein family (Supplementary Table 3). LRP2/Megalin has been found expressed on the apical surface of a number of epithelial cells, including the brush border membrane of Caco-2 cells and to have upregulated expression in the ileum of sucking rats[79-81].

Identification of differentially expressed protein

A total of 168 differentially expressed proteins were in expressed between Caco-2 and HT-29 (57 were upregulated in Caco-2 and 111 were upregulated in HT-29). Using Pathway Studio to generate GO biological processes for the DE proteins (Supplemental Table 1), it was found that there was an over representation of processes linked to Translation, Carbohydrate metabolism and Actin cytoskeleton organisation. For example Insulin-like growth factor 2 mRNA binding protein (IGF2BP1, IMP1) was upregulated 51.58 fold in Caco-2 relative to HT-29. The expression of IGF2BP1 has previously been linked to morphogenesis of the small intestine[82]

Interestingly, the expression of Insulin-like growth factor 2 mRNA binding protein has been linked to SERPINH1 a 47 KDa stress protein, also called Heat Shock Protein 47 (HSP47). HSP47 is upregulated 9.11 fold in this study in Caco-2 relative to HT-29 (Supplementary Table 2). HSP47 is localised to the endoplasmic reticulum where it is a principle chaperone in the collagen biosynthesis pathway. In addition to HSP47's role as a collagen chaperone it has been suggested that it plays an important role in reorganising of the actin cytoskeleton in Caco-2, increasing permeability[83].

The protein showing the biggest down regulation (down regulated 91.89 fold) in Caco-2 relative to HT-29 was the secreted glycoprotein Galectin-3-binding protein (also known as Mac2-binding protein) (Supplementary Table 2). Galectin-3-Binding protein has been linked to the innate immune response[84,85].

While the second most down regulated protein in Caco-2 relative to HT-29 was Annexin A13 (down regulated in 42.38 fold, Supplementary Table 2).

Annexin A13 is found expressed in the small intestine, involved in the localisation of protein to the apical membrane of cells[86,87].

Overlap comparison of individual datasets with already-published studies identifies several common DE gene, protein and miRNA candidates

In order to determine the comparability of our analysis of these cell line models to other published studies on those same cell lines, we overlapped our three individual DE datasets (gene, protein and miRNA) with a selection of two studies that each combined both cell lines (HT-29 and Caco-2) in the one analysis.

For the miRNA lists, we utilised two studies examining the role of miRNAs in colorectal cancer metastasis in the HT-29 and Caco-2 cell lines; Ma *et al*[88] (2011) which reported a DE list of just 8 microRNAs and Zhang *et al*[57] (2012) who disclosed a DE list of 16 microRNAs. Despite the shortness of these previously published lists, we identified the hsa-miR-196a microRNA as commonly DE in both our study and that of Ma *et al*[88] (2011). Additionally, overlapping our 160 microRNAs with the 16 microRNAs identified by Zhang *et al*[57]. (2012) identified a further 3 microRNAs (hsa-let-7a, hsa-miR-10a and hsa-miR-98) which were commonly DE between HT-29 and Caco-2 in both studies (see Table 3)[88].

At the protein level, we incorporated two proteomics profiling studies combining HT-29 and Caco-2; one utilising two-dimensional gel electrophoresis and a newer study incorporating LC-MS/MS[89,90]. Overlap analysis of our DE gene dataset with these two studies identified only one protein, LGALS3 (Galectin-3) as DE between all three studies (Table 3). Individual overlaps with each of the two studies separately identified an additional four proteins [ANXA3 (Annexin A3); NCL (Nucleolin); NPM1 (Nucleophosmin) and SORD (Sorbitol dehydrogenase)] commonly DE between our study and that of Uzozie *et al*[90]., 2014, with a further 12 proteins (ATP5B (ATP synthase subunit beta, mitochondrial); CALR (Calreticulin); CFL1 (Cofilin-1); CTSB (Cathepsin B); ENO1 (Alpha-enolase); HNRNPA2B1 (Heterogeneous nuclear ribonucleoproteins A2/B1); HNRNPL (Heterogeneous nuclear ribonucleoprotein L); HNRNPK (Heterogeneous nuclear ribonucleoprotein K); KRT8 (Keratin, type II cytoskeletal 8); P4HB (Protein disulfide-isomerase); PDIA3 (Protein disulfide-isomerase A3) and PGAM1 (Phosphoglycerate mutase 1) commonly DE between Lenaerts *et al*[89] (2007) and our study (Table 3)[90].

To overlap our DE genes, we utilised a study examining the expression of 377 xenobiotics metabolism genes (incl. xenobiotic-metabolizing enzymes, transporters, and nuclear receptors and transcription factors)[91], as well as a newer study examining Copper homeostasis and distribution, which utilised the same microarray chip that was used in this study[92] but only disclosed data on 33 DE genes. Overlap analysis of our DE gene dataset with these two studies identified only one gene, the ATF7B (ATPase, Cu^{2+} transporting, beta polypeptide) transporter as DE between all three studies (Table 3). Overlapping our dataset with only that of Bourgine *et al*[91]. (2012) identified an additional 25 genes (*ABCA3, ABCB1, AKR1E2, ALDH5A1, ALDH6A1, CDCA2, CYP20A1, CYP27A1, EPHX2, GSTA4, NCOA1, NR5A2, RBP2, SLC15A1, SLC19A3, SLC1A3, SLC22A5, SLC6A4, SLC7A6, SLC7A8, SLCO2B1, SLCO4C1, SULT1C4, THRB* and *VDAC3*) commonly DE between both cell lines[91] . The greater degree of overlap identified was most likely due to the roughly 10-fold greater number of DE genes disclosed (377) by Bourgine *et al*[91] (2012), compared to the 33 genes disclosed by Barresi *et al*[92] (2016).

DE proteins targeted by microRNAs in other studies

In this study, we propose that several of the proteins described here as DE between the HT-29 and Caco-2 cell lines may be targeted by anti-correlated microRNAs (also DE here between these cell lines) and several of these protein-miRNA regulatory interactions have been demonstrated in other cell systems. For example, microRNA-148a has been shown to inhibit the proliferation and promote the paclitaxel-induced apoptosis of ovarian cancer cells by targeting PDIA3[93]. Additionally, YWHAZ (14-3-3 zeta) was confirmed to be a target of miR-302d by proteomic comparison of Human embryonic stem (ES) cells and their differentiated T3DF fibroblasts[94], while LASP1 has been shown to be directly regulated by miR-145 in bladder cancer cell lines[95-97].

In conclusion the intestinal cell lines Caco-2 and HT-29 are commonly used for the creation of *in vitro* models for the intestine. However, the use of such cell lines to model the intestine requires that they are fully characterised which will require a better understanding on the molecular controls that these cells exhibit. One such molecular control is the miRNA control mechanism of translation. This study, by performing a tri-omics analysis (genes, proteomics, miRNAs) on parallel data sets generated from these two cell lines, potential miRNA-protein networks were identified that would not have been immediately apparent otherwise. An advantage of such an approach was that the potential biological noise of the study was reduced by running identical samples in parallel to generate each of the profiles. This has the effect of reducing the potential false negative false positive rates of the *in silico* prediction and allows for high priority list of candidates for functional validation. It is interesting to note that a large number of targets were associated with the actin cytoskeleton and its associated cell processes such as motility, polarisation, endocytosis and cell division. Most of the identified proteins in table Ⅰ and table Ⅱ have important roles in the establishment of apical-basal membrane polarity and the formation of the apical microvilli brush border

Table 3 Overlap of DE genes, proteins, microRNAs with other HT-29/Caco-2 profiling studies

Identifier	Symbol	Description/Family	LinFC	*P* value	Overlapping study	Dataset
hsa-miR-196a_st	hsa-miR-196a	miR-196abc	-5.06	8.53E-05	88	microRNA
hsa-let-7a_st	hsa-let-7a	let-7/98/4458/4500	-2.72	6.34E-04	57	
hsa-miR-10a_st	hsa-miR-10a	miR-10abc/10a-5p	-46.76	7.40E-06	57	
hsa-miR-98_st	hsa-miR-98_st	miR-98	-11.90	4.50E-06	57	
P17931	LGALS3	Galectin-3	2.09	1.10E-03	89; 90	Protein
P06576	ATP5B	ATP synthase subunit beta, mitochondrial	2.07	1.20E-03	89	
P27797	CALR	Calreticulin	1.62	3.35E-02	89	
P23528	CFL1	Cofilin-1	1.53	5.94E-03	89	
P07858	CTSB	Cathepsin B	5.15	5.36E-05	89	
P06733	ENO1	Alpha-enolase	2.06	4.65E-03	89	
P22626	HNRNPA2B1	Heterogeneous nuclear ribonucleoproteins A2/B1	1.72	9.62E-03	89	
P61978	HNRNPK	Heterogeneous nuclear ribonucleoprotein K	1.38	4.38E-04	89	
P14866	HNRNPL	Heterogeneous nuclear ribonucleoprotein L	1.69	4.02E-03	89	
P05787	KRT8	Keratin, type Ⅱ cytoskeletal 8	2.21	1.81E-03	89	
P07237	P4HB	Protein disulfide-isomerase	1.41	3.49E-03	89	
P30101	PDIA3	Protein disulfide-isomerase A3	1.84	7.49E-05	89	
P18669	PGAM1	Phosphoglycerate mutase 1	1.93	1.42E-04	89	
P12429	ANXA3	Annexin A3	2.53	1.55E-06	90	
P19338	NCL	Nucleolin	2.74	4.80E-03	90	
P06748	NPM1	Nucleophosmin	1.51	1.15E-02	90	
Q00796	SORD	Sorbitol dehydrogenase	4.21	7.73E-05	90	
16779311	ATP7B	ATPase, Cu++ transporting, beta polypeptide	3.60	1.57E-05	91; 92	Gene
16823109	ABCA3	ATP-binding cassette, sub-family A (ABC1), member 3	10.07	1.75E-05	91	
17059491	ABCB1	ATP-binding cassette, sub-family B (MDR/TAP), member 1	36.64	2.14E-06		
16701957	AKR1E2	aldo-keto reductase family 1, member E2	4.56	1.09E-05		
17005368	ALDH5A1	aldehyde dehydrogenase 5 family, member A1	3.38	4.08E-06		
16794632	ALDH6A1	aldehyde dehydrogenase 6 family, member A1	2.27	7.54E-05		
17067102	CDCA2	carboxylesterase 1	2.32	2.28E-03		
16889762	CYP20A1	cytochrome P450, family 20, subfamily A, polypeptide 1	2.78	8.71E-04		
16891082	CYP27A1	cytochrome P450, family 27, subfamily A, polypeptide 1	20.68	2.05E-06		
17067284	EPHX2	epoxide hydrolase 2, cytoplasmic	6.51	3.62E-06		
17020103	GSTA4	glutathione S-transferase alpha 4	2.25	4.04E-04		
16877728	NCOA1	nuclear receptor coactivator 1	2.99	7.90E-04		
16675638	NR5A2	nuclear receptor subfamily 5, group A, member 2	2.33	1.73E-03		
16959797	RBP2	retinol binding protein 2, cellular	27.20	2.06E-06		
16780481	SLC15A1	solute carrier family 15 (oligopeptide transporter), member 1	20.05	1.95E-06		
16909257	SLC19A3	solute carrier family 19 (thiamine transporter), member 3	35.13	6.97E-08		
16984056	SLC1A3	solute carrier family 1 (glial high affinity glutamate transporter), member 3	50.97	1.62E-07		
16989018	SLC22A5	solute carrier family 22 (organic cation/carnitine transporter), member 5	2.21	5.49E-04		
16843078	SLC6A4	solute carrier family 6 (neurotransmitter transporter), member 4	9.33	1.33E-06		
16820398	SLC7A6	solute carrier family 7 (amino acid transporter light chain, y+L system), member 6	4.71	5.00E-06		
16790744	SLC7A8	solute carrier family 7 (amino acid transporter light chain, L system), member 8	11.99	4.99E-06		
16729064	SLCO2B1	solute carrier organic anion transporter family, member 2B1	10.15	8.38E-06		
16998551	SLCO4C1	solute carrier organic anion transporter family, member 4C1	11.95	2.59E-03		
16884050	SULT1C4	sulfotransferase family, cytosolic, 1C, member 4	15.89	2.49E-07		
16951567	THRB	thyroid hormone receptor, beta	4.38	1.90E-04		
17068541	VDAC3	voltage-dependent anion channel 3	2.28	3.11E-04		

List of 49 gene, protein and miRNA annotated candidates (6 microRNAs, 17 proteins, 26 genes) which are differentially expressed between the HT-29 and Caco-2 cell lines in this and other published profiling studies that combine both cell lines.

in enterocytes. The data in this study substantially expands the lists of differentially expressed miRNAs, Proteins and mRNAs between Caco-2 and HT-29 cell lines. Furthermore it is to our knowledge the first to provide "tri-omics" analysis (genes, proteomics, miRNAs) on the Caco-2 and HT29 cell lines in combination. It uses the availability of data on multiple levels to identify potential interactions that would not have been identified by a single dataset. Allowing us to provide new information for the characterising of these two cell lines, which are important in intestinal modelling, and help focus on the most likely miRNA candidates for further analysis.

COMMENTS

Background

The development of suitable *in vitro* models of the intestine is of great interest

to the food and pharmaceutical industries. Two commonly used cell lines for the generation of such *in vitro* models are Caco-2 and HT-29. The use of "-omics" studies (transcriptomics, proteomics and metabolomics) has provided insights into how *in vitro* models work in comparison to in vivo scenarios and how to improve them. However, the complexity involved identifying of miRNA targets still remains a significant challenge to researchers. This study addresses that complexity by using a "tri-omics" approach to identify targets.

Research frontiers

The development and maturation of "-omics" technologies has revolutionised our understanding of biological processes. However, while there have been previous studies investigating the differences between theses cell lines, these have focused on only one aspect at a time.

Innovations and breakthroughs

This study is the first to use an integrated "tri-omics" analysis (mRNA, proteomics, miRNAs) on Caco-2 and HT-29 to identify potential miRNA-protein networks were identified that would not have been immediately apparent otherwise. These networks contain a large number of targets associated with the actin cytoskeleton and its associated cell processes such as motility, polarisation, and endocytosis.

Applications

The use of an integrated "tri-omics" analysis will support a better understanding of the molecular events underpinning the different biological behaviours of these two cell lines, which are so important to pharmacological and nutritional research.

Terminology

Ward's method is a robust clustering and is defined as the proximity between two clusters as the increase in squared error that results when two clusters are merged.

Peer-review

This study is well elaborated, uses innovative methodology and supports organoid studies aiming at greater knowledge of enteric epithelial cells.

REFERENCES

1 **Vázquez M**, Calatayud M, Vélez D, Devesa V. Intestinal transport of methylmercury and inorganic mercury in various models of Caco-2 and HT29-MTX cells. *Toxicology* 2013; **311**: 147-153 [PMID: 23793072 DOI: 10.1016/j.tox.2013.06.002]

2 **Pullakhandam R**, Nair KM, Pamini H, Punjal R. Bioavailability of iron and zinc from multiple micronutrient fortified beverage premixes in Caco-2 cell model. *J Food Sci* 2011; **76**: H38-H42 [PMID: 21535765 DOI: 10.1111/j.1750-3841.2010.01993.x]

3 **Gagnon M**, Zihler Berner A, Chervet N, Chassard C, Lacroix C. Comparison of the Caco-2, HT-29 and the mucus-secreting HT29-MTX intestinal cell models to investigate Salmonella adhesion and invasion. *J Microbiol Methods* 2013; **94**: 274-279 [PMID: 23835135 DOI: 10.1016/j.mimet.2013.06.027]

4 **Calatayud M**, Devesa V, Vélez D. Differential toxicity and gene expression in Caco-2 cells exposed to arsenic species. *Toxicol Lett* 2013; **218**: 70-80 [PMID: 23353816 DOI: 10.1016/j.toxlet.2013.01.013]

5 **Nakamura Y**, Yogosawa S, Izutani Y, Watanabe H, Otsuji E, Sakai T. A combination of indol-3-carbinol and genistein synergistically induces apoptosis in human colon cancer HT-29 cells by inhibiting Akt phosphorylation and progression of autophagy. *Mol Cancer* 2009; **8**: 100 [PMID: 19909554 DOI: 10.1186/1476-4598-8-100]

6 **Barker N**. Adult intestinal stem cells: critical drivers of epithelial homeostasis and regeneration. *Nat Rev Mol Cell Biol* 2014; **15**: 19-33 [PMID: 24326621 DOI: 10.1038/nrm3721]

7 **Fogh J**, Wright WC, Loveless JD. Absence of HeLa cell contamination in 169 cell lines derived from human tumors. *J Natl Cancer Inst* 1977; **58**: 209-214 [PMID: 833871]

8 **Rousset M**, Laburthe M, Pinto M, Chevalier G, Rouyer-Fessard C, Dussaulx E, Trugnan G, Boige N, Brun JL, Zweibaum A. Enterocytic differentiation and glucose utilization in the human colon tumor cell line Caco-2: modulation by forskolin. *J Cell Physiol* 1985; **123**: 377-385 [PMID: 2985631 DOI: 10.1002/jcp.1041230313]

9 **Sambuy Y**, De Angelis I, Ranaldi G, Scarino ML, Stammati A, Zucco F. The Caco-2 cell line as a model of the intestinal barrier: influence of cell and culture-related factors on Caco-2 cell functional characteristics. *Cell Biol Toxicol* 2005; **21**: 1-26 [PMID: 15868485 DOI: 10.1007/s10565-005-0085-6]

10 **Shah P**, Jogani V, Bagchi T, Misra A. Role of Caco-2 cell monolayers in prediction of intestinal drug absorption. *Biotechnol Prog* 2006; **22**: 186-198 [PMID: 16454510 DOI: 10.1021/bp050208u]

11 **Huet C**, Sahuquillo-Merino C, Coudrier E, Louvard D. Absorptive and mucus-secreting subclones isolated from a multipotent intestinal cell line (HT-29) provide new models for cell polarity and terminal differentiation. *J Cell Biol* 1987; **105**: 345-357 [PMID: 3611191 DOI: 10.1083/jcb.105.1.345]

12 **Maoret JJ**, Font J, Augeron C, Codogno P, Bauvy C, Aubery M, Laboisse CL. A mucus-secreting human colonic cancer cell line. Purification and partial characterization of the secreted mucins. *Biochem J* 1989; **258**: 793-799 [PMID: 2658973]

13 **Augeron C**, Laboisse CL. Emergence of permanently differentiated cell clones in a human colonic cancer cell line in culture after treatment with sodium butyrate. *Cancer Res* 1984; **44**: 3961-3969 [PMID: 6744312]

14 **Lesuffleur T**, Barbat A, Dussaulx E, Zweibaum A. Growth adaptation to methotrexate of HT-29 human colon carcinoma cells is associated with their ability to differentiate into columnar absorptive and mucus-secreting cells. *Cancer Res* 1990; **50**: 6334-6343 [PMID: 2205381]

15 **Chastre E**, Emami S, Rosselin G, Gespach C. Vasoactive intestinal peptide receptor activity and specificity during enterocyte-like differentiation and retrodifferentiation of the human colonic cancerous subclone HT29-18. *FEBS Lett* 1985; **188**: 197-204 [PMID: 2993022 DOI: 10.1016/0014-5793(85)80371-9]

16 **Mahler GJ**, Shuler ML, Glahn RP. Characterization of Caco-2 and HT29-MTX cocultures in an in vitro digestion/cell culture model used to predict iron bioavailability. *J Nutr Biochem* 2009; **20**: 494-502 [PMID: 18715773 DOI: 10.1016/j.jnutbio.2008.05.006]

17 **Antunes F**, Andrade F, Araújo F, Ferreira D, Sarmento B. Establishment of a triple co-culture in vitro cell models to study intestinal absorption of peptide drugs. *Eur J Pharm Biopharm* 2013; **83**: 427-435 [PMID: 23159710 DOI: 10.1016/j.ejpb.2012.10.003]

18 **Pereira C**, Araújo F, Barrias CC, Granja PL, Sarmento B. Dissecting stromal-epithelial interactions in a 3D in vitro cellularized intestinal model for permeability studies. *Biomaterials* 2015; **56**: 36-45 [PMID: 25934277 DOI: 10.1016/j.biomaterials.2015.03.054]

19 **Tao X**, Xu Z. MicroRNA transcriptome in swine small intestine during weaning stress. *PLoS One* 2013; **8**: e79343 [PMID: 24260202 DOI: 10.1371/journal.pone.0079343]

20 **Liang G**, Malmuthuge N, McFadden TB, Bao H, Griebel PJ, Stothard P, Guan le L. Potential regulatory role of microRNAs in the development of bovine gastrointestinal tract during early life. *PLoS One* 2014; **9**: e92592 [PMID: 24682221 DOI: 10.1371/journal.pone.0092592]

21 **Dalmasso G**, Nguyen HT, Yan Y, Laroui H, Srinivasan S, Sitaraman SV, Merlin D. MicroRNAs determine human intestinal epithelial cell fate. *Differentiation* 2010; **80**: 147-154 [PMID: 20638171 DOI: 10.1016/j.diff.2010.06.005]

22 **Bagga S**, Bracht J, Hunter S, Massirer K, Holtz J, Eachus R, Pasquinelli AE. Regulation by let-7 and lin-4 miRNAs results in target mRNA degradation. *Cell* 2005; **122**: 553-563 [PMID: 16122423 DOI: 10.1016/j.cell.2005.07.031]

23 **Wu L**, Belasco JG. Micro-RNA regulation of the mammalian lin-28 gene during neuronal differentiation of embryonal carcinoma cells. *Mol Cell Biol* 2005; **25**: 9198-9208 [PMID: 16227573 DOI: 10.1128/MCB.25.21.9198-9208.2005]

24 **Pillai RS**, Bhattacharyya SN, Artus CG, Zoller T, Cougot N, Basyuk E, Bertrand E, Filipowicz W. Inhibition of translational initiation by Let-7 MicroRNA in human cells. *Science* 2005; **309**: 1573-1576 [PMID: 16081698 DOI: 10.1126/science.1115079]

25 **Mathonnet G**, Fabian MR, Svitkin YV, Parsyan A, Huck L, Murata T, Biffo S, Merrick WC, Darzynkiewicz E, Pillai RS, Filipowicz W, Duchaine TF, Sonenberg N. MicroRNA inhibition of translation initiation in vitro by targeting the cap-binding complex eIF4F. *Science* 2007; **317**: 1764-1767 [PMID: 17656684 DOI: 10.1126/science.1146067]

26 **Fu L**, Shi Z, Luo G, Tu W, Wang X, Fang Z, Li X. Multiple microRNAs regulate human FOXP2 gene expression by targeting sequences in its 3' untranslated region. *Mol Brain* 2014; **7**: 71 [PMID: 25269856 DOI: 10.1186/s13041-014-0071-0]

27 **Lim LP**, Lau NC, Garrett-Engele P, Grimson A, Schelter JM, Castle J, Bartel DP, Linsley PS, Johnson JM. Microarray analysis shows that some microRNAs downregulate large numbers of target mRNAs. *Nature* 2005; **433**: 769-773 [PMID: 15685193 DOI: 10.1038/nature03315]

28 **John B**, Enright AJ, Aravin A, Tuschl T, Sander C, Marks DS. Human MicroRNA targets. *PLoS Biol* 2004; **2**: e363 [PMID: 15502875 DOI: 10.1371/journal.pbio.0020363]

29 **Lewis BP**, Shih IH, Jones-Rhoades MW, Bartel DP, Burge CB. Prediction of mammalian microRNA targets. *Cell* 2003; **115**: 787-798 [PMID: 14697198 DOI: 10.1016/S0092-8674(03)01018-3]

30 **Krek A**, Grün D, Poy MN, Wolf R, Rosenberg L, Epstein EJ, MacMenamin P, da Piedade I, Gunsalus KC, Stoffel M, Rajewsky N. Combinatorial microRNA target predictions. *Nat Genet* 2005; **37**: 495-500 [PMID: 15806104 DOI: 10.1038/ng1536]

31 **Clarke C**, Henry M, Doolan P, Kelly S, Aherne S, Sanchez N, Kelly P, Kinsella P, Breen L, Madden SF, Zhang L, Leonard M, Clynes M, Meleady P, Barron N. Integrated miRNA, mRNA and protein expression analysis reveals the role of post-transcriptional regulation in controlling CHO cell growth rate. *BMC Genomics* 2012; **13**: 656 [PMID: 23170974 DOI: 10.1186/1471-2164-13-656]

32 **Gallagher C**, Clarke C, Aherne ST, Katikireddy KR, Doolan P, Lynch V, Shaw S, Bobart-Hone A, Murphy C, Clynes M, Power W, O'Sullivan F. Comparative transcriptomic analysis of cultivated limbal epithelium and donor corneal tissue reveals altered wound healing gene expression. *Invest Ophthalmol Vis Sci* 2014; **55**: 5795-5805 [PMID: 25125605 DOI: 10.1167/iovs.14-14664]

33 **Nikitin A**, Egorov S, Daraselia N, Mazo I. Pathway studio--the analysis and navigation of molecular networks. *Bioinformatics* 2003; **19**: 2155-2157 [PMID: 14594725]

34 **Bravo-Cordero JJ**, Magalhaes MA, Eddy RJ, Hodgson L, Condeelis J. Functions of cofilin in cell locomotion and invasion. *Nat Rev Mol Cell Biol* 2013; **14**: 405-415 [PMID: 23778968 DOI: 10.1038/nrm3609]

35 **Ono S**. Mechanism of depolymerization and severing of actin filaments and its significance in cytoskeletal dynamics. *Int Rev Cytol* 2007; **258**: 1-82 [PMID: 17338919 DOI: 10.1016/S0074-7696(07)58001-0]

36 **De La Cruz EM**, Gardel ML. Actin Mechanics and Fragmentation. *J Biol Chem* 2015; **290**: 17137-17144 [PMID: 25957404 DOI: 10.1074/jbc.R115.636472]

37 **Stierum R**, Gaspari M, Dommels Y, Ouatas T, Pluk H, Jespersen S, Vogels J, Verhoeckx K, Groten J, van Ommen B. Proteome analysis reveals novel proteins associated with proliferation and differentiation of the colorectal cancer cell line Caco-2. *Biochim Biophys Acta* 2003; **1650**: 73-91 [PMID: 12922171 DOI: 10.1016/S1570-9639(03)00204-8]

38 **Nagata-Ohashi K,** Ohta Y, Goto K, Chiba S, Mori R, Nishita M, Ohashi K, Kousaka K, Iwamatsu A, Niwa R, Uemura T, Mizuno K. A pathway of neuregulin-induced activation of cofilin-phosphatase Slingshot and cofilin in lamellipodia. *J Cell Biol* 2004; **165**: 465-471 [PMID: 15159416 DOI: 10.1083/jcb.200401136]

39 **Kiuchi T**, Ohashi K, Kurita S, Mizuno K. Cofilin promotes stimulus-induced lamellipodium formation by generating an abundant supply of actin monomers. *J Cell Biol* 2007; **177**: 465-476 [PMID: 17470633 DOI: 10.1083/jcb.200610005]

40 **van Rheenen J**, Condeelis J, Glogauer M. A common cofilin activity cycle in invasive tumor cells and inflammatory cells. *J Cell Sci* 2009; **122**: 305-311 [PMID: 19158339 DOI: 10.1242/jcs.031146]

41 **Staser K**, Shew MA, Michels EG, Mwanthi MM, Yang FC, Clapp DW, Park SJ. A Pak1-PP2A-ERM signaling axis mediates F-actin rearrangement and degranulation in mast cells. *Exp Hematol* 2013; **41**: 56-66.e2 [PMID: 23063725 DOI: 10.1016/j.exphem.2012.10.001]

42 **Mizuno K**. Signaling mechanisms and functional roles of cofilin phosphorylation and dephosphorylation. *Cell Signal* 2013; **25**: 457-469 [PMID: 23153585 DOI: 10.1016/j.cellsig.2012.11.001]

43 **Maizels Y**, Oberman F, Miloslavski R, Ginzach N, Berman M, Yisraeli JK. Localization of cofilin mRNA to the leading edge of migrating cells promotes directed cell migration. *J Cell Sci* 2015; **128**: 1922-1933 [PMID: 25908858 DOI: 10.1242/jcs.163972]

44 **Zhang L**, Luo J, Wan P, Wu J, Laski F, Chen J. Regulation of cofilin phosphorylation and asymmetry in collective cell migration during morphogenesis. *Development* 2011; **138**: 455-464 [PMID: 21205790 DOI: 10.1242/dev.046870]

45 **Wu Q**, Jiang Y, Cui S, Wang Y, Wu X. The role of cofilin-l in vulvar squamous cell carcinoma: A marker of carcinogenesis, progression and targeted therapy. *Oncol Rep* 2016; **35**: 2743-2754 [PMID: 26936386 DOI: 10.3892/or.2016.4625]

46 **Jodoin JN**, Coravos JS, Chanet S, Vasquez CG, Tworoger M, Kingston ER, Perkins LA, Perrimon N, Martin AC. Stable Force Balance between Epithelial Cells Arises from F-Actin Turnover. *Dev Cell* 2015; **35**: 685-697 [PMID: 26688336 DOI: 10.1016/j.devcel.2015.11.018]

47 **Ammer AG**, Weed SA. Cortactin branches out: roles in regulating protrusive actin dynamics. *Cell Motil Cytoskeleton* 2008; **65**: 687-707 [PMID: 18615630 DOI: 10.1002/cm.20296]

48 **Gallo G**. More than one ring to bind them all: recent insights into the structure of the axon. *Dev Neurobiol* 2013; **73**: 799-805 [PMID: 23784998 DOI: 10.1002/dneu.22100]

49 **Weed SA**, Karginov AV, Schafer DA, Weaver AM, Kinley AW, Cooper JA, Parsons JT. Cortactin localization to sites of actin assembly in lamellipodia requires interactions with F-actin and the Arp2/3 complex. *J Cell Biol* 2000; **151**: 29-40 [PMID: 11018051]

50 **Kinley AW**, Weed SA, Weaver AM, Karginov AV, Bissonette E, Cooper JA, Parsons JT. Cortactin interacts with WIP in regulating Arp2/3 activation and membrane protrusion. *Curr Biol* 2003; **13**: 384-393 [PMID: 12620186]

51 **Arpin M,** Chirivino D, Naba A, Zwaenepoel I. Emerging role for ERM proteins in cell adhesion and migration. *Cell Adh Migr* 2011; **5**: 199-206 [PMID: 21343695]

52 **Yang Q**, Onuki R, Nakai C, Sugiyama Y. Ezrin and radixin both regulate the apical membrane localization of ABCC2 (MRP2) in human intestinal epithelial Caco-2 cells. *Exp Cell Res* 2007; **313**: 3517-3525 [PMID: 17825285 DOI: 10.1016/j.yexcr.2007.07.033]

53 **Kobori T**, Harada S, Nakamoto K, Tokuyama S. Radixin influences the changes in the small intestinal P-glycoprotein by etoposide treatment. *Biol Pharm Bull* 2013; **36**: 1822-1828 [PMID: 24189426 DOI: 10.1248/bpb.b13-00511]

54 **Jiang P**, Siggers JL, Ngai HH, Sit WH, Sangild PT, Wan JM. The small intestine proteome is changed in preterm pigs developing necrotizing enterocolitis in response to formula feeding. *J Nutr* 2008; **138**: 1895-1901 [PMID: 18806098]

55 **Kivelä AJ**, Kivelä J, Saarnio J, Parkkila S. Carbonic anhydrases in normal gastrointestinal tract and gastrointestinal tumours. *World J Gastroenterol* 2005; **11**: 155-163 [PMID: 15633208 DOI: 10.3748/wjg.v11.i2.155]

56 **Kuwahara S**, Ikei A, Taguchi Y, Tabuchi Y, Fujimoto N, Obinata M, Uesugi S, Kurihara Y. PSPC1, NONO, and SFPQ are expressed in mouse Sertoli cells and may function as coregulators of androgen receptor-mediated transcription. *Biol Reprod* 2006; **75**: 352-359 [PMID: 16641145 DOI: 10.1095/biolreprod.106.051136]

57 **Zhang P**, Ma Y, Wang F, Yang J, Liu Z, Peng J, Qin H. Comprehensive gene and microRNA expression profiling reveals the crucial role of hsa-let-7i and its target genes in colorectal cancer

metastasis. *Mol Biol Rep* 2012; **39**: 1471-1478 [PMID: 21625861 DOI: 10.1007/s11033-011-0884-1]
58 **Liang G**, Malmuthuge N, Guan le L, Griebel P. Model systems to analyze the role of miRNAs and commensal microflora in bovine mucosal immune system development. *Mol Immunol* 2015; **66**: 57-67 [PMID: 25467799 DOI: 10.1016/j.molimm.2014.10.014]
59 **McKenna LB**, Schug J, Vourekas A, McKenna JB, Bramswig NC, Friedman JR, Kaestner KH. MicroRNAs control intestinal epithelial differentiation, architecture, and barrier function. *Gastroenterology* 2010; **139**: 1654-1664, 1664.e1 [PMID: 20659473 DOI: 10.1053/j.gastro.2010.07.040]
60 **Nakano H**, Miyazawa T, Kinoshita K, Yamada Y, Yoshida T. Functional screening identifies a microRNA, miR-491 that induces apoptosis by targeting Bcl-X(L) in colorectal cancer cells. *Int J Cancer* 2010; **127**: 1072-1080 [PMID: 20039318 DOI: 10.1002/ijc.25143]
61 **Tanaka T**, Arai M, Wu S, Kanda T, Miyauchi H, Imazeki F, Matsubara H, Yokosuka O. Epigenetic silencing of microRNA-373 plays an important role in regulating cell proliferation in colon cancer. *Oncol Rep* 2011; **26**: 1329-1335 [PMID: 21785829 DOI: 10.3892/or.2011.1401]
62 **Kanaan Z**, Rai SN, Eichenberger MR, Barnes C, Dworkin AM, Weller C, Cohen E, Roberts H, Keskey B, Petras RE, Crawford NP, Galandiuk S. Differential microRNA expression tracks neoplastic progression in inflammatory bowel disease-associated colorectal cancer. *Hum Mutat* 2012; **33**: 551-560 [PMID: 22241525 DOI: 10.1002/humu.22021]
63 **Stadthagen G**, Tehler D, Høyland-Kroghsbo NM, Wen J, Krogh A, Jensen KT, Santoni-Rugiu E, Engelholm LH, Lund AH. Loss of miR-10a activates lpo and collaborates with activated Wnt signaling in inducing intestinal neoplasia in female mice. *PLoS Genet* 2013; **9**: e1003913 [PMID: 24204315 DOI: 10.1371/journal.pgen.1003913]
64 **Yang M**, Cui G, Ding M, Yang W, Liu Y, Dai D, Chen L. miR-935 promotes gastric cancer cell proliferation by targeting SOX7. *Biomed Pharmacother* 2016; **79**: 153-158 [PMID: 27044823 DOI: 10.1016/j.biopha.2016.01.011]
65 **Berryman M**, Franck Z, Bretscher A. Ezrin is concentrated in the apical microvilli of a wide variety of epithelial cells whereas moesin is found primarily in endothelial cells. *J Cell Sci* 1993; **105** (Pt 4): 1025-1043 [PMID: 8227193]
66 66 **Kim CY**, Jung WY, Lee HJ, Kim HK, Kim A, Shin BK. Proteomic analysis reveals overexpression of moesin and cytokeratin 17 proteins in colorectal carcinoma. *Oncol Rep* 2012; **27**: 608-620 [PMID: 22076435 DOI: 10.3892/or.2011.1545]
67 **Danielsen EM**, Hansen GH. Lipid raft organization and function in the small intestinal brush border. *J Physiol Biochem* 2008; **64**: 377-382 [PMID: 19391463 DOI: 10.1007/BF03174093]
68 **Stechly L**, Morelle W, Dessein AF, André S, Grard G, Trinel D, Dejonghe MJ, Leteurtre E, Drobecq H, Trugnan G, Gabius HJ, Huet G. Galectin-4-regulated delivery of glycoproteins to the brush border membrane of enterocyte-like cells. *Traffic* 2009; **10**: 438-450 [PMID: 19192249 DOI: 10.1111/j.1600-0854.2009.00882.x]
69 **Nio-Kobayashi J**, Takahashi-Iwanaga H, Iwanaga T. Immunohistochemical localization of six galectin subtypes in the mouse digestive tract. *J Histochem Cytochem* 2009; **57**: 41-50 [PMID: 18796404 DOI: 10.1369/jhc.2008.952317]
70 **Cargnello R**, Celio MR, Schwaller B, Gotzos V. Change of calretinin expression in the human colon adenocarcinoma cell line HT29 after differentiation. *Biochim Biophys Acta* 1996; **1313**: 201-208 [PMID: 8898855]
71 **Häner K**, Henzi T, Pfefferli M, Künzli E, Salicio V, Schwaller B. A bipartite butyrate-responsive element in the human calretinin (CALB2) promoter acts as a repressor in colon carcinoma cells but not in mesothelioma cells. *J Cell Biochem* 2010; **109**: 519-531 [PMID: 19998412 DOI: 10.1002/jcb.22429]
72 **Marilley D**, Schwaller B. Association between the calcium-binding protein calretinin and cytoskeletal components in the human colon adenocarcinoma cell line WiDr. *Exp Cell Res* 2000; **259**: 12-22 [PMID: 10942575 DOI: 10.1006/excr.2000.4942]
73 **Akiyama SK**, Yamada KM. Fibronectin. *Adv Enzymol Relat Areas Mol Biol* 1987; **59**: 1-57 [PMID: 2949539]
74 **Levy P**, Loreal O, Munier A, Yamada Y, Picard J, Cherqui G, Clement B, Capeau J. Enterocytic differentiation of the human Caco-2 cell line is correlated with down-regulation of fibronectin and laminin. *FEBS Lett* 1994; **338**: 272-276 [PMID: 8307193 DOI: 10.1016/0014-5793(94)80282-3]
75 **Vachon PH**, Simoneau A, Herring-Gillam FE, Beaulieu JF. Cellular fibronectin expression is down-regulated at the mRNA level in differentiating human intestinal epithelial cells. *Exp Cell Res* 1995; **216**: 30-34 [PMID: 7813630 DOI: 10.1006/excr.1995.1004]
76 **Rothé B**, Leal-Esteban L, Bernet F, Urfer S, Doerr N, Weimbs T, Iwaszkiewicz J, Constam DB. Bicc1 Polymerization Regulates the Localization and Silencing of Bound mRNA. *Mol Cell Biol* 2015; **35**: 3339-3353 [PMID: 26217012 DOI: 10.1128/MCB.00341-15]
77 **Piazzon N**, Maisonneuve C, Guilleret I, Rotman S, Constam DB. Bicc1 links the regulation of cAMP signaling in polycystic kidneys to microRNA-induced gene silencing. *J Mol Cell Biol* 2012; **4**: 398-408 [PMID: 22641646 DOI: 10.1093/jmcb/mjs027]
78 **Fu Y**, Kim I, Lian P, Li A, Zhou L, Li C, Liang D, Coffey RJ, Ma J, Zhao P, Zhan Q, Wu G. Loss of Bicc1 impairs tubulomorphogenesis of cultured IMCD cells by disrupting E-cadherin-based cell-cell adhesion. *Eur J Cell Biol* 2010; **89**: 428-436 [PMID: 20219263 DOI: 10.1016/j.ejcb.2010.01.002]
79 **Marzolo MP**, Farfán P. New insights into the roles of megalin/LRP2 and the regulation of its functional expression. *Biol Res* 2011; **44**: 89-105 [PMID: 21720686 DOI: 10.4067/S0716-97602011000100012]
80 **Bose S**, Kalra S, Yammani RR, Ahuja R, Seetharam B. Plasma membrane delivery, endocytosis and turnover of transcobalamin receptor in polarized human intestinal epithelial cells. *J Physiol* 2007; **581**: 457-466 [PMID: 17347267 DOI: 10.1113/jphysiol.2007.129171]
81 **Vázquez-Carretero MD**, Palomo M, García-Miranda P, Sánchez-Aguayo I, Peral MJ, Calonge ML, Ilundain AA. Dab2, megalin, cubilin and amnionless receptor complex might mediate intestinal endocytosis in the suckling rat. *J Cell Biochem* 2014; **115**: 510-522 [PMID: 24122887 DOI: 10.1002/jcb.24685]
82 **Hansen TV**, Hammer NA, Nielsen J, Madsen M, Dalbaeck C, Wewer UM, Christiansen J, Nielsen FC. Dwarfism and impaired gut development in insulin-like growth factor II mRNA-binding protein 1-deficient mice. *Mol Cell Biol* 2004; **24**: 4448-4464 [PMID: 15121863 DOI: 10.1128/MCB.24.10.4448-4464.2004]
83 **Han J**, Isoda H, Maekawa T. Analysis of the mechanism of the tight-junctional permeability increase by capsaicin treatment on the intestinal Caco-2 cells. *Cytotechnology* 2002; **40**: 93-98 [PMID: 19003109 DOI: 10.1023/A:1023922306968]
84 **Chen C**, Chi H, Sun BG, Sun L. The galectin-3-binding protein of Cynoglossus semilaevis is a secreted protein of the innate immune system that binds a wide range of bacteria and is involved in host phagocytosis. *Dev Comp Immunol* 2013; **39**: 399-408 [PMID: 23178402 DOI: 10.1016/j.dci.2012.10.008]
85 **Yilmaz Z**, Eralp Inan O, Kocaturk M, Baykal AT, Hacariz O, Hatipoglu I, Tvarijonaviciute A, Cansev M, Ceron J, Ulus IH. Changes in serum proteins after endotoxin administration in healthy and choline-treated calves. *BMC Vet Res* 2016; **12**: 210 [PMID: 27646125 DOI: 10.1186/s12917-016-0837-y]
86 **Iglesias JM**, Morgan RO, Jenkins NA, Copeland NG, Gilbert DJ, Fernandez MP. Comparative genetics and evolution of annexin A13 as the founder gene of vertebrate annexins. *Mol Biol Evol* 2002; **19**: 608-618 [PMID: 11961095 DOI: 10.1016/j.matbio.2007.04.007]
87 **Babusiak M**, Man P, Petrak J, Vyoral D. Native proteomic analysis of protein complexes in murine intestinal brush border membranes. *Proteomics* 2007; **7**: 121-129 [PMID: 17205597 DOI: 10.1002/pmic.200600382]
88 **Ma YL**, Zhang P, Wang F, Moyer MP, Yang JJ, Liu ZH, Peng JY, Chen HQ, Zhou YK, Liu WJ, Qin HL. Human embryonic stem cells and metastatic colorectal cancer cells shared the common endogenous human microRNA-26b. *J Cell Mol*

Med 2011; **15**: 1941-1954 [PMID: 20831567 DOI: 10.1111/j.1582-4934.2010.01170.x]
89 **Lenaerts K**, Bouwman FG, Lamers WH, Renes J, Mariman EC. Comparative proteomic analysis of cell lines and scrapings of the human intestinal epithelium. *BMC Genomics* 2007; **8**: 91 [PMID: 17407598 DOI: 10.1186/1471-2164-8-91]
90 **Uzozie A**, Nanni P, Staiano T, Grossmann J, Barkow-Oesterreicher S, Shay JW, Tiwari A, Buffoli F, Laczko E, Marra G. Sorbitol dehydrogenase overexpression and other aspects of dysregulated protein expression in human precancerous colorectal neoplasms: a quantitative proteomics study. *Mol Cell Proteomics* 2014; **13**: 1198-1218 [PMID: 24567419 DOI: 10.1074/mcp.M113.035105]
91 **Bourgine J**, Billaut-Laden I, Happillon M, Lo-Guidice JM, Maunoury V, Imbenotte M, Broly F. Gene expression profiling of systems involved in the metabolism and the disposition of xenobiotics: comparison between human intestinal biopsy samples and colon cell lines. *Drug Metab Dispos* 2012; **40**: 694-705 [PMID: 22217464 DOI: 10.1124/dmd.111.042465]
92 **Barresi V**, Trovato-Salinaro A, Spampinato G, Musso N, Castorina S, Rizzarelli E, Condorelli DF. Transcriptome analysis of copper homeostasis genes reveals coordinated upregulation of SLC31A1,SCO1, and COX11 in colorectal cancer. *FEBS Open Bio* 2016; **6**: 794-806 [PMID: 27516958 DOI: 10.1002/2211-5463.12060]
93 **Zhao S**, Wen Z, Liu S, Liu Y, Li X, Ge Y, Li S. MicroRNA-148a inhibits the proliferation and promotes the paclitaxel-induced apoptosis of ovarian cancer cells by targeting PDIA3. *Mol Med Rep* 2015; **12**: 3923-3929 [PMID: 26004124 DOI: 10.3892/mmr.2015.3826]
94 **Tsai ZY**, Chou CH, Lu CY, Singh S, Yu SL, Li SS. Proteomic comparison of human embryonic stem cells with their differentiated fibroblasts: Identification of 206 genes targeted by hES cell-specific microRNAs. *Kaohsiung J Med Sci* 2011; **27**: 299-306 [PMID: 21802640 DOI: 10.1016/j.kjms.2011.03.010]
95 **Chiyomaru T,** Enokida H, Kawakami K, Tatarano S, Uchida Y, Kawahara K, Nishiyama K, Seki N, Nakagawa M. Functional role of LASP1 in cell viability and its regulation by microRNAs in bladder cancer. *Urol Oncol* 2012; **30**: 434-443 [PMID: 20843712 DOI: 10.1016/j.urolonc.2010.05.008]
96 **Delanote V**, Vandekerckhove J, Gettemans J. Plastins: versatile modulators of actin organization in (patho)physiological cellular processes. *Acta Pharmacol Sin* 2005; **26**: 769-779 [PMID: 15960882 DOI: 10.1111/j.1745-7254.2005.00145.x]
97 **Chafel MM**, Shen W, Matsudaira P. Sequential expression and differential localization of I-, L-, and T-fimbrin during differentiation of the mouse intestine and yolk sac. *Dev Dyn* 1995; **203**: 141-151 [PMID: 7655078 DOI: 10.1002/aja.1002030203]

P- Reviewer: Gassler N, Rajendran V, Sipahi AM **S- Editor**: Ma YJ
L- Editor: A **E- Editor**: Huang Y

World Journal of Gastroenterology

Submit a Manuscript: http://www.f6publishing.com

World J Gastroenterol 2017 November 7; 23(41): 7387-7396

DOI: 10.3748/wjg.v23.i41.7387

ISSN 1007-9327 (print) ISSN 2219-2840 (online)

ORIGINAL ARTICLE

Retrospective Cohort Study

Fecal calprotectin measurement is a marker of short-term clinical outcome and presence of mucosal healing in patients with inflammatory bowel disease

Athanasios Kostas, Spyros I Siakavellas, Charalambos Kosmidis, Anna Takou, Joanna Nikou, Georgios Maropoulos, John Vlachogiannakos, George V Papatheodoridis, Ioannis Papaconstantinou, Giorgos Bamias

Athanasios Kostas, Spyros I Siakavellas, Charalambos Kosmidis, John Vlachogiannakos, George V Papatheodoridis, Giorgos Bamias, Academic Department of Gastroenterology, University of Athens Medical School, Laiko General Hospital, Athens 11527, Greece

Anna Takou, Joanna Nikou, Georgios Maropoulos, Biochemistry Department, Laiko General Hospital, Athens 11527, Greece

Ioannis Papaconstantinou, 2nd Department of Surgery, University of Athens Medical School, Areteion General Hospital, Athens 11528, Greece

ORCID number: Athanasios Kostas (0000-0002-4411-710X); Spyros I Siakavellas (0000-0001-8217-8950); Charalambos Kosmidis (0000-0002-2734-8475); Anna Takou (0000-0002-2924-9681); Joanna Nikou (0000-0003-3285-5348); Georgios Maropoulos (0000-0001-7545-120X); John Vlachogiannakos (0000-0001-9291-0711); George V Papatheodoridis (0000-0002-3518-4060); Ioannis Papaconstantinou (0000-0002-4614-9041); Giorgos Bamias (0000 -0002-5492 -5717).

Author contributions: Kostas A and Siakavellas SI contributed equally to this work; Kostas A, Siakavellas SI, Papatheodoridis GV, Papaconstantinou I and Bamias G designed the research study; Takou A, Nikou J and Maropoulos G performed the laboratory tests; Kostas A, Siakavellas SI and Kosmidis C collected the data; Siakavellas SI and Bamias G analyzed the data; Kostas A, Siakavellas SI and Bamias G wrote the paper; Vlachogiannakos J, Papatheodoridis GV and Papaconstantinou I provided critical insight regarding paper preparation.

Institutional review board statement: The study was reviewed and approved by the Laika General Hospital Ethics Committee and Institutional Review Board.

Informed consent statement: All study participants, provided informed consent for access to data in their patient files.

Conflict-of-interest statement: The authors have no conflict of interest to declare.

Data sharing statement: No additional data are available.

Manuscript source: Invited Manuscript

Correspondence to: Giorgos Bamias, MD, PhD, Assistant Professor of Gastroenterology, Academic Department of Gastroenterology, University of Athens Medical School, Laiko General Hospital, 17 Agiou Thoma Street Athens 11527, Greece. gbamias@gmail.com
Telephone: +30-213-2061327
Fax: +30-210-7462601

Received: August 12, 2017
Peer-review started: August 19, 2017
First decision: August 30, 2017
Revised: September 18, 2017
Accepted: September 29, 2017
Article in press: September 28, 2017
Published online: November 7, 2017

Abstract

AIM

To evaluate the utility of fecal calprotectin (FC) in predicting relapse and endoscopic activity during follow-

up in an inflammatory bowel disease (IBD) cohort.

METHODS

All FC measurements that were obtained during a 3-year period from patients with inflammatory bowel disease in clinical remission were identified. Data regarding the short-term (6 mo) course of the disease were extracted from the medical files. Exclusion criteria were defined as: (1) An established flare of the disease at the time of FC measurement, (2) Loss to follow up within 6 mo from baseline FC measurement, and, (3) Insufficient data on file. Statistical analysis was performed to evaluate whether baseline FC measurement could predict the short term clinical relapse and/or the presence of mucosal healing.

RESULTS

We included 149 [Crohn's disease (CD) = 113, Ulcerative colitis (UC) = 36, male = 77] IBD patients in our study. Within the determined 6-month period post-FC measurement, 47 (31.5%) had a disease flare. Among 76 patients who underwent endoscopy, 39 (51.3%) had mucosal healing. Baseline FC concentrations were significantly higher in those who had clinical relapse compared to those who remained in remission during follow up (481.0 μg/g, 286.0-600.0 *vs* 89.0, 36.0-180.8, $P < 0.001$). The significant predictive value of baseline median with IQR FC for clinical relapse was confirmed by multivariate Cox analysis [HR for 100μg/g: 1.75 (95%CI: 1.28-2.39), $P = 0.001$]. Furthermore, lower FC baseline values significantly correlated to the presence of mucosal healing in endoscopy (69.0 μg/g, 30.0-128.0 *vs* 481.0, 278.0-600.0, in those with mucosal inflammation, median with IQR, $P < 0.001$). We were able to extract cut-off values for FC concentration with a high sensitivity and specificity for predicting clinical relapse (261 μg/g with AUC = 0.901, sensitivity 87.2%, specificity 85.3%, $P < 0.001$) or mucosal healing (174 μg/g with AUC = 0.956, sensitivity 91.9%, specificity 87.2%, $P < 0.001$). FC was better than CRP in predicting either outcome; nevertheless, having a pathological CRP (> 5 mg/L) in addition to the cut-offs for FC, significantly enhanced the specificity for predicting clinical relapse (95.1% from 85.3%) or endoscopic activity (100% from 87.2%).

CONCLUSION

Serial FC measurements may be useful in monitoring IBD patients in remission, as FC appears to be a reliable predictor of short-term relapse and endoscopic activity.

Key words: Fecal calprotectin; Biomarker; Inflammatory bowel disease; Mucosal healing; Clinical outcome; Relapse; Ulcerative colitis; Crohn's disease

Core tip: Fecal calprotectin (FC) is a novel biomarker aiming to facilitate the assessment of inflammatory bowel disease (IBD) activity as its expression is driven by the presence of intestinal inflammation. Our present retrospective study provides evidence that FC measurement during clinical remission may be helpful in identifying early those cases with a higher risk of recurrence. Moreover, lower FC values seem to correlate with endoscopic quiescence of the disease. Thus, FC monitoring may be effective in recognizing distinct subgroups of IBD patients offering the opportunity to the clinician to tailor their management accordingly in order to achieve optimal disease control.

Kostas A, Siakavellas SI, Kosmidis C, Takou A, Nikou J, Maropoulos G, Vlachogiannakos J, Papatheodoridis GV, Papaconstantinou I, Bamias G. Fecal calprotectin measurement is a marker of short-term clinical outcome and presence of mucosal healing in patients with inflammatory bowel disease. *World J Gastroenterol* 2017; 23(41): 7387-7396 Available from: URL: http://www.wjgnet.com/1007-9327/full/v23/i41/7387.htm DOI: http://dx.doi.org/10.3748/wjg.v23.i41.7387

INTRODUCTION

Inflammatory bowel disease (IBD) encompasses two major clinical phenotypes, ulcerative colitis (UC) and Crohn's disease (CD). Both present with chronic inflammation of the intestines that tends to fluctuate over time, with periods of remission alternating with flares of variable severity. Avoidance of clinical relapse and long-term maintenance of remission is of critical importance in IBD, as failure to control inflammatory activity is associated not only with impaired quality of life of patients but also worse long-term outcomes, including increased potential for colonic carcinogenesis[1,2].

The vital importance of maintaining longitudinal clinical remission emphasizes the need to accurately monitor inflammatory activity in IBD and predict imminent disease flares. Such knowledge would, then, allow for modifications in the treatment strategy, in order to avoid recurrence of overt inflammation. This approach is in line with the recent reappraisal of therapeutic goals in IBD with the introduction of the "treat-to-target" principle[3]. According to the latter concept, clinical remission should be paired with biological and endoscopic evidence of mucosal inflammatory inactivity in IBD patients. Biological inactivity may be indicated by the absence of markers of inflammation in the peripheral blood (ESR, CRP) or feces (calprotectin), whereas mucosal healing is the most accepted endoscopic target. Periodical check for such markers during clinical remission would help to identify those patients in higher risk for recurrence and in need for therapy adjustments. In fact, mucosal healing has emerged as a reliable prognostic marker for disease course[4], as it is associated with lower 2-year probability for clinical flare in both CD and

UC[5]. Nevertheless, repeated colonoscopies are needed to continuously screen patients in remission for the presence of subclinical mucosal inflammation. This may create patient discomfort, increase the risk of procedure-related adverse events, and apply a significant financial burden on the health system. Therefore, discovery of non-invasive biomarkers with high correlation to the presence of mucosal healing would constitute a cost-effective substitute to repeated endoscopies.

In recent years, biomarkers detected in the feces have been proposed as an improved alternative to those measured in the serum for diagnosing residual intestinal inflammation in patients with IBD[6]. The mostly investigated candidate of this category is fecal calprotectin (FC), a calcium and zinc-binding peptide, which originates primarily from neutrophils but also from monocytes[7,8]. It constitutes almost 60% of the total cytosolic protein content in neutrophils and is released upon their activation[9,10]. Thus, the presence of elevated FC is an indicator of mucosal neutrophil infiltration and increased shedding to the intestinal lumen[11]. As these events are typical components of IBD-associated intestinal inflammation, measurement of FC may be useful in this setting[12]. We undertook the present study to evaluate the clinical utility of FC measurement in a large IBD cohort, with a regular follow-up. We report that FC values during remission help to identify those patients with a higher risk of relapse. We also demonstrate that the absence of mucosal healing on follow-up endoscopy correlates strongly with higher FC baseline values. We, further, propose cut-off values for both outcomes (*i.e.* clinical relapse and ongoing endoscopic activity). Finally, we demonstrate that those cut-offs may be significantly lower in patients with post-surgical recurrence of CD in comparison to surgery-free patients.

MATERIALS AND METHODS

Patient population and study outcomes

In this retrospective study, we recovered from the electronic records of our Hospital all FC measurements that were performed between Jan 2014 and Dec 2016 in patients with IBD, who had a regular follow up at our Department. The main aim of our study was to test whether a baseline FC measurement in IBD patients in clinical remission was predictive of clinical relapse in the following 6 mo. Thus, we excluded from analysis those patients with: (1) An established flare of the disease at the time of FC measurement, (2) Loss to follow up within 6 mo from baseline FC measurement, and (3) Insufficient data on file. Disease relapse was defined as: (1) Significant increase in respective clinical activity indices above accepted cut-offs for remission in CD (Harvey-Bradshaw Index $\geqslant$ 5) and UC (Simple Colitis Activity Index $\geqslant$ 3) and/or (2) step-up in the patient's therapeutic regimen, including surgery for intractable disease-related symptoms. A secondary aim of our study was to examine whether the measured FC value could predict the presence or absence of mucosal healing. The latter was defined as an endoscopic Mayo Score of 0 for UC and the absence of mucosal lesions in the colon and terminal ileum for CD, respectively. All endoscopies were performed in our Dpt. by the same experienced endoscopist (GB) thus ensuring uniformity in mucosal healing assessment. For all study participants, demographic, epidemiologic and clinical data were retrieved from the patient files and entered in an SPSS database.

Fecal calprotectin measurement

Fecal samples were collected by patients at home and were brought on the same day to the Biochemical Laboratory of our Hospital. They were stored in deep freeze (-80 ℃) and were unfrozen and used for testing at most two weeks after initial storage. For calprotectin measurement in our Hospital a commercially available monoclonal enzyme-linked immunosorbent assay (ELISA) kit (EK-CAL, Bühlmann, Switzerland) was used according to the manufacturer's instructions. FC levels were expressed as micrograms per gram of feces. The lower limit of detection was at 10 μg/g. Other laboratory markers were routinely done in our Hospital.

Statistical analysis

The SPSS and GraphPad statistical software programs were used for the analysis. Non-parametric tests were used for statistical analysis because of the skewed distribution of FC levels. In particular, comparison between groups was performed by Mann-Whitney (2 groups) or Kruskal-Wallis test (> 2 groups). Values of FC from the same patient were compared by Wilcoxon test. Categorical variables were compared by chi-squared test. Spearman's *r*-test was used to assess correlations of FC with other variables.

Univariable and multivariable Cox regression analysis was performed to evaluate whether FC could serve as independent predictor for disease flare. We accepted the hypothesis that the predictive accuracy of FC for disease flare gradually decreases over time so a 6-mo cut-off time-point was tested as described above. Proportional hazard assumptions of other predictive factors were graphically evaluated using log-minus-log plots. The predictive value of FC was adjusted in multivariable Cox regression for all variables achieving a two-sided $P < 0.20$ in univariable Cox regression. Hazard ratios (HR) were presented per 100 μg/g increment for FC levels.

Receiver operating characteristic (ROC) curve analysis was used to determine specificity, sensitivity and optimal threshold values of FC. The accuracy of FC was evaluated using the area under the curve (AUC) of the ROC and was defined as follows: poor 0.6-0.7;

fair 0.7-0.8; good 0.8-0.9; excellent 0.9-1.0. In all cases, an alpha level of < 0.05 was considered to be significant.

RESULTS

Patients

During the 3-year period under review, 300 measurements of FC were sent from IBD patients in our Department. Among those, we identified 208 measurements which were done in 149 (CD = 113, UC = 36, male = 77) IBD patients with a regular follow-up who fulfilled the inclusion criteria. All patients were in clinical remission when FC baseline measurement was performed. Among those, 47 (31.5%) had a clinical relapse within a 6-mo period whereas 102 remained in remission. In addition, 76 patients (CD = 57, UC = 19) underwent endoscopy within the 6-mo period, among whom 39 (CD = 28, UC = 11) demonstrated mucosal healing, as defined in our study protocol.

Increased baseline fecal calprotectin values in patients with inflammatory bowel disease are associated with elevated risk for clinical relapse within 6 mo

Our main aim in the present study was to investigate whether FC measurements during clinical remission could predict which patients were at higher risk for relapse within a 6-mo period. We, therefore, compared the baseline characteristics, including FC values, between patients who had a relapse (n = 47) and those whose disease remained quiescent during the 6-mo period of f-up (n = 102) (Table 1). No differences were observed between the two groups regarding their basic demographic or clinical characteristics. In contrast, our analysis clearly showed that patients who relapsed had significantly higher FC values at baseline (481.0 μg/g, 286.0-600.0 *vs* 89.0, 36.0-180.8, median with IQR, P < 0.001) (Figure 1). In addition to FC concentration, total WBC count and serum CRP were also statistically different between patients with or without remission within 6 mo (Table 1). FC values significantly correlated with baseline measurements of CRP and WBC (data not shown).

We also observed a dose-response effect of FC concentration on the probability for relapse both at 3- as well as at 6-mo post-measurement. Indeed, as shown in Figure 2, 3.3% and 6.6% patients with a baseline FC concentration of < 250 μg/g relapsed at 3- and 6-mo, respectively, as compared with 25.9% and 63% patients with a baseline value of 250–500 μg/g. Finally, patients with a baseline value greater than 500 μg/g had the highest risk for relapse (40% at 3-mo and 80% at 6-mo, respectively) (P < 0.001 for comparisons at both time points).

To further assess the risk of disease flare according to baseline FC levels, we conducted univariable Cox regression analysis to test baseline variables as predictors for disease relapse. FC levels at baseline were found to be predictive of relapse within 6 mo [HR for 100 μg/g: 1.21 (95%CI: 1.15-1.28), P < 0.001], along with CRP levels and white blood cell count. Moreover, 3 more variables (age, gender and treatment with "aminosalicylates only" at baseline) exhibited a two-sided P < 0.20 in univariable Cox regression and were thus included in the multivariate analysis (Table 2). When conducting multivariate analysis to check for possible interactions, it was shown that FC baseline levels remained a strong independent predictor for disease flare [HR for 100μg/g: 1.75 (95%CI: 1.28-2.39), P = 0.001]. WBC count retained marginal predictive significance in the multivariate analysis, whereas CRP did not (Table 2).

In addition, we used receiver operating characteristic (ROC) curve analysis to determine potential cut-off FC values for the prediction of short-term clinical relapse. The optimal threshold value for elevated risk of disease flare in our cohort of IBD patients was found to be 261 μg/g with excellent accuracy (AUC = 0.901, sensitivity 87.2%, specificity 85.3%, P < 0.001) (Figure 3A and B).

To further validate the significance of FC measurements in discriminating patients with clinical relapse, we compared FC concentrations in 23 individual cases where FC was tested in the same patient before and during disease flare. As shown in Figure 4, FC values were significantly increased during flare episodes (592.0, 394.25-600.0 *vs* 160.5, 98.5-265.8, median with IQR, P < 0.001).

Taken together, these results demonstrate that FC measurement in remission may be useful in distinguishing which patients are at higher risk of relapse.

Lower baseline fecal calprotectin values correlate with mucosal healing

We, next, sought to determine whether baseline FC measurement was associated with the presence of endoscopic remission or inflammation upon follow-up endoscopy. To answer this question, we studied the subgroup of patients (n = 76) that underwent lower gastrointestinal endoscopy within 6 mo of having a FC measurement (mean period between FC measurement and endoscopy was 4.1 mo) (Figure 5A). It should be noted that FC was not assessed in the majority (> 90%) of patients at the time of endoscopy. In our study, we found that FC values were significantly lower in those patients that had mucosal healing (69.0 μg/g, 30.0-128.0, median with IQR) as compared with those who had inflammation in endoscopy (481.0, 278.0-600.0, P < 0.001). Similarly, to clinical relapse, we, also, used receiver operating characteristic (ROC) curve analysis, to determine cut-off FC values for predicting mucosal inflammation. The optimal value that was derived from our study was found to be 174 μg/g, which offered excellent accuracy for predicting the presence of mucosal healing [sensitivity 91.9%, specificity 87.2%, (AUC = 0.956, P < 0.001)] (Figure 5B).

Table 1 Patient characteristics according to clinical course

	Relapse (n = 47)	Remission (n = 102)	P
Age (in yr, mean ± SD, range)	43.9 ± 17.5 (17-76)	38.1 ± 14.6 (17-76)	NS
Male	28 (59.6%)	49 (48.0%)	0.078
Disease duration (in mo, mean ± SD, range)	95.1 ± 118.7 (1-560)	95.3 ± 162.0 (1-1415)	NS
Diagnosis			
Crohn's disease	38 (80.9%)	75 (73.5%)	NS
Ulcerative Colitis	9 (19.1%)	27 (26.5%)	NS
Disease location			NS
Ileal (L1)	16	22	
Colonic (L2)	4	14	
Ileocolonic (L3)	28	29	
Perianal disease (p)	7	11	
Proctitis	1	7	
Left sided	3	8	
Extensive	5	12	
Extraintestinal manifestations	18	35	NS
Fecal calprotectin (in μg/g, median, IQR)	481 (286-600)	89 (36-180.8)	< 0.001
CRP (in yr, mean ± SD, range)	11.3 ± 10.1 (3.0-41.0)	5.1 ± 5.5 (3.1-42.0)	0.002
WBC (in thousands, mean ± SD, range)	8.9 ± 3.3 (3.4-18.2)	7.5 ± 2.4 (3.8-18.4)	0.022
Hgb (in g/dL, mean ± SD, range)	13.2 ± 1.9 (9.7-16.5)	13.6 ± 1.5 (10.0-16.4)	NS
PLT (in thousands, mean ± SD, range)	277.5 ± 99.5 (117-511)	256.0 ± 61.4 (103-450)	NS

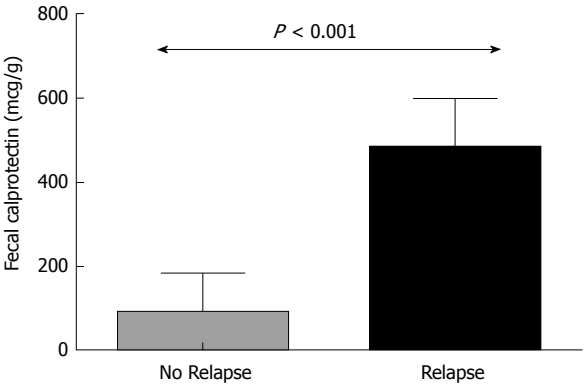

Figure 1 Increased baseline fecal calprotectin values in patients with inflammatory bowel disease are associated with elevated risk for clinical relapse within 6 mo. Patients with disease relapse within 6 mo of follow up have higher FC values at baseline. Column bars represent median values with interquartile range. FC: Fecal calprotectin.

Interestingly when we tried to ascertain the significance of baseline CRP in identifying patients with clinical relapse or mucosal inflammation using ROC curve analysis as described above the results were not as satisfying (AUC = 0.695 for clinical relapse and AUC = 0.599 for mucosal inflammation). Nevertheless, we observed that CRP baseline measurements were useful in improving the specificity of predicting clinical relapse as well as mucosal healing in our study group. In particular, when patients apart from a FC baseline value > 261 μg/g had also CRP higher than normal (> 5 mg/L in our laboratory) clinical relapse could be predicted with a specificity of 95.1%. Similarly, in patients with FC values > 174 μg/g and CRP > 5 mg/dL) identifying the cases with mucosal inflammation could be estimated with a specificity of 100% in our cohort. Thus, CRP measurement may not be very helpful alone in recognizing patients with higher risk for flare. On the other hand, it could be quite useful as a secondary step in reducing false positive cases among those who have already exhibited high FC values, further improving our diagnostic yield of high risk patients.

In our study population, there were also eight patients with CD who developed endoscopic recurrence after right hemicolectomy for L1 disease. We compared this group with 12 surgery-naïve CD patients with ileal disease (L1) who also demonstrated active endoscopic lesions. We found that FC values in the post-surgery group were significantly lower (171.5, 70.8-194.5 *vs* 581.5, 469.0-600.0, median with IQR, P < 0.001) (Figure 6).

In all, these results indicate that elevated FC concentrations are indicative of persistent or impending endoscopic inflammation.

DISCUSSION

Several studies have reported strong associations between increased FC values and clinically active CD or UC[13-15], as well as a potential for FC measurement to predict clinical relapses[16-18] and mucosal healing in patients with IBD[19,20]. Nevertheless, the optimal cut-off values and the particular patient groups that may benefit the most from FC monitoring still remain to be defined. This may be the result of diverse disease characteristics between studies and/or technical considerations regarding FC measurement.

In the present study, we provide evidence that, in IBD patients who are in clinical remission, measurement of the concentration of FC may be used as biological marker for the presence of mucosal inflammation. Serial FC concentration measurements may be effectively used to predict ensuing clinical relapses and/or the existence or development of endoscopically

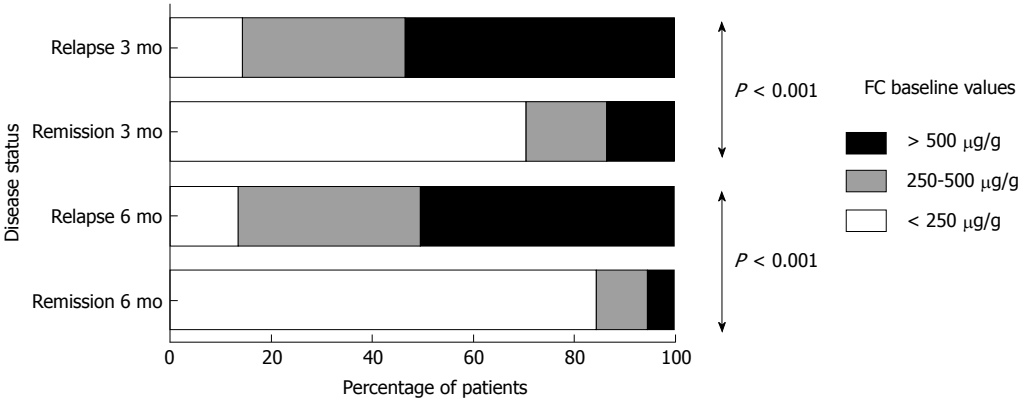

Figure 2 Dose-response effect of fecal calprotectin concentration on the probability for relapse both at 3- as well as at 6-mo post-measurement. Cumulative number of patients with clinical relapse during 6-mo follow-up in relation to baseline concentration of fecal calprotectin. Patients belonging to the groups with higher FC values have an increased probability to relapse within both 3 and 6 mo of follow up. FC: Fecal calprotectin.

Table 2 Cox regression analysis: Fecal calprotectin as predictor of disease flare

	Disease flare			
	Univariate		Multivariate	
	HR (95%CI)	*P*	HR (95%CI)	*P*
FC (HR per 100 μg/g)	1.212 (1.147-1.280)	< 0.001	1.745 (1.275-2.388)	0.001
Age (in yr)	1.018 (0.998-1.037)	0.055	0.973 (0.937-1.011)	NS
Gender (male *vs* female)	0.577 (0.322-1.033)	0.064	0.643 (0.151-2.749)	NS
Disease duration (in mo)	1.000 (0.998-1.002)	> 0.2		
Disease (UC *vs* CD)	1.373(0.664-2.838)	> 0.2		
Extraintestinal manifestations (none *vs* present)	1.085 (0.856-1.375)	> 0.2		
Treatment at baseline	0.915 (0.650-1.287)	> 0.2		
5-ASA	0.408 (0.125-1.331)	0.137	8.805 (0.753-102.913)	NS
Immunomodulators (AZA, 6-MP)	1.193 (0.575-2.474)	> 0.2		
Anti-TNF	0.754 (0.391-1.455)	> 0.2		
Previous Surgery for disease	1.494 (0.591-3.776)	> 0.2		
CRP (HR per 1mg/dL)	1.062 (1.034-1.091)	< 0.001	1.010 (0.935-1.093)	NS
WBC (HR per 1000)	1.144 (1.028-1.273)	0.014	1.197 (1.001-1.432)	0.049
Hgb (HR per 1 g/dL)	0.887 (0.702-1.121)	> 0.2		
PLT (HR per 1000)	1.003 (0.998-1.008)	> 0.2		

FC: Fecal calprotectin; CD: Crohn's disease; UC: Ulcerative colitis.

active disease.

Our findings strongly support the notion that FC concentration is a highly reliable marker of both ongoing clinical activity as well as imminent disease flare in patients with IBD. First, patients with active disease had, as a group, higher FC values that those in remission. Second, more importantly, when paired FC values were tested in individual patients between clinical remission and disease flare, we always observed a clear increase of FC during the latter. This indicates that, in a single patient, FC values accurately reflect the inflammatory status of the disease. Finally, our main finding is that a random measurement of FC concentration highly correlated with the probability of developing clinically active disease during the following 6 mo. This is in line with previous studies that demonstrated a similar predictive significance of FC concentration[21-23]. In fact, recent evidence supports the notion that FC may be the most promising biomarker in providing an estimate of upcoming flare risk[24-26]. In our study, two additional laboratory parameters, CRP and WBC count, were associated with increased probability for relapse in univariate analysis. Nevertheless, among those three, FC performed better and had the most significant difference between patients with sustained clinical remission and those who relapsed within 6 mo of follow-up. Moreover, FC was the only marker that clearly retained its significance to discriminate the two groups of patients in multivariate analysis. The use of FC as an activity biomarker in IBD holds the additional benefit of being specific for intestinal inflammation and not affected by systemic or extraintestinal inflammation, as is the case with CRP or WBC. In fact, other studies have generated conflicting results regarding the value of CRP for this purpose, with some reporting higher CRP levels in IBD patients who relapsed, but the majority showing no such correlation[17,27-29]. Taken together, these previous studies as well as our own present results point to the fact that serial FC measurements may be the best way to follow-up IBD patients in remission inasmuch they may help clinicians to adjust their therapeutic and

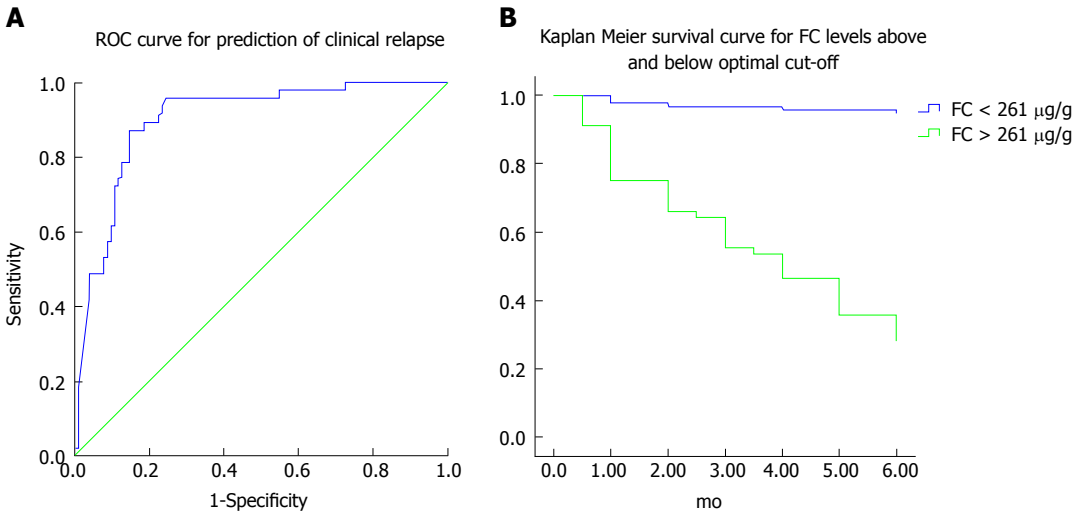

Figure 3 Optimal threshold fecal calprotectin values for predicting elevated risk of disease flare. A: Receiver operating curve analysis: FC baseline levels accurately predict clinical relapse in IBD patients within 6 mo of follow up. B: Disease relapse survival curves (Kaplan-Meier analysis) of patients with FC levels below and above 261 μg/g at baseline. Patients with FC values above this threshold have a substantial risk of disease flare within 6 mo of follow up. FC: Fecal calprotectin; IBD: Inflammatory bowel disease.

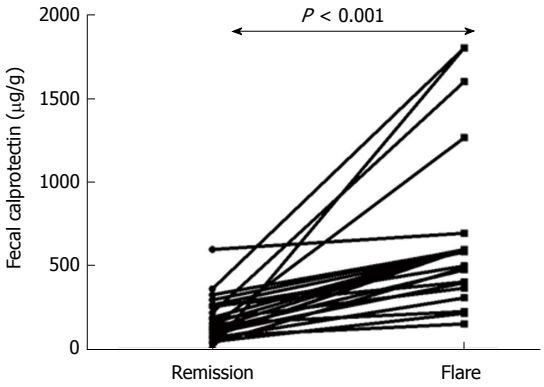

Figure 4 Fecal calprotectin values significantly increase during flare episodes in the same patient. FC values are significantly increased during flare episodes in comparison to remission in the same patients. FC: Fecal calprotectin.

diagnostic approaches in individual cases.

In our patient cohort, we were able to define an optimal cut-off FC value of 261 μg/g, which had a strong predictive value for the discrimination of future relapses *vs* maintenance of remission. Our proposed cut-off is well within the range of FC concentrations that are suitable for predicting a relapse, according to the recent meta-analysis that was reported by Mao *et al*[24]. Indeed, our sensitivity and specificity values are comparable to those observed by other groups[25,29]. Moreover, we show in our cohort that specificity for assessing our study endpoints, may be further improved by additionally testing for CRP in those with FC values over the cut-off. In our study, we chose to focus on a short period (< 6 mo) of follow-up, post-baseline FC testing. This is in line with recent publications that suggest a stronger correlation between high FC values and early (< 12 mo) rather than late relapse[17,21]. Interestingly, contrary to previous indications that FC may be more useful in predicting relapse in UC than CD[30] and in CD with colon involvement compared to L1 disease[18,27], no such significant differences were observed in our cohort. This, however, may be due to the small number of UC and L1 CD patients in our study.

A further important finding from our study is the association of elevated baseline FC values with endoscopically evident mucosal inflammation during the 6-mo follow-up. This is of particular significance as recent studies have shown that not only the presence of symptoms but also the persistence of subclinical mucosal inflammation may be associated with adverse outcomes in IBD. Such residual inflammation may occur in the absence of clinical activity, while the patient is considered to be in remission[17]. In fact, absence of mucosal healing was predictive of disease relapse, as well as hospitalization and IBD-related surgeries[16]. Thus, the potential of FC as a surrogate marker for this endoscopically defined target is intriguing. Early results have showed promising but not conclusive associations[19,30]. Nevertheless, a recent study by D'Haens *et al*[20]. Reported that FC levels below 250 μg/g had 94% sensitivity and 62% specificity in predicting mucosal healing in CD patients[20]. In our analysis, we demonstrated a lower optimal threshold value (174 μg/g) which offered comparable sensitivity and improved specificity for assessing the presence of endoscopic inflammation. Notably, upon further analysis, we were able to detect a subgroup of patients with no clinical activity in whom elevated FC levels were predictive of ongoing endoscopically-evident inflammation (data not shown). We are currently contacting a prospective study on the importance of FC on the selection of patients in remission who may be in need for re-classification of inflammatory activity via endoscopy. This may lead

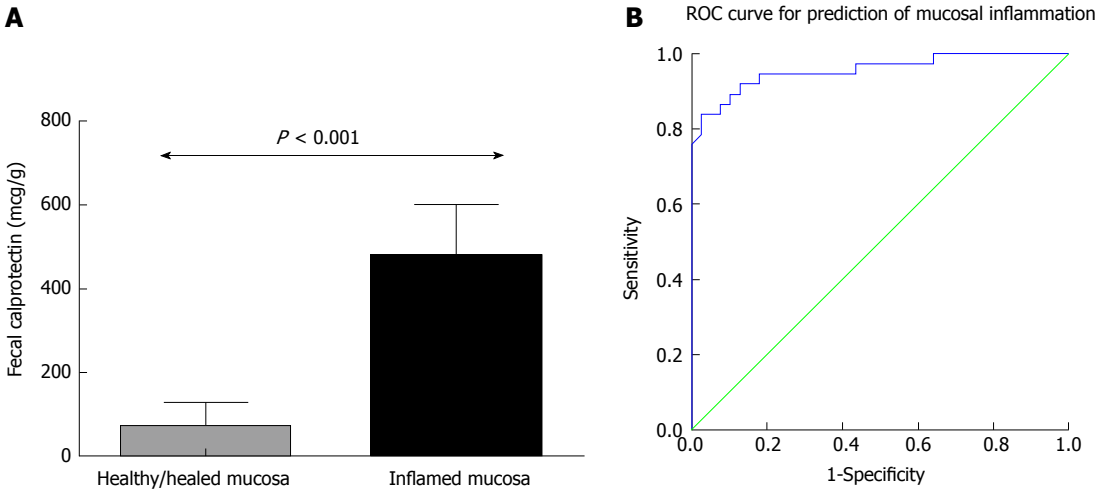

Figure 5 Lower fecal calprotectin baseline values are associated with increased probability of achieving mucosal healing. A: Patients with mucosal healing at endoscopy performed within 6 mo of follow up have lower FC values at baseline. Column bars represent median values with interquartile range. B: Receiver operating curve analysis: FC baseline levels predict accurately the presence of mucosal inflammation in endoscopy performed within 6 mo of FC measurement. FC: Fecal calprotectin.

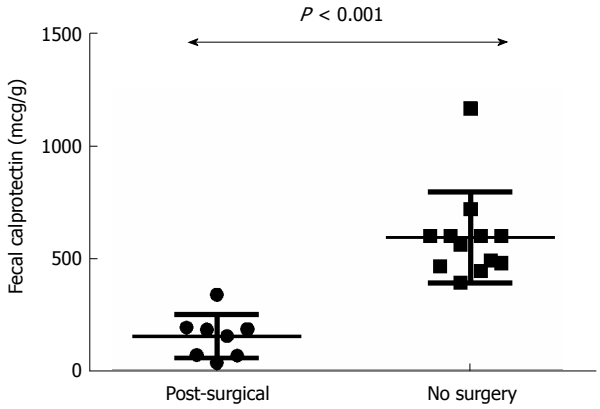

Figure 6 Endoscopic recurrence in post-surgical patients is associated with considerably lower fecal calprotectin values than in surgery-naïve CD patients with inflammation. FC values are significantly lower in post-surgery CD-L1 patients with inflammation in comparison to surgery-naïve CD-L1 patients. Bars represent median values with interquartile range. FC: Fecal calprotectin; CD: Crohn's disease.

to timely therapeutic interventions in high-risk groups and ameliorate the risk for long-term complications. Our results also indicate that FC measurements should always be considered in the appropriate clinical context, as cut-off values may vary in different patient populations. In fact, our findings support the notion that a lower threshold for endoscopy may be needed in CD patients with post-surgery surveillance as endoscopic recurrence was associated with considerably lower FC values than in surgery-naïve CD patients with inflammatory lesions (Figure 6)[31,32].

Our study has important limitations. One such drawback is its retrospective nature as data were collected from the patients' files. This may have led to collection bias. Furthermore, the number of study participants was relatively small. This did not allow us to separate patients with UC from those with CD. Nevertheless, similar trends were observed between the two populations regarding the utility of FC measurements. On the other hand, among the strengths of our study were the fact that we recruited a well-characterized patient cohort with adequate follow-up, and also the considerable percentage of patients who underwent endoscopy, thus allowing us to better estimate the presence of residual inflammation.

In conclusion, we provide evidence for an important role of FC measurement in the prediction of short-term clinical relapse and endoscopic activity in patients with IBD. Further prospective studies with larger number of patients and separation of UC from CD populations are needed to define the exact role of FC in the diagnostic and treatment algorithms in IBD.

ARTICLE HIGHLIGHTS

Research background

Currently, there is increased need for the discovery of simple to perform, non-invasive biomarkers with high correlation to intestinal inflammatory activity in patients with inflammatory bowel disease (IBD). Fecal calprotectin (FC) measurement has shown promise as a candidate marker for this purpose.

Research motivation

Although the value of measuring FC as an indicator for active inflammation is indisputable, the correlation between FC values and future flare of disease activity has not been fully established. Furthermore, uncertainty still exists regarding the optimal cut-off values of FC for this indication and applicability of its measurement in diverse patient groups.

Research objectives

Our principal aim was to study the clinical significance of measuring FC in IBD patients in clinical remission, both as a biomarker for patients stratification according to their risk for relapse, as well as a surrogate marker of endoscopic mucosal healing.

Research methods

We retrospectively analyzed the electronic medical records of all patients

with IBD, with a regular follow up at our department and a FC measurement in a 3-year study period. We specifically focused on patients in stable clinical remission and a medium-term follow-up (at least 6-mo). We then compared two groups of patients: those who remained in remission and those who relapsed (according to pre-defined criteria) during the 6-mo follow-up. A secondary aim of our study was to examine whether the measured FC value could predict the presence or absence of mucosal healing (defined as an endoscopic Mayo Score of 0 for UC and absence of significant mucosal lesions in the colon and terminal ileum for CD, respectively). For all study participants, demographic, epidemiologic and clinical data were retrieved from the patient files and entered in an SPSS database.

Research results

The main findings of our analysis are as follows: First, patients who relapsed within 6-mo from FC measurement had significantly higher baseline FC concentrations than those who remained in remission. Second, patients with mucosal abnormalities in endoscopy (*i.e.* absence of mucosal healing) had significantly higher FC values as compared to patients that demonstrated endoscopic mucosal healing. Third, we were able to define cut-off values for FC concentrations with high sensitivity and specificity for predicting clinical relapse or endoscopical activity in patients with IBD in clinical remission. Fourth, combining FC with CRP measurements further increases the predictive value for short-term clinical flare. Finally, cut-offs may be significantly lower in patients with post-surgical recurrence of CD in comparison to surgery-free patients.

Research conclusions

Our findings clearly indicate that short-term clinical relapse can be predicted with high accuracy by measuring FC concentration in patients with IBD. Consequently, serial FC measurements may prove to be a very useful tool to monitor subclinical inflammatory activity in IBD patients who are in clinical remission. Furthermore, our results show that a high FC value is a surrogate marker of endoscopically active disease. Given the high importance that mucosal healing has gained in recent years for determining disease outcomes in IBD, FC measurements may become a valuable tool for the selection of those patients who need to have an endoscopy while in clinical remission. Subsequently, treatment modifications may be preemptively implemented in such cases, in order to avoid clinical recurrence of symptoms and the systemic consequences of persisting inflammatory activity.

REFERENCES

1 **Vatn MH**. Natural history and complications of IBD. *Curr Gastroenterol Rep* 2009; **11**: 481-487 [PMID: 19903424]
2 **Grivennikov SI**. Inflammation and colorectal cancer: colitis-associated neoplasia. *Semin Immunopathol* 2013; **35**: 229-244 [PMID: 23161445 DOI: 10.1007/s00281-012-0352-6]
3 **Darr U**, Khan N. Treat to Target in Inflammatory Bowel Disease: An Updated Review of Literature. *Curr Treat Options Gastroenterol* 2017; **15**: 116-125 [PMID: 28161818 DOI: 10.1007/s11938-017-0130-6]
4 **Peyrin-Biroulet L**, Ferrante M, Magro F, Campbell S, Franchimont D, Fidder H, Strid H, Ardizzone S, Veereman-Wauters G, Chevaux JB, Allez M, Danese S, Sturm A; Scientific Committee of the European Crohn's and Colitis Organization. Results from the 2nd Scientific Workshop of the ECCO. I: Impact of mucosal healing on the course of inflammatory bowel disease. *J Crohns Colitis* 2011; **5**: 477-483 [PMID: 21939925 DOI: 10.1016/j.crohns.2011.06.009]
5 **Baert F**, Moortgat L, Van Assche G, Caenepeel P, Vergauwe P, De Vos M, Stokkers P, Hommes D, Rutgeerts P, Vermeire S, D' Haens G; Belgian Inflammatory Bowel Disease Research Group; North-Holland Gut Club. Mucosal healing predicts sustained clinical remission in patients with early-stage Crohn's disease. *Gastroenterology* 2010; **138**: 463-468 quiz e10-1 [PMID: 19818785 DOI: 10.1053/j.gastro.2009.09.056]
6 **Tibble JA**, Bjarnason I. Fecal calprotectin as an index of intestinal inflammation. *Drugs Today* (Barc) 2001; **37**: 85-96 [PMID: 12783101]
7 **Angriman I**, Scarpa M, D'Incà R, Basso D, Ruffolo C, Polese L, Sturniolo GC, D'Amico DF, Plebani M. Enzymes in feces: useful markers of chronic inflammatory bowel disease. *Clin Chim Acta* 2007; **381**: 63-68 [PMID: 17368600]
8 **Bjerke K**, Halstensen TS, Jahnsen F, Pulford K, Brandtzaeg P. Distribution of macrophages and granulocytes expressing L1 protein (calprotectin) in human Peyer's patches compared with normal ileal lamina propria and mesenteric lymph nodes. *Gut* 1993; **34**: 1357-1363 [PMID: 8244101]
9 **Poullis A**, Foster R, Northfield TC, Mendall MA. Review article: faecal markers in the assessment of activity in inflammatory bowel disease. *Aliment Pharmacol Ther* 2002; **16**: 675-681 [PMID: 11929384]
10 **Aomatsu T**, Yoden A, Matsumoto K, Kimura E, Inoue K, Andoh A, Tamai H. Fecal calprotectin is a useful marker for disease activity in pediatric patients with inflammatory bowel disease. *Dig Dis Sci* 2011; **56**: 2372-2377 [PMID: 21394462 DOI: 10.1007/s10620-011-1633-y]
11 **Smith LA**, Gaya DR. Utility of faecal calprotectin analysis in adult inflammatory bowel disease. *World J Gastroenterol* 2012; **18**: 6782-6789 [PMID: 23239916 DOI: 10.3748/wjg.v18.i46.6782]
12 **Ikhtaire S**, Shajib MS, Reinisch W, Khan WI. Fecal calprotectin: its scope and utility in the management of inflammatory bowel disease. *J Gastroenterol* 2016; **51**: 434-446 [PMID: 26897740 DOI: 10.1007/s00535-016-1182-4]
13 **Xiang JY**, Ouyang Q, Li GD, Xiao NP. Clinical value of fecal calprotectin in determining disease activity of ulcerative colitis. *World J Gastroenterol* 2008; **14**: 53-57 [PMID: 18176961 DOI: 10.3748/wjg.14.53]
14 **Denis MA**, Reenaers C, Fontaine F, Belaïche J, Louis E. Assessment of endoscopic activity index and biological inflammatory markers in clinically active Crohn's disease with normal C-reactive protein serum level. *Inflamm Bowel Dis* 2007; **13**: 1100-1105 [PMID: 17508418 DOI: 10.1002/ibd.20178]
15 **Schoepfer AM**, Beglinger C, Straumann A, Trummler M, Vavricka SR, Bruegger LE, Seibold F. Fecal calprotectin correlates more closely with the Simple Endoscopic Score for Crohn's disease (SES-CD) than CRP, blood leukocytes, and the CDAI. *Am J Gastroenterol* 2010; **105**: 162-169 [PMID: 19755969 DOI: 10.1038/ajg.2009.545]
16 **Tibble JA**, Bjarnason I. Non-invasive investigation of inflammatory bowel disease. *World J Gastroenterol* 2001; **7**: 460-465 [PMID: 11819811 DOI: 10.3748/wjg.v7.i4.460]
17 **Gisbert JP**, Bermejo F, Pérez-Calle JL, Taxonera C, Vera I, McNicholl AG, Algaba A, López P, López-Palacios N, Calvo M, González-Lama Y, Carneros JA, Velasco M, Maté J. Fecal calprotectin and lactoferrin for the prediction of inflammatory bowel disease relapse. *Inflamm Bowel Dis* 2009; **15**: 1190-1198 [PMID: 19291780 DOI: 10.1002/ibd.20933]
18 **D'Incà R**, Dal Pont E, Di Leo V, Benazzato L, Martinato M, Lamboglia F, Oliva L, Sturniolo GC. Can calprotectin predict relapse risk in inflammatory bowel disease? *Am J Gastroenterol* 2008; **103**: 2007-2014 [PMID: 18802997]
19 **Røseth AG**, Aadland E, Grzyb K. Normalization of faecal calprotectin: a predictor of mucosal healing in patients with inflammatory bowel disease. *Scand J Gastroenterol* 2004; **39**: 1017-1020 [PMID: 15513345]
20 **D'Haens G**, Ferrante M, Vermeire S, Baert F, Noman M, Moortgat L, Geens P, Iwens D, Aerden I, Van Assche G, Van Olmen G, Rutgeerts P. Fecal calprotectin is a surrogate marker for endoscopic lesions in inflammatory bowel disease. *Inflamm Bowel Dis* 2012; **18**: 2218-2224 [PMID: 22344983 DOI: 10.1002/ibd.22917]
21 **Zhulina Y**, Cao Y, Amcoff K, Carlson M, Tysk C, Halfvarson J. The prognostic significance of faecal calprotectin in patients with inactive inflammatory bowel disease. *Aliment Pharmacol Ther* 2016; **44**: 495-504 [PMID: 27402063 DOI: 10.1111/apt.13731]
22 **Lasson A**, Simrén M, Stotzer PO, Isaksson S, Ohman L, Strid H. Fecal calprotectin levels predict the clinical course in patients with new onset of ulcerative colitis. *Inflamm Bowel Dis* 2013; **19**: 576-581 [PMID: 23377170 DOI: 10.1097/MIB.0b013e31827e78be]

23 **Naismith GD**, Smith LA, Barry SJ, Munro JI, Laird S, Rankin K, Morris AJ, Winter JW, Gaya DR. A prospective evaluation of the predictive value of faecal calprotectin in quiescent Crohn's disease. *J Crohns Colitis* 2014; **8**: 1022-1029 [PMID: 24566170 DOI: 10.1016/j.crohns.2014.01.029]

24 **Mao R**, Xiao YL, Gao X, Chen BL, He Y, Yang L, Hu PJ, Chen MH. Fecal calprotectin in predicting relapse of inflammatory bowel diseases: a meta-analysis of prospective studies. *Inflamm Bowel Dis* 2012; **18**: 1894-1899 [PMID: 22238138 DOI: 10.1002/ibd.22861]

25 **Tibble JA**, Sigthorsson G, Bridger S, Fagerhol MK, Bjarnason I. Surrogate markers of intestinal inflammation are predictive of relapse in patients with inflammatory bowel disease. *Gastroenterology* 2000; **119**: 15-22 [PMID: 10889150]

26 **Walkiewicz D**, Werlin SL, Fish D, Scanlon M, Hanaway P, Kugathasan S. Fecal calprotectin is useful in predicting disease relapse in pediatric inflammatory bowel disease. *Inflamm Bowel Dis* 2008; **14**: 669-673 [PMID: 18240279 DOI: 10.1002/ibd.20376]

27 **García-Sánchez V**, Iglesias-Flores E, González R, Gisbert JP, Gallardo-Valverde JM, González-Galilea A, Naranjo-Rodríguez A, de Dios-Vega JF, Muntané J, Gómez-Camacho F. Does fecal calprotectin predict relapse in patients with Crohn's disease and ulcerative colitis? *J Crohns Colitis* 2010; **4**: 144-152 [PMID: 21122498 DOI: 10.1016/j.crohns.2009.09.008]

28 **Kiss LS**, Papp M, Lovasz BD, Vegh Z, Golovics PA, Janka E, Varga E, Szathmari M, Lakatos PL. High-sensitivity C-reactive protein for identification of disease phenotype, active disease, and clinical relapses in Crohn's disease: a marker for patient classification? *Inflamm Bowel Dis* 2012; **18**: 1647-1654 [PMID: 22081542 DOI: 10.1002/ibd.21933]

29 **Kallel L**, Ayadi I, Matri S, Fekih M, Mahmoud NB, Feki M, Karoui S, Zouari B, Boubaker J, Kaabachi N, Filali A. Fecal calprotectin is a predictive marker of relapse in Crohn's disease involving the colon: a prospective study. *Eur J Gastroenterol Hepatol* 2010; **22**: 340-345 [PMID: 19581809 DOI: 10.1097/MEG.0b013e32832bab49]

30 **Costa F**, Mumolo MG, Ceccarelli L, Bellini M, Romano MR, Sterpi C, Ricchiuti A, Marchi S, Bottai M. Calprotectin is a stronger predictive marker of relapse in ulcerative colitis than in Crohn's disease. *Gut* 2005; **54**: 364-368 [PMID: 15710984 DOI: 10.1002/ibd.20490]

31 **Orlando A**, Modesto I, Castiglione F, Scala L, Scimeca D, Rispo A, Teresi S, Mocciaro F, Criscuoli V, Marrone C, Platania P, De Falco T, Maisano S, Nicoli N, Cottone M. The role of calprotectin in predicting endoscopic post-surgical recurrence in asymptomatic Crohn's disease: a comparison with ultrasound. *Eur Rev Med Pharmacol Sci* 2006; **10**: 17-22 [PMID: 16494106]

32 **Scarpa M**, D'Incà R, Basso D, Ruffolo C, Polese L, Bertin E, Luise A, Frego M, Plebani M, Sturniolo GC, D'Amico DF, Angriman I. Fecal lactoferrin and calprotectin after ileocolonic resection for Crohn's disease. *Dis Colon Rectum* 2007; **50**: 861-869 [PMID: 17473939]

P- Reviewer: Day AS, Jadallah KA, Sergi CM **S- Editor**: Wei LJ
L- Editor: A **E- Editor**: Huang Y

World Journal of Gastroenterology

Submit a Manuscript: http://www.f6publishing.com

World J Gastroenterol 2017 November 7; 23(41): 7397-7406

DOI: 10.3748/wjg.v23.i41.7397

ISSN 1007-9327 (print) ISSN 2219-2840 (online)

ORIGINAL ARTICLE

Retrospective Study

Endoscopic balloon dilation of Crohn's disease strictures-safety, efficacy and clinical impact

Susana Lopes, Eduardo Rodrigues-Pinto, Patrícia Andrade, Joana Afonso, Todd H Baron, Fernando Magro, Guilherme Macedo

Susana Lopes, Eduardo Rodrigues-Pinto, Patrícia Andrade, Fernando Magro, Guilherme Macedo, Gastroenterology Department, Faculty of Medicine, Hospital de São João, Porto 4200-319, Portugal

Joana Afonso, Fernando Magro, Department of Pharmacology and Therapeutics, University of Porto, Porto 4200-319, Portugal

Todd H Baron, Division of Gastroenterology and Hepatology, University of North Carolina, Chapel Hill, NC 4200, United States

ORCID number: Susana Lopes (0000-0002-7323-2158); Eduardo Rodrigues-Pinto (0000-0002-2239-1650); Patrícia Andrade (0000-0003-1334-0947); Joana Afonso (0000-0002-9465-937X), Todd H Baron (0000-0003-4934-3090); Fernando Magro (0000-0003-2634-9668); Guilherme Macedo (0000-0002-9387-9872).

Author contributions: Lopes S and Rodrigues-Pinto E contributed equally in the design, conception, analysis, and paper writing; Lopes S, Rodrigues-Pinto E and Magro F conceived and designed the study; Lopes S, Rodrigues-Pinto E and Andrade P collected and analyzed the data; Afonso J performed all laboratorial procedures; Rodrigues-Pinto E and Andrade P were responsible for statistical analysis; Baron TH, Magro F and Macedo G participated in critical revision of the manuscript.

Institutional review board statement: The study was approved by the Ethics Committee of Centro Hospitalar São João, Porto, Portugal.

Informed consent statement: All patients gave informed written consent to participate in the study.

Conflict-of-interest statement: The authors of this manuscript have no conflict of interest to declare.

Data sharing statement: There is no additional data available.

Manuscript source: Unsolicited manuscript

Correspondence to: Guilherme Macedo MD, PhD, Department of Gastroenterology, Centro Hospitalar São João, Alameda Professor Hernani Monteiro, Porto 4200-319, Portugal. guilhermemacedo59@gmail.com
Telephone: +351-22-5513600
Fax: +351-22-5513601

Received: August 16, 2017
Peer-review started: August 19, 2017
First decision: August 30, 2017
Revised: September 11, 2017
Accepted: September 20, 2017
Article in press: September 19, 2017
Published online: November 7, 2017

Abstract

AIM

To evaluate the incidence of anastomotic strictures after intestinal resection in Crohn's disease (CD), demonstrate long-term efficacy and safety of endoscopic balloon dilation (EBD) in CD strictures and its impact on the diagnosis of subclinical postoperative endoscopic recurrence.

METHODS

Retrospective single tertiary center study based on prospectively collected data between 2010 and 2015

including anastomotic and non-anastomotic strictures.

RESULTS

29% of 162 CD patients included developed an anastomotic stricture. 43 patients with anastomotic strictures and 37 with non-anastomotic strictures underwent EBD; technical success was 97.7% and 100%, respectively, however, 63% and 41% needed repeat dilation during the 4.4-year follow-up. Longer periods between surgery and index colonoscopy and higher lactoferrin levels were associated with the presence of stricture after surgery. Calprotectin levels > 83.35 μg/g and current or past history of smoking were associated with a shorter time until need for dilation (HR = 3.877, 95%CI: 1.480-10.152 and HR = 3.041, 95%CI: 1.213-7.627). Anastomotic strictures had a greater need for repeat dilation (63% *vs* 41%, *P* = 0.047). No differences were found between asymptomatic and symptomatic cohorts. Disease recurrence diagnosis was only possible after EBD in a third of patients.

CONCLUSION

EBD is an effective and safe alternative to surgery, with a good short and long-term outcome, postponing or even avoiding further surgery. EBD may allow to diagnose disease recurrence in patients with no clinical signs/biomarkers of disease activity.

Key words: Crohn's disease; Endoscopic recurrence; Anastomotic strictures; Non-anastomotic strictures; Endoscopic balloon dilation

Core tip: This study evaluated the incidence of anastomotic strictures after intestinal resection in Crohn's disease (CD), the long-term efficacy and safety of endoscopic balloon dilation (EBD) in CD strictures and its impact on the diagnosis of subclinical postoperative endoscopic recurrence. Almost one-third of CD patients developed an anastomotic stricture after ileocecal resection/right hemicolectomy. EBD was an effective and safe alternative to surgery, with a good short and long-term outcome, postponing or even avoiding further surgery. EBD also allowed to diagnose disease recurrence in patients with no clinical signs/biomarkers of disease activity. Longer intervals after surgery and higher lactoferrin levels were associated with anastomotic strictures; time until dilation was lower in patients with calprotectin levels > 83.35 μg/g and current/past history of smoking.

Lopes S, Rodrigues-Pinto E, Andrade P, Afonso J, Baron TH, Magro F, Macedo G. Endoscopic balloon dilation of Crohn's disease strictures-safety, efficacy and clinical impact. *World J Gastroenterol* 2017; 23(41): 7397-7406 Available from: URL: http://www.wjgnet.com/1007-9327/full/v23/i41/7397.htm DOI: http://dx.doi.org/10.3748/wjg.v23.i41.7397

INTRODUCTION

Strictures in Crohn's disease (CD) develop during the course of the disease or as the presenting feature[1]. Up to 50% of CD patients undergo surgical resection within the first 10 years of diagnosis[2]. Disease recurrence often occurs at or above the anastomosis due to ongoing inflammatory activity[3,4]. This can result in luminal narrowing, and strictures (non-anastomotic and anastomotic), with up to 70% of patients requiring additional resection[5], though is unpredictable[6].

Medical therapy for stricture management is limited due to the fibrotic nature. Management includes surgical resection and stricturoplasty but with a high rate of recurrence and need for reoperation[7]. Increasing evidence supports endoscopic balloon dilation (EBD) as a safe and effective alternative to surgery, particularly for ileocecal and anastomotic strictures[8,9]. Technical and clinical success rates (resolution of obstructive symptoms) are seen in 73%-100% and 64%-70%, respectively, with a major adverse event (AE) rate of 2%-6.4%[1,10-12]. Balloon diameters of 25 mm are believed to increase risk of AEs[13]. During long-term follow-up patients needing surgery at 1, 3 and 5 years varies form 13%-17%, 28%-42%, and 36%-42% respectively. Strictures recur following dilation, and re-dilation may be required in up to 20% and 50% by 1 and 5 years, respectively[1,14,15]. The best results following dilation are obtained when stricture length is < 4 cm, and for anastomotic strictures when compared to *de novo* strictures[1,12,16].

Anastomotic strictures may represent disease recurrence, but data is limited and contradictory as to whether escalation of medical therapy following dilation may prevent the need for repeat dilation or surgery[10,12]. Other factors such as smoking status and disease activity status at the time of dilation may affect outcome of stricture dilation[12], though many studies are limited by short follow-up durations and small cohorts.

We sought to evaluate anastomotic stricture development after intestinal resection in CD and demonstrate long-term efficacy and safety of EBD in CD anastomotic and *de novo* strictures in a large referral centre cohort and determine the impact of dilation on the diagnosis of subclinical postoperative endoscopic recurrence.

MATERIALS AND METHODS

Retrospective single tertiary center study based on prospectively collected data from a clinical database

created for this purpose. Patients were treated from March 2010 to February 2015 including CD patients who had undergone ileocecal resection/right hemicolectomy. All patients were followed at our Inflammatory Bowel Disease (IBD) outpatient clinic and referred for endoscopic evaluation. Inclusion criteria were definitive diagnosis of CD established by clinical, radiographic, endoscopic, and histological criteria and previous surgery and surgical pathology. Exclusion criteria were previous EBD, age < 18 years, stricture length > 6 cm and fistulae or deep ulceration of the strictured segment.

Clinical disease activity was assessed on the day of endoscopic examination, using the Harvey Bradshaw Index (HBI). Clinically inactive disease was defined as a HBI < 5. Postoperative disease activity of the neoterminal ileum was evaluated according to the Modified Rutgeerts' score[17]. Indication for EBD was to evaluate endoscopic recurrence or symptom/biomarker-driven.

CD patients with non-anastomotic strictures who underwent EBD during the study period were included as a control group (Figure 1).

All procedures were performed in an outpatient setting under propofol sedation, with CO_2 insufflation, by one of two endoscopists (SL and ERP). Polyethylene glycol based bowel preparation was administered the day before colonoscopy. EBD was performed for strictures that would not allow passage with a colonoscope, regardless of patients' symptoms. Dilations were performed endoscopically with a through-the-scope balloon (Boston Scientific, Marlborough, MA), of 10-18 mm diameter and lengths of 55 mm. The balloon was filled with diluted contrast, with diameter of the balloon chosen according to endoscopist discretion. Inflation pressure was maintained for 2 min.

Technical success was defined as the ability to pass the colonoscope through the stricture into the neoileum following dilation. Clinical success was defined as improvement of obstructive symptoms (in symptomatic patients). Major AEs were defined as major bleeding (requiring surgery, blood transfusion or hospital admission) and perforation. Minor, self-limited bleeding was not considered an AE. All patients who underwent dilation were endoscopically reevaluated 6-12 mo later. Long-term efficacy was defined as avoidance of surgical resection or repeat dilation after the initial dilation. Patients were followed until stricture resection, last clinic follow-up, or censor date of March, 2017. Escalation of medical therapy was defined as initiation of a thiopurine or anti-TNF within 6 mo of first dilation, as determined by global physician assessment.

All patients gave informed written consent to participate in the study that was approved by the Ethics Committee of our Institution.

Statistical analysis

Categorical variables were described through absolute and relative frequencies. Continuous variables were described as median, minimum and maximum and dichotomized for analysis using the best cut-off on ROC analysis. Hypotheses were tested about the distribution of continuous variables with non-normal distribution, by using the nonparametric Mann-Whitney. The Chi-squared test and Fisher's exact test were used for differences in proportions of patients experiencing a given outcome. Univariate and multivariate analysis by logistic regression was used to explore the correlation between predictor variables and need of dilation after surgery, as well as need to repeat dilation. To identify independent predictors of need of dilation after surgery, as well as need to repeat dilation, all significant variables evaluated in the univariate analysis were included. Kaplan-Meier survival analysis with log rank statistics was used to assess event-free survival, and Cox conditional proportional hazards regression analysis was used to time-free survival. The results are shown as odds ratio (OR) and hazards ratio (HR) with 95% confidence intervals (CI). All the reported *P* values were two-sided, and *P* values of < 0.05 were considered statistically significant. All data were arranged, processed and analyzed with SPSS® v.24.0 data (Statistical Package for Social Sciences).

RESULTS

Population

A total a 162 CD patients (52.5% males, *n* = 85) who had undergone ileocecal resection/right hemicolectomy were included; the mean age was 42.6 years (SD ± 13.4 years). Baseline demographic characteristics are listed in Table 1. The median follow-up period since colonoscopy index was 4.4 years (1.3-6.8), with a median disease duration of 17.1 years (3.3-52.1). Median time between surgery and index colonoscopy was 7.7 years (range 0.3-37.6 years).

At the time of index colonoscopy, 82% of patients (*n* = 133) were receiving CD medication: 68.5% (*n* = 111) thiopurines and 36.4% (*n* = 59) anti-TNF medication; only 23% of the patients (*n* = 37) were on combination therapy. Seventeen percent of the patients (*n* = 27) had obstructive symptoms, with a median HBI of 1 (0-9). Median labs were: haemoglobin 13.5 g/dL (9.6-18.3), albumin 42 g/dL (24.2-352), C-reactive protein 2.8 mg/L (0.1-105.3), median lactoferrin 4.7 μg/g (0.4-216) and median calprotectin 68.5 μg/g (0.5-2051).

Anastomotic strictures

Twenty-nine percent of patients (*n* = 47) had an anastomotic stricture (17 symptomatic), with 4 also having a non-anastomotic stricture; dilation wasn't

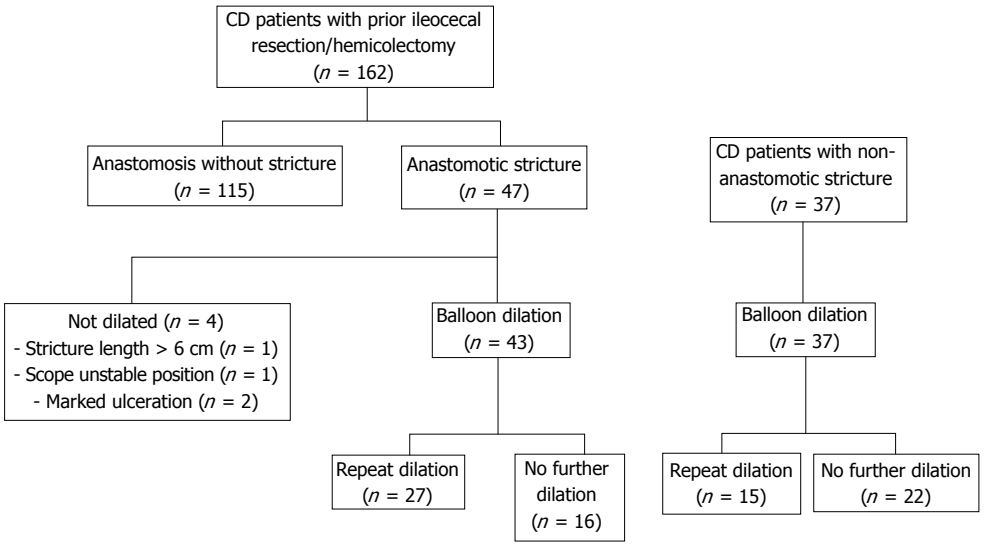

Figure 1 Flowchart with study design.

Table 1 Baseline characteristics of crohn's disease patients with prior ileocecal resection/right hemicolectomy

Characteristic	CD (*n* = 162)
Female/male (*n*)	77/85
Disease duration in years (median; min-max)	17.1 (3.3-52.1)
Follow-up time in years (median; min-max)	4.4 (1.3-6.8)
Time between surgery and index colonoscopy in years (median; min-max)	7.7 (0.3-37.6)
Age at index colonoscopy (mean; standard deviation)	42.6 (± 13.4)
Montreal classification (*n*; %)	
Age at diagnosis	
A1	25 (15.5)
A2	116 (72)
A3	20 (12.4)
Disease location	
L1	89 (54.9)
L2	9 (5.6)
L3	55 (34)
L1-4	7 (4.3)
L3-4	2 (1.2)
Behavior	
B1	6 (3.7)
B2	77 (47.5)
B3	79 (48.8)
Perianal disease	38 (23.5)
Smoking habits (*n*; %)	
Non-smoker	86 (55.1)
Ex-smoker	34 (21.8)
Current smoker	36 (23.1)
Medication at index colonoscopy	
Thiopurines	111 (68.5)
Anti-TNFα	59 (36.4)

TNFα: Tumor necrosis factor α.

performed in 4 patients: 1 due to stricture length > 6 cm, 2 due to marked ulceration and 1 due to unstable scope position.

The presence of stricture after surgery was associated with presence of obstructive symptoms (37% *vs* 9%, OR = 6.3, 95%CI: 2.5-14.9, *P* < 0.001), no medication with thiopurines (74.8% *vs* 53.2%, OR = 2.6, 95%CI: 1.3-5.3, *P* = 0.007), longer duration between surgery and index colonoscopy [132 mo (9-439) *vs* 71 mo (3-415), *P* = 0.001], older age [47 years (16-72) *vs* 39 years (18-77), *P* = 0.031] and lower C-reactive protein levels [2.65 mg/L (0.3-21.9) *vs* 2.85 mg/L (0.1-105.3), *P* = 0.045].

On univariate analysis, the presence of stricture after surgery was associated with longer periods between surgery and index colonoscopy (OR = 1.006, 95%CI: 1.003-1.010, *P* = 0.001), higher lactoferrin levels (OR = 1.010, 95%CI: 1.000-1.021, *P* = 0.049), obstructive symptoms (OR = 6.155, 95%CI: 2.546-14.880, *P* < 0.001), no medication with thiopurines (OR = 2.611, 95%CI: 1.282-5.319, *P* = 0.008) and older age at *index* colonoscopy (OR = 1.028, 95%CI: 1.002-1.055, *P* = 0.033) (Table 2). On multivariate analysis, only longer periods between surgery and index colonoscopy (OR = 1.007, 95%CI: 1.001-1.013, *P* = 0.027) and higher lactoferrin levels (OR = 1.012, 95%CI: 1.000-1.024, *P* = 0.043) were associated with the presence of stricture (Table 2).

In the Cox regression univariate analysis, time until dilation was longer in patients on medication with thiopurines or anti-TNF (HR = 0.476, 95%CI: 0.239-0.946, *P* = 0.034); in further subgroup analysis, thiopurine treatment was the only medication found to be significantly associated with a longer time to dilation (HR = 0.493, 95%CI: 0.275-0.883, *P* = 0.017). Obstructive symptoms and calprotectin levels higher than 83.35 μg/g, on the other hand, were associated with a shorter time until dilation (HR = 2.976, 95%CI: 1.622-5.460, *P* < 0.001 and HR = 3.444, 95%CI: 1.391-8.526, *P* = 0.008, respectively). There was a trend for current or past history of smoking being associated with a shorter time to dilation in the univariate analysis (HR = 1.752, 95%CI: 0.964-3.185, *P* = 0.066). In the Cox multivariate analysis, calprotectin levels > 83.35 μg/g and current

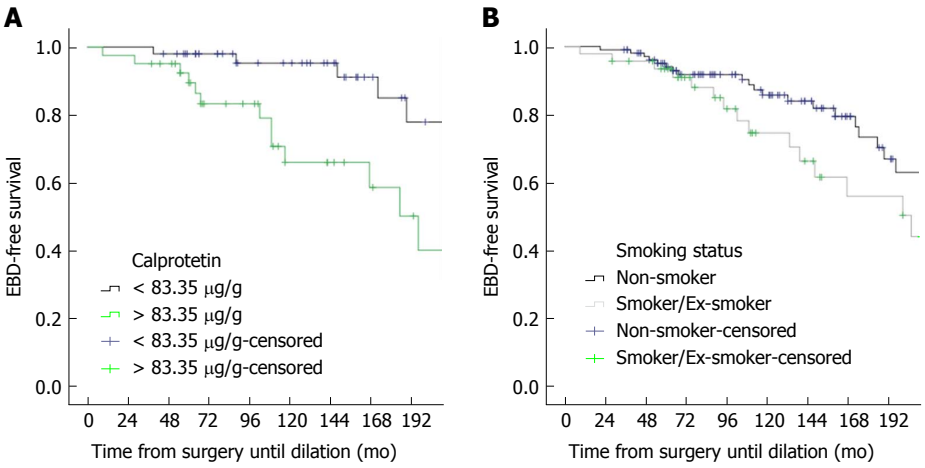

Figure 2 Kaplan-Meier curves showing time from surgery to dilation (in mo) considering calprotectin levels (A) and smoking status (B).

Table 2 Univariate and multivariate analysis of risk factors for need for dilation after surgery

Risk factors	Univariate analysis			Multivariate analysis		
	OR	95%CI	*P* value	OR	95%CI	*P* value
Significant in univariate and multivariate analysis						
Time between surgery and index colonoscopy	1.006	1.003-1.010	0.001	1.007	1.001-1.013	0.027
Lactoferrin levels	1.010	1.000-1.021	0.049	1.012	1.000-1.024	0.043
Significant in univariate analysis						
Subocclusive symptoms	6.155	2.546-14.880	< 0.001	-	-	0.180
No medical treatment with thiopurines	2.611	1.282-5.319	0.008	-	-	0.500
Age at index colonoscopy	1.028	1.002-1.055	0.033	-	-	0.932
Not significant in univariate nor multivariate analysis						
Smoking status	1.877	0.912-3.861	0.087			
B2 behavior	1.221	0.619-2.408	0.565			
B3 behavior	0.895	0.454-1.767	0.750			
Perianal disease	1.376	0.632-2.996	0.421			
Anti-TNF therapy	0.893	0.443-1.799	0.751			
C-reactive protein levels	0.975	0.935-1.016	0.229			
Calprotectin levels	1.001	1.000-1.002	0.125			
Harvey-Bradshaw index	1.111	0.936-1.318	0.229			
Disease duration	1.002	1.000-1.005	0.089			

OR: Odds ratio; CI: Confidence interval; B1: Non-stenosing and non-penetrating behaviour; B2: Stenosing behaviour; B1: Penetrating behaviour; TNF: Tumor necrosis factor.

or past history of smoking were associated with a shorter duration to dilation (HR = 3.877, 95%CI: 1.480-10.152, *P* = 0.006 and HR = 3.041, 95%CI: 1.213-7.627, *P* = 0.018) (Figure 2).

Endoscopic balloon dilation

EBD was performed in 26.5% (*n* = 43) of patients (Table 3). Technical success was achieved in 97.7% (*n* = 42). Repeat dilation was required in 62.8% (*n* = 27) of patients (long-term efficacy: 37.2%), with a total of 85 dilations being performed during the study period [median: 2 (1-5)], with a median balloon dilation of 18mm (range 10-18). Technical success was achieved in 95.3% (*n* = 81) without major AEs, and only one episode of self-limited bleeding (1.2%). All patients (*n* = 17) had improvement of obstructive symptoms. Median time to second dilation was 453.5 d (range: 152-1362).

Endoscopic recurrence, defined as modified Rutgeerts score ⩾ i2b was present in 60 patients (37.7%), of which 20 (33%) were diagnosed only after dilation of the anastomotic stricture. Following initial endoscopy and dilation, medical therapy was escalated in 38.5% of patients (*n* = 15; 3 began thiopurines and 14 began anti-TNF); however, escalation of medical therapy was probably driven by endoscopic recurrence (87%, *n* = 13) and not by anastomotic stricture presence, as suggested by escalation of therapy in 53% (*n* = 21) of the patients with endoscopic recurrence and no anastomotic stricture. No agreement was found between endoscopic recurrence and presence of stricture (*K* = 0.085, *P* = 0.273). Escalation of medical therapy did not decrease the need for repeat dilation; no other risk factors (gender, age, Montreal classification, perianal disease, smoking habits, previous medical therapy, presence of obstructive

Table 3 Baseline characteristics comparison between anastomotic and non-anastomotic strictures *n* (%)

Characteristic	Anastomotic strictures (*n* = 43)	Non-anastomotic strictures (*n* = 37)	*P* value
Female/male (*n*)	19/24	22/15	0.173
Disease duration in years (median; min-max)	19.2 (5.7-52.1)	16.3 (3.0-45.3)	0.236
Follow-up since 1st dilation in years (median; min-max)	4.4 (1.3-6.8)	2.9 (1.2-6.5)	< 0.001
Time between 1st and 2nd dilation in days (median; min-max)	453.5 (152-1362)	368 (157-1705)	0.796
Age at index colonoscopy (mean; standard deviation)	44.9 (± 12.2)	39 (± 12.2)	0.035
Montreal classification			
Age at diagnosis			0.368
A1	6 (14)	4 (12.9)	
A2	29 (67.4)	25 (80.6)	
A3	8 (18.6)	2 (6.5)	
Disease location			0.057
L1	23 (53.5)	9 (29)	
L2	1 (2.3)	4 (12.9)	
L3	17 (39.5%)	14 (45.2%)	
L1-4	2 (4.7%)	3 (9.7%)	
L3-4	-	1 (3.2%)	
Behavior			
B1	1 (2.3)	4 (12.9)	0.071
B2	22 (51.2)	19 (61.3)	0.387
B3	20 (46.5)	8 (25.8)	0.07
Perianal disease	12 (27.9)	9 (29)	0.916
Smoking habits			0.635
Non-smoker	22 (52.4)	11 (44)	
Ex-smoker	8 (19)	9 (36)	
Current smoker	12 (28.6)	5 (20)	
Medication at index colonoscopy			
Thiopurines	23 (53.5)	25 (67.6)	0.200
Anti-TNFα	17 (39.5)	19 (51.4)	0.289
Obstructive symptoms	15 (35.7)	10 (27.8)	0.454
C-reactive protein	2.8 (0.3-18.4)	6.95 (0.2-35.5)	0.126
Calprotectin	103.5 (5.9-1356)	283 (166-321)	0.789
Lactoferrin	7.66 (1.05-204.4)	10.7 (7.1-22.7)	0.429
Need to repeat dilation	27 (62.8)	15 (40.5)	0.047

TNFα: Tumor necrosis factor α.

symptoms, serum/fecal biomarkers) were found to influence need for repeat dilation. After initial dilation, 4.6% of the patients (*n* = 2) required anastomotic stricture resection due to worsening or recurrence of symptoms. The median time to progression to surgery was 35 mo (33.4-36.7).

Non-anastomotic strictures

During the study period, a total of 37 CD patients (40.5% males, *n* = 15) underwent a total of 59 EBD sessions of non-anastomotic strictures (17 in the ileum, 13 in the ileocecal valve, 2 in the ascending colon, 1 in the transverse colon, 3 in the descending colon and 1 in the sigmoid colon) (Table 3). Twenty-seven percent of the patients (*n* = 10) had obstructive symptoms, with a median HBI of 1 (0-10). Technical success was achieved in all patients (*n* = 37). Repeat dilation was required in 40.5% (*n* = 15) of patients (long-term efficacy: 59.5%), with a median balloon dilation of 16.5mm (range 10-18). Technical success and improvement in obstructive symptoms were achieved in all patients without AEs. Following EBD, medical therapy was escalated in 18.9% of patients (*n* = 7; 4 began thiopurines and 6 began anti-TNF). Median time to second dilation was 368 d (range: 157-1705). Only 1 patient (3%) required surgical resection. No risk factors were found to influence need for repeat dilation.

Anastomotic strictures vs non-anastomotic strictures

Baseline characteristics of patients with anastomotic and non-anastomotic strictures are shown in Table 3. Follow-up since 1st dilation was longer in patients with anastomotic strictures. Patients with anastomotic strictures had a greater recurrence of stenosis (63% *vs* 41%, *P* = 0.047). In the univariate analysis, absence of thiopurine medication (OR = 3.1, 95%CI: 1.2-7.9, *P* = 0.019) and anastomotic strictures (OR = 2.5, 95%CI: 1.01-6.1, *P* = 0.049) were the only factors found to influence need for repeat dilation.

Asymptomatic and symptomatic cohorts

No statistical significant differences were found between asymptomatic and symptomatic cohorts when comparing baseline disease characteristics, medical therapy at time of dilation, disease activity,

Table 4 Baseline disease characteristics, endoscopic balloon dilation procedure, need for further dilations, escalation of medical therapy and need for surgery between asymptomatic and symptomatic cohorts *n* (%)

Characteristic	Asymptomatic strictures[1] (*n* = 53)	Symptomatic strictures[1] (*n* = 25)	*P* value
Female/male (*n*)	25/28	16/9	0.165
Disease duration in years (median; min-max)	17.9 (2.9-45.3)	19.9 (5.3-52.1)	0.955
Follow-up since 1st dilation in years (median; min-max)	3.1 (1.3-6.8)	3.9 (2.1-6.7)	0.068
Time between 1st and 2nd dilation in days (median; min-max)	668 (157-2074)	877 (152-2242)	0.790
Age at index colonoscopy (mean ± SD)	41.7 ± 13.8	43 ± 9.3	0.425
Montreal classification			
Age at diagnosis			0.998
A1	7 (14)	3 (13.6)	
A2	36 (72)	16 (72.7)	
A3	7 (14)	3 (13.6)	
Disease location			0.319
L1	22 (44)	9 (40.9)	
L2	5 (10)	-	
L3	21 (42)	9 (40.9)	
L1-4	1 (2)	4 (18.2)	
L3-4	1 (2)	-	
Behavior			0.833
B1	4 (8)	1 (4.5)	
B2	28 (56)	12 (54.5)	
B3	18 (36)	9 (40.9)	
Perianal disease	15 (30)	6 (27.3)	0.815
Smoking habits			0.761
Non-smoker	24 (52.2)	8 (42.1)	
Ex-smoker	8 (17.4)	4 (21.2)	
Current smoker	14 (30.4)	7 (36.8)	
Previous surgery (ileocecal resection/right hemicolectomy)	27 (50.9)	15 (60)	0.454
Medication at index colonoscopy			
Thiopurines	33 (62.3)	13 (52)	0.390
Anti-TNFα	21 (39.6)	14 (56)	0.175
Combo	13 (24.5)	9 (36)	0.293
C-reactive protein	6.2 (0.2-35.5)	3.2 (0.3-19.4)	0.351
Calprotectin	107 (18.2-837)	340 (5.9-1356)	0.449
Lactoferrin	7.1 (1.1-102.6)	37.6 (4.0-204)	0.071
Therapeutic success	52 (98.1)	25 (100%)	0.377
Balloon diameter (median; min - max)	18 (10-18)	18 (13.5-18)	0.201
Adverse events	0 (0)	1 (4)	0.129
Need to repeat dilation	27 (50.9)	15 (60)	0.454
Number of dilations (median; min - max)	2 (1-5)	2 (1-5)	0.463
Escalation of medical therapy after dilation	13 (27.7)	8 (34.8)	0.541
Need for surgery after dilation	2 (4)	1 (4.2)	0.973

[1]Two patients had no information regarding presence of obstructive symptoms (one in each group). TNFα: Tumor necrosis factor α.

EBD procedure, need for further dilations, escalation of medical therapy and need for surgery (Table 4).

DISCUSSION

CD is characterized by chronic, recurrent, transmural inflammation; intestinal strictures are believed to result from partial healing and localized fibrosis[18]. Strictures develop unpredictably after surgery[6]. EBD has emerged as a bridging tool for management of CD strictures with favorable success rates and efficacy[10].

In this study, we found that almost one-third of CD patients develop an anastomotic stricture after ileocecal resection/right hemicolectomy. The mean age at first dilation was 42.6 years, which reflects their etiology as a complication of the surgery. Longer intervals after surgery and higher lactoferrin levels were associated with anastomotic strictures; time until dilation was lower in patients with calprotectin levels > 83.35 μg/g and current/past history of smoking. Previous studies have not studied the development of anastomotic strictures after surgery, however, as a progressive disease, anastomotic strictures will be more likely over time. Both anastomotic and *de novo* strictures have either inflammatory and/or fibrotic elements. Healing occurs in a defined pattern during bouts of activity and remission, with progression to luminal narrowing leading to stricture formation[17]; on the other hand, elevated serologic markers probably reflect the inflammatory component of the neo terminal ileum instead of the presence of an anastomotic stricture. While there is controversy regarding the effect of smoking on the disease phenotype, literature supports smoking as a factor in complicated disease[19].

Regarding EBD, our technical success was 97.7%, similar to literature (88%-100%)[20] and similar to non-

anastomotic strictures (100%), however, this was not associated with a permanent stricture dilation, as 63% of patients with anastomotic strictures and 41% of those with non-anastomotic strictures required additional dilation over a 4.4-year period. The fibrotic pathology of anastomotic strictures may be responsible for the lower response rate of EBD for non-anastomotic strictures. Re-dilation was as technically successful, supporting the evidence that repeated dilations do not reduce the procedural efficacy[20,21]. The rate of major AEs, including bowel perforation and significant bleeding, has been reported to be between 2%-6%[1,8]. AEs have been attributed to balloon size (25 mm diameter), pressure used to dilate and number of dilations per session. Our data confirm safety of EBD for CD strictures. We had no serious AEs, which may be explained by the careful patient selection, fluoroscopy to evaluate stricture characteristics and monitoring, maximum balloon diameter of 18 mm, use of CO_2 insufflation, and endoscopists experience.

Long-term outcome following EBD varies. In our study, a long-term efficacy of 37.2% for anastomotic strictures and 59.5% for non-anastomotic strictures was achieved during a follow-up period of 4.4 years. Even though follow-up was longer, results were somewhat inferior to previous studies (52%-69%) when considering only anastomotic strictures. However, EBD in previous studies was symptom-driven, while in ours, EBD was performed for strictures that did not allow passage with a colonoscope, regardless of patients' symptoms. Besides, EBD delayed time until surgery, with only 3 patients (2 with anastomotic and 1 with non-anastomotic strictures) requiring surgery during follow-up period, suggesting a benefit of EBD. A recent pooled analysis reported a technical success, clinical success, long-term symptomatic and surgical recurrence rates of 89%, 81%, 48% and 29%, respectively[22]; these data are almost exclusively derived from retrospective cohort studies and may somewhat overestimate the actual benefit. In 2013, the European Crohn's and Colitis Organisation stated that EBD was safe and effective and allowed surgery to be avoided in CD patients with anastomotic strictures[23]. The overall technical success rate in the meta-analysis performed by Hassan *et al*[8] was 86% (71%-100%), while 41% of patients required repeated EBD allowing an overall long-term clinical efficacy (avoidance of surgery) rate of 58% during a median follow up of 33 mo.

Risk factors associated with need for subsequent dilation have been inconsistent. Longer disease duration was associated with a shorter time to repeat dilation[12]; technical success of dilation[8,24,25], length of stricture[8,26], and non-ulcerated stricture[27] were found to be associated with a successful procedure. In our study, the only factors found to influence need for repeat dilation (in the univariate analysis) were absence of thiopurine medications and anastomotic strictures. Escalation of medical therapy did not decrease the need for repeat dilation. Considering therapeutic strategy, Thienpont *et al*[10] reported no significant effect of systemic medical therapy after dilation on redilation or surgery, while Honzawa *et al*[28] found that prior use of immunomodulatory drugs improved the clinical outcome of EBD for intestinal strictures in patients with CD. Patients in our study may also have had more severe disease, as demonstrated by the majority receiving immunossupressants at the time of index colonoscopy (immunomodulators: 68.5%; biological therapy: 36.4%), as well as the high rate of repeat dilation. Despite the well-known deleterious association between tobacco use and CD activity, with increased risk of recurrence after surgery and EBD, we did not find any association between smoking and long-term outcome of EBD. Disease activity assessed by serologic markers, endoscopy, and clinical variables such as HBI, disease duration or time between surgery and dilation did not predict the need for repeat dilation, in accordance with previously published data[10,21].

It is controversial whether asymptomatic strictures should be endoscopically treated. Previous studies have found no correlation between patient´s symptoms and clinical scores and endoscopic/radiographic findings after intestinal resection[29-31]. In our study, only 2 patients presented with an HBI > 7 and only 27 patients complained of obstructive symptoms, despite 47 having an anastomotic stricture. Serum biomarkers did not correlate with endoscopic recurrence or presence of strictures, supporting the belief that using only symptoms or C-reactive protein levels to make treatment decisions may increase the risk of disease progression and AEs. Our group believes that dilation of strictures, despite symptoms, has impact on patients' management and disease course, allowing evaluation of disease activity and therapeutic adjustments. If EBD was not performed, a diagnosis of endoscopic recurrence would not have been possible in 33% of patients, all with normal biomarkers. On the other hand, we did not find any differences between asymptomatic and symptomatic cohorts regarding disease characteristics as well EBD peculiarities.

Limitations of our study include its retrospective nature, being conducted in a tertiary referral center (with referral or selection bias), lack of a control group (medical and surgical therapy), uncertainty of the degree of luminal narrowing caused by inflammation *vs* fibrosis and escalation of medical treatment biased toward those having active IBD.

In conclusion, smoking habits and longer disease duration after surgery are associated with a higher risk of anastomotic strictures. EBD is a feasible, simple, effective and safe alternative to surgery, with the possibility of being repeated as needed, with excellent symptomatic response, as well as good short-term and long-term outcomes, postponing or avoiding surgery. Considering that a significant number of patients with significant strictures remain asymptomatic with normal

biomarkers, and the fact that the disease continues to evolve proximal to the strictures, we believe EBD should be considered for all strictures not transposable by a colonoscope, regardless of the presence or absence of symptoms, in order to adjust treatment in an attempt to alter the natural history of the disease. Thus, EBD is useful not only for symptom resolution but also for evaluating mucosal healing.

ARTICLE HIGHLIGHTS

Research background

Strictures in Crohn's disease (CD) develop during the course of the disease or as the presenting feature. More than half of CD patients will need surgery within the first 10 years of diagnosis. Medical therapy for stricture management is limited due to the fibrotic nature. Endoscopic balloon dilation (EBD) has been proposed as a safe and effective therapeutic intervention for CD strictures, particularly for ileocecal and anastomotic strictures.

Research motivation

Data on long term efficacy and safety of EBD are limited due to lack of long-term outcome and small cohorts. Up to now there are also some uncertainties regarding the factors associated with long term success rate. Smoking status and disease activity status at the time of dilation may affect outcome of stricture dilation, though many studies are limited by short follow-up durations and small cohorts. Furthermore, as the primary therapeutic goal of CD has shifted from clinical remission to achieving mucosal healing, it may be important to access the mucosa proximal to strictures to evaluate disease recurrence and escalate therapy if needed.

Research objectives

This study aimed to evaluate anastomotic stricture development after intestinal resection in CD and demonstrate long-term efficacy and safety center of EBD in CD anastomotic and *de novo* strictures in a large referral centre cohort and determine the impact of dilation on the diagnosis of subclinical postoperative endoscopic recurrence.

Research methods

CD patients who had undergone ileocecal resection/right hemicolectomy referred for endoscopic evaluation between March 2010 to February 2015 were included in this study. CD patients with non-anastomotic strictures who underwent EBD during the study period were included as a control group. EBD was performed for strictures that would not allow passage with a colonoscope, regardless of patients' symptoms. Technical success was defined as the ability to pass the colonoscope through the stricture into the neoileum following dilation. Clinical success was defined as improvement of obstructive symptoms (in symptomatic patients). All patients who underwent dilation were endoscopically reevaluated 6-12 mo later. Long-term efficacy was defined as avoidance of surgical resection or repeat dilation after the initial dilation. Patients were followed until stricture resection, last clinic follow-up, or censor date of March, 2017. Escalation of medical therapy was defined as initiation of a thiopurine or anti-TNF within 6 months of first dilation, as determined by global physician assessment.

All data were prospectively collected in a database created for this purpose. After a 5 year follow up period all data were arranged, processed and analyzed with SPSS® v.24.0 data (Statistical Package for Social Sciences).

Research results

In this study we found that almost one-third of CD patients developed an anastomotic stricture after ileocecal resection/right hemicolectomy. Longer periods between surgery and *index* colonoscopy and higher lactoferrin levels were associated with the presence of stricture after surgery. Calprotectin levels > 83.35 μg/g and current or past history of smoking were associated with a shorter time until need for dilation (HR = 3.877, 95%CI: 1.480-10.152 and HR = 3.041, 95%CI: 1.213-7.627). Technical success of EBD was 97.7% and 100% for anastomotic and non-anastomotic strictures, respectively, and 63% and 41% of the patients needed repeat dilation during the 4.4-year follow-up. Anastomotic strictures had a greater need for repeat dilation (63% *vs* 41%, *P* = 0.047). No differences were found between asymptomatic and symptomatic cohorts. Disease recurrence was diagnosed only after EBD in a third of patients.

Research conclusions

EBD is a feasible, simple, effective and safe alternative to surgery, with the possibility of being repeated as needed, with excellent symptomatic response, as well as good short-term and long-term outcomes, postponing or avoiding surgery. Considering that a significant number of patients with significant strictures remain asymptomatic with normal biomarkers, and the fact that the disease continues to evolve proximal to the strictures, we advocate EBD for all strictures regardless of the presence or absence of symptoms, in order to adjust treatment in an attempt to alter the natural history of the disease. Thus, EBD is useful not only for symptom resolution but also for evaluating mucosal healing.

REFERENCES

1 **Morar PS**, Faiz O, Warusavitarne J, Brown S, Cohen R, Hind D, Abercrombie J, Ragunath K, Sanders DS, Arnott I, Wilson G, Bloom S, Arebi N; Crohn's Stricture Study (CroSS) Group. Systematic review with meta-analysis: endoscopic balloon dilatation for Crohn's disease strictures. *Aliment Pharmacol Ther* 2015; **42**: 1137-1148 [PMID: 26358739 DOI: 10.1111/apt.13388]

2 **Bernell O**, Lapidus A, Hellers G. Risk factors for surgery and postoperative recurrence in Crohn's disease. *Ann Surg* 2000; **231**: 38-45 [PMID: 10636100 DOI: 10.1097/00000658-200001000-00006]

3 **Olaison G**, Smedh K, Sjödahl R. Natural course of Crohn's disease after ileocolic resection: endoscopically visualised ileal ulcers preceding symptoms. *Gut* 1992; **33**: 331-335 [PMID: 1568651 DOI: 10.1136/gut.33.3.331]

4 **Rutgeerts P**, Geboes K, Vantrappen G, Kerremans R, Coeneg-rachts JL, Coremans G. Natural history of recurrent Crohn's disease at the ileocolonic anastomosis after curative surgery. *Gut* 1984; **25**: 665-672 [PMID: 6735250 DOI: 10.1136/gut.25.6.665]

5 **Landsend E**, Johnson E, Johannessen HO, Carlsen E. Long-term outcome after intestinal resection for Crohn's disease. *Scand J Gastroenterol* 2006; **41**: 1204-1208 [PMID: 16990206]

6 **Kurer MA**, Stamou KM, Wilson TR, Bradford IM, Leveson SH. Early symptomatic recurrence after intestinal resection in Crohn's disease is unpredictable. *Colorectal Dis* 2007; **9**: 567-571 [PMID: 17573754 DOI: 10.1111/j.1463-1318.2006.01202.x]

7 **Peyrin-Biroulet L**, Loftus EV Jr, Colombel JF, Sandborn WJ. The natural history of adult Crohn's disease in population-based cohorts. *Am J Gastroenterol* 2010; **105**: 289-297 [PMID: 19861953 DOI: 10.1038/ajg.2009.579]

8 **Hassan C**, Zullo A, De Francesco V, Ierardi E, Giustini M, Pitidis A, Taggi F, Winn S, Morini S. Systematic review: Endoscopic dilatation in Crohn's disease. *Aliment Pharmacol Ther* 2007; **26**: 1457-1464 [PMID: 17903236 DOI: 10.1111/j.1365-2036.2007.03532.x]

9 **Gustavsson A**, Magnuson A, Blomberg B, Andersson M, Halfvarson J, Tysk C. Endoscopic dilation is an efficacious and safe treatment of intestinal strictures in Crohn's disease. *Aliment Pharmacol Ther* 2012; **36**: 151-158 [PMID: 22612326 DOI: 10.1111/j.1365-2036.2012.05146.x]

10 **Thienpont C**, D'Hoore A, Vermeire S, Demedts I, Bisschops R, Coremans G, Rutgeerts P, Van Assche G. Long-term outcome of endoscopic dilatation in patients with Crohn's disease is not affected by disease activity or medical therapy. *Gut* 2010; **59**: 320-324 [PMID: 19840991 DOI: 10.1136/gut.2009.180182]

11 **Nanda K**, Courtney W, Keegan D, Byrne K, Nolan B, O' Donoghue D, Mulcahy H, Doherty G. Prolonged avoidance of repeat surgery with endoscopic balloon dilatation of anastomotic strictures in Crohn's disease. *J Crohns Colitis* 2013; **7**: 474-480 [PMID: 22898397 DOI: 10.1016/j.crohns.2012.07.019]

12 **Ding NS**, Yip WM, Choi CH, Saunders B, Thomas-Gibson S, Arebi N, Humphries A, Hart A. Endoscopic Dilatation of Crohn' s Anastomotic Strictures is Effective in the Long Term, and

Escalation of Medical Therapy Improves Outcomes in the Biologic Era. *J Crohns Colitis* 2016; **10**: 1172-1178 [PMID: 26971054 DOI: 10.1093/ecco-jcc/jjw072]
13 **Saunders BP**, Brown GJ, Lemann M, Rutgeerts P. Balloon dilation of ileocolonic strictures in Crohn's disease. *Endoscopy* 2004; **36**: 1001-1007 [PMID: 15520920 DOI: 10.1055/s-2004-825962]
14 **Morini S**, Hassan C, Lorenzetti R, Zullo A, Cerro P, Winn S, Giustini M, Taggi F. Long-term outcome of endoscopic pneumatic dilatation in Crohn's disease. *Dig Liver Dis* 2003; **35**: 893-897 [PMID: 14703886 DOI: 10.1016/j.dld.2003.06.001]
15 **Thomas-Gibson S**, Brooker JC, Hayward CM, Shah SG, Williams CB, Saunders BP. Colonoscopic balloon dilation of Crohn's strictures: a review of long-term outcomes. *Eur J Gastroenterol Hepatol* 2003; **15**: 485-488 [PMID: 12702904 DOI: 10.1097/01.meg.0000059110.41030.bc]
16 **Lian L**, Stocchi L, Remzi FH, Shen B. Comparison of Endoscopic Dilation vs Surgery for Anastomotic Stricture in Patients With Crohn's Disease Following Ileocolonic Resection. *Clin Gastroenterol Hepatol* 2017; **15**: 1226-1231 [PMID: 27816758 DOI: 10.1016/j.cgh.2016.10.030]
17 **Rutgeerts P**, Geboes K, Vantrappen G, Beyls J, Kerremans R, Hiele M. Predictability of the postoperative course of Crohn's disease. *Gastroenterology* 1990; **99**: 956-963 [PMID: 2394349]
18 **Mudter J**, Neurath MF. Insight into Crohn's disease pathomorphology. *Abdom Imaging* 2012; **37**: 921-926 [PMID: 22476334 DOI: 10.1007/s00261-012-9885-3]
19 **Lindberg E**, Järnerot G, Huitfeldt B. Smoking in Crohn's disease: effect on localisation and clinical course. *Gut* 1992; **33**: 779-782 [PMID: 1624159 DOI: 10.1136/gut.33.6.779]
20 **Chen M**, Shen B. Comparable short- and long-term outcomes of colonoscopic balloon dilation of Crohn's Disease and benign non-Crohn's Disease strictures. *Inflamm Bowel Dis* 2014; **20**: 1739-1746 [PMID: 25153504 DOI: 10.1097/MIB.0000000000000145]
21 **Atreja A**, Aggarwal A, Dwivedi S, Rieder F, Lopez R, Lashner BA, Brzezinski A, Vargo JJ, Shen B. Safety and efficacy of endoscopic dilation for primary and anastomotic Crohn's disease strictures. *J Crohns Colitis* 2014; **8**: 392-400 [PMID: 24189349 DOI: 10.1016/j.crohns.2013.10.001]
22 **Bettenworth D**, Gustavsson A, Atreja A, Lopez R, Tysk C, van Assche G, Rieder F. A Pooled Analysis of Efficacy, Safety, and Long-term Outcome of Endoscopic Balloon Dilation Therapy for Patients with Stricturing Crohn's Disease. *Inflamm Bowel Dis* 2017; **23**: 133-142 [PMID: 28002130 DOI: 10.1097/MIB.0000000000000988]
23 **Annese V**, Daperno M, Rutter MD, Amiot A, Bossuyt P, East J, Ferrante M, Götz M, Katsanos KH, Kießlich R, Ordás I, Repici A, Rosa B, Sebastian S, Kucharzik T, Eliakim R; European Crohn's and Colitis Organisation. European evidence based consensus for endoscopy in inflammatory bowel disease. *J Crohns Colitis* 2013; **7**: 982-1018 [PMID: 24184171 DOI: 10.1016/j.crohns.2013.09.016]
24 **Scimeca D**, Mocciaro F, Cottone M, Montalbano LM, D'Amico G, Olivo M, Orlando R, Orlando A. Efficacy and safety of endoscopic balloon dilation of symptomatic intestinal Crohn's disease strictures. *Dig Liver Dis* 2011; **43**: 121-125 [PMID: 20561831 DOI: 10.1016/j.dld.2010.05.001]
25 **Couckuyt H**, Gevers AM, Coremans G, Hiele M, Rutgeerts P. Efficacy and safety of hydrostatic balloon dilatation of ileocolonic Crohn's strictures: a prospective longterm analysis. *Gut* 1995; **36**: 577-580 [PMID: 7737567 DOI: 10.1136/gut.36.4.577]
26 **Mueller T**, Rieder B, Bechtner G, Pfeiffer A. The response of Crohn's strictures to endoscopic balloon dilation. *Aliment Pharmacol Ther* 2010; **31**: 634-639 [PMID: 20047581 DOI: 10.1111/j.1365-2036.2009.04225.x]
27 **Hoffmann JC**, Heller F, Faiss S, von Lampe B, Kroesen AJ, Wahnschaffe U, Schulzke JD, Zeitz M, Bojarski C. Through the endoscope balloon dilation of ileocolonic strictures: prognostic factors, complications, and effectiveness. *Int J Colorectal Dis* 2008; **23**: 689-696 [PMID: 18338175 DOI: 10.1007/s00384-008-0461-9]
28 **Honzawa Y**, Nakase H, Matsuura M, Higuchi H, Toyonaga T, Matsumura K, Yoshino T, Okazaki K, Chiba T. Prior use of immunomodulatory drugs improves the clinical outcome of endoscopic balloon dilation for intestinal stricture in patients with Crohn's disease. *Dig Endosc* 2013; **25**: 535-543 [PMID: 23363364 DOI: 10.1111/den.12029]
29 **Cellier C**, Sahmoud T, Froguel E, Adenis A, Belaiche J, Bretagne JF, Florent C, Bouvry M, Mary JY, Modigliani R. Correlations between clinical activity, endoscopic severity, and biological parameters in colonic or ileocolonic Crohn's disease. A prospective multicentre study of 121 cases. The Groupe d'Etudes Thérapeutiques des Affections Inflammatoires Digestives. *Gut* 1994; **35**: 231-235 [PMID: 7508411 DOI: 10.1136/gut.35.2.231]
30 **Landi B**, Anh TN, Cortot A, Soule JC, Rene E, Gendre JP, Bories P, See A, Metman EH, Florent C. Endoscopic monitoring of Crohn's disease treatment: a prospective, randomized clinical trial. The Groupe d'Etudes Therapeutiques des Affections Inflammatoires Digestives. *Gastroenterology* 1992; **102**: 1647-1653 [PMID: 1568574 DOI: 10.1016/0016-5085(92)91725-J]
31 **Regueiro M**, Kip KE, Schraut W, Baidoo L, Sepulveda AR, Pesci M, El-Hachem S, Harrison J, Binion D. Crohn's disease activity index does not correlate with endoscopic recurrence one year after ileocolonic resection. *Inflamm Bowel Dis* 2011; **17**: 118-126 [PMID: 20848538 DOI: 10.1002/ibd.21355]

P- Reviewer: Dogan UB, Gassler N, Lakatos PL, Shi R
S- Editor: Wei LJ **L- Editor**: A **E- Editor**: Huang Y

World Journal of Gastroenterology

Submit a Manuscript: http://www.f6publishing.com

World J Gastroenterol 2017 November 7; 23(41): 7407-7414

DOI: 10.3748/wjg.v23.i41.7407

ISSN 1007-9327 (print) ISSN 2219-2840 (online)

ORIGINAL ARTICLE

Retrospective Study

Survival analysis based on human epidermal growth factor 2 status in stage Ⅱ-Ⅲ gastric cancer

Jang Ho Cho, Jae Yun Lim, Jae Yong Cho

Jang Ho Cho, Jae Yun Lim, Jae Yong Cho, Division of Medical Oncology, Department of Internal Medicine, Gangnam Severance Hospital, Yonsei University College of Medicine, Seoul 135-720, South Korea

ORCID number: Jang Ho Cho (0000-0002-3429-4321); Jae Yun Lim (0000-0002-7321-9068); Jae Yong Cho (0000-0002-0926-1819).

Author contributions: Lim JY and Cho JY designed the study; Cho JH collected the data, performed data analysis and wrote the manuscript; Cho JH and Cho JY were involved in result interpretation and approved the final version of this manuscript.

Institutional review board statement: The study was approved by the Yonsei University Health System Institutional Review Board (IRB #3-2013-0188).

Informed consent statement: All study participants, or their legal guardian, provided informed written consent prior to study enrollment.

Conflict-of-interest statement: None.

Data sharing statement: No additional data are available.

Manuscript source: Unsolicited manuscript

Correspondence to: Jae Yong Cho, MD, PhD, Department of Medical Oncology, Gangnam Severance Hospital, Yonsei University College of Medicine, Dogok 1-dong, Gangnam-gu, Seoul 135-720, South Korea. chojy@yuhs.ac

Telephone: +82-2-20194363
Fax: +82-2-34633882

Received: July 12, 2017
Peer-review started: July 13, 2017
First decision: August 10, 2017
Revised: August 24, 2017
Accepted: September 6, 2017
Article in press: September 5, 2017
Published online: November 7, 2017

Abstract

AIM

To investigate human epidermal growth factor 2 (HER2) overexpression and validate its prognostic effect in stage Ⅱ-Ⅲ gastric cancer.

METHODS

We reviewed the data of patients who were diagnosed with gastric cancer between March 2008 and October 2013 at the Yonsei University Medical Center. Among these patients, 384 patients who met the inclusion criteria were analyzed retrospectively.

RESULTS

Thirty-two (8.3%) of the 384 stage Ⅱ-Ⅲ gastric cancer patients exhibited HER2 overexpression. The median follow-up duration was 26.0 mo. HER2-negative patients had superior recurrence-free survival (RFS) compared to HER2-positive patients (HR = 0.52, 95%CI: 0.30-0.89; *P* = 0.015). The median overall survival (OS) was significantly prolonged in the HER2-negative group compared with the HER2-positive group (55.0 mo *vs* 38.0 mo, HR = 0.43, 95%CI: 0.21-0.88, *P* = 0.021). OS was also prolonged in HER2-negative patients who received adjuvant chemotherapy compared to HER2-positive patients (55.0 *vs* 38.0

mo, HR = 0.42, 95%CI: 0.18-1.00, *P* = 0.051). In patients who did not receive adjuvant chemotherapy, the median RFS was prolonged in the HER2-negative group compared to the HER2-positive group (not reached *vs* 12.0 mo, HR = 0.17, 95%CI: 0.06-0.49, *P* = 0.001). In a multivariate analysis, HER2 status (HR = 0.421, 95%CI: 0.206-0.861, *P* = 0.018) and Eastern Cooperative Oncology Group performance status (HR = 2.002, 95%CI: 1.530-2.618, *P* < 0.001) were independent predictors of OS.

CONCLUSION

Our findings showed that HER2-positive patients had inferior OS and RFS. Stage Ⅱ-Ⅲ HER2-positive patients might be potential candidates for targeted therapies involving trastuzumab.

Key words: Trastuzumab; Gastric neoplasm; Human epidermal growth factor 2

Core tip: Our study aimed to investigate human epidermal growth factor 2 (HER2) overexpression and validate its prognostic effect in stage Ⅱ-Ⅲ gastric cancer. Clinical data from 384 patients were analyzed. HER2-positive patients had inferior overall survival and recurrence-free survival. Stage Ⅱ-Ⅲ HER2-positive patients might be potential candidates for targeted therapies involving trastuzumab.

Cho JH, Lim JY, Cho JY. Survival analysis based on human epidermal growth factor 2 status in stage Ⅱ-Ⅲ gastric cancer. *World J Gastroenterol* 2017; 23(41): 7407-7414 Available from: URL: http://www.wjgnet.com/1007-9327/full/v23/i41/7407.htm DOI: http://dx.doi.org/10.3748/wjg.v23.i41.7407

INTRODUCTION

Gastric cancer is the fifth most common type of cancer, and half of all cases worldwide occur in East Asia[1]. In addition, gastric cancer is the third leading cause of cancer-related deaths worldwide[1,2]. In South Korea, gastric cancer is the second most commonly diagnosed cancer after thyroid cancer, and remains the third-leading cause of cancer-related mortality after lung cancer and hepatocellular carcinoma. More than 30000 patients are diagnosed annually in South Korea, and more than 10000 patients die annually[3]. Curative resection is the gold standard of treatment, and systemic chemotherapy prolongs the survival of patients with recurrent or metastatic gastric cancer[4]. However, the 5-year survival rates for advanced or metastatic gastric cancer are only approximately 5%-20%, with a median overall survival duration of < 1 year. Classically, only cytotoxic agents have been administered for malignant cancer. Recently, however, molecular pathologic research has been widely conducted, and molecular targeted agents have been applied for cancer treatment, leading to personalized treatment. The identification of biomarkers predictive of prognosis and drug responses is an important issue.

One well-established target is human epidermal growth factor receptor 2 (HER2, ERBB2), one of a family of receptors associated with tumor cell proliferation, apoptosis, adhesion, migration, and differentiation. Increasing evidence suggests that HER2 is an important biomarker and key driver of tumorigenesis in gastric cancer, with studies reporting amplification or overexpression in 7%-34% of tumors[5-7]. Despite conflicting results[8,9], some studies have suggested that HER2 positivity is associated with poor outcomes and an aggressive profile in gastric cancer.

Trastuzumab (Herceptin), a monoclonal antibody that targets HER2, induces antibody-dependent cellular cytotoxicity, inhibits HER2-mediated signaling, and prevents cleavage of the extracellular domain of HER2[10]. In HER2-positive breast cancers, trastuzumab has yielded survival advantages in patients with early and metastatic disease and is now the standard of care. In patients with metastatic breast cancer, high levels of HER2 protein expression and amplification indicate better outcomes with trastuzumab[11-14].

The antitumor activity of trastuzumab, as observed in human gastric cancer xenograft models, warrants the consideration of its use in clinical treatment regimens for gastric cancer patients in combination with various chemotherapeutic agents[15]. In 2010, the Trastuzumab for Gastric Cancer (ToGA) trial, an international phase 3, open-label, randomized controlled trial, demonstrated a significant survival benefit of trastuzumab plus chemotherapy in patients with advanced gastric or gastro-esophageal junction (GEJ) cancer whose tumors were found to overexpress the HER2 protein *via* immunohistochemistry or gene *via* fluorescence *in-situ* hybridization (FISH). This trial revealed significant increases in overall survival (OS, 13.8 mo *vs* 11.1 mo), progression-free survival (PFS, 6.7 mo *vs* 5.5 mo), and overall response rates (47% *vs* 35%). Furthermore, an exploratory analysis identified that patients with strong HER2 protein expression [immunohistochemistry [(IHC) 3(+) or IHC 2(+)/FISH (+)] were more likely to exhibit improved OS with the addition of trastuzumab (16.0 mo *vs* 11.8 mo)[16]. Subsequently, trastuzumab combined with chemotherapy was established as a standard treatment for HER2-positive gastric cancer patients.

Efforts to improve survival among Korean gastric cancer patients begin with an understanding of the clinical practice patterns actually used in Korean hospitals. This study aimed to investigate the frequency of HER2 overexpression among gastric cancer

patients and evaluate the relationship between HER2 overexpression and prognosis.

MATERIALS AND METHODS

Patient characteristics

We reviewed the data of 4680 patients who were diagnosed with gastric cancer between March 2008 and October 2013 at the Yonsei University Medical Center in South Korea. Among these patients, the inclusion criteria were as follows: (1) histologically confirmed gastric adenocarcinoma; (2) diagnosis between 2006 and 2013; and (3) HER2 expression status evaluation in a primary gastric tumor. Patients with a second primary tumor within 5 years were excluded. A total of 384 patients met the eligibility criteria. We analyzed the data of patients who were initially diagnosed stage Ⅱ or Ⅲ on the pathology report (according to the American Joint Committee on Cancer TNM staging, 7th edition). Approximately 15% of the total patient cohort was expected to be HER2-positive based on the proportions and prognostic power of HER2 status[5-7]. The study was approved by the Yonsei University Health System Institutional Review Board (IRB #3-2013-0188).

Clinicopathologic parameters

Clinicopathologic parameters were collected from outpatient clinical or admission records, including age, sex, Eastern Cooperative Oncology Group (ECOG) performance status, diagnosis date, curative resection date, adjuvant chemotherapy (regimen and duration), recurrence date, last follow-up date, date of death, histologic subtype, TNM stage, HER2 IHC, and HER2 FISH; information regarding patient survival was obtained from the Korean National Statistics Registry Database.

Outcome variables

HER2 overexpression and gene amplification were examined with semiquantitative standardized IHC staining using the DAKO-HercepTest™, silver *in situ* hybridization, and FISH. HER2 IHC results were classified as 0/1+/2+/3+. HER2 positivity was defined as (1) IHC of 3+ or (2) IHC of 2+ with *HER2*-FISH amplification. HER2 negativity was defined as (1) IHC of 0/1+ or (2) IHC of 2+ with no *HER2*-FISH amplification. OS was defined as the duration from gastrectomy to gastric cancer-specific death or the last follow-up. RFS was measured from gastrectomy to recurrence in patients diagnosed with stage Ⅱ or Ⅲ gastric cancer.

Statistical analysis

All statistical analyses were performed using SPSS version 21.0 (IBM Co., Armonk, NY, United States). For continuous variables, two-tailed Student's *t*-tests were used to compare the demographic and clinical characteristics. The χ^2 was used for discrete variables. Survival rates and 95%CI were calculated using the Kaplan-Meier method. The influences of covariates on survival length between the two treatment arms were assessed using the log-rank test. A $P < 0.05$ was considered significant. Significant variables in the univariate analysis were entered in the multivariate analysis using the Cox proportional hazards model. Tumor response was assessed using the Response Evaluation Criteria in Solid Tumors version 1.1.

RESULTS

Demographics and baseline disease characteristics

A total of 384 patients with HER2 status data were analyzed in this study. The patients' baseline characteristics are described in Table 1. The median patient age was 61.7 years (range: 28-90 years), and 238 patients (62.0%) were men. Nearly all patients (99.7%) had an ECOG performance status of 0 or 1. Pathologic differentiation was confirmed as well differentiated, moderately differentiated, or poorly differentiated tubular adenocarcinoma, signet ring cell carcinoma, and other in 10 (2.6%), 98 (25.5%), 207 (53.9%), 60 (15.6%), and 9 cases (2.3%), respectively.

HER2 overexpression status was confirmed based on an IHC result of 3+ in 28 patients (7.3%) and based on an IHC of 2+/FISH (+) in 4 patients (1.0%). The HER2 status was confirmed by FISH alone in 5 patients (1.3%).

Clinical outcomes

As shown in Table 1, 32 (8.3%) of the 384 gastric adenocarcinoma patients with stage Ⅱ to Ⅲ disease exhibited HER2 overexpression. Seventeen (8.8%) stage Ⅱ patients and 15 (7.8%) stage Ⅲ patients had HER2 overexpression.

A high correlation between HER2 expression and the intestinal histologic type has been confirmed in recent studies[5]. Our study showed a higher rate of HER2 overexpression in the intestinal type than in the diffuse type (17% *vs* 2.5%, $P < 0.001$; Table 2). In the ToGA trial, HER2 positivity differed significantly by histological subtype (intestinal 34%, diffuse 6%, and mixed 20%)[16]. Moreover, numerous studies have reported that HER2 expression is more common in GEJ cancers than in gastric cancers. Our study found 20% and 9.5% HER2 expression in GEJ and gastric cancers, respectively ($P = 0.008$; Table 2). These results are similar to those of the ToGA study, in which HER2 positivity was found in 32% and 18% of GEJ and gastric cancers, respectively[16].

The median follow-up duration was 26.0 mo (95%CI: 24.9-27.1 mo). In stage Ⅱ and Ⅲ gastric

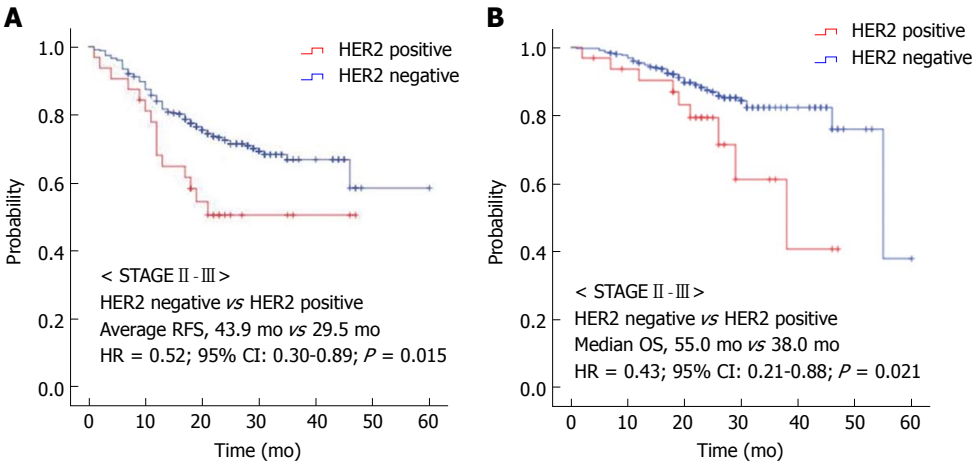

Figure 1 Kaplan-Meier survival curves. A: Recurrence-free survival (RFS) and B: Overall survival (OS) based on human epidermal growth factor 2 (HER2) expression in stage Ⅱ-Ⅲ gastric cancer patients. HR: Hazard ratio.

Table 1 Demographics and baseline characteristics *n* (%)

Characteristic	Stage Ⅱ (*n* = 193, Ⅱ A: 97, Ⅱ B: 96)	Stage Ⅲ (*n* = 191, Ⅲ A: 55, Ⅲ B: 63, Ⅲ C: 73)
Median age (range, yr)	61.27 ± 12.75 (28-90)	62.21 ± 13.20 (33-86)
Gender		
Male	124 (64.2)	114 (59.7)
Female	69 (35.8)	77 (40.3)
ECOG PS		
0	119 (61.7)	76 (39.8)
1	74 (38.3)	114 (59.7)
2	0	1 (0.5)
HER2 status		
HER2 positive		
IHC 3 (+)	15 (7.8)	13 (6.8)
IHC 2 (+)/FISH (+)	2 (1.0)	2 (1.0)
HER2 negative		
IHC 2 (+)/FISH (-)	6 (3.1)	4 (2.1)
IHC 1 (+) or 0	168 (87.1)	169 (88.5)
IHC not done/FISH (-)	2 (1.0)	3 (1.6)
Pathologic differentiation		
WD TA	7 (3.6)	3 (1.6)
MD TA	54 (28.0)	44 (23.0)
PD TA	96 (49.7)	111 (58.1)
Signet ring cell carcinoma	33 (17.1)	27 (14.1)
Others	3 (1.6)	6 (3.2)
T stage		
T1	17 (88.1)	0
T2	48 (24.9)	4 (2.1)
T3	90 (46.6)	51 (26.7)
T4	38 (19.7)	136 (71.2)
N stage		
N0	97 (50.3)	1 (0.5)
N1	60 (31.0)	30 (15.7)
N2	33 (17.1)	52 (27.3)
N3	3 (1.6)	108 (56.5)
Received adjuvant chemotherapy		
Yes	141 (73.1)	161 (84.3)
No	52 (26.9)	30 (15.7)

ECOG PS: Eastern Cooperative Oncology Group Performance Status; HER2: Human epidermal growth factor receptor 2; GEJ: Gastroesophageal junction; IHC: Immunohistochemistry; FISH: Fluorescence in situ hybridization; WD: Well differentiated; MD: Moderately differentiated; PD: Poorly differentiated; TA: Tubular adenocarinoma.

cancer patients, HER2-negative patients had improved RFS compared with HER2-positive patients (HR = 0.52, 95%CI: 0.30-0.89, *P* = 0.015, Figure 1A). The median OS was significantly prolonged in the HER2-negative group compared with the HER2-positive group (55.0 mo *vs* 38.0 mo, HR = 0.43, 95%CI: 0.21-0.88, *P* =

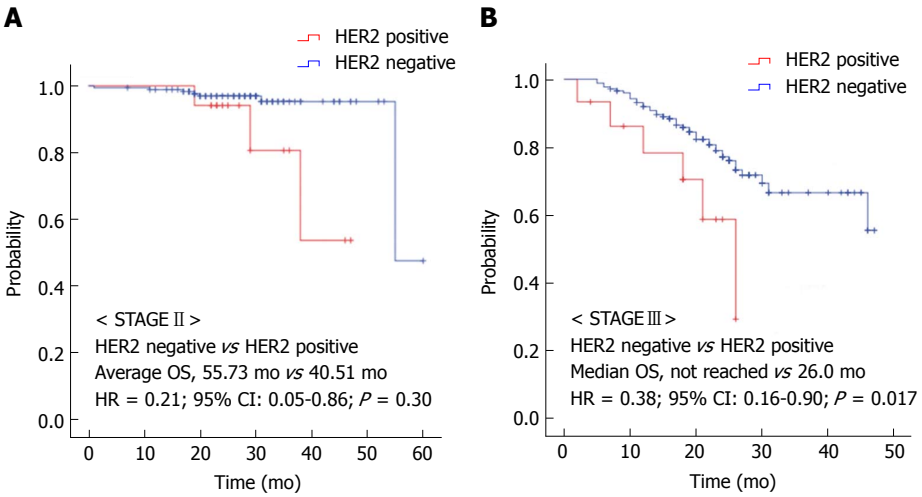

Figure 2 Kaplan-Meier survival curves. Overall survival (OS) based on human epidermal growth factor receptor 2 (HER2) expression in A: Stage Ⅱ and B: Stage Ⅲ gastric cancer patients. HR: Hazard ratio; CI: Confidence interval.

Table 2 Human epidermal growth factor receptor 2 expression and clinicohistologic characteristics

Author	*n*	Histologic type				Localization			Method
		Intestinal (%)	Diffuse (%)	Mixed / unknown (%)	*P*	GEJ (%)	Gastric (%)	*P* value	
Tanner *et al*[6]	231	21.5	2	5	0.005	24	12	-	CISH
Gravalos *et al*[23]	166	16	7	14	0.27	25	9.5	0.01	IHC, FISH
Lordick *et al*[24]	1527	34	6	20	-	32	18	-	IHC, FISH
Present study	384	17	2.5	18	< 0.01	20	9.5	0.008	IHC, FISH

GEJ: Gastro-esophageal junction; CISH: Chromogenic in situ hybridization; FISH: Fluorescence *in situ* hybridization; IHC: Immunochistochemistry.

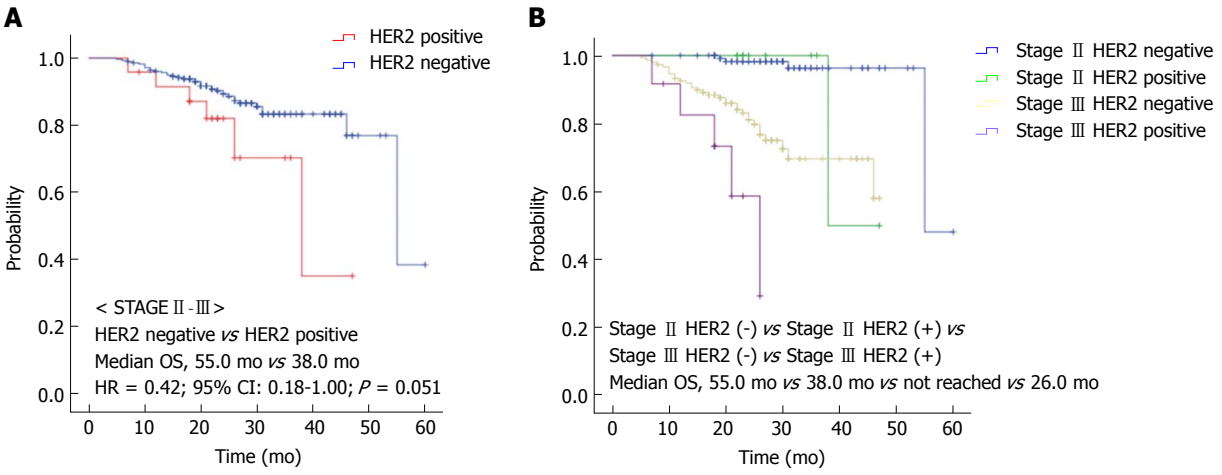

Figure 3 Kaplan-Meier survival curve. Overall survival (OS) based on human epidermal growth factor receptor 2 (HER2) expression in stage Ⅱ and Ⅲ gastric cancer patients who received adjuvant chemotherapy. A: Total patients both stage Ⅱ and Ⅲ; B: Divided by each stage. HR: Hazard ratio; CI: Confidence interval.

0.021, Figure 1B). We also found that in each stage, HER2-negative patients had a significantly improved OS relative to HER2-positive patients. Stage Ⅱ HER2-negative patients had improved OS compared to stage Ⅱ HER2-positive patients, although the difference was not statistically significant (HR = 0.21, 95%CI: 0.05-0.86, *P* = 0.30, Figure 2A). In stage Ⅲ, the median OS was not reached in the HER2-negative group, as compared to 26.0 mo (95%CI: 18.6-33.4 mo) in the HER2-positive group (HR = 0.38, 95%CI: 0.16-0.90, *P* = 0.017, Figure 2B).

We also analyzed survival based on HER2 expression stratifying by the administration of adjuvant chemotherapy. OS was prolonged in the HER2-negative group in stage Ⅱ-Ⅲ patients who received adjuvant chemotherapy relative to the HER2-positive group (55.0 *vs* 38.0 mo, HR = 0.42, 95%CI: 0.18-1.00, *P* = 0.051; Figure 3A and B). In stage Ⅱ-Ⅲ patients who did not

Table 3 Univariate and multivariate analysis showing factors associated with overall survival

Variable	Univariate		Multivariate	
	HR (95%CI)	*P* value	HR (95%CI)	*P* value
HER2 status	0.424 (0.208-0.865)	0.018	0.421 (0.206-0.861)	0.018
WD-MD *vs* PD-SRC	0.694 (0.374-1.290)	0.248		
Sex	1.376 (0.821-2.307)	0.226		
ECOG PS	2.149 (1.648-2.803)	< 0.001	2.002 (1.530-2.618)	< 0.001
Age (< 65)	1.408 (0.837-2.369)	0.197		
Adjuvant chemotherapy	1.750 (0.978-3.128)	0.059		

HR: Hazard ratio; CI: Confidence interval; HER2: Human epidermal growth factor receptor 2; WD: Well differentiated; MD: Moderately differentiated; PD: Poorly differentiated; SRC: Signet ring cell carcinoma; ECOG PS: Eastern Cooperative Oncology Group Performance Status.

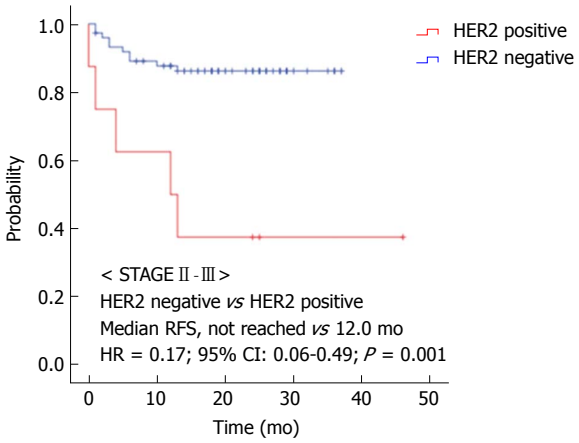

Figure 4 Kaplan-Meier survival curve. Recurrence free survival (RFS) based on human epidermal growth factor receptor 2 (HER2) expression in stage Ⅱ and Ⅲ gastric cancer patients who did not receive adjuvant chemotherapy. HR: Hazard ratio; CI: Confidence interval.

receive adjuvant chemotherapy, the median RFS was prolonged in the HER2-negative group relative to the HER2-positive group (not reached *vs* 12.0 mo, HR = 0.17, 95%CI: 0.06-0.49, *P* = 0.001; Figure 4).

A univariate analysis of all patients identified HER2 status and ECOG performance status as prognostic factors associated with survival. After adjusting for covariates in a multivariate analysis, HER2 status (HR = 0.421, 95%CI: 0.206-0.861, *P* = 0.018) and ECOG performance status (HR = 2.002, 95%CI: 1.530-2.618, *P* < 0.001) remained independent predictors of OS (Table 3).

DISCUSSION

We showed that HER2-positive patients had worse prognosis compared with HER2-negative patients in stage Ⅱ and Ⅲ gastric cancer patients and that HER2 status was independent predictor of OS in multivariate analysis. We also found that only 8.3% of the study patients with stage Ⅱ and Ⅲ gastric cancer exhibited HER2 overexpression.

There is no standard post-operative adjuvant chemotherapy in stage Ⅱ-Ⅲ gastric cancer patients. To the best of our knowledge, there are few studies about targeted therapies in the adjuvant setting. Although many studies have reported on the outcomes of patients with unresectable or metastatic gastric cancer receiving single or combination chemotherapy[4], it is very hard to improve patient outcomes with chemotherapy alone. For some cancers, targeted therapies have been developed, and several targeted agents have been evaluated for gastric cancer[17-19]; however, most did not improve survival relative to standard chemotherapy. In contrast, trastuzumab, a recombinant humanized anti-HER2 monoclonal antibody, has been proven effective in the ToGA trial[16]. This agent is now a standard first-line treatment for HER2-positive metastatic gastric cancer in combination with chemotherapy. In addition, predictive biomarkers of trastuzumab response are known. Recently, ramucirumab yielded impactful results in refractory gastric cancer patients[20,21]; however, predictive markers for this agent have not been validated.

This study aimed to investigate prognosis based on HER2 status in stage Ⅱ-Ⅲ gastric cancer patients. Our study showed that evaluation of the predictive biomarker HER2 was too infrequent among gastric cancer patients. We reviewed medical records from 4680 patients but only found 834 patients with HER2 status information. In other words, only approximately 18% of patients underwent HER2 status testing. Most stage IV gastric cancer patients were tested, but most stage Ⅱ and Ⅲ patients (*i.e.*, those with early or operable gastric cancer) were not tested. Generally, HER2 status is only tested if, following complete resection, gastric cancer recurs. This leads to a significant loss of time. If cancer pathology samples are no longer available, rebiopsy of the recurrent lesion is needed. Therefore, all gastric cancer patients should undergo early HER2 status testing, irrespective of the initial stage.

The carcinogenic role of HER2 in gastric cancer has been investigated. Although the results of the studies have been conflicting, many studies demonstrated that HER2 protein overexpression negatively affects survival in gastric cancer patients[5-7]. Our study also showed that HER2 positivity was an independent factor predictive of OS in a multivariate analysis. We observed a 57% reduction in the risk of death in this

study in HER2-positive patients.

The current study analyzed survival according to HER2 status. In stage Ⅱ-Ⅲ disease, regardless of stage, the median OS was significantly better among HER2-negative patients than among HER2-positive patients. The RFS was also improved among HER2-negative patients with stage Ⅱ-Ⅲ disease than among corresponding HER2-positive patients. Most patients initially diagnosed with stage Ⅱ-Ⅲ disease undergo gastrectomy and are treated with adjuvant chemotherapy to reduce the risk of recurrence. However, the benefit of adjuvant chemotherapy is not convincing. Each patient treated with adjuvant chemotherapy incurs different effects. Trastuzumab was first developed as a targeted agent for HER2-positive breast cancer. Many of the clinical trials that demonstrated clinical efficacy and safety were conducted in a HER2-positive breast cancer adjuvant setting. Accordingly, trastuzumab is currently a component of a standard adjuvant therapy regimen for HER2-positive breast cancer that also includes chemotherapy. We suggest that trastuzumab or other humanized monoclonal antibodies might play a similar role in an adjuvant setting in patients with stage Ⅱ-Ⅲ HER2-positive gastric cancer. Although some experimental studies have been conducted[22], and further studies are required.

In our study of Korean patients with gastric adenocarcinoma, the frequency of HER2 protein overexpression was similar to that reported in other articles. Our findings show that HER2-positive gastric cancer patients have an inferior OS and RFS compared to HER2-negative patients. We suggest that stage Ⅱ-Ⅲ patients exhibiting *HER-2/neu* amplification might be potential candidates for new adjuvant therapies involving the use of humanized monoclonal antibodies. These results will provide essential data for evidence-based strategies of gastric cancer control in South Korea.

COMMENTS

Background

One well-established target is human epidermal growth factor receptor 2 (HER2, ERBB2), one of a family of receptors associated with tumor cell proliferation, apoptosis, adhesion, migration, and differentiation. Increasing evidence suggests that HER2 is an important biomarker and key driver of tumorigenesis in gastric cancer, with studies reporting amplification or overexpression in 7%-34% of tumors. Despite conflicting results, some studies have suggested that HER2 positivity is associated with poor outcomes and an aggressive profile in gastric cancer.

Research frontiers

In 2010, the Trastuzumab for Gastric Cancer (ToGA) trial, an international phase 3, open-label, randomized controlled trial, demonstrated a significant survival benefit of trastuzumab plus chemotherapy in patients with advanced gastric or gastro-esophageal junction cancer whose tumors were found to overexpress the HER2 protein *via* immunohistochemistry or gene *via* fluorescence *in-situ* hybridization (FISH). This trial revealed significant increases in overall survival, progression-free survival, and overall response rates. Efforts to improve survival among Korean gastric cancer patients begin with an understanding of the clinical practice patterns actually used in Korean hospitals. This study aimed to investigate the frequency of HER2 overexpression among gastric cancer patients and evaluate the relationship between HER2 overexpression and prognosis.

Innovations and breakthroughs

The authors showed that HER2-positive patients had worse prognosis compared with HER2-negative patients in stage Ⅱ and Ⅲ gastric cancer patients and that HER2 status was independent predictor of OS in multivariate analysis. OS was also prolonged in HER2-negative patients who received adjuvant chemotherapy compared to HER2-positive patients. In patients who did not receive adjuvant chemotherapy, the median RFS was prolonged in the HER2-negative group compared to the HER2-positive group. In a multivariate analysis, HER2 status and Eastern Cooperative Oncology Group performance status were independent predictors of OS. The study also showed that evaluation of the predictive biomarker HER2 was too infrequent among gastric cancer patients.

Applications

The findings show that HER2-positive gastric cancer patients have an inferior OS and RFS compared to HER2-negative patients. The authors suggest that stage Ⅱ-Ⅲ patients exhibiting *HER-2/neu* amplification might be potential candidates for new adjuvant therapies involving the use of humanized monoclonal antibodies. The authors suggest that trastuzumab or other humanized monoclonal antibodies might play a similar role in an adjuvant setting in patients with stage Ⅱ-Ⅲ HER2-positive gastric cancer. These results will provide essential data for evidence-based strategies of gastric cancer control in South Korea.

Peer-review

This is a well-written manuscript showing survival analysis based on human epidermal growth factor 2 status in stage Ⅱ-Ⅲ gastric cancer.

REFERENCES

1 **Ferlay J**, Soerjomataram I, Dikshit R, Eser S, Mathers C, Rebelo M, Parkin DM, Forman D, Bray F. Cancer incidence and mortality worldwide: sources, methods and major patterns in GLOBOCAN 2012. *Int J Cancer* 2015; **136**: E359-E386 [PMID: 25220842 DOI: 10.1002/ijc.29210]

2 **Jemal A**, Bray F, Center MM, Ferlay J, Ward E, Forman D. Global cancer statistics. *CA Cancer J Clin* 2011; **61**: 69-90 [PMID: 21296855 DOI: 10.3322/caac.20107]

3 **National Cancer Information Center. Cancer registry.** Goyang: National Cancer Information Center, c2012 [cited 2012 July 22]. Available from: URL: http://www. cancer.go.kr/cms/statics/incidence/index.html

4 **Wagner AD**, Grothe W, Haerting J, Kleber G, Grothey A, Fleig WE. Chemotherapy in advanced gastric cancer: a systematic review and meta-analysis based on aggregate data. *J Clin Oncol* 2006; **24**: 2903-2909 [PMID: 16782930 DOI: 10.1200/JCO.2005.05.0245]

5 **Gravalos C**, Jimeno A. HER2 in gastric cancer: a new prognostic factor and a novel therapeutic target. *Ann Oncol* 2008; **19**: 1523-1529 [PMID: 18441328 DOI: 10.1093/annonc/mdn169]

6 **Tanner M**, Hollmén M, Junttila TT, Kapanen AI, Tommola S, Soini Y, Helin H, Salo J, Joensuu H, Sihvo E, Elenius K, Isola J. Amplification of HER-2 in gastric carcinoma: association with Topoisomerase IIalpha gene amplification, intestinal type, poor prognosis and sensitivity to trastuzumab. *Ann Oncol* 2005; **16**: 273-278 [PMID: 15668283 DOI: 10.1093/annonc/mdi064]

7 **Park DI**, Yun JW, Park JH, Oh SJ, Kim HJ, Cho YK, Sohn CI, Jeon WK, Kim BI, Yoo CH, Son BH, Cho EY, Chae SW, Kim EJ, Sohn JH, Ryu SH, Sepulveda AR. HER-2/neu amplification is an independent prognostic factor in gastric cancer. *Dig Dis Sci* 2006; **51**: 1371-1379 [PMID: 16868827 DOI: 10.1007/s10620-005-9057-1]

8 **Tateishi M**, Toda T, Minamisono Y, Nagasaki S. Clinicopathological significance of c-erbB-2 protein expression in human gastric carcinoma. *J Surg Oncol* 1992; **49**: 209-212 [PMID: 1348293 DOI: 10.1002/jso.2930490402]

9 **Sasano H**, Date F, Imatani A, Asaki S, Nagura H. Double immunostaining for c-erbB-2 and p53 in human stomach cancer cells. *Hum Pathol* 1993; **24**: 584-589 [PMID: 8099338 DOI: 10.1016/0046-8177(93)90236-A]

10 **Hudis CA**. Trastuzumab--mechanism of action and use in clinical practice. *N Engl J Med* 2007; **357**: 39-51 [PMID: 17611206 DOI: 10.1056/NEJMra043186]

11 **Piccart-Gebhart MJ**, Procter M, Leyland-Jones B, Goldhirsch A, Untch M, Smith I, Gianni L, Baselga J, Bell R, Jackisch C, Cameron D, Dowsett M, Barrios CH, Steger G, Huang CS, Andersson M, Inbar M, Lichinitser M, Láng I, Nitz U, Iwata H, Thomssen C, Lohrisch C, Suter TM, Rüschoff J, Suto T, Greatorex V, Ward C, Straehle C, McFadden E, Dolci MS, Gelber RD; Herceptin Adjuvant (HERA) Trial Study Team. Trastuzumab after adjuvant chemotherapy in HER2-positive breast cancer. *N Engl J Med* 2005; **353**: 1659-1672 [PMID: 16236737 DOI: 10.1056/NEJMoa052306]

12 **Romond EH**, Perez EA, Bryant J, Suman VJ, Geyer CE Jr, Davidson NE, Tan-Chiu E, Martino S, Paik S, Kaufman PA, Swain SM, Pisansky TM, Fehrenbacher L, Kutteh LA, Vogel VG, Visscher DW, Yothers G, Jenkins RB, Brown AM, Dakhil SR, Mamounas EP, Lingle WL, Klein PM, Ingle JN, Wolmark N. Trastuzumab plus adjuvant chemotherapy for operable HER2-positive breast cancer. *N Engl J Med* 2005; **353**: 1673-1684 [PMID: 16236738 DOI: 10.1056/NEJMoa052122]

13 **Slamon DJ**, Leyland-Jones B, Shak S, Fuchs H, Paton V, Bajamonde A, Fleming T, Eiermann W, Wolter J, Pegram M, Baselga J, Norton L. Use of chemotherapy plus a monoclonal antibody against HER2 for metastatic breast cancer that overexpresses HER2. *N Engl J Med* 2001; **344**: 783-792 [PMID: 11248153 DOI: 10.1056/NEJM200103153441101]

14 **Smith I**, Procter M, Gelber RD, Guillaume S, Feyereislova A, Dowsett M, Goldhirsch A, Untch M, Mariani G, Baselga J, Kaufmann M, Cameron D, Bell R, Bergh J, Coleman R, Wardley A, Harbeck N, Lopez RI, Mallmann P, Gelmon K, Wilcken N, Wist E, Sánchez Rovira P, Piccart-Gebhart MJ; HERA study team. 2-year follow-up of trastuzumab after adjuvant chemotherapy in HER2-positive breast cancer: a randomised controlled trial. *Lancet* 2007; **369**: 29-36 [PMID: 17208639 DOI: 10.1016/S0140-6736(07)60028-2]

15 **Fujimoto-Ouchi K**, Sekiguchi F, Yasuno H, Moriya Y, Mori K, Tanaka Y. Antitumor activity of trastuzumab in combination with chemotherapy in human gastric cancer xenograft models. *Cancer Chemother Pharmacol* 2007; **59**: 795-805 [PMID: 17031648 DOI: 10.1007/s00280-006-0337-z]

16 **Bang YJ**, Van Cutsem E, Feyereislova A, Chung HC, Shen L, Sawaki A, Lordick F, Ohtsu A, Omuro Y, Satoh T, Aprile G, Kulikov E, Hill J, Lehle M, Rüschoff J, Kang YK; ToGA Trial Investigators. Trastuzumab in combination with chemotherapy versus chemotherapy alone for treatment of HER2-positive advanced gastric or gastro-oesophageal junction cancer (ToGA): a phase 3, open-label, randomised controlled trial. *Lancet* 2010; **376**: 687-697 [PMID: 20728210 DOI: 10.1016/S0140-6736(10)61121-X]

17 **Ohtsu A**, Shah MA, Van Cutsem E, Rha SY, Sawaki A, Park SR, Lim HY, Yamada Y, Wu J, Langer B, Starnawski M, Kang YK. Bevacizumab in combination with chemotherapy as first-line therapy in advanced gastric cancer: a randomized, double-blind, placebo-controlled phase III study. *J Clin Oncol* 2011; **29**: 3968-3976 [PMID: 21844504 DOI: 10.1200/JCO.2011.36.2236]

18 **Lordick F**, Kang YK, Chung HC, Salman P, Oh SC, Bodoky G, Kurteva G, Volovat C, Moiseyenko VM, Gorbunova V, Park JO, Sawaki A, Celik I, Götte H, Melezínková H, Moehler M; Arbeitsgemeinschaft Internistische Onkologie and EXPAND Investigators. Capecitabine and cisplatin with or without cetuximab for patients with previously untreated advanced gastric cancer (EXPAND): a randomised, open-label phase 3 trial. *Lancet Oncol* 2013; **14**: 490-499 [PMID: 23594786 DOI: 10.1016/S1470-2045(13)70102-5]

19 **Ohtsu A**, Ajani JA, Bai YX, Bang YJ, Chung HC, Pan HM, Sahmoud T, Shen L, Yeh KH, Chin K, Muro K, Kim YH, Ferry D, Tebbutt NC, Al-Batran SE, Smith H, Costantini C, Rizvi S, Lebwohl D, Van Cutsem E. Everolimus for previously treated advanced gastric cancer: results of the randomized, double-blind, phase III GRANITE-1 study. *J Clin Oncol* 2013; **31**: 3935-3943 [PMID: 24043745 DOI: 10.1200/JCO.2012.48.3552]

20 **Wilke H**, Muro K, Van Cutsem E, Oh SC, Bodoky G, Shimada Y, Hironaka S, Sugimoto N, Lipatov O, Kim TY, Cunningham D, Rougier P, Komatsu Y, Ajani J, Emig M, Carlesi R, Ferry D, Chandrawansa K, Schwartz JD, Ohtsu A; RAINBOW Study Group. Ramucirumab plus paclitaxel versus placebo plus paclitaxel in patients with previously treated advanced gastric or gastro-oesophageal junction adenocarcinoma (RAINBOW): a double-blind, randomised phase 3 trial. *Lancet Oncol* 2014; **15**: 1224-1235 [PMID: 25240821 DOI: 10.1016/S1470-2045(14)70420-6]

21 **Fuchs CS**, Tomasek J, Yong CJ, Dumitru F, Passalacqua R, Goswami C, Safran H, Dos Santos LV, Aprile G, Ferry DR, Melichar B, Tehfe M, Topuzov E, Zalcberg JR, Chau I, Campbell W, Sivanandan C, Pikiel J, Koshiji M, Hsu Y, Liepa AM, Gao L, Schwartz JD, Tabernero J; REGARD Trial Investigators. Ramucirumab monotherapy for previously treated advanced gastric or gastro-oesophageal junction adenocarcinoma (REGARD): an international, randomised, multicentre, placebo-controlled, phase 3 trial. *Lancet* 2014; **383**: 31-39 [PMID: 24094768 DOI: 10.1016/S0140-6736(13)61719-5]

22 **Li W**, Zhao H, Qian W, Li H, Zhang L, Ye Z, Zhang G, Xia M, Li J, Gao J, Li B, Kou G, Dai J, Wang H, Guo Y. Chemotherapy for gastric cancer by finely tailoring anti-Her2 anchored dual targeting immunomicelles. *Biomaterials* 2012; **33**: 5349-5362 [PMID: 22542611 DOI: 10.1016/j.biomaterials.2012.04.016]

23 **Gravalos C**, Márquez A, Colomer R, García-Garbonero R, Sastre J, Rivera F, Saenz Cusi A, Velasco A, Guzman C, Jimeno A. Correlation between HER2/neu overexpression/amplification and clinicopathological parameters in advanced gastric cancer patients: a prospective study 2007. Presented at: Gastrointestinal Cancers Symposium 130: abstract 89. Available from: URL: http://www.asco.org/ASCOv2/Meetings/Abstracts?&vmview=abst_detail_view&confID=45&abstractID=10315

24 **Lordick F**, Bang YJ, Kang YK, Otero Reyes D, Manikhas GM, Shen L, Kulikov E, Stoss O, Jordan BWM, Van Cutsem E. HER2-positive advanced gastric cancer: similar HER2-positivity levels to breast cancer. *Eur J Cancer* 2007; **5**: 271.

P- Reviewer: Giordano A, Li W, Nagahara H **S- Editor**: Wei LJ
L- Editor: A **E- Editor**: Huang Y

World Journal of Gastroenterology

Submit a Manuscript: http://www.f6publishing.com

World J Gastroenterol 2017 November 7; 23(41): 7415-7424

DOI: 10.3748/wjg.v23.i41.7415

ISSN 1007-9327 (print) ISSN 2219-2840 (online)

ORIGINAL ARTICLE

Retrospective Study

Efficacy of postoperative adjuvant transcatheter arterial chemoembolization in hepatocellular carcinoma patients with microvascular invasion

Jia-Zhou Ye, Jun-Ze Chen, Zi-Hui Li, Tao Bai, Jie Chen, Shao-Liang Zhu, Le-Qun Li, Fei-Xiang Wu

Jia-Zhou Ye, Zi-Hui Li, Tao Bai, Jie Chen, Shao-Liang Zhu, Le-Qun Li, Fei-Xiang Wu, Department of Hepatobiliary Surgery, Affiliated Tumor Hospital of Guangxi Medical University, Nanning 530021, Guangxi Zhuang Autonomous Region, China

Jia-Zhou Ye, Tao Bai, Jie Chen, Shao-Liang Zhu, Le-Qun Li, Fei-Xiang Wu, Guangxi Liver Cancer Diagnosis and Treatment Engineering and Technology Research Center, Nanning 530021, Guangxi Zhuang Autonomous Region, China

Jia-Zhou Ye, Tao Bai, Jie Chen, Shao-Liang Zhu, Le-Qun Li, Fei-Xiang Wu, Key Laboratory of Early Prevention and Treatment for Regional High Frequency Tumor, Ministry of Education, Nanning 530021, Guangxi Zhuang Autonomous Region, China

Jun-Ze Chen, Department of General Surgery, The Ninth Affiliated Hospital of Guangxi Medical University, Beihai 536000, Guangxi Zhuang Autonomous Region, China

Author contributions: Ye JZ and Chen JZ equally contributed to this work; Ye JZ, Li LQ and Wu FX designed the research; Ye JZ, Chen JZ, Bai T, Chen J, Zhu SL, Li LQ, and Wu FX performed the research; Ye JZ, Chen JZ, and Li ZH analyzed the data; Ye JZ and Chen JZ wrote the paper.

Supported by Key Laboratory of Early Prevention and Treatment for Regional High Frequency Tumor, Ministry of Education, No. GKZ201604; Key Project of Guangxi Health and Family Planning Commission, China, No. S201513; and Key Project of Guangxi Science and Technology Department, China, No. Gui Ke AB16380242.

Institutional review board statement: The study was reviewed and approved by the Clinical Research Ethics Committee of Affiliated Tumor Hospital of Guangxi Medical University.

Informed consent statement: Informed consent was not required from the patients for the study as the analysis used anonymous clinical data. Individuals cannot be identified based on the data presented.

Conflict-of-interest statement: The authors declare no conflicts of interest.

Data sharing statement: No additional data are available.

Manuscript source: Unsolicited manuscript

Correspondence to: Fei-Xiang Wu, MD, Department of Hepatobiliary Surgery, Affiliated Tumor Hospital of Guangxi Medical University, No. 71, Hedi Road, Nanning 530021, Guangxi Zhuang Autonomous Region, China. wufeixiang@gxmu.edu.cn
Telephone: +86-771-5320971
Fax: +86-771-5320971

Received: July 26, 2017
Peer-review started: July 26, 2017
First decision: August 10, 2017
Revised: September 9, 2017
Accepted: September 20, 2017
Article in press: September 19, 2017
Published online: November 7, 2017

Abstract

AIM

To investigate the efficacy and safety of postoperative adjuvant transcatheter arterial chemoembolization (PA-

TACE) in preventing tumor recurrence and improving survival in Barcelona Clinic Liver Cancer (BCLC) early (A) and intermediate (B) stage hepatocellular carcinoma (HCC) patients with microvascular invasion (MVI).

METHODS

A total of 519 BCLC A or B HCC patients treated by liver resection alone or followed by PA-TACE between January 2012 and December 2015 were studied retrospectively. Univariate and multivariate analyses were performed to investigate the risk factors for recurrence-free survival (RFS) and overall survival (OS). Multiple logistic regression was used to identify the clinicopathological characteristics associated with MVI. The rates of RFS and OS were compared among patients with or without MVI treated with liver resection alone or followed by PA-TACE.

RESULTS

Univariate and multivariate analyses demonstrated that serum AFP level > 400 ng/mL, tumor size > 5 cm, tumor capsule invasion, MVI, and major hepatectomy were risk factors for poor OS. Tumor capsule invasion, MVI, tumor size > 5 cm, HBV-DNA copies > 1 x 10^4 IU/mL, and multinodularity were risk factors for poor RFS. Multiple logistic regression identified serum AFP level > 400 ng/mL, tumor size > 5 cm, and tumor capsule invasion as independent predictors of MVI. Both OS and DFS were significantly improved in patients with MVI who received PA-TACE as compared to those who underwent liver resection alone. Patients without MVI did not show a significant difference in OS and RFS between those treated by liver resection alone or followed by PA-TACE.

CONCLUSION

PA-TACE is a safe adjuvant intervention and can efficiently prevent tumor recurrence and improve the survival of BCLC early- and intermediate-stage HCC patients with MVI.

Key words: Hepatocellular carcinoma; Microvascular invasion; Postoperative adjuvant transcatheter arterial chemoembolization; Recurrence-free survival; Overall survival

Core tip: Microvascular invasion (MVI) is an independent risk factor attributed to frequent tumor recurrence in Barcelona Clinic Liver Cancer (BCLC) early- and intermediate-stage hepatocellular carcinoma (HCC) patients. Postoperative adjuvant transcatheter arterial chemoembolization (PA-TACE) has been confirmed to be effective in preventing early recurrence and delaying the progression of recurrent tumors, thereby improving the overall survival (OS) of HCC patients with macrovascular invasion. However, whether PA-TACE could provide the survival benefit to HCC patients with MVI remains unclear. The present study showed that PA-TACE is an effective method that can safely prevent tumor recurrence and improve the survival of BCLC early- and intermediate-stage HCC patients with MVI. However, it failed to provide obvious OS or RFS benefits to patients without MVI.

Ye JZ, Chen JZ, Li ZH, Bai T, Chen J, Zhu SL, Li LQ, Wu FX. Efficacy of postoperative adjuvant transcatheter arterial chemoembolization in hepatocellular carcinoma patients with microvascular invasion. *World J Gastroenterol* 2017; 23(41): 7415-7424 Available from: URL: http://www.wjgnet.com/1007-9327/full/v23/i41/7415.htm DOI: http://dx.doi.org/10.3748/wjg.v23.i41.7415

INTRODUCTION

Hepatocellular carcinoma (HCC) is the fifth most common cancer worldwide in males and the second leading cause of cancer-related deaths[1,2], especially in the Asia-Pacific region[3,4]. With advances in surgical techniques, surgical resection has been the most effective curative strategy for early- and intermediate-stage HCC[5,6]; however, the postoperative 5-year recurrence rate is 70%-80%, leading to poor overall survival (OS)[7-9].

Macrovascular invasion and macrovascular thrombosis, such as the invasion of the portal vein, hepatic vein, or hepatic artery, are the hallmarks of HCC[10]. Macrovascular invasion has been well accepted as a major mechanism promoting the growth of residual tumors as well as intrahepatic metastasis, thereby contributing to early recurrence and poor survival in HCC patients after liver resection[11-15]. Recently, microvascular invasion (MVI) has been demonstrated as an independent risk factor associated with early tumor recurrence in patients with single HCC without macrovascular invasion[16-21], which accounts for approximately 15%-60% of HCC patients[22,23]. MVI may promote metastasis by acting as a "seed" to give rise to micro-metastases in the liver parenchyma, and such metastasis is common among patients whose more than five vessels are affected by MVI[24].

Routinely, postoperative adjuvant intervention is recommended for preventing the recurrence in HCC patients with residual tumors after liver resection. Previous studies[13,25-28] confirmed that postoperative adjuvant transcatheter arterial chemoembolization (PA-TACE) prevented early recurrence and delayed the progression of recurrent tumors, thereby improving the OS in HCC patients with macrovascular invasion. However, whether PA-TACE can provide the survival benefit to HCC patients with MVI is yet unclear and necessitates further investigation.

Therefore, the current study investigated the

efficacy of PA-TACE in preventing tumor recurrence and improving survival in HCC patients with MVI. The study involved only patients with early- or intermediate-stage HCC based on the Barcelona Clinic Liver Cancer (BCLC) staging system[29], who did not present macrovascular invasion.

MATERIALS AND METHODS

The present study was approved by the Clinical Research Ethics Committee of the Affiliated Tumor Hospital of Guangxi Medical University and performed in compliance with the Helsinki Declaration. Patients were not required to give informed consent to the study as the analysis used anonymous clinical data and individuals cannot be identified based on the data presented. The results of the study were reported according to the Transparent Reporting of a Multivariable Prediction Model for Individual Prognosis or Diagnosis statement[30].

Patients and study design

All HCC patients diagnosed with BCLC early- or intermediate-stage disease who underwent curative resection at the Affiliated Tumor Hospital of Guangxi Medical University between January 1, 2012 and December 31, 2015 were considered for this retrospective study. Patients who fulfilled the following inclusion criteria were eligible for the study: (1) they initially underwent liver resection with curative intent without any prior treatment for HCC; (2) complete gross resection was achieved, with no residual tumor in the remnant liver as determined by intraoperative visual inspection and a negative resection (R0) margin based on the histological examination; (3) HCC and MVI were confirmed by postoperative histopathology of the surgical samples, and MVI was defined as the microscopic tumor invasion identified in the portal or hepatic vein of the surrounding liver tissue, contiguous to the tumor[31]; (4) no macrovascular invasion was present; (5) no other simultaneous malignancies or distant lymph node metastasis were present; (6) no cardiopulmonary, renal, or cerebral dysfunction was present before liver resection. The patients were excluded if they received treatments (such as TACE and radiotherapy) before liver resection, died of surgical complications or postoperative liver failure, received postoperative sorafenib treatment, or were lost to follow-up within 60 d after discharge.

Univariate and multivariate analyses were used to investigate the risk factors for recurrence-free survival (RFS) and overall survival (OS). Multiple logistic regression was performed to investigate the potential associations between clinicopathological characteristics and MVI. Patients were stratified into four groups depending on whether they had MVI or not and whether they were treated by liver resection alone or with resection followed by PA-TACE. Postoperative RFS and OS rates were compared among the four groups using the Kaplan-Meier method, and significant differences were identified using log-rank analysis.

Treatments

All patients were treated by curative resection, which was defined as no residual tumor and a negative resection (R0) margin based on the histological examination. Surgical procedures were performed as described previously[20,32]. Decisions about liver resection approaches were based on liver function, tumor location, and estimated volume of residual liver according to volume computed tomography (CT). Major hepatectomy was defined as the resection of three or more Couinaud segments, whereas minor hepatectomy as resection of one to two segments[20]. In patients with multiple tumors, the largest lesion was used as the index lesion.

In a subset of patients with MVI, PA-TACE was performed at 1, 3, and 6 mo after hepatectomy. During this procedure, a hepatic arterial catheter was inserted through the femoral artery using the Seldinger technique; the catheter was inserted selectively into the tumor-feeding artery as technically possible. An emulsion of lobaplatin (50 mg), raltitrexed (4 mg), and lipiodol (3-5 mL) was infused into the remnant liver through this catheter. Simultaneously, hepatic angiography and/or CT angiography was carried out to detect any obvious residual tumor in the remnant liver. TACE was conducted on the entire remnant liver.

Follow-up

Serum AFP level and other laboratory tests were routinely monitored. In case of patients treated by curative resection associated with adjuvant TACE, contrast-enhanced dynamic CT or magnetic resonance imaging (MRI) scan was performed before and two weeks after TACE. Moreover, digital subtraction angiography (DSA) was performed concurrently with adjuvant TACE. Recurrent HCC was confirmed when CT or MRI showed stable tumor staining in the pre-contrast phase accompanied by an increase in the serum AFP level. In case of patients who underwent liver resection alone, contrast-enhanced dynamic CT or MRI scans were performed to routinely monitor the condition of the patient since the end of the first month after resection and then at monthly intervals. Recurrent HCC was confirmed by CT or MRI images showing rapid tumor staining in the arterial phase that disappeared in the early venous phase together with an increase in the serum AFP level. DSA was supplemented when tumor lesions were < 1 cm. All patients were followed until death or May 31, 2016.

Table 1 Baseline clinicopathological characteristics of hepatocellular carcinoma patients, stratified by microvascular invasion status and use of postoperative adjuvant transcatheter arterial chemoembolization *n* (%)

		No MVI (*n* = 259)			MVI (*n* = 260)		
Characteristic	Category	No TACE (*n* = 187)	TACE (*n* = 72)	*P*	No TACE (*n* = 174)	TACE (*n* = 86)	*P*
Age (yr)	≤ 60	146 (78.1)	65 (90.3)	0.024	140 (80.5)	73 (84.9)	0.383
	> 60	41 (21.9)	7 (9.7)		34 (19.5)	13 (15.1)	
Sex	Female	29 (15.5)	9 (12.5)	0.540	24 (13.8)	11 (12.8)	0.824
	Male	158 (84.5)	63 (87.5)		150 (86.2)	75 (87.2)	
HBsAg	Negative	19 (10.2)	6 (8.3)	0.656	18 (10.3)	14 (16.3)	0.171
	Positive	168 (89.8)	66 (91.7)		156 (89.7)	72 (83.7)	
Total bilirubin, μmol/L		11 (3-118.3)	11.2 (4.9-33.2)	0.423	11.2 (2.8-30.9)	11.75 (5.1-33.1)	0.330
Prothrombin time (s)		13.10 ± 1.18	13.55 ± 1.21	0.006	13.31 ± 1.38	13.31 ± 1.22	0.978
AFP (ng/mL)	≤ 400	128 (68.4)	44 (61.1)	0.263	89 (51.1)	49 (57.0)	0.376
	> 400	59 (31.6)	28 (38.9)		85 (48.9)	37 (43.0)	
HBV-DNA (IU/mL)	≤ 10^4	95 (50.8)	43 (59.7)	0.197	89 (51.1)	52 (60.5)	0.156
	> 10^4	92 (49.2)	29 (40.3)		85 (48.9)	34 (39.5)	
Pathology data							
Size of largest tumor (cm)	≤ 5	121 (64.7)	38 (52.8)	0.077	76 (43.7)	41 (47.7)	0.542
	> 5	66 (35.3)	34 (47.2)		98 (56.3)	45 (52.3)	
No. of nodules	Single	155 (82.9)	62 (86.1)	0.528	137 (78.7)	73 (84.9)	0.237
	Multiple	32 (17.1)	10 (13.9)		37 (21.3)	13 (15.1)	
Differentiation	Edmondson 1-2	129 (69)	37 (51.4)	0.008	91 (52.3)	49 (57)	0.477
	Edmondson 3-4	58 (31)	35 (48.6)		83 (47.7)	37 (43)	
Capsule	Complete	143 (76.5)	52 (72.2)	0.478	105 (60.3)	51 (59.3)	0.872
	Incomplete	44 (23.5)	20 (27.8)		69 (39.7)	35 (40.7)	
Cirrhosis	No	31 (16.6)	9 (12.5)	0.416	31 (17.8)	14 (16.3)	0.758
	Yes	156 (83.4)	63 (87.5)		143 (82.2)	72 (83.7)	
Surgical data							
Type of resection	Minor	118 (63.1)	48 (66.7)	0.592	93 (53.4)	47 (54.7)	0.855
	Major	69 (36.9)	24 (33.3)		81 (46.6)	39 (45.3)	
Hepatic inflow occlusion	No	79(42.2)	25 (34.7)	0.268	53 (30.5)	32 (37.2)	0.275
	Yes	108 (57.8)	47 (65.3)		121 (69.5)	54 (62.8)	
Child-Pugh classification	A	180 (96.3)	70 (97.2)	1.000	172 (98.9)	84 (97.7)	0.601
	B	7 (3.7)	2 (2.8)		2 (1.1)	2 (2.3)	
Hypersplenism	No	169 (90.4)	67 (93.1)	0.497	155 (89.1)	83 (96.5)	0.043
	Yes	18 (9.6)	5 (6.9)		19 (10.9)	3 (3.5)	
BCLC	0	18 (9.6)	1 (1.4)	0.002	6 (3.4)	1 (1.2)	0.158
	A	151 (80.7)	54 (75)		121 (69.5)	69 (80.2)	
	B	18 (9.6)	17 (23.6)		47 (27)	16 (18.6)	
Recurrence	Yes	56 (29.9)	20 (27.8)	0.731	102 (58.6)	34 (39.5)	0.004
	No	131 (70.1)	52 (72.2)		72 (41.4)	52 (60.5)	

HBsAg: Hepatitis B surface antigen; AFP: Alpha-fetoprotein; BCLC: Barcelona Clinic Liver Cancer; MVI: Microvascular invasion.

Statistical analysis

Intergroup differences in continuous variables were assessed for significance using Student's *t*-test (normally distributed data) or Mann-Whitney *U* test (skewed data). Intergroup differences in categorical data were assessed using χ^2 or Fisher's exact test as appropriate. Survival was analyzed using the Kaplan-Meier method, and survival curves were compared using the log-rank test. Uni- and multivariate analyses were carried out using a Cox proportional hazards stepwise model in order to identify independent factors related to OS and RFS. Factors with $P < 0.1$ in univariate analysis were incorporated into the multivariate analysis. Patient characteristics that independently predicted the MVI were identified using multiple logistic regression. All statistical analyses were performed using SPSS 22.0 (IBM, Chicago, IL, United States). The threshold of significance was defined as $P < 0.05$, and all *P*-values were two-tailed.

RESULTS

Between January 2012 and December 2015, 1,110 patients underwent liver resection at the Affiliated Tumor Hospital of Guangxi Medical University. Of these, 103 were excluded as they had other malignancies (*n* = 34), metastatic carcinoma (*n* = 14), or recurrent HCC (*n* = 13) or they had received preoperative TACE treatment (*n* = 42). The resulting 1007 potentially eligible patients diagnosed with primary liver cancer and treated by liver resection with curative intent for HCC were considered for this retrospective study. Of these patients, 488 were excluded due to the following reasons: 353 had macrovascular invasion (BCLC stage C disease), 120 did not have MVI determined by postoperative histopathological examination, and 15

Table 2 Uni- and multivariate analyses to identify predictors of overall survival or recurrence-free survival in hepatocellular carcinoma patients after potentially curative resection

Factor	Univariate				Multivariate			
	OS		RFS		OS		RFS	
	HR (95%CI)	*P*	HR (95%CI)	*P*	HR (95%CI)	*P*	HR (95%CI)	*P*
Sex (male)	1.487 (0.773-2.864)	0.235	1.354 (0.885-2.071)	0.163				
Age (> 60 yr)	1.091 (0.627-1.772)	0.723	1.017 (0.723-1.430)	0.923				
HBsAg (+)	1.275 (0.618-2.630)	0.511	1.365 (0.842-2.214)	0.207				
Total bilirubin (μmol/L)	0.992 (0.964-1.021)	0.586	0.966 (0.979-1.013)	0.653				
Prothrombin time (s)	1.071 (0.931-1.232)	0.340	1.064 (0.966-1.173)	0.210				
Child-Pugh classification (B)	1.423 (0.523-3.875)	0.490	2.074 (1.098-3.915)	0.024				
Hypersplenism (yes)	0.949 (0.477-1.887)	0.882	1.158 (0.738-1.817)	0.524				
AFP (> 400 ng/mL)	2.063 (1.379-3.086)	0.000	1.321 (1.007-1.733)	0.044	1.738 (1.152-2.622)	0.008		
HBV-DNA (> 1×10^4 IU/mL)	1.191 (0.798-1.777)	0.393	1.259 (0.962-1.649)	0.094			1.316 (1.002-1.729)	0.048
Tumor size (> 5 cm)	2.219 (1.456-3.382)	0.000	1.694 (1.291-2.223)	0.000	1.858 (1.213-2.848)	0.004	1.600 (1.216-2.105)	0.001
Nodule no. (multinodular)	1.425 (0.885-2.294)	0.145	1.370 (0.985-1.905)	0.061			1.427 (1.024-1.989)	0.036
Differentiation (grades 3-4)	1.396 (0.934-2.085)	0.103	1.347 (1.027-1.766)	0.031				
Incomplete tumor capsule (yes)	2.366 (1.582-3.537)	0.000	1.664 (1.266-2.187)	0.000	1.998 (1.329-3.006)	0.001	1.468 (1.114-1.935)	0.006
MVI (yes)	3.412 (2.135-5.452)	0.000	2.180 (1.646-2.888)	0.000	2.524 (1.564-4.075)	0.000	1.959 (1.472-2.606)	0.000
Cirrhosis (yes)	0.922 (0.522-1.541)	0.757	1.359 (0.918-2.031)	0.125				
Approach of resection (major)	1.576 (1.054-2.357)	0.027	1.177 (0.896-1.547)	0.242	1.611 (1.073-2.419)	0.021		
Hepatic inflow occlusion (yes)	0.784 (0.519-1.185)	0.248	0.919 (0.649-1.217)	0.556				

OS: Overall survival; RFS: Recurrence-free survival; AFP: Alpha-fetoprotein; MVI: Microvascular invasion.

Table 3 Logistic regression to identify independent predictors of microvascular invasion in hepatocellular carcinoma patients

Predictor	HR (95%CI)	*P*
AFP (> 400 ng/mL)	1.680 (1.167-2.418)	0.005
Tumor size (> 5 cm)	1.767 (1.235-2.527)	0.002
Incomplete tumor capsule (yes)	1.960 (1.335-2.878)	0.001

AFP: Alpha-fetoprotein.

were lost to follow-up < 2 mo after discharge. Finally, 519 patients who fulfilled the inclusion criteria were enrolled and studied retrospectively.

Clinicopathological characteristics

Based on the postoperative histopathological examination, 260 patients presented MVI; of these, 86 (33.1%) underwent PA-TACE following liver resection; 259 did not have MVI, of these 72 (27.8%) underwent PA-TACE. The remaining patients were treated by liver resection alone (Table 1). Patients with or without MVI who did or did not receive PA-TACE presented similar peri- or postoperative clinicopathological characteristics and surgical resection procedures. Among patients with MVI, those who received PA-TACE showed a significantly lower postoperative recurrence rate than those who underwent resection alone (39.5 *vs* 58.6%, $P = 0.004$). The same result was not observed among patients without MVI.

Risk factors for poor RFS and OS

Uni- and multivariate analyses demonstrated that serum AFP level > 400 ng/mL, tumor size > 5 cm, incomplete tumor capsule, MVI, and major hepatectomy were risk factors for poor OS, whereas incomplete tumor capsule, MVI, tumor size > 5 cm, HBV-DNA copies > 1 x 10^4 IU/mL, and multi-nodularity were independent risk factors for poor RFS. Sex, age, HBsAg, serum total bilirubin level, prothrombin time, hypersplenism, Child-Pugh classification B, degree of HCC differentiation, cirrhosis, and hepatic inflow occlusion were not significantly related to OS or RFS (Table 2).

Multiple logistic regression identified serum AFP level > 400 ng/mL, tumor size > 5 cm, and incomplete tumor capsule as independent predictors of MVI (Table 3).

Efficacy and safety of PA-TACE in the prevention of recurrence and improvement of survival

Among patients with MVI, OS was significantly improved in patients treated by PA-TACE than those treated by liver resection alone (1 year, 92.7% *vs* 81.3%; 2 years, 86.5% *vs* 65.7%; 3 years, 73.1% *vs* 58.8%; 4 years, 67.5% *vs* 53.9%; $P = 0.019$; Figure 1B and Table 4). Similarly, RFS was significantly better in patients treated by PA-TACE (median RFS, 37 mo *vs* 13 mo; RFS at 1 year, 72.1% *vs* 52.0%; 2 years, 58.3% *vs* 41.1%; 3 years, 54.9% *vs* 33.7%; 4 years, 30.9% *vs* 28.4%; $P = 0.002$; Figure 1D). Among patients without MVI, OS was similar between those with or without PA-TACE (1 year, 94.2% *vs* 98.8%; 2 years, 91.9% *vs* 91.5%; 3 years, 87.6% *vs* 82.8%; 4 years, 87.6% *vs* 82.8%; $P = 0.872$; Figure 1A). Similar results were obtained for RFS (1 year, 83.0% *vs* 80.7%; 2 years, 71.8% *vs* 70.1%; 3 years, 61.9%

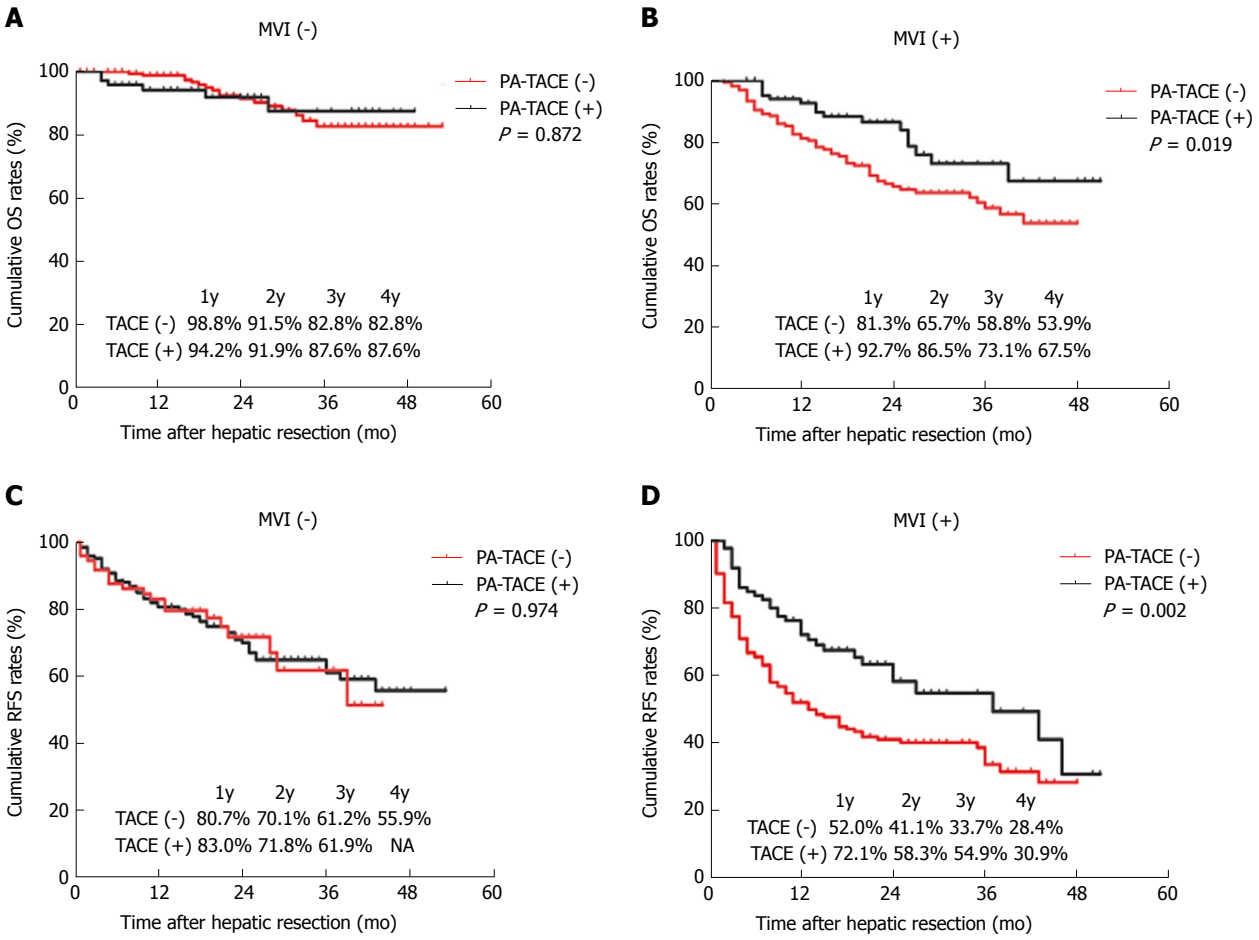

Figure 1 Overall survival and recurrence-free survival curves of hepatocellular carcinoma patients who either underwent liver resection alone or followed by postoperative adjuvant transcatheter arterial chemoembolization. A: OS for HCC/MVI (-) patients (P = 0.872); B: OS for HCC/MVI (+) patients (P = 0.019); C: RFS for HCC/MVI (-) patients (P = 0.974); D: RFS for HCC/MVI (+) patients (P = 0.002). OS: Overall survival; HCC: Hepatocellular carcinoma; MVI: Microvascular invasion; RFS: Recurrence-free survival.

Table 4 Survival rates of hepatocellular carcinoma patients in different groups

Group	OS rate (%)					RFS rate (%)				
	1 yr	2 yr	3 yr	4 yr	*P*	1 yr	2 yr	3 yr	4 yr	*P*
MVI (-), TACE (-)	98.8	91.5	82.8	82.8	0.872	80.7	70.1	61.2	55.9	0.974
MVI (-), TACE (+)	94.2	91.9	87.6	87.6		83.0	71.8	61.9	NA	
MVI (+), TACE (-)	81.3	65.7	58.8	53.9	0.019	52.0	41.1	33.7	28.4	0.002
MVI (+), TACE (+)	92.7	86.5	73.1	67.5		72.1	58.3	54.9	30.9	

OS: Overall survival; RFS: Recurrence-free survival; MVI: Microvascular invasion; TACE: Transcatheter arterial chemoembolization.

vs 61.2%; 4 years, not available *vs* 55.9%; P = 0.974; Figure 1C). Since recurrence did not occur in > 50% of patients without MVI, we could not compare median RFS duration between those who did or did not receive PA-TACE.

Moreover, complications of TACE were summarized in Table 5. Owing to PA-TACE as an adjuvant preventative therapy with a low dose of lipiodol (3-5 mL) and chemotherapeutic drugs lobaplatin (50 mg) and raltitrexed (4 mg), no serious complications were observed in all patients who received PA-TACE in the current study.

DISCUSSION

With advances in surgical techniques, liver resection remains the most effective curative strategy for HCC[5,6]. Nevertheless, the high incidence of postoperative recurrence usually leads to poor survival[7-9]. Vascular invasion promotes the growth of residual tumors and intrahepatic metastasis, which contributes to early recurrence post liver resection[11-15]. Invisible

Table 5 Complications and adverse events after postoperative adjuvant transcatheter arterial chemoembolization *n* (%)

Complication	Events
Nausea and vomiting	46 (29.11)
Fever	35 (22.2)
Pain	49 (31.0)
Alopecia	5 (3.2)
Liver failure	0 (0.0)
Bleeding of esophageal venous plexus	0 (0.0)
Gastrointestinal hemorrhage	0 (0.0)
Heart failure	0 (0.0)
Infection	0 (0.0)
Ectopic embolism syndrome	0 (0.0)
Refractory ascites	0 (0.0)
Pulmonary complication	2 (1.3)
Therapy-related death	0 (0.0)

intra-hepatic micro-metastases likely distribute *via* the hepatic artery and portal vein system, readily escaping detection during preoperative imaging or intra-operative observation. Recently, MVI has been associated with intrahepatic metastasis after curative resection[33,34]. MVI may promote metastasis by acting as a "seed" to give rise to micro-metastases in the liver parenchyma, and such metastasis is a common occurrence among patients in whom MVI affects more than five vessels[24]. Recent studies revealed that MVI is an independent risk factor for early recurrence in single HCC without macrovascular invasion[16-21,24], which is in agreement with our findings. In the present study, uni- and multivariate analyses showed that MVI is closely related to OS and RFS in HCC patients with early disease.

We conducted multiple logistic regression to identify that serum AFP level > 400 ng/mL, tumor size > 5 cm, and incomplete tumor capsule were closely related to MVI. Our finding that MVI incidence increases with increasing tumor diameter is in agreement with previous reports[35,36]. Nonetheless, tumor size is one of the major prognostic factors in HCC[36], and the aggressive or infiltrative tendency of HCC increases when the tumor diameter is > 3 cm[37,38]. In addition, MVI incidence tends to be high in patients with incomplete tumor capsule, which is associated with an aggressive physiological behavior[39]. Such tumors potentially invade normal tissue containing microvessels, giving rise to MVI[14,40]. A CT scan study showed that the presence of incomplete tumor capsule closely correlated with the absence of MVI. Moreover, the incidence of MVI was high among patients in our cohort with AFP level > 400 ng/mL, which is consistent with previous studies associating elevated AFP level with MVI[35,41].

Postoperative adjuvant intervention is routinely recommended for suppressing the progression of invisible micro-metastatic lesions and preventing recurrence. Normal liver parenchyma receives about 70% of its basic blood supply from the portal venous system, whereas HCC growth, including invisible micro-metastases, depends primarily on the blood supply by the hepatic artery[42-44]. Therefore, lipiodol injection *via* TACE is speculated to selectively accumulate in the invisible metastatic HCC to block the nutrient vessels when delivered intra-arterially while serving as a carrier of anticancer drugs that allow the sustainable chemotherapeutic killing of microscopic HCC cells[45-47]. Previous studies have shown that PA-TACE can prevent the early recurrence and delay the progression of recurrent tumors, thereby improving OS in HCC patients with macrovascular invasion. However, only a few studies have examined whether PA-TACE can prevent recurrence and improve the survival of HCC patients with MVI.

In the present study, the early-stage HCC patients were stratified according to the MVI status and subgroup analysis was performed. We found that PA-TACE after liver resection significantly prolonged the OS and RFS in patients with MVI. These results were in agreement with a previous study, which showed that PA-TACE at 4 wk after R0 hepatectomy in HCC patients with MVI significantly prolonged the RFS and OS, as well as reduced the rate of early recurrence[20]. On the other hand, in case of patients without MVI in the current study, PA-TACE did not significantly improve OS or RFS. Furthermore, we observed that none of the patients presented serious complications after PA-TACE. These findings suggest that when HCC patients experience postoperative MVI, immediate TACE, as a safe management, may prevent recurrence. However, when MVI is absent, PA-TACE is not strongly recommended for patients with BCLC early- or intermediate-stage HCC. These findings could be utilized for clinical guidance of the treatment and management of early-stage HCC.

The conclusions of the present study should be noted for several limitations. The present study was retrospective and involved patients from only one medical center, thereby highlighting the need for verification through large, multicenter, preferably prospective trials. Furthermore, PA-TACE drugs and dosages can vary across medical centers. The current cohort may have shown selection bias since we excluded patients whose MVI was not assessed through postoperative histopathology. The current follow-up time was only 4 years; thus, long-term outcomes are yet controversial. Moreover, the AFP levels were not evaluated before and after TACE. Hence, further prospective studies to verify the efficacy of PA-TACE for the prevention of recurrence and improvement of survival in early-stage HCC with MVI

remains to be investigated in larger populations.

COMMENTS

Background

Microvascular invasion (MVI) is associated with a high rate of recurrence in patients with hepatocellular carcinoma (HCC). Currently, postoperative adjuvant transcatheter arterial chemoembolization (PA-TACE) is an efficient method for preventing early recurrence and delaying the progression of recurrent tumors, thereby improving the overall survival in HCC patients with macrovascular invasion. However, whether PA-TACE could provide a survival benefit to HCC patients with MVI remains unclear. This study aimed to investigate the efficacy and safety of PA-TACE in the prevention of recurrence and improvement of survival in Barcelona Clinic Liver Cancer (BCLC) early- and intermediate-stage HCC patients with MVI.

Research frontiers

This study aimed to evaluate the efficacy and safety of PA-TACE to prevent recurrence and improve survival in BCLC early- and intermediate-stage HCC patients with or without MVI who were treated by liver resection alone or followed by PA-TACE. The results indicate that PA-TACE is an effective and safe method to prevent the recurrence and improve the survival in BCLC early- and intermediate-stage HCC patients with MVI. Nevertheless, the study failed to provide obvious OS or RFS benefits in patients without MVI.

Innovations and breakthroughs

This study indicates that PA-TACE is an effective and safe approach to prevent recurrence and improve survival in BCLC early- and intermediate-stage HCC patients with MVI. However, obvious OS or RFS benefits in patients without MVI could not be detected.

Applications

This study suggests that PA-TACE is effective and safe for preventing recurrence and improving the survival in patients with BCLC A and B stage HCC with MVI; however, it is not essential when MVI is absent. These findings could be utilized for clinical decision with respect to the treatment and management of BCLC A and B stage HCC.

Terminology

PA-TACE is a minimally invasive procedure performed in interventional radiology to block the blood supply of the tumors by lipiodol and/or drug-loaded microspheres that simultaneously serve as a carrier of anticancer drugs to allow the sustainable chemotherapeutic killing of microscopic HCC cells. PA-TACE was performed at 1, 3, and 6 mo after hepatectomy. During this procedure, a hepatic arterial catheter was inserted through the femoral artery using the Seldinger technique; the catheter was inserted selectively into the tumor-feeding artery as technically plausible. An emulsion of lobaplatin (50 mg), raltitrexed (4 mg), and lipiodol (3-5 mL) was infused into the remnant liver through the catheter. Simultaneously, hepatic angiography and/or computed tomography angiography detected any obvious residual tumor in the remnant liver. TACE was conducted on the entire remnant liver.

Peer-review

This is a retrospective study comprising of 519 HCC patients with BCLC stage A or B disease treated by curative liver resection between 2012 and 2015. Based on the histology, the whole series was divided into 259 cases without and 260 cases with MVI. The study found that PA-TACE is effective and safe for the prevention of recurrence and improvement in the survival of BCLC A and B stage HCC patients with MVI.

REFERENCES

1 **McGuire S**. World Cancer Report 2014. Geneva, Switzerland: World Health Organization, International Agency for Research on Cancer, WHO Press, 2015. *Adv Nutr* 2016; **7**: 418-419 [PMID: 26980827 DOI: 10.3945/an.116.012211]

2 **Torre LA**, Bray F, Siegel RL, Ferlay J, Lortet-Tieulent J, Jemal A. Global cancer statistics, 2012. *CA Cancer J Clin* 2015; **65**: 87-108 [PMID: 25651787 DOI: 10.3322/caac.21262]

3 **Lavanchy D**. Hepatitis B virus epidemiology, disease burden, treatment, and current and emerging prevention and control measures. *J Viral Hepat* 2004; **11**: 97-107 [PMID: 14996343]

4 **Gao JD**, Shao YF, Xu Y, Ming LH, Wu ZY, Liu GT, Wang XH, Gao WH, Sun YT, Feng XL, Liang LM, Zhang YH, Sun ZT. Tight association of hepatocellular carcinoma with HBV infection in North China. *Hepatobiliary Pancreat Dis Int* 2005; **4**: 46-49 [PMID: 15730918]

5 **Bruix J**, Sherman M; American Association for the Study of Liver Diseases. Management of hepatocellular carcinoma: an update. *Hepatology* 2011; **53**: 1020-1022 [PMID: 21374666 DOI: 10.1002/hep.24199]

6 **Bruix J**, Llovet JM. Prognostic prediction and treatment strategy in hepatocellular carcinoma. *Hepatology* 2002; **35**: 519-524 [PMID: 11870363 DOI: 10.1053/jhep.2002.32089]

7 **Lim KC**, Chow PK, Allen JC, Siddiqui FJ, Chan ES, Tan SB. Systematic review of outcomes of liver resection for early hepatocellular carcinoma within the Milan criteria. *Br J Surg* 2012; **99**: 1622-1629 [PMID: 23023956 DOI: 10.1002/bjs.8915]

8 **Belghiti J**, Panis Y, Farges O, Benhamou JP, Fekete F. Intrahepatic recurrence after resection of hepatocellular carcinoma complicating cirrhosis. *Ann Surg* 1991; **214**: 114-117 [PMID: 1714267]

9 **European Association For The Study Of The Liver.**; European Organisation For Research And Treatment Of Cancer. EASL-EORTC clinical practice guidelines: management of hepatocellular carcinoma. *J Hepatol* 2012; **56**: 908-943 [PMID: 22424438 DOI: 10.1016/j.jhep.2011.12.001]

10 **Hanahan D**, Weinberg RA. Hallmarks of cancer: the next generation. *Cell* 2011; **144**: 646-674 [PMID: 21376230 DOI: 10.1016/j.cell.2011.02.013]

11 **Edge SB**, Compton CC. The American Joint Committee on Cancer: the 7th edition of the AJCC cancer staging manual and the future of TNM. *Ann Surg Oncol* 2010; **17**: 1471-1474 [PMID: 20180029 DOI: 10.1245/s10434-010-0985-4]

12 **Llovet JM**, Brú C, Bruix J. Prognosis of hepatocellular carcinoma: the BCLC staging classification. *Semin Liver Dis* 1999; **19**: 329-338 [PMID: 10518312 DOI: 10.1055/s-2007-1007122]

13 **Kudo M**, Kitano M, Sakurai T, Nishida N. General Rules for the Clinical and Pathological Study of Primary Liver Cancer, Nationwide Follow-Up Survey and Clinical Practice Guidelines: The Outstanding Achievements of the Liver Cancer Study Group of Japan. *Dig Dis* 2015; **33**: 765-770 [PMID: 26488173 DOI: 10.1159/000439101]

14 **Gouw AS**, Balabaud C, Kusano H, Todo S, Ichida T, Kojiro M. Markers for microvascular invasion in hepatocellular carcinoma: where do we stand? *Liver Transpl* 2011; **17** Suppl 2: S72-S80 [PMID: 21714066 DOI: 10.1002/lt.22368]

15 **Rodríguez-Perálvarez M**, Luong TV, Andreana L, Meyer T, Dhillon AP, Burroughs AK. A systematic review of microvascular invasion in hepatocellular carcinoma: diagnostic and prognostic variability. *Ann Surg Oncol* 2013; **20**: 325-339 [PMID: 23149850 DOI: 10.1245/s10434-012-2513-1]

16 **Roayaie S**, Blume IN, Thung SN, Guido M, Fiel MI, Hiotis S, Labow DM, Llovet JM, Schwartz ME. A system of classifying microvascular invasion to predict outcome after resection in patients with hepatocellular carcinoma. *Gastroenterology* 2009; **137**: 850-855 [PMID: 19524573 DOI: 10.1053/j.gastro.2009.06.003]

17 **Sparrelid E**, Del Chiaro M. Microvascular Invasion in Hepatitis B Virus-Related Hepatocellular Carcinoma: Another Step Toward Preoperative Evaluation? *JAMA Surg* 2016; **151**: 364 [PMID: 26579990 DOI: 10.1001/jamasurg.2015.4267]

18 **Du M**, Chen L, Zhao J, Tian F, Zeng H, Tan Y, Sun H, Zhou J, Ji Y.

Microvascular invasion (MVI) is a poorer prognostic predictor for small hepatocellular carcinoma. *BMC Cancer* 2014; **14**: 38 [PMID: 24460749 DOI: 10.1186/1471-2407-14-38]

19 **Lim KC**, Chow PK, Allen JC, Chia GS, Lim M, Cheow PC, Chung AY, Ooi LL, Tan SB. Microvascular invasion is a better predictor of tumor recurrence and overall survival following surgical resection for hepatocellular carcinoma compared to the Milan criteria. *Ann Surg* 2011; **254**: 108-113 [PMID: 21527845 DOI: 10.1097/SLA.0b013e31821ad884]

20 **Barreto SG**, Brooke-Smith M, Dolan P, Wilson TG, Padbury RT, Chen JW. Cirrhosis and microvascular invasion predict outcomes in hepatocellular carcinoma. *ANZ J Surg* 2013; **83**: 331-335 [PMID: 22943449 DOI: 10.1111/j.1445-2197.2012.06196.x]

21 **Ünal E**, İdilman İS, Akata D, Özmen MN, Karçaaltıncaba M. Microvascular invasion in hepatocellular carcinoma. *Diagn Interv Radiol* 2016; **22**: 125-132 [PMID: 26782155 DOI: 10.5152/dir.2015.15125]

22 **Faber W**, Stockmann M, Kruschke JE, Denecke T, Bahra M, Seehofer D. Implication of microscopic and macroscopic vascular invasion for liver resection in patients with hepatocellular carcinoma. *Dig Surg* 2014; **31**: 204-209 [PMID: 25196847 DOI: 10.1159/000365257]

23 **Sun JJ**, Wang K, Zhang CZ, Guo WX, Shi J, Cong WM, Wu MC, Lau WY, Cheng SQ. Postoperative Adjuvant Transcatheter Arterial Chemoembolization After R0 Hepatectomy Improves Outcomes of Patients Who have Hepatocellular Carcinoma with Microvascular Invasion. *Ann Surg Oncol* 2016; **23**: 1344-1351 [PMID: 26714945 DOI: 10.1245/s10434-015-5008-z]

24 **Hirokawa F**, Hayashi M, Asakuma M, Shimizu T, Inoue Y, Uchiyama K. Risk factors and patterns of early recurrence after curative hepatectomy for hepatocellular carcinoma. *Surg Oncol* 2016; **25**: 24-29 [PMID: 26979637 DOI: 10.1016/j.suronc.2015.12.002]

25 **Sumie S**, Kuromatsu R, Okuda K, Ando E, Takata A, Fukushima N, Watanabe Y, Kojiro M, Sata M. Microvascular invasion in patients with hepatocellular carcinoma and its predictable clinicopathological factors. *Ann Surg Oncol* 2008; **15**: 1375-1382 [PMID: 18324443 DOI: 10.1245/s10434-008-9846-9]

26 **Kanai T**, Hirohashi S, Upton MP, Noguchi M, Kishi K, Makuuchi M, Yamasaki S, Hasegawa H, Takayasu K, Moriyama N. Pathology of small hepatocellular carcinoma. A proposal for a new gross classification. *Cancer* 1987; **60**: 810-819 [PMID: 2439190]

27 **EDMONDSON HA**, STEINER PE. Primary carcinoma of the liver: a study of 100 cases among 48,900 necropsies. *Cancer* 1954; **7**: 462-503 [PMID: 13160935]

28 **Sumie S**, Nakashima O, Okuda K, Kuromatsu R, Kawaguchi A, Nakano M, Satani M, Yamada S, Okamura S, Hori M, Kakuma T, Torimura T, Sata M. The significance of classifying microvascular invasion in patients with hepatocellular carcinoma. *Ann Surg Oncol* 2014; **21**: 1002-1009 [PMID: 24254204 DOI: 10.1245/s10434-013-3376-9]

29 **Zhong C**, Guo RP, Li JQ, Shi M, Wei W, Chen MS, Zhang YQ. A randomized controlled trial of hepatectomy with adjuvant transcatheter arterial chemoembolization versus hepatectomy alone for Stage III A hepatocellular carcinoma. *J Cancer Res Clin Oncol* 2009; **135**: 1437-1445 [PMID: 19408012 DOI: 10.1007/s00432-009-0588-2]

30 **Jin YJ**, Lee JW, Lee OH, Chung HJ, Kim YS, Lee JI, Cho SG, Jeon YS, Lee KY, Ahn SI, Shin WY. Transarterial chemoembolization versus surgery/radiofrequency ablation for recurrent hepatocellular carcinoma with or without microvascular invasion. *J Gastroenterol Hepatol* 2014; **29**: 1056-1064 [PMID: 24372785 DOI: 10.1111/jgh.12507]

31 **Wang SN**, Chuang SC, Lee KT. Efficacy of sorafenib as adjuvant therapy to prevent early recurrence of hepatocellular carcinoma after curative surgery: A pilot study. *Hepatol Res* 2014; **44**: 523-531 [PMID: 23672310 DOI: 10.1111/hepr.12159]

32 **Bruix J**, Takayama T, Mazzaferro V, Chau GY, Yang J, Kudo M, Cai J, Poon RT, Han KH, Tak WY, Lee HC, Song T, Roayaie S, Bolondi L, Lee KS, Makuuchi M, Souza F, Berre MA, Meinhardt G, Llovet JM; STORM investigators. Adjuvant sorafenib for hepatocellular carcinoma after resection or ablation (STORM): a phase 3, randomised, double-blind, placebo-controlled trial. *Lancet Oncol* 2015; **16**: 1344-1354 [PMID: 26361969 DOI: 10.1016/S1470-2045(15)00198-9]

33 **Fan J**, Zhou J, Wu ZQ, Qiu SJ, Wang XY, Shi YH, Tang ZY. Efficacy of different treatment strategies for hepatocellular carcinoma with portal vein tumor thrombosis. *World J Gastroenterol* 2005; **11**: 1215-1219 [PMID: 15754408 DOI: 10.3748/wjg.v11.i8.1215]

34 **Llovet JM**, Schwartz M, Mazzaferro V. Resection and liver transplantation for hepatocellular carcinoma. *Semin Liver Dis* 2005; **25**: 181-200 [PMID: 15918147 DOI: 10.1055/s-2005-871198]

35 **Nagano Y**, Shimada H, Takeda K, Ueda M, Matsuo K, Tanaka K, Endo I, Kunisaki C, Togo S. Predictive factors of microvascular invasion in patients with hepatocellular carcinoma larger than 5 cm. *World J Surg* 2008; **32**: 2218-2222 [PMID: 18642045 DOI: 10.1007/s00268-008-9585-x]

36 **Pawlik TM**, Delman KA, Vauthey JN, Nagorney DM, Ng IO, Ikai I, Yamaoka Y, Belghiti J, Lauwers GY, Poon RT, Abdalla EK. Tumor size predicts vascular invasion and histologic grade: Implications for selection of surgical treatment for hepatocellular carcinoma. *Liver Transpl* 2005; **11**: 1086-1092 [PMID: 16123959 DOI: 10.1002/lt.20472]

37 **Esnaola NF**, Lauwers GY, Mirza NQ, Nagorney DM, Doherty D, Ikai I, Yamaoka Y, Regimbeau JM, Belghiti J, Curley SA, Ellis LM, Vauthey JN. Predictors of microvascular invasion in patients with hepatocellular carcinoma who are candidates for orthotopic liver transplantation. *J Gastrointest Surg* 2002; **6**: 224-232; discussion 232 [PMID: 11992808]

38 **Jun L**, Zhenlin Y, Renyan G, Yizhou W, Xuying W, Feng X, Yong X, Kui W, Jian L, Dong W, Hongyang W, Lehua S, Mengchao W, Feng S. Independent factors and predictive score for extrahepatic metastasis of hepatocellular carcinoma following curative hepatectomy. *Oncologist* 2012; **17**: 963-969 [PMID: 22653882 DOI: 10.1634/theoncologist.2011-0447]

39 **Lu XY**, Xi T, Lau WY, Dong H, Xian ZH, Yu H, Zhu Z, Shen F, Wu MC, Cong WM. Pathobiological features of small hepatocellular carcinoma: correlation between tumor size and biological behavior. *J Cancer Res Clin Oncol* 2011; **137**: 567-575 [PMID: 20508947 DOI: 10.1007/s00432-010-0909-5]

40 **Groeschl RT**, Gamblin TC, Turaga KK. Ablation for hepatocellular carcinoma: validating the 3-cm breakpoint. *Ann Surg Oncol* 2013; **20**: 3591-3595 [PMID: 23720072 DOI: 10.1245/s10434-013-3031-5]

41 **Chandarana H**, Robinson E, Hajdu CH, Drozhinin L, Babb JS, Taouli B. Microvascular invasion in hepatocellular carcinoma: is it predictable with pretransplant MRI? *AJR Am J Roentgenol* 2011; **196**: 1083-1089 [PMID: 21512074 DOI: 10.2214/AJR.10.4720]

42 **Portolani N**, Coniglio A, Ghidoni S, Giovanelli M, Benetti A, Tiberio GA, Giulini SM. Early and late recurrence after liver resection for hepatocellular carcinoma: prognostic and therapeutic implications. *Ann Surg* 2006; **243**: 229-235 [PMID: 16432356 DOI: 10.1097/01.sla.0000197706.21803.a1]

43 **Cucchetti A**, Piscaglia F, Caturelli E, Benvegnù L, Vivarelli M, Ercolani G, Cescon M, Ravaioli M, Grazi GL, Bolondi L, Pinna AD. Comparison of recurrence of hepatocellular carcinoma after resection in patients with cirrhosis to its occurrence in a surveilled cirrhotic population. *Ann Surg Oncol* 2009; **16**: 413-422 [PMID: 19034578 DOI: 10.1245/s10434-008-0232-4]

44 **Wang J**, Li Q, Sun Y, Zheng H, Cui Y, Li H, Zhou H, Hao X. Clinicopathologic features between multicentric occurence and intrahepatic metastasis of multiple hepatocellular carcinomas related to HBV. *Surg Oncol* 2009; **18**: 25-30 [PMID: 18640032 DOI: 10.1016/j.suronc.2008.05.009]

45 **Inayoshi J**, Ichida T, Sugitani S, Tsuboi Y, Genda T, Honma N,

Asakura H. Gross appearance of hepatocellular carcinoma reflects E-cadherin expression and risk of early recurrence after surgical treatment. *J Gastroenterol Hepatol* 2003; **18**: 673-677 [PMID: 12753149]

46 **Iguchi T**, Aishima S, Sanefuji K, Fujita N, Sugimachi K, Gion T, Taketomi A, Shirabe K, Maehara Y, Tsuneyoshi M. Both fibrous capsule formation and extracapsular penetration are powerful predictors of poor survival in human hepatocellular carcinoma: a histological assessment of 365 patients in Japan. *Ann Surg Oncol* 2009; **16**: 2539-2546 [PMID: 19533247 DOI: 10.1245/s10434-009-0453-1]

47 **Ng IO**, Lai EC, Ng MM, Fan ST. Tumor encapsulation in hepatocellular carcinoma. A pathologic study of 189 cases. *Cancer* 1992; **70**: 45-49 [PMID: 1318778]

P- Reviewer: Al-Shamma S, Sergi CM, Tai DI **S- Editor**: Ma YJ
L- Editor: Wang TQ **E- Editor**: Huang Y

World Journal of Gastroenterology

Submit a Manuscript: http://www.f6publishing.com

World J Gastroenterol 2017 November 7; 23(41): 7425-7432

DOI: 10.3748/wjg.v23.i41.7425

ISSN 1007-9327 (print) ISSN 2219-2840 (online)

ORIGINAL ARTICLE

Retrospective Study

Value of gamma-glutamyltranspeptidase-to-platelet ratio in diagnosis of hepatic fibrosis in patients with chronic hepatitis B

Yan-Chao Hu, Hao Liu, Xiao-Yan Liu, Li-Na Ma, Yu-Hua Guan, Xia Luo, Xiang-Chun Ding

Yan-Chao Hu, Xiao-Yan Liu, Li-Na Ma, Yu-Hua Guan, Xia Luo, Xiang-Chun Ding, Department of Infectious Diseases, General Hospital of Ningxia Medical University, Yinchuan 750001, Ningxia Hui Autonomous Region, China

Hao Liu, Department of Gastroenterology, General Hospital of Ningxia Medical University, Yinchuan 750001, Ningxia Hui Autonomous Region, China

ORCID number: Yan-Chao Hu (0000-0002-9179-1375); Hao Liu (0000-0002-2235-6177); Xiao-Yan Liu (0000-0002-6062-1656); Li-Na Ma (0000-0002-2524-9473); Yu-Hua Guan (0000-0002-6244-7997); Xia Luo (0000-0003-4090-9279); Xiang-Chun Ding (0000-0003-0283-9419).

Author contributions: Hu YC, Liu H, Liu XY, Ma LN, Guan YH, and Ding XC performed the study; Hu YC, Liu H, and Luo X collected and analyzed the data; and Hu YC designed the study and wrote the manuscript.

Supported by National Natural Science Foundation of China, No. 81460301 and No. 81760363; Key Project of Natural Science Foundation of Ningxia, No. NZ15134.

Conflict-of-interest statement: The authors declare that there are no conflicts of interest related to this study.

Data sharing statement: No additional data are available.

Manuscript source: Unsolicited manuscript

Correspondence to: Dr. Xiang-Chun Ding, Department of Infectious Disease, General Hospital of Ningxia Medical University, 804 Shengli Street, Yinchuan 750004, Ningxia Hui Autonomous Region, China. dingxiangchun@nyfy.com.cn
Telephone: +86-136-19511768

Received: August 5, 2017
Peer-review started: August 7, 2017
First decision: September 4, 2017
Revised: September 14, 2017
Accepted: September 29, 2017
Article in press: September 28, 2017
Published online: November 7, 2017

Abstract

AIM

To investigate the value of the gamma-glutamyl-traspeptidase (GGT)-to-platelet (PLT) ratio (GPR) in the diagnosis of hepatic fibrosis in patients with chronic hepatitis B (CHB).

METHODS

We included 390 untreated CHB patients in this study. The GPR, aspartate aminotransferase (AST)-to-PLT ratio index (APRI), and fibrosis-4 (FIB-4) of all patients were analysed to determine if these parameter were correlated with age, gender, medical history, liver function [total bilirubin (TBil), alanine aminotransferase (ALT), and AST], GGT, PLT count, or hepatic fibrosis stage. The GPR, APRI, and FIB-4, as well as the combination of the GPR and APRI or the GPR and FIB-4 were assessed in different cirrhosis stages using receiver operating characteristic (ROC) curve analysis to evaluate their value in diagnosing hepatic fibrosis in CHB patients.

RESULTS

The GPR, APRI, and FIB-4 were not correlated with

CHB patients' age, gender, or disease duration (P > 0.05), but all of these parameters were positively correlated with serum ALT, AST, GGT, and PLT count (P < 0.01). Additionally, the GPR, APRI, and FIB-4 were positively correlated with hepatic fibrosis (P < 0.01); the areas under the ROC curve for the GPR in F1, F2, F3, and F4 stages were 0.723, 0.741, 0.826, and 0.833, respectively, which were significantly higher than the respective values for the FIB-4 and APRI (F1: 0.581, 0.612; F2: 0.706, 0.711; F3: 0.73, 0.751; and F4: 0.799, 0.778). The respective diagnostic cut-off points for each stage were 0.402, 0.448, 0.548, and 0.833, respectively. The diagnostic sensitivity and specificity were, respectively, 88.8% and 87.5% in F1, 72.7% and 89.7% in F2, 81.3% and 98.6% in F3, and 80% and 97.4% in F4 when the GPR and APRI were connected in parallel; 86.6% and 90.2%, 78.4% and 96%, 78.6% and 97.4%, and 73.2% and 97.9%, respectively, when the GPR and APRI were connected in series; 80.2% and 89%, 65% and 89%, 70.3% and 98.5%, and 78.8% and 96.8%, respectively, when the GPR and FIB-4 were connected in parallel; and 83.6% and 87.9%, 76.8% and 96.6%, 72.7% and 98%, and 74.4% and 97.7%, respectively, when the GPR and FIB-4 were connected in series.

CONCLUSION

The GPR, as a serum diagnostic index of liver fibrosis, is more accurate, sensitive, and easy to use than the FIB-4 and APRI, and the GPR can significantly improve the sensitivity and specificity of hepatic fibrosis diagnosis in CHB when combined with the FIB-4 or APRI.

Key words: Gamma-glutamyltraspeptidase-to-platelet ratio; APRI; FIB-4; Chronic hepatitis B; Hepatic fibrosis

Core tip: Hepatic fibrosis is a precursor of cirrhosis for chronic hepatitis B patients. Severe hepatic fibrosis and cirrhosis can increase the incidence and mortality of primary liver cancer. Although liver biopsy is still the gold standard for the diagnosis of liver fibrosis, it is not widely used as a routine examination because of its invasiveness, high cost, and lack of repeatability. Identification of a simple, convenient, cheap, and noninvasive index to assess patients' hepatic fibrosis level is thus urgently needed. The aim of the present study was to investigate the value of the gamma-glutamyltranspeptidase-to-platelet ratio in the diagnosis of hepatic fibrosis in patients with chronic hepatitis B.

Hu YC, Liu H, Liu XY, Ma LN, Guan YH, Luo X, Ding XC. Value of gamma-glutamyltranspeptidase-to-platelet ratio in diagnosis of hepatic fibrosis in patients with chronic hepatitis B. *World J Gastroenterol* 2017; 23(41): 7425-7432 Available from: URL: http://www.wjgnet.com/1007-9327/full/v23/i41/7425.htm DOI: http://dx.doi.org/10.3748/wjg.v23.i41.7425

INTRODUCTION

Hepatic fibrosis is a precursor of cirrhosis in patients with chronic hepatitis B (CHB)[1]. Severe hepatic fibrosis and cirrhosis can increase the incidence and mortality of primary liver cancer[2]. Although liver biopsy is still the gold standard for the diagnosis of liver fibrosis, it is not widely used as a routine examination because of its invasiveness, high cost, and lack of repeatability. The aspartate aminotransferase (AST)-to-platelet (PLT) ratio index (APRI) and fibrosis-4 (FIB-4) are commonly used in the clinic as two noninvasive serum models; but their complicated calculation, poor sensitivity, and requirement for combination with other indexes for comprehensive evaluation of the degree of hepatic fibrosis actually increase the workload. As an alternative, transient elastography (Fibroscan) by imaging is considered a good tool for the diagnosis of hepatic fibrosis, but its performance is restricted by several factors, such as diet, obesity, ascites, and rib gap width. In recent years, researchers have tried to identify a simple, convenient, cheap, and noninvasive index to assess patients' hepatic fibrosis level, which could assist in early diagnosis to achieve timely treatment, delay cirrhosis or liver cancer incidence, improve patients' quality of life, and prolong patients' survival time.

The gamma-glutamyltraspeptidase (GGT)-to-PLT ratio (GPR) is a newly reported model for evaluating the grade of hepatic fibrosis, which is of great value in predicting hepatic fibrosis[3-11]. In June 2015, Lemoine *et al*[3] first reported that the GPR could be widely used as an independent predictor to assess hepatic fibrosis in CHB patients in West Africa, and that the sensitivity of the GPR is higher than that of the APRI and FIB-4. In November 2015, Boyd *et al*[9] showed that in patients with HBV and HIV superinfection in France, the GPR can predict the level of significant hepatic fibrosis. In November 2016, Li *et al*[11] reported that GPR was better than other noninvasive serum models in assessing hepatic fibrosis in CHB patients with high HBV DNA (≥ 5 $\log_{10}$ copies/mL) and normal or mildly elevated alanine transaminase (ALT) [≤ 2 times upper limit of normal (ULN)] in a Chinese population. Moreover, Lemoine *et al*[4] and Park *et al*[5] each reported that the GPR could be used as an independent factor in the preoperative evaluation of patients with primary liver cancer caused by CHB. However, likely due to the small sample size, they did not carry out an in-depth stratified pathological study of hepatic fibrosis. Based on these findings, to further explore the value of the GPR in the diagnosis of hepatic fibrosis, we retrospectively analysed a total of 652 outpatients and inpatients diagnosed with CHB at the General Hospital of Ningxia Medical University from May 2010 to January 2016, among whom 390 newly diagnosed CHB patients with complete data without previous

therapy were examined by correlation analysis and receiver operating characteristic curve (ROC) analysis. The correlations among patient's general information, medical history, and laboratory examination results were determined.

MATERIALS AND METHODS

Case selection

There were 652 outpatients and inpatients diagnosed with CHB at the General Hospital of Ningxia Medical University from May 2010 to January 2017. Patients with severe heart, brain or kidney disease; severe infection; super infection with hepatitis A virus, hepatitis C virus, hepatitis D virus, or hepatitis E virus or autoimmune liver disease; heavy drinking; or pregnancy were excluded. The remaining 390 newly diagnosed CHB patients, who did not undergo hepatoprotective, anti-hepatic fibrosis drug or antiviral drug treatments, were selected for the study, which included 283 males and 107 females. All CHB patients in the study had a complete medical history; data on HBV serum markers, serum HBV DNA, and liver function; and liver biopsy results. According to the clinical diagnostic criteria in the Guidelines for prevention and treatment of chronic hepatitis B published in 2001, all of the CHB patients were classified and analysed based on liver function and liver fibrosis.

Clinical indexes

The clinical characteristics of the CHB patients in this study, including their medical history, HBV serum markers, liver function, blood platelets, serum GGT, hepatic fibrosis indexes (APRI, FIB-4, and GPR), and pathological grade of hepatic fibrosis, were statistically analysed.

HBV serum marker detection: Chemiluminescence detection was used to assess HBV serum markers. The equipment and reagents were provided by Abbott Company (United States).

Liver function and GGT detection: A kinetic method was used to assess liver function and GGT. An ACX9 automatic biochemical analyser (Beckman Company, United States) was employed for this purpose. The biochemical test kit was also from Beckman. GGT normal range was 10-60 U/L.

Platelet detection: An automatic blood cell analyser was used for platelet detection. The normal range was 100-300 × 10^9/L.

APRI and FIB-4 calculation formulas: The formulas for calculating the APRI and FIB-4 indexes were as follows: APRI = (AST/ULN) × 100/PLT count (10^9/L) and FIB-4 = (age × AST)/(PLT count × ALT square root). Total bilirubin (TBIL) normal range was 3.4-17.1 μmol/L. AST normal range was 15-40 U/L. ALT normal range was 9-50 U/L.

Hepatic tissue pathological fibrosis analysis: The degree of fibrosis was graded from F1 to F4 according to the guidelines on CHB published in 2015.

Statistical method: A database of all data was established in Excel2000. The data, expressed as the mean ± SD, were statistically analysed using SPSS17.0 software. Normally distributed data were compared by *t*-test, and non-normally distributed data were compared using the χ^2 test. In addition, correlations were determined by Pearson correlation analysis. $P < 0.05$ indicated that the difference was statistically significant. ROC curves were plotted for the GPR, APRI and FIB-4; and the areas under the curve (AUCs) were calculated to determine the optimal cut-off points on the ROC curves corresponding to the greatest sum of the sensitivity and specificity and to calculate the rate of diagnostic accuracy. ROC curve is a graphical plot that illustrates the diagnostic ability of a binary classifier system as its discrimination threshold varies. The ROC curve is created by plotting the true positive rate (TPR) against the false positive rate (FPR) at various threshold settings. The TPR is also known as sensitivity, recall or probability of detection in machine learning. The FPR is also known as the fall-out or probability of false alarm and can be calculated as (1 - specificity). The ROC curve is thus the sensitivity as a function of fall-out. In general, if the probability distributions for both detection and false alarm are known, the ROC curve can be generated by plotting the cumulative distribution function of the detection probability on the Y-axis *vs* the cumulative distribution function of the false-alarm probability on the x-axis.

The value of the GPR, APRI, and FIB-4, as well as the combination of the GPR and APRI or the GPR and FIB-4, in the diagnosis of CHB associated liver fibrosis was evaluated according to the test results. A difference was considered statistically significant at $P < 0.05$.

RESULTS

Correlation analysis of GPR, APRI, and FIB-4 and clinical data

A total of 390 patients with CHB were enrolled in this study, including 283 males and 107 females, with a mean age of 38.94 ± 11.39 years. Pearson correlation analysis showed that the GPR, APRI and FIB-4 were not associated with the CHB patients' age, gender, or the disease course, but were associated with TBil, AST, ALT, GGT, and PLT count ($P < 0.01$; Table 1).

Correlation analysis of GPR, APRI, and FIB-4 and CHB liver function classification

To investigate the relationships between the GPR, APRI

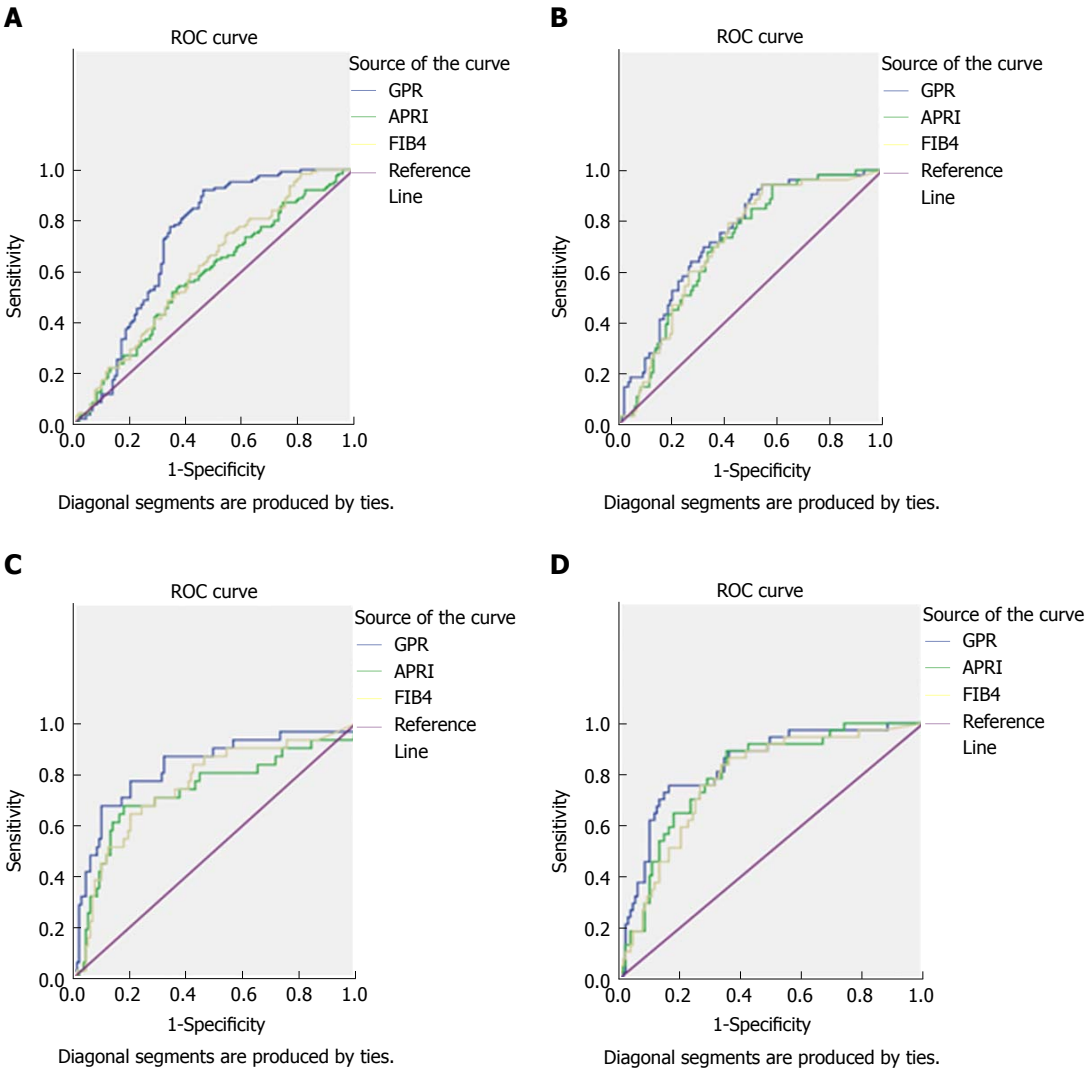

Figure 1 ROC curves of GPR, APRI, and FIB-4 for diagnosing liver fibrosis. A: F = 1; B: F = 2; F = 3; F = 4.

and FIB-4 and CHB disease, the CHB patients were divided into three groups according to their condition: 244 mild cases, 57 moderate cases, and 80 severe cases. Spearman correlation analysis showed that the GPR, APRI, and FIB-4 were positively related to the grade of the CHB patients' liver function ($P < 0.01$; Table 2).

Correlation analysis of GPR, APRI, and FIB-4 and hepatic fibrosis stages of CHB

According to the liver biopsy results, the degrees of hepatic fibrosis was divided into F1 to F4, and the Spearman rank correlation analysis showed that the GPR, APRI, and FIB-4 were positively correlated with the stage of hepatic fibrosis ($P < 0.01$; Table 3).

ROC analysis of GPR, APRI, and FIB-4 in diagnosis of hepatic fibrosis in CHB

The AUC values for the GPR in F1, F2, F3, and F4 were 0.723, 0.741, 0.826, and 0.833, respectively, which were significantly higher than the values for the FIB-4 and APRI (F1: 0.581 and 0.612; F2: 0.706 and 0.711; F3: 0.73 and 0.751; and F4: 0.799 and 0.778). The diagnostic cut-off points for each stage were, respectively, 0.402, 0.448, 0.548, and 0.833. The diagnostic sensitivity and specificity had a gradually increasing trend with the aggravation of hepatic fibrosis. In particular, the diagnostic sensitivity and specificity were, respectively, 88.8% and 87.5% in F1, 72.7% and 89.7% in F2, 81.3% and 98.6% in F3, and 80% and 97.4% in F4 when GPR and APRI were connected in parallel; 86.6% and 90.2 %, 78.4% and 96%, 78.6% and 97.4%, and 73.2% and 97.9%, respectively, when GPR and APRI were connected in series; 80.2% and 89%, 65% and 89%, 70.3% and 98.5%, and 78.8% and 96.8%, respectively, when GPR and APRI were connected in parallel; and 83.6% and 87.9%, 76.8% and 96.6%, 72.7% and 98%, and 74.4% and 97.7%, respectively, when GPR and APRI were connected in series (Figure 1, Table 4).

DISCUSSION

CHB is an inevitable stage for patients with HBV

Table 1 Correlation of the GPR, APRI, and FIB-4 (mean ± SD) with the baseline characteristics of patients

Parameter		GPR	APRI	FIB-4	
	Mean ± SD	*r*	*r*	*r*	*P*
TBIL (μmol/L)	22.70 ± 28.53	0.275	0.205	0.258	< 0.01
AST (IU/L)	81.71 ± 146.11	0.183	0.644	0.834	< 0.01
ALT (IU/L)	125.71 ± 246.43	0.113	0.547	0.764	< 0.01
GGT (IU/L)	225.21 ± 1008.88	0.779	0.222	0.235	< 0.01
PLT count (10^9/L)	160.82 ± 66.61	-0.285	-0.285	-0.26	< 0.01
GPR	0.73 ± 1.79	1.000	0.385	0.255	< 0.01
APRI	65.44 ± 140.77	0.385	1.000	0.847	< 0.01
FIB-4	417.93 ± 1367.85	0.255	0.847	1.000	< 0.01

TBIL: Total bilirubin; AST: Aspartate transaminase; ALT: Alanine transaminase; GGT: Gamma-glutamyltranspeptidase; PLT: Platelet; GPR: the gamma-glutamyltranspeptidase-to-platelet ratio; APRI: (AST)-to-platelet ratio index; FIB-4: Fibrosis-4.

Table 2 Correlation of the GPR, APRI, and FIB-4 (mean ± SD) with the liver function severity classification

Parameter	*n*	GPR	APRI	FIB-4
Liver function grade mild				
Mild	244	0.50 ± 0.92	30.71 ± 76.73	68.39 ± 126.12
r		0.213	0.091	0.219
P		< 0.01	< 0.01	< 0.01
Moderate	57	1.57 ± 3.59	101.20 ± 202.09	511.23 ± 1234.61
r		0.11	0.16	0.191
P		< 0.01	< 0.01	< 0.01
Severe	80	0.84 ± 1.74	145.90 ± 192.51	1417.54 ± 2544.58
r		0.016	0.563	0.720
P		< 0.01	< 0.01	< 0.01

Table 3 Correlation of the GPR, APRI, and FIB-4 (mean ± SD) with the fibrosis grade

Parameter	*n*	GPR	APRI	FIB-4
Fibrosis grade				
F1	122	0.54 ± 1.23	53.18 ± 134.37	331.04 ± 1152.78
r		0.077	0.089	0.077
P		< 0.01	< 0.01	< 0.01
F2	52	0.66 ± 2.02	47.55 ± 120.04	278.98 ± 1053.17
r		0.223	0.069	0.037
P		< 0.01	< 0.01	< 0.01
F3	61	0.60 ± 0.95	61.15 ± 152.26	406.94 ± 1580.52
r		0.278	0.226	0.183
P		< 0.01	< 0.01	< 0.01
F4	41	0.52 ± 0.85	49.43 ± 125.04	287.50 ± 1092.13
r		0.186	0.121	0.064
P		< 0.01	< 0.01	< 0.01

infection, developing from hepatic fibrosis to cirrhosis and leading to chronic liver failure and HBV-related hepatocellular carcinoma. Assessment of the degree of hepatic fibrosis and the progression of CHB is important in determining the treatment strategy for and prognosis of CHB patients[12,13]. Currently, liver biopsy is still the gold standard for evaluating the degree of hepatic fibrosis in certain high-risk liver cirrhosis and liver cancer patients and is an indicator for clinicians to guide patients, especially CHB patients with mildly elevated AIT, to start antiviral therapy in a timely fashion. However, as an invasive examination, liver biopsy can cause serious complications[14-18]; thus, it is not preferred by most CHB patients in the clinic. Given this situation, strategies for avoiding and reducing the frequency of liver biopsy and obtaining reliable liver pathological data are urgently needed[19-21]. The APRI and FIB-4 were developed as serum models in recent years and have been widely used in the assessment of hepatic fibrosis classification[22-26]. However, for patients with severe liver inflammation, the hepatic fibrosis results yielded by the APRI and FIB-4 are variable. Therefore, these indexes are predominantly used for hepatic fibrosis evaluation in patients with mildly abnormal liver function before treatment. Recently, Lemoine *et al*[3] analysed the combination of GGT and PLT count and found that the GPR was significantly better than the FIB-4 and APRI in predicting significant liver fibrosis. However, due to the sample size, the depth of the study was limited. To further explore the value of applying the GPR, a correlation analysis of 390 newly diagnosed CHB patients who were not treated with hepatoprotective therapy, anti-liver fibrosis drugs, or antiviral drugs to assess the correlation of the GPR, APRI, and FIB-4 with age, gender, medical history, liver function (TBil, ALT, AST), GGT, PLT count, and liver tissue fibrosis stage. The results showed that the GPR, APRI, and FIB-4 had no correlation with the CHB patients' age, gender, or duration, but were correlated with TBil, AST, ALT, GGT, and PLT count. Furthermore, the GPR, APRI, and FIB-4 were positively associated with liver function and liver tissue pathological grade ($P < 0.01$). These results indicate that the GPR, as well as the APRI and FIB-4, can not only be used as an index to judge the severity of acute liver injury, but also has potential value in evaluating the degree of hepatic fibrosis in patients with CHB.

To further analyse the value of the GPR for the diagnosis of hepatic fibrosis, we performed ROC analysis of the GPR, APRI, and FIB-4 according to the stage of liver fibrosis. The results showed that the AUC values for GPR in F1, F2, F3, and F4 were 0.723, 0.741, 0.826 and 0.833, respectively, which were significantly better than the values for the APRI and FIB-4 (F1: 0.581 and 0.612; F2: 0.706 and 0.711; F3: 0.73 and

Table 4 GPR, APRI, and FIB-4 results relative to hepatic fibrosis stage (F1, F2, F3, and F4) in CHB patients

	Parameter	GPR	APRI	FIB-4	GPR + APRI (in parallel)	GPR + APRI (in series)	GPR + FIB-4 (in parallel)	GPR + FIB-4 (in series)
	AUC	0.723	0.581	0.612	-	-	-	-
	Cut-off	0.448	0.166	0.201	-	-	-	-
F1	Sensitivity	90.6%	88.8%	62.1%	88.8%	86.8%	80.2%	83.6%
	Specificity	54.2%	87.5%	66.3%	87.5%	90.2%	89%	87.9%
	AUC	0.741	0.706	0.711	-	-	-	-
	Cut-off	0.402	0.361	0.4	-	-	-	-
F2	Sensitivity	57.1%	75.8%	47.4%	72.7%	78.4%	65%	76.8%
	Specificity	89.5%	92.5%	89.3%	89.7%	96%	89%	96.6%
	AUC	0.826	0.73	0.751	-	-	-	-
	Cut-off	0.548	0.496	0.44	-	-	-	-
F3	Sensitivity	74.1%	70.6%	64.7%	81.3%	78.6%	70.3%	72.7%
	Specificity	91.8%	90.5%	88%	98.6%	97.4%	98.5%	98%
	AUC	0.833	0.799	0.778	-	-	-	-
	Cut-off	0.591	0.538	0.503	-	-	-	-
F4	Sensitivity	83.2%	74%	75.4%	80%	73.2%	78.8%	74.4%
	Specificity	96.5%	95.4%	94.5%	97.4%	97.9%	96.8%	97.7%

In parallel: Both parameters are met simultaneously; In series: One of two parameters is met.

0.751; and F4: 0.799 and 0.778). The diagnostic cut-off points for each stage were, respectively, 0.402, 0.448, 0.548, and 0.833. The diagnostic sensitivity and specificity showed a gradually increasing trend with the aggravation of liver fibrosis. Thus, the combined detection of the GPR and FIB-4 or the GPR and APRI could improve the sensitivity and specificity the diagnosis of CHB-associated hepatic fibrosis in each stage. These results indicate that the GPR can accurately differentiate the stages of hepatic fibrosis in CHB patients, and that the diagnostic value of the GPR is superior to those of the APRI and FIB-4. Thus, the combined detection of the GPR and FIB-4 or the GPR and APRI can significantly improve the diagnostic sensitivity and specificity of hepatic fibrosis diagnosis in CHB. However, serum GGT levels may increase slightly to moderately in acute hepatitis, chronic active hepatitis, decompensated cirrhosis, obstructive jaundice, alcoholism, and hepatocellular carcinoma cases[16,27-28], which may lead to variation of the GPR. Due to the sample size in this study, we did not further stratify the cohort by liver function. The value of the GPR in evaluating the degree of hepatic fibrosis in CHB patients with different levels of liver function is thus still unknown. Further research involving stratified analyses and verification of our results with increased sample sizes is needed.

ARTICLE HIGHLIGHTS

Research background

Hepatic fibrosis is a precursor of cirrhosis in patients with chronic hepatitis B (CHB). Severe hepatic fibrosis and cirrhosis can increase the incidence and mortality of primary liver cancer. Looking for a non-invasive, simple, easy to operate, cheap way to assess liver fibrosis is very important.

Liver biopsy is still the gold standard for the diagnosis of liver fibrosis, but it is not widely used as a routine examination because of its invasiveness, high cost, and lack of repeatability. As an alternative, transient elastography (Fibroscan) by imaging is considered a good tool for the diagnosis of hepatic fibrosis, but its performance is restricted by several factors.

Researchers have tried to identify a simple, convenient, cheap, and noninvasive index to assess patients' hepatic fibrosis level, which could assist in early diagnosis to achieve timely treatment, delay cirrhosis or liver cancer occurrence, improve patients' quality of life, and prolong patients' survival time.

Research motivation

At present, liver biopsy is still the gold standard for the diagnosis of liver fibrosis, but liver biopsy can cause serious complications; thus, it is not preferred by most CHB patients in the clinic. Our study aimed to identify a simple, convenient, cheap, and noninvasive index to assess patients' hepatic fibrosis level.

Research objectives

Our study aimed to identify a simple, convenient, cheap, and noninvasive index to assess patients' hepatic fibrosis level. In the future, in our clinical work, assessing the level of liver fibrosis in patients is faster and easier, effectively avoiding the complications caused by liver biopsy.

Research methods

There were 652 outpatients and inpatients diagnosed with CHB at the General Hospital of Ningxia Medical University. Patients with severe heart, brain or kidney disease; severe infection; superinfection with hepatitis A virus, hepatitis C virus, hepatitis D virus, or hepatitis E virus or autoimmune liver disease; heavy drinking; or pregnancy were excluded. The remaining 390 newly diagnosed CHB patients, who did not undergo hepatoprotective, anti-hepatic fibrosis drug, or antiviral drug treatments, were selected for the study. We chose multiple noninvasive indicators for comparison, to illustrate that GPR is an optimal noninvasive index. Meanwhile, the sample size was large to enhance persuasiveness. Statistically analysed using SPSS17.0 software, the data are expressed as the mean ± SD. Normal distributed data were compared by *t*-test, and non-normally distributed data were compared using the Chi-square test. In addition, correlations were determined by Pearson correlation analysis; $P < 0.05$ indicated that the difference was statistically significant.

Research results

The GPR is a simple, convenient, cheap, and noninvasive index to assess patients' hepatic fibrosis level, and it can significantly improve the sensitivity and specificity of hepatic fibrosis diagnosis in CHB when combined with the FIB-4 or APRI.

Research conclusions

The GPR is a newly reported model for evaluating the grade of hepatic fibrosis, which is of great value in predicting hepatic fibrosis. In June 2015, Lemoine *et al* first reported that the GPR could be widely used as an independent predictor to

assess hepatic fibrosis in CHB patients in West Africa, and that the sensitivity of the GPR is higher than those of the APRI and FIB-4. GPR is a simple, convenient, cheap, and noninvasive index to assess patients' hepatic fibrosis level, and it can significantly improve the sensitivity and specificity of hepatic fibrosis diagnosis in CHB when combined with the FIB-4 or APRI. In the future, in our clinical work, assessing the level of liver fibrosis in patients is faster and easier, effectively avoiding the complications caused by liver biopsy.

Research perspectives

In the future work, it is required to look for more noninvasive, convenient and efficient methods to assess the level of liver fibrosis in patients with chronic hepatitis B.

REFERENCES

1 **Liang P**, Zu J, Yin J, Li H, Gao L, Cui F, Wang F, Liang X, Zhuang G. The independent impact of newborn hepatitis B vaccination on reducing HBV prevalence in China, 1992-2006: A mathematical model analysis. *J Theor Biol* 2015; **386**: 115-121 [PMID: 26375372 DOI: 10.1016/j.jtbi.2015.08.030]

2 **Wu JF**, Chang MH. Natural history of chronic hepatitis B virus infection from infancy to adult life - the mechanism of inflammation triggering and long-term impacts. *J Biomed Sci* 2015; **22**: 92 [PMID: 26487087 DOI: 10.1186/s12929-015-0199-y]

3 **Lemoine M**, Shimakawa Y, Nayagam S, Khalil M, Suso P, Lloyd J, Goldin R, Njai HF, Ndow G, Taal M, Cooke G, D'Alessandro U, Vray M, Mbaye PS, Njie R, Mallet V, Thursz M. The gamma-glutamyl transpeptidase to platelet ratio (GPR) predicts significant liver fibrosis and cirrhosis in patients with chronic HBV infection in West Africa. *Gut* 2016; **65**: 1369-1376 [PMID: 26109530 DOI: 10.1136/gutjnl-2015-309260]

4 **Lemoine M**, Thursz M, Mallet V, Shimakawa Y. Diagnostic accuracy of the gamma-glutamyl transpeptidase to platelet ratio (GPR) using transient elastography as a reference. *Gut* 2017; **66**: 195-196 [PMID: 26921348 DOI: 10.1136/gutjnl-2016-311554]

5 **Park YE**, Kim BK, Park JY, Kim DY, Ahn SH, Han KH, Han S, Jeon MY, Heo JY, Song K, Kim SU. Gamma-glutamyl transpeptidase-to-platelet ratio is an independent predictor of hepatitis B virus-related liver cancer. *J Gastroenterol Hepatol* 2017; **32**: 1221-1229 [PMID: 27859587 DOI: 10.1111/jgh.13653]

6 **Wang WL,** Zheng XL, Zhang ZY, Zhou Y, Hao J, Tang G, Li O, Xiang JX, Wu Z, Wang B. Preoperative γ-glutamyl transpeptidase to platelet ratio (GPR) is an independent prognostic factor for HBV-related hepatocellular carcinoma after curative hepatic resection. *Medicine* (Baltimore) 2016; **95**: 27 (e4087) [PMID: 27399101 DOI: 10.1097/MD.0000000000004087]

7 **Pang Q**, Bi JB, Wang ZX, Xu XS, Qu K, Miao RC, Chen W, Zhou YY, Liu C. Simple models based on gamma-glutamyl transpeptidase and platelets for predicting survival in hepatitis B-associated hepatocellular carcinoma. *Onco Targets Ther* 2016; **9**: 2099-2109 [PMID: 27110127 DOI: 10.2147/OTT.S101465]

8 **Li Q**, Song J, Huang Y, Li X, Zhuo Q, Li W, Chen C, Lu C, Qi X, Chen L. The Gamma-Glutamyl-Transpeptidase to Platelet Ratio Does not Show Advantages than APRI and Fib-4 in Diagnosing Significant Fibrosis and Cirrhosis in Patients With Chronic Hepatitis B: A Retrospective Cohort Study in China. *Medicine* (Baltimore) 2016; **95**: e3372 [PMID: 27100421 DOI: 10.1097/MD.0000000000003372]

9 **Boyd A,** Bottero J, Lacombe K. Theγ-glutamyltranspeptidase-to-plateletratio as a predictor of liverfibrosisinpatients co-infect-edwith HBV and HIV. *Gut* 2016; **65**: 718-720 [DOI: 10.1136/gutjnl-2015-310607]

10 **Schiavon LL**, Narciso-Schiavon JL, Ferraz MLG, Silva AEB, Carvalho-Filho RJ. The γ-glutamyl transpeptidase to platelet ratio (GPR) in HBV patients: just adding up? *Gut* 2017; **66**: 1169-1170 [PMID: 27534672 DOI: 10.1136/gutjnl-2016-312658]

11 **Li Q**, Lu C, Li W, Huang Y, Chen L. Globulin-platelet model predicts significant fibrosis and cirrhosis in CHB patients with high HBV DNA and mildly elevated alanine transaminase levels. *Clin Exp Med* 2017; Epub ahead of print [PMID: 28884309 DOI: 10.1007/s10238-017-0472-3]

12 **Trépo C**, Chan HL, Lok A. Hepatitis B virus infection. *Lancet* 2014; **384**: 2053-2063 [PMID: 24954675 DOI: 10.1016/S0140-6736(14)60220-8]

13 **Imamura H**, Matsuyama Y, Tanaka E, Ohkubo T, Hasegawa K, Miyagawa S, Sugawara Y, Minagawa M, Takayama T, Kawasaki S, Makuuchi M. Risk factors contributing to early and late phase intrahepatic recurrence of hepatocellular carcinoma after hepatectomy. *J Hepatol* 2003; **38**: 200-207 [PMID: 12547409 DOI: 10.1016/S0168-8278(02)00360-4]

14 **Sorbi D**, Boynton J, Lindor KD. The ratio of aspartate aminotransferase to alanine aminotransferase: potential value in differentiating nonalcoholic steatohepatitis from alcoholic liver disease. *Am J Gastroenterol* 1999; **94**: 1018-1022 [PMID: 10201476 DOI: 10.1111/j.1572-0241.1999.01006.x]

15 **McGill DB**, Rakela J, Zinsmeister AR, Ott BJ. A 21-year experience with major hemorrhage after percutaneous liver biopsy. *Gastroenterology* 1990; **99**: 1396-1400 [PMID: 2101588 DOI: 10.1016/0016-5085(90)91167-5]

16 **Shukla A**, Kapileswar S, Gogtay N, Joshi A, Dhore P, Shah C, Abraham P, Bhatia S. Simple biochemical parameters and a novel score correlate with absence of fibrosis in patients with nonalcoholic fatty liver disease. *Indian J Gastroenterol*2015; **34**: 281-285 [PMID: 26341864 DOI: 10.1007/s12664-015-0580-5]

17 **Liaw YF**, Leung N, Kao JH, Piratvisuth T, Gane E, Han KH, Guan R, Lau GK, Locarnini S; Chronic Hepatitis B Guideline Working Party of the Asian-Pacific Association for the Study of the Liver. Asian-Pacific consensus statement on the management of chronic hepatitis B: a 2008 update. *Hepatol Int* 2008; **2**: 263-283 [PMID: 19669255 DOI: 10.1007/s12072-008-9080-3]

18 **Lok AS,** McMahon BJ. Chronic hepatitis B: update 2009. *Hepatology* 2009; **50**: 661-662 [DOI: 10.1002/hep.23190]

19 **Chen J**, Liu C, Chen H, Liu Q, Yang B, Ou Q. Study on noninvasive laboratory tests for fibrosis in chronic HBV infection and their evaluation. *J Clin Lab Anal* 2013; **27**: 5-11 [PMID: 23292737 DOI: 10.1002/jcla.21554]

20 **Lee IC**, Chan CC, Huang YH, Huo TI, Chu CJ, Lai CR, Lee PC, Su CW, Hung HH, Wu JC, Lin HC, Lee SD. Comparative analysis of noninvasive models to predict early liver fibrosis in hepatitis B e Antigen-negative Chronic Hepatitis B. *J Clin Gastroenterol* 2011; **45**: 278-285 [PMID: 20505530 DOI: 10.1097/MCG.0b013e3181dd5357]

21 **Pinto J**, Matos H, Nobre S, Cipriano MA, Marques M, Pereira JM, Gonçalves I, Noruegas MJ. Comparison of acoustic radiation force impulse/serum noninvasive markers for fibrosis prediction in liver transplant. *J Pediatr Gastroenterol Nutr* 2014; **58**: 382-386 [PMID: 24164902 DOI: 10.1097/MPG.0000000000000226]

22 **Sebastiani G**, Halfon P, Castera L, Mangia A, Di Marco V, Pirisi M, Voiculescu M, Bourliere M, Alberti A. Comparison of three algorithms of non-invasive markers of fibrosis in chronic hepatitis C. *Aliment Pharmacol Ther* 2012; **35**: 92-104 [PMID: 22035045 DOI: 10.1111/j.1365-2036.2011.04897.x]

23 **Arora A**, Sharma P. Non-invasive Diagnosis of Fibrosis in Non-alcoholic Fatty Liver Disease. *J Clin Exp Hepatol* 2012; **2**: 145-155 [PMID: 25755423 DOI: 10.1016/S0973-6883(12)60103-0]

24 **Xiao G**, Yang J, Yan L. Comparison of diagnostic accuracy of aspartate aminotransferase to platelet ratio index and fibrosis-4 index for detecting liver fibrosis in adult patients with chronic hepatitis B virus infection: a systemic review and meta-analysis. *Hepatology* 2015; **61**: 292-302 [PMID: 25132233 DOI: 10.1002/hep.27382]

25 **Sumida Y**, Yoneda M, Hyogo H, Itoh Y, Ono M, Fujii H, Eguchi Y, Suzuki Y, Aoki N, Kanemasa K, Fujita K, Chayama K, Saibara T, Kawada N, Fujimoto K, Kohgo Y, Yoshikawa T, Okanoue T; Japan Study Group of Nonalcoholic Fatty Liver Disease (JSG-NAFLD). Validation of the FIB4 index in a Japanese nonalcoholic fatty liver disease population. *BMC Gastroenterol* 2012; **12**: 2 [PMID: 22221544 DOI: 10.1186/1471-230X-12-2]

26 **Shah AG**, Lydecker A, Murray K, Tetri BN, Contos MJ, Sanyal AJ; Nash Clinical Research Network. Comparison of noninvasive

markers of fibrosis in patients with nonalcoholic fatty liver disease. *Clin Gastroenterol Hepatol* 2009; **7**: 1104-1112 [PMID: 19523535 DOI: 10.1016/j.cgh.2009.05.033]

27 **Elawdi HA**, Franzini M, Paolicchi A, Emdin M, Fornaciari I, Fierabracci V, De Simone P, Carrai P, Filipponi F. Circulating gamma-glutamyltransferase fractions in cirrhosis. *Liver Int* 2014; **34**: e191-e199 [PMID: 24387676 DOI: 10.1111/liv.12455]

28 **Eminler AT**, Irak K, Ayyildiz T, Keskin M, Kiyici M, Gurel S, Gulten M, Dolar E, Nak SG. The relation between liver histopathology and GGT levels in viral hepatitis: more important in hepatitis B. *Turk J Gastroenterol* 2014; **25**: 411-415 [PMID: 25254524 DOI: 10.5152/tjg.2014.3693]

P- Reviewer: Sirin G, Jin B, He ST, Komatsu H, Koch TR, Ikura Y
S- Editor: Qi Y **L- Editor**: Wang TQ
E- Editor: Huang Y

World Journal of Gastroenterology

Submit a Manuscript: http://www.f6publishing.com

World J Gastroenterol 2017 November 7; 23(41): 7433-7439

DOI: 10.3748/wjg.v23.i41.7433

ISSN 1007-9327 (print) ISSN 2219-2840 (online)

ORIGINAL ARTICLE

Observational Study

Anatomic isolated caudate lobectomy: Is it possible to establish a standard surgical flow?

Yun Jin, Liang Wang, Yuan-Quan Yu, Dong-Er Zhou, Da-Ren Liu, Jun-Jie Yang, Shu-You Peng, Jiang-Tao Li

Yun Jin, Liang Wang, Yuan-Quan Yu, Dong-Er Zhou, Da-Ren Liu, Shu-You Peng, Jiang-Tao Li, Department of General Surgery, The Second Affiliated Hospital, College of Medicine, Zhejiang University, Hangzhou 310009, Zhejiang Province, China

Jun-Jie Yang, Department of General Surgery, Xinchang People's Hospital, Shaoxing 312500, Zhejiang Province, China

ORCID number: Yun Jin (0000-0002-3073-4043); Liang Wang (0000-0001-5345-2818); Yuan-Quan Yu (0000-0002-1109-1652); Dong-Er Zhou (0000-0003-3673-5001); Da-Ren Liu (0000-0001-7022-8033); Jun-Jie Yang (0000-0003-0263-4501); Shu-You Peng (0000-0003-3989-3056); Jiang-Tao Li (0000-0001-7538-2910).

Author contributions: Peng SY and Li JT conceived and designed the study; Jin Y, Wang L, Yu YQ and Yang JJ performed the study; Jin Y and Yang JJ wrote the paper; Zhou DE, Liu DR, Peng SY and Li JT reviewed and edited the manuscript; All authors read and approved the manuscript.

Supported by the National Natural Science Foundation of China, No. 81570559 and No. 81272673; 2014 Zhejiang Provincial Program for the Cultivation of High-level Innovative Health Talents.

Institutional review board statement: The study was reviewed and approved by the Second Affiliated Hospital Zhejiang University School of Medicine Institutional Review Board.

Informed consent statement: All study participants, or their legal guardian, provided informed written consent prior to study enrollment.

Conflict-of-interest statement: We declare that we have no conflict of interest related to this work.

Data sharing statement: Technical appendix, statistical code, and dataset available from the Jiang-Tao Li at zrljt@zju.edu.cn.

Manuscript source: Unsolicited manuscript

Correspondence to: Jiang-Tao Li, MD, FACS, Department of General Surgery, The Second Affiliated Hospital, School of Medicine, Zhejiang University, 88 Jiefang Road, Hangzhou 310009, Zhejiang Province, China. zrljt@zju.edu.cn
Telephone: +86-571-89713727

Received: July 4, 2017
Peer-review started: July 5, 2017
First decision: July 28, 2017
Revised: August 10, 2017
Accepted: September 13, 2017
Article in press: September 13, 2017
Published online: November 7, 2017

Abstract

AIM

To establish the surgical flow for anatomic isolated caudate lobe resection.

METHODS

The study was approved by the ethics committee of the Second Affiliated Hospital Zhejiang University School of Medicine (SAHZU). From April 2004 to July 2014, 20 patients were enrolled who underwent anatomic isolated caudate lobectomy at SAHZU. Clinical and postoperative pathological data were analyzed.

RESULTS

Of the total 20 cases, 4 received isolated complete caudate lobectomy (20%) and 16 received isolated partial caudate lobectomy (80%). There were 4 cases

with the left approach (4/20, 20%), 6 cases with the right approach (6/20, 30%), 7 cases with the bilateral combined approach (7/20, 35%), 3 cases with the anterior approach (3/20, 15%), and the hanging maneuver was also combined in 2 cases. The median tumor size was 5.5 cm (2-12 cm). The median intra-operative blood loss was 600 mL (200-5700 mL). The median intra-operative blood transfusion volume was 250 mL (0-2400 mL). The median operation time was 255 min (110-510 min). The median post-operative hospital stay was 14 d (7-30 d). The 1- and 3-year survival rates for malignant tumor were 88.9% and 49.4%, respectively.

CONCLUSION

Caudate lobectomy was a challenging procedure. It was demonstrated that anatomic isolated caudate lobectomy can be done safely and effectively.

Key words: Caudate lobectomy; Surgical flow; Anatomic liver resection

Core tip: Caudate lobe resection is still a challenging procedure for the vast majority of surgeons because of the difficult anatomical location and intraoperative bleeding. According to prior experience, six steps were established and validated on the patient. Anatomic isolated caudate lobectomy can be done safely and effectively following the surgical flow.

Jin Y, Wang L, Yu YQ, Zhou DE, Liu DR, Yang JJ, Peng SY, Li JT. Anatomic isolated caudate lobectomy: Is it possible to establish a standard surgical flow? *World J Gastroenterol* 2017; 23(41): 7433-7439 Available from: URL: http://www.wjgnet.com/1007-9327/full/v23/i41/7433.htm DOI: http://dx.doi.org/10.3748/wjg.v23.i41.7433

INTRODUCTION

The caudate lobe (CL), situated in a tricky location, lies deep in the liver and is adjacent to major blood vessels. CL consists of a Spiegel lobe on the left, a caudate process on the right, and a paracaval portion between them[1]. Surgical resection is the most suitable strategy to eradicate hepatic malignant lesions in this area. In recent years, the number of caudate lobectomies has increased with the improvement of imaging[2-5]. However, CL resection remains a challenging procedure for the vast majority of surgeons because of the difficult anatomical location and intraoperative bleeding.

Overall survival (OS) can be achieved by anatomic liver resection for hepatocellular carcinoma (HCC) patients[6,7]. However, reports of anatomic resection usually refer to segment Ⅱ to segment Ⅷ, excepting CL. The implement of more CL resection is limited due to a lack of standard flow. Therefore, the aim of this study was to establish the surgical flow for anatomic isolated CL resection.

MATERIALS AND METHODS

Patients

The study was approved by the ethics committee of the Second Affiliated Hospital Zhejiang University School of Medicine. Twenty patients who underwent anatomic isolated caudate lobectomy between April 2004 to July 2014, performed by our group, were enrolled in this study, including 13 males (13/20, 65%) and 7 females (7/20, 35%). The median age of patients was 55.5 years, ranging from 24-72 years. Postoperative pathological examinations included 14 cases of HCC (14/20, 70%), 2 cases of adenocarcinoma (2/20, 10%), 1 case of hepatic hemangioma (1/20, 5%), 1 case of hepatosarcoma (1/20, 5%), 1 case of angioleiomyoma (1/20, 5%), and 1 case of adenoma (1/20, 5%) (Table 1).

Surgical approach

The procedures were performed according to the results of computed tomography (CT) or magnetic resonance imaging (MRI) before surgery (Figure 1). Based on the location of the tumor, four different flows were planned before surgery (Figure 2).

Step 1: Mobilization of the liver. For all patients, a reversed L-shaped incision was adopted from xiphoid to the tip of 12th rib. For resection of the caudate process, the right ligamentum teres, falciform ligament, coronary ligament and triangular ligament were divided (Figure 3A). The hepatorenal ligament was dissected and the right adrenal gland was separated from the right liver with a right approach. For resection of the Spiegel lobe, usually, the ligaments of the left liver were dissected, Arantius ligament was divided until the tip of the CL and the Spiegel lobe was exposed completely with a left approach (Figure 4). For complete CL resection, usually, both left and right liver were mobilized. For giant CL tumors or the paracaval portion, sometimes, the transection of the liver parenchyma along Cantilie's line were conducted.

Step 2: Ligation of short hepatic veins. For a right approach, liver was turned to the left and the inferior vena cava (IVC) was exposed. The inferior right hepatic vein was divided firstly and short hepatic veins were ligated gradually along the IVC (Figure 3B). The caudate process was exposed and dissociated from the IVC. For a left approach, the liver was turned to the right and short hepatic veins were isolated as well as divided until the Spiegel lobe was separated from the

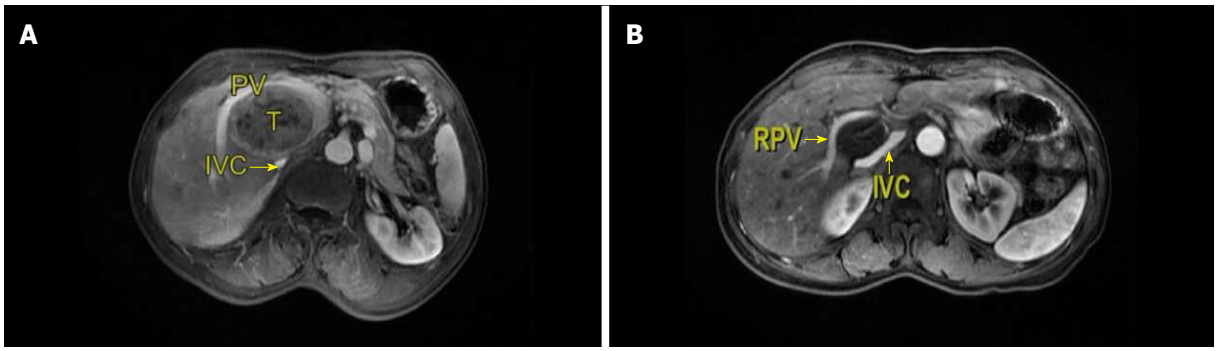

Figure 1 Magnetic resonance images for caudate lesions. A: T located between PV and IVC; B: Hepatic hemangioma located between RPV and IVC. IVC: Inferior vena cava; PV: Portal vein; RPV: Right portal vein; T: Tumor.

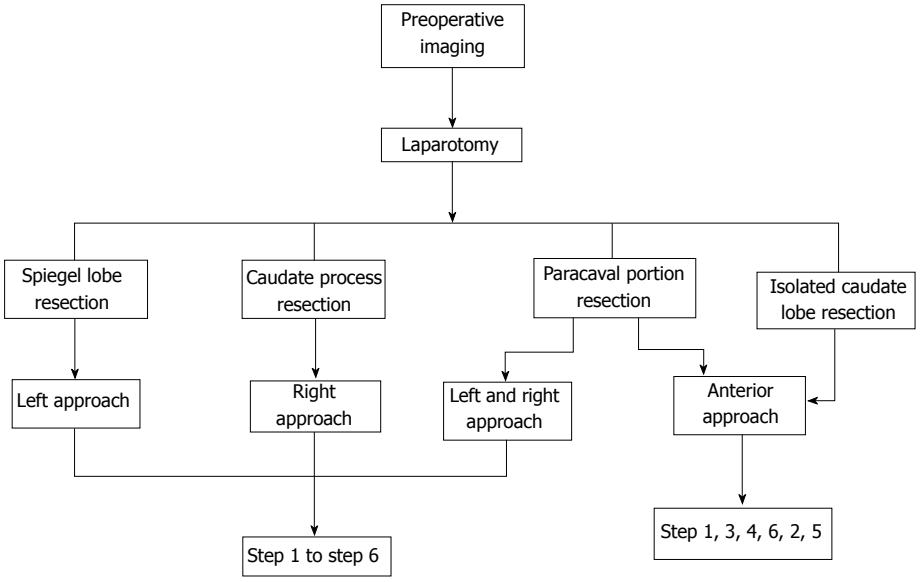

Figure 2 Surgical flow.

Table 1 Clinical data for all 20 patients with isolated caudate lobectomy

n = 20	Data
Sex	
Female	7 (35)
Male	13 (65)
Age in yr	55.5 (24-72)
Pathological examinations	
Hepatocellular carcinoma	14 (70)
Intrahepatic cholangia carcinoma	2 (10)
Hepatic hemangioma	1 (5)
Hepatosarcoma	1 (5)
Angiomyolipoma	1 (5)
Adenoma	1 (5)
Tumor size in cm	5.5 (2-12)

Data are presented as *n* (%) or median (range).

IVC completely.

Step 3: Isolation and taping of three major hepatic veins. The liver was pushed down medially, and the fossa was exposed between the right hepatic vein (RHV) and the middle hepatic vein (MHV) (Figure 3C). A tape was positioned around the common trunk of the MHV and the left hepatic vein (LHV). The hepatocaval ligament (Makuuchi ligament[8]) was extra-hepatically dissected from the right side and another tape was positioned around the RHV carefully.

Step 4: Controlling the inflow blood supply. The hepatoduodenal ligament was exposed and a tape was encircled around the hepatic hilum to control hepatic blood inflow if necessary. The occlusion time was usually 5 min, 8 min and 10 min during the first three times and then 10 min with 2 min interruption every time. The branch of portal triads to the CL was divided and ligated. Afterwards, ischemia landmarks could be found easily (Figure 3D).

Step 5: Identification of the CL boundary. The left boundary was established as the Arantius ligament, the right boundary was described as Peng's line from the CL tip to the caudate process[9] (Figure 5). The tip

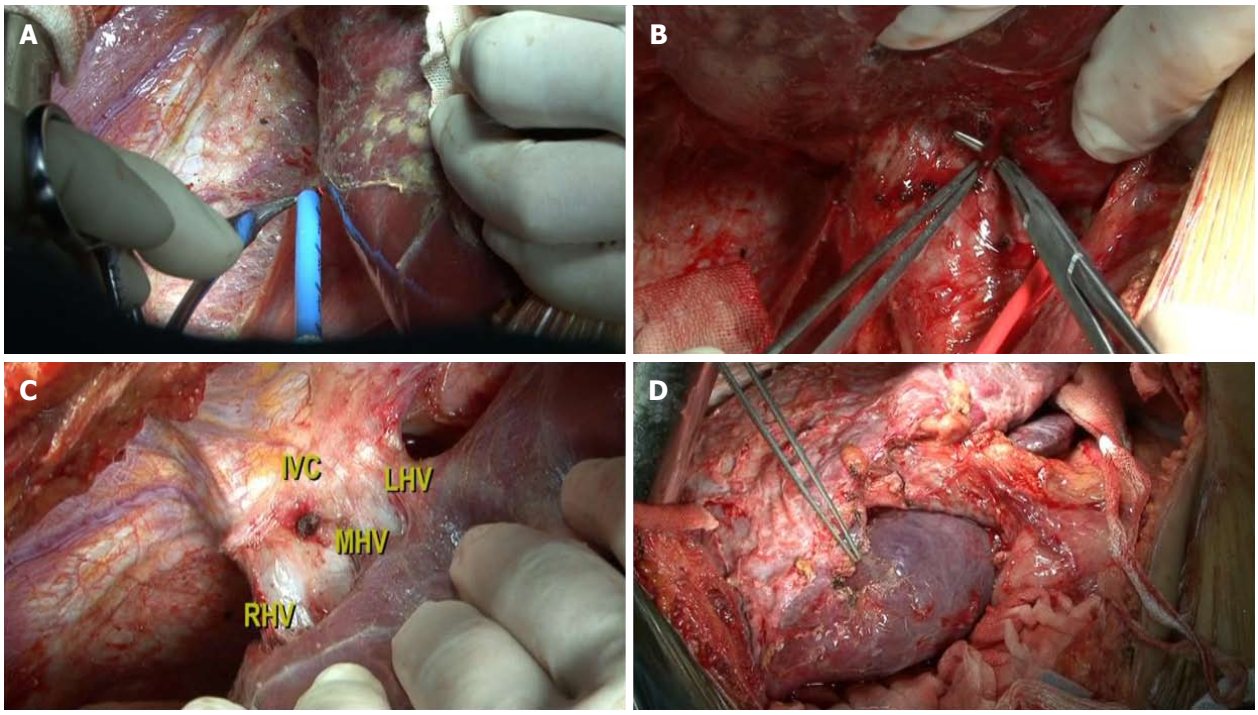

Figure 3 Flow of the caudate lobectomy. A: Liver mobilization; B: Short hepatic veins isolated and divided; C: Three hepatic veins isolated; D: Ischemia landmark of the caudate lobe is shown.

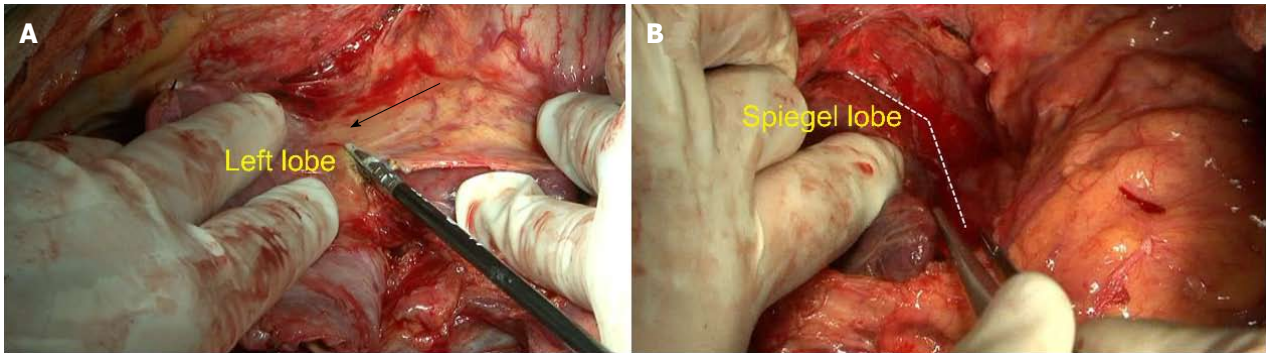

Figure 4 Marking of the left boundary of the caudate lobe. A: Divided Arantius ligament (black arrow); B: Left boundary of caudate lobe (white dotted line).

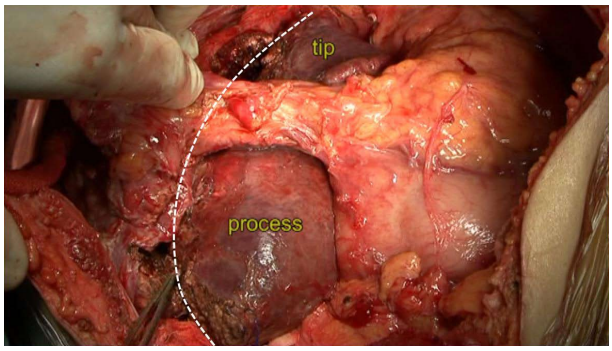

Figure 5 Identification of the right boundary of the caudate lobe. Peng's line was marked as the right boundary, which was from the upper tip to the process (white arc).

of the CL was located between the LHV and the IVC.

Step 6: Liver transection. Hepatic parenchyma was transected with the curettage and aspiration dissection technique using Peng's multifunction operative dissector[4,10].

The anatomic isolated caudate lobectomy is presented in the accompanying video (Supplement 1).

Statistical analysis

Clinical variables were described as median or mean ± SD. Discrete and continuous variables were analyzed by chi-square test and *t*-test, respectively. Survival time was analyzed by the Kaplan-Meier method. All data were analyzed by SPSS 16.0 software (SPSS Inc,

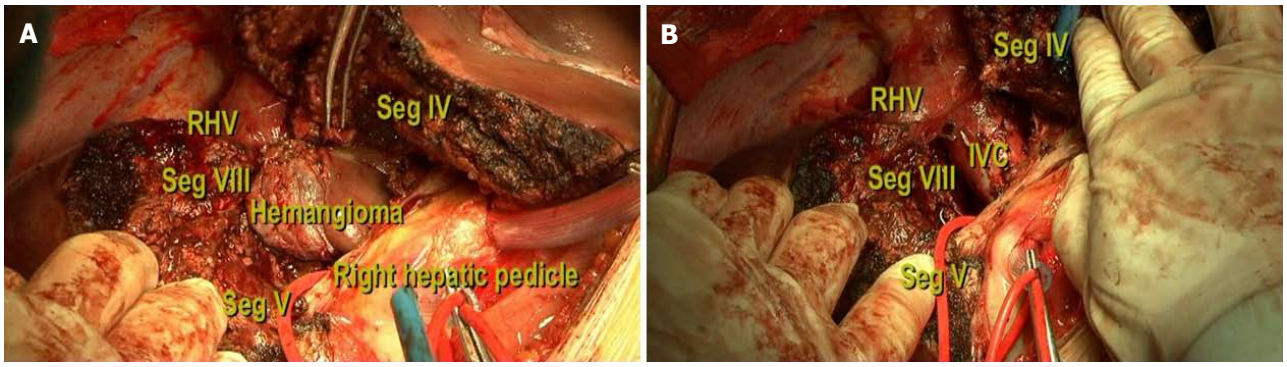

Figure 6 Splitting the liver by the anterior approach. A: The hemangioma was exposed; B: The hemangioma was removed and the major vessels were identified.

Table 2 Surgical data for all 20 patients with isolated caudate lobectomy

Surgical feature	Data
Approach	
LSR	4 (20)
RSR	6 (30)
CSR	7 (35)
AR	3 (15)
Procedure	
ICCL	4 (20)
IPCL	16 (80)
Blood loss in mL	600 (200-5700)
VIBT in mL	250 (0-2400)
Operation time in min	255 (110-510)
HSPO in d	14 (7-30)
Postoperative complication	
Incision infection	1 (5)
Ascites	3 (15)
Pleural effusion	2 (10)

Data are presented as *n* (%) or median (range). AR:Anterior resection; CSR: Combined sides resection; HSPO: Hospital stay post operation ; ICCL: Isolated complete caudate lobectomy; IPCL: Isolated partial caudate lobectomy; LSR: Left side resection; RSR: Right side resection; VIBT: Volume of intraoperative blood transfusion.

Chicago, IL, United States).

RESULTS

Among all patients, 4 cases received isolated complete caudate lobectomy (4/20, 20%), while 16 cases received isolated partial caudate lobectomy (16/20, 80%). Based on the type of dissection, there were 4 cases with the left approach (4/20, 20%), 6 cases with the right approach (6/20, 30%), 7 cases with the bilateral combined approach (7/20, 35%), 3 cases with the anterior approach (3/20, 15%) (Figure 6), and the hanging maneuver was also combined in 2 cases. The median tumor size was 5.5 cm (2-12 cm). The median intra-operative blood loss was 600 mL (200-5700 mL). The median intra-operative blood transfusion volume was 250 mL (0-2400 mL). The median operation time was 255 min (110-510 min), and the median post-operative hospital stay was 14 d (7-30 d).

There was 1 case of incision infection (1/20, 5%), 3 cases of ascites (3/20, 15%), and 2 cases of pleural effusion (2/20, 10%) (Table 2). There was no mortality and the median survival time for malignant tumor was 48 mo, with 1- and 3-year survival rates of 88.9% and 49.4%, respectively.

DISCUSSION

Due to abundant adjacent blood vessels of the CL, chemoembolization, radiofrequency ablation and other treatments are not appropriate for CL lesions[11]. Surgical resection is considered as the preferred method and anatomic resection can improve prognosis[7,12]. Hasegawa *et al*[6] believed that anatomic resection was one of the independent predictors of improved OS for HCC. However, the majority of anatomic resection refers to the segment Ⅱ to segment Ⅷ, excepting segment Ⅰ. Caudate lobectomy was once called a 'bloody gultch'[13]. While the resection of the tumor in the CL is not difficult today, it is still difficult to perform isolated anatomic resection for CL; the vast majority reports are from case reports. In this study, we mainly explored the possibility to establish a standard surgical flow for anatomical isolated caudate lobectomy[5,14,15].

Chaib *et al*[16] classified CL tumors into five types, depending on their locations, and this classification has clinical significance for small size tumors. However, in China, HCC is usually large and concurrent with cirrhosis. And, anatomic resection is necessary for longer survival. Blumgart's group[17] performed 150 cases of caudate resection, which led to a median survival for HCC of 32 mo. In 2013, Philips *et al*[18] reported their experience of caudate resection, having a median OS of 21 mo. Our results showed a median survival time of 48 mo for malignant patients, though this was not a comparison study.

Like other anatomic resections, the identification of the blood supply to one part or the whole CL is a prerequisite. The key steps are preoperative assessment and intra-operative identification of the precise boundary. We called this boundary as two tips, two boundaries and one virtual plane. The confluence of Arantius ligament and IVC was the upper tip, while the converging point of the right lobe and the caudate

process was the lower tip. The Arantius ligament is regarded as the left border of CL, while Peng's line is the right border. The plane of the retro-CL is the surface of the retro-hepatic IVC. In practice, resection of the CL along the Peng's line shows similar effects as intra-operative dye labeling, which is safe and convenient[5].

The advantages of the different surgical approaches are to perform CL resection easily. Left approach is suitable for the tumor located in the Spiegel lobe. Right approach is for resection of tumor located in the caudate process. For complete CL resection, we usually used the left and right approach. For giant CL tumors or the paracaval portion, the anterior approach should be used. The disadvantage of the anterior approach is that incidence of biliary fistula will be high because of hepatic parenchyma transection. The laparoscopic resection of the CL has been reported sporadically, and we will be working on this in the future.

During the resection, other surgical techniques can be used to reduce bleeding and increase surgical safety. These techniques include the selective control of inflow, the liver hanging maneuver and retrograde resection of the CL[15,19,20].

In conclusion, as an individual anatomic segment, caudate lobectomy remains a substantially challenging procedure. Our experience demonstrated that anatomic isolated caudate lobectomy can be done safely and effectively by establishing a surgical flow.

COMMENTS

Background

Caudate lobe (CL) is an important part of the liver and adjacent to the major blood vessels. Surgical resection is the preferred treatment for patients with malignant lesions in this area. However, CL resection remains a challenging procedure.

Research frontiers

The implementation of more CL resections is limited due to a lack of standard flow. The hotspot of this study is the establishment a standard surgical flow for anatomic isolated caudate lobectomy.

Innovations and breakthroughs

In recent years, the number of caudate lobectomies has increased. However, anatomic isolated caudate lobectomy is not common because of the difficult anatomical location and intraoperative bleeding. This study presents the recommendation of a surgical flow which facilitates the performance of anatomic isolated caudate lobectomy safely.

Applications

The surgical flow in this study was established according to prior experience and validated on the patient. Anatomic isolated caudate lobectomy can be done safely and effectively based on this flow.

Terminology

Peng's line is the right boundary of CL, from the CL tip to the right border of the caudate process. Peng's multifunction operative dissector is an electrosurgical instrument, which was used for transection hepatic parenchyma.

Peer-review

CL isolated resection is a rare and challenging procedure. I think that the strength of the paper is the description of the different techniques, detailed with intraoperative pictures. The authors deserve praise for having done a difficult job - the article has described a series of 20 resections in a decade. It may be expected that the authors will come up with a larger series in future. The description of operative steps is one of the strong points of this article.

REFERENCES

1 **Kumon M.** Anatomy of the caudate lobe with special refefence to portal vein and bile duct. *Acta Hepatol Jpn* 1985; **26**:1193-1199

2 **Dai WD**, Huang JS, Hu JX. Isolated caudate lobe resection for huge hepatocellular carcinoma (10 cm or greater in diameter). *Am Surg* 2014; **80**: 159-165 [PMID: 24480216]

3 **Cai X**, Li Z, Yu H, Liu K, Liang X, Wang Y, Liang Y. Isolated laparoscopic resection of the hepatic caudate lobe. *Chin Med J* (Engl) 2014; **127**: 3194-3195 [PMID: 25189971]

4 **Yang JH**, Gu J, Dong P, Chen L, Wu WG, Mu JS, Li ML, Wu XS, Zhao YL, Zhang L, Weng H, Ding Q, Ding QC, Liu YB. Isolated complete caudate lobectomy for hepatic tumor of the anterior transhepatic approach: surgical approaches and perioperative outcomes. *World J Surg Oncol* 2013; **11**: 197 [PMID: 23947911 DOI: 10.1186/1477-7819-11-197]

5 **Peng SY,** Qian HR, Xu B, Wang YF, Wang XA. Surgical treatment of the caudate lobe diseases. *J Clin Surg* 2009; **17**: 581-583 [DOI: 10.3969/j.issn.1005-6483.2009.09.002]

6 **Hasegawa K**, Kokudo N, Imamura H, Matsuyama Y, Aoki T, Minagawa M, Sano K, Sugawara Y, Takayama T, Makuuchi M. Prognostic impact of anatomic resection for hepatocellular carcinoma. *Ann Surg* 2005; **242**: 252-259 [PMID: 16041216]

7 **Jia CK**, Weng J, Chen YK, Fu Y. Anatomic resection of liver segments 6-8 for hepatocellular carcinoma. *World J Gastroenterol* 2014; **20**: 4433-4439 [PMID: 24764684 DOI: 10.3748/wjg.v20.i15.4433]

8 **Makuuchi M**, Yamamoto J, Takayama T, Kosuge T, Gunvén P, Yamazaki S, Hasegawa H. Extrahepatic division of the right hepatic vein in hepatectomy. *Hepatogastroenterology* 1991; **38**: 176-179 [PMID: 1649789]

9 **Peng SY.** Hepatic caudate lobe resection: Springer Verlag Berlin Heidelberg, 2010; 9-11 [DOI: 10.1007/978-3-642-05105-0]

10 **Peng SY**, Li JT. "Curettage and aspiration dissection technique" using PMOD for liver resection. *HPB* (Oxford) 2008; **10**: 285-288 [PMID: 18773106 DOI: 10.1080/13651820802167151]

11 **Asahara T**, Dohi K, Hino H, Nakahara H, Katayama K, Itamoto T, Ono E, Moriwaki K, Yuge O, Nakanishi T, Kitamoto M. Isolated caudate lobectomy by anterior approach for hepatocellular carcinoma originating in the paracaval portion of the caudate lobe. *J Hepatobiliary Pancreat Surg* 1998; **5**: 416-421 [PMID: 9931391]

12 **Yoo PS**, Enestvedt CK, Kulkarni S. Anatomic considerations in the surgical resection of hepatocellular carcinoma. *J Clin Gastroenterol* 2013; **47** Suppl: S11-S15 [PMID: 23632343 DOI: 10.1097/MCG.0b013e318280ce5f]

13 **Colonna JO 2nd**, Shaked A, Gelabert HA, Busuttil RW. Resection of the caudate lobe through "bloody gultch". *Surg Gynecol Obstet* 1993; **176**: 401-402 [PMID: 8460420]

14 **Peng SY**, Li JT, Mou YP, Liu YB, Wu YL, Fang HQ, Cao LP, Chen L, Cai XJ, Peng CH. Different approaches to caudate lobectomy with "curettage and aspiration" technique using a special instrument PMOD: a report of 76 cases. *World J Gastroenterol* 2003; **9**: 2169-2173 [PMID: 14562371 DOI: 10.3748/wjg.v9.i10.2169]

15 **Peng SY**, Liu YB, Wang JW, Li JT, Liu FB, Xue JF, Xu B, Cao LP, Hong DF, Qian HR. Retrograde resection of caudate lobe of liver. *J Am Coll Surg* 2008; **206**: 1232-1238 [PMID: 18501825 DOI: 10.1016/j.jamcollsurg.2007.11.013]

16 **Chaib E**, Ribeiro MA Jr, Silva Fde S, Saad WA, Cecconello I.

Caudate lobectomy: tumor location, topographic classification, and technique using right- and left-sided approaches to the liver. *Am J Surg* 2008; **196**: 245-251 [PMID: 18571618 DOI: 10.1016/j.amjsurg.2007.11.020]

17 **Hawkins WG**, DeMatteo RP, Cohen MS, Jarnagin WR, Fong Y, D'Angelica M, Gonen M, Blumgart LH. Caudate hepatectomy for cancer: a single institution experience with 150 patients. *J Am Coll Surg* 2005; **200**: 345-352 [PMID: 15737844 DOI: 10.1016/j.jamcollsurg.2004.10.036]

18 **Philips P**, Farmer RW, Scoggins CR, McMasters KM, Martin RC 2nd. Caudate lobe resections: a single-center experience and evaluation of factors predictive of outcomes. *World J Surg Oncol* 2013; **11**: 220 [PMID: 24010947 DOI: 10.1186/1477-7819-11-220]

19 **Kim SH**, Park SJ, Lee SA, Lee WJ, Park JW, Kim CM. Isolated caudate lobectomy using the hanging maneuver. *Surgery* 2006; **139**: 847-850 [PMID: 16782444 DOI: 10.1016/j.surg.2006.01.004]

20 **Li Z**, Sun YM, Wu FX, Yang LQ, Lu ZJ, Yu WF. Controlled low central venous pressure reduces blood loss and transfusion requirements in hepatectomy. *World J Gastroenterol* 2014; **20**: 303-309 [PMID: 24415886 DOI: 10.3748/wjg.v20.i1.303]

P- Reviewer: Bandyopadhyay SK, Garcia-Olmo D, Petrucciani N
S- Editor: Qi Y **L- Editor**: Filipodia **E- Editor**: Huang Y

World Journal of Gastroenterology

Submit a Manuscript: http://www.f6publishing.com

World J Gastroenterol 2017 November 7; 23(41): 7440-7449

DOI: 10.3748/wjg.v23.i41.7440

ISSN 1007-9327 (print) ISSN 2219-2840 (online)

ORIGINAL ARTICLE

Observational Study

Circulating miRNAs as biomarkers for severe acute pancreatitis associated with acute lung injury

Xiao-Guang Lu, Xin Kang, Li-Bin Zhan, Li-Min Kang, Zhi-Wei Fan, Li-Zhi Bai

Xiao-Guang Lu, Xin Kang, Zhi-Wei Fan, Li-Zhi Bai, Department of Emergency, Zhongshan Hospital, Dalian University, Dalian 116001, Liaoning Province, China

Li-Bin Zhan, College of Basic Medicine, Nanjing University of Chinese Medicine, Nanjing 210000, Jiangsu Province, China

Li-Min Kang, Department of Hepatobiliary and Pancreatic Surgery, Puer People's Hospital, Puer 665000, Yunnan Province, China

ORCID number: Xiao-Guang Lu (0000-0001-8741-9928); Xin Kang (0000-0002-6754-9802); Li-Bin Zhan (0000-0002-2146-7158); Li-Min Kang (0000-0002-3062-897X); Zhi-Wei Fan (0000-0002-2385-5277); Li-Zhi Bai (0000-0002-3567-2072).

Author contributions: Lu XG and Kang X contributed equally to this work and should be regarded as co-first authors; Lu XG, Kang X, Zhan LB and Kang LM designed the study and drafted the manuscript; Kang X and Kang LM analyzed the data; Kang X, Kang LM, Fan ZW and Bai LZ provided blood plasma samples and edited the manuscript; All authors read and approved the final manuscript.

Supported by the National Natural Science Foundation of China, No. 30971626 and No. 81473512.

Institutional review board statement: This study was reviewed and approved by the Institutional Review Board (IRB) of the Affiliated Zhongshan Hospital of Dalian University (IRB No. 2011-60).

Informed consent statement: All study participants, or their legal guardian, provided informed written consent prior to study enrollment. All clinical data were obtained anonymously and innocuously.

Conflict-of-interest statement: The authors have no conflicts of interest to disclose.

Data sharing statement: No additional data are available.

Manuscript source: Unsolicited manuscript

Correspondence to: Xiao-Guang Lu, MD, Department of Emergency, Zhongshan Hospital, Dalian University, Dalian 116001, Liaoning Province, China. dllxg@126.com
Telephone: +86-411-62893126
Fax: +86-411-62893555

Received: May 29, 2017
Peer-review started: June 2, 2017
First decision: July 27, 2017
Revised: August 23, 2017
Accepted: September 20, 2017
Article in press: September 19, 2017
Published online: November 7, 2017

Abstract

AIM

To identify circulating micro (mi)RNAs as biological markers for prediction of severe acute pancreatitis (SAP) with acute lung injury (ALI).

METHODS

Twenty-four serum samples were respectively collected and classified as SAP associated with ALI and SAP without ALI, and the miRNA expression profiles were determined by microarray analysis. These miRNAs were validated by quantitative reverse transcription-polymerase chain reaction, and their putative targets were predicted by the online software TargetScan, miRanda and PicTar database. Gene ontology (GO) and Kyoto encyclopedia of genes and genomes (commonly known as KEGG) were used to predict their possible

functions and pathways involved.

RESULTS

We investigated 287 miRNAs based on microarray data analysis. Twelve miRNAs were differentially expressed in the patients with SAP with ALI and those with SAP without ALI. Hsa-miR-1260b, 762, 22-3p, 23b and 23a were differently up-regulated and hsa-miR-550a*, 324-5p, 484, 331-3p, 140-3p, 342-3p and 150 were differently down-regulated in patients with SAP with ALI compared to those with SAP without ALI. In addition, 85 putative target genes of the significantly dysregulated miRNAs were found by TargetScan, miRanda and PicTar. Finally, GO and pathway network analysis showed that they were mainly enriched in signal transduction, metabolic processes, cytoplasm and cell membranes.

CONCLUSION

This is the first study to identify 12 circulating miRNAs in patients with SAP with ALI, which may be biomarkers for prediction of ALI after SAP.

Key words: miRNAs; Severe acute pancreatitis; Acute lung injury; Biomarker; Microarray analysis

Core tip: Early diagnosis of severe acute pancreatitis (SAP) associated with acute lung injury (ALI) is still difficult. Our study is the first to identify 12 differentially expressed circulating microRNAs in patients with SAP with ALI, which may be used as circulating biomarkers for prediction of acute lung injury induced by SAP.

Lu XG, Kang X, Zhan LB, Kang LM, Fan ZW, Bai LZ. Circulating miRNAs as biomarkers for severe acute pancreatitis associated with acute lung injury. *World J Gastroenterol* 2017; 23(41): 7440-7449 Available from: URL: http://www.wjgnet.com/1007-9327/full/v23/i41/7440.htm DOI: http://dx.doi.org/10.3748/wjg.v23.i41.7440

INTRODUCTION

Acute pancreatitis is a potentially fatal disease characterized by wide clinical variation, ranging from a mild self-limiting to severe disease complicated with sepsis and multiple organ failure, leading to high morbidity and mortality[1]. Severe acute pancreatitis (SAP) develops in 10%-25% of the patients, which is also a systemic disease and usually induces injury to extra-pancreatic organs, such as lung, liver and kidney, leading to multiple organ failure and even death[2,3]. Acute lung injury (ALI) is a common and serious complication of SAP. It can develop into acute respiratory distress syndrome (ARDS) without timely intervention[4,5]. At present, the early diagnosis of SAP associated with ALI is still difficult. Some biochemical parameters, such as high-mobility group box (HMGB)-1, pre-B cell colony-enhancing factor (PBEF) and surfactant protein (SP)-A, have been used for diagnosis of ALI[6-9]. However, there are few research studies in this area and there are no definitive diagnostic markers; additionally, sometimes the concentration of the markers can be affected by other factors. So, it is important to choose several biomarkers that might be used jointly to improve the diagnostic rate and establish the mechanism of SAP associated with ALI.

Micro (mi)RNAs are a family of naturally occurring, small noncoding RNA molecules that play an important regulatory role in gene expression. They are involved in numerous pathophysiological processes within cells and represent major regulators of gene expression by virtue of their preponderance to target transcription factors. miRNAs have been proposed as ideal biomarkers of disease, including diagnosis, prognosis and monitoring of treatment responses. Circulating miRNAs, presenting in a stable form protected from endogenous RNase activation, are highly stable in blood serum. Hence, in view of their potential use as novel, noninvasive biomarkers, the profiles of circulating miRNAs have been explored in diseases such as cancer, heart failure, myocardial infarction and spinal cord injury[10-17]. miRNA analysis of plasma from patients with SAP associated with ALI might yield new biomarkers for diagnosis and identify potential treatment targets for ALI[18,19].

The present study was designed to test the hypotheses that circulating miRNAs are closely related to the incidence of SAP associated with ALI, they are be involved in a variety of pathophysiological processes of ALI, and can be used as a circulating marker to predict the disease. This study aimed to identify expression of the different circulating miRNAs and their target genes in patients with SAP associated with ALI, and in those with SAP without ALI. The findings from this study will contribute to early diagnosis and treatment of SAP associated with ALI.

MATERIALS AND METHODS

Patients

All patients with SAP were admitted within 72 h after onset of symptoms to the Medical or Surgical Intensive Care Units of the Affiliated Zhongshan Hospital of Dalian University and Nanjing General Hospital of Nanjing Military Command from January 2010 to December 2013. Twelve of 30 SAP patients were not complicated with ALI. All patients met the criteria of the Atlanta definition of SAP. Specifically, SAP diagnosis should meet at least one of the following criteria: (1) APACHE Ⅱ score ⩾ 8; (2) Ranson score ⩾ 3; (3) organ failure (*i.e.* transient and persistent); and (4) local complications (*i.e.* necrosis, abscess

Table 1 Clinical features of the participants who contributed plasma

Characteristic	SAP with ALI cases	SAP without ALI cases	*P* value
Age	43.85 ± 1.70	44.25 ± 1.47	0.8602
Men/Women	8/4	7/5	0.6733
Current smoker	6 (50)	4 (33.3)	0.6802
Etiology			
Biliary	10 (83.3)	9 (75)	0.1606
Alcohol	1 (8.3)	2 (16.7)	0.1261
Other	1 (8.3)	1 (8.3)	1.0000
APACHE Ⅱ	18.92 ± 1.00	13.17 ± 0.81	0.0002
Mechanical ventilation	8	0	0.0013
Hospital mortality	2	0	0.4783

ALI: Acute lung injury; APACHE: Acute Physiology and Chronic Health Evaluation; SAP: Severe acute pancreatitis.

or pseudocyst). To ensure inclusion of only eligible patients with a first attack of SAP, patients with recurrent SAP, chronic pancreatitis or pancreatic cancer were excluded. ALI was defined by the American-European Consensus Conference[20].

Patient demographic and clinical characteristics are summarized in Table 1. Six SAP patients were finally excluded for not meeting all inclusion criteria, and 24 patients met the criteria; six of 24 serum samples of patients were randomly selected for miRNA microarray analysis. This study was approved by the Ethics Committee of the Affiliated Zhongshan Hospital of Dalian University and Nanjing General Hospital of Nanjing Military Command. All of the patients gave written informed consent.

Serum samples and RNA isolation

Four-milliliter serum specimens from each patient were collected immediately after grouping of patients into SAP without ALI and SAP with ALI. Serum samples were immediately frozen in liquid nitrogen and then stored at -80 ℃ for later determination. Total RNA was extracted from serum specimens using a mirVana PARIS kit (Ambion, Austin, TX, United States). The quantity and quality of total RNA were determined using an ultraviolet spectrophotometer at 260 and 280 nm.

miRNA microarray analysis

miRNA microarrays were manufactured by Agilent Technologies (Santa Clara, CA, United States). Total RNA samples (4-8 μg) were 3'-extended with a poly(A) tail using poly(A) polymerase. An oligonucleotide tag was then ligated to the poly(A) tail for later fluorescent dye staining (Atactic Technologies, Houston, TX, United States)[21-23]. Similar methods reported in a previous work were used in this section[24,25]. All raw data were transformed to $\log^2$ values, and each expression was normalized by having zero mean and unit sample variance. In order to screen significantly differentially expressed miRNAs, we compared expression in serum between the patients with SAP with ALI and those with SAP without ALI.

The relative miRNA expression levels were further normalized using the overall median value for patients with SAP with ALI, which gave each patient a median log ratio of 0 for normalized expression levels. The weighted differences in miRNA expression between patients with SAP with ALI and those with SAP without ALI were calculated using the random variance model *t*-test, in which fold-change > 1.5 was considered significant. The heatmap analysis and hierarchical cluster analysis of data were performed using Multi-Experiment Viewer (MeV) v4.7.1 from the TM4 software package available as open-source software at http://www.tm4.org[26]. Hierarchical clustering was performed using the Euclidean distance metric with complete linkage option.

Verification of miRNA expression by quantitative reverse transcription-polymerase chain reaction (qRT-PCR)

qRT-PCR was used to verify miRNA expression identified by microarray analysis. Of 24 serum samples of patients, 18 were assessed by qRT-PCR. The primers for RT-PCR were used to amplify miRNAs, and were designed using Premier 5.0.RNase inhibitor (Toyobo, Osaka, Japan). The reverse primer, M-MLV reverse transcriptase and U6B were purchased from Guangzhou RiboBio Co. Ltd. (China), and U6B was used as internal control. Mixtures of 1 μg total RNA, 50 nmol/L reverse primer, 5 U M-MLV reverse transcriptase (Toyobo), 2 U RNase inhibitor (Toyobo) and 0.5 μmol/L dNTP were incubated for 30 min at 16 ℃, 30 min at 42 ℃, and 15 min at 70 ℃. The reaction mixtures were used as templates for qRT-PCR. PCR product amplification was determined by the level of fluorescence emitted by SYBR Green Realtime PCR Master Mix-Plus (Takara, Dalian, China) and MX3000P qPCR system (Stratagene, Santa Clara, CA, United States). The PCR mixture, containing 1 μL reverse transcriptase product of total RNA, 10 μL SYBR-Green Real-time PCR Master Mix-plus, 2 μL Plus solution, 2 μL each specific forward and reverse primer, and 3 μL diethyl pyrocarbonate water, was prepared in a total final volume of 20 μL. The reaction was performed at 95 ℃ for 2 min, followed by 40 cycles at 95 ℃ for 15 s and 60 ℃ for 1 min. Each sample was run in triplicate. Melting curves were used to verify the specificity of each PCR. The procedure for qRT-PCR was described previously[27].

miRNA target prediction, gene ontology (GO) and pathway network analysis

The putative target prediction of validated miRNAs by qRT-PCR was performed using three online software programs: PicTar: http://www.pictar.org/; miRanda: http://www.microrna.org/microrna/home.do/; and TargetScan: http://www.targetscan.org. We used PicTar, miRanda and TargetScan together to enhance the credibility of the study. PicTar identified a list of putative targets, searching for almost

fully complementary sites between miRNAs and 3′-untranslated region (UTR) mRNAs. The free energy between the binding sites was then calculated and the results were ranked by means of a score obtained using a hidden Markov model (HMM). miRNAs with multiple binding sites were highly scored. The miRanda algorithm searched for target sites on the 3′-UTRs of mRNAs. It considered both the binding energy for the duplex stability and the conservation of the target site among different species. The TargetScan algorithm was based on the identification of fully complementary zones between the miRNA seed (nucleotides 2-8) and 3′-UTR mRNA. Starting from those sites, TargetScan searched for larger interactions, ranking the results in three groups according to the length of the matches. In particular, the presence of an adenine in the first position of the target site was highly scored because of its evolutionary conservation. The prediction followed the rules: (1) perfect match at the seed region (2-8 nucleotides from the 5′ end of miRNA); (2) minimum free energy of the miRNA/target duplex should be smaller than -20 kcal/mol; and (3) total score for miRNA-mRNA pairs should be > 140. GO was performed for analysis of the biological process (BP), cellular component (CC) and molecular function (MF) of miRNA target genes based on the GO database (http://www.geneontology.org/). Fisher's two-side exact test and χ^2 test were used to classify the GO categories, and the false discovery rate (FDR) was calculated to correct the *P* values. We chose only GOs that had a *P* value < 0.05 and FDR < 0.05.

The Kyoto Encyclopedia of Genes and Genomes (KEGG) pathway analysis was performed to identify the enriched pathways of miRNA target genes based on the KEGG database (http://www.genome.jp/kegg/). This analysis provided a better understanding of gene expression information as a complete network. KEGG pathway annotation of the miRNA targets was found using the Database for Annotation, Visualization and Integrated Discovery (DAVID) gene annotation tool (http://david.abcc. ncifcrf.gov/). Fisher's exact test and the threshold of significance were defined by the *P* value and FDR. The screening criterion was *P* < 0.05. To calculate the enrichment ratio and *P* value for KEGG analysis, we defined N as number of genes annotated by pathway chip and M as number of differentially expressed genes annotated by pathway in predicted miRNA targets. We recorded the intersecting genes belonging to GO and the pathway at the same time. According to the attributes of the intersecting target genes and miRNAs, the miRNA gene network, representing the critical miRNAs and their targets, was established in accordance with the miRNA degree. The key miRNA and gene in the network had the largest extent. The most important biological metabolic pathway and signal transduction pathway could be determined using pathway enrichment.

Statistical analysis

Statistical analyses were performed using GraphPad Prism 6.0 software (San Diego, CA, United States). Fisher's exact test and *t*-test were used to assess differences in clinical features between the participants in the two groups. A value of *P* < 0.05 was considered statistically significant.

RESULTS

Differential expression of miRNAs in patients with SAP with ALI and SAP without ALI

We investigated 287 miRNAs based on microarray data analysis. The miRNAs with fold-changes > 1.5 or < 1/2 and *P* < 0.05 were selected for further study. Twelve miRNAs met these criteria and were differentially expressed in patients with SAP with ALI, and in those with SAP without ALI. The 12 miRNAs are summarized in Figure 1.

Validation of differentially expressed miRNAs by qRT-PCR

In order to validate the microarray results, qRT-PCR was performed for the identified 12 miRNAs (*P* < 0.05). We found that five miRNAs (hsa-miR-22-3p, hsa-miR-1260b, hsa-miR-762, hsa-miR-23b and hsa-miR-23a) were significantly up-regulated and seven (hsa-miR-550a*, hsa-miR-324-5p, hsa-miR-484, hsa-miR-331-3p, hsa-miR-140-3p, hsa-miR-342-3p and hsa-miR-150) were down-regulated in patients with SAP with ALI and in those with SAP without ALI (Figure 2).

Analysis of miRNA target genes

Eighty-five putative target genes of the 12 validated miRNAs were found in patients with SAP with ALI and those with SAP without ALI by TargetScan, miRanda and PicTar database.

GO analysis

GO analysis showed annotation of the genes from three ontologies: BP, MF and CC. GO enrichment analysis of 12 validated miRNAs indicated that 4817 GOs were regulated by the down-regulated miRNAs, whereas 5088 GOs were regulated by the up-regulated miRNAs. In BP terms, they were enriched in signal transduction and metabolic processes. In CC terms, they focused on cytoplasm, cell membranes and plasma membranes, and were enriched in protein binding and in receptor activity terms in MF (Figure 3).

KEGG pathway enrichment analysis and miRNA-KEGG network

KEGG pathway analysis showed that the target genes of up-regulated miRNAs were involved in glutathione metabolism, Wnt signaling pathway, cytokine-cytokine receptor interaction, complement and coagulation cascades, methionine metabolism, apoptosis, cytosolic

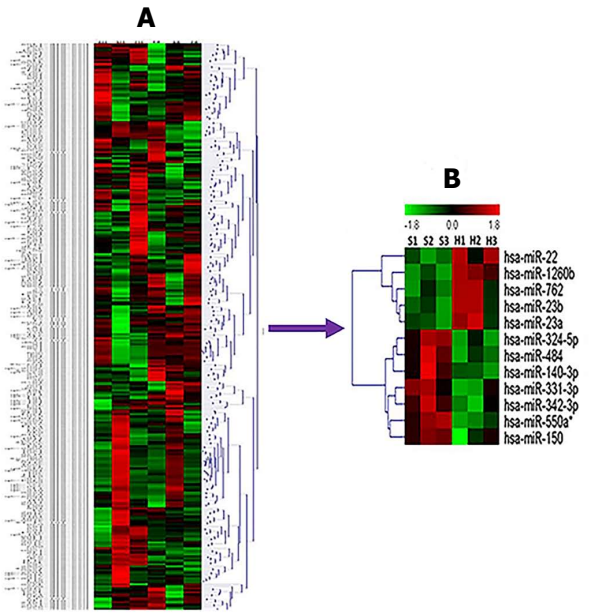

C

Index	Reporter name	Target sequence (5′ to 3′)	Strand
1	hsa-miR-550a*	AGUGCCUGAGGGAGUAAGAGCCC	-
2	hsa-miR-324-5p	CGCAUCCCCUAGGGCAUUGGUGU	-
3	hsa-miR-484	UCAGGCUCAGUCCCCUCCCGAU	-
4	hsa-miR-331-3p	GCCCCUGGGCCUAUCCUAGAA	-
5	hsa-miR-22-3p	AAGCUGCCAGUUGAAGAACUGU	+
6	hsa-miR-140-3p	UACCACAGGGUAGAACCACGG	-
7	hsa-miR-1260b	AUCCCACCACUGCCACCAU	+
8	hsa-miR-342-3p	UCUCACACAGAAAUCGCACCCGU	-
9	hsa-miR-762	GGGGCUGGGGCCGGGGCCGAGC	+
10	hsa-miR-23b	AUCACAUUGCCAGGGAUUACC	+
11	hsa-miR-23a	AUCACAUUGCCAGGGAUUUCC	+
12	hsa-miR-150	UCUCCCAACCCUUGUACCAGUG	-

Figure 1 Circulating miRNA expression in patients with SAP with ALI and those with SAP without ALI. A and B: Differentially expressed miRNAs ($P < 0.05$) were analyzed by hierarchical clustering of the $\log^2$ values of miRNA microarray signals. Red: Up-regulation; Green: Down-regulation; Black: No change. The legend on the right displays the miRNA represented in the corresponding row. The bar code on the top represents the color scale of the $\log^2$ values. The heatmap shows 12 significantly expressed circulating miRNAs in patients with SAP with ALI and SAP without ALI using miRNA array data; C: Information and expression of 12 circulating miRNAs. ALI: Acute lung injury; miRNA: microRNA; SAP: Severe acute pancreatitis.

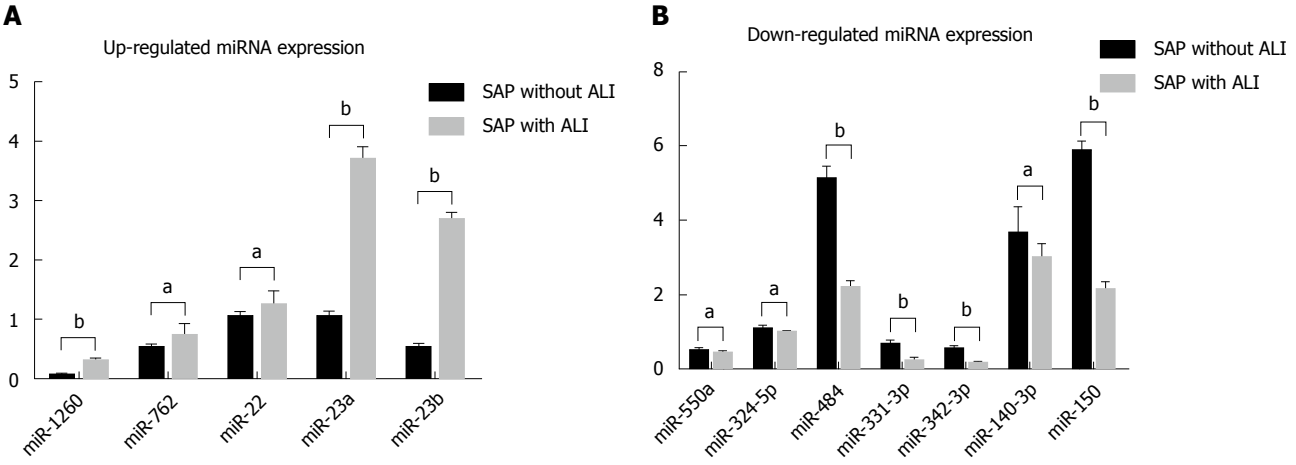

Figure 2 Differential expression of 12 circulating miRNAs were validated by quantitative reverse transcription-polymerase chain reaction. A: Validation of up-regulated expressed miRNAs. Hsa-miR-22-3p, hsa-miR-1260b, hsa-miR-762, hsa-miR-23b and hsa-miR-23a in patients with SAP with ALI were significantly up-regulated compared to patients with SAP without ALI; B: Validation of down-regulated expressed miRNAs. hsa-miR-550a*, hsa-miR-324-5p, hsa-miR-484, hsa-miR-331-3p, hsa-miR-140-3p, hsa-miR-342-3p and hsa-miR-150 were down-regulated in patients with SAP with ALI in comparison with patients with SAP without ALI. $^aP < 0.05$, $^bP < 0.01$. ALI: Acute lung injury; miRNA: microRNA; SAP: Severe acute pancreatitis.

DNA-sensing pathway, Notch signaling pathway, chemokine signaling pathway, and mitogen-activated protein kinase (MAPK) signaling pathway. Target genes of down-regulated miRNAs were related to the insulin signaling pathway, transforming growth factor (TGF)-β signaling pathway, T-cell receptor signaling pathway, amino sugar and nucleotide sugar metabolism, and starch and sucrose metabolism. As an example, the Wnt signaling pathway involved in up-regulated miRNAs and regulation of Rab GTPase activity by down-regulated miRNAs is shown in Figure 4A and B.

DISCUSSION

In this study, we identified that 12 miRNAs, including five up-regulated (has-miR-22-3p, 1260b, 762, 23b and 23a) and 7 down-regulated (has-miR-550a-5p, 324-5p, 484, 331-3p, 22-3p, 140-3p and 342-3p) were significantly expressed in patients with SAP with ALI and in those with SAP without ALI. Furthermore,

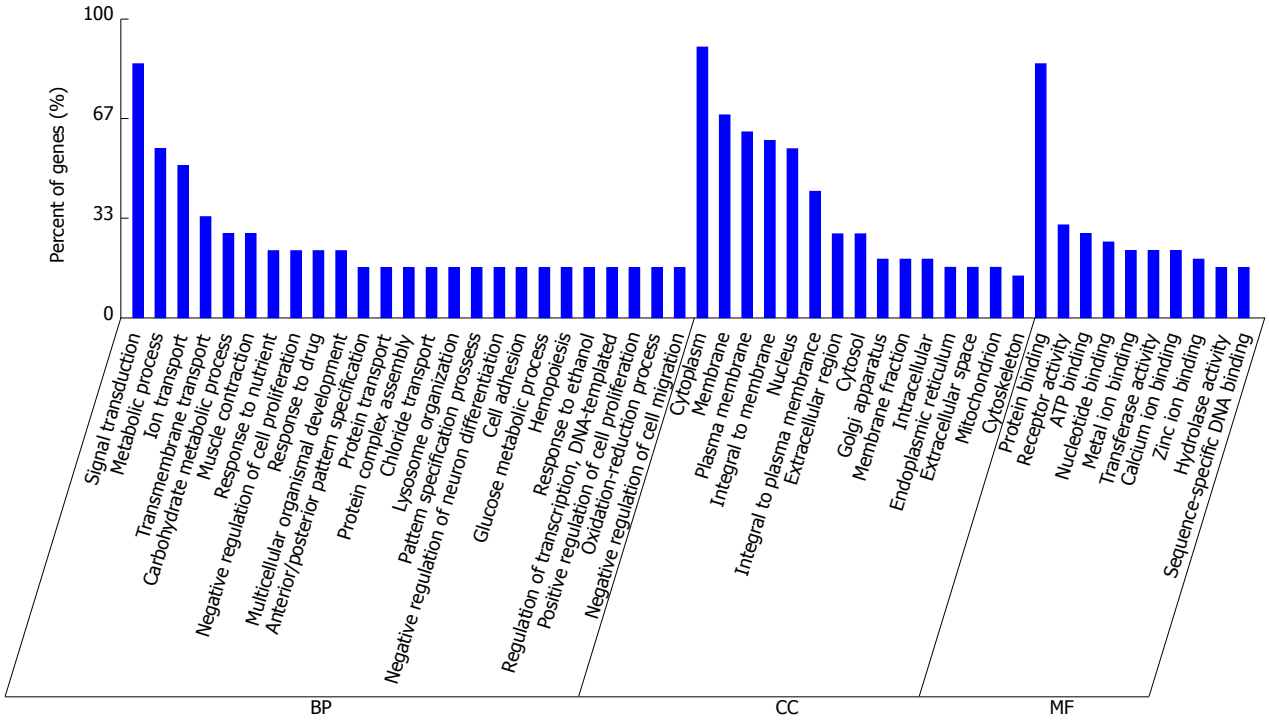

Figure 3 Gene ontology analysis of genes. In BP terms, they were enriched in signal transduction and metabolic processes. In CC terms, they focused on cytoplasm, cell membranes and plasma membranes, and were enriched in protein binding and receptor activity terms in MF. In each ontology, the first at least 10 enriched terms are listed. BP: Biological process; CC: Cellular component; MF: Molecular function.

we found that 4817 GOs regulated by the seven down-regulated miRNAs and 5088 GOs regulated by the five up-regulated miRNAs were involved in SAP with ALI. These miRNAs may be candidate novel biomarkers and were involved in many biological processes of SAP with ALI, such as signal transduction, metabolic processes, cytoplasm, cell membranes, and receptor activity terms. Moreover, the 85 putative target genes were regulated by 12 specific miRNAs, and the Wnt signaling pathway and Rab GTPase activity were important metabolic pathways that were up-regulated and down-regulated by miRNAs, respectively.

miRNAs are short non-coding RNAs involved in post-transcriptional regulation of gene expression. An increasing body of evidence indicates that miRNAs have investigated the potential involvement of miRNAs in ALI or ARDS. Liu *et al*[28] found that miRNA-200c-3p is crucial in ALI/ARDS and that the inhibition of miR-200c-3p ameliorated the ALI induced by H5N1 virus infection *in vivo*, indicating a potential therapeutic target. Vaporidi *et al*[29] investigated pulmonary miRNA profiling in a mouse model of high tidal volume ventilation (HVTV)-induced lung injury and results showed that of the 335 miRNAs examined, the expression of 50 miRNAs increased > 2-fold, expression of 15 miRNAs decreased by more than half and the miRNAs with the greatest increase in expression after 4 h of HVT were miR-7b, miR-189 and miR-223, whereas the miRNAs with the greatest decrease in expression were miR-503 and miR-211. However, circulating miRNAs as biomarkers of SAP with ALI are still unclear.

In our study, 12 circulating miRNAs were differentially expressed in patients with SAP with ALI and SAP without ALI. Among these, five miRNAs (hsa-miR-22-3p, 1260b, 762, 23b and 23a) were significantly up-regulated and seven (hsa-miR-550a*, 324-5p, 484, 331-3p, 22-3p, 140-3p and 342-3p) were down-regulated. qRT-PCR was performed to verify the gene expression levels of these regulated circulating miRNA. In the five differentially overexpressed miRNAs, the expression of hsa-miR-1260b, 23b and 23a showed a fold-change > 5 with $P < 0.01$, while hsa-miR-22-3p and 762 showed only a > 2 but < 5 fold-change < 5 with $P < 0.05$. Xu *et al*[30] found that overexpression of miR-1260b in non-small cell lung cancer (NSCLC) with lymph node metastasis can be regarded as a specific signature for early progression and prognosis of NSCLC.

Sarrion *et al*[31] reported that expression of miR23a was correlated with pulmonary function, and silencing of miR23a resulted in increased expression of PGC1α, as well as its well-known regulated genes CYC, SOD, NRF2 and HO1 in patients with idiopathic pulmonary arterial hypertension. Begum *et al*[32] found that overexpression of miR-23b in H1838 cells significantly increased cell proliferation, while inhibition of miR-23b in H1437 and H1944 cell lines significantly reduced cell doubling time. In addition, our miRNA network analysis predicted that these up-regulated miRNAs modulate glutathione metabolism, cytokine-cytokine receptor interaction, complement and coagulation cascades, methionine metabolism, apoptosis, cytosolic DNA-

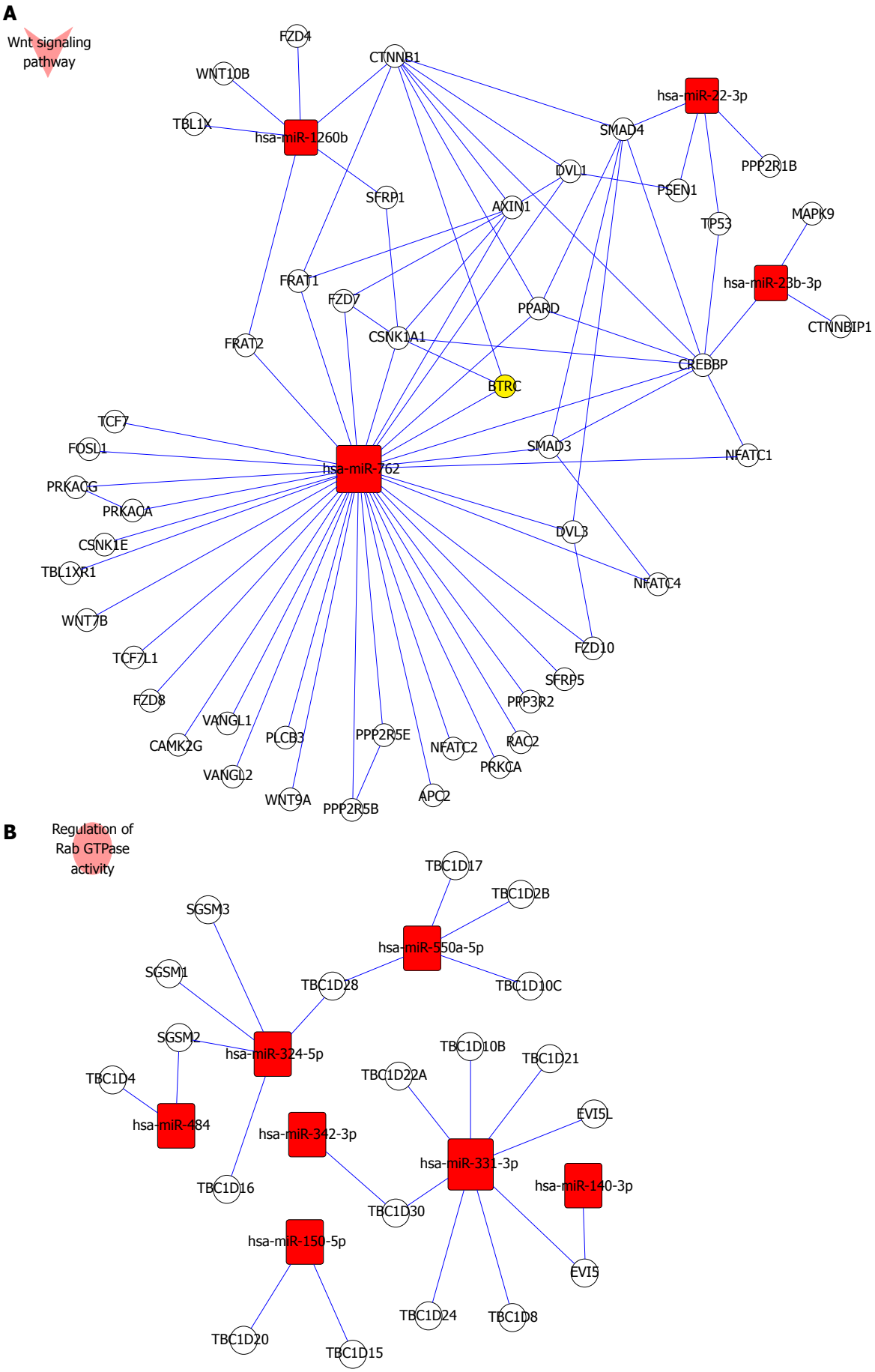

Figure 4 Wnt receptor signaling pathway and regulation of Rab GTPase activity involved in miRNA expression. A: Up-regulated miRNAs (has-miR-762, has-miR-1260b, has-miR-22-3p and has-miR-23b-3p) take part in regulation of the Wnt receptor signaling pathway. B: All down-regulated miRNAs (hsa-miR-550a*, hsa-miR-324-5p, hsa-miR-484, hsa-miR-331-3p, hsa-miR-140-3p, hsa-miR-342-3p and hsa-miR-150) were involved in regulating Rab GTPase activity. miRNA: microRNA.

sensing pathway, Notch signaling pathway, chemokine signaling pathway, and MAPK signaling pathway.

Ell *et al*[33] found that the miRNA-23b/27b/24 cluster promoted breast cancer lung metastasis by targeting the metastasis-suppressive gene prosaposin. Thus, these results show that the significantly overexpressed hsa-miR-1260b, 23a and 23b may be important biomarkers of SAP with ALI. Nevertheless, there is a lack of relevant studies on their role of pathological processes in ALI induced by ASP. Moreover, there is still no report about the reports with hsa-miR-22-3p and hsa-miR-762 and lung diseases.

We also identified seven down-regulated miRNAs (hsa-miR-550a*, 324-5p, 484, 331-3p, 140-3p, 342-3p and 150) by microarray analysis in patients with SAP with ALI and SAP without ALI. Expression of hsa-miR-484, 331-3p, 342-3p and 150 showed a fold-change < 0.5 with $P < 0.01$. miRNA-550a acts as a pro-metastatic gene and directly targets cytoplasmic polyadenylation element binding protein 4 in hepatocellular carcinoma[34]. Moreover, the miR550a-5p/RNF43/Wnt signaling axis acts as a Brg-1 target for regulating colorectal cancer metastasis, and miR150 likely regulates miR124a expression and thus augments expression of inflammatory mediators in myeKlf2$^{-/-}$ macrophages[35,36]. Cai *et al*[37] found that miR-199a and miR-16 were the most significantly down-regulated miRNAs in lipopolysaccharide-induced mouse ALI.

In our study, miR-199a and miR-16 expression did not differ between patients with SAP with ALI and those with SAP without ALI. This discrepancy may have been caused by different inducing factors of ALI. In addition, the results of KEGG pathway enrichment analysis and miRNA-KEGG network showed that the target genes of down-regulated miRNAs were related to the Wnt signaling pathway, insulin signaling pathway, TGF-β signaling pathway, T-cell receptor signaling pathway, and amino sugar and nucleotide sugar metabolism. Previous studies have shown that signaling pathways are involved in the pathogenesis of ALI. Guo *et al*[38] reported that Wnt3a over-rode the effect of P2X7R on Wnt/β-catenin signaling to prevent death of alveolar epithelial type Ⅰ cells and restrict the severity of ALI. Pittet *et al*[39] reported that TGF-beta was a critical mediator of acute lung injury. Mu *et al*[40] also reported that the TGF-β1/Smad signaling (p-Smad 2 and p-Smad 3) pathway was an important mechanism in the course of ALI.

In conclusion, we identified 12 significantly expressed circulating miRNAs in patients with SAP with ALI. These miRNAs may be specifically involved in the pathological mechanism of SAP with ALI. miRNAs and their target genes, as novel therapeutic targets, look promising. At present, the study regarding the mechanism of miRNAs in ALI remains at its nascent stage. miRNAs and their role of pathological processes in ALI induced by SAP remain to be elucidated. There were some limitations in this study. The main limitation was the small sample size. The results need to be verified in multicenter clinical trials. In addition, the molecular mechanism of circulating miRNAs regulating downstream signaling pathways should be further studied in patients with SAP with ALI.

COMMENTS

Background

Severe acute pancreatitis (SAP) is a potentially fatal disease characterized by wide clinical variation. Acute lung injury (ALI) is a common and serious complication of SAP. At present, the early diagnosis of SAP with ALI is still difficult. So, it is important to choose several biomarkers that may be used jointly to improve the diagnostic rate and establish the mechanism of SAP with ALI.

Research frontiers

Some biochemical parameters have been used for diagnosis of ALI, but there are no definitive diagnostic markers and few research studies in this area. We identify circulating biomarkers for prediction of SAP with ALI.

Innovations and breakthrough

The authors identify 12 significantly expressed circulating miRNA in SAP with ALI patients. The information on these miRNAs shed light on potential pathological mechanisms underlying SAP associated with ALI and open new doors for the development of circulating biomarkers for SAP associated with ALI.

Applications

This observational study contributes to finding relevant biomarkers for prediction of SAP with ALI.

Terminology

ALI is defined as a syndrome of inflammation and increased permeability that is associated with a constellation of clinical, radiologic and physiologic abnormalities that cannot be explained by, but may coexist with, left atrial or pulmonary capillary hypertension.

Peer-review

SAP associated with ALI is a critical situation in clinic; therefore, it is important to find relevant biomarkers for detecting SAP associated with ALI in patients. In the present study, the authors demonstrated that 12 circulating microRNAs are associated with SAP patients with ALI. In conclusion, this observational study is novel, interesting and has potential clinical application.

REFERENCES

1 **Liu Y**, Zhou D, Long FW, Chen KL, Yang HW, Lv ZY, Zhou B, Peng ZH, Sun XF, Li Y, Zhou ZG. Resolvin D1 protects against inflammation in experimental acute pancreatitis and associated lung injury. *Am J Physiol Gastrointest Liver Physiol* 2016; **310**: G303-G309 [PMID: 26702138 DOI: 10.1152/ajpgi.00355.2014]

2 **Lytras D**, Manes K, Triantopoulou C, Paraskeva C, Delis S, Avgerinos C, Dervenis C. Persistent early organ failure: defining the high-risk group of patients with severe acute pancreatitis? *Pancreas* 2008; **36**: 249-254 [PMID: 18362837 DOI: 10.1097/MPA.0b013e31815acb2c]

3 **Fedorkiv MB**. [Prevention and correction of pulmonary complications for severe acute pancreatitis]. *Klin Khir* 2015; **(6)**: 22-24 [PMID: 26521460]

4 **Wei M**, Gong YJ, Tu L, Li J, Liang YH, Zhang YH. Expression

of phosphatidylinositol-3 kinase and effects of inhibitor Wortmannin on expression of tumor necrosis factor-α in severe acute pancreatitis associated with acute lung injury. *World J Emerg Med* 2015; **6**: 299-304 [PMID: 26693266 DOI: 10.5847/wjem.j.1920-8642.2015.04.009]

5 **De Campos T**, Deree J, Coimbra R. From acute pancreatitis to end-organ injury: mechanisms of acute lung injury. *Surg Infect (Larchmt)* 2007; **8**: 107-120 [PMID: 17381402 DOI: 10.1089/sur.2006.011]

6 **Li G**, Zhou CL, Zhou QS, Zou HD. Galantamine protects against lipopolysaccharide-induced acute lung injury in rats. *Braz J Med Biol Res* 2016; **49**: e5008 [PMID: 26648090 DOI: 10.1590/1414-431X20155008]

7 **Lee KA**, Gong MN. Pre-B-cell colony-enhancing factor and its clinical correlates with acute lung injury and sepsis. *Chest* 2011; **140**: 382-390 [PMID: 21565968 DOI: 10.1378/chest.10-3100]

8 **Hong SB**, Huang Y, Moreno-Vinasco L, Sammani S, Moitra J, Barnard JW, Ma SF, Mirzapoiazova T, Evenoski C, Reeves RR, Chiang ET, Lang GD, Husain AN, Dudek SM, Jacobson JR, Ye SQ, Lussier YA, Garcia JG. Essential role of pre-B-cell colony enhancing factor in ventilator-induced lung injury. *Am J Respir Crit Care Med* 2008; **178**: 605-617 [PMID: 18658108 DOI: 10.1164/rccm.200712-1822OC]

9 **Chen XY**, Wang SM, Li N, Hu Y, Zhang Y, Xu JF, Li X, Ren J, Su B, Yuan WZ, Teng XR, Zhang RX, Jiang DH, Mulet X, Li HP. Creation of lung-targeted dexamethasone immunoliposome and its therapeutic effect on bleomycin-induced lung injury in rats. *PLoS One* 2013; **8**: e58275 [PMID: 23516459 DOI: 10.1371/journal.pone.0058275]

10 **Chen X**, Ba Y, Ma L, Cai X, Yin Y, Wang K, Guo J, Zhang Y, Chen J, Guo X, Li Q, Li X, Wang W, Zhang Y, Wang J, Jiang X, Xiang Y, Xu C, Zheng P, Zhang J, Li R, Zhang H, Shang X, Gong T, Ning G, Wang J, Zen K, Zhang J, Zhang CY. Characterization of microRNAs in serum: a novel class of biomarkers for diagnosis of cancer and other diseases. *Cell Res* 2008; **18**: 997-1006 [PMID: 18766170 DOI: 10.1038/cr.2008.282]

11 **Mitchell PS**, Parkin RK, Kroh EM, Fritz BR, Wyman SK, Pogosova-Agadjanyan EL, Peterson A, Noteboom J, O'Briant KC, Allen A, Lin DW, Urban N, Drescher CW, Knudsen BS, Stirewalt DL, Gentleman R, Vessella RL, Nelson PS, Martin DB, Tewari M. Circulating microRNAs as stable blood-based markers for cancer detection. *Proc Natl Acad Sci USA* 2008; **105**: 10513-10518 [PMID: 18663219 DOI: 10.1073/pnas.0804549105]

12 **Schwarzenbach H**, Hoon DS, Pantel K. Cell-free nucleic acids as biomarkers in cancer patients. *Nat Rev Cancer* 2011; **11**: 426-437 [PMID: 21562580 DOI: 10.1038/nrc3066]

13 **Zhao DS**, Chen Y, Jiang H, Lu JP, Zhang G, Geng J, Zhang Q, Shen JH, Zhou X, Zhu W, Shan QJ. Serum miR-210 and miR-30a expressions tend to revert to fetal levels in Chinese adult patients with chronic heart failure. *Cardiovasc Pathol* 2013; **22**: 444-450 [PMID: 23660476 DOI: 10.1016/j.carpath.2013.04.001]

14 **Hsu A**, Chen SJ, Chang YS, Chen HC, Chu PH. Systemic approach to identify serum microRNAs as potential biomarkers for acute myocardial infarction. *Biomed Res Int* 2014; **2014**: 418628 [PMID: 24900964 DOI: 10.1155/2014/418628]

15 **Peng L**, Chun-guang Q, Bei-fang L, Xue-zhi D, Zi-hao W, Yun-fu L, Yan-ping D, Yang-gui L, Wei-guo L, Tian-yong H, Zhen-wen H. Clinical impact of circulating miR-133, miR-1291 and miR-663b in plasma of patients with acute myocardial infarction. *Diagn Pathol* 2014; **9**: 89 [PMID: 24885383 DOI: 10.1186/1746-1596-9-89]

16 **Hachisuka S**, Kamei N, Ujigo S, Miyaki S, Yasunaga Y, Ochi M. Circulating microRNAs as biomarkers for evaluating the severity of acute spinal cord injury. *Spinal Cord* 2014; **52**: 596-600 [PMID: 24891009 DOI: 10.1038/sc.2014.86]

17 **Zhou X**, Wen W, Shan X, Qian J, Li H, Jiang T, Wang W, Cheng W, Wang F, Qi L, Ding Y, Liu P, Zhu W, Chen Y. MiR-28-3p as a potential plasma marker in diagnosis of pulmonary embolism. *Thromb Res* 2016; **138**: 91-95 [PMID: 26702486 DOI: 10.1016/j.thromres.2015.12.006]

18 **Wang JF**, Zha YF, Li HW, Wang F, Bian Q, Lai XL, Yu G. Screening plasma miRNAs as biomarkers for renal ischemia-reperfusion injury in rats. *Med Sci Monit* 2014; **20**: 283-289 [PMID: 24553149 DOI: 10.12659/MSM.889937]

19 **Kinet V**, Halkein J, Dirkx E, Windt LJ. Cardiovascular extracellular microRNAs: emerging diagnostic markers and mechanisms of cell-to-cell RNA communication. *Front Genet* 2013; **4**: 214 [PMID: 24273550 DOI: 10.3389/fgene.2013.00214]

20 **Bernard GR**, Artigas A, Brigham KL, Carlet J, Falke K, Hudson L, Lamy M, Legall JR, Morris A, Spragg R. The American-European Consensus Conference on ARDS. Definitions, mechanisms, relevant outcomes, and clinical trial coordination. *Am J Respir Crit Care Med* 1994; **149**: 818-824 [PMID: 7509706 DOI: 10.1164/ajrccm.149.3.7509706]

21 **Beier M**, Hoheisel JD. Analysis of DNA-microarrays produced by inverse in situ oligonucleotide synthesis. *J Biotechnol* 2002; **94**: 15-22 [PMID: 11792449]

22 **Gao X**, Gulari E, Zhou X. In situ synthesis of oligonucleotide microarrays. *Biopolymers* 2004; **73**: 579-596 [PMID: 15048782 DOI: 10.1002/bip.20005]

23 **Zhu Q**, Hong A, Sheng N, Zhang X, Matejko A, Jun KY, Srivannavit O, Gulari E, Gao X, Zhou X. microParaflo biochip for nucleic acid and protein analysis. *Methods Mol Biol* 2007; **382**: 287-312 [PMID: 18220239]

24 **Gui Z**, Li S, Liu X, Xu B, Xu J. Oridonin alters the expression profiles of microRNAs in BxPC-3 human pancreatic cancer cells. *BMC Complement Altern Med* 2015; **15**: 117 [PMID: 25880988 DOI: 10.1186/s12906-015-0640-5]

25 **Wang Y**, Lan Q, Zhao X, Xu W, Li F, Wang Q, Chen R. Comparative Profiling of microRNA Expression in Soybean Seeds from Genetically Modified Plants and their Near-Isogenic Parental Lines. *PLoS One* 2016; **11**: e0155896 [PMID: 27214227 DOI: 10.1371/journal.pone.0155896]

26 **Saeed AI**, Sharov V, White J, Li J, Liang W, Bhagabati N, Braisted J, Klapa M, Currier T, Thiagarajan M, Sturn A, Snuffin M, Rezantsev A, Popov D, Ryltsov A, Kostukovich E, Borisovsky I, Liu Z, Vinsavich A, Trush V, Quackenbush J. TM4: a free, open-source system for microarray data management and analysis. *Biotechniques* 2003; **34**: 374-378 [PMID: 12613259]

27 **Wu ZB**, Li WQ, Lin SJ, Wang CD, Cai L, Lu JL, Chen YX, Su ZP, Shang HB, Yang WL, Zhao WG. MicroRNA expression profile of bromocriptine-resistant prolactinomas. *Mol Cell Endocrinol* 2014; **395**: 10-18 [PMID: 25064468 DOI: 10.1016/j.mce.2014.07.014]

28 **Liu Q**, Du J, Yu X, Xu J, Huang F, Li X, Zhang C, Li X, Chang J, Shang D, Zhao Y, Tian M, Lu H, Xu J, Li C, Zhu H, Jin N, Jiang C. miRNA-200c-3p is crucial in acute respiratory distress syndrome. *Cell Discov* 2017; **3**: 17021 [PMID: 28690868 DOI: 10.1038/celldisc.2017.21]

29 **Vaporidi K**, Vergadi E, Kaniaris E, Hatziapostolou M, Lagoudaki E, Georgopoulos D, Zapol WM, Bloch KD, Iliopoulos D. Pulmonary microRNA profiling in a mouse model of ventilator-induced lung injury. *Am J Physiol Lung Cell Mol Physiol* 2012; **303**: L199-L207 [PMID: 22659882 DOI: 10.1152/ajplung.00370.2011]

30 **Xu L**, Li L, Li J, Li H, Shen Q, Ping J, Ma Z, Zhong J, Dai L. Overexpression of miR-1260b in Non-small Cell Lung Cancer is Associated with Lymph Node Metastasis. *Aging Dis* 2015; **6**: 478-485 [PMID: 26618049 DOI: 10.14336/AD.2015.0620]

31 **Sarrion I**, Milian L, Juan G, Ramon M, Furest I, Carda C, Cortijo Gimeno J, Mata Roig M. Role of circulating miRNAs as biomarkers in idiopathic pulmonary arterial hypertension: possible relevance of miR-23a. *Oxid Med Cell Longev* 2015; **2015**: 792846 [PMID: 25815108 DOI: 10.1155/2015/792846]

32 **Begum S**, Hayashi M, Ogawa T, Jabboure FJ, Brait M, Izumchenko E, Tabak S, Ahrendt SA, Westra WH, Koch W, Sidransky D, Hoque MO. An integrated genome-wide approach to discover deregulated microRNAs in non-small cell lung cancer: Clinical significance of miR-23b-3p deregulation. *Sci Rep* 2015; **5**: 13236 [PMID: 26314549 DOI: 10.1038/srep13236]

33 **Ell B**, Qiu Q, Wei Y, Mercatali L, Ibrahim T, Amadori D, Kang Y. The microRNA-23b/27b/24 cluster promotes breast cancer lung

metastasis by targeting metastasis-suppressive gene prosaposin. *J Biol Chem* 2014; **289**: 21888-21895 [PMID: 24966325 DOI: 10.1074/jbc.M114.582866]

34 **Tian Q**, Liang L, Ding J, Zha R, Shi H, Wang Q, Huang S, Guo W, Ge C, Chen T, Li J, He X. MicroRNA-550a acts as a pro-metastatic gene and directly targets cytoplasmic polyadenylation element-binding protein 4 in hepatocellular carcinoma. *PLoS One* 2012; **7**: e48958 [PMID: 23145039 DOI: 10.1371/journal.pone.0048958]

35 **Wang G**, Fu Y, Yang X, Luo X, Wang J, Gong J, Hu J. Brg-1 targeting of novel miR550a-5p/RNF43/Wnt signaling axis regulates colorectal cancer metastasis. *Oncogene* 2016; **35**: 651-661 [PMID: 25961913 DOI: 10.1038/onc.2015.124]

36 **Manoharan P**, Basford JE, Pilcher-Roberts R, Neumann J, Hui DY, Lingrel JB. Reduced levels of microRNAs miR-124a and miR-150 are associated with increased proinflammatory mediator expression in Krüppel-like factor 2 (KLF2)-deficient macrophages. *J Biol Chem* 2014; **289**: 31638-31646 [PMID: 25248747 DOI: 10.1074/jbc.M114.579763]

37 **Cai ZG**, Zhang SM, Zhang Y, Zhou YY, Wu HB, Xu XP. MicroRNAs are dynamically regulated and play an important role in LPS-induced lung injury. *Can J Physiol Pharmacol* 2012; **90**: 37-43 [PMID: 22185353 DOI: 10.1139/y11-095]

38 **Guo Y**, Mishra A, Weng T, Chintagari NR, Wang Y, Zhao C, Huang C, Liu L. Wnt3a mitigates acute lung injury by reducing P2X7 receptor-mediated alveolar epithelial type I cell death. *Cell Death Dis* 2014; **5**: e1286 [PMID: 24922070 DOI: 10.1038/cddis.2014.254]

39 **Pittet JF**, Griffiths MJ, Geiser T, Kaminski N, Dalton SL, Huang X, Brown LA, Gotwals PJ, Koteliansky VE, Matthay MA, Sheppard D. TGF-beta is a critical mediator of acute lung injury. *J Clin Invest* 2001; **107**: 1537-1544 [PMID: 11413161 DOI: 10.1172/jci11963]

40 **Mu E**, Ding R, An X, Li X, Chen S, Ma X. Heparin attenuates lipopolysaccharide-induced acute lung injury by inhibiting nitric oxide synthase and TGF-β/Smad signaling pathway. *Thromb Res* 2012; **129**: 479-485 [PMID: 22035631 DOI: 10.1016/j.thromres.2011.10.003]

P- Reviewer: Zaja I, Zhao J **S- Editor**: Gong ZM
L- Editor: Filipodia **E- Editor**: Huang Y

World Journal of Gastroenterology

Submit a Manuscript: http://www.f6publishing.com

World J Gastroenterol 2017 November 7; 23(41): 7450-7458

DOI: 10.3748/wjg.v23.i41.7450

ISSN 1007-9327 (print) ISSN 2219-2840 (online)

ORIGINAL ARTICLE

Prospective Study

Scoring systems for peptic ulcer bleeding: Which one to use?

Ivan Budimir, Sanja Stojsavljević, Neven Baršić, Alen Bišćanin, Gorana Mirošević, Sven Bohnec, Lora Stanka Kirigin, Tajana Pavić, Neven Ljubičić

Ivan Budimir, Sanja Stojsavljević, Neven Baršić, Alen Bišćanin, Tajana Pavić, Neven Ljubičić, Division of Gastroenterology, Department of Internal Medicine, "Sestre Milosrdnice" University Hospital Center, Zagreb 10000, Croatia

Gorana Mirošević, Lora Stanka Kirigin, Division of Endocrinology, Department of Internal Medicine, "Sestre Milosrdnice" University Hospital Center, Medical and Dental Faculty, University of Zagreb, Zagreb 10000, Croatia

Sven Bohnec, Gastronterologie, Allgemeine Innere Medizin und Geriatrie, Rems-Murr Klinik Winnenden, 71364 Winnenden, Germany

ORCID number: Ivan Budimir (0000-0003-4198-8329); Sanja Stojsavljević (0000-0002-1626-3003); Neven Baršić (0000-0002-4416-4520); Alen Bišćanin (0000-0003-2923-4110); Gorana Mirošević (0000-0002-9922-2687); Sven Bohnec (0000-0002-3381-3783); Lora Stanka Kirigin (0000-0001-5003-7627); Tajana Pavić (0000-0002-0370-5001); Neven Ljubičić (0000-0002-5207-4357).

Author contributions: Budimir I, Stojsavljević S and Baršić N contributed equally to this work; Budimir I and Ljubičić N designed the research; Budimir I, Stojsavljević S, Baršić N Bišćanin A and Pavić T performed the research; Budimir I, Stojsavljević S, Baršić N, Mirošević G, Bohnec S, Kirigin LS and Pavić T analyzed the data; Budimir I, Stojsavljević S and Baršić N wrote the paper.

Institutional review board statement: The study was reviewed and approved by the Ethics Board of the Clinical Hospital Center ''Sestre Milosrdnice'', Vinogradska cesta 29, Zagreb.

Clinical trial registration statement: The study was registered in the Clinical Hospital Center ''Sestre Milosrdnice'' clinical trials register.

Informed consent statement: All study participants, or their legal guardian, provided informed written consent prior to study enrollment.

Conflict-of-interest statement: None declared.

Data sharing statement: No additional data are available.

Manuscript source: Unsolicited manuscript

Correspondence to: Sanja Stojsavljević, MD, Division of Gastroenterology, Department of Internal Medicine, "Sestre Milosrdnice" University Hospital Center, Vinogradska ul. 29, Zagreb 10000, Croatia. sanja.stojsavljevic@kbcsm.hr
Telephone: +385-1-3787178
Fax: +385-1-3787448

Received: July 26, 2017
Peer-review started: July 26, 2017
First decision: August 10, 2017
Revised: August 24, 2017
Accepted: September 13, 2017
Article in press: September 13, 2017
Published online: November 7, 2017

Abstract

AIM

To compare the Glasgow-Blatchford score (GBS), Rockall score (RS) and Baylor bleeding score (BBS) in predicting clinical outcomes and need for interventions in patients with bleeding peptic ulcers.

METHODS

Between January 2008 and December 2013, 1012

consecutive patients admitted with peptic ulcer bleeding (PUB) were prospectively followed. The pre-endoscopic RS, BBS and GBS, as well as the post-endoscopic diagnostic scores (RS and BBS) were calculated for all patients according to their urgent upper endoscopy findings. Area under the receiver-operating characteristics (AUROC) curves were calculated for the prediction of lethal outcome, rebleeding, needs for blood transfusion and/or surgical intervention, and the optimal cutoff values were evaluated.

RESULTS

PUB accounted for 41.9% of all upper gastrointestinal tract bleeding, 5.2% patients died and 5.4% patients underwent surgery. By comparing the AUROC curves of the aforementioned pre-endoscopic scores, the RS best predicted lethal outcome (AUROC 0.82 *vs* 0.67 *vs* 0.63, respectively), but the GBS best predicted need for hospital-based intervention or 30-d mortality (AUROC 0.84 *vs* 0.57 *vs* 0.64), rebleeding (AUROC 0.75 *vs* 0.61 *vs* 0.53), need for blood transfusion (AUROC 0.83 *vs* 0.63 *vs* 0.58) and surgical intervention (0.82 *vs* 0.63 *vs* 0.52) The post-endoscopic RS was also better than the post-endoscopic BBS in predicting lethal outcome (AUROC 0.82 *vs* 0.69, respectively).

CONCLUSION

The RS is the best predictor of mortality and the GBS is the best predictor of rebleeding, need for blood transfusion and/or surgical intervention in patients with PUB. There is no one 'perfect score' and we suggest that these two tests be used concomitantly.

Key words: Upper gastrointestinal bleeding; Peptic ulcer bleeding; Glasgow-Blatchford score; Rockall score; Baylor bleeding score

Core tip: Endoscopic hemostasis represents the cornerstone of upper gastrointestinal bleeding treatment, and several scores have been developed for the prediction of rebleeding. This is a first study on Croatian patients to include over 1000 participants with peptic ulcer bleeding, and the aim was to compare three scores (Glasgow Blatchford score, Rockall score and Baylor bleeding score) in the prediction of peptic ulcer bleeding treatment outcome, including need for hospital-based intervention or 30-d mortality, 30-d rebleeding rate, 30-d mortality rate, and needs for surgical intervention and blood transfusion, and to find optimal cutoff values that indicate high-risk patients.

Budimir I, Stojsavljević S, Baršić N, Bišćanin A, Mirošević G, Bohnec S, Kirigin LS, Pavić T, Ljubičić N. Scoring systems for peptic ulcer bleeding: Which one to use? *World J Gastroenterol* 2017; 23(41): 7450-7458 Available from: URL: http://www.wjgnet.com/1007-9327/full/v23/i41/7450.htm DOI: http://dx.doi.org/10.3748/wjg.v23.i41.7450

INTRODUCTION

Upper gastrointestinal bleeding (UGIB) is a common medical emergency. Incidence rates of UGIB demonstrate variations ranging from 48 to 160 cases per 100000 population[1]. The most common causes of acute UGIB are non-variceal, where 28% to 59% are caused by peptic ulcer bleeding (PUB)[1-3]. Endoscopic hemostasis represents the cornerstone of UGIB treatment, and several scores have been developed for the prediction of clinical intervention (*i.e*. Rockall score (RS), Glasgow-Blatchford score (GBS), Baylor bleeding score (BBS), Cedars-Sinai Medical Center predictive index, Almela score, AIMS65 score)[4-14]. The recently published American College of Gastroenterology practice guidelines on the management of patients with ulcer bleeding recommend risk assessment in all patients in order to stratify them into high or low risk categories, since it may assist in initial decisions regarding the timing of endoscopy, time of discharge, and level of care[15].

The GBS is a pre-endoscopic score and contains the following parameters: initial hemoglobin levels, urea, blood pressure, pulse, known syncope, melena, and liver or cardiac failure. Each variable has an appointed numeric value and the maximal number of points is 23 (Table 1). The GBS was designed to predict lower risk bleeds, and a GBS value of 1 or lower indicates very low risk category[8,9]. The most commonly used RS consists of a pre-endoscopic evaluation part, which includes age, signs of shock and comorbidities, along with an endoscopic part, which evaluates high-risk endoscopic characteristics as well (known as the post-endoscopic RS) (Table 2). Each variable is appointed a numeric value and every value > 2 indicates a high-risk patient[7]. The maximal pre-endoscopic RS value is 7, and the maximal post-endoscopic value is 11. The post-endoscopic RS can be calculated if bleeding is diagnosed and evaluated with upper endoscopy[7,16,17]. The BBS contains a pre-endoscopic evaluation part, which includes age, severity and duration of associated diseases, along with a post-endoscopic part, which evaluates the position and type of fresh bleeding (Table 3). The maximal pre-endoscopic BBS is 15, and the maximum total (pre-endoscopic and post-endoscopic) BBS is 24[18].

The RS was primarily developed to predict mortality and the GBS to evaluate need for clinical intervention[6-14]. Secondarily, they can be applied to asses rebleeding risk. The BBS was primarily developed to identify patients at high risk for rebleeding after endoscopic hemostasis[6,16]. In previous studies,

Table 1 Glasgow-Blatchford score

		Assigned score
Blood urea, mmol/L	6.5 -7.9	2
	8.0-9.9	3
	10.0-24.9	4
	⩾ 25	6
Hemoglobin for men, g/dL	12 -12.9	1
	10-11.9	3
	< 10	6
Hemoglobin for women, g/dL	10-11.9	1
	< 10	6
Systolic blood pressure, mmHg	100-109	1
	90-99	2
	< 90	3
Other markers	Pulse ⩾ 100	1
	Melena	1
	Syncope	2
	Hepatic disease	2
	Cardiac failure	2

the GBS has been shown to be better than the pre-endoscopic and post-endoscopic RS in predicting the need for hospital-based intervention in patients with UGIB[6,13,19]. On the other hand, the RS appeared to be better at predicting mortality after rebleeding, contributing to more accurate diagnostics and shorter hospital stay[7,13,14]. Recent studies have shown that early endoscopy (within 24 h of presentation) is performed in only half of patients with UGIB, demonstrating the need for reliable and accurate pre-endoscopic risk assessment[6-15,20-25].

This is the first prospective study in Croatia to include over 1000 patients with PUB, and the aim was to compare the GBS, pre-endoscopic RS and pre-endoscopic BBS, as well as the post-endoscopic RS and post-endoscopic BBS, in the prediction of PUB treatment outcome, need for hospital-based intervention (endoscopic treatment, transfusion, surgery intervention) or 30-d mortality, including 30-d rebleeding rate, 30-d mortality rate, and needs for surgical intervention and blood transfusion, and to find optimal cutoff values that indicate high-risk patients.

MATERIALS AND METHODS

This prospective study was conducted in the University Hospital Center "Sestre Milosrdnice" that covers a population of approximately 300000 in the City of Zagreb, Croatia. All patients presenting to the Emergency Unit between January 2008 and December 2013 with hematemesis, melena, hematochezia, or blood admixture upon nasogastric insertion were considered for study enrolment. If initial work-up indicated the need for hospitalization, patients were admitted to the Interventional Gastroenterology Unit.

Upper gastrointestinal endoscopy was performed in all patients within 24 h of admission. Only patients with gastric and/or duodenal ulcers, or an ulcer at the site of gastro-enteric anastomosis found during emergency endoscopy, without any other possible cause of bleeding were included in the study. All patients with high-risk ulcer stigmata and patients selected depending on clinical judgment received high-dose acid suppression therapy (pantoprazole or esomeprazole 80 mg as an intravenous bolus, followed by 40 mg intravenously 2 times daily or 200 mg daily in the form of continuous infusion for at least 48 h followed by 40 mg daily by mouth). The institution's ethics committee approved the study. Data was prospectively entered into a database, with patient details stored in a depersonalized manner to protect patient confidentiality.

Data collection

The following data were collected for each patient: demographic data, history of ulcer or liver disease, coexisting and past illnesses, medication use, clinical characteristics of the bleeding episode, laboratory results, endoscopic diagnosis including stigmata of ongoing or recent hemorrhage, endoscopic intervention, medical treatment, rebleeding, surgical therapy, duration of hospitalization and cause of death. The grading of overall health and co-morbidity was performed according to the American Society of Anesthesiology (ASA) classification (grade 1, normal healthy patients; grade 2, mild systemic illness; grade 3, severe but incapacitating systemic illness; grade 4, life-threatening illness). Stigmata of hemorrhage were defined according to the Forrest classification (Forrest Ia, spurting bleeding; Forrest Ib, oozing bleeding; Forrest Ⅱa, non-bleeding visible vessel; Forrest Ⅱb, adherent clot; Forrest Ⅱc, hematin on ulcer base; Forrest Ⅲ, clean ulcer base).

Shock was defined as syncope or signs of shock at physical examination, including systolic blood pressure less than 100 mmHg and pulse rate more than 100 beats/min.

Post-hemorrhagic anemia was corrected with red blood cell transfusion (2 units, approximately 500 mL) at a hemoglobin threshold of 70-80 g/L.

All patients diagnosed with PUB and high-risk stigmata underwent initial hemostasis (injection of dilute epinephrine into and around the bleeding point, positioning of clips or thermal coagulation, or both, but never epinephrine alone). Two biopsy specimens were obtained from the gastric antrum and body in all patients and the presence of *Helicobacter pylori (H. pylori)* infection was assessed by histopathological examination of the specimens using hematoxylin-eosin (HE) stain.

All patients with negative histology for *H. pylori* at index endoscopy had a control endoscopy with repeating biopsy samples, or urea breath test (UBT), performed 2 wk after proton-pump inhibitor treatment was discontinued. Patients in whom the described protocol was not followed were excluded from the study about *H. pylori* infection.

Table 2 Rockall score

		Points			
	Variable	0	1	2	3
Pre-endoscopic score	Age, yr	< 60	60-79	⩾ 80	
	Shock	Systolic blood pressure ⩾ 100 Pulse < 100/min	Systolic blood pressure ⩾ 100 mmHg Pulse ⩾ 100/min	Systolic blood pressure < 100	
	Comorbidity	No major comorbidity		Cardiac failure, ischemic heart disease, any major comorbidity	Renal failure, liver failure, disseminated malignancy
Post-endoscopic score	Diagnosis	Mallory-Weiss tear, no lesion identified and no signs of recent hemorrhage	All other diagnosis	Malignancy of upper gastrointestinal tract	
	Major signs of recent hemorrhage	None or dark spot only		Blood in upper gastrointestinal tract, adherent clot, visible or spurting vessel	

Table 3 Baylor bleeding score

Assigned score	Age, yr	No. of parallel illnesses	Severity of illnesses	Site of bleeding	Stigmata of bleeding
0	< 30	0			
1	30-49	1 or 2			Clot
2	50-59				
3	60-69				Visible vessel
4		3 or 4	Chronic	Posterior wall bulb	
5	⩾ 70	⩾ 5	Acute		Active bleeding
Score		Pre-endoscopic		Post-endoscopic	

Rebleeding was defined as one or more signs of recurrent bleeding, including fresh hematemesis or melena, hematochezia, aspiration of fresh blood *via* nasogastric tube, instability of vital signs, and reduction of hemoglobin levels by 2 g/dL or more, occurring 24-h after the primary bleeding was stopped.

For all patients with gastric ulcer in whom recurrent bleeding was not observed, control endoscopy was performed 4-5 d after initial hemostasis and biopsy specimens were obtained from the margins and base of gastric ulcers to exclude malignancy. Control endoscopy with histology had been planned to be performed in all patients with gastric ulcer.

Documented clinical outcomes were: need for hospital-based intervention or 30-d mortality, 30-d rebleeding, 30-d mortality and interventions (transfer to the Department of Surgery and the need for blood transfusion).

The collected data was used to calculate the GBS score, as well as the pre-endoscopic RS and pre-endoscopic BBS for each patient presenting with UGIB. The post-endoscopic RS and BBS were calculated if bleeding from gastric, duodenal or gastro-enteric ulcers was endoscopically diagnosed. Methods for calculating the GBS, RS and BBS were as previously described. Pre-endoscopic and post-endoscopic scores were separately evaluated.

Statistical analysis

The Mann-Whitney *U*-test and Kruskal-Wallis analysis of variance test were used to analyze differences in quantitative data. The discriminative ability of the scoring systems to predict outcomes was evaluated by receiver operating characteristics curves (ROC) with 95%CI. The areas under ROC (AUROC) curves were compared using the method of Delong *et al*[26] (1988) for the calculation of the standard error of the Area Under the Curve (AUC) and of the difference between two AUCs. The optimal thresholds of the GBS, RS and BBS for the prediction of rebleeding, death, and needs for blood transfusion and/or surgical intervention were identified as the threshold associated with the highest Youden index[27]. A two-tailed significance level of 5% was used in all comparisons. All analyses were performed using a statistical package MedCalc for Windows, version 15.8 (MedCalc Software, Ostend, Belgium).

RESULTS

The analysis included 2643 patients with UGIB, of that 2326 (88%) patients had non-variceal bleeding, 225 (8.5%) had variceal bleeding, and 92 (3.5%) had an unidentified cause of bleeding.

From 2418 patients with non-variceal bleeding, 41.9% (1012) had PUB; specifically, the cause of bleeding in 49% (496) was gastric ulcer, in 47% (476) duodenal ulcer, in 2.4% (24) both gastric and duodenal ulcer, and in 1.6% (16) gastro-enteric anastomosis ulcer. Endoscopic treatment was required in 58% of

Table 4 Patient characteristics and clinical outcomes

Age	
Median, yr	65.3 (20-100)
Sex	
Male/Female	638 (63)/374 (37)
Findings at endoscopy	
Gastric ulcers	496 (49)
Duodenal ulcers	476 (47)
Gastric and duodenal ulcers	24 (2.4)
Ulcer on gastro-enteric anastomosis	16 (1.6)
High-risk ulcers (Forrest Ⅰa-Ⅱb)	526 (52)
Forrest Ⅰa	61 (6)
Forrest Ⅰb	111 (11)
Forrest Ⅱa	212 (21)
Forrest Ⅱb	142 (14)
Low- risk ulcers (Forrest Ⅱc-Ⅲ)	486 (48)
Forrest Ⅱc	172 (17)
Forrest Ⅲ	314 (31)
Hemodynamic shock	111 (11)
Comorbidity	
Ischemic and valvular heart disease	213 (21.5)
Liver disease	172 (17)
Renal failure	111 (11)
Any malignancy	131 (12.9)
Comorbidity (ASA class)	
ASA Ⅰ	142 (14)
ASA Ⅱ	283 (28)
ASA Ⅲ-Ⅳ	587 (58)
H. pylori	
Tested	760 (75.1)
H. pylori-positive	324 (42.6)
Drugs	
Without previous therapy	433 (42.8)
NSAIDs	284 (28.1)
Acetylsalicylic acid	203 (20)
Antiplatelet therapy	31 (3.1)
Anticoagulant therapy	41 (4)
NOAC	20 (2)
Treatment	
Endoscopic therapy	587 (58)
Epinephrine	213 (36.3)
Hemoclips	156 (26.6)
Hemoclips + epinephrine	180 (30.7)
Thermocoagulation	26 (4.4)
Thermocoagulation + epinephrine	12 (2)
Repeated endoscopic therapy	71 (7)
Blood transfusion required	496 (49)
Red blood cell	406 (40.1)
Median (range), unit	2.5 (1-16)
Fresh frozen plasma	81 (8)
Median (range), unit	2 (1-6)
Platelet	9 (0.9)
Median (range), unit	6 (4-8)
Whole blood	0 (0)
Surgery	55 (5.4)
Outcome	
Rebleeding	95 (9.4)
Rebleeding (anticoag. and NOAC)	9 (14.8)
30-d mortality	53 (5.2)
Median hospital stay, d	6 (0-45)

Data are presented as *n* (%) or mean (range). ASA: American society of anesthesiology; NOAC: New(er) oral anticoagulant; NSAIDs: Non-steroidal anti-inflammatory drugs.

patients with ulcer bleeding, and in 57.3% hemostasis was achieved with hemoclips or with combination

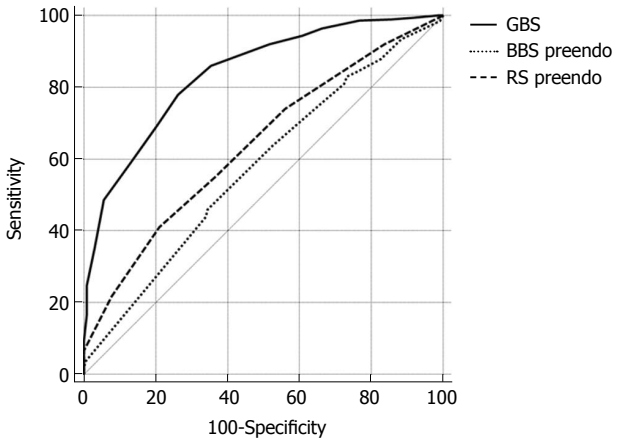

Figure 1 Comparison of Glasgow-Blatchford score, pre-endoscopic Rockall score and pre-endoscopic Baylor bleeding score in predicting need for hospital-based intervention or 30-d mortality. AUROC [0.83 (95%CI: 0.81-0.86)] *vs* [0.63 (95%CI: 0.59-0.68)] *vs* [0.57 (95%CI: 0.53-0.61)]. GBS: Glasgow-Blatchford score; BBS: Baylor bleeding score; RS: Rockall score.

hemoclips/diluted epinephrine. The rate of rebleeding was 9.4%, and in patients that were on anticoagulant therapy the rebleeding rate was 14.8% (P = 0.245), which was not statistically significant. In total, 5.4% of the patients were transferred to the Department of Surgery. The 30-d mortality was 5.2% and the median length of hospitalization was 6 d. Transfusion of red blood cells was performed in 49% of patients. Patients were predominantly men (median age 65.3). In 52% of patients, high-risk ulcers were verified (Forrest Ia-Ⅱb), 11% of the patients presented with shock, and moderate to severe comorbidity was found in 58%. Furthermore, 28.1% patients with peptic ulcer had been taking nonsteroidal anti-inflammatory drugs, 20% acetylsalicylic acid, 3.1% antiplatelet medication and 6% anticoagulant therapy.

H. pylori testing was performed in 760 (75.1%) patients, of which 324 (42.6%) tested positive. Table 4 shows the patient characteristics and clinical outcomes.

Using ROC curve analysis we found that the GBS was clearly superior to pre-endoscopic RS and pre-endoscopic BBS, in predicting need for hospital-based intervention or 30-d mortality (AUROC 0.84 *vs* 0.57 *vs* 0.64 respectively) (Figure 1).

The cutoff value that maximized the sum of the sensitivity and specificity for predicting 30-d mortality for the pre-endoscopic RS was 4 (sensitivity 0.63, specificity 0.85, total 1.48), and 5 for the post-endoscopic RS (sensitivity 0.83, specificity 0.68, total 1.51).

Based on ROC analysis of sensitivity and specificity, the optimal cutoff value of the pre-endoscopic BBS for 30-d mortality was 8 (0.63 sensitivity, 0.58 specificity, total 1.21), and the optimal cutoff post-endoscopic BBS value for 30-d mortality was 9 (0.88 sensitivity, 0.40 specificity, total 1.28).

When assessing scores for the prediction of lethal outcome in patients with PUB, the pre-endoscopic

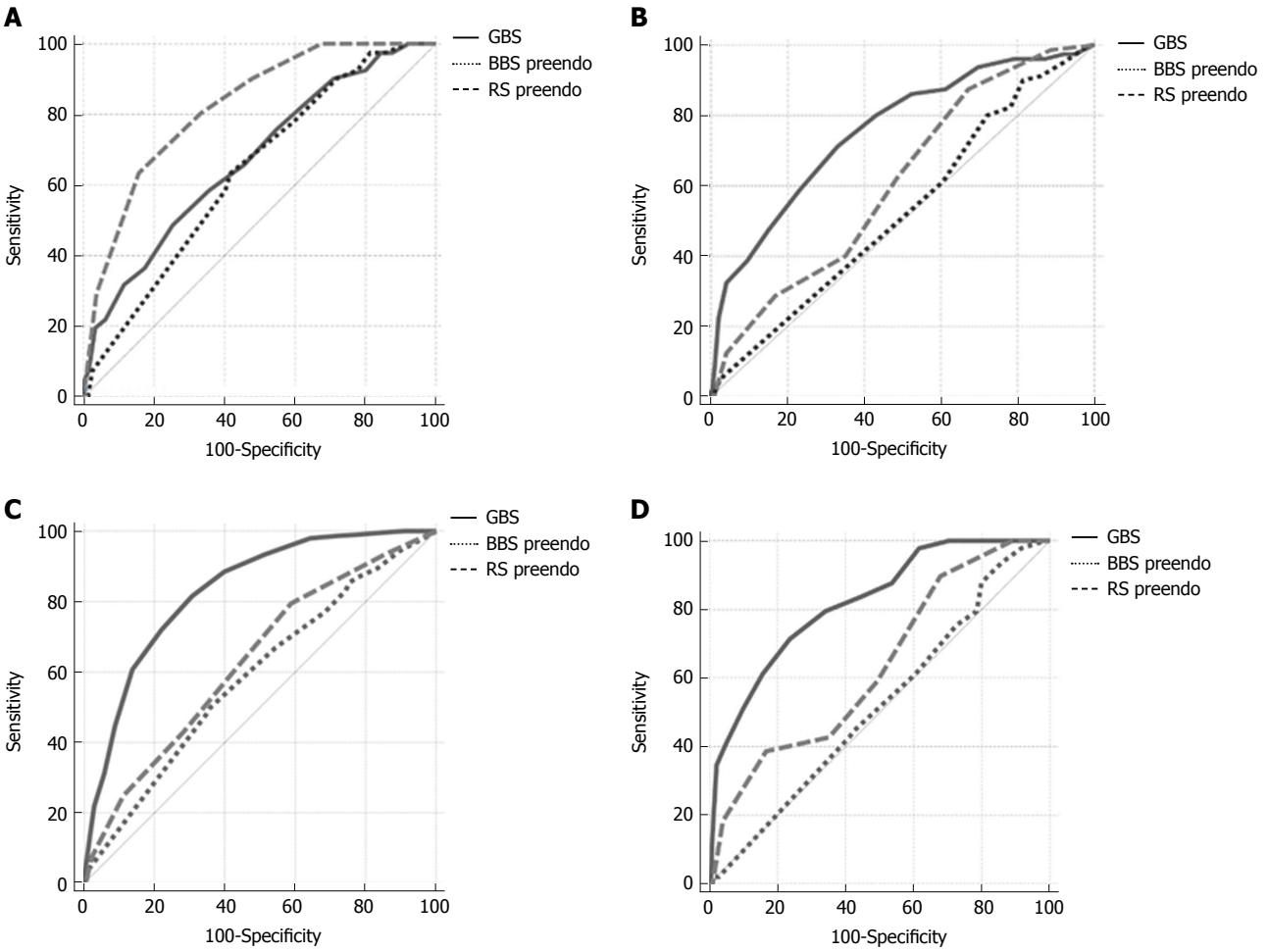

Figure 2 Comparison of the Glasgow-Blatchford score, pre-endoscopic Rockall score and pre-endoscopic Baylor bleeding score for the prediction of death, recurrent bleeding, transfusion or surgical intervention. A: AUROC [0.67 (95%CI: 0.64-0.70)] *vs* [0.82 (95%CI: 0.79-0.84)] *vs* [0.63 (95%CI: 0.60-0.66)]; B: AUROC [0.75 (95%CI: 0.72-0.78)] *vs* [0.61 (95%CI: 0.57-0.64)] *vs* [0.52 (95%CI: 0.49- 0.56)]; C: AUROC [0.83 (95%CI: 0.80-0.85)] *vs* [0.63 (95%CI: 0.59-0.66)] *vs* [0.58 (95%CI: 0.55-0.62)]; D: AUROC [0.82 (95%CI: 0.79-0.84)] *vs* [0.63 (95%CI: 0.60-0.66)] *vs* [0.52 (95%CI: 0.48-0.55)]. GBS: Glasgow-Blatchford score; BBS: Baylor bleeding score; RS: Rockall score.

RS was superior compared to the GBS and the pre-endoscopic BBS (AUROC 0.82 *vs* 0.67 *vs* 0.63, respectively) (Figure 2A).

Based on the ROC analysis of sensitivity and specificity, the optimal cutoff GBS value for 30-d mortality was 12 (0.49 sensitivity, 0.75 specificity, total 1.24), for rebleeding 11 (0.71 sensitivity, 0.67 specificity, total 1.38), for blood transfusion 9 (0.71 sensitivity, 0.67 specificity, total 1.38) and for surgery 12 (0.71 sensitivity, 0.76 specificity, total 1.47).

The GBS score was superior to the pre-endoscopic RS and BBS in the prediction of rebleeding (AUROC 0.75 *vs* 0.61 *vs* 0.52) (Figure 2B).

The GBS score was superior to the pre-endoscopic RS and BBS in predicting the need for blood transfusion (AUROC 0.83 *vs* 0.63 *vs* 0.59, respectively) (Figure 2C) and transfer to the Department of Surgery (AUROC 0.82 *vs* 0.63 *vs* 0.52, respectively) (Figure 2D). Also, the post-endoscopic RS was superior to the post-endoscopic BBS (AUROC 0.82 *vs* 0.69) in the prediction of lethal outcome (Figure 3A).

There was no significant difference between the post-endoscopic RS and BBS in the prediction of rebleeding (AUROC 0.70 *vs* 0.73) (Figure 3B).

The rebleeding cutoff point that maximized the sum of the sensitivity and specificity for the pre-endoscopic BBS was 3 (sensitivity 0.90, specificity 0.19, total 1.09), and 11 for the post-endoscopic BBS (sensitivity 0.66, specificity 0.76, total 1.42).

There was no significant difference between the post-endoscopic RS and BBS in predicting the need for blood transfusion (AUROC 0.68 *vs* 0.71) (Figure 3C) and transfer to the Department of Surgery (AUROC 0.68 *vs* 0.74) (Figure 3D).

DISCUSSION

UGIB is the most important cause of emergency gastroenterological admissions and the most frequent condition requiring emergency endoscopy[1]. The most common causes of acute UGIB are non-variceal, of which 30% to 60% are attributed to PUB[28]. In our study, 42% of all non-variceal bleeding was caused by PUB. In order to assess the adequate timing of

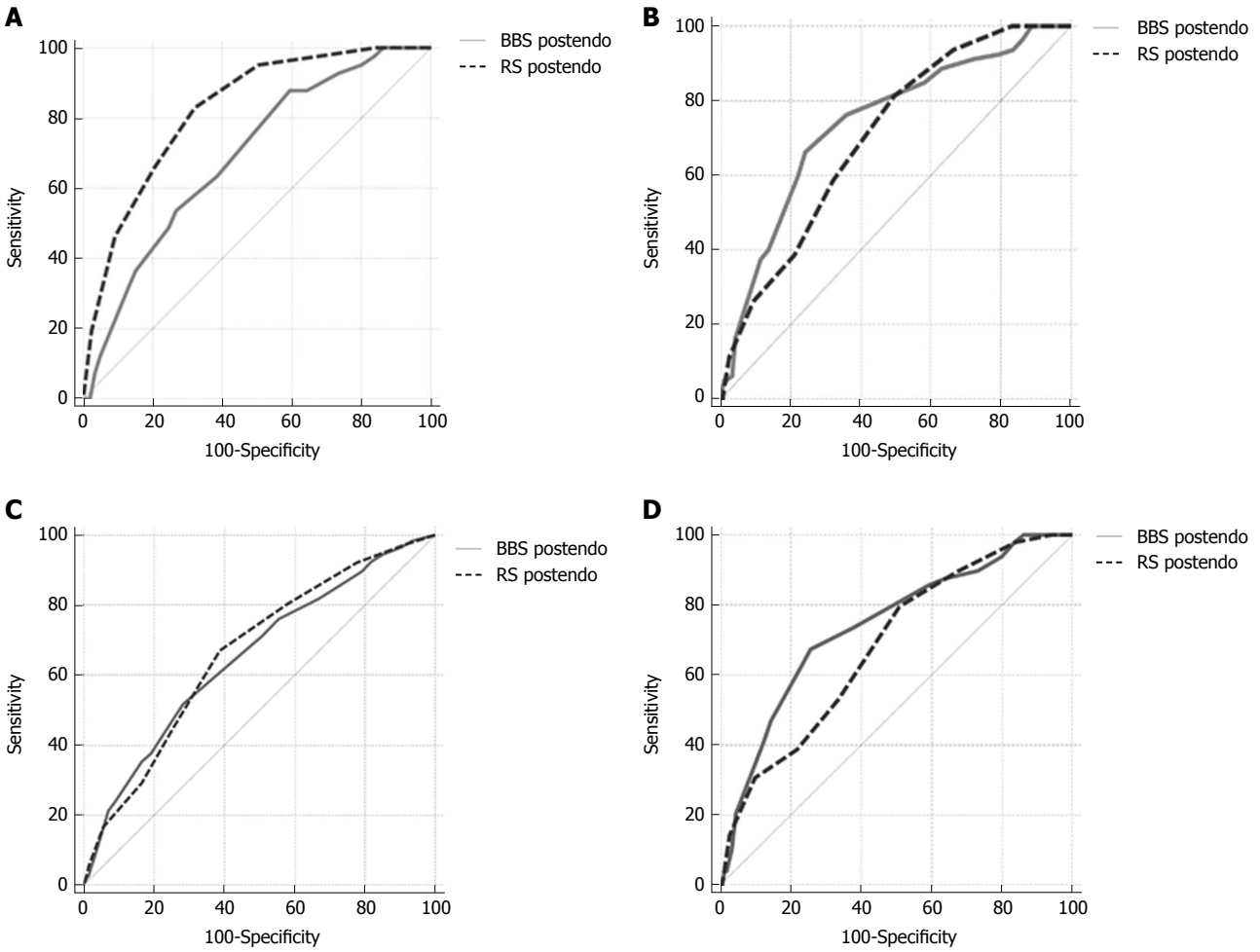

Figure 3 Comparison of the post-endoscopic Rockall score and post-endoscopic Baylor bleeding score for the prediction of death recurrent bleeding, transfusion or surgical intervention. AUROC: [0.82 (95%CI: 0.79-0.84)] *vs* [0.69 (95%CI: 0.65-0.72)]; B: AUROC [0.70 (95%CI: 0.67-0.73)] *vs* [0.73 (95%CI: 0.70-0.76)]; C: AUROC [0.66 (95%CI: 0.62-0.70)] *vs* [0.65 (95%CI: 0.61-0.69)]; D: AUROC [0.68 (95%CI: 0.65-0.71)] *vs* [0.74 (95%CI: 0.71-0.77)]. BBS: Baylor bleeding score; RS: Rockall score.

endoscopy and selection of patients for hospital admission, several scoring systems for risk estimation have been developed. With the array of available scoring systems, it is often difficult to select the ideal scoring system for a particular patient or clinical outcome of interest. Therefore, in this study, we compared the performance of these scoring systems in the risk assessment of various clinical outcomes.

Our study showed that the GBS is superior to the pre-endoscopic RS and BBS in predicting need for hospital-based intervention or 30-d mortality. This is in concordance with the results from a study by Laursen[22] and a study by Bryant *et al*[19]. Our study also showed that the GBS is superior to the pre-endoscopic RS and BBS in predicting peptic ulcer re-bleeding. An explanation for why the GBS best predicts peptic ulcer rebleeding is that it incorporates hemoglobin and serum urea values. Serum urea is a good biochemical marker for UGIB because it rises rapidly when there is catabolism of isoleucine-poor hemoglobin[8,29]. The maximal level of hemoglobin and urea account for half of the maximal sum of points in the GBS score.

Our study showed that there is no significant difference between the post-endoscopic BBS and post-endoscopic RS in predicting peptic ulcer rebleeding. This is in concordance with the results from a study by Laursen *et al*[6]. Similar data was published by Italian and Dutch researchers, who also found low values under the ROC curve [(0.59-0.68) and 0.61] and concluded that the RS is not appropriate for prediction of rebleeding[16,30].

Our study showed that the GBS is superior to the pre-endoscopic RS and pre-endoscopic BBS in predicting the needs for blood transfusion and/or transfer to the Department of Surgery. The ROC curve for GBS rebleeding was similar to the GBS ROC curve for blood transfusion requirement and transfer to the Department of Surgery because peptic ulcer rebleeding is the main cause of blood transfusion requirement and need for surgical intervention. Bryant *et al*[19] published similar data.

Our study showed that the pre-endoscopic RS was superior to the GBS and pre-endoscopic BBS

in predicting mortality. The RS best predicted fatal outcome because it incorporated the majority of risk factors (age, shock, moderate to severe co-morbidities and high-risk endoscopic signs for rebleeding), which was valuable in a multivariate analysis of risk for fatal outcome[7,13,30,31]. Our study showed that the post-endoscopic RS is superior to the post-endoscopic BBS in predicting lethal outcome in patients with PUB. Laursen[22] did not find any significant difference in AUROC among post-endoscopic BBS and post-endoscopic RS.

According to studies by Hyett *et al*[14] and Bryant *et al*[19], the GBS cutoff points for high-risk of lethal outcome and rebleeding were ⩾ 10 and ⩾ 12, respectively. In a recent retrospective study, Lim *et al*[32] suggested urgent endoscopy in the first 13 h after clinical presentation in high-risk patients with GBS > 12, in the first 24 h in patients with GBS > 7 and for patients with GBS values between 4 and 7 urgent endoscopy in the first 24 h is recommended, but not necessary.

Our cutoff points for high-risk of rebleeding and lethal outcome in PUB patients are significantly different in comparison with original research papers (GBS ⩾ 2, pre-endoscopic BBS > 5, post-endoscopic BBS ⩾ 10, post-endoscopic RS ⩾ 4), which all refer to UGIB[6-9,13,14]. An explanation for this could be that the original series included an unselected group of patients with UGIB, with a significant proportion of patients with a low-risk of death, recurrent bleeding, and needs for blood transfusion and/or surgical intervention. These were patients that presented with low-risk bleeding ulcers (Forrest Ⅱc and Forrest Ⅲ), Mallory-Weiss syndrome, ulcerative esophagitis, angiodysplasia and portal hypertensive gastropathy.

When considering possible limitations of our study, there is always a certain level of subjectivity in the endoscopic classification of ulcers and variation in endoscopic treatment. Furthermore, our study had a relatively short follow-up period of 30 d.

By comparing the ROC curves of the aforementioned pre-endoscopic scores, the RS proved to be the best score for predicting lethal outcome. The post-endoscopic RS was also better than the post-endoscopic BBS in predicting lethal outcome in patients with PUB. On the other hand, among the three pre-endoscopic scores, the GBS best predicted need for hospital-based intervention or 30-d mortality, rebleeding, and needs for blood transfusion and/or surgical intervention.

COMMENTS

Background

This paper delivers a prospective single-center study, with a sample size of more than 1000 patients, that compared the scoring systems of the Glasgow-Blatchford score, Rockall score and Baylor bleeding score in predicting clinical outcomes and need for interventions in patients with bleeding peptic ulcers.

Research frontiers

Endoscopic hemostasis represents the cornerstone of upper gastrointestinal bleeding treatment, and several scores have been developed for the prediction of rebleeding.

Innovations and breakthroughs

The authors concluded that although there is no 'perfect score', the Rockall score is the best predictor of mortality and the Glasgow-Blatchford score is the best predictor of need for hospital-based intervention or 30-d mortality, rebleeding, and needs for blood transfusion and/or surgical intervention in patients with peptic ulcer bleeding.

Peer-review

A detailed description is provided to allow other investigators to reproduce or validate the results. The statistical methods used are appropriate. The results provide sufficient experimental evidence to draw firm scientific conclusions. The discussion is well organized and provides systematic theoretical analysis and valuable conclusions.

REFERENCES

1 **Holster IL**, Kuipers EJ. Management of acute nonvariceal upper gastrointestinal bleeding: current policies and future perspectives. *World J Gastroenterol* 2012; **18**: 1202-1207 [PMID: 22468083 DOI: 10.3748/wjg.v18.i11.1202]

2 **Hearnshaw SA**, Logan RF, Lowe D, Travis SP, Murphy MF, Palmer KR. Acute upper gastrointestinal bleeding in the UK: patient characteristics, diagnoses and outcomes in the 2007 UK audit. *Gut* 2011; **60**: 1327-1335 [PMID: 21490373 DOI: 10.1136/gut.2010.228437]

3 **Bardou M**, Benhaberou-Brun D, Le Ray I, Barkun AN. Diagnosis and management of nonvariceal upper gastrointestinal bleeding. *Nat Rev Gastroenterol Hepatol* 2012; **9**: 97-104 [PMID: 22230903 DOI: 10.1038/nrgastro.2011.260]

4 **Laine L**, Jensen DM. Management of patients with ulcer bleeding. *Am J Gastroenterol* 2012; **107**: 345-60; quiz 361 [PMID: 22310222 DOI: 10.1038/ajg.2011.480]

5 **Gralnek IM**, Dumonceau JM, Kuipers EJ, Lanas A, Sanders DS, Kurien M, Rotondano G, Hucl T, Dinis-Ribeiro M, Marmo R, Racz I, Arezzo A, Hoffmann RT, Lesur G, de Franchis R, Aabakken L, Veitch A, Radaelli F, Salgueiro P, Cardoso R, Maia L, Zullo A, Cipolletta L, Hassan C. Diagnosis and management of nonvariceal upper gastrointestinal hemorrhage: European Society of Gastrointestinal Endoscopy (ESGE) Guideline. *Endoscopy* 2015; **47**: a1-46 [PMID: 26417980 DOI: 10.1055/s-0034-1393172]

6 **Laursen SB**, Hansen JM, Schaffalitzky de Muckadell OB. The Glasgow Blatchford score is the most accurate assessment of patients with upper gastrointestinal hemorrhage. *Clin Gastroenterol Hepatol* 2012; **10**: 1130-1135.e1 [PMID: 22801061 DOI: 10.1016/j.cgh.2012.06.022]

7 **Rockall TA**, Logan RF, Devlin HB, Northfield TC. Risk assessment after acute upper gastrointestinal haemorrhage. *Gut* 1996; **38**: 316-321 [PMID: 8675081]

8 **Blatchford O**, Murray WR, Blatchford M. A risk score to predict need for treatment for upper-gastrointestinal haemorrhage. *Lancet* 2000; **356**: 1318-1321 [PMID: 11073021 DOI: 10.1016/S0140-6736(00)02816-6]

9 **Blatchford O**, Davidson LA, Murray WR, Blatchford M, Pell J. Acute upper gastrointestinal haemorrhage in west of Scotland: case ascertainment study. *BMJ* 1997; **315**: 510-514 [PMID: 9329304]

10 **Forrest JA**, Finlayson ND, Shearman DJ. Endoscopy in gastrointestinal bleeding. *Lancet* 1974; **2**: 394-397 [PMID: 4136718]

11 **Budimir I**, Gradišer M, Nikolić M, Baršić N, Ljubičić N, Kralj D, Budimir I Jr. Glasgow Blatchford, pre-endoscopic Rockall and AIMS65 scores show no difference in predicting rebleeding rate and mortality in variceal bleeding. *Scand J Gastroenterol* 2016; **51**: 1375-1379 [PMID: 27356670 DOI: 10.1080/00365521.2016.1200138]

12 **Almela P**, Benages A, Peiró S, Añón R, Pérez MM, Peña A, Pascual I, Mora F. A risk score system for identification of patients with upper-GI bleeding suitable for outpatient management. *Gastrointest Endosc* 2004; **59**: 772-781 [PMID: 15173788]

13 **Stanley AJ**, Dalton HR, Blatchford O, Ashley D, Mowat C, Cahill A, Gaya DR, Thompson E, Warshow U, Hare N, Groome M, Benson G, Murray W. Multicentre comparison of the Glasgow Blatchford and Rockall Scores in the prediction of clinical end-points after upper gastrointestinal haemorrhage. *Aliment Pharmacol Ther* 2011; **34**: 470-475 [PMID: 21707681 DOI: 10.1111/j.1365-2036.2011.04747.x]

14 **Hyett BH**, Abougergi MS, Charpentier JP, Kumar NL, Brozovic S, Claggett BL, Travis AC, Saltzman JR. The AIMS65 score compared with the Glasgow-Blatchford score in predicting outcomes in upper GI bleeding. *Gastrointest Endosc* 2013; **77**: 551-557 [PMID: 23357496 DOI: 10.1016/j.gie.2012.11.022]

15 **Barkun AN**, Bardou M, Kuipers EJ, Sung J, Hunt RH, Martel M, Sinclair P; International Consensus Upper Gastrointestinal Bleeding Conference Group. International consensus recommendations on the management of patients with nonvariceal upper gastrointestinal bleeding. *Ann Intern Med* 2010; **152**: 101-113 [PMID: 20083829 DOI: 10.7326/0003-4819-152-2-201001190-00009]

16 **Vreeburg EM**, Terwee CB, Snel P, Rauws EA, Bartelsman JF, Meulen JH, Tytgat GN. Validation of the Rockall risk scoring system in upper gastrointestinal bleeding. *Gut* 1999; **44**: 331-335 [PMID: 10026316]

17 **Masaoka T**, Suzuki H, Hori S, Aikawa N, Hibi T. Blatchford scoring system is a useful scoring system for detecting patients with upper gastrointestinal bleeding who do not need endoscopic intervention. *J Gastroenterol Hepatol* 2007; **22**: 1404-1408 [PMID: 17716345 DOI: 10.1111/j.1440-1746.2006.04762.x]

18 **Saeed ZA**, Ramirez FC, Hepps KS, Cole RA, Graham DY. Prospective validation of the Baylor bleeding score for predicting the likelihood of rebleeding after endoscopic hemostasis of peptic ulcers. *Gastrointest Endosc* 1995; **41**: 561-565 [PMID: 7672549]

19 **Bryant RV**, Kuo P, Williamson K, Yam C, Schoeman MN, Holloway RH, Nguyen NQ. Performance of the Glasgow-Blatchford score in predicting clinical outcomes and intervention in hospitalized patients with upper GI bleeding. *Gastrointest Endosc* 2013; **78**: 576-583 [PMID: 23790755 DOI: 10.1016/j.gie.2013.05.003]

20 **Srirajaskanthan R**, Conn R, Bulwer C, Irving P. The Glasgow Blatchford scoring system enables accurate risk stratification of patients with upper gastrointestinal haemorrhage. *Int J Clin Pract* 2010; **64**: 868-874 [PMID: 20337750 DOI: 10.1111/j.1742-1241.2009.02267.x]

21 **Cameron EA**, Pratap JN, Sims TJ, Inman S, Boyd D, Ward M, Middleton SJ. Three-year prospective validation of a pre-endoscopic risk stratification in patients with acute upper-gastrointestinal haemorrhage. *Eur J Gastroenterol Hepatol* 2002; **14**: 497-501 [PMID: 11984147]

22 **Laursen SB**. Treatment and prognosis in peptic ulcer bleeding. *Dan Med J* 2014; **61**: B4797 [PMID: 24547604]

23 **Hearnshaw SA**, Logan RF, Lowe D, Travis SP, Murphy MF, Palmer KR. Use of endoscopy for management of acute upper gastrointestinal bleeding in the UK: results of a nationwide audit. *Gut* 2010; **59**: 1022-1029 [PMID: 20357318 DOI: 10.1136/gut.2008.174599]

24 **Maggio D**, Barkun AN, Martel M, Elouali S, Gralnek IM; Reason Investigators. Predictors of early rebleeding after endoscopic therapy in patients with nonvariceal upper gastrointestinal bleeding secondary to high-risk lesions. *Can J Gastroenterol* 2013; **27**: 454-458 [PMID: 23936874]

25 **Imperiale TF**, Dominitz JA, Provenzale DT, Boes LP, Rose CM, Bowers JC, Musick BS, Azzouz F, Perkins SM. Predicting poor outcome from acute upper gastrointestinal hemorrhage. *Arch Intern Med* 2007; **167**: 1291-1296 [PMID: 17592103 DOI: 10.1001/archinte.167.12.1291]

26 **DeLong ER**, DeLong DM, Clarke-Pearson DL. Comparing the areas under two or more correlated receiver operating characteristic curves: a nonparametric approach. *Biometrics* 1988; **44**: 837-845 [PMID: 3203132]

27 **Youden WJ**. Index for rating diagnostic tests. *Cancer* 1950; **3**: 32-35 [PMID: 15405679]

28 **van Leerdam ME**. Epidemiology of acute upper gastrointestinal bleeding. *Best Pract Res Clin Gastroenterol* 2008; **22**: 209-224 [PMID: 18346679 DOI: 10.1016/j.bpg.2007.10.011]

29 **Olde Damink SW**, Dejong CH, Deutz NE, van Berlo CL, Soeters PB. Upper gastrointestinal bleeding: an ammoniagenic and catabolic event due to the total absence of isoleucine in the haemoglobin molecule. *Med Hypotheses* 1999; **52**: 515-519 [PMID: 10459831 DOI: 10.1054/mehy.1998.0026]

30 **Camellini L**, Merighi A, Pagnini C, Azzolini F, Guazzetti S, Scarcelli A, Manenti F, Rigo GP. Comparison of three different risk scoring systems in non-variceal upper gastrointestinal bleeding. *Dig Liver Dis* 2004; **36**: 271-277 [PMID: 15115340 DOI: 10.1016/j.dld.2003.10.017]

31 **Kim BJ**, Park MK, Kim SJ, Kim ER, Min BH, Son HJ, Rhee PL, Kim JJ, Rhee JC, Lee JH. Comparison of scoring systems for the prediction of outcomes in patients with nonvariceal upper gastrointestinal bleeding: a prospective study. *Dig Dis Sci* 2009; **54**: 2523-2529 [PMID: 19104934 DOI: 10.1007/s10620-008-0654-7]

32 **Lim LG**, Ho KY, Chan YH, Teoh PL, Khor CJ, Lim LL, Rajnakova A, Ong TZ, Yeoh KG. Urgent endoscopy is associated with lower mortality in high-risk but not low-risk nonvariceal upper gastrointestinal bleeding. *Endoscopy* 2011; **43**: 300-306 [PMID: 21360421 DOI: 10.1055/s-0030-1256110]

P- Reviewer: Beales ILP, Chiu KW, Huang CM, Sugimoto M
S- Editor: Ma YJ **L- Editor**: Filipodia **E- Editor**: Huang Y

World Journal of Gastroenterology

Submit a Manuscript: http://www.f6publishing.com

World J Gastroenterol 2017 November 7; 23(41): 7459-7469

DOI: 10.3748/wjg.v23.i41.7459

ISSN 1007-9327 (print) ISSN 2219-2840 (online)

ORIGINAL ARTICLE

Randomized Controlled Trial

Tenofovir *vs* lamivudine plus adefovir in chronic hepatitis B: TENOSIMP-B study

Manuel Rodríguez, Juan Manuel Pascasio, Enrique Fraga, Javier Fuentes, Martín Prieto, Gloria Sánchez-Antolín, José Luis Calleja, Esther Molina, María Luisa García-Buey, María Ángeles Blanco, Javier Salmerón, María Lucía Bonet, José Antonio Pons, José Manuel González, Miguel Ángel Casado, Francisco Jorquera; the TENOSIMP-B Research Group

Manuel Rodríguez, Division of Gastroenterology and Hepatology. Hospital Universitario Central de Asturias, Oviedo 33011, Spain

Juan Manuel Pascasio, Unit for the Clinical Management of Digestive Diseases, IBIS, Hospital Universitario Virgen del Rocío, Sevilla 41013, Spain and CIBERehd

Enrique Fraga, Liver Transplantation and Hepatology Unit, Gastroenterology Service, Hospital Universitario Reina Sofía, Córdoba 14004, Spain

Javier Fuentes, Digestive Medicine Service, Hospital Universitario Miguel Servet, Zaragoza 50009, Spain

Martín Prieto, Hepatology Unit, Digestive Medicine Service, Hospital Universitari i Politècnic La Fe, Valencia 46026, Spain and CIBERehd

Gloria Sánchez-Antolín, Hepatology Unit, Hospital Universitario Rio Hortega, Valladolid 47012, Spain

José Luis Calleja, Liver Unit, Hospital Universitario Puerta de Hierro de Majadahonda, Universidad Autónoma de Madrid, Madrid 28049, Spain

Esther Molina, Digestive Medicine Service, Hospital Clínico de Santiago de Compostela, La Coruña 15706, Spain

María Luisa García-Buey, Liver Unit, Hospital Universitario de La Princesa, Madrid 28006, Spain and CIBERehd

María Ángeles Blanco, Digestive Medicine Service, Hospital General Universitario Gregorio Marañón, Madrid 28007, España

Javier Salmerón, Digestive Medicine Unit, Complejo Hospitalario de Granada, Granada 18014, Spain

María Lucía Bonet, Digestive Medicine Service, Hospital Universitario Son Espases, Palma de Mallorca 07120, Spain

José Antonio Pons, Hepatology Unit, IMIB Hospital Universitario Virgen de la Arrixaca, Murcia 30120, Spain

José Manuel González, Digestive Medicine Service, Hospital Clínico Universitario de Valladolid, Valladolid 47003, Spain

Miguel Ángel Casado, Pharmacoeconomics and Outcomes Research Iberia, Madrid 28224, Spain

Francisco Jorquera, Division of Gastroenterology and Hepatology, Complejo Asistencial Universitario de León, León 24001, Spain CIBERehd and IBIOMED León.

Author contributions: Rodríguez M and Jorquera F participated in the recruitment of patients, data collection and wrote the manuscript; Pascasio JM, Fraga E, Fuentes J, Prieto M, Sánchez-Antolín G, Calleja JL, Molina E, García-Buey ML, Blanco MÁ, Salmerón J, Bonet ML, Pons JA, González JM participated in the recruitment of patients and data collection; Casado MA was involved in data analysis and wrote the manuscript.

Institutional review board statement: The study was approved and authorized by the Medication Research Ethics Committee [Comité de Ética de la Investigación con medicamentos (CEIm)] of the Hospital Universitario Central de Asturias (Oviedo, Asturias, Spain), and the Spanish Pharmaceutical and Healthcare Products Agency [Agencia Española de Medicamentos y Productos Sanitarios (AEMPS)] was notified of the study.

Conflict-of-interest statement: Manuel Rodríguez consults for and is on the speaker's bureau for Gilead and AbbVie. Juan Manuel Pascasio consults for and expert advice for BMS, Gilead, AbbVie, MSD and Janssen. Enrique Fraga consults for and is on the speaker's bureau for Gilead, MSD, BMS and AbbVie. Martín Prieto participates in advisory board for AbbVie, Bristol-Myers, Gilead, Janssen and MSD and in lectures for Bristol-Myers, Gilead, Janssen, Janssen and MSD. José Luis Calleja consults for and is on the speaker's bureau for: BMS and Gilead. María Luisa Garcia-Buey consults for and is on the speakers´s bureau for

AbbVie, Janssen, and Gilead. The remaining authors declare that they have no conflicts of interest.

Manuscript source: Unsolicited manuscript

Correspondence to: Manuel Rodríguez, MD, Liver Unit, Division of Gastroenterology and Hepatology, Hospital Universitario Central de Asturias, 33011 Oviedo, Spain. amunoz@porib.com
Telephone: +34-609-744058

Received: March 25, 2017
Peer-review started: March 29, 2017
First decision: April 20, 2017
Revised: May 22, 2017
Accepted: June 18, 2017
Article in press: June 19, 2017
Published online: November 7, 2017

Abstract

AIM

To demonstrate the non-inferiority (15% non-inferiority limit) of monotherapy with tenofovir disoproxil fumarate (TDF) *vs* the combination of lamivudine (LAM) plus adefovir dipivoxil (ADV) in the maintenance of virologic response in patients with chronic hepatitis B (CHB) and prior failure with LAM.

METHODS

This study was a Phase IV prospective, randomized, open, controlled study with 2 parallel groups (TDF and LAM+ADV) of adult patients with hepatitis B e antigen (HBeAg)-negative CHB, prior failure with LAM, on treatment with LAM+ADV for at least 6 mo, without prior resistance to ADV and with an undetectable viral load at the start of the study, in 14 Spanish hospitals. The follow-up time for each patient was 48 wk after randomization, with quarterly visits in which the viral load, biochemical and serological parameters, adverse effects, adherence to treatment and consumption of hospital resources were analysed.

RESULTS

Forty-six patients were evaluated [median age: 55.4 years (30.2-75.2); 84.8% male], including 22 patients with TDF and 24 with LAM+ADV. During study development, hepatitis B virus DNA (HBV-DNA) remained undetectable, all patients remained HBeAg negative, and hepatitis B surface antigen (HBsAg) positive. Alanine aminotransferase (ALT) values at the end of the study were similar in the 2 groups (25.1 ± 7.65, TDF *vs* 24.22 ± 8.38, LAM+ADV, $P = 0.646$). No significant changes were observed in creatinine or serum phosphorus values in either group. No significant differences between the 2 groups were noted in the identification of adverse effects (AEs) (53.8%, TDF *vs* 37.5%, LAM+ADV, $P = 0.170$), and none of the AEs which occurred were serious. Treatment adherence was 95.5% and 83.3% in the TDF and the LAM+ADV groups, respectively ($P = 0.488$). The costs associated with hospital resource consumption were significantly lower with the TDF treatment than the LAM+ADV treatment (€4943 ± 1059 *vs* €5811 ± 1538, respectively, $P < 0.001$).

CONCLUSION

TDF monotherapy proved to be safe and not inferior to the LAM+ADV combination therapy in maintaining virologic response in patients with CHB and previous LAM failure. In addition, the use of TDF generated a significant savings in hospital costs.

Key words: Tenofovir; Lamivudine+Adefovir; Efficacy; Safety; Adherence; Costs; Hepatitis B

Core tip: The Tenosimp-B study was performed to demonstrate the non-inferiority (15% non-inferiority limit) of tenofovir disoproxil fumarate (TDF) monotherapy versus the combination of lamivudine+adefovir (LAM+ADF) in 46 patients with chronic hepatitis B (CHB) and resistance to LAM (22 with TDF and 24 with LAM+ADV). TDF demonstrated its safety (no significant differences in adverse events (AEs), kidney function or liver function) and non-inferiority in maintaining virologic response [undetectable hepatitis B virus DNA (HBV-DNA) and negative for hepatitis B e antigen (HBeAg)] during the study, without differences in adherence to treatment. Additionally, the use of TDF resulted in significant savings in hospital costs.

Rodríguez M, Pascasio JM, Fraga E, Fuentes J, Prieto M, Sánchez-Antolín G, Calleja JL, Molina E, García-Buey LM, Blanco MÁ, Salmerón J, Bonet ML, Pons JA, González JM, Casado MA, Jorquera F; the TENOSIMP-B Research Group. Tenofovir vs lamivudine plus adefovir in chronic hepatitis B: TENOSIMP-B study. *World J Gastroenterol* 2017; 23(41): 7459-7469 Available from: URL: http://www.wjgnet.com/1007-9327/full/v23/i41/7459.htm DOI: http://dx.doi.org/10.3748/wjg.v23.i41.7459

INTRODUCTION

Approximately 400 million people worldwide are infected by the hepatitis B virus (HBV)[1]. Given that a significant portion of these patients receive treatment for management of chronic hepatitis B (CHB) over

a long period of time[2-4], it is necessary to use new antivirals with potent action and an adequate long-term safety profile. Likewise, it is important that these medications possess a high genetic barrier that will lead to reduced HBV resistance rates[5]. The establishment of CHB treatment has, as its objective, the sustained suppression of virus replication to prevent disease progression and increase survival.

Sustained viral suppression with lamivudine (LAM) has been shown to reduce the progression of the disease, preventing the development of cirrhosis and the occurrence of complications, which include liver failure, hepatocellular carcinoma and liver-related mortality[6]. However, while LAM is an effective medication, its use has been limited due to the development of mutations in the polymerase region of HBV that promote resistance, causing loss of antiviral activity and its clinical benefit[7]. The rate of appearance of resistance is in the range of 15%-20% per year of treatment and may increase to up to 80% at 5 years after the start of treatment[8]. Management of LAM resistance has evolved in recent years. Initially, the recommended therapeutic option was to switch to adefovir dipivoxil (ADV)[9]. However, it was found that this strategy favoured the appearance of ADV resistance[10]. One randomized study demonstrated that the probability of developing ADV resistance at 3 years of treatment in patients with resistance to LAM was significantly higher in the patient group treated with ADV monotherapy than in the group receiving a combination of LAM plus ADV[11]. The Clinical Guidelines of the European Association for the Study of the Liver (EASL) recommend that patients with CHB and LAM resistance be changed to tenofovir disoproxil fumarate (TDF) or have ADV added if TDF is not available[12].

TDF, a prodrug of tenofovir, is a potent nucleotide analogue with high efficacy in CHB treatment[13]. Phase Ⅲ clinical trials showed that TDF is superior to ADV in the suppression of viral replication and in histological improvement in both hepatitis B e antigen- (HBeAg-) positive and HBeAg-negative patients[5]. Furthermore, it is a drug with a high genetic barrier to resistance, with no reported cases of resistance during 6 years of treatment[14]. Additionally, the antiviral activity of TDF is maintained against HBV strains resistant to LAM[5,15,16].

The antiviral efficacy of TDF monotherapy has been demonstrated in patients with HBV infection and a partial prior response to ADV, including patients with a history of LAM resistance; its efficacy is similar to that of TDF in combination with emtricitabine (FTC)[17]. Based on these results and on the fact that, at the current time, there are no reports of TDF resistance, several authors have purposed TDF monotherapy treatment in patients with LAM resistance[12,18].

Patients who have previously failed LAM treatment and who have previously received combination treatment with LAM+ADV would be the ideal population to determine whether TDF monotherapy is equivalent to standard treatment (LAM+ADV) in maintaining a virologic response. As a result, the primary objective of the TENOSIMP-B study was to demonstrate the non-inferiority (with a limit of 15%) of TDF monotherapy in maintaining an undetectable viral load *vs* the combination LAM+ADV treatment in patients with CHB and prior failure of LAM. The secondary objectives of the study were to compare the safety profiles in each treatment group, especially the incidence of renal safety; to calculate adherence to treatment; and to determine the differences in hospital expenses for patients assigned to each of the treatment strategies.

MATERIALS AND METHODS

TENOSIMP-B is a Phase IV open, randomized, controlled study of non-inferiority with 2 parallel arms (TDF and LAM+ADV) and prospective follow-up. The trial was performed in 14 Spanish public hospitals with the participation of adult patients with chronic HBV infection. The recruitment period was between August 2011 and January 2013. Patients were followed for 48 wk with intermediate visits during weeks 12, 24 and 36.

During the study period, patients were treated with the medication to be studied, and data were collected every 12 wk using an electronic case report form (eCRF). Variables collected included those related to the patient's clinical data (HBV-DNA load and hepatitis B biochemical and serological parameters), information on possible adverse events (AEs) during study tracking and adherence to therapy using dispensation records provided by Hospital Pharmacy Services. In addition, through the use of a patient diary, information was compiled at each visit regarding the use of hospital resources by patients during the study period.

The randomization process was performed in blocks to ensure that each centre had a 1:1 ratio of patients with TDF (300 mg/d) or LAM (100 mg/d) plus ADV (10 mg/d). All drugs were administered orally.

The study was authorized by the Medication Research Ethics Committee (MREC) of the Hospital Universitario Central de Asturias (Oviedo, Asturias, Spain), which acted as the reference committee in coordination with committees from the other participating centres. The study was developed in accordance with the ethical principles stated in the Declaration of Helsinki and was consistent with the guidelines for good clinical practice and the applicable local regulatory requirements. All patients gave informed written consent for participation in the study.

Study population

Included in the study were patients with HBV infection with previous LAM failure who were rescued with LAM+ADV, who received this treatment for at least

6 mo and with undetectable viral load [HBV-DNA below the lower limit of quantification (LOQ)] before randomization, with compensated liver disease and with positive hepatitis B surface antigen (HBsAg) in the baseline visit.

Patients who were co-infected with another virus (hepatitis C, hepatitis D or HIV); were intolerant to one of the components of the therapeutic regimen; had HBV mutations associated with ADV resistance (as evidenced by resistance tests or history of virologic rebound reported in the case history); had hepatocellular carcinoma; had a liver or kidney transplant; had serious pulmonary or neurologic disease that might interfere with their participation in the study; were pregnant or lactating; were undergoing treatment with any experimental (unapproved) medications 30 d prior to the baseline visit; and/or had moderate to severe renal insufficiency with one of the following conditions were not included in this study: a glomerular filtration rate (GFR) $\leqslant$ 60 mL/min [using the abbreviated Modification of Diet in Renal Disease (MDRD) formula] and/or creatinine clearance (CrCl) $\leqslant$ 60 mL/min (according to the Cockcroft-Gault equation).

Primary variable: viral load

The primary variable in this study was the proportion of patients who maintained a sustained virologic response, defined as HBV-DNA levels that were undetectable (below the LOQ) at 48 wk of study using the quantitative HBV-DNA detection technique used in routine clinical practice in each of the participating centres. Additionally, during weeks 12, 24 and 36, the following parameters were evaluated: percentage of patients with sustained virologic response, percentage of patients with virologic rebound in each arm of treatment who developed resistance to ADV or TDF, percentage of patients with loss of HBsAg and percentage of patients with seroconversion to anti-HBs.

Secondary variables

During each visit, the patient's levels of alanine aminotransferase (ALT), aspartate aminotransferase (AST), creatinine, CrCl and serum phosphate were measured. Other measured parameters included safety, using the registry of serious AEs and the relationship of AEs to drugs administered in each visit; the degree of therapeutic compliance in each group; and the costs associated with each treatment group.

Safety: Safety analyses included all patients who received at least 1 drug dose during the study and all events that occurred during treatment. The safety parameters evaluated in this study included all AEs and all anomalies (in laboratory parameters) that were symptomatic or clinically significant (documented as AEs). All AEs were registered in the patient's clinical record and in the eCRF. To assess toxicity of the AEs, the World Health Organization (WHO) recommendations were used. Patients with adverse reactions (ARs), that is, AEs related to the studied medication, were monitored using the pertinent clinical evaluations and laboratory analyses until satisfactory resolution of the event or stabilization.

Adherence: Adherence to treatment was calculated using the Morisky-Green test[19] and the dispensation records of the Pharmacy Service. The Morisky-Green test consists of 4 questions scored as 0 (negative response) or 1 (affirmative response). The dispensation records noted, in a retrospective form, the quantity of medication dispensed to the patient at the prior visit and the units returned to the hospital Pharmacy Service following 12 wk of treatment. Patients with missing data for these variables were considered non-adherent.

The calculation of the percentage of adherence to LAM and ADV was performed separately, and the lower adherence value was used to determine whether the patient was adherent; in these patients, it was considered failure to comply if only 1 of the 2 drugs used in treatment was taken.

A patient was considered adherent when the adherence percentage in the dispensation record was greater than or equal to 80% and the score obtained from the Morisky-Green test was between 0 and 1.

Analysis of expenses: Hospital resources consumed by patients were recorded throughout the 48 wk of the study with the objective of quantifying the cost in euros associated with the management of these patients. The costs calculation was obtained by finding the product of resources consumed multiplied by the unit cost associated with each resource. Unit costs (euros, 2014) of the resources were obtained from the healthcare cost database eSalud (eHealth)[20]. Pharmaceutical costs were estimated based on laboratory sale price (LSP) established in the medication catalogue of the General Council of Official Associations of Pharmacists[21], applying the deduction corresponding to each drug established by Royal Decree-Law 8/2010[22].

Statistical analysis

Except for safety analyses, in which the safety population was used, statistical analyses were performed in the population per protocol (PPP) function of statistical software R version 3.10.0[23]. For the hypothesis contrasts, an alpha risk of 0.05 was assumed. The included *P*-values were calculated based on bilateral contrast without adjustment for the performance of multiple contrasts.

For comparison of the percentage of patients maintaining a sustained virologic response at 48 wk of study and to evaluate differences in AE incidence in the 2 arms, Fisher's exact text was used.

To evaluate differences in the evolution of hepatic and renal function, differences between baseline values and those obtained at weeks 12, 24, 36 and 48 were compared by hypothesis contrast using the Friedman test.

In the cost analysis, differences between costs were compared using the Mann-Whitney *U* test.

RESULTS

Study population

In total, 53 patients were randomized; of these, 4 patients did not comply with all study selection criteria (3 due to moderate or severe renal insufficiency and 1 due to not having a documented failure on LAM). Of the 49 remaining patients, 2 left the study by personal petition (1 after the baseline visit and another at the week-12 visit) and 1 due to lack of follow-up. For the study's data analysis, the data of 46 patients was considered, which constituted the final PPP of the study. Of the randomized patients, 22 were assigned to the group administered 300 mg TDF/d and 24 patients were assigned to the group administered 100 mg LAM/d + 10 mg ADV/d (Figure 1).

The average age of the patients included in the analysis was 54.82 ± 11.88 years. Males comprised 84.8% of the study population. Obesity was present in 19.6% of the patients, and 8 patients (17.4%) had diabetes or hypertension. Globally, 19.6% of the patients had comorbidities in the gastrointestinal, cardiovascular or skeletal systems. A small proportion of patients (8.7%) had liver cirrhosis (Table 1).

A patient was considered to have LAM resistance when, after a negative HBV DNA result was obtained, virologic rebound was found without stopping LAM administration. All researchers verified the presence of LAM resistance in clinical records. In 21.7% of patients, LAM resistance was corroborated using a resistance test (Table 1).

No significant differences were found between both groups of therapy regarding sociodemographic, clinical and biochemical characteristics at baseline (Tables 1 and 2).

Primary variable: viral load

The HBV-DNA viral load remained below the LOQ for the length of the study (weeks 12, 24, 26 and 48) in 100% of patients in both treatment groups. As a result, no patient presented virologic rebound during the study period. HBeAg remained negative in all patients for the duration of the study. No patient cleared HBsAg during the 48 wk of the study.

Secondary variables

Safety: Of the 53 patients evaluated in the safety analysis, none were found to have a serious AE (SAE) during study tracking, nor was there any discontinuation in either treatment group due to lack of efficacy prior to week 48.

A total of 25 AEs were evaluated during the study period; the common cold was the most frequent (10.89% of cases). Twenty-three of those cases were unrelated events, including 9 in 4 patients from the LAM+ADV group and 14 in 9 patients from the TDF group. The other 2 AEs occurred in the same patient and were considered moderate-intensity adverse reactions (RA) and not serious (digestive intolerance and muscle pains) (Table 3). In this case, the research team decided to discontinue the studied medication two weeks after randomization, abating the RA.

No statistically significant differences between the 2 study groups were found in the evolution of ALT and AST transaminase values (Figure 2), which were used to evaluate liver function, from the baseline visit to 48 wk of study.

With respect to kidney function, no differences between the 2 groups were found in phosphorus levels (Figure 3), urea, serum creatinine, GFR or CrCl (Figure 4) at 48 wk of tracking (Table 2). Over the length of the study, 4 patients changed to a state of renal insufficiency. Two belonging to the LAM+ADV arm moved from moderate insufficiency (stage Ⅲ) to mild (stage Ⅱ) insufficiency and returned to stage Ⅲ prior to the study's end, and a third changed from stage Ⅱ to stage Ⅲ at the final visit. The 4th patient from the TDF group moved from stage Ⅱ to stage Ⅲ and back to stage Ⅱ prior to the conclusion of the study.

Adherence: Overall, 89.1% of the patients in the study were considered adherent, and there was no significant difference between the 2 groups concerning adherence (TDF 95.5%; LAM+ADV 83.3%; $P = 0.745$). Three patients (1 in the TDF group and 2 in the LAM+ADV group) were considered non-adherent due to missing values for this variable, although they did not present with virologic rebound (their HBV-DNA was negative at the end of tracking).

Cost analysis: The total average hospital expense per patient treated with TDF and LAM+ADV was €4943 and €5811, respectively. These numbers indicate that, in patients undergoing TDF treatment, an average savings of €868 per patient was observed over the 48 wk of the study. The difference in average cost per patient between those treated with TDF and those treated with LAM+ADV was statistically significant. In concomitant medication costs and analytic and diagnostic tests, there were no statistically significant differences between the 2 treatment groups. Furthermore, there were statistically significant differences in drug costs, with an average cost savings per TDF patient *vs* LAM+ADV patient of €1252 (Table 4).

DISCUSSION

LAM, the first nucleoside analogue that has been

Table 1 Sociodemographic characteristics of the study population *n* (%)

Characteristic	TDF (*n* = 22)	LAM+ADV (*n* = 24)	Total (*n* = 46)	*P* value
Age - average (range)	53.14 ± 11.95	56.35 ± 11.86	54.82 ± 11.88	0.377
Gender				
Male	17 (77.3)	22 (91.7)	39 (84.4)	
Female	5 (22.7)	2 (8.3)	7 (15.2)	
Weight - average (range)	75.37 (46 - 105)	78.72 (62 - 107)	77.08 (46 - 107)	0.663
Height - average (range)	1.68 (1.48 - 1.93)	1.70 (1.56 - 1.80)	1.69 (1.48 - 1.93)	0.30
BMI - average (range)	26.59 (17.10 - 32.96)	27.17 (21.45-34.54)	26.89 (17.1-34.54)	0.883
< 18.50 - Underweight	2 (9.10)	1 (4.20)	3 (6.50)	
18.50 - 24.99 - Normal	7 (31.80)	8 (33.30)	15 (32.60)	
25.0 - 29.9 - Overweight	9 (40.90)	10 (41.70)	19 (41.30)	
⩾ 30.0 - Obese	4 (18.20)	5 (20.8)	9 (19.60)	
LAM resistance establishment				0.725
Clinical records	18 (81.8)	18 (75.0)	36 (78.3)	
Resistance test	4 (18.2)	6 (25.0)	10 (21.7)	
Cirrhosis, F4 state	3 (13.6)	1 (4.2)	4 (8.7)	0.336
Diabetes mellitus and/ or hypertension	2 (9.1)	6 (25.0)	8 (17.4)	0.247

ADV: Adefovir dipivoxil; BMI: Body mass index; F: Fibrosis; LAM: Lamivudine; TDF: Tenofovir dipivoxil fumarate.

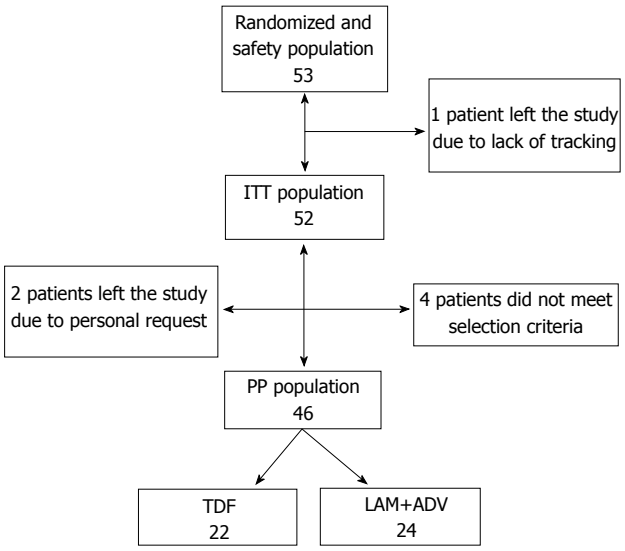

Figure 1 Study Population analysed. ADV: Adefovir dipivoxil; LAM: Lamivudine; TDF: Tenofovir dipivoxil fumarate; ITT: Intent-to-treat; PP: Per protocol.

proven effective against HBV, was widely used during the 1990s in CHB treatment. As a consequence of its previous use and due to its low genetic barrier to resistance, a significant portion of patients with CHB who received this treatment have developed resistance[8]. For years, the addition of ADV to LAM has been the recommended regimen for the management of patients with LAM resistance[11]. A retrospective multi-centre study analysed the effectiveness of TDF monotherapy in patients who had failed treatment with LAM and/or ADV, noting a cumulative probability of virologic response of 79% after an average treatment duration of 23 mo. In this study, it was observed that the presence of LAM resistance did not influence the response to TDF monotherapy, whereas the presence of ADV resistance did influence the response[24]. In recent years, various randomized studies have shown that TDF monotherapy is as effective as a combined treatment with TDF and FTC or entecavir (ETV) in the rescue of patients with not only LAM resistance[25,26] but also resistance to other analogues such as ADV or ETV[27,28].

In the present study, the effectiveness and safety of a simplification of the therapeutic regimen consisting of TDF monotherapy was evaluated in patients who had failed treatment with LAM and who had been satisfactorily rescued with a combination of LAM+ADV. The simplification with TDF could, at least theoretically, encourage adherence to treatment, reduce adverse effects over the long term and decrease hospital expenses.

In this randomized study, it has been demonstrated that TDF monotherapy is as effective as the combination of LAM+ADV in maintaining a complete virologic response. During the 48 wk of the study, all patients maintained an undetectable HBV-DNA load. The preliminary results of a similar study carried out in Taiwan showed reappearance of HBV-DNA in 9.4% of patients assigned to TDF monotherapy and in 16.7% of those assigned to LAM+ADV, although in all cases the reappearance of viremia was transitory[29]. Another prospective study conducted in China demonstrated that TDF monotherapy was superior to a combination of LAM+ADV in achieving complete virologic response in patients with LAM resistance and suboptimal response to LAM+ADV[30]. Finally, a retrospective study carried out in the United States evaluated the strategy of simplifying treatment to TDF or ETV monotherapy in patients who had not completely responded to ETV and who had been satisfactorily rescued with the ETV+TDF combination[31]. In this study, it was observed that virologic rebound rates at 6 mo from the start of monotherapy were significantly higher (88%)

Table 2 Biochemical parameters: Baseline visit *vs* final visit

	Baseline visit			Visit at 48 wk		
	TDF average (range)	LAM+ADV average (range)	*P* value	TDF average (range)	LAM+ADV average (range)	*P* value
AST (UI/mL)	26.66 (9.00-74.00)	26.69 (15.00-69.00)	0.904	26.41 (14.00-71.00)	26.05 (18.00-52.00)	0.916
ALT (UI/mL)	25.41 (12.00-62.00)	23.62 (13.60-40.00)	0.646	26.32 (12.00-55.00)	27.29 (17.00-51.00)	0.965
Phosphorus (mmol/dL)	3.00 (1.80-4.00)	2.84 (1.90-3.80)	0.263	3.08 (1.70-4.40)	2.95 (2.00-3.70)	0.832
Urea (mg/dL)	36.14 (20.00-53.00)	36.96 (18.00-61.90)	0.698	38.29 (25.00-57.00)	38.69 (22.00-53.00)	0.479
Serum creatinine (mg/dL)	0.88 (0.70-1.16)	0.89 (0.60-1.35)	0.912	0.88 (0.69-1.16)	0.92 (0.60-1.27)	0.396
Glomerular filtration rate (mL/min/1.73 m^2)	94.13 (66.95-121.03)	97.48 (60.47-157.83)	0.922	93.11 (66.75-123.55)	93.14 (59.14-151.26)	0.468
Creatinine clearance (mL/min)	103.52 (65.57-185.25)	105.43 (64.79-166.22)	0.831	100.85 (60.84-149.66)	102.32 (60.26-157.5)	0.308

ADV: Adefovir dipivoxil; ALT: Alanine aminotransferase; AST: Aspartate aminotransferase; LAM: Lamivudine; TDF: Tenofovir dipivoxil fumarate.

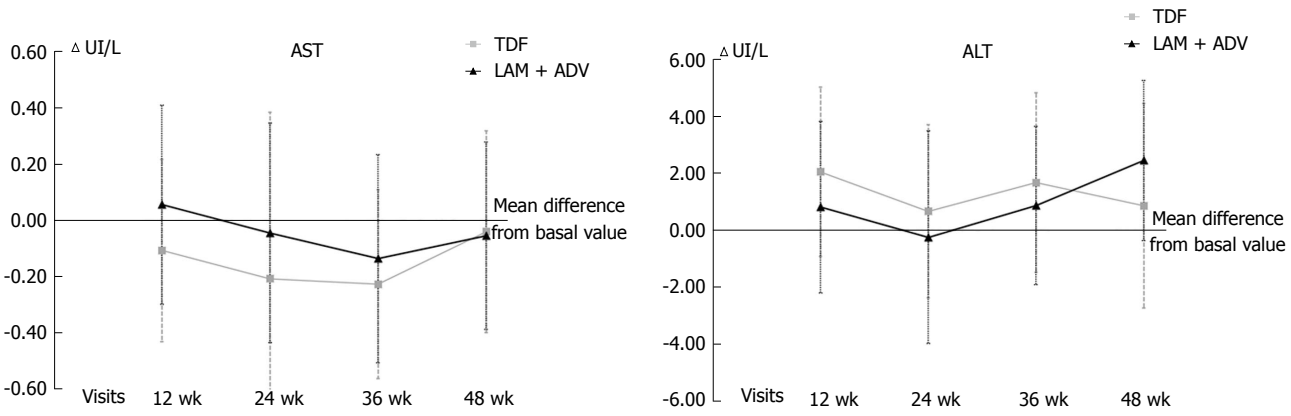

Figure 2 Changes in the transaminases levels: Alanine aminotransferase and aspartate aminotransferase. ADV: Adefovir dipivoxil; LAM: Lamivudine; TDF: Tenofovir dipivoxil fumarate. *P* value > 0.05 for each visit.

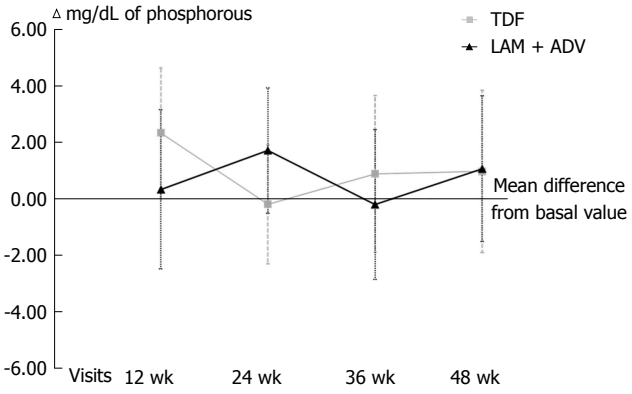

Figure 3 Changes in the phosphorus levels. ADV: Adefovir dipivoxil; LAM: Lamivudine; TDF: Tenofovir dipivoxil fumarate. *P* value > 0.05 for each visit.

in patients who received ETV than in those treated with TDF (39%). One of the factors associated in this report with the risk of presenting a virologic rebound was a duration of complete virologic response of less than 12 mo prior to simplification of treatment to monotherapy[31].

Regarding the biochemical response, in our study, we observed that ALT levels at the end of the study were similar to baseline levels and that there was no difference in ALT levels between patients who received monotherapy with TDF and those who continued combined treatment with LAM+ADV. On the other hand, during the 48 wk of the study, none of the patients lost HBsAg, an unsurprising finding given the reduced clearance rate of HBsAg in patients with HBeAg-negative CHB treated with nucleos(t)ide analogues, even when a potent analogue with a high generic barrier to resistance, such as TDF, is used[13].

In the safety evaluation, no serious adverse effects were observed during the study, and the rate of adverse effects was similar in the 2 study groups, with the most frequent adverse effect being the common cold. A patient from the TDF group presented with a drug-related adverse effect (digestive intolerance and muscle pains), which resulted in the interruption of treatment. As for renal safety, although both ADV and TDF can, on rare occasions, produce a Fanconi-like renal tubular acidosis, during the present study, no significant changes in the levels of serum phosphorus were observed in either of the 2 groups. Regarding kidney function, no differences were observed between the baseline visit and the end of treatment in either group, nor were there differences at the end of the study between patients who received TDF and those treated with LAM+ADV. Three patients, 2 in the LAM+ADV group and 1 in the TDF group, displayed mild and transitory deterioration in kidney function during the study, and 1 patient belonging to the LAM+ADV group moved from stage Ⅱ at the start to stage Ⅲa at the end of the study.

Table 3 Adverse clinical events at week 48 *n* (%)

Event	Intensity	TDF (*n* = 26)	LAM+ADV (*n* = 27)	Total (*n* = 53)	*P* value
Adverse reactions		2 (7.70)	0	2 (3.57)	0.236
Digestive intolerance	moderate	1 (3.85)	0	1 (1.89)	1.000
Muscle pains	moderate	1 (3.85)	0	1 (1.89)	1.000
Adverse events		14 (53.85)	9 (37.5)	23 (43.40)	0.17
Common cold	mild	3 (11.54)	2 (7.41)	5 (9.43)	0.699
Headache	mild	1 (3.85)	1 (3.70)	2 (3.77)	1.000
Retrosternal oppression with heartburn	moderate	0	1 (3.70)	1 (1.89)	1.000
Otitis	mild	1 (3.85)	0	1 (1.89)	0.491
Molar extraction	mild	1 (3.85)	0	1 (1.89)	0.491
Right- and left-flank pain	mild	1 (3.85)	0	1 (1.89)	0.491
Vomiting	mild	1 (3.85)	0	1 (1.89)	0.491
Osteoarticular pain in hands	mild	0	1 (3.70)	1 (1.89)	1.000
Hypophosphatemia and hypomagnesemia	moderate	0	1 (3.70)	1 (1.89)	1.000
Renal colic	mild	1 (3.85)	0	1 (1.89)	0.491
Epigastric pain	mild	1 (3.85)	0	1 (1.89)	0.491
Back pain	mild	1 (3.85)	0	1 (1.89)	0.491
Chronic prostatitis	mild	0	1 (3.70)	1 (1.89)	1.000
Epidermoid carcinoma	moderate	1 (3.85)	0	1 (1.89)	0.491
Vertiginous syndrome	mild	0	1 (3.70)	1 (1.89)	1.000
Itching (eyes, nose and mouth)	mild	1 (3.85)	0	1 (1.89)	0.491
Vertigo	mild	0	1 (3.70)	1 (1.89)	1.000
Choluria	mild	1 (3.85)	0	1 (1.89)	0.491

ADV: Adefovir dipivoxil; LAM: Lamivudine; TDF: Tenofovir dipivoxil fumarate.

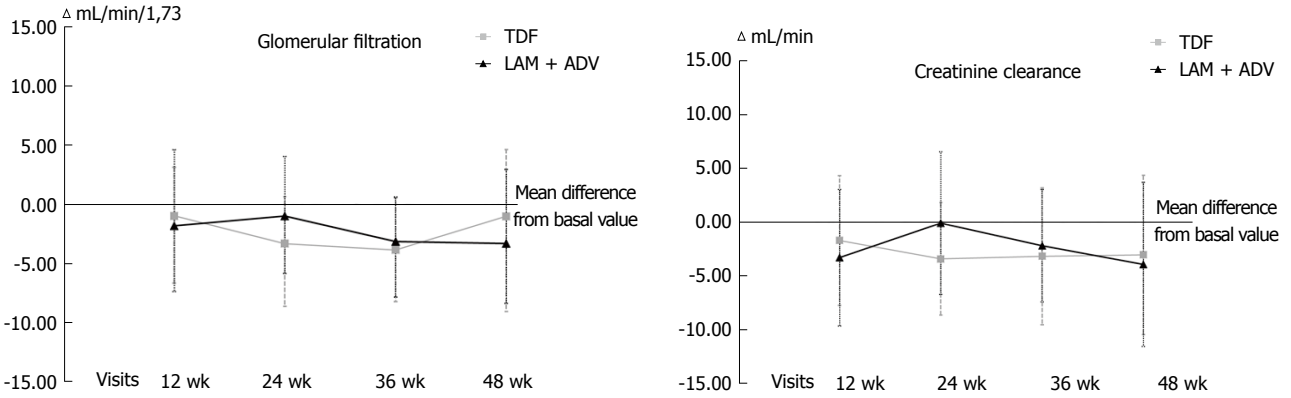

Figure 4 Changes in the glomerular filtration rate and creatinine clearance. ADV: Adefovir dipivoxil; LAM: Lamivudine; TDF: Tenofovir dipivoxil fumarate. *P* value > 0.05 for each visit.

An observational study conducted in France in 214 patients who were treated with analogues for a median period of 2.4 years showed that kidney function decreased significantly in patients treated with ADV in monotherapy or combination therapy, whereas kidney function remained stable in those treated with LAM, TDF or ETV[32]. Although no differences were observed between the treatment groups in our study, likely due to its short duration and to the limited number of patients, it could be inferred that changing from the LAM+ADV combination to TDF may be beneficial for kidney function over the long term. Additionally, a new formulation of tenofovir, tenofovir alafenamide (TAF), has shown lower renal toxicity than TDF[33].

Another of the potential beneficial effects of treatment simplification may be greater treatment adherence. In our study, although adherence was greater in the TDF monotherapy group (95.3%) than in the combined treatment group (87.5%), the differences were not significant. It is possible that with a larger number of patients and a longer study period, these differences might have reached statistical significance.

Among the most relevant result of this study is the significant difference in average overall cost between the TDF-monotherapy group and the LAM+ADV group due to the reduction in drug costs. This finding may have a beneficial impact on the approach to this disease from the perspective of the health system.

On the other hand, the main limitations of the present study are the small number of patients included and the relatively short period of tracking the data.

Although in randomized studies, there is an established preference for analysis of a population using intention-to-treat (ITT) *vs* PPP due to a reduced risk of bias; given that our study is a non-inferiority study, the more restrictive analysis were chosen

Table 4 Average costs per patient (€, 2014)

Costs - average, € (SD)	TDF (*n* = 22)	LAM+ADV (*n* = 24)	Difference TDF *vs* LAM+ADV	*P* value
Studied medication	2966 (69)	4218 (558)	-1252	< 0.001[1]
Concomitant medication	218 (599)	82 (213)	136	0.484
Medical visits	505 (158)	500 (137)	5	0.942
Tests	1388 (182)	1363 (242)	25	0.834
Admissions and surgeries	0 (0)	0 (0)	0 (0)	NA
Total	4943 (1059)	5811 (1538)	-868	< 0.001[1]

[1]Statistically significant difference. ADV: Adefovir dipivoxil; ALT: Alanine aminotransferase; AST: Aspartate aminotransferase; LAM: Lamivudine; TDF: Tenofovir dipivoxil fumarate.

because ITT analysis tends to bias the results towards a lack of difference[34]. In this study, patient assignment was performed without blinding, a factor that may be related to selection bias[34], even though assignment without blinding is closer to routine clinical practice.

The results presented here in suggest that treatment simplification from the LAM+ADV combination to TDF monotherapy, in patients with HBeAg-negative CHB, LAM-treatment failure and complete virologic response under LAM+ADV treatment, is an efficient strategy. The current results are similar to the ones obtained with combined treatment in terms of effectiveness and safety. The treatment used was shown to decrease the cost of management of patients. It is likely that this simplification strategy would be equally efficient in patients with the same characteristics who are under LAM+TDF treatment.

COMMENTS

Background

Approximately 400 million people worldwide are infected by the hepatitis B virus. Given that a significant portion of these patients receive treatment for management of chronic hepatitis B (CHB) over a long period of time, it is necessary to use new antivirals with potent action and an adequate long-term safety profile. Likewise, it is important that these medications possess a high genetic barrier that will lead to reduced HBV resistance rates. The establishment of CHB treatment has, as its objective, the sustained suppression of virus replication to prevent disease progression and increase survival.

Research frontiers

Tenofovir disoproxil fumarate (TDF), a prodrug of tenofovir, is a potent nucleotide analogue with high efficacy in CHB treatment. Phase Ⅲ clinical trials showed that TDF is superior to ADV in the suppression of viral replication and in histological improvement in both hepatitis B e antigen- (HBeAg-) positive and HBeAg-negative patients[5].

Innovations and breakthroughs

In this study, it was observed that virologic rebound rates at 6 mo from the start of monotherapy were significantly higher (88%) in patients who received ETV than in those treated with TDF (39%). One of the factors associated in this report with the risk of presenting a virologic rebound was a duration of complete virologic response of less than 12 mo prior to simplification of treatment to monotherapy.

Applications

The treatment used was shown to decrease the cost of management of patients. It is likely that this simplification strategy would be equally efficient in patients with the same characteristics who are under LAM+TDF treatment.

Peer-review

This study focused on the efficacy and safety of Tenofovir disoproxil fumarate versus Lamivudine + adefovir in patients with chronic hepatitis B with prior failure with Lamivudine.

ACKNOWLEDGMENTS

The study's authors would like to thank the medical department of Gilead Sciences SL for supplying the medications used in this study and its funding regardless of the study results; Miguel Ángel Casado, María Yébenes, Álvaro Muñoz, Fernando de Andrés, Eliazar Sabater and Araceli Casado of Pharmacoeconomics and Outcomes Research Iberia (PORIB) for management, coordination and monitoring of the study; Mireia Riera and Jordi Cantoni of BioClever for support and follow-up on the electronic case report forms; and the pharmacy services of the participating centres for their collaboration in obtaining dispensation records, with special thanks to University of Leon Hospital for its participation in the destruction of the study's medications.

Research Group TENOSIMP-B: Principal researchers: Rodríguez M (Hospital Universitario de Central Asturias), Jorquera F (Complejo Asistencial Universitario de León), , Pascasio JM (Hospital Universitario Virgen del Rocío), Fraga E (Hospital Universitario Reina Sofía), Fuentes J (Hospital Universitario Miguel Servet), Prieto M (Hospital Universitari i Politècnic La Fe), Sánchez-Antolín G (Hospital Universitario Rio Hortega), Calleja JL (Hospital Universitario Puerta de Hierro de Majadahonda), Molina E (Hospital Clínico de Santiago de Compostela), García-Buey ML (Hospital Universitario de La Princesa), Blanco MÁ (Hospital General Universitario Gregorio Marañón), Salmerón J (Complejo Hospitalario de Granada), Bonet ML (Hospital Universitario Son Espases), Pons JA, (Hospital Universitario Virgen de la Arrixaca) and González JM (Hospital Clínico Universitario de Valladolid).

Collaborating researchers: González-Diéguez ML (Hospital Universitario Central de Asturias), Linares

P, Olcoz JL (Complejo Asistencial Universitario de León), Cuaresma M, Ferrer MT, Giráldez A, Márquez JL, Ruiz R, Sousa JM (Hospital Universitario Virgen del Rocío), Aguilar P, Barrera P, Costan G, Mata M, Montero JL, Núñez F, Poyato A (Hospital Universitario Reina Sofía), Barrao E, Lázaro M (Hospital Universitario Miguel Servet), Aguilera V, Berenguer M, Casterá F, García M, Rubín A, Zaragoza A (Hospital Universitari i Politècnic La Fe), Almohalla C, García F (Hospital Universitario Rio Hortega), Pons F, Revilla J, Gómez M, Rodríguez LA (Hospital Universitario Puerta de Hierro de Majadahonda), Fernández J, Otero E, Martínez ST (University of Santiago Hospital Complex), Alonso MJ, Real Y (La Princesa University Hospital), Clemente G (Hospital General Universitario Gregorio Marañón), Gila A, Quintero D (Complejo Hospitalario de Granada), Aller R and Gómez S (Valladolid University Clinical Hospital).

REFERENCES

1 **Lai CL**, Yuen MF. Chronic hepatitis B--new goals, new treatment. *N Engl J Med* 2008; **359**: 2488-2491 [PMID: 19052131 DOI: 10.1056/NEJMe0808185]

2 **Feld JJ**, Heathcote EJ. Hepatitis B e antigen-positive chronic hepatitis B: natural history and treatment. *Semin Liver Dis* 2006; **26**: 116-129 [PMID: 16673290 DOI: 10.1055/s-2006-939750]

3 **Hadziyannis SJ**, Papatheodoridis GV. Hepatitis B e antigen-negative chronic hepatitis B: natural history and treatment. *Semin Liver Dis* 2006; **26**: 130-141 [PMID: 16673291 DOI: 10.1055/s-2006-939751]

4 **Zones JS**, Schroeder SA. Evolving residency requirements for ambulatory care training for five medical specialties, 1961 to 1989. *West J Med* 1989; **151**: 676-678 [PMID: 2618049 DOI: 10.5152/eurasianjmed.2015.052]

5 **Marcellin P**, Heathcote EJ, Buti M, Gane E, de Man RA, Krastev Z, Germanidis G, Lee SS, Flisiak R, Kaita K, Manns M, Kotzev I, Tchernev K, Buggisch P, Weilert F, Kurdas OO, Shiffman ML, Trinh H, Washington MK, Sorbel J, Anderson J, Snow-Lampart A, Mondou E, Quinn J, Rousseau F. Tenofovir disoproxil fumarate versus adefovir dipivoxil for chronic hepatitis B. *N Engl J Med* 2008; **359**: 2442-2455 [PMID: 19052126 DOI: 10.1056/NEJMoa0802878]

6 **Fung J**. Management of chronic hepatitis B before and after liver transplantation. *World J Hepatol* 2015; **7**: 1421-1426 [PMID: 26052387 DOI: 10.4254/wjh.v7.i10.1421]

7 **Liaw YF**, Sung JJ, Chow WC, Farrell G, Lee CZ, Yuen H, Tanwandee T, Tao QM, Shue K, Keene ON, Dixon JS, Gray DF, Sabbat J; Cirrhosis Asian Lamivudine Multicentre Study Group. Lamivudine for patients with chronic hepatitis B and advanced liver disease. *N Engl J Med* 2004; **351**: 1521-1531 [PMID: 15470215 DOI: 10.1056/NEJMoa033364]

8 **Buti M**, García-Samaniego J, Prieto M, Rodríguez M, Sánchez-Tapias JM, Suárez E, Esteban R. [Consensus document of the Spanish Association for the Study of the Liver on the treatment of hepatitis B infection (2012)]. *Gastroenterol Hepatol* 2012; **35**: 512-528 [PMID: 22749508 DOI: 10.1016/j.gastrohep.2012.04.006]

9 **Peters MG**, Hann Hw Hw, Martin P, Heathcote EJ, Buggisch P, Rubin R, Bourliere M, Kowdley K, Trepo C, Gray Df Df, Sullivan M, Kleber K, Ebrahimi R, Xiong S, Brosgart CL. Adefovir dipivoxil alone or in combination with lamivudine in patients with lamivudine-resistant chronic hepatitis B. *Gastroenterology* 2004; **126**: 91-101 [PMID: 14699491 DOI: 10.1053/j.gastro.2003.10.051]

10 **Lee YS**, Suh DJ, Lim YS, Jung SW, Kim KM, Lee HC, Chung YH, Lee YS, Yoo W, Kim SO. Increased risk of adefovir resistance in patients with lamivudine-resistant chronic hepatitis B after 48 weeks of adefovir dipivoxil monotherapy. *Hepatology* 2006; **43**: 1385-1391 [PMID: 16729316 DOI: 10.1002/hep.21189]

11 **Rapti I**, Dimou E, Mitsoula P, Hadziyannis SJ. Adding-on versus switching-to adefovir therapy in lamivudine-resistant HBeAg-negative chronic hepatitis B. *Hepatology* 2007; **45**: 307-313 [PMID: 17256746 DOI: 10.1002/hep.21534]

12 European Association For The Study Of The Liver. EASL clinical practice guidelines: Management of chronic hepatitis B virus infection. *J Hepatol* 2012; **57**: 167-185 [PMID: 22436845 DOI: 10.1016/j.jhep.2012.02.010]

13 **Marcellin P**, Gane E, Buti M, Afdhal N, Sievert W, Jacobson IM, Washington MK, Germanidis G, Flaherty JF, Aguilar Schall R, Bornstein JD, Kitrinos KM, Subramanian GM, McHutchison JG, Heathcote EJ. Regression of cirrhosis during treatment with tenofovir disoproxil fumarate for chronic hepatitis B: a 5-year open-label follow-up study. *Lancet* 2013; **381**: 468-475 [PMID: 23234725 DOI: 10.1016/S0140-6736(12)61425-1]

14 **Kitrinos KM**, Corsa A, Liu Y, Flaherty J, Snow-Lampart A, Marcellin P, Borroto-Esoda K, Miller MD. No detectable resistance to tenofovir disoproxil fumarate after 6 years of therapy in patients with chronic hepatitis B. *Hepatology* 2014; **59**: 434-442 [PMID: 23939953 DOI: 10.1002/hep.26686]

15 **Brunelle MN**, Lucifora J, Neyts J, Villet S, Holy A, Trepo C, Zoulim F. In vitro activity of 2,4-diamino-6-[2-(phosphonomethoxy)ethoxy]-pyrimidine against multidrug-resistant hepatitis B virus mutants. *Antimicrob Agents Chemother* 2007; **51**: 2240-2243 [PMID: 17371827 DOI: 10.1128/AAC.01440-06]

16 **Delaney WE**, Ray AS, Yang H, Qi X, Xiong S, Zhu Y, Miller MD. Intracellular metabolism and in vitro activity of tenofovir against hepatitis B virus. *Antimicrob Agents Chemother* 2006; **50**: 2471-2477 [PMID: 16801428 DOI: 10.1128/AAC.00138-06]

17 **Berg T**, Marcellin P, Zoulim F, Moller B, Trinh H, Chan S, Suarez E, Lavocat F, Snow-Lampart A, Frederick D, Sorbel J, Borroto-Esoda K, Oldach D, Rousseau F. Tenofovir is effective alone or with emtricitabine in adefovir-treated patients with chronic-hepatitis B virus infection. *Gastroenterology* 2010; **139**: 1207-1217 [PMID: 20600025 DOI: 10.1053/j.gastro.2010.06.053]

18 **Lok AS**. Drug therapy: tenofovir. *Hepatology* 2010; **52**: 743-747 [PMID: 20597070 DOI: 10.1002/hep.23788]

19 **Morisky DE**, Green LW, Levine DM. Concurrent and predictive validity of a self-reported measure of medication adherence. *Med Care* 1986; **24**: 67-74 [PMID: 3945130]

20 Oblikue Consulting. Base de datos de costes sanitarios eSalud [Internet]. Barcelona: Oblikue Consulting; 2014 [citado 10 ago 2016]. Available from: URL: http: //www.oblikue.com/bddcostes/

21 Bot Plus 2.0 [Internet]. Madrid: Consejo General de Colegios Oficiales de Farmacéuticos; 2014 [citado 10 ago. 2016]. Available from: URL: https: //botplusweb.portalfarma.com/

22 Real Decreto-ley 8/2010, de 20 de mayo, por el que se adoptan medidas extraordinarias para la reducción del déficit público. Available from: URL: http: //www.boe.es/boe/dias/2010/05/24/pdfs/BOE-A-2010-8228.pdf

23 R Core Team (2015). R: A language and environment for statistical computing. R Foundation for Statistical Computing, Vienna, Austria. Available from: URL: https: //www.R-project.org

24 **van Bömmel F**, de Man RA, Wedemeyer H, Deterding K, Petersen J, Buggisch P, Erhardt A, Hüppe D, Stein K, Trojan J, Sarrazin C, Böcher WO, Spengler U, Wasmuth HE, Reinders JG, Möller B, Rhode P, Feucht HH, Wiedenmann B, Berg T. Long-term efficacy of tenofovir monotherapy for hepatitis B virus-monoinfected patients after failure of nucleoside/nucleotide analogues. *Hepatology* 2010; **51**: 73-80 [PMID: 19998272 DOI: 10.1002/hep.23246]

25 **Fung S**, Kwan P, Fabri M, Horban A, Pelemis M, Hann HW, Gurel S, Caruntu FA, Flaherty JF, Massetto B, Dinh P, Corsa A, Subramanian GM, McHutchison JG, Husa P, Gane E. Randomized comparison of tenofovir disoproxil fumarate vs emtricitabine and tenofovir disoproxil fumarate in patients with lamivudine-resistant chronic hepatitis B. *Gastroenterology* 2014; **146**: 980-988 [PMID: 24368224 DOI: 10.1053/j.gastro.2013.12.028]

26 **Fung S**, Kwan P, Fabri M, Horban A, Pelemis M, Hann HW,

Gurel S, Caruntu FA, Flaherty JF, Massetto B, Kim K, Kitrinos KM, Subramanian GM, McHutchison JG, Yee LJ, Elkhashab M, Berg T, Sporea I, Yurdaydin C, Husa P, Jablkowski MS, Gane E. Tenofovir disoproxil fumarate (TDF) vs. emtricitabine (FTC)/TDF in lamivudine resistant hepatitis B: A 5-year randomised study. *J Hepatol* 2017; **66**: 11-18 [PMID: 27545497 DOI: 10.1016/j.jhep.2016.08.008]

27 **Lim YS**, Byun KS, Yoo BC, Kwon SY, Kim YJ, An J, Lee HC, Lee YS. Tenofovir monotherapy versus tenofovir and entecavir combination therapy in patients with entecavir-resistant chronic hepatitis B with multiple drug failure: results of a randomised trial. *Gut* 2016; **65**: 852-860 [PMID: 25596179 DOI: 10.1136/gutjnl-2014-308353]

28 **Lim YS**, Yoo BC, Byun KS, Kwon SY, Kim YJ, An J, Lee HC, Lee YS. Tenofovir monotherapy versus tenofovir and entecavir combination therapy in adefovir-resistant chronic hepatitis B patients with multiple drug failure: results of a randomised trial. *Gut* 2016; **65**: 1042-1051 [PMID: 25800784 DOI: 10.1136/gutjnl-2014-308435]

29 **Huang YH**, Yu ML, Peng CY, et al. Y.-H, Chen JJ, Chen CY, Su CW, Lin WY, Lai HC, Wang YJ, Dai CY, Chuang WL, Lin HC. Multicenter randomized controlled trial of switching to tenofovir disoproxil fumarate monotherapy in lamivudine-resistant chronic hepatitis B patients with undetectable HBV viral load under lamivudine/adefovir add-on therapy; interim analysis. *J Hepatol* 2016; **64** (suppl 2): S605 [DOI: 10.1016/S0168-8278(16)01118-1]

30 **Yang DH**, Xie YJ, Zhao NF, Pan HY, Li MW, Huang HJ. Tenofovir disoproxil fumarate is superior to lamivudine plus adefovir in lamivudine-resistant chronic hepatitis B patients. *World J Gastroenterol* 2015; **21**: 2746-2753 [PMID: 25759545 DOI: 10.3748/wjg.v21.i9.2746]

31 **Kim LH**, Chaung KT, Ha NB, Kin KC, Vu VD, Trinh HN, Nguyen HA, Nguyen MH. Tenofovir monotherapy after achieving complete viral suppression on entecavir plus tenofovir combination therapy. *Eur J Gastroenterol Hepatol* 2015; **27**: 871-876 [PMID: 25919771 DOI: 10.1097/MEG.0000000000000368]

32 **Mallet V**, Schwarzinger M, Vallet-Pichard A, Fontaine H, Corouge M, Sogni P, Pol S. Effect of nucleoside and nucleotide analogues on renal function in patients with chronic hepatitis B virus monoinfection. *Clin Gastroenterol Hepatol* 2015; **13**: 1181-8.e1 [PMID: 25460550 DOI: 10.1016/j.cgh.2014.11.021]

33 **Buti M**, Gane E, Seto WK, Chan HL, Chuang WL, Stepanova T, Hui AJ, Lim YS, Mehta R, Janssen HL, Acharya SK, Flaherty JF, Massetto B, Cathcart AL, Kim K, Gaggar A, Subramanian GM, McHutchison JG, Pan CQ, Brunetto M, Izumi N, Marcellin P; GS-US-320-0108 Investigators. Tenofovir alafenamide versus tenofovir disoproxil fumarate for the treatment of patients with HBeAg-negative chronic hepatitis B virus infection: a randomised, double-blind, phase 3, non-inferiority trial. *Lancet Gastroenterol Hepatol* 2016; **1**: 196-206 [PMID: 28404092 DOI: 10.1016/S2468-1253(16)30107-8]

34 **Dossing A**, Tarp S, Furst DE, Gluud C, Beyene J, Hansen BB, Bliddal H, Christensen R. Interpreting trial results following use of different intention-to-treat approaches for preventing attrition bias: a meta-epidemiological study protocol. *BMJ Open* 2014; **4**: e005297 [PMID: 25260368 DOI: 10.1136/bmjopen-2014-005297]

P- Reviewer: Jarcuska P, Tang ZH, Yang YL **S- Editor**: Qi Y
L- Editor: A **E- Editor**: Huang Y

World Journal of Gastroenterology

Submit a Manuscript: http://www.f6publishing.com

World J Gastroenterol 2017 November 7; 23(41): 7470-7477

DOI: 10.3748/wjg.v23.i41.7470

ISSN 1007-9327 (print) ISSN 2219-2840 (online)

ORIGINAL ARTICLE

Randomized Controlled Trial

Clinical outcomes of transcatheter selective superior mesenteric artery urokinase infusion therapy *vs* transjugular intrahepatic portosystemic shunt in patients with cirrhosis and acute portal vein thrombosis

Ting-Ting Jiang, Xiao-Ping Luo, Jian-Ming Sun, Jian Gao

Ting-Ting Jiang, Jian Gao, Department of Gastroenterology and Hepatology, Second Affiliated Hospital, Chongqing Medical University, Chongqing 400010, China

Xiao-Ping Luo, Department of Radiology, Second Affiliated Hospital, Chongqing Medical University, Chongqing 400010, China

Jian-Ming Sun, Department of Vascular Surgery, Second Affiliated Hospital, Chongqing Medical University, Chongqing 400010, China

ORCID number: Ting-Ting Jiang (0000-0000-2815-3556); Xiao-Ping Luo (0000-0001-9142-9037); Jian-Ming Sun (0000-0002-7168-2809); Jian Gao (0000-0002-9799-160X).

Author contributions: Jiang TT and Gao J designed the research; Jiang TT, Luo XP, and Sun JM performed the research and participated in data acquisition and analysis; Jiang TT wrote the paper.

Supported by the National Natural Science Foundation of China, No. 81572888.

Institutional review board statement: The study was reviewed and approved by the ethics committee of the Second Affiliated Hospital of Chongqing Medical University (Number: 2012-076).

Informed consent statement: All study participants provided written informed consent prior to study enrollment.

Conflict-of-interest statement: None declared.

Data sharing statement: None declared.

Manuscript source: Unsolicited manuscript

Correspondence to: Jian Gao, PhD, Professor, Chief, Department of Gastroenterology and Hepatology, Second Affiliated Hospital of Chongqing Medical University, 76 Linjiang Road, Yuzhong District, Chongqing 400010, China. ykdxdeyy@public.cta.cq.cn
Telephone: +86-23-63693325
Fax: +86-23-63693323

Received: July 23, 2017
Peer-review started: July 25, 2017
First decision: August 30, 2017
Revised: September 10, 2017
Accepted: September 29, 2017
Article in press: September 28, 2017
Published online: November 7, 2017

Abstract

AIM

To compare the outcomes of transcatheter superior mesenteric artery (SMA) urokinase infusion and transjugular intrahepatic portosystemic shunt (TIPS) for acute portal vein thrombosis (PVT) in cirrhosis.

METHODS

From January 2013 to December 2014, patients with liver cirrhosis and acute symptomatic PVT who met the inclusion criteria were randomly assigned to either an SMA group or a TIPS group. The two groups accepted transcatheter selective SMA urokinase infusion therapy

and TIPS, respectively. The total follow-up time was 24 mo. The primary outcome measure was the change in portal vein patency status which was evaluated by angio-computed tomography or Doppler ultrasound. Secondary outcomes were rebleeding and hepatic encephalopathy.

RESULTS

A total of 40 patients were enrolled, with 20 assigned to the SMA group and 20 to the TIPS group. The symptoms of all patients in the two groups improved within 48 h. PVT was improved in 17 (85%) patients in the SMA group and 14 (70%) patients in the TIPS group. The main portal vein (MPV) thrombosis was significantly reduced in both groups ($P < 0.001$), and there was no significant difference between them ($P = 0.304$). In the SMA group, superior mesenteric vein (SMV) thrombosis and splenic vein (SV) thrombosis were significantly reduced ($P = 0.048$ and $P = 0.02$), which did not occur in the TIPS group. At 6-, 12-, and 24-mo follow-up, in the SMA group and the TIPS group, the cumulative rates free of the first episode of rebleeding were 80%, 65%, and 45% *vs* 90%, 80%, and 60%, respectively ($P = 0.320$); the cumulative rates free of the first episode of hepatic encephalopathy were 85%, 80%, and 65% *vs* 50%, 40%, and 35%, respectively ($P = 0.022$).

CONCLUSION

Transcatheter selective SMA urokinase infusion and TIPS are safe and effective for acute symptomatic PVT in cirrhosis.

Key words: Cirrhosis; Portal vein thrombosis; Superior mesenteric artery; Urokinase; Transjugular intrahepatic portosystemic shunt

Core tip: Transcatheter selective superior mesenteric artery urokinase infusion therapy and transjugular intrahepatic portosystemic shunt can both significantly reduce acute portal vein thrombosis in cirrhosis, and there was no significant difference between them. Moreover, the two strategies did not result in serious adverse events such as bleeding.

Jiang TT, Luo XP, Sun JM, Gao J. Clinical outcomes of transcatheter selective superior mesenteric artery urokinase infusion therapy *vs* transjugular intrahepatic portosystemic shunt in patients with cirrhosis and acute portal vein thrombosis. *World J Gastroenterol* 2017; 23(41): 7470-7477 Available from: URL: http://www.wjgnet.com/1007-9327/full/v23/i41/7470.htm DOI: http://dx.doi.org/10.3748/wjg.v23.i41.7470

INTRODUCTION

Portal vein thrombosis (PVT) is defined as thrombosis occurring in the trunk of the portal vein or portal branches (mesenteric and splenic veins)[1]. The prevalence of non-neoplastic PVT in liver cirrhosis ranges from 7.2% to 17%[2-4], and is higher at the decompensated or advanced stage[3,5]. Acute thrombosis can be severe and may lead to mesenteric ischemia and variceal bleeding. Recent studies have shown that acute PVT influences the outcomes of liver cirrhosis and results in worse survival and a significant increase in the risk of gastroesophageal variceal rebleeding[6-10].

Up to now, there has been no consensus on the treatment of liver cirrhosis with acute PVT in any guideline. Anticoagulation is usually used as a first-line treatment, and has been confirmed to be effective by some studies[11,12], whereas systemic and local thrombolysis, percutaneous portal vein recanalization, and transjugular intrahepatic portosystemic shunt (TIPS) are often considered as second-line choices[13]. Recently, endovascular selective catheterization thrombolytic therapy has been increasingly successfully implemented, which can be administered directly *via* percutaneous transhepatic or transjugular intrahepatic route or indirectly *via* the superior mesenteric artery (SMA) through femoral or radial artery infusion of thrombolytic agents[14,15]. The aim of this study was to compare the clinical outcomes of transcatheter selective SMA urokinase infusion therapy and TIPS in patients with cirrhosis and acute PVT to evaluate their effectiveness and safety.

MATERIALS AND METHODS

Patients

From January 2013 to December 2014, all patients with cirrhosis and acute PVT treated at the Second Hospital of Chongqing Medical University were enrolled. All patients provided informed consent before admission. The ethics committee approved our research program. The inclusion criteria were as follows: (1) patients with liver cirrhosis; (2) clear thrombosis in the portal vein system as seen through Doppler ultrasound, angio-computed tomography (CTA), and/or angio-magnetic resonance imaging analyses (MRA); (3) onset of acute thrombosis within 1 wk; (4) continued abdominal pain or abdominal distension. The exclusion criteria were as follows: (1) contraindications to anticoagulation therapy; (2) severe cardiac or lung disease; (3) previous TIPS or thrombolytic therapy; (4) PVT after liver transplantation; (5) malignant tumor; and (6) refusing interventional therapy or follow-up.

Evaluation of PVT status

Before the study, clinical symptoms, physical examination, and laboratory examination were recorded. All patients had an endoscopy to check for varices prior to thrombolysis and band ligation would be used to prevent variceal bleeding in patients with varices.

Doppler ultrasound, CTA, and/or MRA were used to estimate thrombosis from the aspects of location

and severity. The PVT location was divided into the main portal vein (MPV), superior mesenteric vein (SMV), and splenic vein (SV). The PVT severity was divided into four levels: grade 0 (thrombus deficiency), grade Ⅰ (MPV thrombus < 50% or only SMV and SV thrombus existed), grade Ⅱ (MPV thrombus accounted for 50%-100%), and grade Ⅲ (complete blocking or cavernous transformation of the portal vein).

Randomization

Using randomly generated numbers, patients who met the inclusion criteria were randomly allocated to the SMA group or the TIPS group.

Intervention

In the SMA group, we used the transfemoral approach for transcatheter selective SMA urokinase infusion therapy. Transcatheter thrombolysis was completed as follows: a catheter was selected for the SMA and remained in place. Contrast agent was injected through the SMA catheter. The first impact volume was 500000 IU. After the completion of angiography, urokinase was continuously pumped *via* the indwelling SMA catheter, depending on the patient's weight (250000-500000 IU, twice daily, for a total of 15000 IU/kg/d). Thrombolysis time depended on the improvement of the patient's clinical symptoms, a decrease in D-dimer, and imaging data. Anticoagulant therapy was completed as follows: patients were given subcutaneous heparin (2000 IU, twice daily) to maintain an international normalized ratio (INR) between 2 and 3. Patients were constantly monitored during thrombolytic therapy, including D-dimer, coagulation function, and routine blood tests. In addition, at intervals of 72 h and before removal of the catheter, angiography was re-performed. We considered ending thrombolysis and removing the indwelling SMA catheter when: (1) Superior mesenteric venography showed improvement of portal vein and SMV obstruction; (2) CT-enhanced examination showed that the PVT had obviously absorbed (stale thrombus occupying < 50% after treatment); or (3) vascular recanalization was achieved. After leaving the hospital, the patients continued taking oral warfarin for at least 3 mo.

In the TIPS group, TIPS was performed by two experienced physicians in accordance with standard procedures. After balloons were used to expand the obstructive passageway, a covered stent was embedded into the passageway. Additional bare-metal stents were placed into other obstructive veins of the portal venous system. After the procedure, the patients were given hypodermic low-molecular-weight heparin to prevent acute thrombosis (6000 IU, three time daily, consecutively for 1 wk). After discharge, all patients were treated with warfarin to achieve an INR of 2 to 3 for 6 mo.

Follow-up

All patients were followed at 1, 3, 6, 12, 18, and 24 mo after the procedure. Physical examinations and laboratory testing (coagulation function, routine blood test) were performed in both groups at each arranged follow-up visit, and CTA or Doppler ultrasound was performed at 6, 12, and 18 mo or whenever clinically required (*e.g.,* for ascites, black stools, or abdominal pain). During follow-up, no blind method was adopted for patients taking warfarin.

Outcome measurements

The primary outcome measure was the change in portal vein patency status, which was evaluated by CTA or Doppler ultrasound. Secondary outcomes were rebleeding and hepatic encephalopathy. Changes in portal vein patency status were defined as follows: (1) recanalization, with complete disappearance or reconstruction of cavernous transformation; (2) improved, with recanalization improvement from grade Ⅲ or Ⅱ to grade Ⅱ or Ⅰ, or disappearance of an SMV or SV thrombus; (3) stable; and (4) worsened, with worsening from grade Ⅰ or Ⅱ to grade Ⅱ or Ⅲ, progression of thrombus to cavernous transformation, or formation of an SMV or SV thrombus.

Statistical analysis

Statistical analyses were performed using SPSS software version 19.0. All tests of significance were two-sided, and a P value < 0.05 was considered significant. A Student's t-test was used to compare the differences in continuous variables between the two groups. Bivariate associations between categorical variables were analyzed with the χ^2 test and Fisher exact test. Category ordinal variables, including Child-Pugh class and MPV thrombus severity, were analyzed using the Mann-Whitney U test. Survival analysis was performed by the Kaplan-Meier method and compared by log-rank test.

RESULTS

Patients

A total of 40 patients were included in our study. Figure 1 shows the patient inclusion and exclusion process. Twenty patients were assigned to the SMA group, and the other 20 patients were assigned to the TIPS group. Between the two groups, the baseline characteristics (*i.e.,* age, sex, etiology, liver function, splenectomy, and status of PVT) had no significant difference (Table 1). There were 29 (72.5%) men and 11 (27.5%) women. The mean patient age was 49.3 ± 11.0 years (range, 27-72 yr). There were 31 (77.5%) patients with cirrhosis caused by hepatitis B virus (HBV), 1 patient (2.5%) by hepatitis C virus (HCV), 6 patients (15%) by alcohol, 1 patient (2.5%) by an autoimmune disorder, and 1 patient (2.5%) had a cryptogenic etiology. The average Child-Pugh score was 8.98 ± 1.79, and the average MELD score was 8.56 ± 5.98. There was no significant difference between the two groups in the MPV status; SMV thrombosis

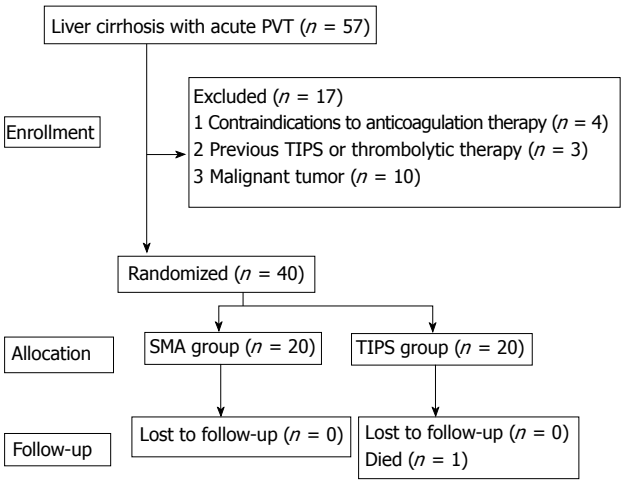

Figure 1 The process of patient inclusion and exclusion. PVT: Portal vein thrombosis; TIPS: Transjugular intrahepatic portosystemic shunt; SMA: Superior mesenteric artery.

and SV thrombosis occurred in 16 patients and 15 patients, respectively.

Intervention and follow-up

The technical success rate was 100% in both groups, and no fatal complications occurred.

In the SMA group, after treatment for 24 h, abdominal pain and abdominal distension were reduced by 80.0% (16/20), and 15.0% (3/20) of patients had no re-aggravation of their symptoms. At 48 h after the start of treatment, all of the 20 patients had a definite improvement in symptoms, and no patient had abdominal pain or distention before the end of thrombolysis (SMA catheter withdrawal). The mean time of indwelling SMA catheter placement was 8.75 ± 2.31 d, and the average dose of urokinase was 3705000.0 ± 1437000.1 IU. Before removing the catheter, contrast studies showed that in 15 cases, PVT had completely disappeared; another five cases of PVT had been absorbed (compared with before treatment, residual thrombus was < 10%).

During the follow-up period, no patients died. Oral warfarin (1.5-3.0 mg/d) for at least 3 mo was administered to patients to achieve an INR of 2 to 3. One patient stopped using warfarin and was treated with vitamin K1 after discharge for 1 mo; this patient had an INR of 9.27 and an activated partial thromboplastin time of 66.8 s during follow-up. Two patients were diagnosed with malignant tumors.

In the TIPS group, after treatment for 24 h, abdominal pain and abdominal distension were reduced by 75.0% (15/20), and 15.0% (3/20) of patients maintained the original symptoms. At 48 h after the start of treatment, all of the 20 patients had a definite improvement in symptoms.

The average value of portal pressure decreased from 46.30 ± 11.50 mmHg to 32.30 ± 7.47 mmHg. The last ultrasound scan before discharge showed that PVT had completely disappeared in 14 cases, and another 6 cases of PVT had been absorbed. During the follow-up period, one patient died of liver failure 14 mo after treatment. Ten patients had gastrointestinal rebleeding. Six patients had hepatic encephalopathy. Shunt dysfunction occurred in eight patients, six of whom underwent stent recanalization. Three patients were diagnosed with hepatocellular carcinoma, and one patient was diagnosed with suspected liver cancer.

Outcomes

Changes in PVT: At the 6-mo follow-up, in the SMA group, 15 patients maintained sustained recanalization, four improved, and one remained stable; no patient had a worsened condition. In the TIPS group, 12 patients maintained sustained recanalization, four improved, and four remained stable; no patient had a worsened condition (P = 0.239). At the 12-mo follow-up, in the SMA group, compared with the 6-mo follow-up, the patients' status of thrombus did not change. In the TIPS group, 13 patients achieved continuous recanalization, two improved, two remained stable, and three worsened due to shunt dysfunction (P = 0.307). At the 24-mo follow-up, 13 patients maintained sustained recanalization, four improved, three remained stable, and no one worsened in the SMA group. In the TIPS group, 11 patients maintained sustained recanalization, three improved, two remained stable, and four worsened (one died of liver failure). For the thrombolytic result, there was no significant difference between the two groups (P = 0.304) (Table 2). One patient with MPV complete blocking and cavernous transformation (grade Ⅲ), with severe abdominal pain and black stool, was treated by transcatheter SMA urokinase infusion therapy; 6 mo later, the MPV achieved sustained recanalization (Figure 2). In summary, the thrombus was significantly reduced in both groups (P < 0.001) (Tables 3 and 4) and patients with grade Ⅰ and Ⅱ PVT benefitted the most. In addition, in the SMA group, SMV thrombosis and SV thrombosis were significantly reduced (P = 0.048, P = 0.02).

Rebleeding: A total of 11 patients in the SMA group and eight patients in the TIPS group had rebleeding. In the SMA group, recurrent variceal bleeding occurred in seven patients; no explicit causation was found in the remaining four patients. In the TIPS group, gastrointestinal bleeding after shunt dysfunction occurred in four patients; no explicit causation was found in any of the four patients. The cumulative rates free of the first episode of rebleeding at months 6, 12, and 24 in the SMA group and in the TIPS group were 80%, 65%, and 45% *vs* 90%, 80%, and 60%, respectively (P = 0.320) (Figure 3A).

Hepatic encephalopathy: Hepatic encephalopathy occurred in seven and 13 patients in the SMA group

Table 1 Baseline characteristics of the study population

Characteristic	SMA group (n = 20)	TIPS group (n = 20)	P value
Age (yr)[1]	48.4 ± 13.2	50.1 ± 8.6	0.632
Male sex	14	15	1.000[3]
Etiology			0.156[3]
HBV	14	17	
HCV	0	1	
Alcohol	5	1	
Autoimmune	0	1	
Cryptogenic	1	0	
Child-Pugh class			0.065[2]
A	6	1	
B	8	9	
C	6	10	
Child-Pugh score[1]	8.6 ± 1.7	9.4 ± 1.8	0.135
MELD score[1]	8.0 ± 6.9	9.1 ± 5.1	0.582
Splenectomy	6	3	0.451[3]
Past esophageal or gastric varices	13	18	0.127[3]
Past gastrointestinal bleeding	12	18	0.065[3]
MPV thrombus			0.938[2]
Grade Ⅰ	6	7	
Grade Ⅱ	13	11	
Grade Ⅲ	1	2	
SMV thrombus	11	5	0.105[3]
SV thrombus	8	7	1.000[3]

[1]Data are mean plus or minus standard deviation; [2]Determined using Mann-Whitney *U* test; [3]Determined using Fisher exact test. Data are numbers of patients. MELD: Model for end-stage liver disease; MPV: Main portal vein; SMV: Superior mesenteric vein, SV: Splenic vein.

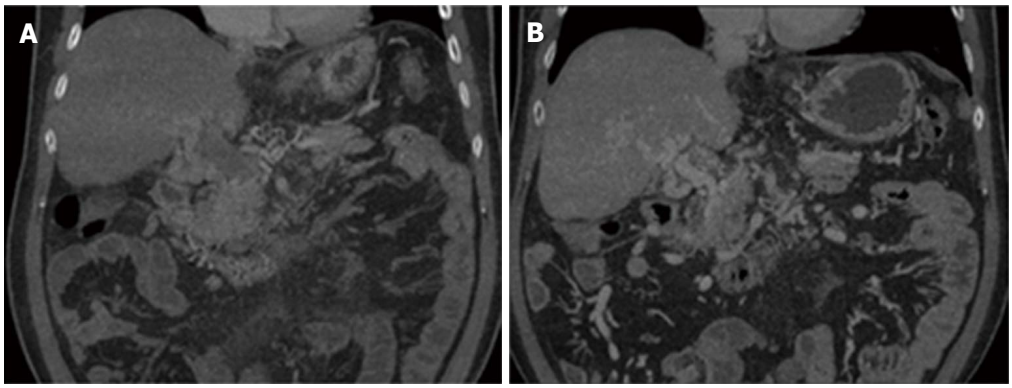

Figure 2 Contrast images of angio-computed tomography before and after transcatheter selective superior mesenteric artery urokinase infusion therapy in a patient. A: A patient with MPV complete blocking and cavernous transformation (grade Ⅲ) before urokinase infusion; B: 6 mo after urokinase infusion, MPV achieved sustained recanalization, but there was still cavernous transformation.

and the TIPS group, respectively. The cumulative rates free of the first episode of hepatic encephalopathy at months 6, 12, and 24 in the SMA group and in the TIPS group were 85%, 80%, and 65% *vs* 50%, 40%, and 35%, respectively (P = 0.022) (Figure 3B).

DISCUSSION

To date, the primary treatments for PVT include anticoagulation, thrombectomy, thrombolysis, and TIPS[16]. Although there is general agreement that anticoagulant therapy is needed for most symptomatic cases of PVT[17], there is no consensus on the treatment of liver cirrhosis with acute PVT. It was reported that simple anticoagulant therapy had a better curative effect on the patients with mild symptoms and limited scope of thrombus[18,19]. Compared to anticoagulation therapy, catheter-directed thrombolysis and TIPS are used infrequently, but they can: (1) decrease the risk of rebleeding in cirrhotic patients with previous variceal bleeding; (2) increase the rate of portal vein recanalization; and (3) be used in patients with cavernous transformation of the portal vein[14,20-23].

In our study, acute PVT greatly improved after catheter-directed thrombolysis and TIPS, and there was no significant difference between the two groups. Evidence about the use of thrombolytics for the treatment of acute PVT in patients with cirrhosis is relatively rare; some studies showed that PVT disappearance occurs in 100% of cases, with no recurr-

Table 2 Comparison of portal vein thrombosis changes between the two groups

	SMA group (n = 20)			TIPS group (n = 20)			
Time (mo)	6	12	24	6	12	24	*P* value
Recanalization	15	15	13	12	13	11	0.239 (6 mo)
Improved	4	4	4	4	2	3	0.307 (12 mo)
Stable	1	1	3	4	2	2	0.304 (24 mo)
Worse	0	0	0	0	3	4	

Data are numbers of patients. Determined using Mann-Whitney *U* test. TIPS: Transjugular intrahepatic portosystemic shunt; SMA: Superior mesenteric artery.

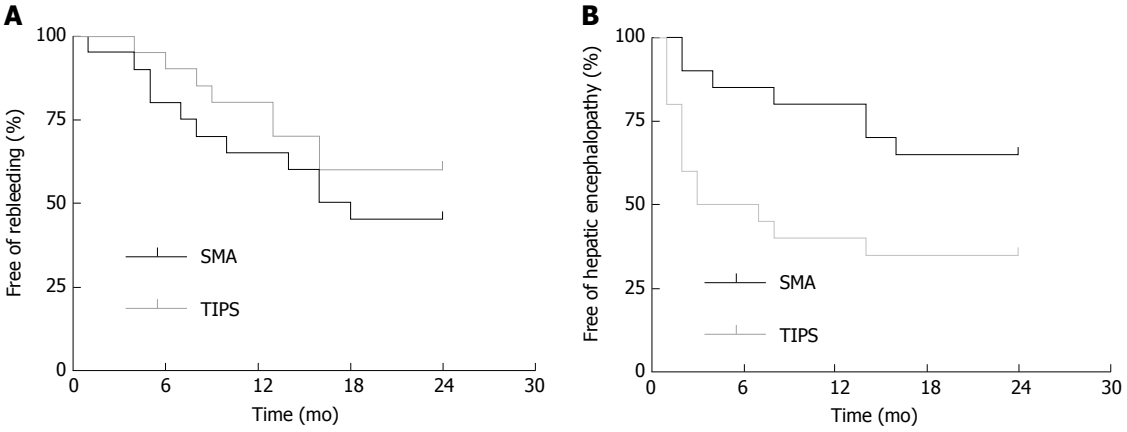

Figure 3 Rebleeding and hepatic encephalopathy in the two groups. A: Cumulative rate free of the first episode of rebleeding in the superior mesenteric artery (SMA) group and transjugular intrahepatic portosystemic shunt (TIPS) group (P = 0.320, log-rank test); B: Cumulative rate free of the first episode of hepatic encephalopathy in the SMA group and TIPS group (P = 0.022, log-rank test).

ence during follow-up[14]. Acute PVT in 70% of patients was improved after TIPS treatment, which is consistent with previous studies that PVT disappearance occurred in 57% to 100% of patients[22,24]. We consider that this is consistent with the view that a reduced portal vein flow velocity is the key risk factor for PVT formation[7,14,25]. Patients with concomitant cirrhosis have significantly slower portal vein flow rates than the healthy population[14]. In addition, old thrombus often cannot be cleared completely, which aggravates local blood circulation disorder. Moreover, we observed that SMV thrombolysis and SV thrombolysis disappeared significantly in the SMA group, and no phenomenon occurred in the TIPS group. Previous reports showed that the treatment of acute PV-SMV thrombosis by transcatheter superior mesenteric artery catheter urokinase infusion therapy *via* the radial artery was effective[14]. This method is simple, easy to operate, and very safe. Because the thrombolytic agent circulates into the branch of the intestinal vein, the treatment of mesenteric venous thrombosis is better. All in all, acute PVT improved after SMA and TIPS; in addition, transcatheter selective SMA infusion therapy is better for the treatment of fresh thrombus in the mesentery.

Another problem that we are particularly concerned about is rebleeding. We observed that the rates of rebleeding were lower and the time to rebleeding was delayed in the TIPS group compared with the SMA group, although there was no significant difference between the two groups (P = 0.320). It has been confirmed that TIPS decreases the incidence of rebleeding as the second-line treatment for variceal hemorrhage[22,25,26]. In our study, infusion of relatively low-dose urokinase, no simultaneous peripheral venous infusion, and close monitoring of blood coagulation (which may cause the incidence of rebleeding) kept complications relatively low.

In the TIPS group, the patency rate in 24 mo was consistent with those reported in previous studies using covered stents[27]. TIPS is related to an increased risk of hepatic encephalopathy[22,23]. Our study showed that occurrences of hepatic encephalopathy in the TIPS group were markedly higher than those in the SMA group, and 50% of patients with hepatic encephalopathy, which was caused by the portosystemic shunting, had this occurrence within of 6 mo after TIPS treatment, whereas patients in the SMA group had hepatic encephalopathy caused by deterioration of liver function.

There are some limitations to our study. First, the lack of a large sample of participants is the major limitation, and further large-scale studies are needed. Second, our study was not a double-blind study, because patients in our study needed to be closely followed for blood clotting, and to detect complications that may be life-threatening.

In conclusion, transcatheter SMA infusion therapy and TIPS are both safe and effective treatments for

Table 3 Changes in portal vein thrombosis before and after urokinase infusion in the superior mesenteric artery group

	Before	After	*P* value
MPV thrombus			< 0.001
Grade 0	0	13	
Grade Ⅰ	6	4	
Grade Ⅱ	13	3	
Grade Ⅲ	1	0	
SMV thrombus	11	4	0.048[1]
SV thrombus	8	1	0.02[1]

[1]Determined using Fisher exact test. *P* value was obtained from a comparison at 24-mo follow-up. Data are numbers of patients. Determined using Mann-Whitney *U* test.

Table 4 Changes in portal vein thrombosis before and after transjugular intrahepatic portosystemic shunt in the transjugular intrahepatic portosystemic shunt group

	Before	After	*P* value
MPV thrombus			< 0.001
Grade 0	0	11	
Grade Ⅰ	7	3	
Grade Ⅱ	11	2	
Grade Ⅲ	2	4	
SMV thrombus	5	7	0.731[1]
SV thrombus	7	3	0.273[1]

[1]Determined using Fisher exact test. *P* value was obtained from a comparison at 24-mo follow-up. Data are numbers of patients. Determined using Mann-Whitney *U* test. SMA: Superior mesenteric artery; MPV: Main portal vein.

patients with cirrhosis and acute PVT, particularly for grade Ⅰ and Ⅱ PVT, and transcatheter SMA urokinase infusion therapy is more ideal for the treatment of fresh thrombus in the mesentery.

ARTICLE HIGHLIGHTS

Research background

Acute portal vein thrombosis is a common complication of cirrhosis and would lead to adverse prognosis. Endovascular selective catheterization thrombolytic therapy and transjugular intrahepatic portosystemic shunt has been increasingly successfully implemented, which brings new opportunities for the treatment of acute portal vein thrombosis (PVT).

Research motivation

The aim of this study was to compare the clinical outcomes of transcatheter selective superior mesenteric artery (SMA) urokinase infusion therapy and transjugular intrahepatic portosystemic shunt (TIPS) in patients with cirrhosis and acute PVT to evaluate their effectiveness and safety for acute PVT.

Research objectives

To evaluate the effectiveness and safety of transcatheter selective SMA urokinase infusion therapy and TIPS in patients with cirrhosis and acute PVT to provide theoretical support for the implementation of new therapies.

Research methods

A randomized controlled trial was performed, and the total follow-up time was 24 mo. The outcome measures were the change in portal vein patency status, rebleeding, and hepatic encephalopathy.

Research results

Both treatments can quickly relieve symptoms within 48 h. The main portal vein thrombosis was significantly reduced in both groups and there was no significant difference between them. No fatal complications occurred.

Research conclusions

Transcatheter SMA infusion therapy and TIPS are both safe and effective treatments for patients with cirrhosis and acute PVT, particularly for grade Ⅰ and Ⅱ PVT, and transcatheter SMA urokinase infusion therapy is more ideal for the treatment of fresh thrombus in the mesentery.

Research perspectives

Further large-scale studies are needed. It is better to have a separate anticoagulant group as a control.

REFERENCES

1 **Primignani M**. Portal vein thrombosis, revisited. *Dig Liver Dis* 2010; **42**: 163-170 [PMID: 19766546 DOI: 10.1016/j.dld.2009.08.003]

2 **Violi F**, Corazza RG, Caldwell SH, Perticone F, Gatta A, Angelico M, Farcomeni A, Masotti M, Napoleone L, Vestri A, Raparelli V, Basili S; PRO-LIVER Collaborators. Portal vein thrombosis relevance on liver cirrhosis: Italian Venous Thrombotic Events Registry. *Intern Emerg Med* 2016; **11**: 1059-1066 [PMID: 27026379 DOI: 10.1007/s11739-016-1416-8]

3 **Stine JG**, Shah PM, Cornella SL, Rudnick SR, Ghabril MS, Stukenborg GJ, Northup PG. Portal vein thrombosis, mortality and hepatic decompensation in patients with cirrhosis: A meta-analysis. *World J Hepatol* 2015; **7**: 2774-2780 [PMID: 26644821 DOI: 10.4254/wjh.v7.i27.2774]

4 **Aman**N, Gul H, Roghani IS, Afridi Z. Frequency of portal vein thrombosis in cirrhosis on ultrasound. *J Med Sci* 2015; **23**: 11-13

5 **Turon** F, Baiges A, Garcia-Criado A, Nuñez I, Gilabert R, Bru C, Hernández-Gea V. Portal Vein Thrombosis in Patients with Cirrhosis. Incidence and Factors Associated with Its Development. *J Hepatol* 2016; **64**: S260 [DOI: 10.1016/S0168-8278(16)00290-7]

6 **Qi X**, Li H, Liu X, Yao H, Han G, Hu F, Shao L, Guo X. Novel insights into the development of portal vein thrombosis in cirrhosis patients. *Expert Rev Gastroenterol Hepatol* 2015; **9**: 1421-1432 [PMID: 26325361 DOI: 10.1586/17474124.2015.1083856]

7 **Qi X**, Dai J, Yang M, Ren W, Jia J, Guo X. Association between Portal Vein Thrombosis and Survival in Non-Liver-Transplant Patients with Liver Cirrhosis: A Systematic Review of the Literature. *Gastroenterol Res Pract* 2015; **2015**: 480842 [PMID: 25810714 DOI: 10.1155/2015/480842]

8 **Qi X**, Dai J, Jia J, Ren W, Yang M, Li H, Fan D, Guo X. Association between portal vein thrombosis and survival of liver transplant recipients: a systematic review and meta-analysis of observational studies. *J Gastrointestin Liver Dis* 2015; **24**: 51-59, 4 p following 59 [PMID: 25822434 DOI: 10.15403/jgld.2014.1121.qix]

9 **Qi X**, Su C, Ren W, Yang M, Jia J, Dai J, Xu W, Guo X. Association between portal vein thrombosis and risk of bleeding in liver cirrhosis: A systematic review of the literature. *Clin Res Hepatol Gastroenterol* 2015; **39**: 683-691 [PMID: 25956490 DOI: 10.1016/j.clinre.2015.02.012]

10 **Zang L**, Sun Z, Li W, Liu X. [Meta-analysis of risk factors of gastroesophageal varices rebleeding after therapeutic endoscopy]. *Zhonghua Gan Zang Bing Za Zhi* 2015; **23**: 275-280 [PMID: 26133819 DOI: 10.3760/cma.j.issn.1007-3418.2015.04.009]

11 **Loffredo L**, Pastori D, Farcomeni A, Violi F. Effects of Anticoagulants in Patients With Cirrhosis and Portal Vein Thrombosis: A Systematic Review and Meta-analysis. *Gastroenterology* 2017; **153**: 480-487.e1 [PMID: 28479379 DOI: 10.1053/j.gastro.2017.04.042]

12 **Tonon**M, Piano S, Sacerdoti D, Dalla Valle F, Grbec M, Spiezia L, AngeliP. Efficacy and safety of treatment of acute nonmalignant portal vein thrombosis with subcutaneous fondaparinux in patients with cirrhosis and marked thrombocytopenia. *Hepatology* 2015;

62: 591A [DOI: 10.1016/j.dld.2015.12.066]
13 **Tsochatzis EA**, Senzolo M, Germani G, Gatt A, Burroughs AK. Systematic review: portal vein thrombosis in cirrhosis. *Aliment Pharmacol Ther* 2010; **31**: 366-374 [PMID: 19863496 DOI: 10.1111/j.1365-2036.2009.04182.x]
14 **Wang MQ**, Guo LP, Lin HY, Liu FY, Duan F, Wang ZJ. Trans-radial approach for transcatheter selective superior mesenteric artery urokinase infusion therapy in patients with acute extensive portal and superior mesenteric vein thrombosis. *Cardiovasc Intervent Radiol* 2010; **33**: 80-89 [PMID: 20033163 DOI: 10.1007/s00270-009-9777-2]
15 **Wang MQ**, Liu FY, Duan F, Wang ZJ, Song P, Fan QS. Acute symptomatic mesenteric venous thrombosis: treatment by catheter-directed thrombolysis with transjugular intrahepatic route. *Abdom Imaging* 2011; **36**: 390-398 [PMID: 20652243 DOI: 10.1007/s00261-010-9637-1]
16 **Sharma AM**, Zhu D, Henry Z. Portal vein thrombosis: When to treat and how? *Vasc Med* 2016; **21**: 61-69 [PMID: 26584887 DOI: 10.1177/1358863X15611224]
17 **European Association for the Study of the Liver.** Electronic address: easloffice@easloffice.eu. EASL Clinical Practice Guidelines: Vascular diseases of the liver. *J Hepatol* 2016; **64**: 179-202 [PMID: 26516032 DOI: 10.1016/j.jhep.2015.07.040]
18 **Harnik IG**, Brandt LJ. Mesenteric venous thrombosis. *Vasc Med* 2010; **15**: 407-418 [PMID: 20926500 DOI: 10.1177/1358863X10379673]
19 **Bergqvist D**, Svensson PJ. Treatment of mesenteric vein thrombosis. *Semin Vasc Surg* 2010; **23**: 65-68 [PMID: 20298951 DOI: 10.1053/j.semvascsurg.2009.12.008]
20 **Liu K**, Li WD, Du XL, Li CL, Li XQ. Comparison of Systemic Thrombolysis Versus Indirect Thrombolysis via the Superior Mesenteric Artery in Patients with Acute Portal Vein Thrombosis. *Ann Vasc Surg* 2017; **39**: 264-269 [PMID: 27671456 DOI: 10.1016/j.avsg.2016.06.029]
21 **Qi X**, Han G, Fan D. The preferable treatment for cirrhotic portal vein thrombosis: anticoagulation or transjugular intrahepatic portosystemic shunt? *Hepatology* 2010; **51**: 713-714 [PMID: 20104582 DOI: 10.1002/hep.23217]
22 **Han G**, Qi X, He C, Yin Z, Wang J, Xia J, Yang Z, Bai M, Meng X, Niu J, Wu K, Fan D. Transjugular intrahepatic portosystemic shunt for portal vein thrombosis with symptomatic portal hypertension in liver cirrhosis. *J Hepatol* 2011; **54**: 78-88 [PMID: 20932597 DOI: 10.1016/j.jhep.2010.06.029]
23 **Luca A**, Miraglia R, Caruso S, Milazzo M, Sapere C, Maruzzelli L, Vizzini G, Tuzzolino F, Gridelli B, Bosch J. Short- and long-term effects of the transjugular intrahepatic portosystemic shunt on portal vein thrombosis in patients with cirrhosis. *Gut* 2011; **60**: 846-852 [PMID: 21357252 DOI: 10.1136/gut.2010.228023]
24 **D'Avola D**, Bilbao JI, Zozaya G, Pardo F, Rotellar F, Iñarrairaegui M, Quiroga J, Sangro B, Herrero JI. Efficacy of transjugular intrahepatic portosystemic shunt to prevent total portal vein thrombosis in cirrhotic patients awaiting for liver transplantation. *Transplant Proc* 2012; **44**: 2603-2605 [PMID: 23146469 DOI: 10.1016/j.transproceed.2012.09.050]
25 **Stine JG**, Wang J, Shah PM, Argo CK, Intagliata N, Uflacker A, Caldwell SH, Northup PG. Decreased portal vein velocity is predictive of the development of portal vein thrombosis: A matched case-control study. *Liver Int* 2017; Epub ahead of print [PMID: 28632958 DOI: 10.1111/liv.13500]
26 **Qi X**, He C, Guo W, Yin Z, Wang J, Wang Z, Niu J, Bai M, Yang Z, Fan D, Han G. Transjugular intrahepatic portosystemic shunt for portal vein thrombosis with variceal bleeding in liver cirrhosis: outcomes and predictors in a prospective cohort study. *Liver Int* 2016; **36**: 667-676 [PMID: 26235541 DOI: 10.1111/liv.12929]
27 **Perarnau JM**, Le Gouge A, Nicolas C, d'Alteroche L, Borentain P, Saliba F, Minello A, Anty R, Chagneau-Derrode C, Bernard PH, Abergel A, Ollivier-Hourmand I, Gournay J, Ayoub J, Gaborit C, Rusch E, Giraudeau B; STIC-TIPS group. Covered vs. uncovered stents for transjugular intrahepatic portosystemic shunt: a randomized controlled trial. *J Hepatol* 2014; **60**: 962-968 [PMID: 24480619 DOI: 10.1016/j.jhep.2014.01.015]

P- Reviewer: Memeo R, Tripathi D **S- Editor**: Qi Y
L- Editor: Wang TQ **E- Editor**: Huang Y

World Journal of Gastroenterology

Submit a Manuscript: http://www.f6publishing.com

World J Gastroenterol 2017 November 7; 23(41): 7478-7488

DOI: 10.3748/wjg.v23.i41.7478

ISSN 1007-9327 (print) ISSN 2219-2840 (online)

CASE REPORT

Extraordinary response of metastatic pancreatic cancer to apatinib after failed chemotherapy: A case report and literature review

Cheng-Ming Li, Zhi-Chao Liu, You-Ting Bao, Xin-Dong Sun, Lin-Lin Wang

Cheng-Ming Li, Zhi-Chao Liu, School of Medicine and Life Sciences, University of Jinan-Shandong Academy of Medical Sciences, Jinan 250101, Shandong Province, China

Cheng-Ming Li, Zhi-Chao Liu, You-Ting Bao, Xin-Dong Sun, Lin-Lin Wang, Department of Radiation Oncology, Shandong Cancer Hospital Affiliated to Shandong University, Shandong Academy of Medical Sciences, Jinan 250117, Shandong Province, China

Lin-Lin Wang, School of Medicine, Shandong University, Jinan 250012, Shandong Province, China

You-Ting Bao, Department of Oncology, Weifang Medical University, Weifang 261042, Shandong Province, China

ORCID number: Cheng-Ming Li (0000-0002-1111-3268); Zhi-Chao Liu (0000-0001-7313-2504); You-Ting Bao (0000-0001-6349-5125); Xin-Dong Sun (0000-0003-2325-1366); Lin-Lin Wang (0000-0002-2873-4204).

Author contributions: Li CM collected the case data and wrote the paper; Sun XD and Wang LL treated the patient; Li CM, Liu ZC and Bao YT contributed to the literature search; Wang LL reviewed and revised the manuscript; All authors have read and approved the final manuscript.

Supported by The National Natural Science Foundation of China, No. 81402299; the Project of Postdoctoral Innovation of Shandong Province, No. 201501010; and the Project of Postdoctoral Science Foundation of China, No. 2016M590640.

Institutional review board statement: The case report was reviewed and approved by the Institutional Review Board of Shandong Cancer Hospital Affiliated to Shandong University, Jinan, China.

Informed consent statement: The husband of the patient provided written informed consent.

Conflict-of-interest statement: All the authors declare that there is no conflict of interest.

Data sharing statement: No additional data are available.

Manuscript source: Unsolicited manuscript

Correspondence to: Lin-Lin Wang, MD, PhD, Department of Radiation Oncology, Shandong Cancer Hospital Affiliated to Shandong University, Shandong Academy of Medical Sciences, No. 440, Jiyan Road, Jinan 250117, Shandong Province, China. 13793187739@163.com
Telephone: +86-531-67626142
Fax: +86-531-67626141

Received: July 14, 2017
Peer-review started: August 1, 2017
First decision: August 31, 2017
Revised: September 13, 2017
Accepted: September 26, 2017
Article in press: September 26, 2017
Published online: November 7, 2017

Abstract

Chemotherapy has limited efficacy in the treatment of advanced and metastatic pancreatic cancer (PC), and has serious side effects. The development of novel effective agents, especially targeted therapy, is essential

for patients with PC. We present a 58-year-old Chinese woman initially diagnosed with locally advanced PC. As the disease progressed to Stage Ⅳ, the patient was unable to tolerate chemotherapy after the fourth-line treatment. She was then treated with apatinib, a novel and highly selective tyrosine kinase inhibitor of vascular endothelial growth factor receptor-2 and achieved a progression-free-survival of 7 mo. All drug-related side effects were well controlled with medication. To the best of our knowledge, this is the first case of PC which responded to apatinib. Considering this remarkable response, apatinib may be a promising agent in the treatment of PC. We also reviewed the literature on chemotherapy and targeted therapy, especially the anti-angiogenesis therapy for patients with PC, and investigated the effect of apatinib in other solid tumors as well.

Key words: Anti-angiogenesis; Apatinib; Pancreatic cancer; Targeted therapy; Vascular endothelial growth factor receptor-2

Core tip: As chemotherapy has limited efficacy in the treatment of advanced and metastatic pancreatic cancer, targeted therapy is becoming increasingly important in patients with pancreatic cancer. The case reported herein suggests that apatinib, a novel and highly selective tyrosine kinase inhibitor of vascular endothelial growth factor receptor-2, may be a promising and useful agent in the treatment of pancreatic cancer.

Li CM, Liu ZC, Bao YT, Sun XD, Wang LL. Extraordinary response of metastatic pancreatic cancer to apatinib after failed chemotherapy: A case report and literature review. *World J Gastroenterol* 2017; 23(41): 7478-7488 Available from: URL: http://www.wjgnet.com/1007-9327/full/v23/i41/7478.htm DOI: http://dx.doi.org/10.3748/wjg.v23.i41.7478

INTRODUCTION

Pancreatic cancer (PC) is a malignant tumor with a poor prognosis, and is the seventh most common cancer worldwide[1]. Chemotherapy or chemoradiation are recommended as primary therapy according to the National Comprehensive Cancer Network (NCCN) guideline for advanced and metastatic PC[2]. However, the therapeutic outcomes are unsatisfactory, with 1-year survival rates of only 17%-23%[3-5]. Given that there is limited evidence that further systemic therapy provides meaningful benefit for patients who have progressed on chemotherapy, the development of novel effective agents, including targeted therapy, to improve patient outcome is required.

Tumor angiogenesis has been found to be essential in the proliferation, invasion and metastasis of PC[6-9]. Vascular endothelial growth factor receptor-2 (VEGFR-2) is a major element involved in pancreatic tumor angiogenesis[10-13]. Therefore, interference with the VEGFR-2 signaling pathway may have therapeutic efficacy in the treatment of PC by preventing angiogenesis.

Apatinib (Hengrui Pharmaceutical Co., Ltd., Shanghai, China), also known as YN968D1, is a multiple kinase inhibitor with *in vitro* activity against VEGFR-2, PDGFR-beta, c-Kit, and c-src[14,15]. It was shown to have a survival benefit in gastric cancer in a Phase Ⅱ[16] and Ⅲ[17] trial and is currently being studied in multiple solid tumor types, such as colon and breast cancers[18-20]. Because of its easy administration, better compliance, reduced toxicity and improved outcomes, apatinib has demonstrated substantial potential as a new therapeutic option in a variety of tumor types[17,21].

Here, we report a patient with PC who was treated with apatinib following failure of the fourth-line therapy and achieved a progression-free survival (PFS) of 7 mo, demonstrating the potential of apatinib in the treatment of PC. To the best of our knowledge, this is the first case of PC which responded to apatinib.

CASE REPORT

In November 2014, a 58-year-old woman attended our hospital complaining of persistent pain in the upper abdomen and back, following dyspepsia for approximately 4 d. Physical examination suggested tenderness in the upper abdomen but without rebound pain. The serum carbohydrate antigen 19-9 (CA19-9) level was 148 U/mL (normal range, 0-39 U/mL). An upper abdominal contrast-enhanced computed tomography (CT) scan revealed a 3.1 cm × 1.7 cm mass at the body of the pancreas (Figure 1A), with the mass having an intimate connection to the splenic artery and vein. An enlarged lymph node was detected behind the aorta abdominalis (Figure 1B). An ^{18}F-FDG positron emission tomography scan also displayed a mass in the body of the pancreas with an SUV of 6.2 and an enlarged lymph node with an SUV of 4.8 (Figure 1C and D). Subsequently, an endoscopic biopsy of the mass showed a moderately differentiated adenocarcinoma (Figure 2). The patient was diagnosed with locally advanced, unresectable PC (cT4N1M0, Stage Ⅲ).

Concurrent chemoradiotherapy (CCRT) with gemcitabine (GEM) weekly and 30 fractions of radiotherapy were administered from November 7 to December 18, 2014. When CCRT was completed, the tumor response was considered stable disease (SD) on a repeat abdominal CT according to the modified

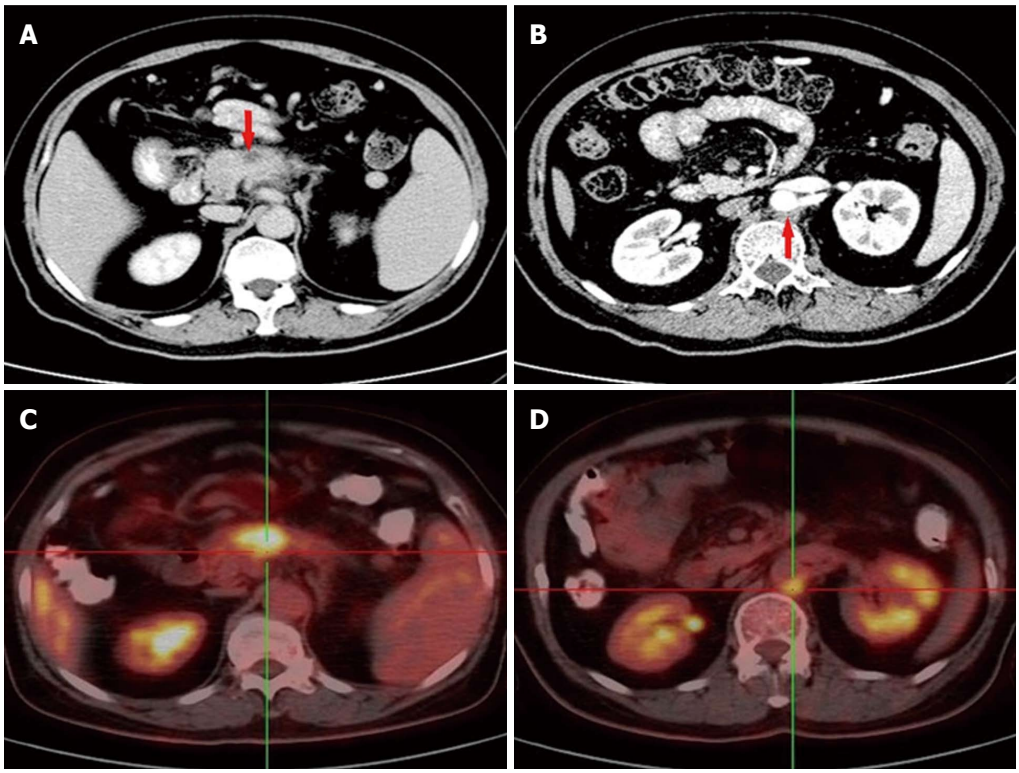

Figure 1 Abdominal CT and ^{18}F-FDG PET/CT show lesions located in the pancreas and behind the aorta abdominalis. A: A 3.1 cm × 1.7 cm mass at the body of the pancreas; B: An enlarged lymph node behind the aorta abdominalis; C: The mass in the body of the pancreas with an SUV of 6.2; D: The enlarged lymph node with an SUV of 4.8. CT: Computed tomography; PET: Positron emission tomography.

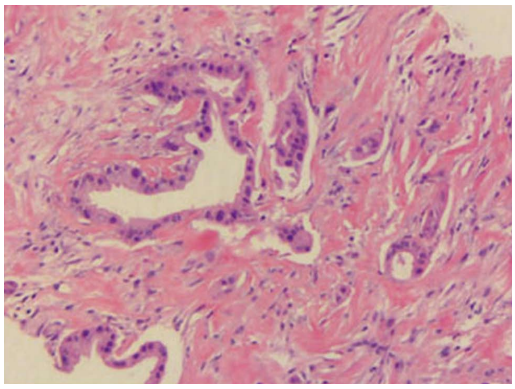

Figure 2 Hematoxylin and eosin staining of a tumor section (× 200). The pathological diagnosis was moderately differentiated adenocarcinoma.

Response Evaluation Criteria in Solid Tumors (RECIST) criteria. The CA19-9 level gradually decreased to 125.6 U/mL. GEM with oxaliplatin was then administered for 4 cycles. An abdominal CT scan revealed a partial response, while serum CA19-9 level gradually decreased to a normal value (24.4 U/mL). The timeline of treatment and trend in CA19-9 during treatment are displayed in Figure 3.

However, 1 mo later, the patient attended our hospital again because of recurrence of upper abdominal pain. The CT scan showed metastatic lesions in the right pleura and lungs (Figure 4A-D), while the lesion in the pancreas and enlarged lymph node remained stable (Figure 4E and F). Clinical restaging showed cT4N1M1, Stage IV. The CA19-9 level increased to 150.8 U/mL. From June 27, 2015, 4 cycles of paclitaxel-albumin with S-1 were administered. The response after 2 courses and 4 courses was SD. The CA19-9 level gradually decreased to 46.87 U/mL, which was almost a normal value (Figure 3).

Approximately 4 mo later, a CT scan showed that the primary as well as the metastatic lesions had progressed. The CA19-9 level was 107.6 U/mL. As the patient had good performance status (PS), the fourth-line therapy with FOLFOX4 was administered. After 3 cycles, the CT scan showed that response to treatment was SD. However, the CA19-9 level had gradually increased from 107.6 U/mL to 302.3 U/mL. The patient was unable to tolerate this regimen due to gastrointestinal toxicity, and refused further chemotherapy. From June 3, 2016, the patient received apatinib (500 mg p.o. qd) as the fifth-line treatment. The CA19-9 level after 15 d of apatinib treatment decreased sharply from 302.3 U/mL to 88.8 U/mL. The CA19-9 level was tested every 2 wk and a CT scan was performed every 8 wk during the follow-up. The CA19-9 level was maintained between 56.8 U/mL and 92.4 U/mL (Figure 3) and the primary mass decreased from 1.7 cm to 1.2 cm, and then to 1.0 cm (Figure 5D-F) while other lesions showed no obvious

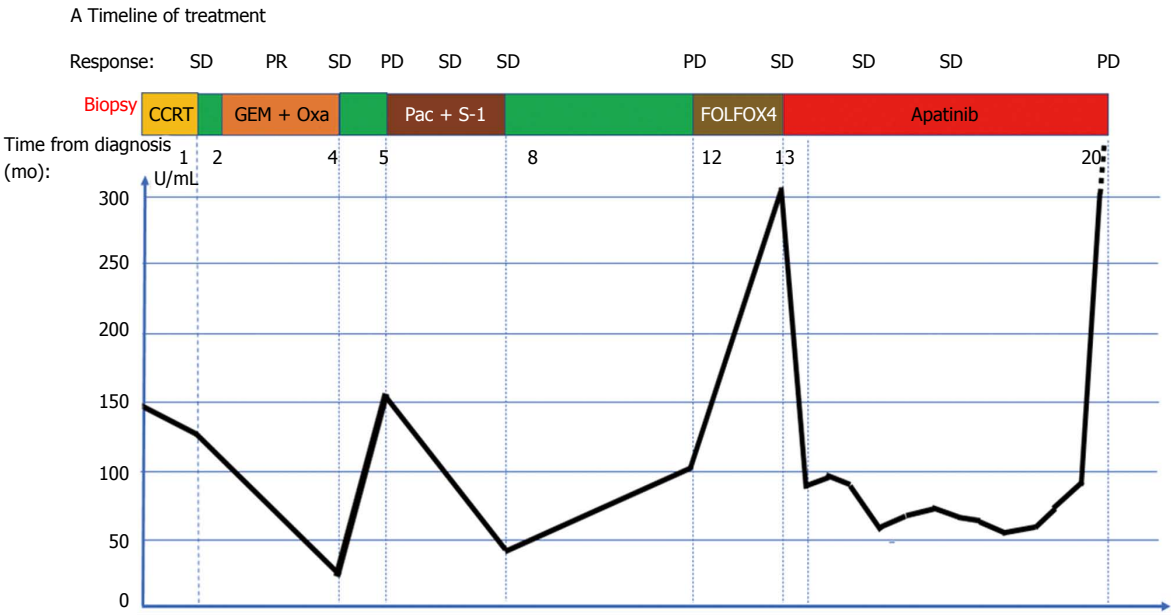

Figure 3 Timeline of treatment (A) and trend in carbohydrate antigen 19-9 level during treatment. Oxa: Oxaliplatin; Pac: Paclitaxel-albumin. Green color indicates time without treatment.

change (Figure 5A-C, G-I). The response to treatment with apatinib was SD.

On January 13, 2017, the patient attended our hospital complaining of difficulty in breathing and the recurrence of upper abdominal pain, a CT scan revealed several metastatic lesions in the liver and pleural effusion (Figure 6). In addition, the CA19-9 level had markedly increased to 1978.0 U/mL. Her PS diminished rapidly with a score of 3, and the disease had progressed. The patient finally died of multiple organ dysfunction resulting from pulmonary infection.

During apatinib treatment, this patient developed the primary side effects of hypertension (grade 2), dental ulcer (grade 2) and a higher serum alanine transaminase level (grade 1) according to the Common Terminology Criteria for Adverse Events (CTCAE) v4.0 criteria. All side effects were well controlled with drug treatment and she had a PS score of 2.

This study was approved by the Institutional Review Board of Shandong Cancer Hospital Affiliated to Shandong University. The husband of the patient provided written informed consent.

DISCUSSION

To date, there has been no effective therapy for improving the survival of a PC patient due to its aggressive nature. In this case, we administered CCRT as first-line therapy and the tumor response was SD. GEM and oxaliplatin were administered as second-line therapy and PFS was only 3 mo. Paclitaxel-albumin with S-1 was then administered as third-line therapy and FOLFOX4 regimen as the fourth-line therapy. The tumor response was SD but the CA19-9 level gradually increased. Due to chemotherapy intolerance, apatinib was then given as the fifth-line therapy to this patient. PFS following apatinib therapy was 7 mo. In addition, the patient tolerated apatinib well, with satisfactory quality of life.

With current chemotherapy regimens for PC, including GEM, paclitaxel-albumin, S-1, oxaliplatin, 5-FU, leucovorin and irinotecan, the median survival for patients with unresectable or metastatic PC is 9-11 mo[4,22,23]. In recent years, an increasing number of targeted drugs for PC have been studied. Erlotinib is the only targeted drug approved by the Federal Drug Administration to treat PC. In a randomized Phase Ⅲ trial[3], the median survival and 1-year survival rate both increased in patients treated with GEM plus erlotinib, compared to those treated with only GEM. Although these results seem positive, the median overall survival (OS) was only prolonged by 9.9 d (6.24 mo *vs* 5.91 mo, $P = 0.038$) and the objective response rates (ORR) were not significantly different between the two treatment arms (57.5% *vs* 49.2%, $P = 0.07$). Furthermore, a higher incidence of some adverse events was observed with erlotinib plus GEM. In a small-sample study, sorafenib plus erlotinib also did not improve either survival or PFS rate as compared to a historical control[24]. The ViP trial, a Phase Ⅱ double-blind, multicenter, randomized placebo-controlled trial, showed that vandetanib combined with GEM in patients with advanced PC did not improve OS (8.83 mo *vs* 8.95 mo, $P = 0.303$)[25]. In addition, a meta-analysis showed that there was no statistically significant improvement in survival when PC patients

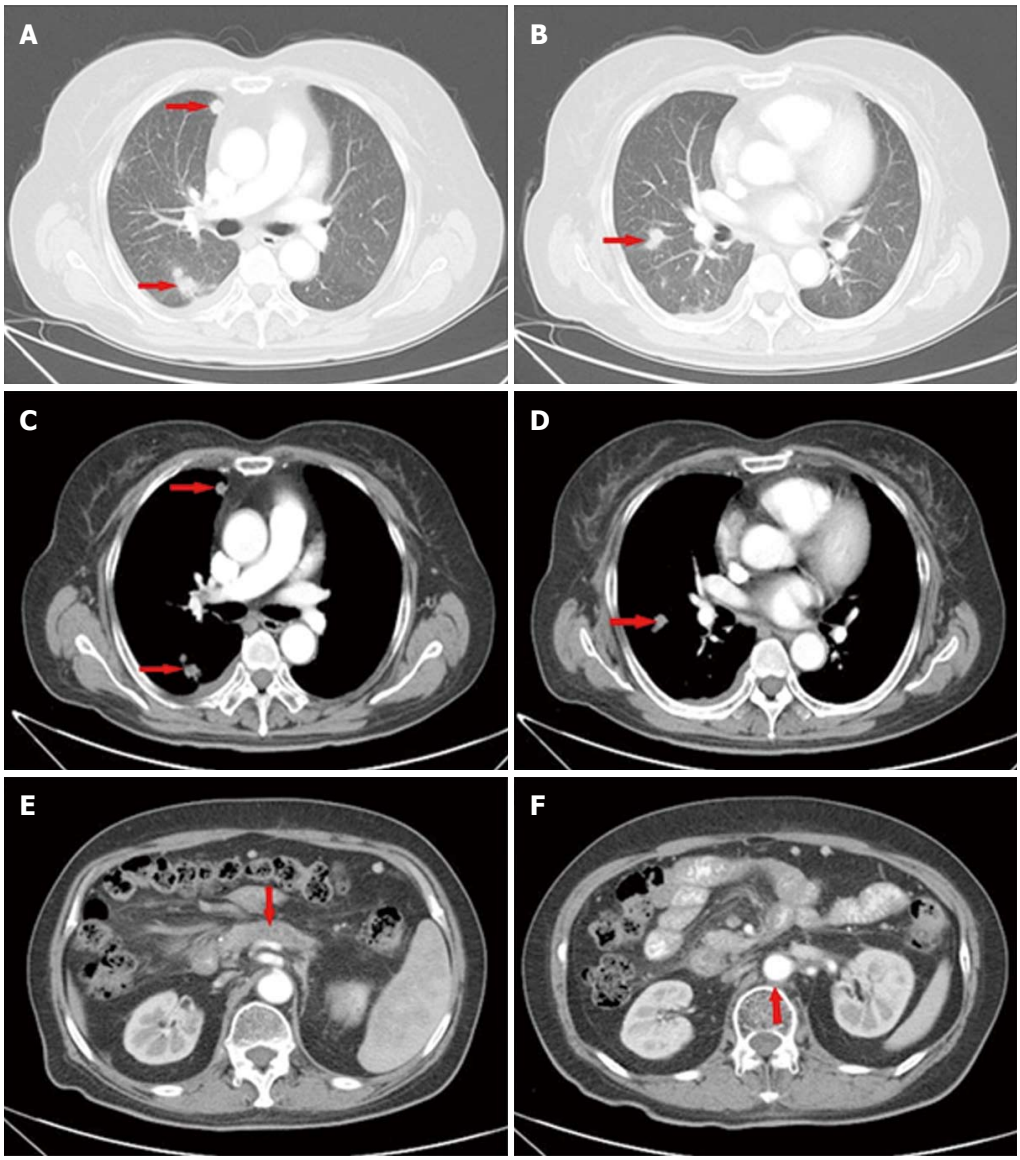

Figure 4 Computed tomography scan showed that the disease had progressed to stage Ⅳ. Metastatic lesions in the right pleura and lungs (lung window A, B; mediastinal window C, D); The lesion in the pancreas and enlarged lymph node remained stable (E, F).

Table 1 Clinical trials using targeted agents for advanced or metastatic pancreatic cancer

Target medicine	Mechanism	Phase	Stage	*n*	Arm	PFS, mo	OS, mo	ORR
Cetuximab[27]	EGFR	Ⅲ	Locally advanced/ metastatic	746	A: GEM + cetuximab B: GEM	3.4 *vs* 3.0 *P* = 0.18	6.3 *vs* 5.9 *P* = 0.23	49% *vs* 44% *P* = 0.59
Nimotuzumab[28]	EGFR	Ⅲ	Locally advanced/ metastatic	18	GEM + nimotuzumab	3.71	9.29	55.50%
Lapatinib[29]	EGFR + Her-2	Ⅱ	Metastatic	17	Lapatinib + capecitabine	2.6	5.2	-
Cixutumumab[30]	IGF-1R	Ⅰb/Ⅱ	Metastatic	116	A: Erlotinib + cixutumumab + GEM B: Erlotinib + GEM	3.6 *vs* 3.6 *P* = 0.97	7.0 *vs* 6.7 *P* = 0.64	12.28% *vs* 15.25%
Cetuximab +Everolimus[31]	EGFR + mTOR	Ⅱ	Locally advanced/ metastatic	31	Everolimus+ cetuximab + capecitabine	-	5.0	22.60%
Cetuximab + trastuzumab[32]	EGFR + Her-2	Ⅰ - Ⅱ	Metastatic	33	Cetuximab + trastuzumab	1.8	4.6	-
Erlotinib + Selumetinib[33]	EGFR + MEK1/2	Ⅱ	Locally advanced/ metastatic	46	Erlotinib + selumetinib	1.9	7.3	-

EGFR: Epidermal growth factor receptor; GEM: Gemcitabine; ORR: Objective response rate.

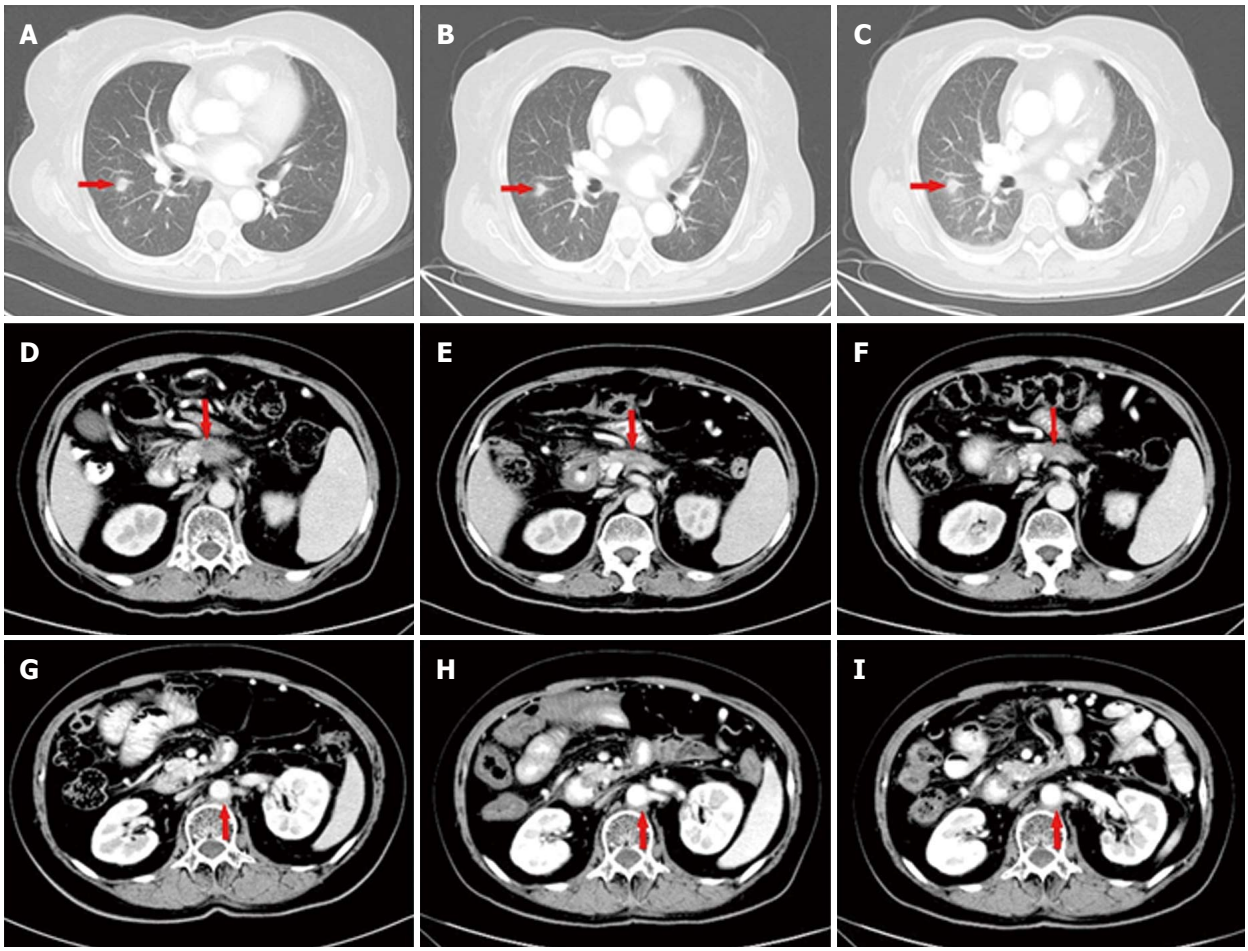

Figure 5 The primary mass in the pancreas shrunk gradually during apatinib treatment: (D) 1.7 cm (E) 1.2 cm (F) 1.0 cm. The metastatic lesions showed no obvious change (A-C; G-I).

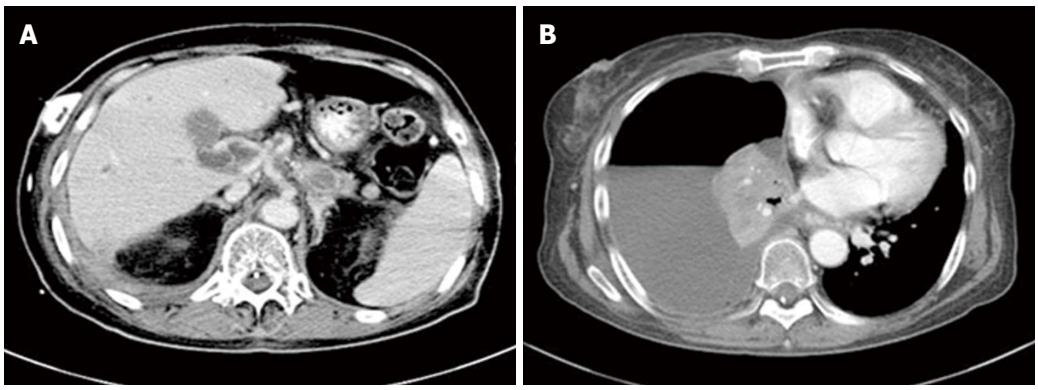

Figure 6 Disease progression. CT scan revealed several metastatic lesions in the liver (A) and pleural effusion (B). CT: Computed tomography.

were treated with erlotinib or cetuximab[26]. Other trials where one[27-30] or a combination of two targeted agents[31-33] were administered for advanced or metastatic PC also did not show significant positive results (Table 1).

Angiogenesis is an essential and significant step in tumor growth as it supplies necessary oxygen, growth factors and nutrients, and is generally considered an attractive target in cancer therapy[34-37]. Some studies have confirmed that PC is indeed angiogenesis-dependent[6-9]. Bevacizumab, an anti-angiogenesis agent, is currently the most frequently studied drug for PC in clinical trials. A double-blind phase Ⅲ trial of bevacizumab in combination with GEM and erlotinib for metastatic PC showed that the addition of bevacizumab led to a statistically significant

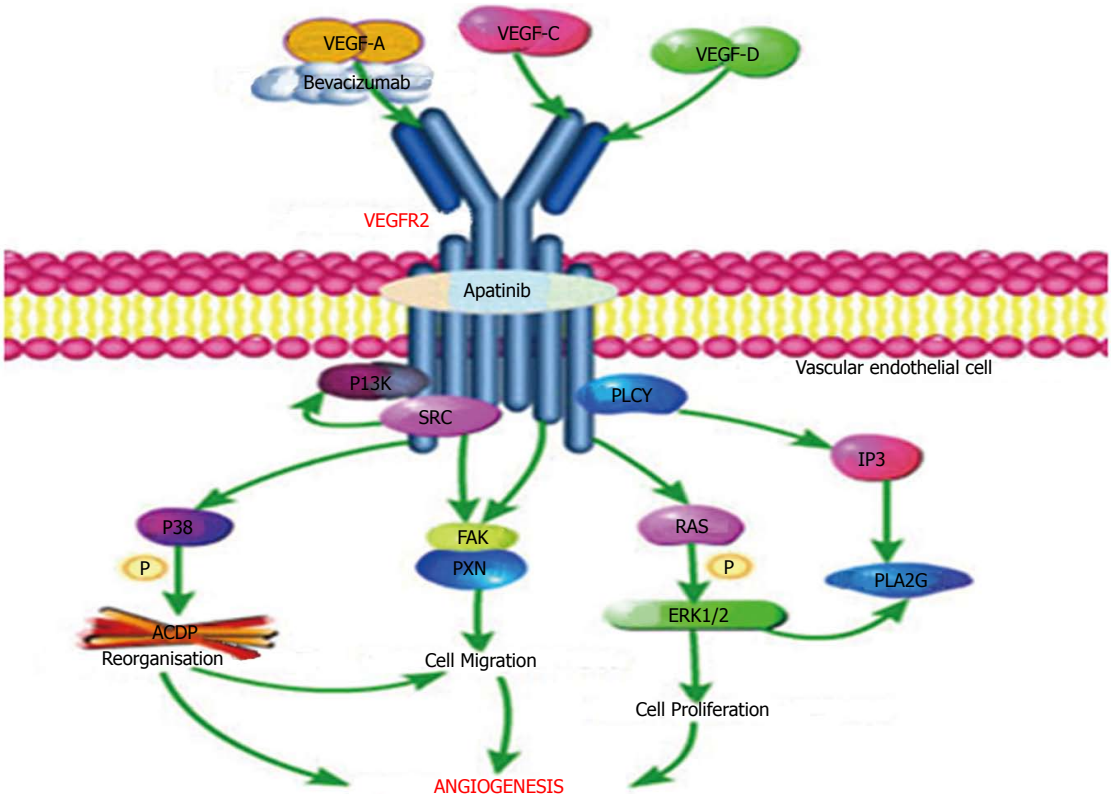

Figure 7 Pathway of VEGFR-2 (produced using the Pathway Builder Tool). Bevacizumab targets VEGF-A to prevent its interaction with VEGFR-2; apatinib mainly targets VEGFR-2. VEGF: Vascular endothelial growth factor; VEGFR: Vascular endothelial growth factor receptor.

improvement in PFS (P = 0.0002). However, there was no significant improvement in OS (7.1 mo *vs* 6.0 mo, P = 0.2087)[38]. Moreover, in the CALGB 80303 trial[39], median PFS and ORR were similar in the two treatment arms (for PFS, 3.8 mo *vs* 2.9 mo, P = 0.07; for ORR, 13% *vs* 10%, respectively). However, in the subgroup analysis, the median survival was 7.9 mo in PS 0 patients, 4.8 mo in PS 1 patients and only 2.4 mo in PS 2 patients. These findings suggested that bevacizumab is much more effective in PS 0 and 1 patients. In another Phase Ⅱ study[40] of bevacizumab combined with chemotherapy, median PFS was 5.9 mo and median OS was 7.4 mo. Partial response and stable disease occurred in 30% and 45% of patients, respectively, which met the study's primary endpoint. These studies[39-41] demonstrated that further efforts should be focused on identifying subsets of PC patients who are more likely to benefit from bevacizumab. These findings indicate that anti-angiogenesis treatment has great potential in PC.

Tumors produce various angiogenic factors and cytokines to induce angiogenesis, which is essential for tumor growth. Among these tumor-derived factors, the VEGF family including VEGF-A to -D was initially identified as endothelial cell-specific mitogens with the ability to induce physiologic and pathologic angiogenesis[42-46]. It has been reported that VEGF displays these broad vascular functions by the binding and activation of VEGFR[46-49], especially VEGFR-2[50-52], mainly expressed in vascular endothelial cells. As described in Figure 7, bevacizumab, a humanized monoclonal antibody that only targets VEGF-A to prevent its interaction with VEGFR-2, was the first targeted antiangiogenic agent approved for use in oncology[53]. Apatinib, the first generation of oral anti-angiogenesis drugs, mainly targets VEGFR-2 through the intracellular ATP-binding site that inhibits all VEGF-stimulated endothelial cell migration and proliferation, decreases tumor microvascular density and promotes apoptosis[11,54,55]. Therefore, it seems that apatinib may have more potential in anti-angiogenesis than bevacizumab by affecting the VEGFR-2 pathway of angiogenesis.

Apatinib shows antitumor efficacy and good tolerance in mice when administered alone or in combination with chemotherapeutic drugs against a broad range of human tumor xenografts[15]. In patients with advanced gastric or gastroesophageal junction adenocarcinoma, a Phase Ⅱ study[16] and a Phase Ⅲ study[20] showed that both OS and median PFS were significantly improved in the apatinib group. Furthermore, other clinical trials[17,56] concluded that apatinib has substantial clinical activity without significant additional toxicity in patients with advanced

non-squamous and non-small cell lung cancer and hepatocellular carcinoma. Whether apatinib has an important role in the treatment of PC is unknown.

The reason for the use of apatinib in our case were unsatisfactory treatment efficacy after the fourth-line chemotherapy, but the patient still wished to continue the treatment. According to the general condition of the patient who had a PS 2, she was treated with apatinib at a daily dose of 500 mg. After 15 d of apatinib treatment, the CA19-9 level decreased sharply from 302.3 U/mL to 88.8 U/mL. Following a period of treatment, the primary mass was reduced in size and other metastatic diseases were well controlled for 7 mo. Although this is an individual case, apatinib did demonstrate its curative effect in PC. As an anti-angiogenesis therapy, it seems that apatinib may be effective in the treatment of PC.

Here, we report the first case of PC which responded to apatinib. It seems that apatinib may provide an additional option for the targeted treatment of PC. Nevertheless, further large-scale prospective studies on apatinib are required to verify its efficacy in the treatment of PC.

COMMENTS

Case characteristics

A 58-year-old woman with no significant medical history attended our hospital complaining of persistent pain in the upper abdomen and back, following dyspepsia for approximately 4 d.

Clinical diagnosis

Physical examination suggested tenderness in her upper abdomen but without rebound pain.

Differential diagnosis

Pancreatitis, pancreatic neuroendocrine tumor, cholecystitis, ampullary carcinoma.

Laboratory diagnosis

The serum carbohydrate antigen 19-9 level was 148 U/mL when diagnosed.

Imaging diagnosis

Computed tomography revealed a 3.1 cm × 1.7 cm mass at the body of the pancreas, and an enlarged lymph node was detected behind the aorta abdominalis. ^{18}F-FDG positron emission tomography displayed a mass in the body of the pancreas with an SUV of 6.2 and an enlarged lymph node with an SUV of 4.8.

Pathological diagnosis

Moderately differentiated adenocarcinoma.

Treatment

Chemotherapy, radiotherapy, and targeted therapy.

Related reports

Recently, many targeted drugs for pancreatic cancer have been studied. Erlotinib is the only targeted drug approved by the Federal Drug Administration to treat pancreatic cancer. Apatinib, the first generation of oral anti-angiogenesis drugs, mainly targets vascular endothelial growth factor receptor-2 (VEGFR-2). In patients with advanced gastric or gastroesophageal junction adenocarcinoma, a Phase Ⅱ study and a Phase Ⅲ study showed that both overall survival and median progression-free survival were significantly improved in the apatinib group. Furthermore, other clinical trials concluded that apatinib has substantial clinical activity without significant additional toxicity in patients with advanced non-squamous and non-small cell lung cancer and hepatocellular carcinoma. Therefore, apatinib seems have potential in anti-angiogenesis by affecting the VEGFR-2 pathway of angiogenesis.

Term explanation

Apatinib, also known as YN968D1, is a multiple kinase inhibitor with *in vitro* activity against VEGFR-2, PDGFR-beta, c-Kit, and c-src.

Experiences and lessons

Apatinib may provide an additional option for the targeted treatment of pancreatic cancer, and further large-scale prospective studies on apatinib are required to verify its efficacy in the treatment of pancreatic cancer.

Peer-review

In this study, it showed that apatinib, a first-generation anti-angiogenesis drug targeting VEGFR-2, indeed improved the life of a patient with metastatic pancreatic cancer.

ACKNOWLEDGMENTS

We thank our colleagues from Shandong Cancer Hospital for the treatment of this case, and the patient and her family members who agreed to publication of this case.

REFERENCES

1 **Ferlay J**, Soerjomataram I, Dikshit R, Eser S, Mathers C, Rebelo M, Parkin DM, Forman D, Bray F. Cancer incidence and mortality worldwide: sources, methods and major patterns in GLOBOCAN 2012. *Int J Cancer* 2015; **136**: E359-E386 [PMID: 25220842 DOI: 10.1002/ijc.29210]

2 **Tempero MA**, Malafa MP, Behrman SW, Benson AB 3rd, Casper ES, Chiorean EG, Chung V, Cohen SJ, Czito B, Engebretson A, Feng M, Hawkins WG, Herman J, Hoffman JP, Ko A, Komanduri S, Koong A, Lowy AM, Ma WW, Merchant NB, Mulvihill SJ, Muscarella P 2nd, Nakakura EK, Obando J, Pitman MB, Reddy S, Sasson AR, Thayer SP, Weekes CD, Wolff RA, Wolpin BM, Burns JL, Freedman-Cass DA. Pancreatic adenocarcinoma, version 2.2014: featured updates to the NCCN guidelines. *J Natl Compr Canc Netw* 2014; **12**: 1083-1093 [PMID: 25099441]

3 **Moore MJ**, Goldstein D, Hamm J, Figer A, Hecht JR, Gallinger S, Au HJ, Murawa P, Walde D, Wolff RA, Campos D, Lim R, Ding K, Clark G, Voskoglou-Nomikos T, Ptasynski M, Parulekar W; National Cancer Institute of Canada Clinical Trials Group. Erlotinib plus gemcitabine compared with gemcitabine alone in patients with advanced pancreatic cancer: a phase III trial of the National Cancer Institute of Canada Clinical Trials Group. *J Clin Oncol* 2007; **25**: 1960-1966 [PMID: 17452677 DOI: 10.1200/JCO.2006.07.9525]

4 **Conroy T**, Desseigne F, Ychou M, Bouché O, Guimbaud R, Bécouarn Y, Adenis A, Raoul JL, Gourgou-Bourgade S, de la Fouchardière C, Bennouna J, Bachet JB, Khemissa-Akouz F, Péré-Vergé D, Delbaldo C, Assenat E, Chauffert B, Michel P, Montoto-Grillot C, Ducreux M; Groupe Tumeurs Digestives of Unicancer; PRODIGE Intergroup. FOLFIRINOX versus gemcitabine for metastatic pancreatic cancer. *N Engl J Med* 2011; **364**: 1817-1825 [PMID: 21561347 DOI: 10.1056/NEJMoa1011923]

5 **Burris HA 3rd**, Moore MJ, Andersen J, Green MR, Rothenberg ML, Modiano MR, Cripps MC, Portenoy RK, Storniolo AM, Tarassoff P, Nelson R, Dorr FA, Stephens CD, Von Hoff DD. Improvements in survival and clinical benefit with gemcitabine as first-line therapy for patients with advanced pancreas cancer: a randomized trial. *J Clin Oncol* 1997; **15**: 2403-2413 [PMID: 9196156 DOI: 10.1200/JCO.1997.15.6.2403]

6 **Kuwahara K**, Sasaki T, Kuwada Y, Murakami M, Yamasaki S, Chayama K. Expressions of angiogenic factors in pancreatic ductal carcinoma: a correlative study with clinicopathologic parameters and patient survival. *Pancreas* 2003; **26**: 344-349 [PMID: 12717266]

7 **Kisker O**, Onizuka S, Banyard J, Komiyama T, Becker CM, Achilles EG, Barnes CM, O'Reilly MS, Folkman J, Pirie-Shepherd SR. Generation of multiple angiogenesis inhibitors by human pancreatic cancer. *Cancer Res* 2001; **61**: 7298-7304 [PMID: 11585769]

8 **Ikeda N**, Adachi M, Taki T, Huang C, Hashida H, Takabayashi A, Sho M, Nakajima Y, Kanehiro H, Hisanaga M, Nakano H, Miyake M. Prognostic significance of angiogenesis in human pancreatic cancer. *Br J Cancer* 1999; **79**: 1553-1563 [PMID: 10188906 DOI: 10.1038/sj.bjc.6690248]

9 **Chung GG**, Yoon HH, Zerkowski MP, Ghosh S, Thomas L, Harigopal M, Charette LA, Salem RR, Camp RL, Rimm DL, Burtness BA. Vascular endothelial growth factor, FLT-1, and FLK-1 analysis in a pancreatic cancer tissue microarray. *Cancer* 2006; **106**: 1677-1684 [PMID: 16532435 DOI: 10.1002/cncr.21783]

10 **Solorzano CC**, Baker CH, Bruns CJ, Killion JJ, Ellis LM, Wood J, Fidler IJ. Inhibition of growth and metastasis of human pancreatic cancer growing in nude mice by PTK 787/ZK222584, an inhibitor of the vascular endothelial growth factor receptor tyrosine kinases. *Cancer Biother Radiopharm* 2001; **16**: 359-370 [PMID: 11776753 DOI: 10.1089/108497801753354267]

11 **Büchler P**, Reber HA, Ullrich A, Shiroiki M, Roth M, Büchler MW, Lavey RS, Friess H, Hines OJ. Pancreatic cancer growth is inhibited by blockade of VEGF-RII. *Surgery* 2003; **134**: 772-782 [PMID: 14639356 DOI: 10.1016/S0039-6060(03)00296-4]

12 **Guo P**, Hu B, Gu W, Xu L, Wang D, Huang HJ, Cavenee WK, Cheng SY. Platelet-derived growth factor-B enhances glioma angiogenesis by stimulating vascular endothelial growth factor expression in tumor endothelia and by promoting pericyte recruitment. *Am J Pathol* 2003; **162**: 1083-1093 [PMID: 12651601 DOI: 10.1016/S0002-9440(10)63905-3]

13 **Yamagishi S**, Yonekura H, Yamamoto Y, Fujimori H, Sakurai S, Tanaka N, Yamamoto H. Vascular endothelial growth factor acts as a pericyte mitogen under hypoxic conditions. *Lab Invest* 1999; **79**: 501-509 [PMID: 10212003]

14 **Wilhelm SM**, Carter C, Tang L, Wilkie D, McNabola A, Rong H, Chen C, Zhang X, Vincent P, McHugh M, Cao Y, Shujath J, Gawlak S, Eveleigh D, Rowley B, Liu L, Adnane L, Lynch M, Auclair D, Taylor I, Gedrich R, Voznesensky A, Riedl B, Post LE, Bollag G, Trail PA. BAY 43-9006 exhibits broad spectrum oral antitumor activity and targets the RAF/MEK/ERK pathway and receptor tyrosine kinases involved in tumor progression and angiogenesis. *Cancer Res* 2004; **64**: 7099-7109 [PMID: 15466206 DOI: 10.1158/0008-5472.CAN-04-1443]

15 **Tian S**, Quan H, Xie C, Guo H, Lü F, Xu Y, Li J, Lou L. YN968D1 is a novel and selective inhibitor of vascular endothelial growth factor receptor-2 tyrosine kinase with potent activity in vitro and in vivo. *Cancer Sci* 2011; **102**: 1374-1380 [PMID: 21443688 DOI: 10.1111/j.1349-7006.2011.01939.x]

16 **Li J**, Qin S, Xu J, Guo W, Xiong J, Bai Y, Sun G, Yang Y, Wang L, Xu N, Cheng Y, Wang Z, Zheng L, Tao M, Zhu X, Ji D, Liu X, Yu H. Apatinib for chemotherapy-refractory advanced metastatic gastric cancer: results from a randomized, placebo-controlled, parallel-arm, phase II trial. *J Clin Oncol* 2013; **31**: 3219-3225 [PMID: 23918952 DOI: 10.1200/JCO.2013.48.8585]

17 **Li J**, Qin S, Xu J, Xiong J, Wu C, Bai Y, Liu W, Tong J, Liu Y, Xu R, Wang Z, Wang Q, Ouyang X, Yang Y, Ba Y, Liang J, Lin X, Luo D, Zheng R, Wang X, Sun G, Wang L, Zheng L, Guo H, Wu J, Xu N, Yang J, Zhang H, Cheng Y, Wang N, Chen L, Fan Z, Sun P, Yu H. Randomized, Double-Blind, Placebo-Controlled Phase III Trial of Apatinib in Patients With Chemotherapy-Refractory Advanced or Metastatic Adenocarcinoma of the Stomach or Gastroesophageal Junction. *J Clin Oncol* 2016; **34**: 1448-1454 [PMID: 26884585 DOI: 10.1200/JCO.2015.63.5995]

18 **Scott AJ**, Messersmith WA, Jimeno A. Apatinib: a promising oral antiangiogenic agent in the treatment of multiple solid tumors. *Drugs Today* (Barc) 2015; **51**: 223-229 [PMID: 26020064 DOI: 10.1358/dot.2015.51.4.2320599]

19 **Hu X**, Cao J, Hu W, Wu C, Pan Y, Cai L, Tong Z, Wang S, Li J, Wang Z, Wang B, Chen X, Yu H. Multicenter phase II study of apatinib in non-triple-negative metastatic breast cancer. *BMC Cancer* 2014; **14**: 820 [PMID: 25376790 DOI: 10.1186/1471-2407-14-820]

20 **Hu X**, Zhang J, Xu B, Jiang Z, Ragaz J, Tong Z, Zhang Q, Wang X, Feng J, Pang D, Fan M, Li J, Wang B, Wang Z, Zhang Q, Sun S, Liao C. Multicenter phase II study of apatinib, a novel VEGFR inhibitor in heavily pretreated patients with metastatic triple-negative breast cancer. *Int J Cancer* 2014; **135**: 1961-1969 [PMID: 24604288 DOI: 10.1002/ijc.28829]

21 **Liu L**, Yu H, Huang L, Shao F, Bai J, Lou D, Chen F. Progression-free survival as a surrogate endpoint for overall survival in patients with third-line or later-line chemotherapy for advanced gastric cancer. *Onco Targets Ther* 2015; **8**: 921-928 [PMID: 25960663 DOI: 10.2147/OTT.S82365]

22 **Vaccaro V**, Sperduti I, Milella M. FOLFIRINOX versus gemcitabine for metastatic pancreatic cancer. *N Engl J Med* 2011; **365**: 768-769; author reply 769 [PMID: 21864184 DOI: 10.1056/NEJMc1107627]

23 **Von Hoff DD**, Ervin T, Arena FP, Chiorean EG, Infante J, Moore M, Seay T, Tjulandin SA, Ma WW, Saleh MN, Harris M, Reni M, Dowden S, Laheru D, Bahary N, Ramanathan RK, Tabernero J, Hidalgo M, Goldstein D, Van Cutsem E, Wei X, Iglesias J, Renschler MF. Increased survival in pancreatic cancer with nab-paclitaxel plus gemcitabine. *N Engl J Med* 2013; **369**: 1691-1703 [PMID: 24131140 DOI: 10.1056/NEJMoa1304369]

24 **Cardin DB**, Goff L, Li CI, Shyr Y, Winkler C, DeVore R, Schlabach L, Holloway M, McClanahan P, Meyer K, Grigorieva J, Berlin J, Chan E. Phase II trial of sorafenib and erlotinib in advanced pancreatic cancer. *Cancer Med* 2014; **3**: 572-579 [PMID: 24574334 DOI: 10.1002/cam4.208]

25 **Middleton G**, Palmer DH, Greenhalf W, Ghaneh P, Jackson R, Cox T, Evans A, Shaw VE, Wadsley J, Valle JW, Propper D, Wasan H, Falk S, Cunningham D, Coxon F, Ross P, Madhusudan S, Wadd N, Corrie P, Hickish T, Costello E, Campbell F, Rawcliffe C, Neoptolemos JP. Vandetanib plus gemcitabine versus placebo plus gemcitabine in locally advanced or metastatic pancreatic carcinoma (ViP): a prospective, randomised, double-blind, multicentre phase 2 trial. *Lancet Oncol* 2017; **18**: 486-499 [PMID: 28259610 DOI: 10.1016/S1470-2045(17)30084-0]

26 **Ottaiano A**, Capozzi M, De Divitiis C, De Stefano A, Botti G, Avallone A, Tafuto S. Gemcitabine mono-therapy versus gemcitabine plus targeted therapy in advanced pancreatic cancer: a meta-analysis of randomized phase III trials. *Acta Oncol* 2017; **56**: 377-383 [PMID: 28256961 DOI: 10.1080/0284186X.2017.1288922]

27 **Philip PA**, Benedetti J, Corless CL, Wong R, O'Reilly EM, Flynn PJ, Rowland KM, Atkins JN, Mirtsching BC, Rivkin SE, Khorana AA, Goldman B, Fenoglio-Preiser CM, Abbruzzese JL, Blanke CD. Phase III study comparing gemcitabine plus cetuximab versus

gemcitabine in patients with advanced pancreatic adenocarcinoma: Southwest Oncology Group-directed intergroup trial S0205. *J Clin Oncol* 2010; **28**: 3605-3610 [PMID: 20606093 DOI: 10.1200/JCO.2009.25.7550]

28 **Su D**, Jiao SC, Wang LJ, Shi WW, Long YY, Li J, Bai L. Efficacy of nimotuzumab plus gemcitabine usage as first-line treatment in patients with advanced pancreatic cancer. *Tumour Biol* 2014; **35**: 2313-2318 [PMID: 24142531 DOI: 10.1007/s13277-013-1306-x]

29 **Wu Z**, Gabrielson A, Hwang JJ, Pishvaian MJ, Weiner LM, Zhuang T, Ley L, Marshall JL, He AR. Phase II study of lapatinib and capecitabine in second-line treatment for metastatic pancreatic cancer. *Cancer Chemother Pharmacol* 2015; **76**: 1309-1314 [PMID: 26507197 DOI: 10.1007/s00280-015-2855-z]

30 **Philip PA**, Goldman B, Ramanathan RK, Lenz HJ, Lowy AM, Whitehead RP, Wakatsuki T, Iqbal S, Gaur R, Benedetti JK, Blanke CD. Dual blockade of epidermal growth factor receptor and insulin-like growth factor receptor-1 signaling in metastatic pancreatic cancer: phase Ib and randomized phase II trial of gemcitabine, erlotinib, and cixutumumab versus gemcitabine plus erlotinib (SWOG S0727). *Cancer* 2014; **120**: 2980-2985 [PMID: 25041791 DOI: 10.1002/cncr.28744]

31 **Kordes S**, Richel DJ, Klümpen HJ, Weterman MJ, Stevens AJ, Wilmink JW. A phase I/II, non-randomized, feasibility/safety and efficacy study of the combination of everolimus, cetuximab and capecitabine in patients with advanced pancreatic cancer. *Invest New Drugs* 2013; **31**: 85-91 [PMID: 22367239 DOI: 10.1007/s10637-012-9802-1]

32 **Assenat E**, Azria D, Mollevi C, Guimbaud R, Tubiana-Mathieu N, Smith D, Delord JP, Samalin E, Portales F, Larbouret C, Robert B, Bibeau F, Bleuse JP, Crapez E, Ychou M, Pèlegrin A. Dual targeting of HER1/EGFR and HER2 with cetuximab and trastuzumab in patients with metastatic pancreatic cancer after gemcitabine failure: results of the "THERAPY"phase 1-2 trial. *Oncotarget* 2015; **6**: 12796-12808 [PMID: 25918250 DOI: 10.18632/oncotarget.3473]

33 **Ko AH**, Bekaii-Saab T, Van Ziffle J, Mirzoeva OM, Joseph NM, Talasaz A, Kuhn P, Tempero MA, Collisson EA, Kelley RK, Venook AP, Dito E, Ong A, Ziyeh S, Courtin R, Linetskaya R, Tahiri S, Korn WM. A Multicenter, Open-Label Phase II Clinical Trial of Combined MEK plus EGFR Inhibition for Chemotherapy-Refractory Advanced Pancreatic Adenocarcinoma. *Clin Cancer Res* 2016; **22**: 61-68 [PMID: 26251290 DOI: 10.1158/1078-0432.CCR-15-0979]

34 **Liotta LA**, Steeg PS, Stetler-Stevenson WG. Cancer metastasis and angiogenesis: an imbalance of positive and negative regulation. *Cell* 1991; **64**: 327-336 [PMID: 1703045]

35 **Schuch G**, Kisker O, Atala A, Soker S. Pancreatic tumor growth is regulated by the balance between positive and negative modulators of angiogenesis. *Angiogenesis* 2002; **5**: 181-190 [PMID: 12831059]

36 **Hanahan D**, Folkman J. Patterns and emerging mechanisms of the angiogenic switch during tumorigenesis. *Cell* 1996; **86**: 353-364 [PMID: 8756718]

37 **Costache MI**, Ioana M, Iordache S, Ene D, Costache CA, Săftoiu A. VEGF Expression in Pancreatic Cancer and Other Malignancies: A Review of the Literature. *Rom J Intern Med* 2015; **53**: 199-208 [PMID: 26710495 DOI: 10.1515/rjim-2015-0027]

38 **Van Cutsem E**, Vervenne WL, Bennouna J, Humblet Y, Gill S, Van Laethem JL, Verslype C, Scheithauer W, Shang A, Cosaert J, Moore MJ. Phase III trial of bevacizumab in combination with gemcitabine and erlotinib in patients with metastatic pancreatic cancer. *J Clin Oncol* 2009; **27**: 2231-2237 [PMID: 19307500 DOI: 10.1200/JCO.2008.20.0238]

39 **Kindler HL**, Niedzwiecki D, Hollis D, Sutherland S, Schrag D, Hurwitz H, Innocenti F, Mulcahy MF, O'Reilly E, Wozniak TF, Picus J, Bhargava P, Mayer RJ, Schilsky RL, Goldberg RM. Gemcitabine plus bevacizumab compared with gemcitabine plus placebo in patients with advanced pancreatic cancer: phase III trial of the Cancer and Leukemia Group B (CALGB 80303). *J Clin Oncol* 2010; **28**: 3617-3622 [PMID: 20606091 DOI: 10.1200/JCO.2010.28.1386]

40 **Martin LK**, Li X, Kleiber B, Ellison EC, Bloomston M, Zalupski M, Bekaii-Saab TS. VEGF remains an interesting target in advanced pancreas cancer (APCA): results of a multi-institutional phase II study of bevacizumab, gemcitabine, and infusional 5-fluorouracil in patients with APCA. *Ann Oncol* 2012; **23**: 2812-2820 [PMID: 22767582 DOI: 10.1093/annonc/mds134]

41 **Ko AH**, Dito E, Schillinger B, Venook AP, Xu Z, Bergsland EK, Wong D, Scott J, Hwang J, Tempero MA. A phase II study evaluating bevacizumab in combination with fixed-dose rate gemcitabine and low-dose cisplatin for metastatic pancreatic cancer: is an anti-VEGF strategy still applicable? *Invest New Drugs* 2008; **26**: 463-471 [PMID: 18379729 DOI: 10.1007/s10637-008-9127-2]

42 **Ferrara N**, Gerber HP, LeCouter J. The biology of VEGF and its receptors. *Nat Med* 2003; **9**: 669-676 [PMID: 12778165 DOI: 10.1038/nm0603-669]

43 **Cao Y**. Positive and negative modulation of angiogenesis by VEGFR1 ligands. *Sci Signal* 2009; **2**: re1 [PMID: 19244214 DOI: 10.1126/scisignal.259re1]

44 **Leung DW**, Cachianes G, Kuang WJ, Goeddel DV, Ferrara N. Vascular endothelial growth factor is a secreted angiogenic mitogen. *Science* 1989; **246**: 1306-1309 [PMID: 2479986]

45 **Dvorak HF**. Vascular permeability factor/vascular endothelial growth factor: a critical cytokine in tumor angiogenesis and a potential target for diagnosis and therapy. *J Clin Oncol* 2002; **20**: 4368-4380 [PMID: 12409337 DOI: 10.1200/JCO.2002.10.088]

46 **Kieran MW**, Kalluri R, Cho YJ. The VEGF pathway in cancer and disease: responses, resistance, and the path forward. *Cold Spring Harb Perspect Med* 2012; **2**: a006593 [PMID: 23209176 DOI: 10.1101/cshperspect.a006593]

47 **Carmeliet P**, Jain RK. Angiogenesis in cancer and other diseases. *Nature* 2000; **407**: 249-257 [PMID: 11001068 DOI: 10.1038/35025220]

48 **Coultas L**, Chawengsaksophak K, Rossant J. Endothelial cells and VEGF in vascular development. *Nature* 2005; **438**: 937-945 [PMID: 16355211 DOI: 10.1038/nature04479]

49 **Glade-Bender J**, Kandel JJ, Yamashiro DJ. VEGF blocking therapy in the treatment of cancer. *Expert Opin Biol Ther* 2003; **3**: 263-276 [PMID: 12662141 DOI: 10.1517/14712598.3.2.263]

50 **Gille H**, Kowalski J, Li B, LeCouter J, Moffat B, Zioncheck TF, Pelletier N, Ferrara N. Analysis of biological effects and signaling properties of Flt-1 (VEGFR-1) and KDR (VEGFR-2). A reassessment using novel receptor-specific vascular endothelial growth factor mutants. *J Biol Chem* 2001; **276**: 3222-3230 [PMID: 11058584 DOI: 10.1074/jbc.M002016200]

51 **Hamerlik P**, Lathia JD, Rasmussen R, Wu Q, Bartkova J, Lee M, Moudry P, Bartek J Jr, Fischer W, Lukas J, Rich JN, Bartek J. Autocrine VEGF-VEGFR2-Neuropilin-1 signaling promotes glioma stem-like cell viability and tumor growth. *J Exp Med* 2012; **209**: 507-520 [PMID: 22393126 DOI: 10.1084/jem.20111424]

52 **Ferrara N**. Role of vascular endothelial growth factor in regulation of physiological angiogenesis. *Am J Physiol Cell Physiol* 2001; **280**: C1358-C1366 [PMID: 11350730]

53 **Ferrara N**, Hillan KJ, Gerber HP, Novotny W. Discovery and development of bevacizumab, an anti-VEGF antibody for treating cancer. *Nat Rev Drug Discov* 2004; **3**: 391-400 [PMID: 15136787 DOI: 10.1038/nrd1381]

54 **Peng H**, Zhang Q, Li J, Zhang N, Hua Y, Xu L, Deng Y, Lai J, Peng Z, Peng B, Chen M, Peng S, Kuang M. Apatinib inhibits VEGF signaling and promotes apoptosis in intrahepatic cholangiocarcinoma. *Oncotarget* 2016; **7**: 17220-17229 [PMID: 26967384 DOI: 10.18632/oncotarget.7948]

55 **Peng S**, Zhang Y, Peng H, Ke Z, Xu L, Su T, Tsung A, Tohme

S, Huang H, Zhang Q, Lencioni R, Zeng Z, Peng B, Chen M, Kuang M. Intracellular autocrine VEGF signaling promotes EBDC cell proliferation, which can be inhibited by Apatinib. *Cancer Lett* 2016; **373**: 193-202 [PMID: 26805764 DOI: 10.1016/j.canlet.2016.01.015]

56 **Qin S.** Apatinib in Chinese patients with advanced hepatocellular carcinoma: A phase II randomized, open-label trial. Asco Meeting Abstracts. 2014

P- Reviewer: Barreto S, Chowdhury P **S- Editor**: Gong ZM
L- Editor: Filipodia **E- Editor**: Huang Y

World Journal of Gastroenterology

Submit a Manuscript: http://www.f6publishing.com

World J Gastroenterol 2017 November 7; 23(41): 7489-7494

DOI: 10.3748/wjg.v23.i41.7489

ISSN 1007-9327 (print) ISSN 2219-2840 (online)

CASE REPORT

3D-printed "fistula stent" designed for management of enterocutaneous fistula: An advanced strategy

Jin-Jian Huang, Jian-An Ren, Ge-Fei Wang, Zong-An Li, Xiu-Wen Wu, Hua-Jian Ren, Song Liu

Jin-Jian Huang, Jian-An Ren, Ge-Fei Wang, Xiu-Wen Wu, Hua-Jian Ren, Department of Surgery, Jinling Hospital, Nanjing 210002, Jiangsu Province, China

Jin-Jian Huang, School of Medicine, Southeast University, Nanjing 210009, Jiangsu Province, China

Zong-An Li, NARI School of Electrical and Automation Engineering, Nanjing Normal University, Nanjing 210042, Jiangsu Province, China

Song Liu, Department of General Surgery, Nanjing Drum Tower Hospital, Nanjing 210008, Jiangsu Province, China

ORCID number: Jin-Jian Huang (0000-0002-8951-8935); Jian-An Ren (0000-0002-4697-4762); Ge-Fei Wang (0000-0002-6017-2291); Zong-An Li (0000-0002-3580-5891); Xiu-Wen Wu (0000-0001-5319-2665); Hua-Jian Ren (0000-0002-2205-4072); Song Liu (0000-0002-4780-9697).

Author contributions: Huang JJ and Ren JA designed this report; Wang GF performed the 3D-reconstructed fistulography; Huang JJ and Li ZA fabricated this 3D-printed fistula stent; Ren JA and Ren HJ implanted the fistula stent; Wu XW and Liu S followed up the patient and recorded his medical information.

Supported by the National Natural Science Foundation of China, No. 81571881.

Informed consent statement: Written informed consent was obtained from the patient.

Conflict-of-interest statement: We declared no potential conflicts of interest with respect to the research, authorship and publication of this article.

Manuscript source: Unsolicited manuscript

Correspondence to: Jian-An Ren, MD, FACS, Director, Department of Surgery, Jinling Hospital, 305 East Zhongshan Road, Nanjing 210002, Jiangsu Province, China. jiananr@gmail.com
Telephone: +86-13605169808
Fax: +86-25-80860376

Received: September 19, 2017
Peer-review started: September 20, 2017
First decision: September 27, 2017
Revised: September 29, 2017
Accepted: October 18, 2017
Article in press: October 17, 2017
Published online: November 7, 2017

Abstract

Enterocutaneous fistulas (ECFs) are great challenges during the open abdomen. The loss of digestive juice, water-electrolyte imbalance and malnutrition are intractable issues during management of ECF. Techniques such as "fistula patch" and vacuum-assisted closure therapy have been applied to prevent contamination of open abdominal wounds by intestinal fistula drainage. However, failures are encountered due to high-output fistula and anatomical complexity. Here, we report 3D-printed patient-personalized fistula stent for ECF treatment based on 3D reconstruction of the fistula image. Subsequent follow-up demonstrated that this stent was well-implanted and effective to reduce the volume of enteric fistula effluent.

Key words: Enterocutaneous fistula; 3D printing; Open abdomen; Isolation technique

Core tip: There are few reports about how to manage enterocutaneous fistulas (ECFs) after open abdomen, especially those that are unlikely to achieve spontaneous closure. This case report describes how to use 3D printing technique to fabricate a fistula stent in accordance with the ECF anatomy, and how the stent can improve enteric effluent, patient's nutrition and physical strength, and surrounding wound inflammation.

Huang JJ, Ren JA, Wang GF, Li ZA, Wu XW, Ren HJ, Liu S. 3D-printed "fistula stent" designed for management of enterocutaneous fistula: An advanced strategy. *World J Gastroenterol* 2017; 23(41): 7489-7494 Available from: URL: http://www.wjgnet.com/1007-9327/full/v23/i41/7489.htm DOI: http://dx.doi.org/10.3748/wjg.v23.i41.7489

INTRODUCTION

Enterocutaneous fistula (ECF) is defined as an abnormal, unintentional connection between the gastrointestinal (GI) tract and the skin or the GI tract and the atmosphere (enteroatmospheric fistula, EAF) in the open abdomen (OA)[1]. Protective strategies such as Bogota bag, mesh products, Wittman patch and vacuum-assisted closure (VAC) therapy have been devised, which nevertheless fail to prevent the occurrence of ECF with an incidence of 5.7%-54.5%[2]. Patients with ECF have life-threatening malnutrition and sepsis, with a mortality rate 6%-33%[3].

Since the enteric effluent consists of pancreatic fluid, bile and intestinal secretions, uncontrolled effluent of ECF leads to repeated inflammation of surrounding skin. In addition, the loss of excessive digestive juice adds to the severity of water-electrolyte imbalance. Therefore, controlling the enteric effluent has become the key step during the management of ECF[4].

Recent progress of negative pressure wound therapy (NPWT) has been achieved in OA management, which could significantly improve the healing process and induce spontaneous fistula closure. However, it appears to be impossible for the ECF to achieve spontaneous closure with mucosal protrusion[5]. For those who are unlikely to achieve spontaneous closure, definitive fistula resection is required after relief from all (or most) associated complications, and the abdominal cavity has become a less hostile environment. For this purpose, we introduced a novel isolation technique using 3D-printed "fistula stent" designed from 3D reconstruction of the fistula image to prevent the loss of enteric effluent.

CASE REPORT

A 45-year-old man was admitted to the local hospital after a traffic accident on January 2, 2017. His abdomen was struck directly by the handlebar of a motorcycle. Physical examination revealed abdominal tenderness and pelvic deformity. X-ray imaging suggested digestive tract perforation and pelvic fracture. Emergency laparotomy found two lesions of GI tract rupture that were surgically repaired. Pelvic fracture fixation was performed as well. On postoperative day 1, the patient presented with high fever, chill, dysphoria and fluid leakage from the surgical incision, which was confirmed as digestive juice by amylase. The patient was immediately transferred to the First Affiliated Hospital of Zhengzhou University. After carrying out open abdomen and double-pipe drainage, and administration of antibacterial agents, antacids and parenteral nutrition, the symptoms were relieved. However, the fistula did not show any tendency to achieve spontaneous closure and the surrounding tissues were severely contaminated by enteric effluent. Therefore, the patient was transferred to our hospital on June 8.

In order to reduce the surrounding tissue inflammation and maintain homeostasis, we tried to implant the "fistula patch" to block the enteric effluent[6], but failed because the patch did not match with the structure of the ECF. After investigating the anatomy of the ECF using 3D-reconstructed fistulography of contrast-mediated, high-resolution CT scanning, we found an angled GI tract connecting the ECF (Figure 1A and B, Supplementary Figure 1). In this case, fistula patch did not fit the shape of the GI tract. Therefore, we set our sights on the advanced technique of 3D printing. Two parameters were measured on the 3D reconstructive image: (1) the diameters of the proximal and distal GI tract (15 mm and 12 mm, respectively); (2) the angle between the proximal and distal GI tract (105°). These parameters were used to design a model of the fistula stent using Solidwork software (Supplementary Figure 2), followed by saving as an STL file for recognition by the 3D printer.

Thermoplastic urethane (TPU) is a biocompatible material with flexible mechanical properties, and has been used in medical devices such as catheters, pace-maker leads and vascular grafts[7]. TPU fuses at 230-260 ℃ and is deposited at room temperature. Therefore, TPU was chosen as the raw material to print the fistula stent. TPU powder of pharmaceutical grade was purchased from Shanghai JiangLai CO. LTD and processed into filaments using hot extrusion machine.

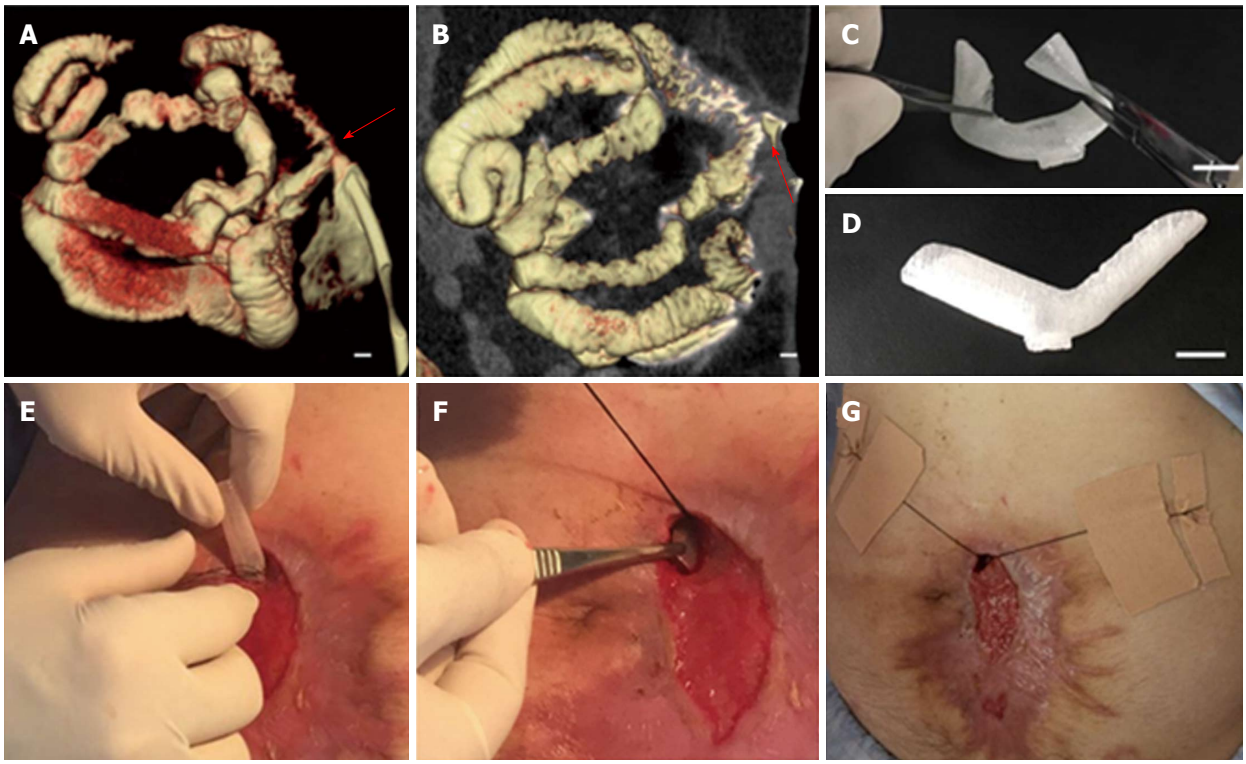

Figure 1 Fabrication and implantation of 3D-printed fistula stent. A and B: 3D-reconstructed fistulography of the ECF: the diameters of the proximal and distal GI tract were 15 mm and 12 mm, respectively, bar = 1 mm (red arrow: ECF); C: Flexibility of fistula stent made of TPU, bar = 15 mm; D: Shape memory of the fistula stent after application of an external force, bar = 15 mm; E and G: The process of the fistula stent implantation. ECF: Enterocutaneous fistula.

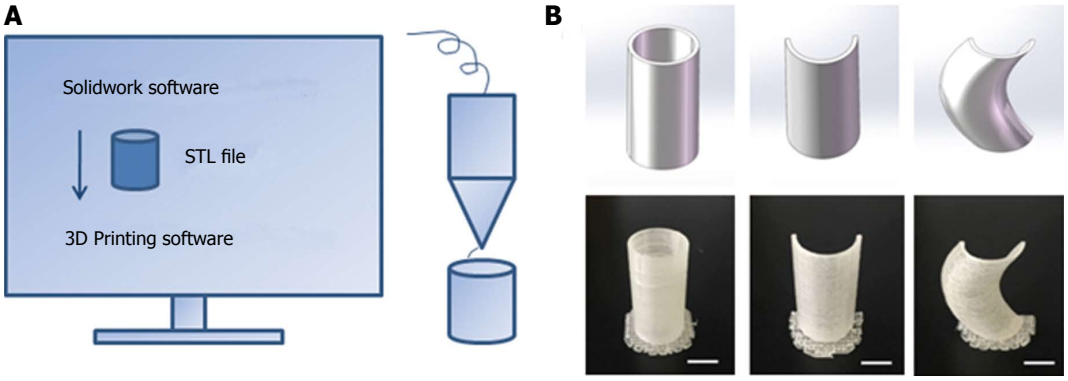

Figure 2 3D printing technique. A: Schematic diagram of the 3D printing technique; B: 3D-printed models: Column, semi-column and tortuous semi-column, bar = 1 cm.

A 3D printer of FDM pattern was used to print the fistula stent from STL file (Video 1). The 3D printing technique was capable of making the real product from the designed image regardless of the column, semi-column and tortuous semi-column (Figure 2). The stent was also consistent with the design, and had the ability to bend (Figure 1C) and recover (Figure 1D) the shape. A protuberance was located at the corner of the stent for sewing and immobilization.

The safety of the stent was detected using MTT assay[8]. Generally, the leachate was obtained by immersion of stent in 10 mL DMEM with 10% FBS. 10×10^4 fibroblasts (L929) was seeded into 200 μL fresh DMED or 200 μL leachate in a 96-well plate, followed by incubation at 37 ℃ for 24 h, 48 hand 72 h. Then, MTT (5 mg/mL) reagent was added to each well and further incubated for 4 h. Afterwards, the formazan salt was dissolved with 200 μL DMSO. As soon as thoroughly dissolved, the solution was added to a new plate and measured with a microplate Spectrophotometer at 570 nm (n = 3). As shown in Supplementary Figure 3, the result indicated the leachate of stent did not influence the cell viability and exhibited a good biocompatibility.

The fistula stent was trimmed on its two sides. It was then implanted through the fistula orifice,

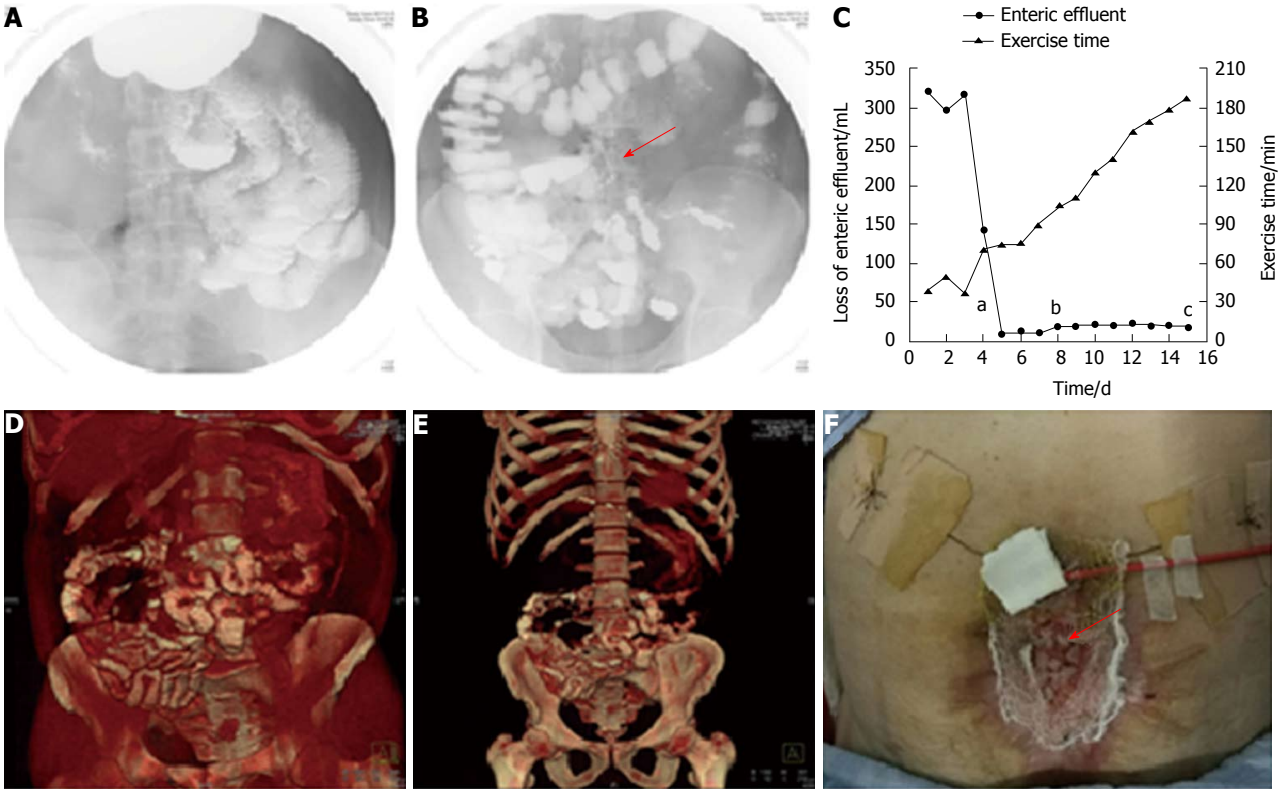

Figure 3 Follow-up after stent implantation. A: Image of small intestine after barium meal, indicating no obstruction; B: Image of colon after barium meal, indicating that contrast passed through the stent smoothly (red arrow: fistula stent); C: Loss of enteric effluent and the time of exercise tolerance before and after stent implantation. [a]Time point of stent insertion; [b]Time point of starting EN; [c]Time point of skin transplantation; D and E: 3D-reconstructed images after barium meal, indicating no abnormity after starting EN; G: Skin transplantation for abdominal wall reconstruction (red arrow: skin graft). EN: Enteral nutrition.

and fixed with threads and adhesive tapes on June 17(Figure 1E-G, Video 2).

Two days after implantation, a barium meal examination was carried out to investigate patency of the GI tract. The barium was able to pass through the GI tract smoothly without obstruction (Figure 3A), and the fistula stent was ambiguously displayed (Figure 3B). Therefore, octreotide was stopped and enteral nutrition (EN) began on June 21 to prepare for the future definitive fistula resection. On June 26, a barium meal indicated that the bowel was well tolerated to EN without obstruction (Figure 3D and E). The loss of enteric effluent was recorded from 3 d before implantation. At that point, the amount of lost enteric effluent was calculated using the following formula: $V_{loss} = V_{drainage} - V_{irrigation}$; where $V_{drainage}$ represented the amount of drainage fluid from the fistula orifice, and $V_{irrigation}$ the volume of fistula irrigation fluid. After stent insertion, the V_{loss} was equivalent to the amount of drainage fluid as follows: $V_{loss} = V_{drainage}$. As shown in Figure 3C, the patient presented with low output ECF (< 500 mL/24 h) before implantation. On the day of implantation, V_{loss} was significantly decreased. Subsequently, the loss of enteric effluent was maintained at a low level even when EN was administered. Leakage of enteric effluent only occurred during postural change, especially from standing to lying. Simply lying, standing or walking did not lead to the leakage. In that case, it was convenient to remove the leaked enteric effluent and take good care of the surrounding granulation tissues. The patient had greater tolerance to physical rehabilitation, potentially due to reduced loss of enteric effluent and regaining EN. Abdominal wall reconstruction was performed by skin transplantation (Figure 3F) and the skin graft survived after 7 d. Afterwards, the patient was discharged to a rehabilitation center for wound healing and future ECF resection. On September 20, the patient received ECF resection and was discharged 10 d later.

DISCUSSION

In this report, we described a novel fistula stent using both 3D reconstruction of an ECF image and 3D printing technique. The fistula stent complied with the complicated ECF anatomy. Two points are very important to design the stent: bowel diameters and angle.

This method is an ideal supplement to NPWT

techniques since the stent can create an isolated environment for ECFs that cannot achieve spontaneous closure. Compared with our previous plugging strategies such as fistula patch and fibrin glue[9], this fistula stent complies with the shape and direction of the ECF, which leads to less mechanical damage to the surrounding GI mucosa. Moreover, it could reduce the loss of enteric effluent, thus preventing water-electrolyte imbalance. It has been reported that fistuloclysis lessens the loss of enteric effluent *via* collecting the proximal ECF output and reinfusing through the fistula feeding tube[3]. However, it still has several disadvantages such as distal location of the fistula, inability to cannulate the fistula to obtain distal enteral access, or rejection by patients to infuse the enteric contents after they have left the body. The fistula stent was capable of overcoming these difficulties by its patient-personalized design and restoration of GI tract integrity.

Rebibo *et al*[10] reported a new treatment to manage ECFs by stent placement under the endoscopic guidance in patients with terminal ileostomy. However, their method was different from the fistula stent in our study. First, it was not necessary for us to enroll patients with terminal ileostomy because the stent was short and flexible enough for implantation. Second, the process of the implantation was simpler. Third, the cross-section of our stent was not a full circle, which meant less GI mucosa was influenced by this intervention. Based on the superiority of the 3D-printed fistula stent, a study with a larger number of patients is needed to confirm the applicability of this treatment.

In conclusion, as a tailored GI isolation technique, a 3D-printed fistula stent was fabricated under the guidance of 3D-reconstructed fistulography, and was effective for control of the loss of enteric effluent in this ECF patient. Therefore, this method should be advocated, and the clinical outcomes merit further investigation.

COMMENTS

Case characteristics
A 45-year-old man was referred to our hospital because of non-healing enterocutaneous fistula after open abdomen.

Clinical diagnosis
The clinical diagnosis was enterocutaneous fistula of small intestine.

Differential diagnosis
Intestinal perforation, surgical site infections, or abdominal wall deformity.

Laboratory diagnosis
Enterocutaneous fistula of small intestine by detection of amylase in drainage fluid.

Imaging diagnosis
Enterocutaneous fistula of small intestine by X-ray.

Treatment
3D-printed fistula stent was highlight during management of the enterocutaneous fistula (ECF) patient.

Related reports
Previously, traditional stent was reported to manage ECF in patients with terminal ileostomy.

Term explanation
ECF is defined as an abnormal, unintentional connection between the gastrointestinal (GI) tract and the skin or the GI tract and the atmosphere in the open abdomen.

Experiences and lessons
The 3D-printed fistula stent can be designed to match with ECF anatomy and reduce the loss of enteric effluent and prevent the contamination of surrounding granulation tissues, thus leading to making a good preparation of ECF resection.

Peer-review
Authors reported how to use 3D-printed fistula stent to manage ECF. The method was novel and very interesting.

REFERENCES

1 **Schecter WP**, Hirshberg A, Chang DS, Harris HW, Napolitano LM, Wexner SD, Dudrick SJ. Enteric fistulas: principles of management. *J Am Coll Surg* 2009; **209**: 484-491 [PMID: 19801322 DOI: 10.1016/j.jamcollsurg.2009.05.025]

2 **Di Saverio S**, Tarasconi A, Walczak DA, Cirocchi R, Mandrioli M, Birindelli A, Tugnoli G. Classification, prevention and management of entero-atmospheric fistula: a state-of-the-art review. *Langenbecks Arch Surg* 2016; **401**: 1-13 [PMID: 26867939 DOI: 10.1007/s00423-015-1370-3]

3 **Ortiz LA**, Zhang B, McCarthy MW, Kaafarani HMA, Fagenholz P, King DR, De Moya M, Velmahos G, Yeh DD. Treatment of Enterocutaneous Fistulas, Then and Now. *Nutr Clin Pract* 2017; **32**: 508-515 [PMID: 28358595 DOI: 10.1177/0884533617701402]

4 **Yetisir F**, Sarer AE, Aldan M. New isolation technique for enteroatmospheric fistula in Björck 4 open abdomen. *Hernia* 2017; **21**: 809–812 [PMID: 28417280 DOI: 10.1007/s10029-017-1614-y]

5 **Bobkiewicz A**, Walczak D, Smoliński S, Kasprzyk T, Studniarek A, Borejsza-Wysocki M, Ratajczak A, Marciniak R, Drews M, Banasiewicz T. Management of enteroatmospheric fistula with negative pressure wound therapy in open abdomen treatment: a multicentre observational study. *Int Wound J* 2017; **14**: 255-264 [PMID: 27000995 DOI: 10.1111/iwj.12597]

6 **Wang G**, Ren J, Liu S, Wu X, Gu G, Li J. "Fistula patch": making the treatment of enteroatmospheric fistulae in the open abdomen easier. *J Trauma Acute Care Surg* 2013; **74**: 1175-1177 [PMID: 23511162 DOI: 10.1097/TA.0b013e318282705e]

7 **Santerre JP**, Woodhouse K, Laroche G, Labow RS. Understanding the biodegradation of polyurethanes: from classical implants to tissue engineering materials. *Biomaterials* 2005; **26**: 7457-7470 [PMID: 16024077 DOI: 10.1016/j.biomaterials.2005.05.079]

8 **Zhang S**, Guo Y, Dong Y, Wu Y, Cheng L, Wang Y, Xing M, Yuan Q.A Novel Nanosilver/Nanosilica Hydrogel for Bone Regeneration in Infected Bone Defects. *ACS Appl Mater Interfaces* 2016; **8**: 13242-13250 [PMID: 27167643 DOI: 10.1021/acsami.6b01432]

9 **Papavramidis ST**, Eleftheriadis EE, Apostolidis DN, Kotzampassi KE.Endoscopic fibrin sealing of high-output non-healing

gastrocutaneous fistulas after vertical gastroplasty in morbidly obese patients.*Obes Surg* 2001; **11**: 766-769 [PMID: 11775579 DOI: 10.1381/09608920160558759]

10 **Rebibo L**, Wacrenier A, Thiebault H, Delcenserie R, Regimbeau JM. Combined endoscopic and surgical covered stent placement: a new tailored treatment for enteroatmospheric fistula in patients with terminal ileostomy. *Endoscopy* 2017; **49**: E35-E36 [PMID: 28068698 DOI: 10.1055/s-0042-121489]

P- Reviewer: FujinoY, Garg P **S- Editor**: Wei LJ **L- Editor**: A
E- Editor: Huang Y

Published by **Baishideng Publishing Group Inc**
7901 Stoneridge Drive, Suite 501, Pleasanton, CA 94588, USA
Telephone: +1-925-223-8242
Fax: +1-925-223-8243
E-mail: bpgoffice@wjgnet.com
Help Desk: http://www.f6publishing.com/helpdesk
http://www.wjgnet.com

ISSN 1007-9327